Multiply Functionalized Low-Valent Silicon and Germanium Compounds: Novel Building Blocks for Extended Group 14 Systems

Dissertation
zur Erlangung des Grades
des Doktors der Naturwissenschaften
der Naturwissenschaftlich-Technischen Fakultät
der Universität des Saarlandes

Von

M. Sc. David Nieder

Saarbrücken

April/2017

Tag des Kolloquiums:	04.Juli 2017
Dekan:	Prof. Dr. Guido Kickelbick
Berichterstatter:	Prof. Dr. David Scheschkewitz
	Prof. Dr. Dr. h.c. Michael Veith
Vorsitz:	Prof. Dr. Johann Jauch
Akademischer Mitarbeiter:	Dr. Volker Huch

Diese Arbeit entstand in der Zeit von Oktober 2013 bis April 2017, in der Fachrichtung 8.1 Chemie der Universität des Saarlandes unter der Leitung von Herrn Prof. Dr. David Scheschkewitz (Allgemeine und Anorganische Chemie).

Abstract

The transfer and incorporation of intact unsaturated heavier Group 14 motifs into organic and inorganic substrates is one major target of the modern Group 14 chemistry with regard on expanded, possibly conjugated systems in order to gain access to e.g. novel polymers.

This work aimed to provide for a better understanding in view of the prerequisite incorporation of several unsaturated donor-coordinated Si_2Ge-scaffolds into mono- and di-functionalized organic systems, all the while retaining a reactive low-valent heavier Group 14 center. In this context, the isolation of previously proposed highly reactive unsaturated Si_2Ge-intermediates (formed upon reaction of a base-stabilized heavier silyl substituted version of vinylidene with differently sized anionic nucleophiles) was achieved.

As disilenides, silicon versions of vinyl anions, have been the preparative point of entry into the Si_2Ge chemistry, the availability of digermenides could be expected to allow for investigations into the corresponding Ge_3 chemistry. Herein, the synthesis and isolation of the first fully characterized digermenide is presented, as well as first reactivity studies toward different organic and inorganic substrates.

Zusammenfassung

Die Übertragung und Einarbeitung von intakten, ungesättigten schweren Gruppe 14 Strukturmotiven auf organische und anorganische Substrate ist eines der Hauptziele der modernen Gruppe 14 Chemie mit Hinblick auf erweiterte, möglicherweise konjugierter Systeme, die beispielsweise den selektiven Zugang zu neuartigen Polymeren erlauben.

Diese Arbeit trägt zu einem besseren Verständnis bezüglich der Einarbeitung verschiedener ungesättigter Donor-koordinierter Si_2Ge-Gerüste in mono- und difunktionalisierten organischen Systemen bei, die über die ganze Zeit hinweg ein reaktives niedervalentes schweres Gruppe 14 Zentrum beibehalten. In diesem Zusammenhang gelang die Isolierung von zuvor vorausgesagten hoch reaktiven ungesättigten Si_2Ge-Zwischenprodukten (gebildet in Reaktion eines Basen-stabilisierten schweren Silyl-funktionalisierten Vinylidene Analogons mit unterschiedlich großen anionischen Nukleophilen).

Da Disilenide, schwere Versionen von Vinylanionen, den präparativen Zugangspunkt in die Si_2Ge-Chemie bildeten, könnte die Verfügbarkeit von Digermeniden eine Erforschung in die entsprechende Ge_3-Chemie ermöglichen. Hier wird nun die Synthese und Isolierung des ersten vollständig charakterisierten Digermenids präsentiert, sowie erste Reaktivitätsstudien gegenüber verschiedenen organischen und anorganischen Substraten durchgeführt.

Annotation

This thesis has been published in parts in:

- D. Nieder, C. B. Yildiz, A. Jana, M. Zimmer, V. Huch and D. Scheschkewitz, **„Dimerization of a marginally stable disilenyl germylene to tricyclic systems: evidence for reversible NHC-coordination“**, *Chem. Commun.* **2016**, *52*, 2799–2802.

- D. Nieder, V. Huch, C. B. Yildiz and D. Scheschkewitz, **„Regiodiscriminating Reactivity of Isolable NHC-Coordinated Disilenyl Germylene and Its Cyclic Isomer“**, *J. Am. Chem. Soc.* **2016**, *138*, 13996–14005.

Danksagung

Bei **Prof. Dr. David Scheschkewitz** möchte ich mich herzlich dafür bedanken, dass ich nach meiner Masterarbeit die Möglichkeit und das Vertrauen bekam, in die anorganische Molekülchemie zu wechseln. Ebenfalls danke ich ihm für die außerordentlich interessante Themenstellung und die fachliche Hilfe, indem er mir auch in schwierigen Phasen stets zur Seite gestanden und immer eine Lösung gefunden hat.

Weiterhin möchte ich **Prof. Dr. Dr. h.c. Michael Veith** herzlich danken, dass er sich bereit erklärt hat, das Zweitgutachten zu übernehmen.

Prof. Dr. Johann Jauch danke ich an dieser Stelle für die Unterstützung während meines gesamten Studiums.

Ebenso möchte ich mich bei **Dr. André Schäfer** bedanken.

Ein herzliches Dankeschön geht auch an meinen Vertiefungsstudenten **Nicolas Zapp** und alle anderen Studenten, die ich während verschiedener Praktika betreut habe. Vielen Dank auch an alle Kommilitonen.

Ein besonderer Dank geht an **Lukas Klemmer**, **Yvonne Kaiser**, **Yannic Heider** und **Thomas Büttner**, mit denen mir die Arbeit im Labor immer genauso viel Freude bereitet hat wie auch die Feierabendbiere.

Ein weiterer großer Dank geht an **Dr. Cem B. Yildiz**, der unermüdlich DFT-Rechnungen für mich durchgeführt hat und immer für einen Scherz aufgelegt war.

Bei **Dr. Carsten Präsang** möchte ich mich für sein ständiges Interesse, seine Hilfe und den immer guten Ratschlägen in Laborangelegenheiten bedanken.

Vielen Dank an alle vergangenen und jetzigen Gruppenmitglieder: **Dr. Moumita Majumdar**, **Dr. Anukul Jana**, **Dr. Prasenjit Bag**, **Hui Zhao**, **Naim M. Obeid**, **Isabell Omlor**, **Nadine Poitiers**, **Marcel Lambert**, **Dr. Kinga Leszczyńska**, **Dr. Andreas Rammo**, **Ramona Cullmann**, **Evelyne Altmeyer**, **Andreas Adolf**, **Bettina Piro** und **Günther Berlin**.
Bei **Susanne Harling** möchte ich mich für die immer zügigen Messungen der Elementaranalysen herzlich bedanken.

Dr. Volker Huch danke ich sehr für die Mühe bei der Kristallstrukturanalytik, da die Kristallgüte sicher nicht immer die Beste war und er trotzdem das Maximum herausgeholt hat.

Bei **Dr. Michael Zimmer** möchte ich mich für die Unterstützung bei den teilweise sehr länglichen VT-NMR-Experimenten bedanken. Hierbei war auch immer wieder sein Einfallsreichtum gefragt.

Bianca Iannuzzi möchte ich ganz herzlich für die immer unterhaltsamen Gespräche danken. Vielen Dank auch für das Abnehmen einiger bürokratischer Hürden.

Dr. Philipp Willmes möchte ich für die schönen gemeinsamen Jahre, in denen wir stets zusammen gelernt, gearbeitet und ausgiebig gefeiert haben, danken. Des Weiteren bedanke ich mich für den ständigen wissenschaftlichen Austausch und sein Interesse an meiner Arbeit.

Besonders herzlich möchte ich mich bei all meinen Familienmitgliedern bedanken, die immer ein offenes Ohr für mich hatten und mich unterstützten.

Roswitha und **Rüdiger Müller** sowie **Anneliese Gabriel** danke ich für die ständige herzliche Unterstützung während der ganzen letzten Jahre.

Vielen Dank an meinen **Bruder Simon**, meine **Schwester Nora** und **Anna**, die es immer verstanden haben, mich auch in stressigen Zeiten auf besondere Art und Weise zum Lachen zu bringen.

Ein ganz besonderer Dank geht hiermit an meine Großeltern **Oma Irmgard** und **Opa Hermann**, die mich während meiner Kindheit und Jugend sehr geprägt haben. Ich bin ihnen für alles, was sie für mich getan haben über alles dankbar und werde sie niemals vergessen.

Der wohl größte Dank, den ich aussprechen kann, geht aber an drei ganz besondere Menschen, die schon immer an mich glaubten und mir die nötige Kraft gaben, um diese Arbeit zu bewältigen.

Meinem **Vater Karl-Hermann** danke ich für seine spaßige und immer ermutigende Art und meiner **Mutter Christine** für ihre zahlreichen Gespräche, die mich immer ein Stück weiterbrachten.

Meiner **Partnerin Tina** möchte ich an dieser Stelle noch einmal ganz besonders danken, obwohl es mir schwer fällt, dies überhaupt in Worte zu fassen. Sie war in jeder Situation für mich da und hatte immer die richtigen Worte parat. Mit ihrer liebevollen, warmherzigen, aber doch kritischen und zugleich motivierenden Art ist und bleibt sie die Beste.

Table of Contents

List of Abbreviations

Å	**A**ngström
Ar	**Ar**omatic substituent
Bbi	$Si(^{i}Pr)(CH(SiMe_3)_2))_2$
Bbt	$2,6\text{-}[(Me_3Si)_2CH]_2\text{-}4\text{-}[(Me_3Si)_3C]\text{-}C_6H_2)$
B3LYP	**B**ecke hybrid-**3**-parameter functional and the correlation functional of **L**ee, **Y**ang and **P**arr
C	**C**elsius
cAAC	**c**yclic **A**lkyl **A**mino **C**arbene
CGMT	**C**arter-**G**oddard-**M**alrieu-**T**rinquier
Cy	**Cy**clohexyl
dem	**Di**ethoxy**m**ethane
Dec.	**Dec**omposition
DFT	**D**ensity **F**unctional **T**heorie
Dip	2,6-**Di**isopropyl**p**henyl
dme	1,2-**Dim**ethoxy**e**thane
Dur	**Dur**yl, 2,3,5,6-Tetrametylphenyl
Dsi	$CH(SiMe_3)_2)$
EMind	1,1,3,3,7,7-Hexaethyl-5,5-dimethyl-s-hydrindacen-4-yl
equ	**equ**ivalent
Et	**Et**hyl, $-C_2H_5$
Et_2O	Diethylether
h	**h**our
HOMO	**H**ighest **O**ccupied **M**olecular **O**rbital
^{i}Pr	*iso*-**Pr**opyl, $-C_3H_7$
IR	**I**nfra**r**ed
LUMO	**L**owest **U**noccupied **M**olecular **O**rbital
M	**M**olar
Me	**M**ethyl, $-CH_3$
Mes	2,4,6-Trimethylphenyl
Mes*	2,4,6-Tri-*tert*.-butylphenyl
MO	**M**olecular **O**rbital
M. p.	**M**elting **p**oint

Naph	**Naph**thalene
NHC	***N*-H**eterocyclic **C**arbene
NMR	**N**uclear **M**agnetic **R**esonance
Ph	**Ph**enyl
rt	**r**oom **t**emperature
Tbt	2,4,6-**T**ris[**b**is(**t**rimethylsilyl)methyl]phenyl
^{t}Bu	***tert***.-**Bu**tyl, -C_4H_9
thf	**t**etra**h**ydro**f**urane
Tip	2,4,6-**T**ri**i**sopropyl**p**henyl
Tol	**Tol**uene
UV	**U**ltra**v**iolet
vis	**vis**ible
VT	**V**ariable **T**emperature
Xyl	**Xyl**yl, 2,6-Dimethylphenyl

List of Figures

List of Schemes

Foreword

The element germanium has only a low abundance in the Earth's crust ($1.5*10^{-4}$ mass%, position 53) in stark contrast to its lighter congener silicon, which is the second most abundant element after oxygen (27.7 mass%).[1–3] Postulated in 1871 by Dimitri Ivanovich Mendeleev as eka-silicon, germanium was discovered in 1886 by Clemens Winkler and thereby provided considerable support for the Periodic Table of the Elements.[4–7] Winkler extracted germanium from the mineral argyrodite (Ag_8GeS_6, 6% Ge-content), which was found in the silver mine "*Himmelfürst Fundgrube*" in Freiberg. The name of the element refers to the Latin word for Germany, Winkler's homeland.[6] Germanium occurs in low concentrations in rare minerals (2 to 6% Ge-content) or in sphalerite (ZnS) and therefore extraction processes are complex and expensive.[3,8] It was also up to Winkler to synthesize tetraethyl germane, the first organo-germanium compound.[6]

In 1948, germanium's excellent semiconducting properties were demonstrated by the invention of the first transistor, a triode containing a germanium-block as base (germanium-transistor).[9] The major application field of germanium in the last decades is the utilization in high-end technologies e.g. solar modules, satellites, night-vision devices, IR-optics and especially fiber-optics (Figure 1).[2] Another commercial application is the use of GeO_2 as a catalyst for polymerization in the process of polyethylene terephthalate (PET).[10]

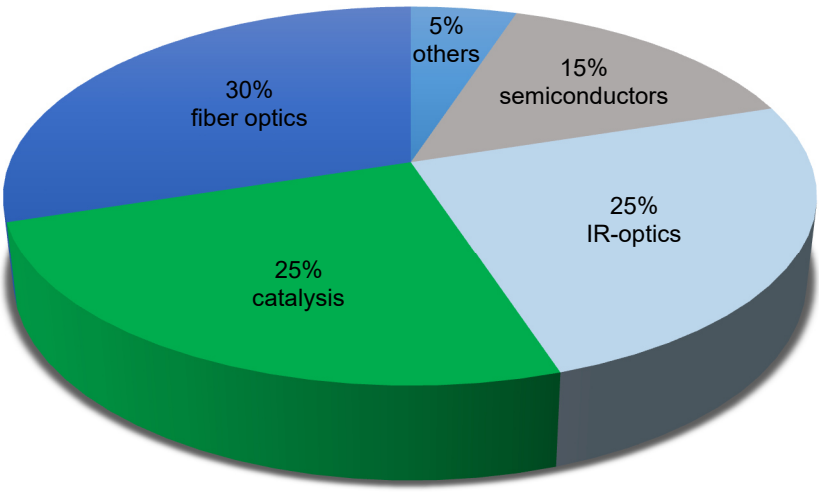

Figure 1. Applications of germanium.

Taking all these facts into account, it is evident that germanium chemistry needs to be further investigated in detail for a most efficient utilization of this scarce element.

1. Introduction

In 1976, the first heavier alkene analogues were isolated by Lappert *et al.*: digermene **1** and distannene **2**, although at that time only the structure of distannene **2** was determined by single-crystal X-ray diffraction.[11,12] The molecular structure in the solid state of digermene **1** was confirmed by Lappert *et al.* in 1984.[13] Notably, both species show a strongly *trans*-bent structure with surprisingly long germanium-germanium and tin-tin bonds, respectively, and – moreover – dissociate in solution to the constituting carbene-like fragments. These observations raised severe doubts about their doubly-bonded nature. In 1981, however, West, Michl and Fink achieved a breakthrough by the synthesis of the stable disilene **3** which is protected by four bulky mesityl substituents (Scheme 1), but still maintains its dimeric nature in solution.[14] The key to the stability of such unsaturated systems is the kinetic protection by substituents with carefully chosen steric demand.[15,16] In the subsequent decades a variety of different substituted digermenes[17] and disilenes[18] (as well as distannenes and even diplumbenes)[15–17,19] have been synthesized *via* different synthetic pathways (see Chapter 1.4.).

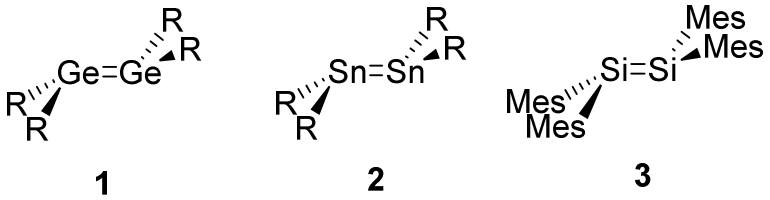

Scheme 1. First heavier Group 14 alkene analogues: digermene **1**, distannene **2** (R = $CH(SiMe_3)_2$) and disilene **3** (Mes = 2,4,6-Me_3-C_6H_2).

Theory has constantly evolved in parallel and the bonding situation in heavier multiply bonded compounds is textbook material by now.[20] In the following paragraphs, heavier alkenes will initially be introduced from a theoretical perspective including the discussion of stabilizing effects in their constituting carbene-like fragments. Subsequently, an overview of experimentally available unsaturated species of silicon and germanium will be provided in order of increasing complexity. Thus, the literature on heavier carbene analogues as well as their base adducts will be reviewed followed by heavier alkenes and finally mixed systems with both functionalities in a single molecule.

1.1. Triplet- and Singlet-Tetrylenes

In general, carbenes (:CR_2) are neutral compounds possessing a divalent C-atom with only six electrons in the valence shell. The 2e2c-bonds to the substituents utilize four of these electrons, leaving two electrons of non-bonding nature. Two electronic states are relevant for the non-bonding electrons of carbenes: triplet and singlet. While triplet carbenes have two singly occupied orbitals with parallel spin (diradical character), the ambiphilic singlet carbenes exhibit two paired electrons in a sp^2-type hybrid orbital (nucleophilic, high s-character) and a vacant p-orbital (electrophilic, Figure 2). The idealized case for a triplet methylene fragment features a HCH-angle of 180° thus allowing for two perfectly degenerate p orbitals. In reality, however, triplet carbenes deviate considerably from linearity due to secondary orbital interactions giving rise to an angle of 134°. For singlet methylene a HCH-angle of 90° would be ideal, as a pure p-type interaction with the substituents maximized the s character of the lone pair. In reality the angle for singlet methylene is with 102° somewhat larger, but still considerably smaller than the 120° expected on purely steric arguments.

Theoretical calculations predict that the singlet-triplet energy difference ΔE_{ST} for tetrylene fragments is much higher than in the case of carbenes. For example, the singlet-triplet energy difference (ΔE_{ST}) for GeH_2 is predicted to be 21.8 kcal mol^{-1} in contrast to the difference in CH_2 which was found to be –14.0 kcal mol^{-1}. This means the triplet state is lying much higher in energy for carbene-like tetrylene fragments than the singlet state and consequently leads to the pronounced preference of the singlet state in heavier Group 14 carbene analogues.[21–26]

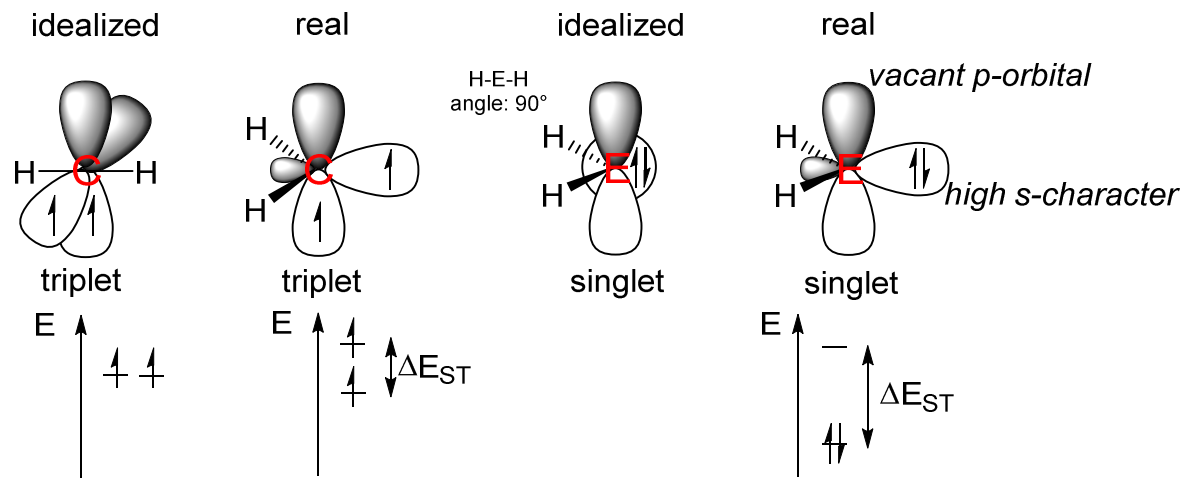

Figure 2. Difference between the ground state of carbenes and heavier tetrylenes (ΔE_{ST} = $E_{Singlet}$ – $E_{Triplet}$).

As steric repulsion at a carbene center maximizes the angle enclosed by the pending groups, bulky substituents tend to stabilize the triplet state. Ideal substituents to stabilize singlet tetrylenes preserve the electroneutrality of the tetrylene center: two π-donor σ-attractor groups, for example, create a push, push-mesomeric (lower HOMO) and pull, pull-inductive (higher LUMO) substitution pattern such as in diamino tetrylenes.[19,21,27,28]

1.2. Carter-Goddard-Malrieu-Trinquier (CGMT)-Model

In contrast to the planar geometry of alkenes, their heavier congeners incorporating silicon, germanium, tin or lead into the double bond show a more or less pronounced deviation from planarity. Therefore, heavier alkene analogues are characterized by a non-classical electron distribution, which is best described by the Carter-Goddard-Malrieu-Trinquier (CGMT) model. In this model, the double bond is considered as formally originating from the combination of two carbene-like fragments.[29–31] In the case of carbenes themselves, the triplet state is the ground state (singlet state for methylene: ca. 14 kcal/mol higher in energy).[22] When two triplet carbene fragments are combined, the result is the classical planar double bond, which is typical for alkenes (Figure 3). In contrast, the singlet state is inherently more stable for heavier carbene homologues (Chapter 1.1., ΔE_{ST} for SiH_2: 16.7 kcal mol^{-1}, ΔE_{ST} for GeH_2: 21.8 kcal mol^{-1} and ΔE_{ST} for SnH_2: 24.8 kcal mol^{-1}).[32–34] Unlike in the carbon case, a direct interaction of two tetrylene fragments is not possible due to Coulomb-repulsion between the lone pairs. Therefore, the formally sp^2-hybridized lone pairs of each tetrylene fragment form a donor-acceptor bond with the empty p_z-orbital of the other fragment resulting in the typically "non-classical", *trans*-bent structure known for heavier alkene analogues. An alternative rationalization of the trans-bending of heavier double bonds was provided by Power *et al.* that heavier alkene analogues **I** can also be regarded as zwitterionic and/or diradical-species **I'** and **I''** (Scheme 2).[16,35]

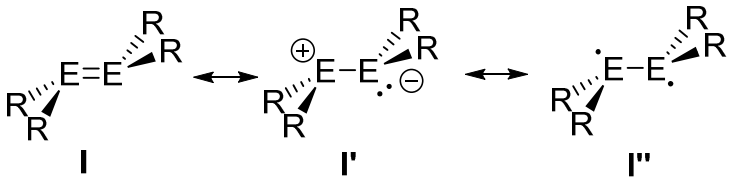

Scheme 2. Zwitterionic and diradical resonance forms **I'** and **I''** of heavier alkene analogues **I** reported by Power and co-workers (E = heavier Group 14 element, R = bulky substituent).

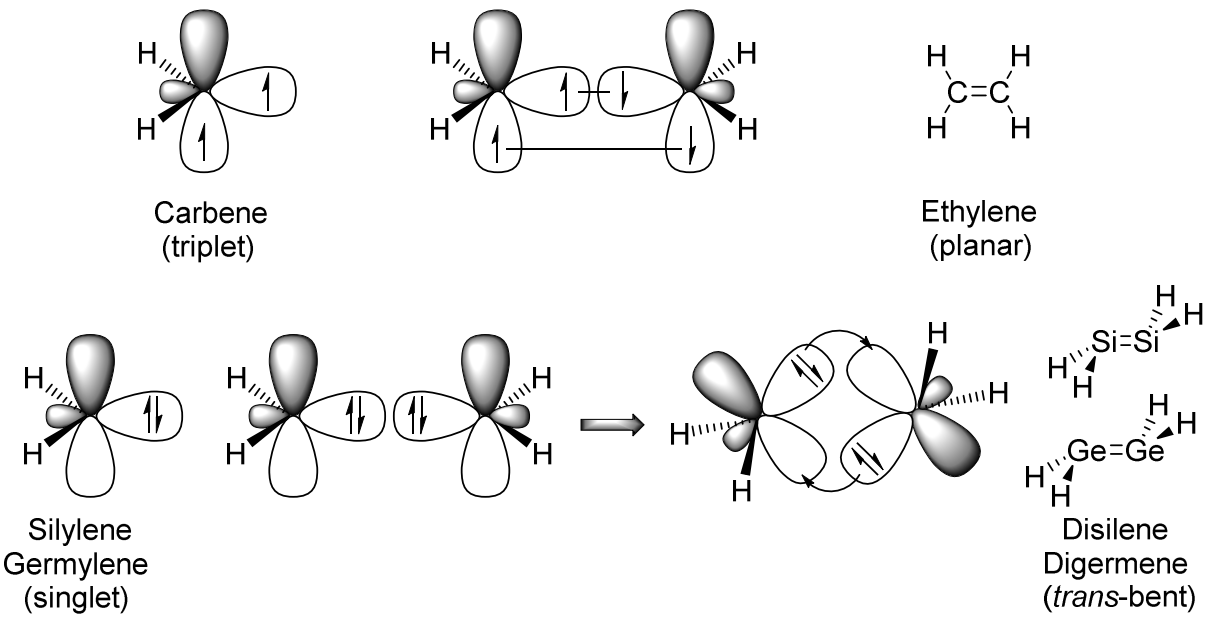

Figure 3. Formation of double bonds in case of carbon and heavier Group 14 congeners according to the CGMT-model.

Three parameters are typically employed to characterize the deviation from planarity of heavier Group 14 E=E-double bonds (Figure 4):[36]

1) The *trans*-bent angle θ (or *cis*-bent angle) quantifies the degree of pyramidalization at the heavier group 14 element atoms.

2) The twist angle τ is a measure for dihedral distortion and defined by the normals of the planes of the E-atoms (E = heavier Group 14 element) and the bonds to the pending substituents.

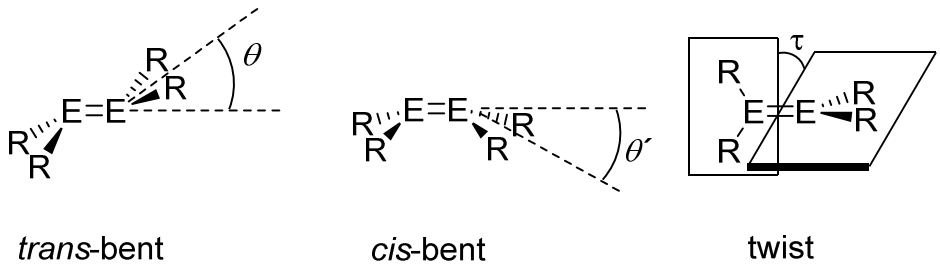

Figure 4. Typical distortion modes for heavier Group 14 E=E-bonds.

The calculated *trans*-bent angle in $H_2Ge{=}GeH_2$ is with $\theta = 34°$ much higher than in the calculated disilene case ($\theta = 13°$).[37,38].

In a sense, *trans*-bending of the double bonds is therefore a direct consequence of the increased stability of the constituting carbene-like fragments. Nevertheless, even for the Group 14 elements heavier than silicon these fragments are unstable in molecular

form unless gas phase or cold matrix conditions are applied.[39–41] As will be detailed in the following, additional measures are necessary in order to gain access to compounds that can be handled under standard laboratory conditions.

1.3. Stable Subvalent Germanium and Silicon-Species

In general the stabilization of tetrylene fragments can be realized by kinetic measures (extremely bulky substituents) or electronically by inclusion of heteroatoms (N, O, P) with their inductive and mesomeric effects.[23,42,43] For example, the first exclusively monomeric dialkyl germylene $(Me_3Si)_3CGeCH(SiMe_3)_2$ both in solution and in the solid state was reported by the Jutzi group.[44] A first stable Si(II)-species was then obtained by West and co-workers by incorporation of the Si(II)-center into an *N*-heterocyclic framework in analogy to the Arduengo carbenes.[45] While these are examples for the *intra*molecular stabilization of heavier carbene analogues, the focus in the following will rest on the *inter*molecular stabilization by an external base, more precisely on *N*-heterocyclic carbene (NHC)-coordinated low-valent Ge- and Si-species:

In 1991, Arduengo *et al.* reported for the first time of a crystalline sample of an *N*-heterocyclic carbene (NHC) **5**.[46] To date a vast number of modified NHCs has been synthesized with varying substitution pattern as well as various peripheral functional groups (Scheme 3).[47]

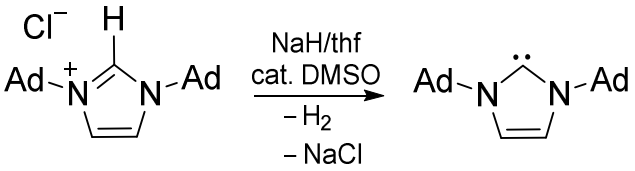

4 **5**

Scheme 3. Synthesis of NHC **5** by deprotonation of **4** reported by Arduengo *et al.* (Ad = adamantyl).

The applications of NHCs is a rapidly growing field,[48] especially in transition metal catalysis,[49,50] organocatalysis,[51] or in coordination chemistry.[52] In addition, a vast number of donor-stabilized main-group compounds has been reported to date.[53,54] Despite the fact that silicon is closer to carbon in the Periodic Table of the Elements, germanium is in many ways more comparable to carbon. In fact, the introduction of the popular Allred-Rochow[55] electronegativity scale was prompted by the observation that while silane (SiH_4) violently reacts with oxygen, germane (GeH_4) is like methane (CH_4) virtually inert to oxidation by excess oxygen at room temperature.[56]

In this light, it is not surprising that many of the newly discovered compound classes in low-valent Group 14 chemistry were initially described as the germanium species.

1.3.1. NHC-Stabilized Low-Valent Germanium-Species

$GeCl_2$·dioxane was first reported by Nefedov and co-workers in 1966 by reaction of $HGeCl_3$ with 1,4-dioxane.[57] Dichloro germylene is stabilized by the coordination of 1,4-dioxane as Lewis-base to the vacant p-orbital on the germanium(II)-center (Scheme 4).

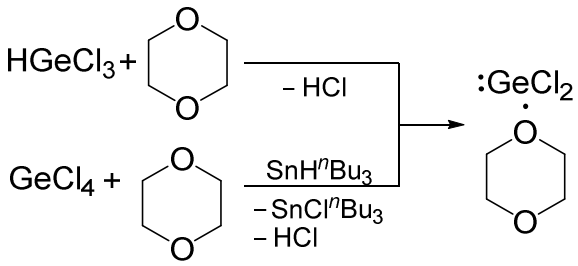

Scheme 4. Synthesis of $GeCl_2$·dioxane by Nefedov *et el.*[57] and Lappert *et al.*[58]

Pioneering contributions to the field of NHC-stabilized germylenes were reported by Arduengo *et al.* in 1993 and by Lappert in 2000.[59,60] Arduengo made use of GeI_2 **6** for the synthesis of the first NHC-stabilized dihalo germylene **7** (Scheme 5), while Lappert *et al.* synthesized an NHC-stabilized *N*-heterocyclic germylene.[59,60]

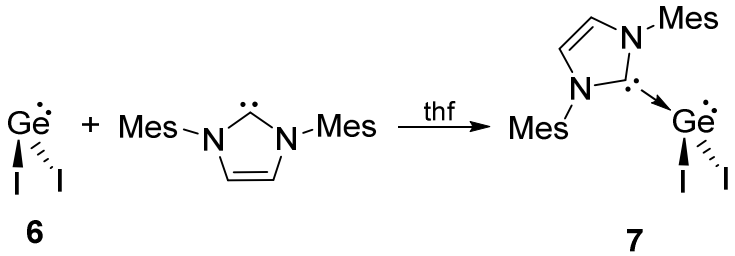

Scheme 5. Reaction of GeI_2 **6** with NHC^{Mes2} leading to the first dihalo germylene NHC-adduct **7** reported by Arduengo *et al.* (Mes = 2,4,6-Me_3-C_6H_2).

In 2007, Baines *et al.* utilized $GeCl_2$·dioxane as starting material for $NHC^{iPr2Me2}$-coordinated dichloro germylene **8** obtained from the replacement of dioxane by $NHC^{iPr2Me2}$ as a stronger σ-donor ($NHC^{iPr2Me2}$ = 1,3-diisopropyl-4,5-dimethylimidazol-2-ylidene). Furthermore, by addition of an excess $NHC^{iPr2Me2}$ to GeI_2·$NHC^{iPr2Me2}$ **9** an unique germanium-centered dication **10** was synthesized, which carries a lone-pair of electrons at the metal-center and a double positive charge (Scheme 6).[61]

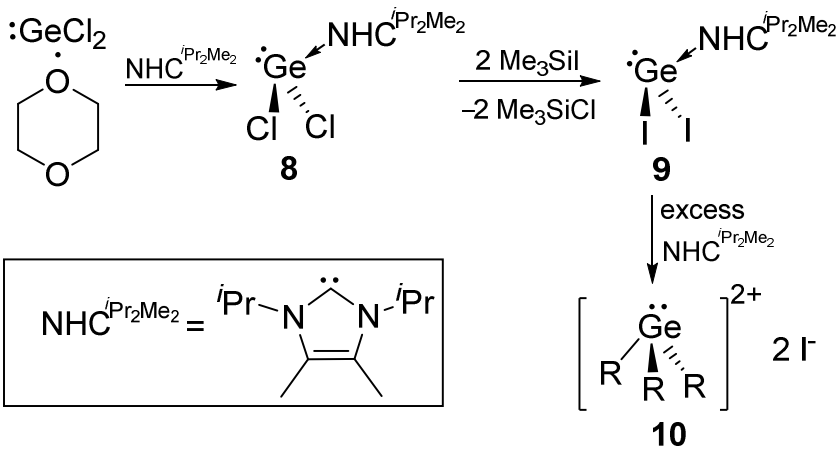

Scheme 6. Synthesis of Ge^{2+}-dication **10** starting from NHC-stabilized $GeCl_2$-adduct **8** *via* NHC-coordinated GeI_2-adduct **9** (R = $NHC^{iPr_2Me_2}$ = 1,3-diisopropyl-4,5-dimethylimidazol-2-ylidene).

In the following years, Baines and co-workers intensely studied the reactions of NHC-stabilized germylenes and showed that one chlorine-atom of **8** can be substituted selectively by different groups yielding NHC-germylene-adducts **11-13** (Scheme 7).[62–64]

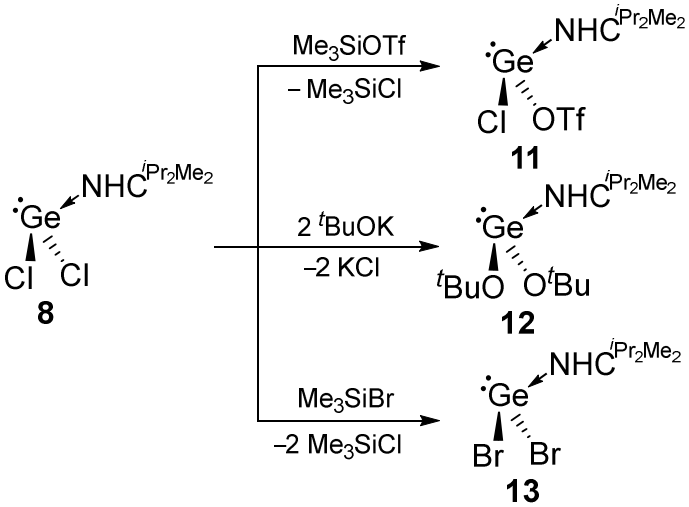

Scheme 7. Examples for different substituted NHC-stabilized germylenes **11-13** starting from $GeCl_2 \cdot NHC^{iPr_2Me_2}$ **8** ($NHC^{iPr_2Me_2}$ = 1,3-diisopropyl-4,5-dimethylimidazol-2-ylidene, OTf = O_3SCF_3).

In 2007, Baines and co-workers obtained the first example of a stable NHC-coordinated germylene with two organic substituents **15** by homolytic cleavage of the Ge=Ge-double bond of $Mes_2Ge{=}GeMes_2$ **14** (Scheme 8).[65] In the reaction with 2,3-dimethylbutadiene, the NHC-stabilized germylene **15** plausibly dissociates to the free NHC and free germylene, which is trapped by 2,3-dimethylbutadiene.

The same group could also demonstrate that the NHC in the germylene adduct **15** can be displaced from the Ge(II)-center by MeLi leading to **16** (Scheme 8).

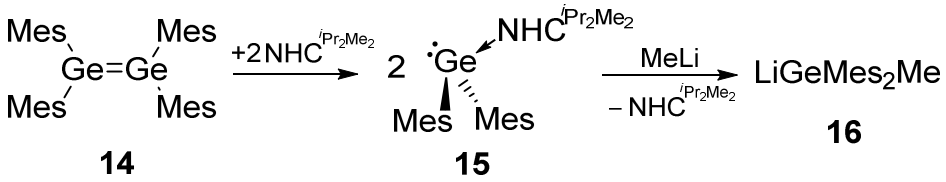

Scheme 8. Cleavage of the Ge-Ge-double bond in $Mes_2Ge{=}GeMes_2$ **14** with NHC^{iPr_2Me_2} (1,3-diisopropyl-4,5-dimethylimidazol-2-ylidene) resulting in two NHC-coordinated germylene fragments **15** (Mes = 2,4,6-Me_3-C_6H_2).

In 2008, by treatment of NHC-stabilized germylene **11** with cryptand [2.2.2], the synthesis of a cryptand-encapsulated Ge(II)-cation **17** with concomitant formation of the cationic dicarbene complex **18** was reported by the Baines group. Dicationic germanium compound **17** could potentially be a starting material for functionalized Ge-species (Scheme 9).[66]

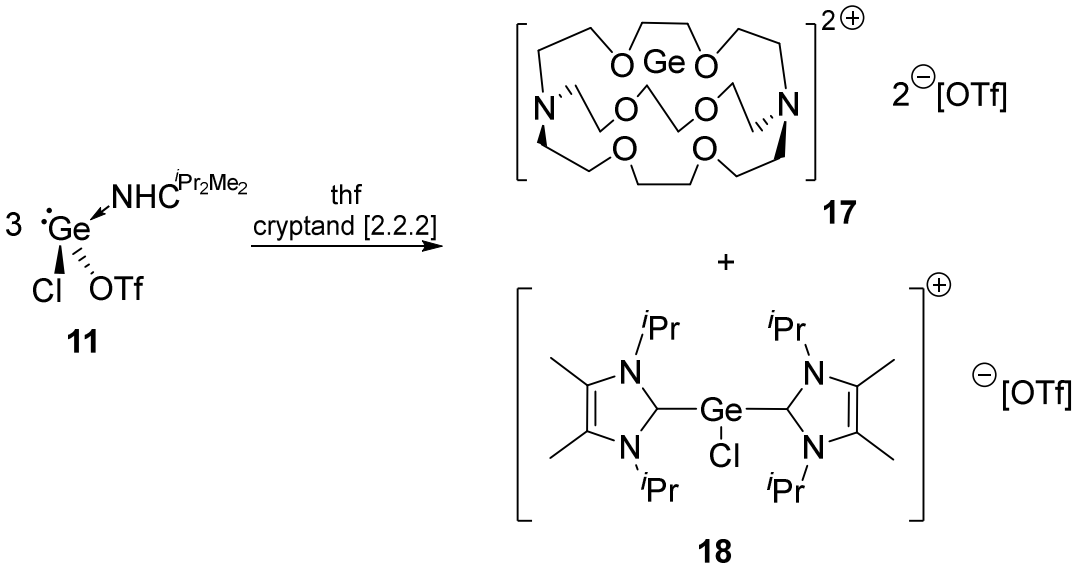

Scheme 9. Synthesis of cryptand-encapsulated Ge(II)-cation **17** and monocationic species **18** starting form germylene **11** reported by Baines *et al.* (NHC^{iPr_2Me_2} = 1,3-diisopropyl-4,5-dimethylimidazol-2-ylidene, OTf = O_3SCF_3).

A further contribution to germylene chemistry was recently reported by the group of Aldridge. An acyclic two-coordinate monocationic germylene **20** was synthesized in the reaction of an NHC-coordinated germylene **19** with the salt Na[BAr$^f_4$] (Scheme 10).[67]

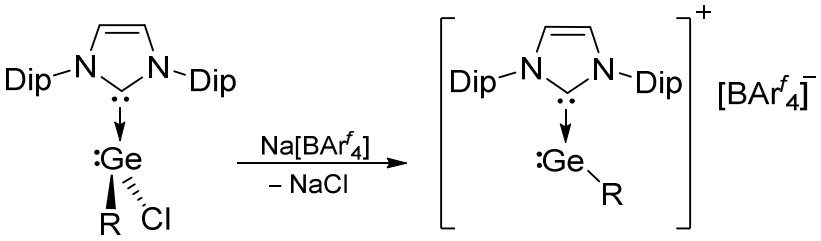

Scheme 10. Synthesis of [R(NHC)Ge]$^+$-cation **20** starting from NHC-coordinated germylene **19** disclosed by Aldridge *et al.* (R = $CH(SiMe_3)_2$, Dip = 2,6-^{i}Pr$_2$-C_6H_3, [BAr$^f_4$]$^-$ = 3,5-$(CF_3)_2$-C_6H_3).

Two NHC-stabilized arylhalo germylenes **23a**,**b** with sterically demanding groups were synthesized by the group of Filippou starting either from NHC-coordinated $GeCl_2$ **21** or from free monomeric arylchloro germylene **22** (Scheme 11).[68,69]

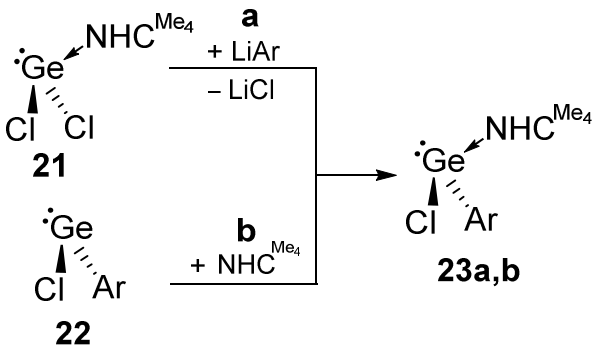

Scheme 11. Synthesis of arylchloro germylenes **23a**,**b** by Filippou *et al.* (**a**: Ar = 2,6-Mes_2-C_6H_3, Mes = 2,4,6-Me_3-C_6H_2, **b**: Ar = 2,6-Tip_2-C_6H_3, Tip = 2,4,6-^{i}Pr$_3$-C_6H_2, NHC^{Me_4} = 1,3,4,5-tetramethylimidazol-2-ylidene).

A clear highlight of the versatile reactions of Ge(II)-compounds, which is particularly relevant for this thesis, was disclosed by Jones and co-workers in 2009. The reduction of $GeCl_2$·NHC^{Dip2} **24** with a Mg(I)-compound yielded the NHC-coordinated $Ge(0)_2$-species **25**, which can also be regarded as zwitterionic **25'** (Scheme 12).[70–73] Although the classification of **25** (and preceding related species) as being of the formal oxidation state zero is somewhat contentious,[74,75] this study together with the earlier report on related silicon systems (page 15, Scheme 18) provided a tremendous stimulus to low-valent main group chemistry with numerous other examples to follow.

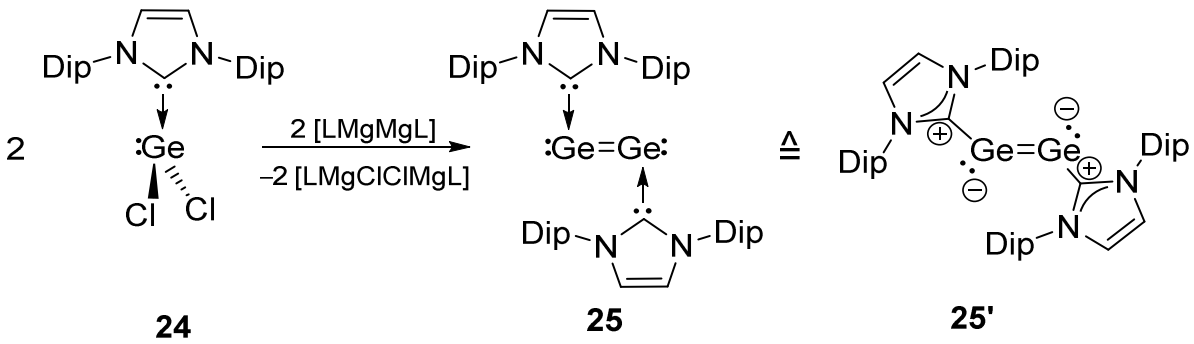

Scheme 12. Synthesis of NHC-stabilized digermanium(0) **25** by Jones *et al.* (Dip = 2,6-$^{i}Pr_2$-C_6H_3, L = $[N(Mes)CMe]_2CH$, Mes = 2,4,6-Me_3-C_6H_2).

For example, the group of Scheschkewitz reported in 2015 the synthesis of a donor-acceptor coordinated formal $Ge(0)_2$-species **28** starting from $Fe(CO)_4$-$GeCl_2 \cdot NHC^{iPr2Me2}$-complex **26** (Scheme 13).[76,77]

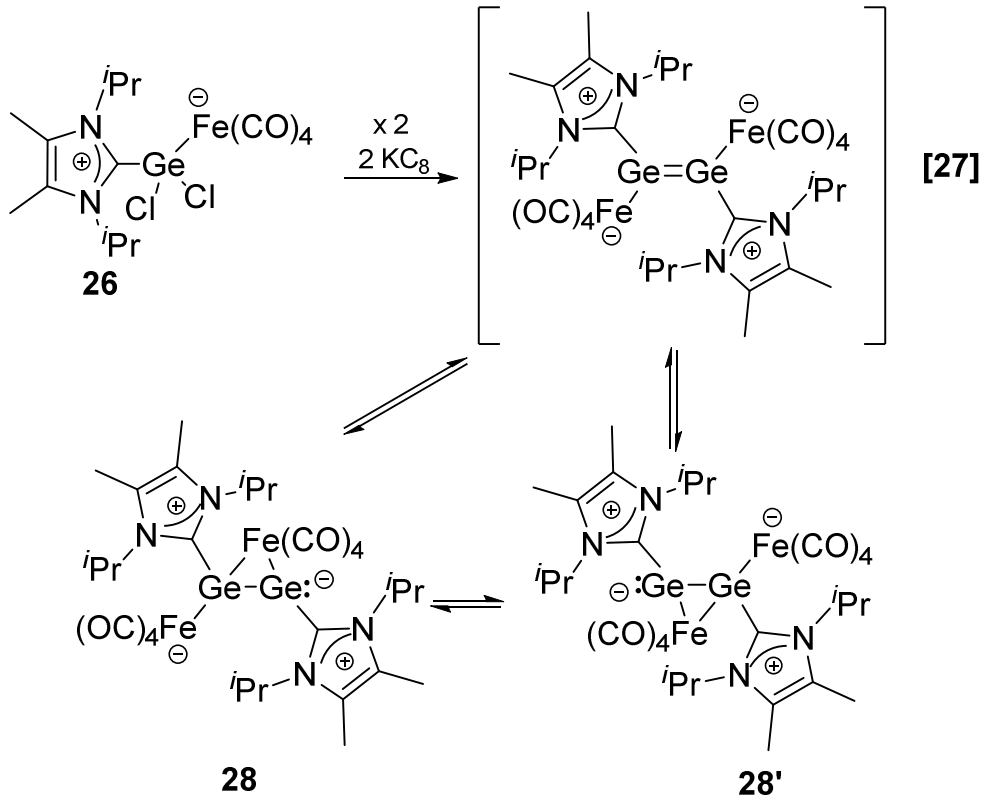

Scheme 13. Synthesis of donor-acceptor coordinated Ge(0)-species **28** (Tip = 2,4,6-$^{i}Pr_3$-C_6H_2).

Driess *et al.* reported the synthesis of a so-called germylone **31** upon reduction of a bis-carbene stabilized chloro germyliumylidene cation **30** with Na/naphthalene.[78] Germylone **31** is the first example for a Ge(0)-complex with only one germanium-atom stabilized by a dicarbene.

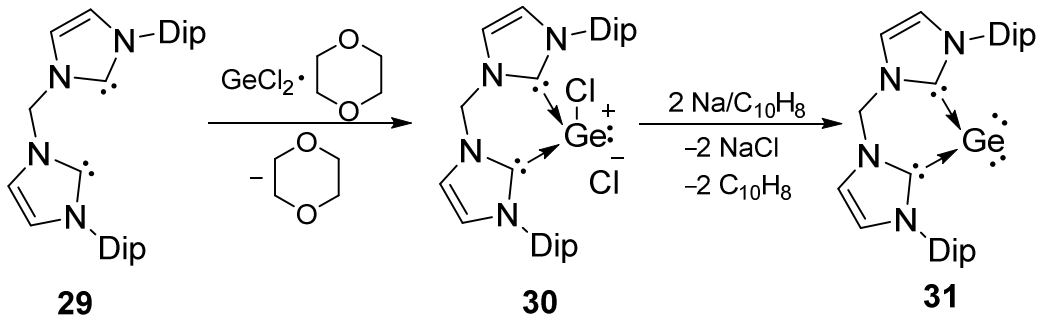

Scheme 14. Synthesis of germylone **31** reported by Driess *et al.* starting form ionic precursor **30** (Dip = 2,6-^{i}Pr$_2$-C$_6$H$_3$).

1.3.2. NHC-Stabilized Low-Valent Silicon-Species

In 1995, Kuhn and Kratz reported the first NHC-adduct of a silicon species **32** together with other derivatives **33** and **34** by simple mixing of the corresponding free chloro silanes with the free carbene (Scheme 15).[79]

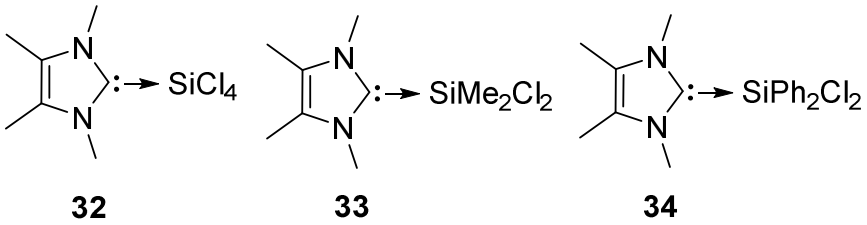

Scheme 15. Examples for NHC-adducts of Si(IV)-species **32-34**.

While the first carbene adduct of a low-valent germanium species was reported as early as 1993 by Arduengo (page 8, Scheme 5),[60] it took until 2009 before Roesky *et al.* succeeded in the synthesis of the first stable NHC-stabilized dichloro silylene with the bulky NHC^{Dip2}. The reaction of two equivalents of NHC^{Dip2} with HSiCl$_3$ *via* HCl elimination led to NHC-coordinated silylene **35** beside imidazolium chloride **36** (Scheme 16).[80]

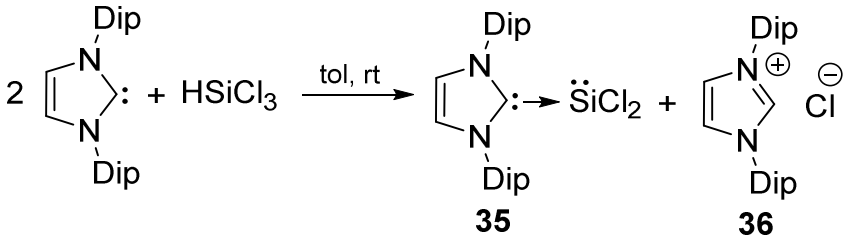

Scheme 16. Synthesis of the first NHC-stabilized dichloro silylene **35** by Roesky *et al.* (Dip = 2,6-^{i}Pr$_2$-C$_6$H$_3$).

In the same issue of Angewandte Chemie, Filippou *et al.* reported on the synthesis of dibromo silylene **38** stabilized by an NHC upon reduction of ionic precursor **37** with two equivalents of KC_8 (Scheme 17).[81]

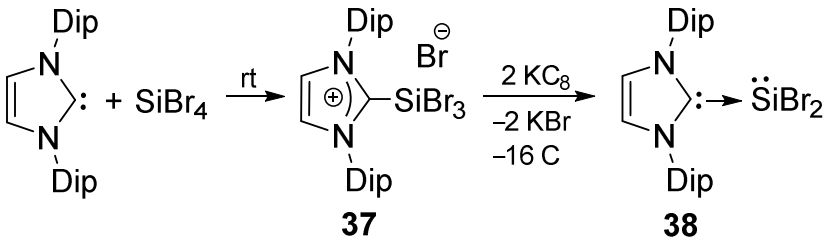

Scheme 17. Synthesis of NHC-stabilized $SiBr_2$-species **38** by the group of Filippou by reduction of ionic precursor **37** (Dip = 2,6-^{i}Pr$_2$-C$_6$H$_3$).

The initial breakthrough in the chemistry of NHC-coordinated low-valent Group14 species, however, was actually the synthesis of a $Si(0)_2$-species **40** coordinated by two NHCs reported by Robinson in 2008.[82] $Si(0)_2$-species **40** can also be regarded as a zwitterionic **40'** with a negative charge at both silicon centers. The NHC-$SiCl_4$-complex **39** was reduced by KC_8 forming $Si(0)_2$-species **40** (Scheme 18). Recently, the reaction of disilicon(0) **40** with N_2O and O_2 led to unique NHC-stabilized Si_2O_3 and Si_2O_4-species **41** and **42** (Scheme 18).[83]

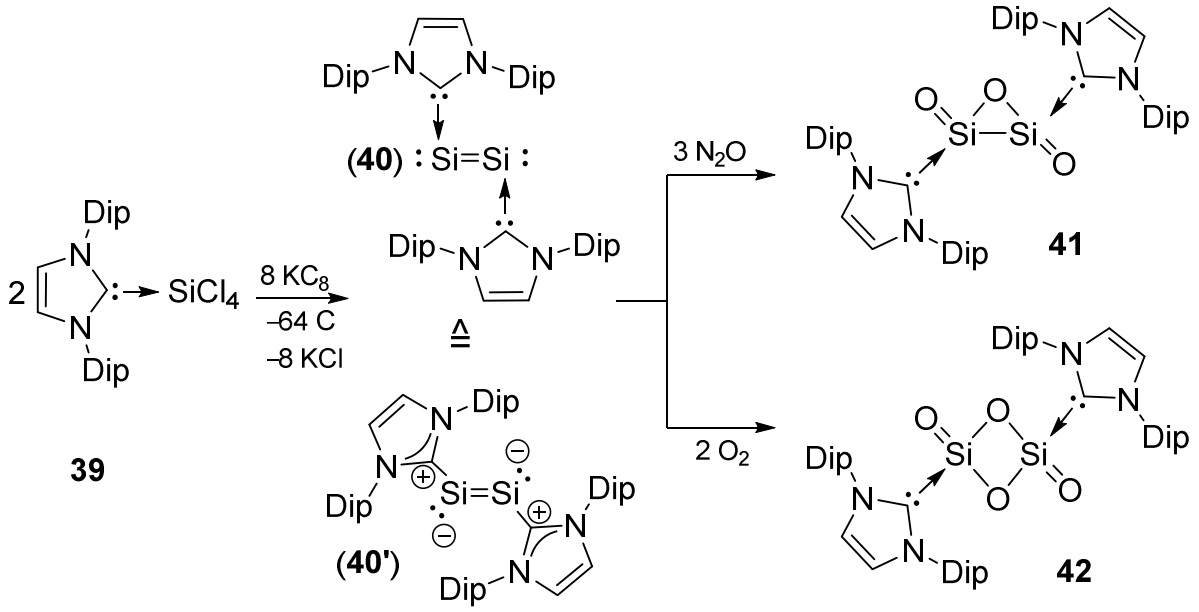

Scheme 18. Synthesis of NHC-stabilized disilicon(0) **40** by Robinson *et al.* and reactivity toward N_2O and O_2 resulting in **41** and **42** (Dip = 2,6-^{i}Pr$_2$-C$_6$H$_3$).

In the last years, Filippou and co-workers used NHC-stabilized Si(0)$_2$ **40** to study the electrochemical behavior and reactivity of **40** toward small electrophiles E^+ (H^+, Me^+, Et^+) resulting in disilicon(I) compounds.[84–86]

In 2013, the group of Driess succeeded in the synthesis of a so-called silylone **44** (Scheme 19) by reduction of precursor **43** with Na/naphthalene, in analogy to their synthesis of germylone **30** (page 13, Scheme 14).[87]

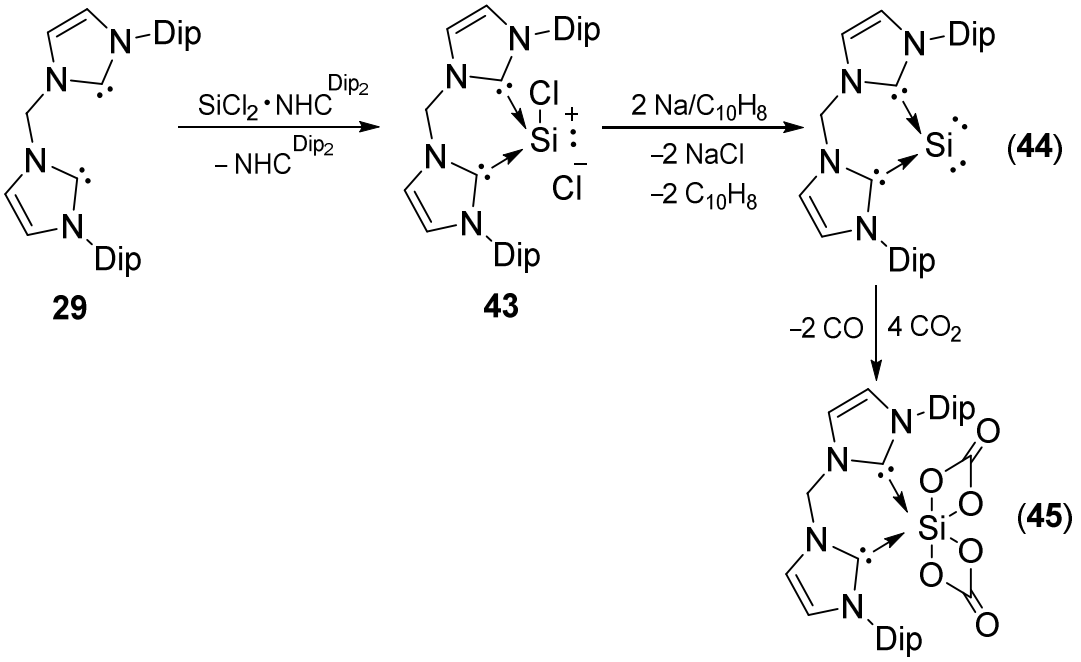

Scheme 19. Synthesis of silylone **44** and reaction of **44** with 4 eq CO_2 resulting in silicon dicarbonate complex **45** reported by Driess *et al.* (Dip = 2,6-^{i}Pr$_2$-C$_6$H$_3$).

Silylone **44** turns out to be a versatile starting material for the synthesis of bis(carbene) complexes of otherwise elusive silicon species. For instance, the reaction of **44** with CO_2 results in the isolable molecular silicon dicarbonate complex **45**.[88] A silicon dioxide complex was proven to be the intermediate of this reaction.

1.4. Synthesis of Digermenes, Disilenes and Silagermenes

Lappert's digermene **1** had been synthesized by reaction of germanium diamide **46** with to equivalents of $Li(CH(SiMe_3)_2$. While digermene **1** has been characterized as a heavier alkene in the solid state, it dissociates into two tetrylene fragments **47** in solution (Scheme 20).[11–13] In the meantime, the dissociation of digermenes into tetrylene fragments in solution is a well-established phenomenon, which indicates the lower bond dissociation energy of the Ge-Ge-double bond in comparison to the Si=Si-bond.[19,89]

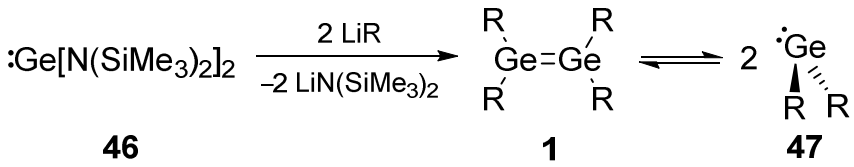

Scheme 20. Synthesis of Lappert's digermene **1** and illustration of equilibrium in solution into tetrylene fragments **47** (R = $CH(SiMe_3)_2$).

The first stable digermene **49** in solution was reported in 1984 by Masamune and Williams by irradiation of linear cyclotrigermane **48** (Scheme 21).[90,91]

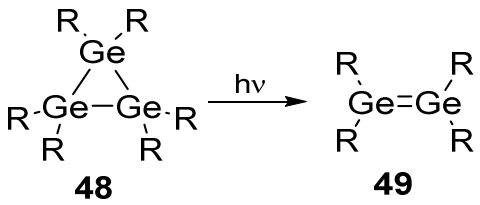

Scheme 21. Synthesis of the first solution stable digermene **49** (R = 2,6-diethylphenyl).

A classical approach for the construction of a Ge=Ge-bond is, like in the case of disilenes, the simple reduction of dichloro germanes. In 1989, digermenes **51** and **53** were synthesized upon reduction of dichloro germanes **50** and **52** reported by Masamune.[91] In 1999, Weidenbruch *et al.* disclosed the synthesis of digermene **51** by reaction of germanium diamide **46** with two equivalents of TipLi in analogy to the synthesis of Lappert's digermene **1** (Scheme 22).[94]

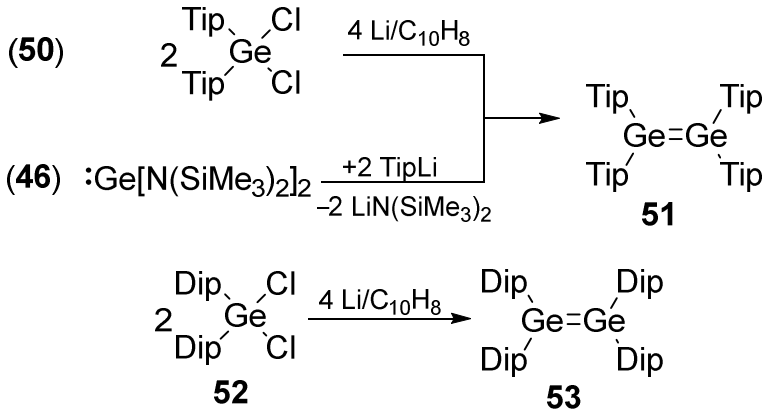

Scheme 22. Synthesis of digermenes **51** and **53** by Masamune *et al.* and synthesis of digermene **51** by Weidenbruch and co-workers (Dip = 2,6-^{i}Pr$_2$-C$_6$H$_3$, Tip = 2,4,6-^{i}Pr$_3$-C$_6$H$_2$).

In the same year Ando *et al.* disclosed a different approach in analogy to the synthesis of West's disilene **3** without confirming the molecular structure of tetramesityl digermene **14** in the solid state.[93,95,96] In 2007, the group of Baines synthesized digermene **14** by photolysis of cyclotrigermane **55** and confirmed the predicted structure of **14** by X-ray diffraction on single crystals (Scheme 23).[97,98]

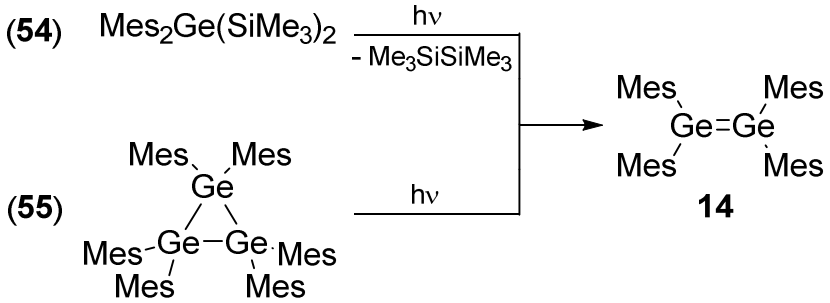

Scheme 23. Synthesis of digermene **14** by Ando *et al.* and the group of Baines (Mes = 2,4,6-Me$_3$-C$_6$H$_2$).

An example for a symmetrically substituted tetrasilyl digermene was presented by the group of Sekiguchi. They reduced dichlorodisilyl germane **56** with KC_8 which afforded blue digermene **57** (Scheme 24, for the silicon analogue see page 20, Scheme 28, **70b**).[99]

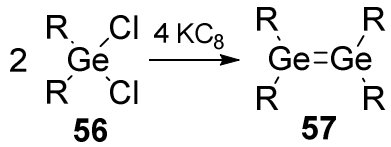

Scheme 24. Synthesis of blue digermene **57** by Sekiguchi and co-workers (R = SiMe^{t}Bu$_2$).

In the last years numerous of examples and synthetic methods for digermenes have been successfully applied as well as reactivity studies toward different organic and inorganic substrates have been investigated.[17,100]

In 1981, the first crystalline sample of a disilene was obtained by West *et al.* by irradiation of the linear trisilane **58** (Scheme 25).[14]

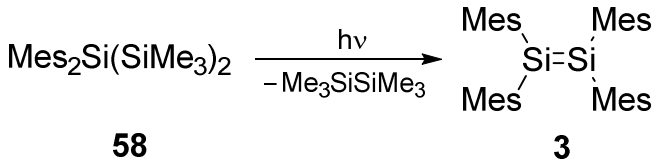

Scheme 25. Synthesis of the first stable disilene **3** reported by West, Fink and Michl in 1981 (Mes = 2,4,6-Me_3-C_6H_2).

Masamune and co-workers reported of disilene **61** by irradiation of cyclotrisilane **60**, which in turn had been obtained by reduction of chloro silane **59**. In 1987, the same group used the reductive dehalogenation of silane **62** with Li/naphthalene to synthesize disilene **63** (Scheme 26).[101,102]

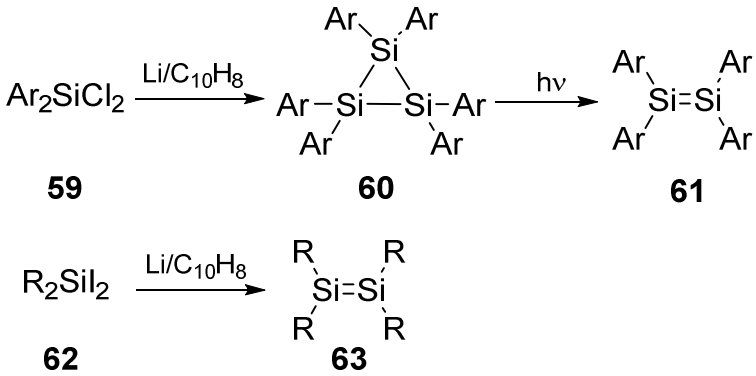

Scheme 26. Synthesis of disilenes **61**and **63** by Masamune *et al.* (Ar = 2,6-Me_2-C_6H_3, R = $(Me_3Si)_2CH$).

The same approach was used by Watanabe and co-workers in the same year by reduction of Tip_2SiCl_2 **64** with four equivalents of Li/naphthalene resulting in the "almost air-stable" disilene **65** with an unusual (for a tetraaryl disilene) perfectly planar Si=Si framework (Scheme 27).[103]

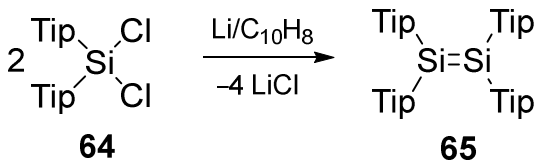

Scheme 27. Reduction of Tip_2SiCl_2 **64** with Li/naphthalene resulting in disilene **65**.

Further input was provided by the group of Sakurai synthesizing yellow silyl-substituted disilene **70a** by irradiation of the sterically less congested cyclotrisilane **66** (Scheme 28).[104] In 2004, the group of Sekiguchi obtained disilene **70b** in reaction of dilithiated silane **67** with dibromo silane **68** or by simple reduction of silane **69** with KC_8 (Scheme 28).[105] Disilene **70a** is nearly planar in stark contrast to the significant twisted blue disilene **70b** (τ = 54°) due to the steric repulsion of the bulky substituents at both silicon centers.

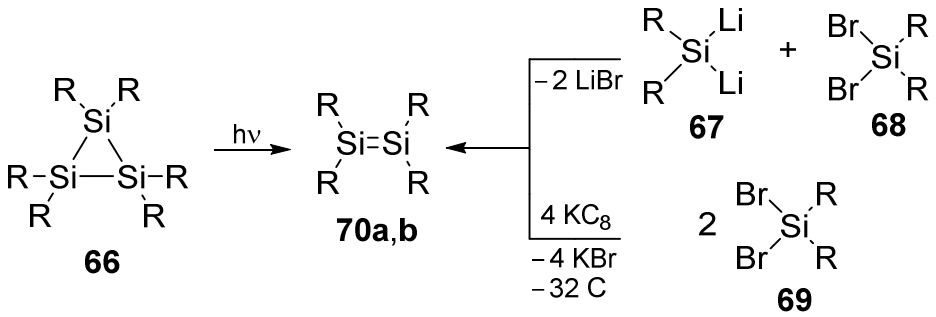

Scheme 28. Synthesis of yellow disilene **70a** by Sakurai *et al.*, blue disilene **70b** by Sekiguchi and co-workers (**66**: R = $SiMe_2{}^tBu$, **67**, **68**, **69**: R = $SiMe{}^tBu_2$, **70a**: R = $SiMe_2{}^tBu$, **70b**: R = $SiMe{}^tBu_2$).

While stable digermenes and disilenes are well studied compounds, less is known about the heteronuclear germasilenes. The first germasilene **72** was reported by the Baines group in 1992 by irradiation of siladigermirane **71** (Scheme 29).[106] An isolable example was obtained by the group of Sekiguchi who were able to characterize germasilene **75** in the solid state by reaction of dilithio silane **73** and dichloro germane **74** (Scheme 29).[107] Further silagermenes were to follow in the last decades and were summarized in several review articles.[19,108–110]

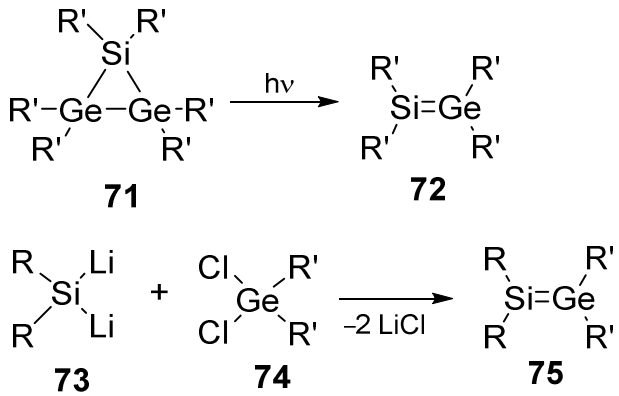

Scheme 29. Synthesis of germasilenes **72** and **75** presented by the groups of Baines and Sekiguchi (R = $Si{}^tBu_3$, R' = Mes).

1.5. Heavier Analogues of Alkynes: Disilynes and Digermynes

Alkynes play a pivotal role in organic chemistry as building blocks for the construction of a variety of molecules.[111–113] The first heavier alkyne analogue, a diplumbyne was reported by Power and co-workers in 2000.[114]

Two years later, Power *et al.* were able to isolate the first digermyne **77** upon reduction of the bulky chloro germylene **76** with potassium (Scheme 30).[115] A year later the same group reported dianionic reduction products e.g. **78** from the reduction of digermyne **77** with excess lithium (Scheme 30).[116,117]

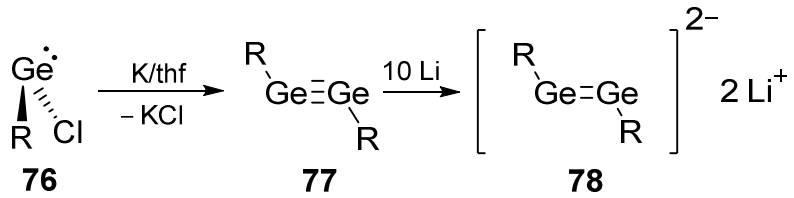

Scheme 30. First stable digermyne **77** and its reduction product **78** reported by Power *et al.* (R = 2,6-Dip_2-C_6H_3; Dip = 2,6-$^iPr_2$-C_6H_3).

In 2006, Tokitoh *et al.* synthesized digermyne **80** upon reduction of dibromo digermene **79** with KC_8 (Scheme 31).[118]

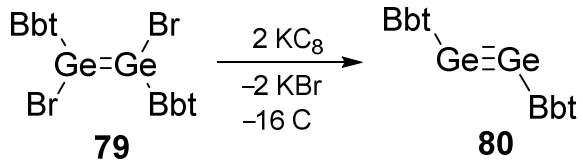

Scheme 31. Synthesis of digermyne **80** reported by Tokitoh *et al.* (Bbt =2,6-[$(Me_3Si)_2CH]_2$-4-[$(Me_3Si)_3C$]-C_6H_2).

Recently, the group of Jones reported the first example of an amido-digermyne[119] and the activation with H_2 leading to a hydrido-digermene.[120]

The first stable molecule containing a Si≡Si-bond was reported by Sekiguchi *et al.* in 2004 by reduction of disilane **81** with KC_8 which yielded disilyne **82**. The silicon centers are protected by extremely bulky silyl substituents, which are responsible for the stability of the Si-Si-triple-bond (Scheme 32).[121,122]

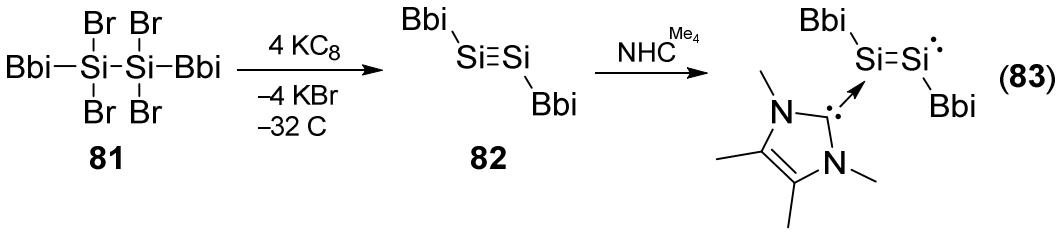

Scheme 32. Synthesis of Sekiguchi's disilyne **82** and reactivity with NHC^{Me4} leading to disilyne-complex **83** reported by Driess and Sekiguchi (Bbi = $Si^{i}PrDsi_2$, Dsi = $CH(SiMe_3)_2$).

A remarkable reactivity of disilyne **82** was disclosed by Sekiguchi and Driess in 2010 showing the irreversible reaction of disilyne **82** with NHC^{Me4} resulting in the polar disilyne-complex **83** with a *trans*-geometry of the Si=Si moiety and a lone-pair of electrons located at one double-bonded silicon-atom (Scheme 32).[123]

In the following years some further examples of disilynes have been reported. Diaryl substituted disilyne **85** was synthesized in the reaction of dibromo disilene **84** with 2 equivalents ^{t}BuLi by Tokitoh *et al.* (Scheme 33).[124] Unsymmetrically substituted disilyne **87** was obtained by the group of Sekiguchi upon reduction of disilane **86** with 4 equivalents KC_8 (Scheme 33).[125]

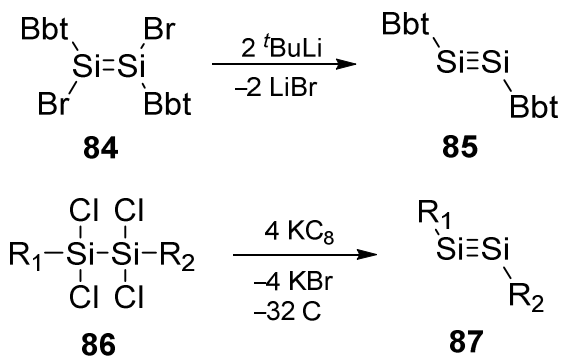

Scheme 33. Synthesis of disilynes **85** and **87** (Bbt = 2,6-$[(Me_3Si)_2CH]_2$-4-$[(Me_3Si)_3C]$-C_6H_2), R_1 = $SiNpDsi_2$, R_2 = $Si^{i}PrDsi_2$, Np = $CH_2{}^{t}Bu$, Dsi = $CH(SiMe_3)_2$).

It should be noted that in none of these cases, isomerization processes of the heavier alkynes to the corresponding heavier vinylidene analogues were observed (see Chapter 1.6.2).

1.6. Doubly Functionalized Low-Valent Group 14 Systems

1.6.1. Digermenides and Disilenides

A major target of the modern low-valent Group 14 chemistry is the incorporation or transfer of intact unsaturated functionalities to different organic and inorganic moieties to obtain expanded systems with low-valent Group 14 functionalities.[126,127] A breakthrough in this field was the development of Group 14 vinyllithium analogues, which will be discussed in the following chapter. Heavier Group 14 vinyl anions **II** feature two functionalities (anionic-center and double-bond). On grounds of the comparatively weak E=E-bonds, they can also be considered in the mesomeric form e.g. as silylene silyl-anion of type **II'** (Scheme 34).

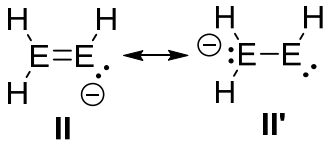

Scheme 34. Mesomeric resonance structures **II** and **II'** of heavier vinyl anions.

In 1989, Masamune *et al.* reduced digermene **53** with Li/naphthalene and isolated a red crystalline material, which was analyzed as the corresponding digermenide **88** by NMR and UV/vis spectroscopy. As an X-ray diffraction analyses to confirm the molecular structure in the solid state could not be obtained, the methanolysis of proposed digermenide **88** to digermane **89** provided circumstantial evidence (Scheme 35).[92]

A second synthetic approach was reported by Weidenbruch *et al.* in 2000 also starting from a digermene. By reduction of $Tip_2Ge{=}GeTip_2$ **51** with lithium in dme, the isolation of digermenide **90** was equally impossible, but the addition of TipBr to the reaction mixture resulted in the formation of tetragermabutadiene **92** (Scheme 35).

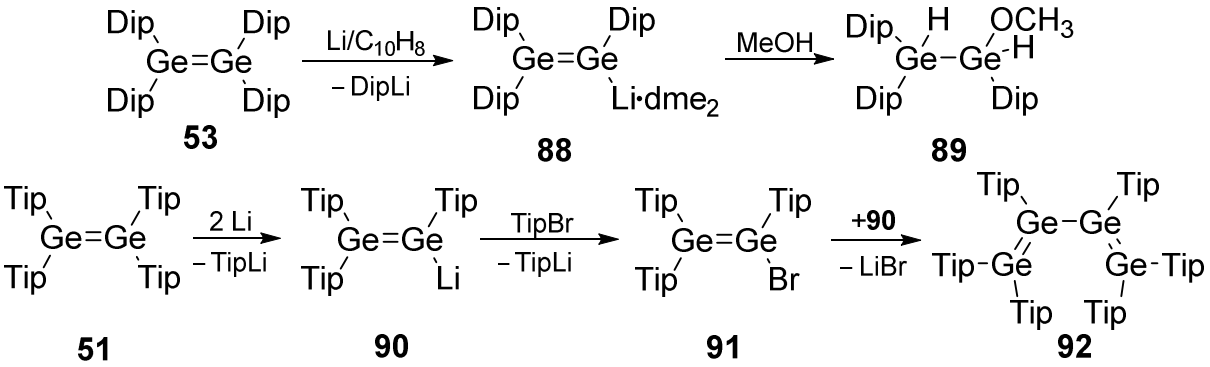

Scheme 35. Attempts to synthesize digermenides **88** and **90** by reduction of **53** and **51** presented by Masamune and Weidenbruch (Dip = 2,6-^{i}Pr$_2$-C$_6$H$_3$, Tip = 2,4,6-^{i}Pr$_3$-C$_6$H$_2$, dme = 1,2-dimethoxyethane).

The proposed digermenide **90** had most likely been formed as an intermediate, which may have been partially brominated by TipBr to bromo digermene **91** and then finally reacted with excess of digermenide **90**. Tetragermabutadiene **92** was the first example for a system with conjugated Ge=Ge-double bonds.[128] In 2003, Weidenbruch *et al.* reported a higher yielding synthesis for tetragermabutadiene **92** starting from $GeCl_2$·dioxane in reaction with TipMgBr and Mg.[129,130]

Inspired by an earlier report on a similar germanium species by the group of Masamune (Scheme 35), Weidenbruch *et al.* reduced symmetrical disilene $Tip_2Si{=}SiTip_2$ **65**[103] with two equivalents lithium to obtain disilenyllithium **93** by reductive abstraction of one aryl substituent.

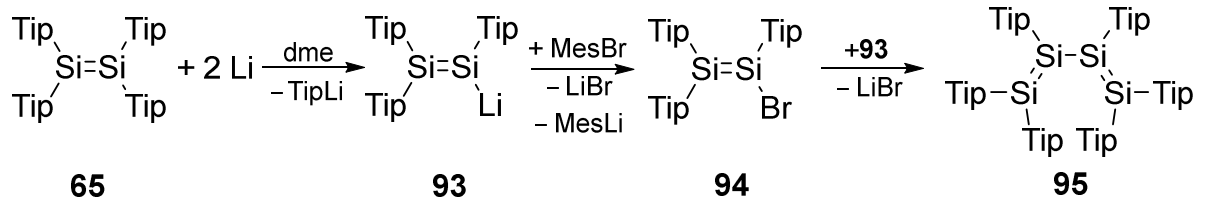

Scheme 36. Weidenbruch's synthesis of tetrasilabutdiene **95** *via* proposed intermediate disilenyllithium **93** (Tip = 2,4,6-^{i}Pr$_3$-C$_6$H$_2$).

As the isolation of the plausible intermediate disilenide **93** failed, again circumstantial evidence was employed to prove its formation. The addition of MesBr to the reaction mixture yielded tetrasilabutadiene **95**, which was the first example of a Si=Si-double bond containing conjugated system (Scheme 36).[131]

Seven years later Scheschkewitz was able to isolate and fully characterize Weidenbruch's *et al.* proposed disilenyllithium **93** upon reduction of Tip_2SiCl_2 **64** with Li-powder in dme (Scheme 37).[132]

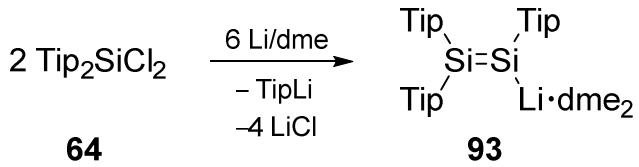

Scheme 37. Synthesis of Scheschkewitz's disilenide **93** (Tip = 2,4,6-$^{i}Pr_3$-C_6H_2, dme = 1,2-dimethoxyethane).

A few months later, Sekiguchi *et al.* reported that lithium disilenide **97** is obtained by reaction of ^{t}BuLi with the unsymmetrical substituted tetrasilabutadiene **96** (Scheme 38).[133]

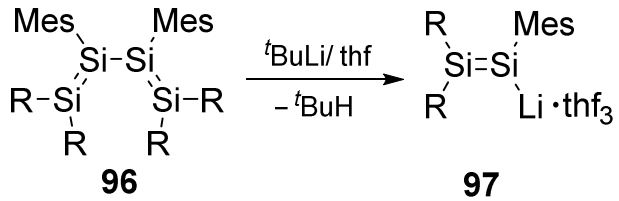

Scheme 38. Synthesis of Sekiguchi's disilenide **97** in 2004 (R = $^{t}Bu_2MeSi$, Mes = 2,4,6-Me_3-C_6H_2).

Examples of cyclic substituted disilenides **100a**,**b** were obtained by Iwamoto *et al.* upon reduction of chloro disilanes **99a**,**b** with KC_8 (Scheme 39).[134,135]

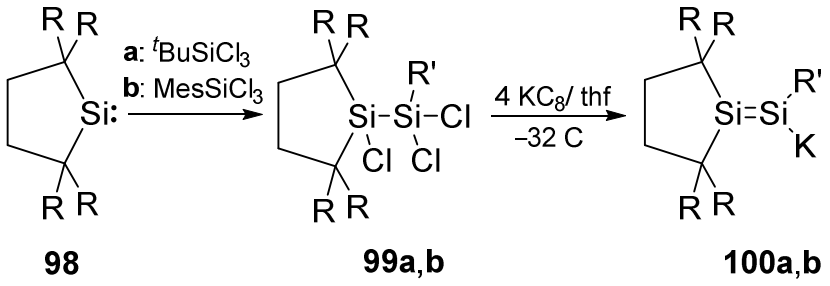

Scheme 39. Synthesis of cyclic trialkyl disilenide **100a** and aryl substituted dialkyl disilenide **100b** presented by Iwamoto *et al.* (R = $SiMe_3$, **a**: R' = ^{t}Bu, **b**: R' = Mes = 2,4,6-Me_3-C_6H_2).

In the last decade, disilenides turned out to be suitable building blocks in Group 14 chemistry for a variety of molecules in which the unsaturated Si=Si moiety stays intact or is converted into another low-valent functionality.[126,136,137]

1.6.2. Heavier Group 14 Vinylidene Analogues

The simplest unsaturated carbene is vinylidene **IV**, which constitutes the only electron-precise isomer of acetylene **III** (Scheme 40). In the case of carbon, derivatives have only been observed in cold matrices[138–140] or as transition metal complexes, the latter being known as catalysts of alkene- or alkyne-metathesis.[141–143] Vinylidene **IV** provides two highly reactive centers (carbene- and C=C-functionality) and heavier congeners could therefore serve as suitable building blocks for the synthesis of unsaturated Group 14 molecules. By extension of the acetylene backbone **III** by just one methyl group, propyne is formally obtained and the number of possible isomers is drastically increased. In addition to the alkyne and vinylidene isomers **V** and **VI** an open-chained vinyl carbene-type isomer **VII** can be envisaged, which is like vinylidene **IV** an example for a molecule containing a double functionality. The E_3H_4 ring-isomers **VIII-X** are now possible as well, albeit they would be expected to display a high reactivity because of the ring strain and the lone-pair of electrons at one E-center.

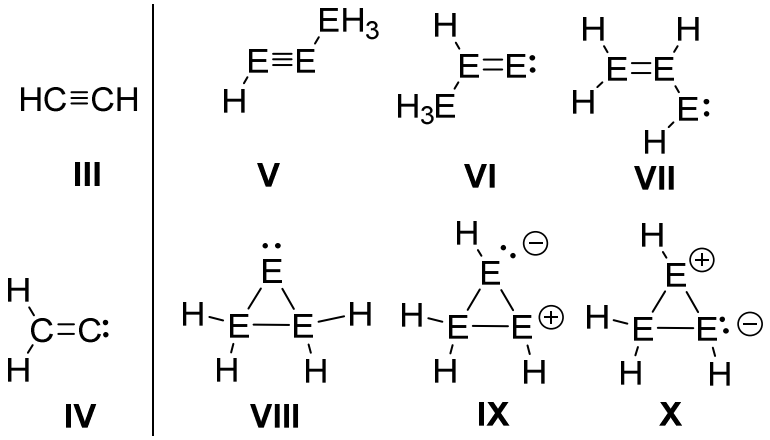

Scheme 40. Acetylene **III**, vinylidene **IV** and isomers **V-X** arising from chain expansion by one EH_3-group (E = Group 14 element).

The first stable monomeric NHC-coordinated heavier vinylidene analogue, silagermenylidene **101**, was synthesized by Scheschkewitz and co-workers in 2013.[144] The synthetic approach is the straightforward reductive dehalogenation of a 1:1 mixture of Tip_2SiCl_2 **64** and $GeCl_2{\cdot}NHC^{iPr2Me2}$ **8** with Li/naphthalene in thf, which afforded silagermenylidene **101** in 8% yield – low, but respectable for a reductive heterocoupling reaction (Scheme 41).

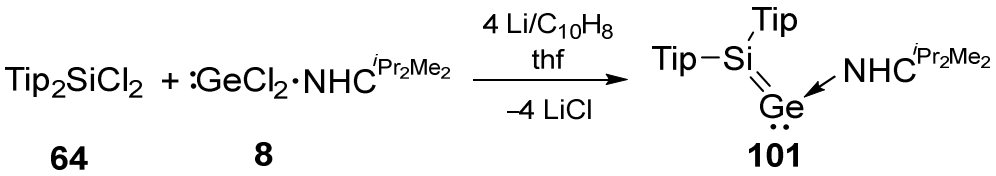

Scheme 41. Synthesis of first stable monomeric NHC-coordinated heavier vinylidene analogue **101** (Tip = 2,4,6-$^{i}Pr_3$-C_6H_2, NHC^{iPr2Me2} = 1,3-diisopropyl-4,5-dimethylimidazol-2-ylidene).

Proof-of-principle for the high synthetic potential of silagermenylidene **101** was provided by treatment with phenylacetylene, which resulted in the formation of the base-stabilized cyclic germylene **102** *via* a regioselective [2 + 2] cycloaddition (Scheme 42).[144]

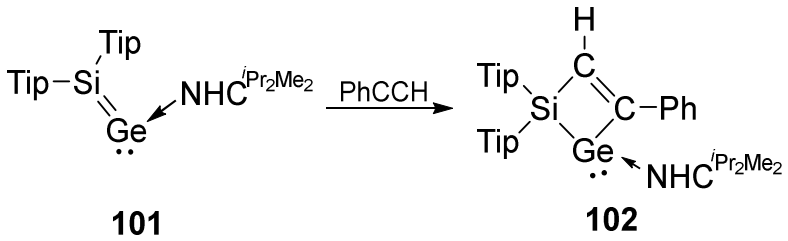

Scheme 42. [2 + 2] Cycloaddition of **101** with phenylacetylene leading to the cyclic germylene **102** (Tip = 2,4,6-$^{i}Pr_3$-C_6H_2, NHC^{iPr2Me2} = 1,3-diisopropyl-4,5-dimethylimidazol-2-ylidene).

In 2014, an α-chloro-silyl substituted silagermenylidene **104** was synthesized by Scheschkewitz and co-workers in a reaction of disilenide **93** with GeCl$_2$·NHC ^{iPr2Me2} **8**. The plausible mechanism for the formation of **104** is a salt elimination followed by a fast 1,3-migration of the chlorine atom from the proposed unobserved transient chloro disilenyl germylene **[103]** to the β-silicon atom (Scheme 43).[145]

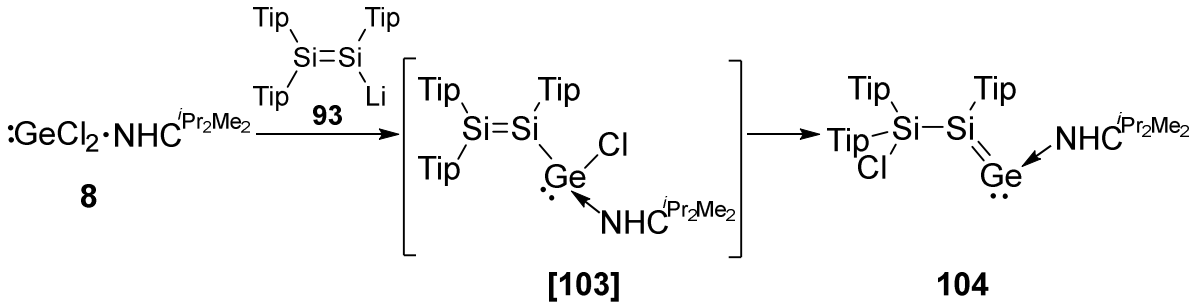

Scheme 43. Synthesis of NHC-stabilized silagermenylidene **104** (Tip = 2,4,6-$^{i}Pr_3$-C_6H_2, NHC^{iPr2Me2} = 1,3-diisopropyl-4,5-dimethylimidazol-2-ylidene).

Due to the high degree of functionalization (double bond between Si and Ge, lone pair at the germanium(II)-center, base coordination, β-chlorosilyl-group),silyl substituted silagermenylidene **104** provides various opportunities for further manipulations (Scheme 44).

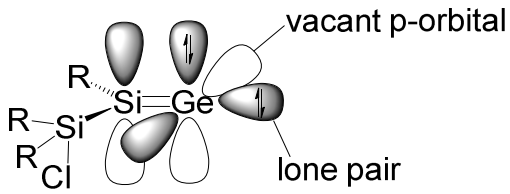

Scheme 44. Silagermenylidene **104** and its functionalities.

For example, silagermenylidene **104** reacts with nucleophiles leading to different cyclic NHC-stabilized Si_2Ge-systems.[146] It has also been demonstrated that **104** can be used as a ligand in a transition-metal complex.[145] With regards to expanded systems, silagermenylidene **104** was reacted with xylyl isocyanide (XylNC) to form an NHC-coordinated cyclic germylene under mild conditions and the reversibility of the NHC coordination has been established.[147] In depth discussion of these findings will follow in “Results and Discussion” of this thesis in the corresponding chapter.

In 2015, the group of Filippou disclosed an NHC-stabilized phosphasilenylidene **106** which was obtained by the reaction of $SiCl_2{\cdot}NHC^{Dip2}$ **35** with $LiP(Mes^*)(SiMe_3)$ *via* the proposed intermediate **105** followed by a 1,2-elimination of Me_3SiCl (Scheme 45).[148]

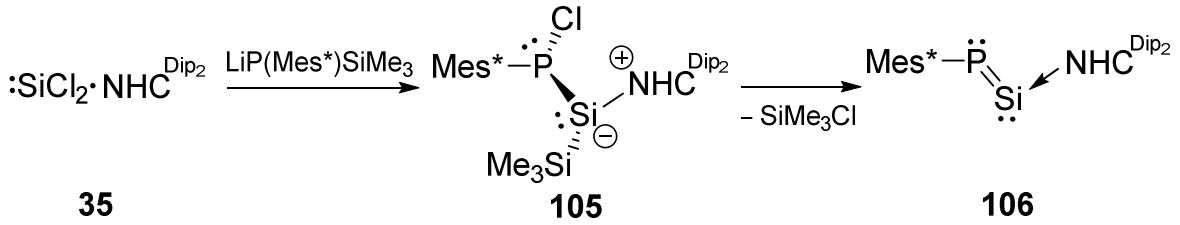

Scheme 45. Synthesis of phosphasilenylidene **106** reported by Filippou *et al.* (Mes* = 2,4,6-^{t}Bu$_3$-C$_6$H$_2$, NHC^{Dip2} = 1,3-bis(2,6-diisopropylphenyl)imidazolin-2-ylidene, Dip = 2,6-^{i}Pr$_2$-C$_6$H$_3$).

In the same year, Filippou *et al.* also presented another example of a heavier vinylidene analogue. The NHC-stabilized disilavinylidene **108** was synthesized by a two-electron reduction of NHC-stabilized silylene **107** with KC_8 (Scheme 46).[149] Recently, a transient base-free disilavinylidene (H_2SiSi:) was observed by crossing beams of atomic silicon with SiH_4 in the gas-phase. Based on calculations, it was concluded that

the highly reactive $H_2Si{=}Si$: exists in equilibrium with the mono-bridged (Si-(H)SiH) and di-bridged ($Si(H_2)Si$) isomers.[150]

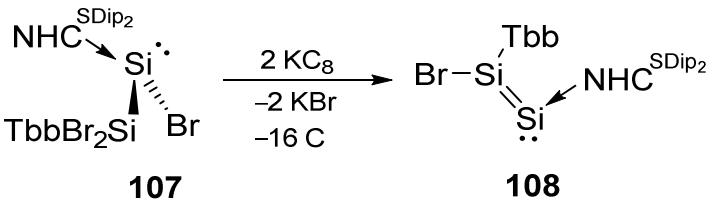

Scheme 46. Synthesis of NHC-stabilized disilavinylidene **108** by Filippou *et al.* (Tbb = 2,6-[CH-$(SiMe_3)_2]_2$-4-^{t}Bu-C_6H_2, NHC^{SDip2} = $C[N(2,6\text{-}^i Pr_2\text{-}C_6H_3)CH_2]_2$).

Very recently, the first base-free heavier vinylidene analogue, digermavinylidene **113**, was obtained by Aldridge *et al.*[151,152] by a sequence of reactions starting from the NHC-stabilized borylchloro germylene **110**, which in turn had been synthesized from the borylanion **109**[153] and $GeCl_2{\cdot}NHC^{iPr2Me2}$ **8** (Scheme 47).

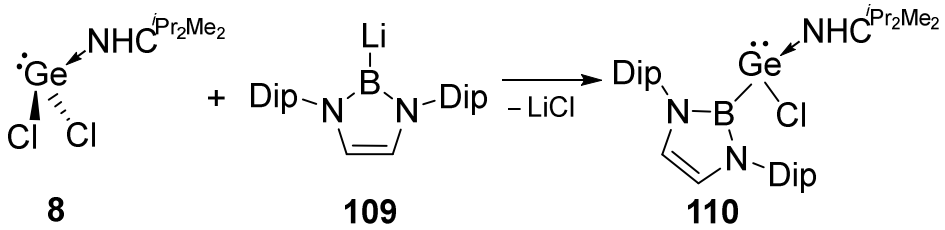

Scheme 47. Synthesis of NHC-stabilized borylchloro germylene **110** by Aldridge *et al.* (Dip = 2,6-$^i Pr_2$-C_6H_3).

Reduction of NHC-stabilized germylene **110** with K or KC_8 yielded the formal $Ge(0)_2$-compound **112** similar to dianionic systems reported by the Power group.[116,117,154] Oxidation of $Ge(0)_2$-compound **112** with $[Ph_3C][B(C_6F_5)_4]$ resulted in digermavinylidene **113** with an unique 1,1-disubstitution pattern of the boryl ligands around the Ge_2-fragment. The 1,2-substitution pattern of **112** can be reestablished by reduction of digermavinylidene **113** by KC_8 (Scheme 48).

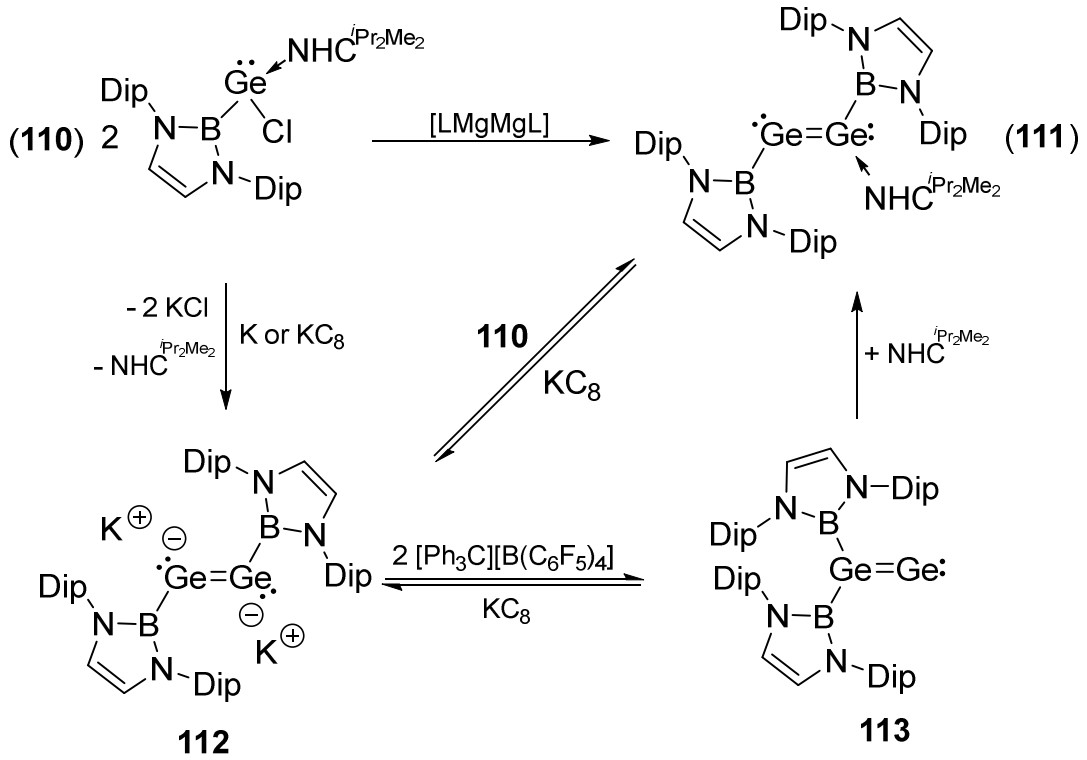

Scheme 48. Synthesis of base-free digermavinylidene **113** by Aldridge *et al*. (Dip = 2,6-^{i}Pr$_2$-C$_6$H$_3$, LMgMgL = [(HC(MeCMesN)$_2$)Mg]$_2$, Mes = 2,4,6-Me$_3$-C$_6$H$_2$).

A further important contribution was reported by Scheschkewitz *et al.* in 2013 with the synthesis of an isolable NHC-stabilized disilenyl silylene **116**, which dissociates into free NHC^{iPr2Me2} and the corresponding cyclotrisilene **114** in solution (Scheme 49).[155] Disilenyl silylene **116** is a further impressive example that in the case of silicon two unsaturated functionalities (Si=Si moiety, silylene) can be tolerated when trapped with an NHC, which are inaccessible in the case of carbon. At low temperature, with the cyclotrisilene NHC-adduct **115** a proposed intermediate of ring opening **114** to **116** was observed.

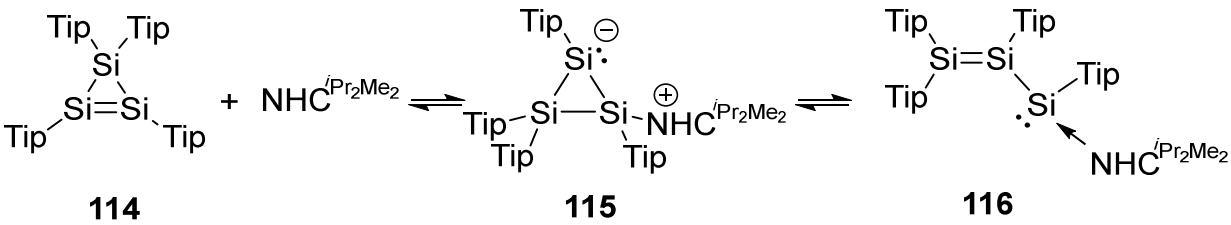

Scheme 49. Equilibrium between cyclotrisilene **114**, NHC and NHC-coordinated disilenyl silylene **116** (Tip = 2,4,6-^{i}Pr$_3$-C$_6$H$_2$, NHC^{iPr2Me2} = 1,3-diisopropyl-4,5-dimethylimidazol-2-ylidene).

2. Aims and Scope

The main target of this work was the construction of unsaturated, highly functionalized germanium-based building blocks for the incorporation into organic frameworks, most preferably conjugated systems.

Recently, our group reported on the synthesis of the first two isolable heavier versions of vinylidene (**101** and **104**) as donor-acceptor complexes with an NHC. In particular, the α-chloro silyl substituted silagermenylidene **104** is a versatile precursor due to the high degree of functionalization (Scheme 50).[144–147]

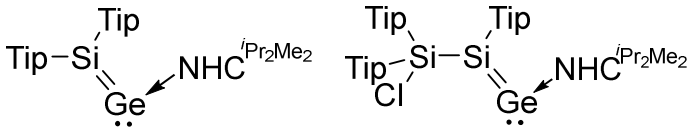

101 **104**

Scheme 50. Heavier analogues of vinylidene: silagermenylidenes **101** and **104**.

As had been reported previously, **104** readily reacts with nucleophiles. In particular, the replacement of the chlorine-atom with different organolithium nucleophiles (Chapter 3.1.) should be useful for the construction of extended systems with Si=Ge containing repeat units. An initial task of this thesis was to develop a better understanding of the experimental parameters that lead to the formation of the possible isomers **XII** to **XV** and to investigate the possible differences in reactivity of **XI** to **XIII** (Scheme 51).

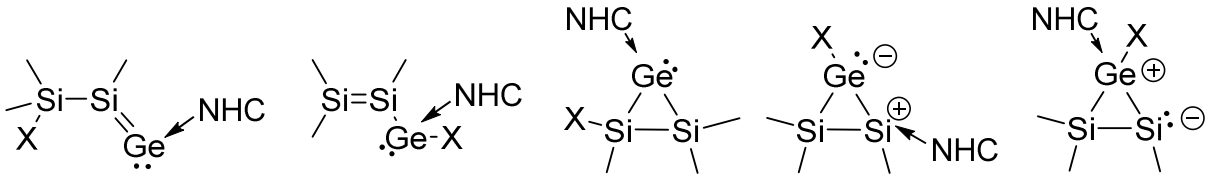

XI **XII** **XIII** **XIV** **XV**

Scheme 51. Isomers **XII** to **XV** (X = alkyl- or aryl-substituent) of silagermenylidene **XI** (X = Cl).

In a second step, this knowledge was to be applied for the incorporation of different mono- or doubly functionalized organic molecules into the unsaturated scaffold of the isomeric NHC-coordinated Si_2Ge-systems **XI-XIII** in order to furnish difunctional precursor molecules that could, at least in principle be employed for the construction of extended unsaturated Group 14 aggregates (Scheme 52).

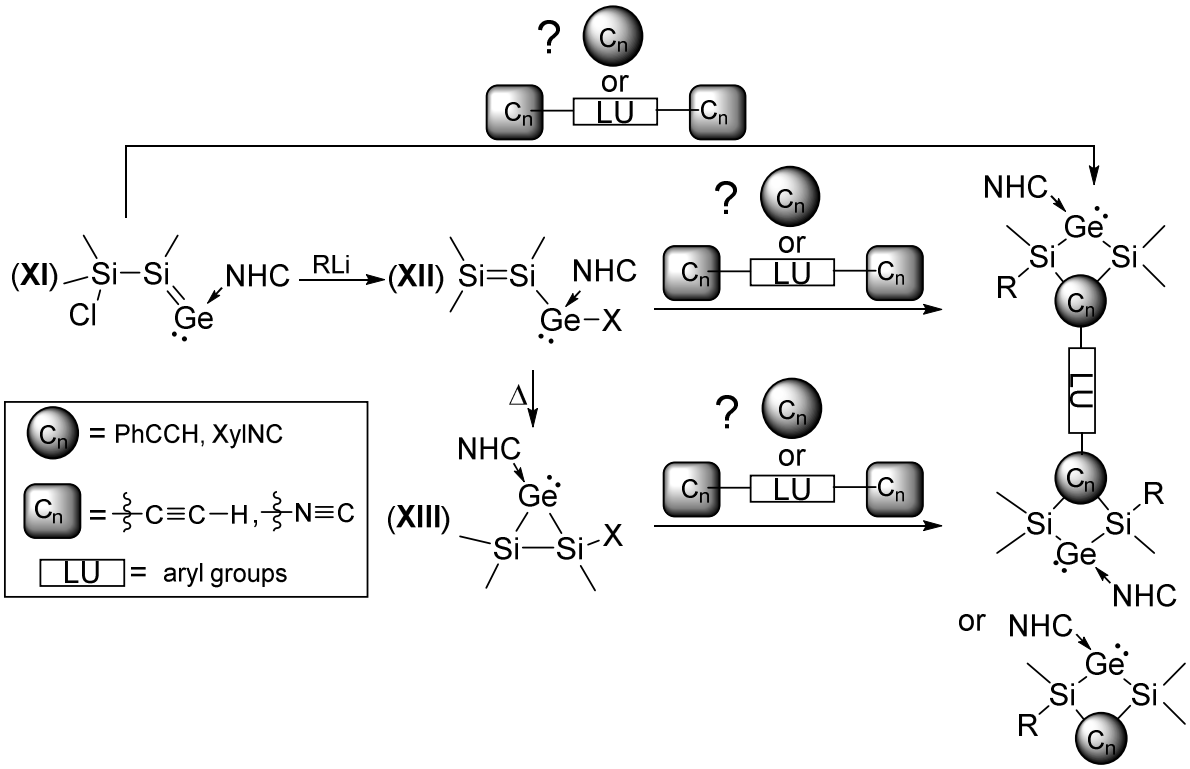

Scheme 52. Proposed reactions of silagermenylidene **XI** (X = Cl) and its isomers **XII** and **XIII** with different functionalized organic molecules (X = alkyl or aryl group).

In order to broaden the scope of heavier vinylidenes, the variation of the heavier Group 14 elements constituting the double bond was to be investigated through different strategies. Although other groups have provided alternative strategies in the meantime (Chapter 1.6.2.), the two following classes of precursors should be suitable to access heavier vinylidenes (Scheme 53):

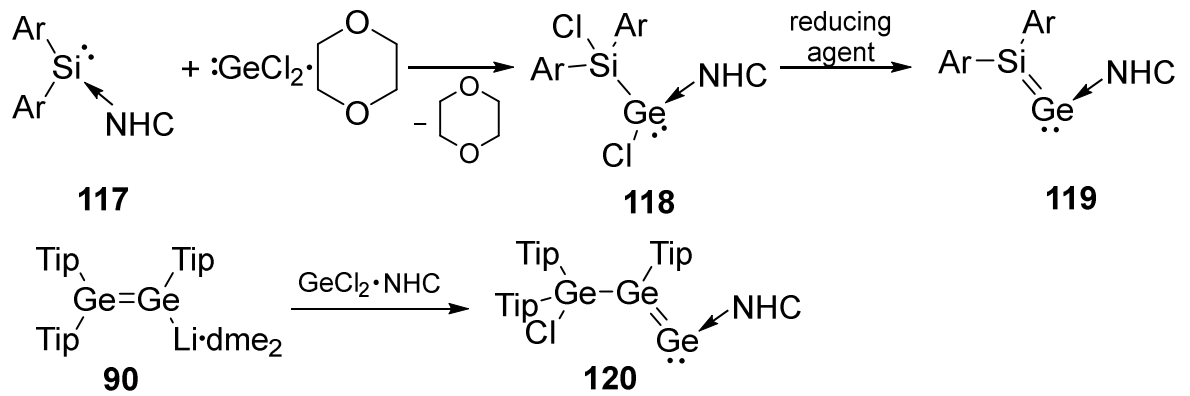

Scheme 53. Possible precursors for the synthesis of heavier vinylidene analgoues: (1) NHC-stabilized diaryl silylene **117** (Ar = aryl group), (2) digermenyllithium **90**.

(1) NHC-stabilized diaryl silylene **117** could be reacted with $GeCl_2$·dioxane leading to NHC-stabilized chloro silyl germylene **118** by a 1,2-shift of a chlorine atom from the Ge(II)-center to the adjacent silicon. In a next step, a reduction should in principle lead to a silagermenylidene.

(2) Digerma analogues of vinyllithium could react with a $GeCl_2$·NHC-adduct to form germyl digermavinylidene **120** in analogy to the formation of silyl substituted silagermenylidene **104** (page 27, Scheme 43).

As both types of compounds were unknown in preparative quantities, the third major task of this PhD thesis was the development of synthetic protocols for the isolation and full characterization of suitable examples.

3. Results and Discussion

3.1. Versatile Reactivity of Silagermenylidene 104 toward Anionic Nucleophiles

In order to exploit its high degree of functionalization, the α-chloro silyl substituted silagermenylidene **104** had been investigated with regards to various reagents.[145–147] With a relatively loosely bound NHC ligand, a vacant p-orbital could be readily made available for derivatization of **104** by neutral and anionic nucleophiles. Indeed, the stepwise reaction of heavier vinylidene analogue **104** with two equivalents of NHC^{Me4} initially resulted in the exchange of the NHC to afford **121**. Upon addition of the second equivalent NHC^{Me4} the residual chloro-substituent in **121** is expelled as chloride to yield the ion pair **122**. The reaction of **104** with the anionic nucleophile MesLi led to the formation of the heavier NHC-coordinated cyclopropylidene analogue **123a** and cyclosilagermene **124a** (Scheme 54).[146] It had been proposed that the site of the nucleophilic attack by MesLi could either have been at the Ge(II)-center or the formal sp^2-silicon center of silagermenylidene **104**.

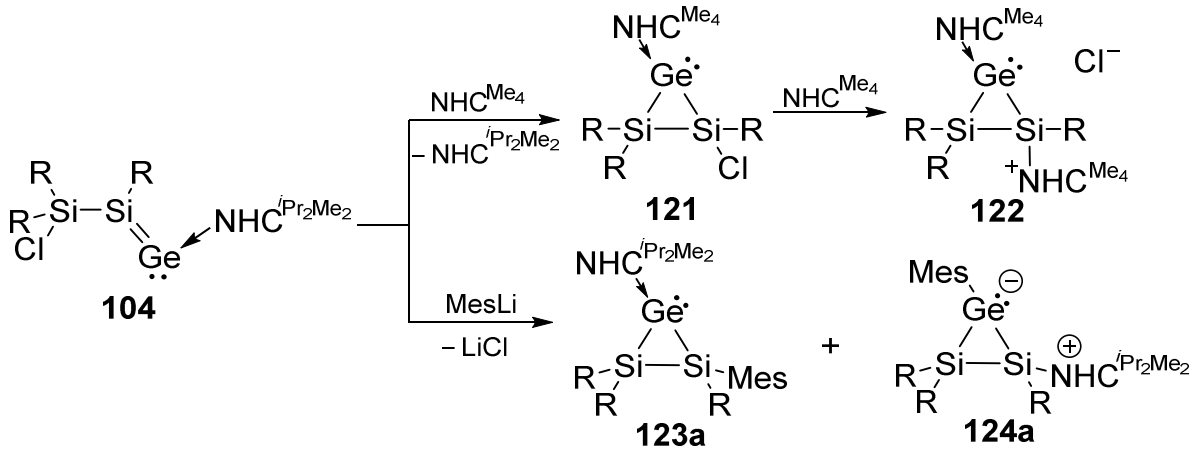

Scheme 54. Reactions of silagermenylidene **104** with neutral and anionic nucleophiles resulting in Si_2Ge-rings **121-124a** (R = Tip).

In the present thesis, a detailed reactivity study of the heavier vinylidene analogue **104** toward anionic nucleophiles of different sizes was therefore to be conducted in order to shed a light on the mechanism of formation and interconversion of isomers **XII-XV** (Scheme 55). Furthermore, the isolation of an NHC-stabilized disilenyl germylene **XII**, which was suggested to be a transient intermediate in previous reports by our group was a target of central importance.[145,146]

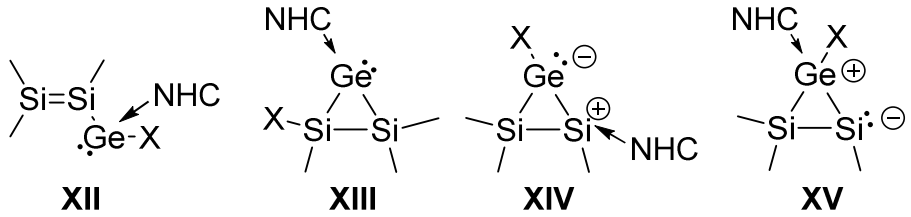

Scheme 55. Isomers **XII-XV** (X = alkyl or aryl) of silagermenylidene **104**.

3.1.1. Dimerization of Marginally Stable Disilenyl Germylene to Tricyclic Si_4Ge_2-Systems: Evidence for Reversible NHC-Coordination

Recently, NHC-coordinated disilenyl silylene **116** was reported by the group of Scheschkewitz. The homoleptic cyclotrisilene **114** gives rise to reversible ring opening by the NHC to disilenyl silylene **116** (Scheme 56).[155]

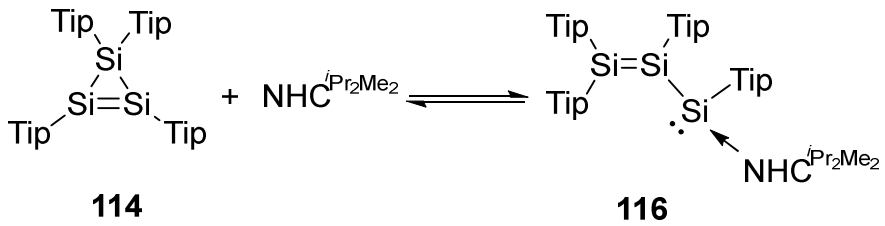

Scheme 56. Equilibrium of homonuclear disilenyl silylene **116** and cyclotrisilene **114**.

Attempts to prepare a related disilenyl germylene have so far not met with success: disilenyl-substituted germanium(II)chloride **[125]** was proposed as an unstable intermediate of the reaction of disilenide **93** with $GeCl_2$·dioxane adduct. Although no spectroscopic evidence for **[125]** was forthcoming, the in situ-reduction with lithium/naphthalene yielded the unsaturated heteronuclear cluster **126**, which in turn slowly rearranges to the thermodynamically more stable bridged propellane **127**.[156] The related NHC-adduct of chloro disilenyl germylene **[103]** was invoked as transient intermediate that undergoes a 1,3-chlorine atom shift to afford the NHC-complex of silagermenylidene **104** (Scheme 57).[145]

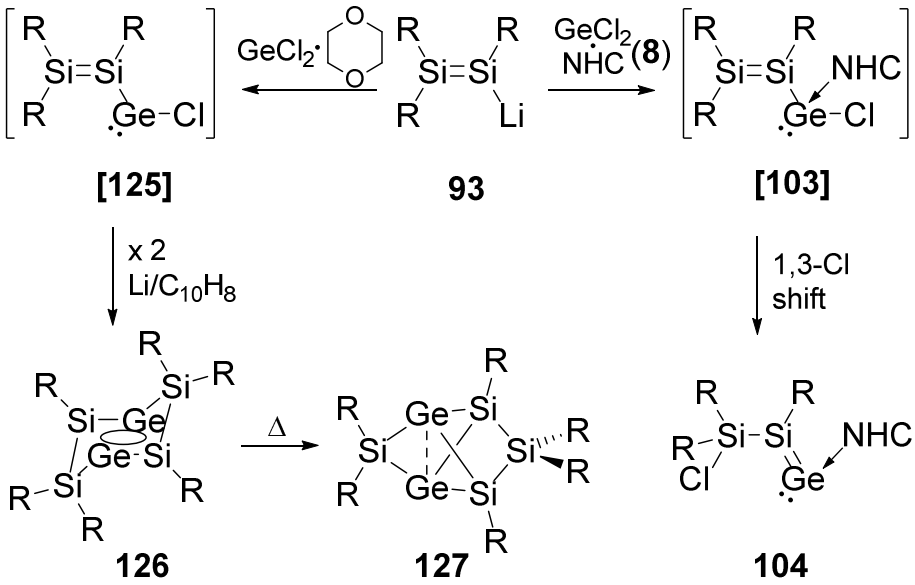

Scheme 57. Reaction of disilenide **93** with $GeCl_2{\cdot}NHC^{iPr2Me2}$ **8** via **[103]** to NHC-stabilized silagermenylidene **104** and reaction of disilenide **93** with $GeCl_2$·dioxane *via* **[125]** to dismutational Ge_2Si_4 isomer **126** which is thermally converted in **127** (R = Tip).

The chloro functionalities of the proposed germylene intermediates **[103]** and **[125]** with their high propensity for migration are likely the key to their instability. It was therefore investigated whether it is possible to substitute the chloro group by an electronically and sterically innocent methyl group. As discussed previously in the context of the reactivity of **104** with bulkier nucleophiles such as mesityl lithium, nucleophilic attack can either occur at the germanium(II)-center, the chlorosilyl group or the formal sp^2-silicon center.[146] If the nucleophilic attack took place at the Ge(II)-center, a subsequent LiCl elimination would result in a Si-Si double bond and thus give access to the NHC-stabilized disilenyl germylene **128a** (Scheme 58).

Therefore, a solution of MeLi (3.0 M in dem) was added to a precooled (−78 °C) solution of silagermenylidene **104** in toluene-d_8. A ^{29}Si NMR spectrum recorded at −60 °C reveals only signals of the starting material **104** at δ = 163.47 and 8.37 ppm (Figure 8a).

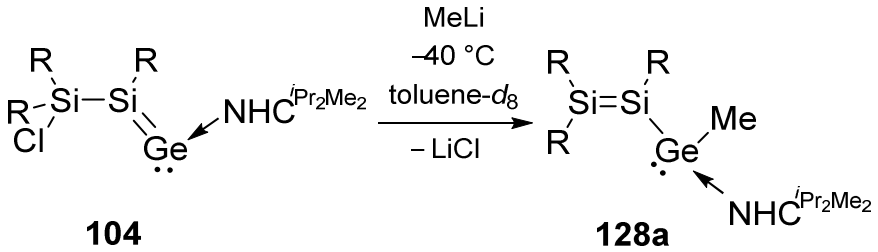

Scheme 58. Reaction of **104** with MeLi leading to thermally unstable disilenyl germylene **128a** (R = Tip).

Upon warming to −40 °C, however, two new ^{29}Si NMR signals appear at δ = 90.10 and 85.27 ppm in an approximate ratio of 1:1 (Figure 8b), which is consistent with the presence of a Si=Si double bond. Almost full conversion is reached at −20 °C (Figure 5).

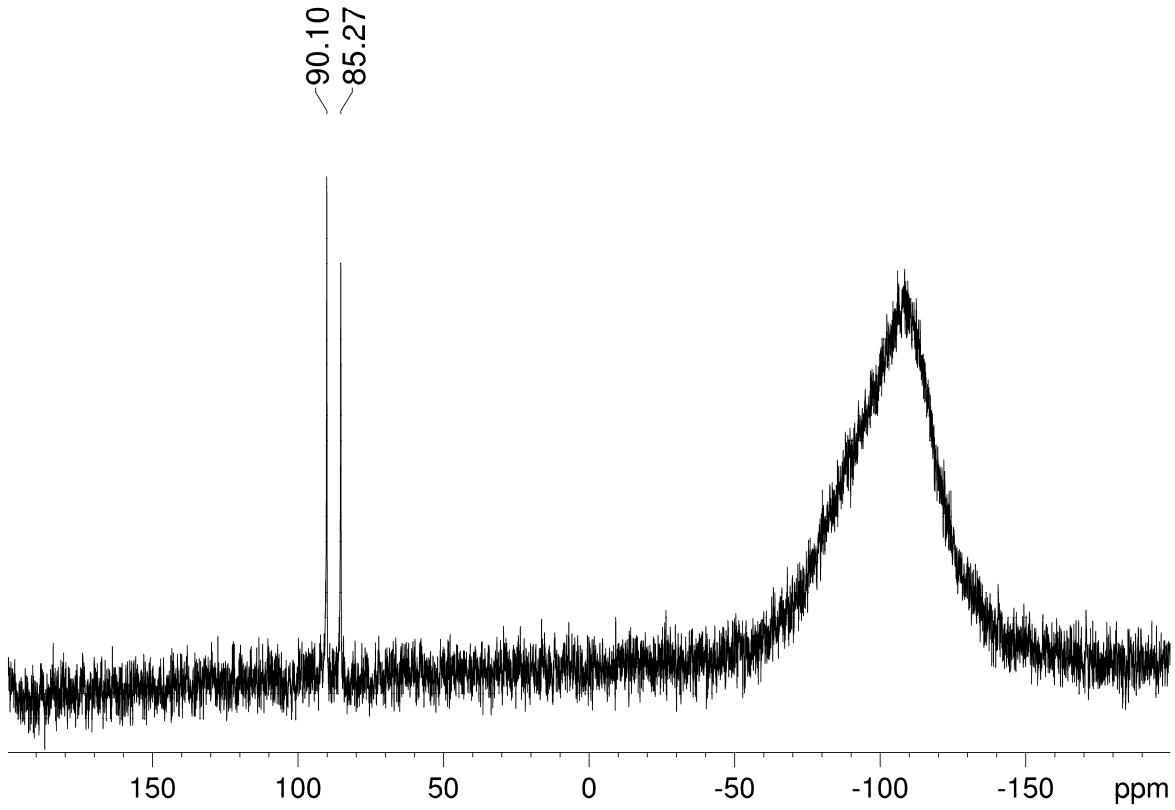

Figure 5. ^{29}Si NMR spectrum of the low temperature NMR study: intermediate **128a** in toluene-d_8 at −20 °C.

A multiplet at δ = 5.70 ppm in the ^{1}H NMR spectrum (for comparison **104**: septet at 5.41 ppm for C*H*CH$_3$ of NHC) and a ^{13}C NMR resonance at δ = 174.88 ppm are indicative of the coordination of the NHC to the Ge(II)-center.[144,145] These spectroscopic data (Figure 6 and Figure 7) strongly support the formulation of the initial reaction product as an NHC-coordinated disilenyl germylene **128a**. Unfortunately, all attempts to isolate **128a** failed, even when the entire workup of the crude reaction mixture was carried out at −10 °C.

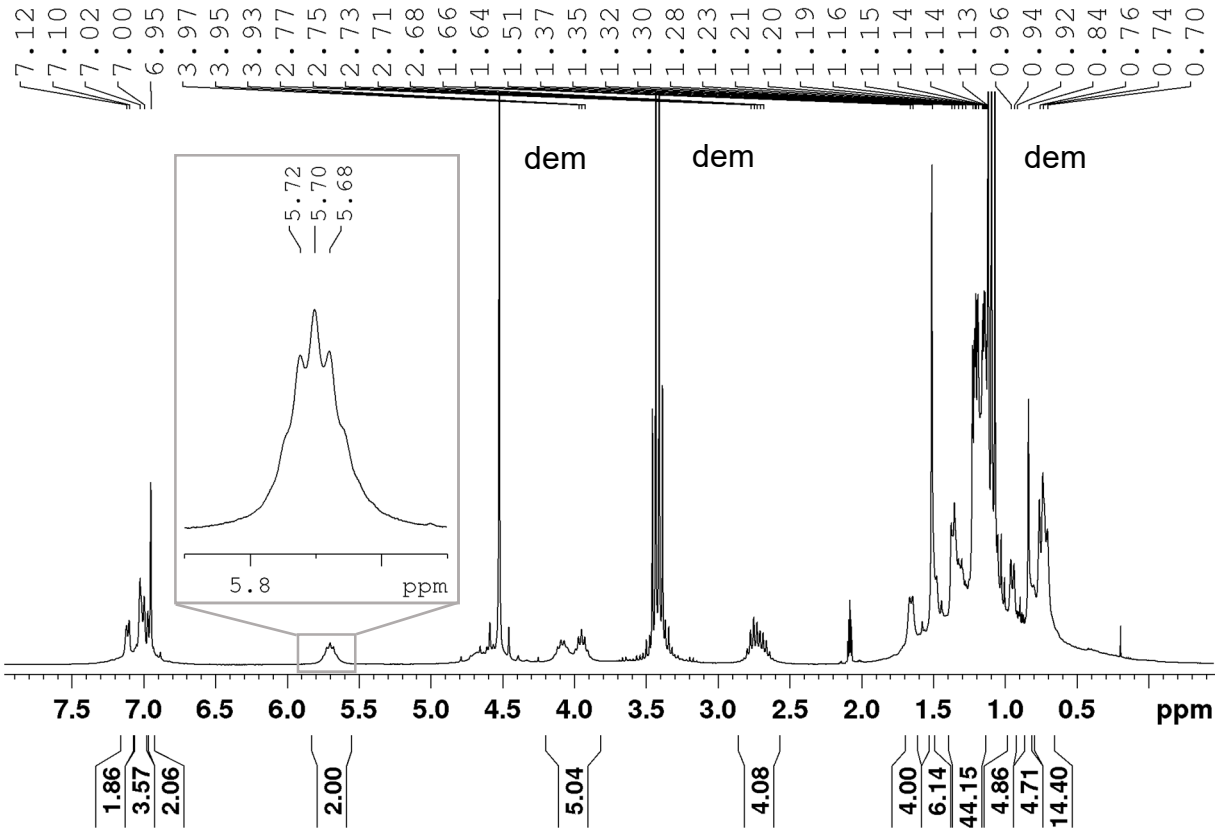

Figure 6. ^{1}H NMR spectrum of the low temperature NMR study: proposed intermediate **128a** in toluene-d_8 at −20 °C (dem: diethoxymethane). The excerpt shows the methine protons of the NHC which coordinates to **128a**.

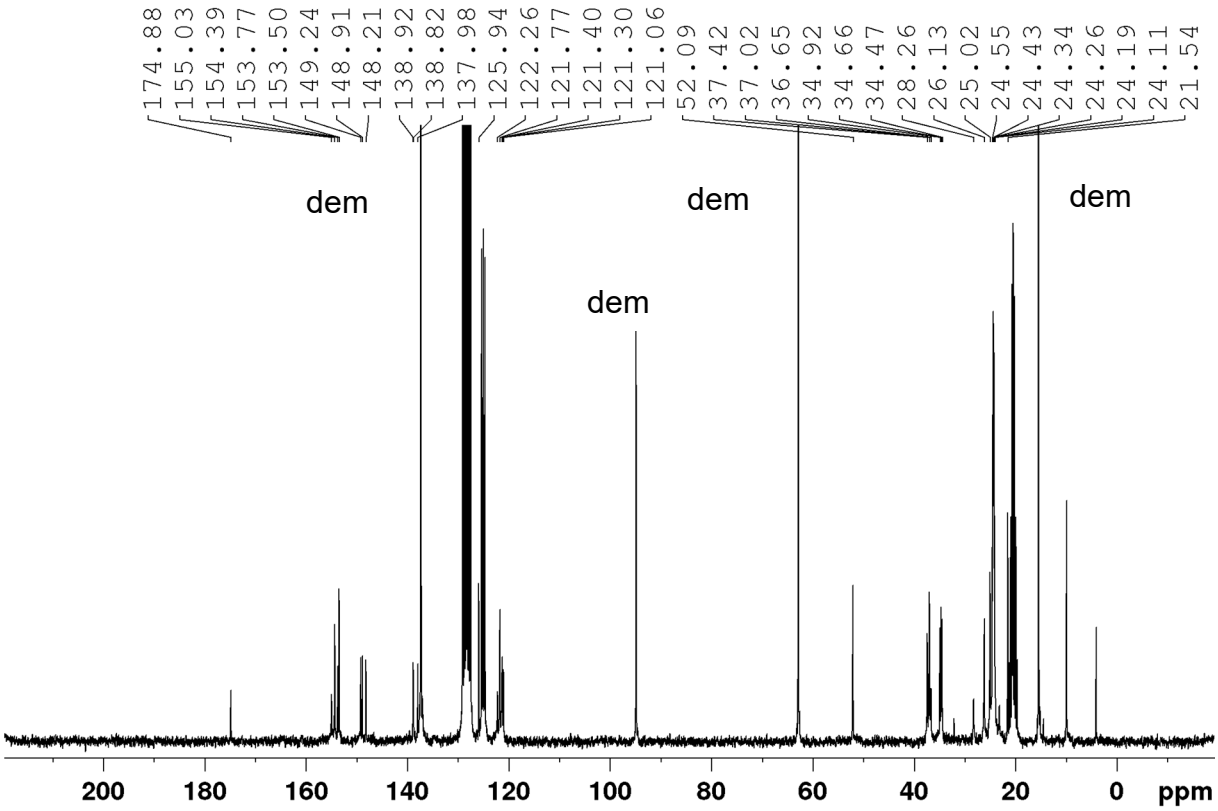

Figure 7. ^{13}C NMR spectrum of the low temperature NMR study: intermediate **128a** in toluene-d_8 at −20 °C (dem: diethoxymethane).

When a sample is further warmed to room temperature, new ^{29}Si NMR signals at δ = −64.92 and −66.51 ppm (Figure 8d) start growing in, in accordance with the formation of a three-membered ring. A characteristic ^{13}C NMR signal at δ = 175.90 ppm proves the coordination of NHC to the germanium center (see above). On the basis of the spectroscopic data it is concluded that the product corresponds to **129**, the NHC-adduct of a 2,3-disilagermirene analogous to the previously reported stable example with the bulkier mesityl group in place of methyl (Scheme 59).[146] It cannot be excluded beyond doubt that the methyl group is intermittently attached to silicon although this is an unlikely scenario based on the relatively low propensity of methyl groups for migration. Stable disilagermirenes without base-coordination, but with sterically demanding substituents at all three ring atoms have been reported.[157–159]

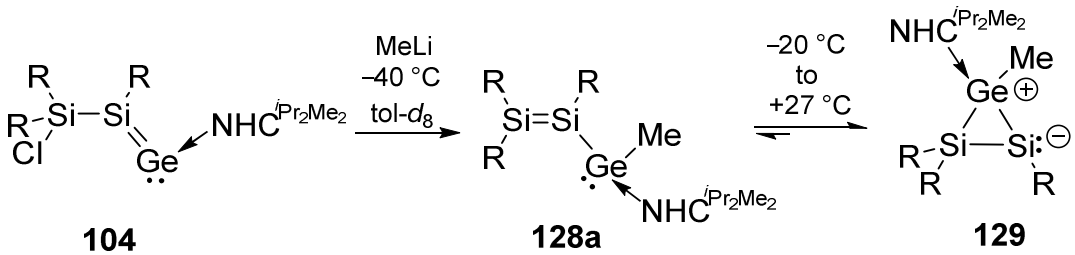

Scheme 59. Reaction of **104** with MeLi leading to intermediate disilenyl germylene **128a** and NHC-adduct of 2,3-disilagermirene **129** (R = Tip).

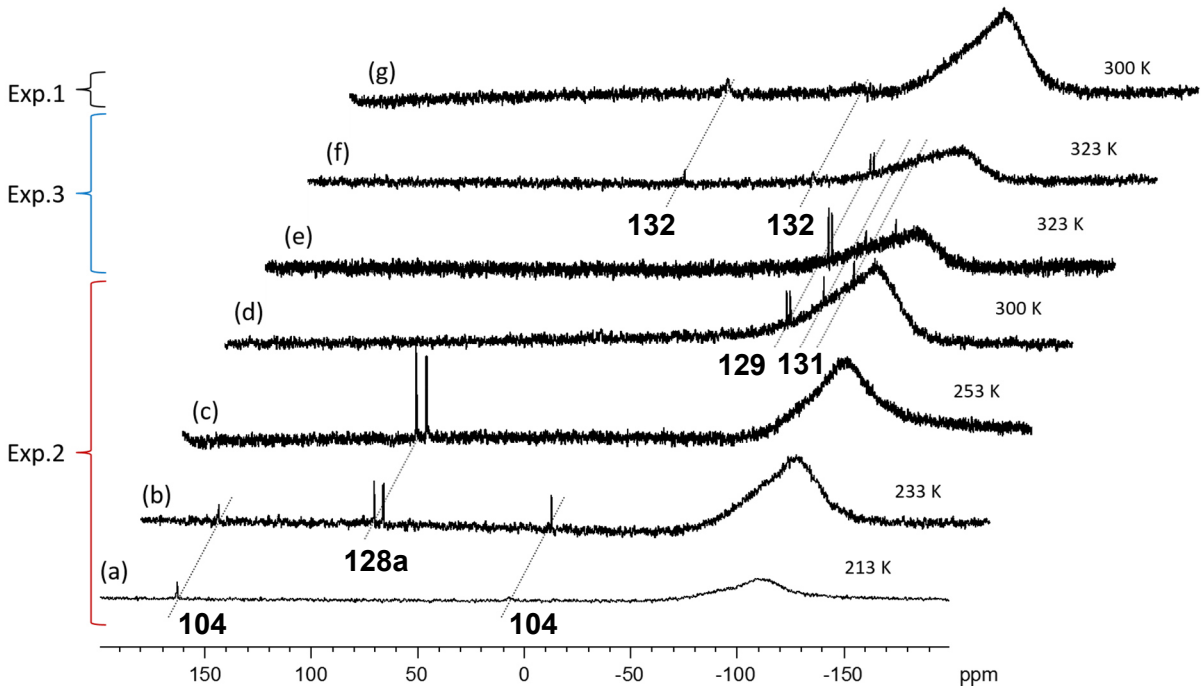

Figure 8. Stacked plot of ^{29}Si NMR spectra of different VT-NMR experiments with identical starting conditions. *Experiment 2*: (a) starting material **104** at −60 °C, (b) **104** and disilenyl germylene **128a** at −40 °C, (c) **128a** at −20 °C, (d) mixture of **129** and **131** after 30 h at 27 °C. *Experiment 3*: (e) mixture of **129** and **131** after 1 h at 50 °C, (f) mixture of **129** and doubly bridged tetrahedron **132** after 2 h at 50 °C. *Experiment 1*: (g) **132** at 27 °C (crystalline sample); all spectra recorded in toluene-d_8.

Well before complete conversion to **129**, however, an additional set of signals at higher field starts appearing in the ^{29}Si NMR spectrum at δ = −82.55 and −96.42 ppm (Figure 8d) with concomitant formation of free NHC. It is speculated that the addition of excess NHC to **128a** may slow down this process (Scheme 60).

Indeed, in a separate NMR experiment in the presence of 3.8 eq of NHC only ^{29}Si NMR signals at δ = −64.92 and −66.51 ppm for **129** (Figure 9b) were observed even after heating of the mixture to 50 °C for 5 h. Interestingly, the stability of the disilenyl germylene **128a** (stable for 1 hour at 27 °C) is similarly increased by excess NHC (Figure 9a) as in the case of disilenyl silylene **116**.[155]

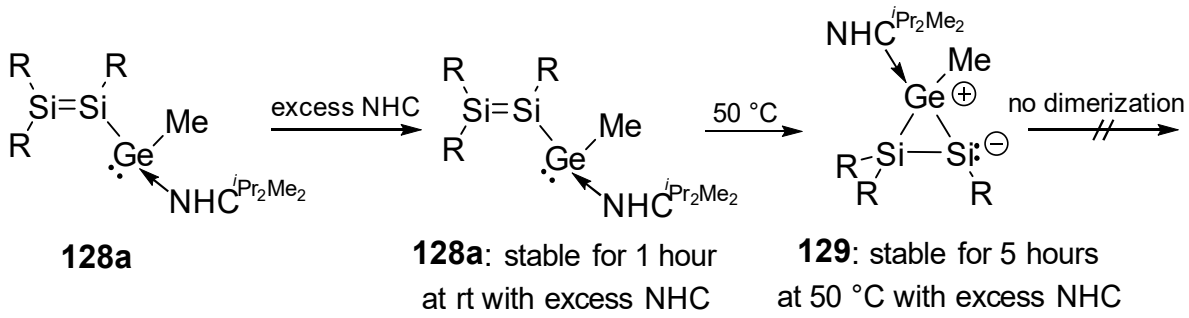

Scheme 60. Treatment of disilenyl germylene **128a** with 3.8 eq of NHC resulting in stable **128a** by heating to 50 °C for 30 min (R = Tip).

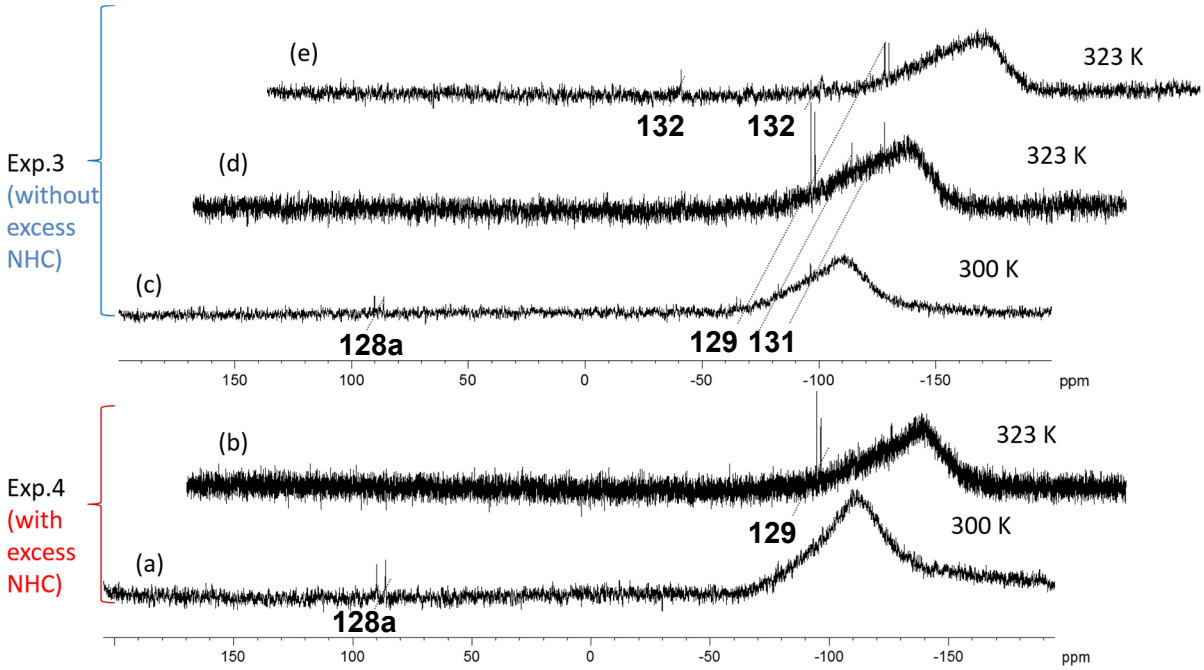

Figure 9. Stacked plots of ^{29}Si NMR spectra of NMR experiments with or without added NHC. *Experiment 4 with 3.8 eq of NHC*: (a) after 50 min at 27 °C **128a** is still the major component, (b) after 1 h at 50 °C clean conversion to **129** has occurred. *Experiment 3 without added NHC*: (c) after 50 min at 27 °C a mixture of **128a**, three-membered ring **129** and chair form of $Si_4Ge_2R_6$ **131** are obtained, (d) after 1 h at 50 °C a mixture of **129** and **131** are observed, (e) after 2 h at 50 °C a mixture of **129** and $Si_4Ge_2R_6$ doubly bridged tetrahedron **132** are observed; all spectra recorded in toluene-d_8 (R = Tip).

To prove these findings another sample containing only **128a** was warmed to 27 °C (Figure 9c) and after 50 min at 27 °C three sets of signals were observed in the ^{29}Si NMR spectrum: δ = 90.07 and 85.40 ppm (**128a**), δ = −64.92 and −66.51 ppm (**129**) and δ = −82.55 and −96.42 ppm (**131**). The temperature was increased to 50 °C for 1 hour as in the case with 3.8 eq of NHC and two sets of signals (Figure 9d) were observed at δ = −64.92 and −66.51 ppm (**129**) and δ = −82.55 and −96.42 ppm (**131**). After 2 hours at 50 °C only resonances at δ = −64.92 and −66.51 ppm (**129**) and δ = 21.97, –37.74 ppm (**132**) were observed (Figure 9e).

In the absence of excess NHC, keeping the mixture of **128a**, **129** and **131** (Figure 9c) at room temperature overnight results in the complete disappearance of the ^{29}Si NMR signals of **129**. In addition to the two sharp resonances at δ = −82.60 and −96.58 ppm, a second set of broad signals at δ = 21.97 and −37.74 (**132**) ppm in the integrated ratio of 3:3:2:2 (Figure 10) is observed together with a small amount of an unknown CH-insertion product (^{29}Si NMR: δ = −65.94 ppm, ^{1}H NMR: characteristic singlet for SiH at δ = 5.57 ppm). Insertion into CH bonds is typically observed for highly reactive heavier main group species.[160,161]

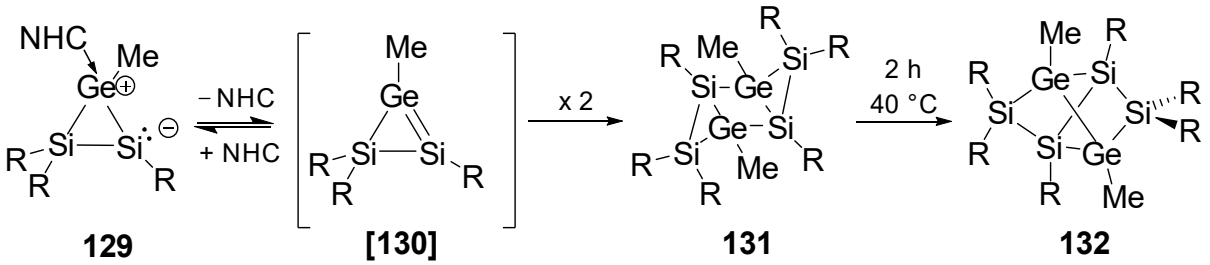

Scheme 61. Dimerization of heavier NHC-coordinated cyclopropene analogue **129** to tricyclic Si_4Ge_2-isomers **131** and **132** *via* unobserved base free heavier cyclopropene **[130]** (R = Tip).

It is therefore concluded that the formation of **131** and **132** is preceded by the reversible dissociation of the NHC from **129** to give the transient (and unobservable) base-free heavier cyclopropene **[130]** (Scheme 61). In case of the related homonuclear cyclotrisilene **114** the species corresponding to **128a** and **[130]** coexist at room temperature, which can be attributed to the higher stability of cyclotrisilene **114** due to sterically more demanding substitution pattern (Tip instead of Me at the low-valent center).

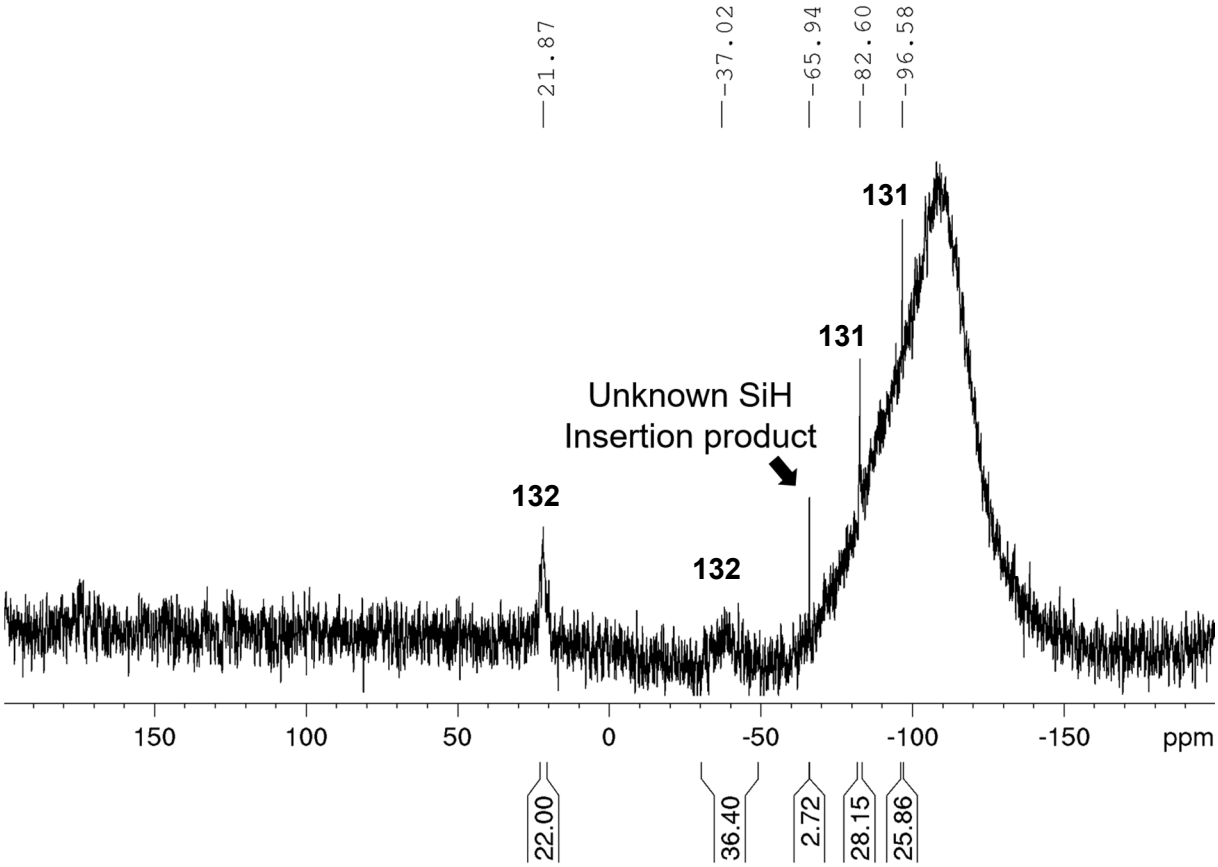

Figure 10. ^{29}Si NMR spectrum of the mixture of tricyclic Si_4Ge_2-isomers **131** and **132** and an unknown CH insertion product (Experiment 1).

The ^{1}H and ^{13}C NMR spectra prove the formation of considerable amounts of free NHC^{iPr2Me2} upon standing overnight. After removal of free NHC by sublimation, crystallization from toluene at −26 °C afforded a few pale red crystals of **131** co-crystallized with a large amount of colorless crystals of **132**.

The X-ray diffraction study on the pale red crystals finally established the connectivity of the chair-like tetrasila-2,5-digermatricyclohexane **131** (Figure 11). The central four-membered ring contains the two methyl-substituted germanium centers in 1,3-position with no apparent Ge-Ge bonding (Ge1-Ge2: 3.1984(4) Å). The Ge-Si bond distances of the central four-membered Si_2Ge_2 ring of **131** (between 2.3725(8) Å and 2.4174(8) Å; folding angle: 165.38°) are similar to those of the unsaturated version **127** with "naked" germanium atoms.[156]

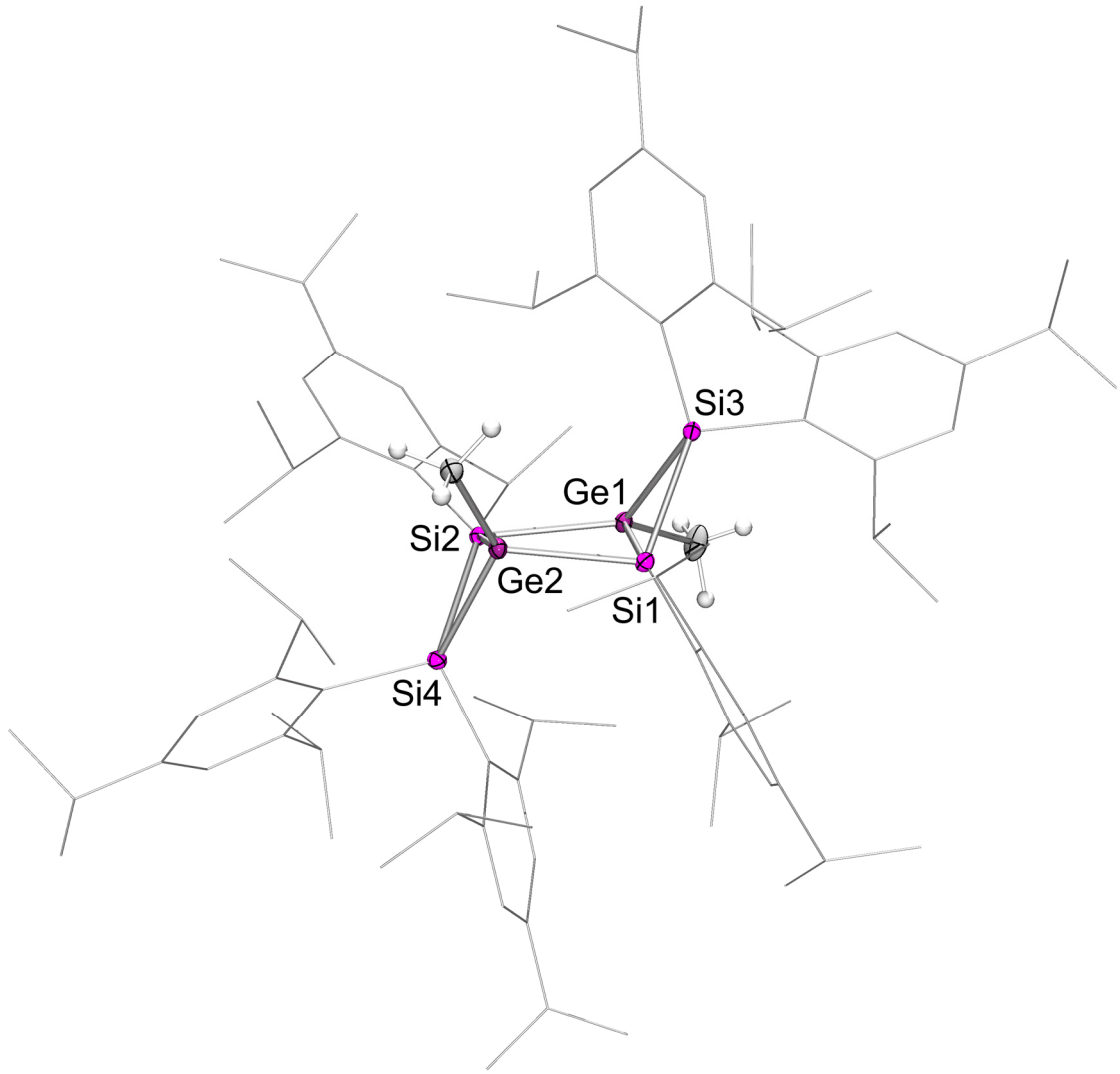

Figure 11. Molecular structure of **131**·C_7H_8 in the solid state (ellipsoids are at 30%, hydrogen atoms, co-crystallized toluene and disorder omitted for clarity). Selected bond lengths [Å]: Ge1-Si1 2.4099(8), Ge1-Si2 2.4174(8), Ge1-Si3 2.4596(8), Ge2-Si1 2.3725(8), Ge2-Si2 2.4163(8), Ge2-Si4 2.4568(8), Si1-Si3 2.3395(10), Si2-Si4 2.3881(10).

In contrast, the X-ray diffraction study of the colorless crystals reveals a different tricyclic system with a remarkable change in connectivity compared to that of **131**. The tetrasila-4,5-digermatricyclo[2.2.0.0^{2,5}]hexane **132** is best described as a doubly edge-bridged tetrahedron with a direct bond between the two germanium atoms (Figure 12). The Ge1-Ge2 distance of 2.4534(5) Å is within the typical range of a single bond.[162,163] The Si1-Si2 bond in **132** (2.4809(11) Å) is significantly longer than in analogous homonuclear silicon systems, whether unsaturated[164] or saturated.[165–167] The chair-like isomer **131**, the apparent kinetic product of the dimerization of the transient heavier cyclopropene **[130]**, is unstable in solution and therefore a clean sample could not be obtained yet.

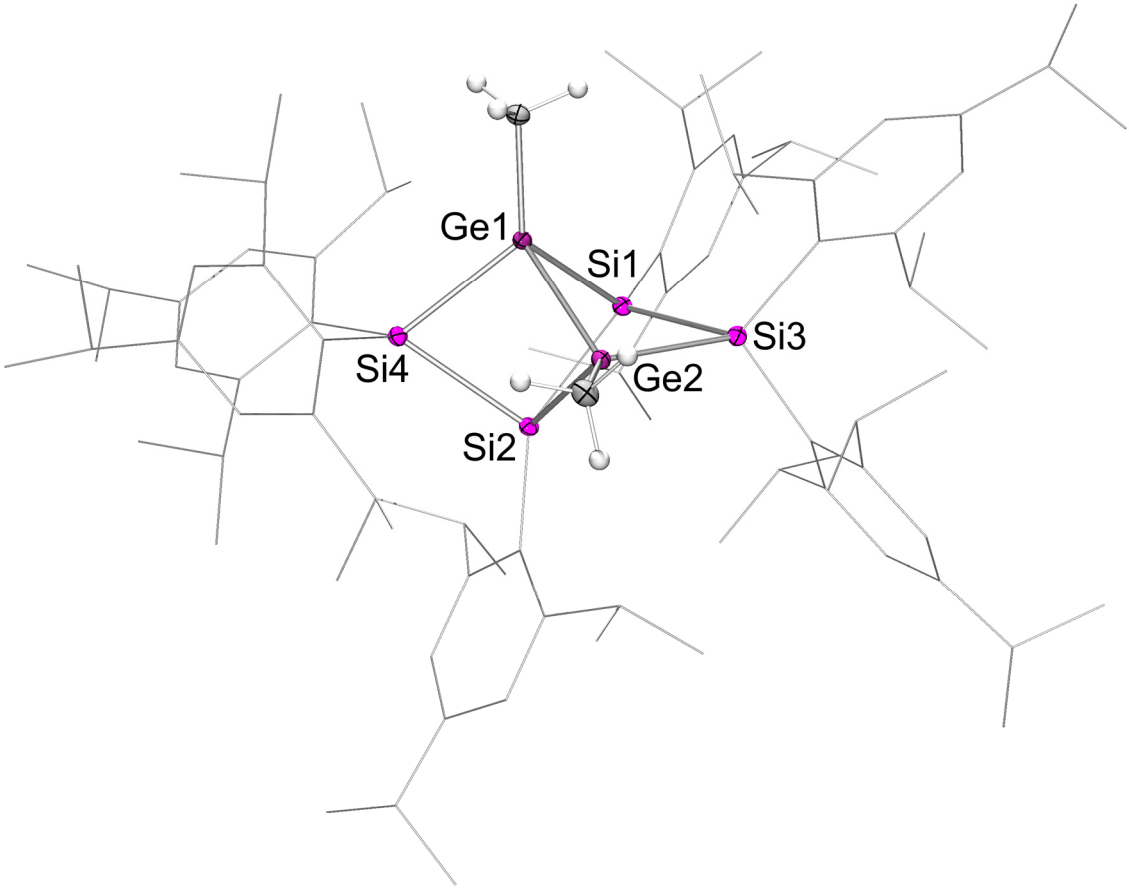

Figure 12. Molecular structure in the solid state of **132**·0.5 C_7H_8 (thermal ellipsoids are drawn at 30%, hydrogen atoms and co-crystallized half toluene molecules and disorder are omitted for clarity). Selected bond lengths [Å]: Ge1-Si4 2.4072(8), Ge1-Si1 2.4344(8), Ge1-Ge2 2.4534(5), Ge2-Si3 2.3956(8), Ge2-Si2 2.4398(8), Si1-Si3 2.3993(11), Si1-Si2 2.4809(11), Si2-Si4 2.4464(11).

Full conversion of **132** is achieved by heating the mixture to 40 °C for two hours, affording predominantly **132**. A similar, albeit photochemical isomerization has been reported for a homonuclear Si_6R_8 derivative (R = Si^{t}BuMe$_2$) by Kira and co-workers.[166]

In the present heteronuclear case, the change in connectivity of the germanium atoms from 1,3 in **131** to 1,2 in **132** is in stark contrast to the case of the 1,4-digermatetrasilabenzene isomer **126**, which is thermally converted into the likely global minimum isomer **127** without such a change in connectivity (Scheme 58).[156] A pure sample of **132** was obtained by crystallization in 63% yield. Doubly edge-bridged tetrahedron **132** is stable in benzene solution for at least 4 weeks and thermally stable up to 220 °C where it decomposes to a mixture of unknown compounds.

The comparison of the ^{29}Si NMR data of pure **132** with the reaction mixture of **131** and **132**, shows that the broad signals at δ = 21.97 and −37.74 ppm (Figure 8g) belong to **132** and that the signals at δ = −82.60 and −96.58 ppm must consequently be assigned to chair-like isomer **131**. The ^{29}Si NMR resonances are comparable to those of homonuclear derivatives of tricyclohexasilane.[165–167] The conclusion at this point is that the initial attack of the sterically innocent methyl anion exclusively was observed at the Ge(II)-center resulting in the NHC-coordinated disilenyl germylene **128a** which was identified by NMR-spectroscopy. The following ring-closure led to the unobserved heavier cyclopropene analogue **[130]**, which than dimerizes to the two saturated tricyclic Ge_2Si_4-scaffolds **131** and **132**. Furthermore the reversibility of the NHC coordination was shown by NMR-spectroscopy.

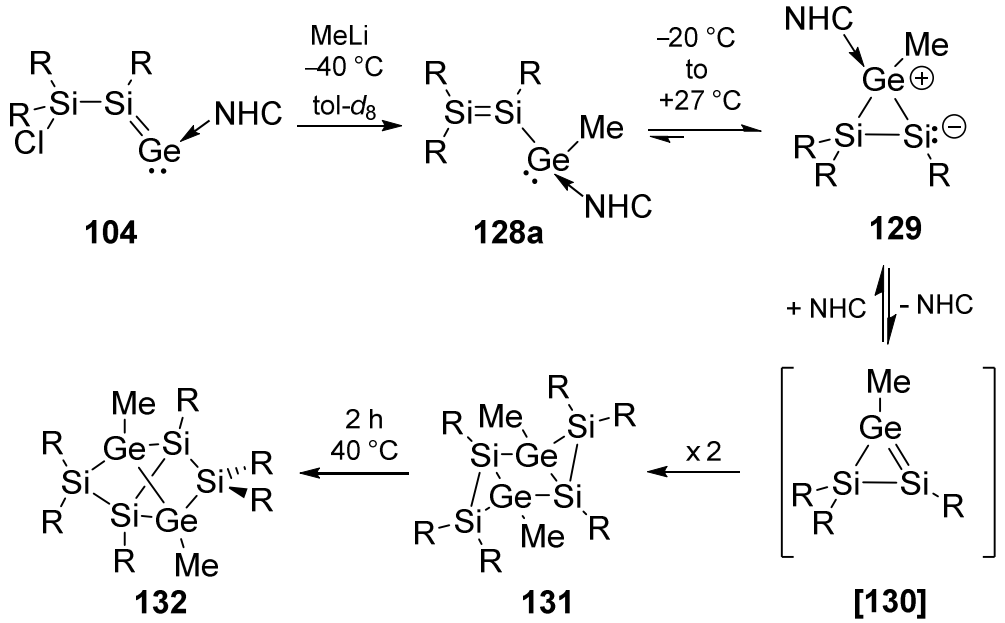

Scheme 62. Overview of the reaction of silagermenylidene **104** with MeLi resulting in unstable disilenyl germylene **128a** leading to **129** and **[130]** which dimerizes to Si_4Ge_2-scaffolds **131** and **132** (R = Tip, NHC = 1,3-diisopropyl-4,5-dimethylimidazol-2-ylidene).

In order to shed some light on the relative thermodynamic stabilities of **128a**, **129**, and **[130]**, Dr. Cem B. Yildiz (now at Aksaray University, Turkey) performed DFT calculations on truncated model systems (Me instead of Tip substituents; see Figure 13) at the B3LYP/6-31+G(d,p) level of theory. The calculated gain in free energy from **128a-Me** to **129-Me** of $\Delta G = -5.2$ kcal mol^{-1} with an activation barrier of $\Delta G^{\neq} = +8.7$ kcal mol^{-1} is fully in line with the observed equilibrium in favor of **129**. The dissociation of NHC from **129-Me** to give **130-Me** is strongly endergonic in Gibbs energy ($\Delta G = +21.7$ kcal mol^{-1}), albeit the larger Tip groups would likely decrease this value considerably in the experimental case. Although the dimerization of **130-Me** to **131-Me** is calculated to proceed without apparent barrier with a gain in free energy of $\Delta G = -64.9$ kcal mol^{-1}, **131-Me** is still by $\Delta G = -25.1$ kcal mol^{-1} higher in energy than **132-Me** (Figure 13), which reflects the experimental observation that **131** is formed as a kinetic product prior to its rearrangement to **132**.

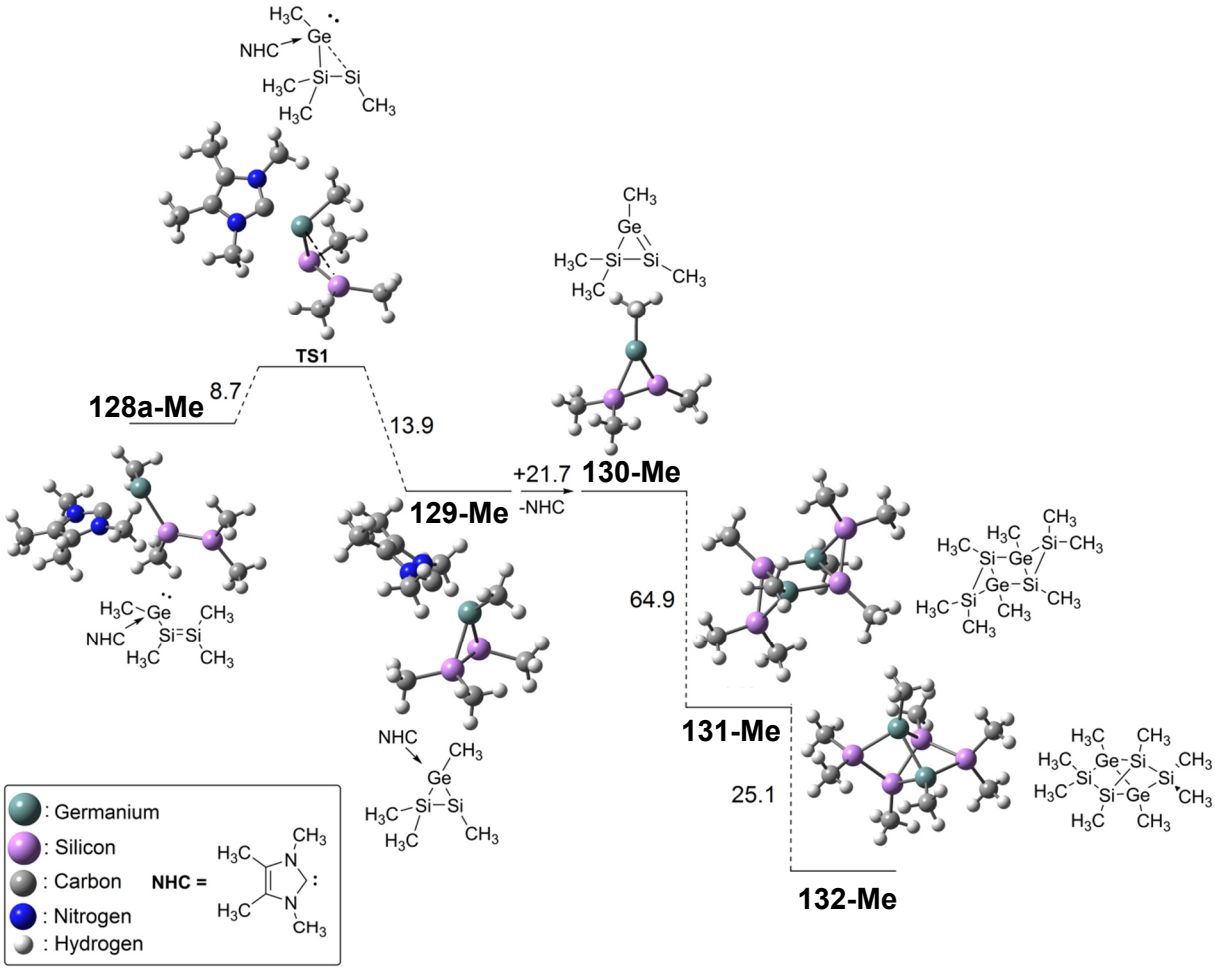

Figure 13. Proposed mechanism and intermediates for the formation of **130-Me** using a simplified model system with methyl groups instead of Tip substituents at B3LYP/6-31+G(d,p) level of theory. ΔG energy values at 298 K are given in kcal mol^{-1}.[168]

In summary, we have gathered spectroscopic evidence for two reactive intermediates on the way toward saturated Ge_2Si_4 dimeric aggregates **131** and **132** with saturated scaffolds that structurally resemble the recently reported unsaturated Ge_2Si_4 systems. Initial attack of the sterically innocent methyl anion equivalent at germanium results in formation of an NHC-stabilized disilenyl germylene **128a**, followed by ring-closure to an NHC-adduct of a heavier cyclopropene **129**. The reversibility of the NHC coordination to **129** is unambiguously proven. The stabilization by excess NHC is a concept resembling common strategies in the stabilization of catalytically active species in the transition metal series and we conclude that this approach will also have an impact in further developments in main group chemistry.

3.1.2. Reaction of Silagermenylidene 104 with EtLi

The observation of NHC-stabilized disilenyl germylene **128a** at low temperatures encouraged us to investigate larger organolithium species as anionic nucleophiles in order to confer higher stability to the NHC-stabilized disilenyl germylene intermediate for the purpose of possible isolation (Scheme 63).

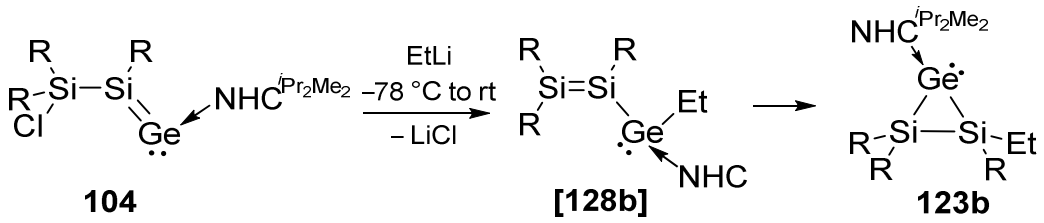

Scheme 63. Reaction of **104** with EtLi resulting in Si_2Ge-species **123b** *via* the proposed intermediate disilenyl germylene **[128b]** (R = Tip).

The addition of EtLi (0.5 M in benzene/cyclohexane) to silagermenylidene **104** at −78 °C in toluene solution results in an immediate change in color from pale red to deep red. Upon warming to room temperature the color turned from red into orange. The ^{29}Si NMR spectrum at room temperature shows two signals at δ = −61.52 and −70.09 ppm, indicating that the plausible NHC-coordinated disilenyl germylene **[128b]** if formed is already completely converted to a saturated species at room temperature (Figure 14). Instead, the ^{29}Si NMR resonances are comparable to the Si_2Ge-rings **123a** and **124a** with the mesityl-group (**123a**: δ = −63.43 and −71.91 ppm, **124a**: δ = −56.08

and −78.10 ppm, Scheme 64) as well as for the three-membered ring **129** with the Me-group (^{29}Si NMR resonances of **129**: δ = −64.92 and −66.51 ppm).

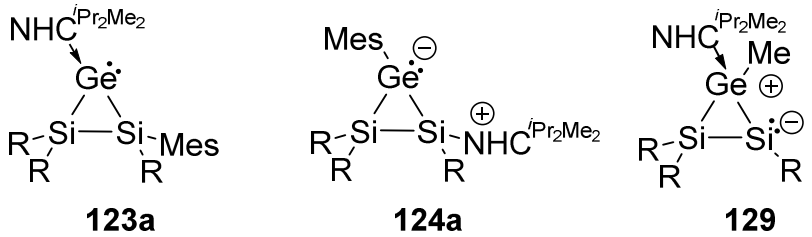

Scheme 64. NHC-stabilized heavier cyclopropylidene analogue **123a** and heavier cyclopropene analogues **124a** and **129** (R = Tip).

The ^{13}C NMR spectrum shows a resonance at δ = 173.52 ppm, comparable to the carbenic C-atom attached to the Ge(II)-center in **123a** (δ = 173.47 ppm),[146] suggesting that Si_2Ge-ring **123b** is generated. An isolation of the proposed heavier cyclopropylidene analogue **123b** in a repeat experiment failed.

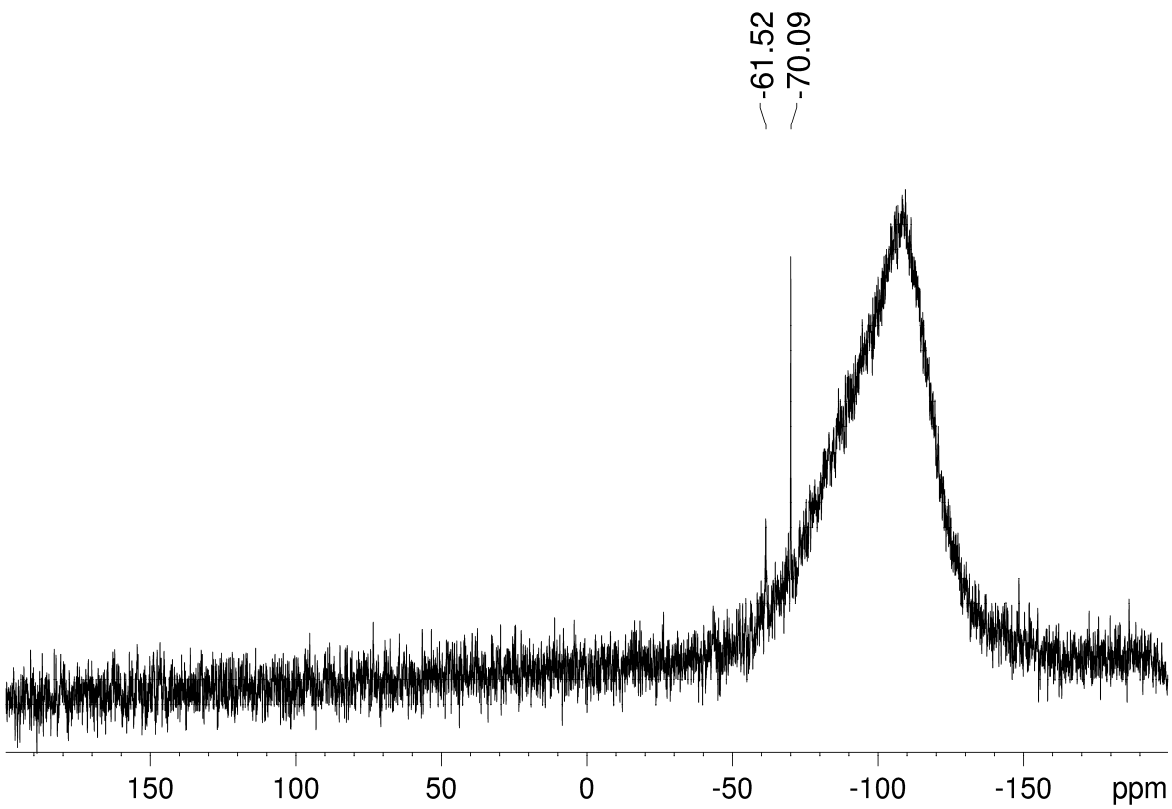

Figure 14. ^{29}Si NMR spectrum of the reaction mixture of **104** with EtLi.

3.1.3. Synthesis of an Isolable Disilenyl Germylene and Its Cyclic Isomer

As reported in Chapter 3.1.1., the reaction of MeLi with silagermenylidene **104** affords methyl-substituted disilenyl germylene **128a** as initial product at low temperature, which could not be characterized in the solid state due to its thermal instability. A sterically more demanding substituent, however, could provide sufficient inertness to a disilenyl germylene to allow for its isolation and full characterization.

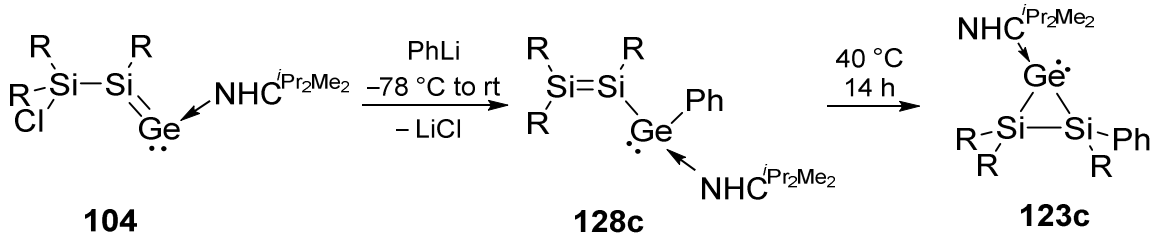

Scheme 65. Reaction of heavier vinylidene analogue **104** with PhLi resulting in persistent NHC-coordinated disilenyl germylene **128c** and its thermal rearrangement to **123c** (R = Tip).

Treatment of **104** with one equivalent of the steric more demanding nucleophile PhLi (1.9 M in *n*-dibutylether) at −78 °C in toluene induced an immediate change in color from pale to deep red. After warming to room temperature, the ^{29}Si NMR signals at δ = 95.06 and 73.88 ppm indicate the quantitative conversion to a new product consistent with the constitution of disilenyl germylene NHC-adduct **128c** (Scheme 65). The ^{1}H NMR spectrum shows a diagnostic broad signal at δ = 5.69 ppm, which is typical for the methine protons of the C*H*Me$_2$ group of a NHC^{iPr_2Me_2} coordinated to a Ge(II)-center.[61,145] In addition, the ^{13}C NMR resonance at δ = 172.91 ppm provides further support for NHC coordination to the Ge(II)-center.

Red crystals for X-ray diffraction were initially obtained from a concentrated solution of **128c** in toluene at −26 °C. As the co-crystallized toluene molecule turned out to be disordered in the solid state structure of **128c**·toluene, the solvent was changed to mesitylene (1,3,5-trimethylbenzene). Indeed, red crystals suitable for X-ray diffraction were obtained after three days at −26 °C without disorder due to the more symmetric mesitylene molecule (Figure 15). The molecular structure of **128c** is in line with the NMR spectroscopic data and confirms the presence of a Si=Si moiety and the coordination of the NHC^{iPr_2Me_2} to the Ge(II)-center. The Si=Si moiety in **128c** is moderately twisted (τ = 11.4°) and only slightly *trans*-bent (θ, SiTip$_2$ = 3.1°; θ, SiTipGe

= 1.8°).[155] As expected, the Ge-Si2 distance corresponds to a typical Ge-Si single bond (2.4206(6) Å). The Ge-C7 bond at 2.056(2) Å is comparable to the corresponding distance of silagermenylidene **104** (2.061 Å),[145] but shorter than that of $GeCl_2$·NHC^{iPr2Me2} **8** (2.106 Å).[61] The Si=Si bond is with 2.1706(8) Å in the typical range of disilenes[18] and very similar to that of the recently reported NHC^{iPr2Me2}-adduct of disilenyl silylene **116** (2.179 Å).[155]

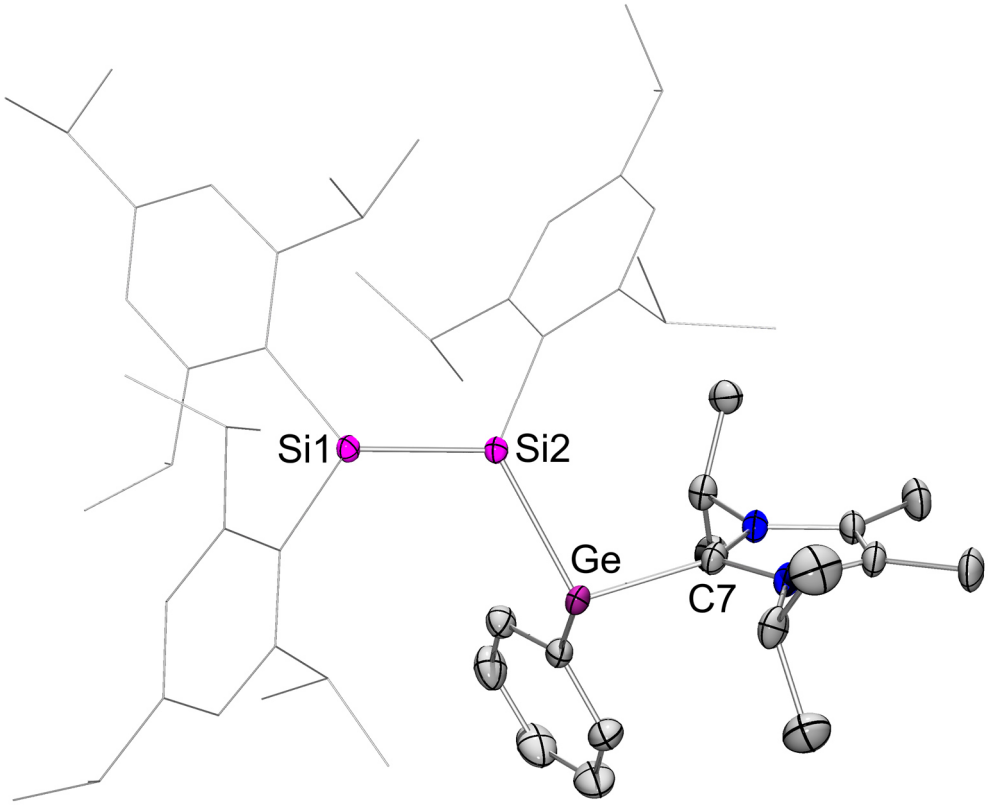

Figure 15. Molecular structure of **128c**·C_9H_{12} in the solid state (thermal ellipsoids at 30%, H atoms and co-crystallized mesitylene omitted for clarity). Selected bond lengths [Å]: Ge-C7 2.056(2), Ge-Si2 2.4206(6), Si1-Si2 2.1706(8).

The red color of **128c** is attributed to the longest wavelength absorption in the UV/vis spectrum at λ_{max} = 452 nm (ε = 10900 Lmol^{-1}cm^{-1}), which is identical to that of silagermenylidene **104** (λ_{max} = 452 nm)[145] and blue-shifted in comparison to that of the NHC-stabilized disilenyl silylene **116** (λ_{max} = 568 nm).[155] At room temperature in solution, **128c** slowly, but selectively, rearranges to a new species with ^{29}Si NMR resonances at δ = −62.74 and −68.81 ppm, which are very similar to those of previously reported heavier cyclopropylidene analogue **123a** and therefore indicative of the formation of **123c**.[146] Accordingly, the characteristic ^{13}C NMR resonance at δ = 172.75

ppm is retained suggesting that NHC^{iPr2Me2} is still coordinated to the Ge(II)-center. In contrast to the mesityl-substituted cases, **123a** and **124a** (Scheme 64), complete conversion to **123c** requires heating of **128c** in toluene to 40 °C for 14 h. Moreover, in case of **123c** no trace of an isomeric cyclization product of type **124a** was observed. Yellow crystals of **123c** suitable for X-ray diffraction (Figure 16) were obtained from a concentrated toluene solution at room temperature after one day.

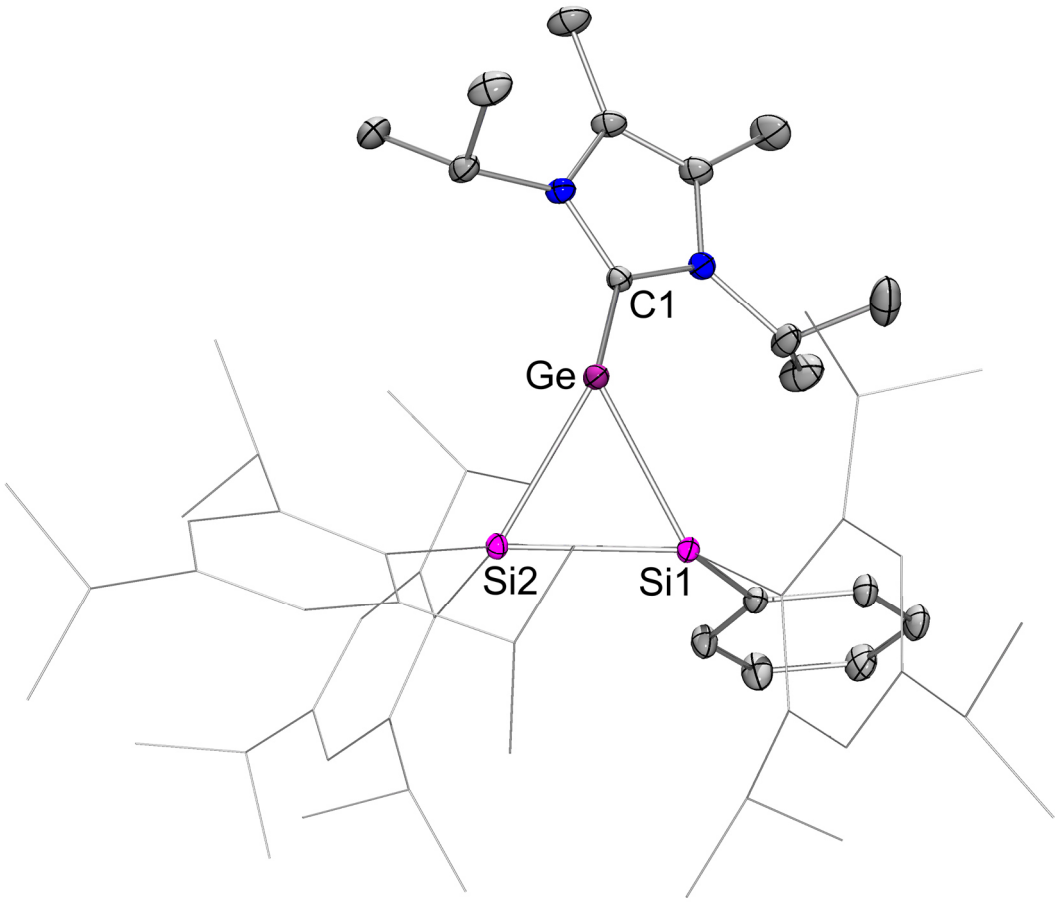

Figure 16. Molecular structure of **123c**·3 C_7H_8 in the solid state (thermal ellipsoids at 30%, H atoms and co-crystallized toluene omitted for clarity). Selected bond lengths [Å] and angles [°]: Ge-C1 2.0589(17), Ge-Si1 2.4232(5), Ge-Si2 2.4452(5), Si1-Si2 2.3775(7); C1-Ge-Si1 116.96(5), C1-Ge-Si2 121.69(5), Si1-Ge-Si2 58.46(17).

The molecular structure in the solid state confirms the connectivity of the three-membered ring of **123c** predicted on the basis of multinuclear NMR spectroscopy. The Si1-Si2 bond length (2.3775(7) Å) is much shorter than that of the mesityl-substituted Si_2Ge-cyclopropylidene of **123a**, (Scheme 64, **123a** = Mes: 2.4448 Å[146]), which could be explained by the sterically more demanding mesityl-group. The Ge-Si bond lengths of Ge-Si1 2.4232(5) and Ge-Si2 2.4452(5) Å in **123c**, however, are not significantly differing (Scheme 64, **123a** = Mes: Ge-Si2 2.4319; Ge-Si1 2.4320 Å[146]). The distance

between the Ge(II)-center and the carbenic carbon of 2.0589(17) Å is slightly elongated suggesting a somewhat weakened NHC-coordination. The yellow color of **123c** is due to the longest wavelength absorption in the UV/vis spectrum at λ_{max} = 438 nm (ε = 6400 $Lmol^{-1}cm^{-1}$), which is slightly blue-shifted in comparison to the mesityl-substituted version (λ_{max} = 454 nm[146]).

3.1.4. Reaction of Silagermenylidene 104 with MesLi

The spectroscopic evidence for NHC-coordinated disilenyl germylene **128a** at −20 °C and the isolation of the persistent disilenyl germylene **128c**, encouraged us to have a closer look at the reaction of MesLi with **104**. The proposed disilenyl germylene had not been detected at 0 °C in Et_2O in the original study, seemingly directly affording the Si_2Ge-species **123a** and **124a**.[146] Changing the solvent and reaction conditions, however, could have a significant influence on the outcome of the reaction and might allow for the detection of disilenyl germylene **128d** (Scheme 66).

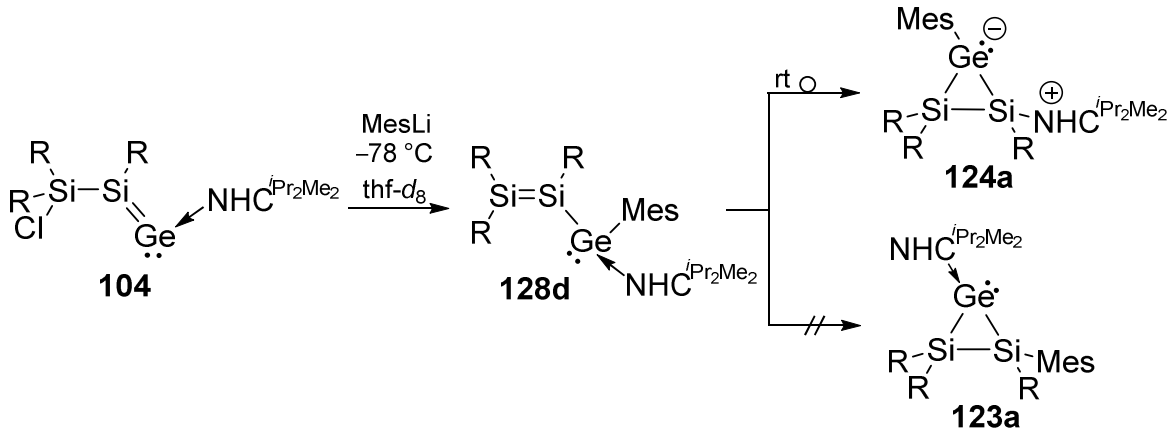

Scheme 66. Reaction of **104** with MesLi at −78 °C leading to **128d** which rearranges to **124a** at room temperature (R = Tip).

A −78 °C cold solution of silagermenylidene **104** in thf-d_8 was added to a −78 °C cold solution of MesLi in thf-d_8. The mixture was stirred for 2 hours at this temperature to guarantee a homogenous system because of the low solubility of MesLi. A part of the reaction mixture is transferred *via* a precooled glass pipette into an NMR-tube (both −78 °C).

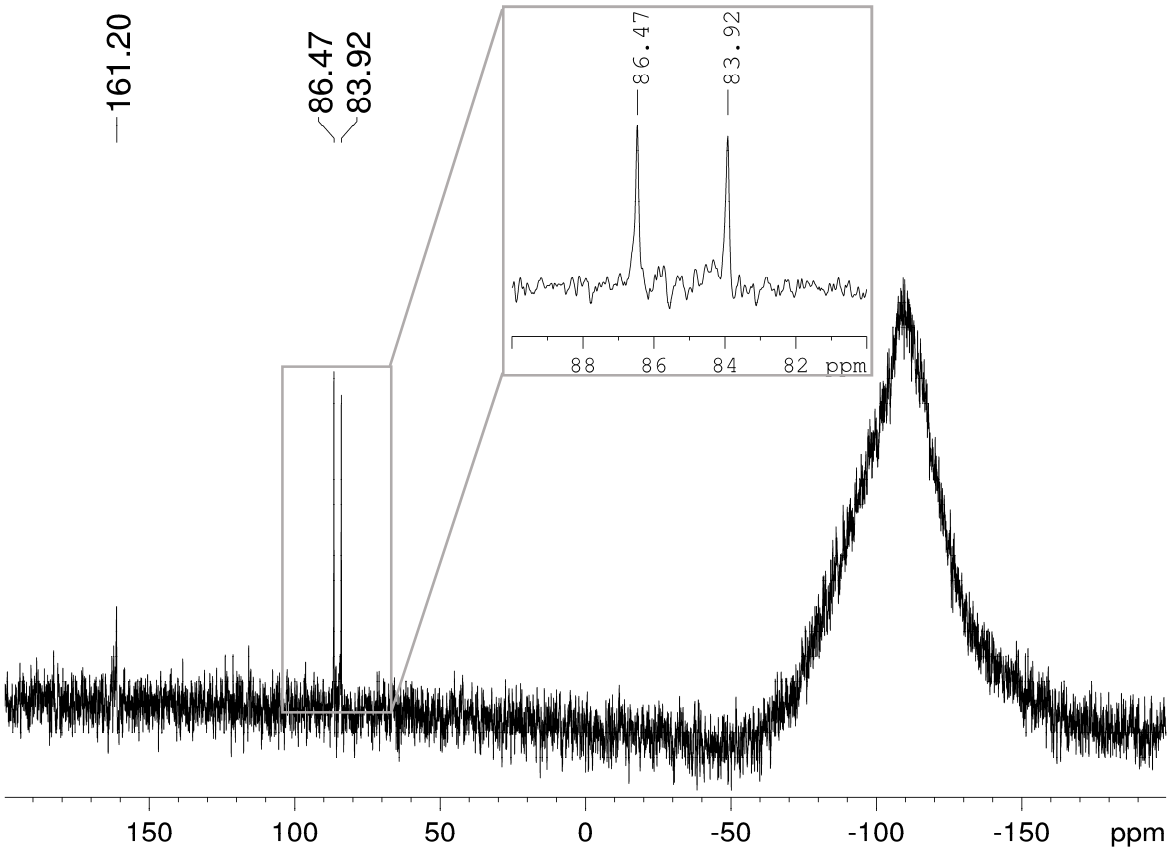

Figure 17. ^{29}Si NMR spectrum of the reaction mixture of **104** with MesLi at −60 °C in thf-d_8. The excerpt shows the signals of disilenyl germylene **128d**.

A ^{29}Si NMR spectrum was recorded at −60 °C and two new signals appeared at δ = 86.47 and 83.92 ppm (Figure 17), which were in the typical range of a Si=Si moiety and in good agreement with the ^{29}Si NMR data of NHC-stabilized disilenyl germylenes **128a** and **128c** (**128a** (Me): δ = 90.10 and 85.27 ppm; **128c** (Ph): δ = 95.06 and 73.88 ppm). A small amount of starting material **104** was detected due to concentration gradients in the NMR tube (only the downfield shift at δ = 161.20 ppm was observed). The ^{13}C NMR spectrum as well as the ^{1}H NMR spectrum show signals typical for the coordination of an NHC to the Ge(II)-center (^{13}C NMR: δ = 172.54 ppm (Figure 18), ^{1}H NMR: δ = 5.34 ppm (Figure 19)). In contrast to disilenyl germylenes **128a** and **128c**, **128d** is thermally extremely unstable leading to the disappearance of the ^{29}Si NMR signals at −40 °C already.

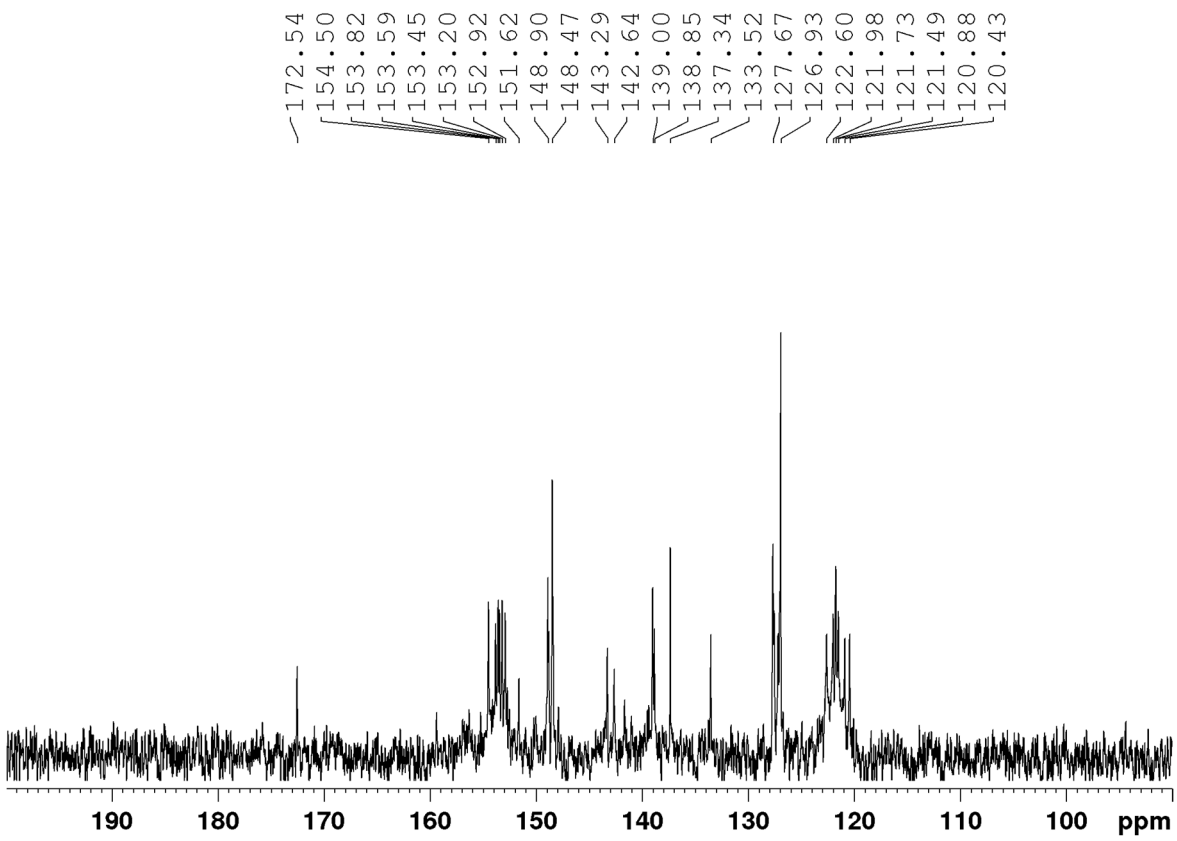

Figure 18. Excerpt of the aryl-region of the ^{13}C NMR spectrum of the reaction mixture of **104** with MesLi at −60 °C in thf-d_8.

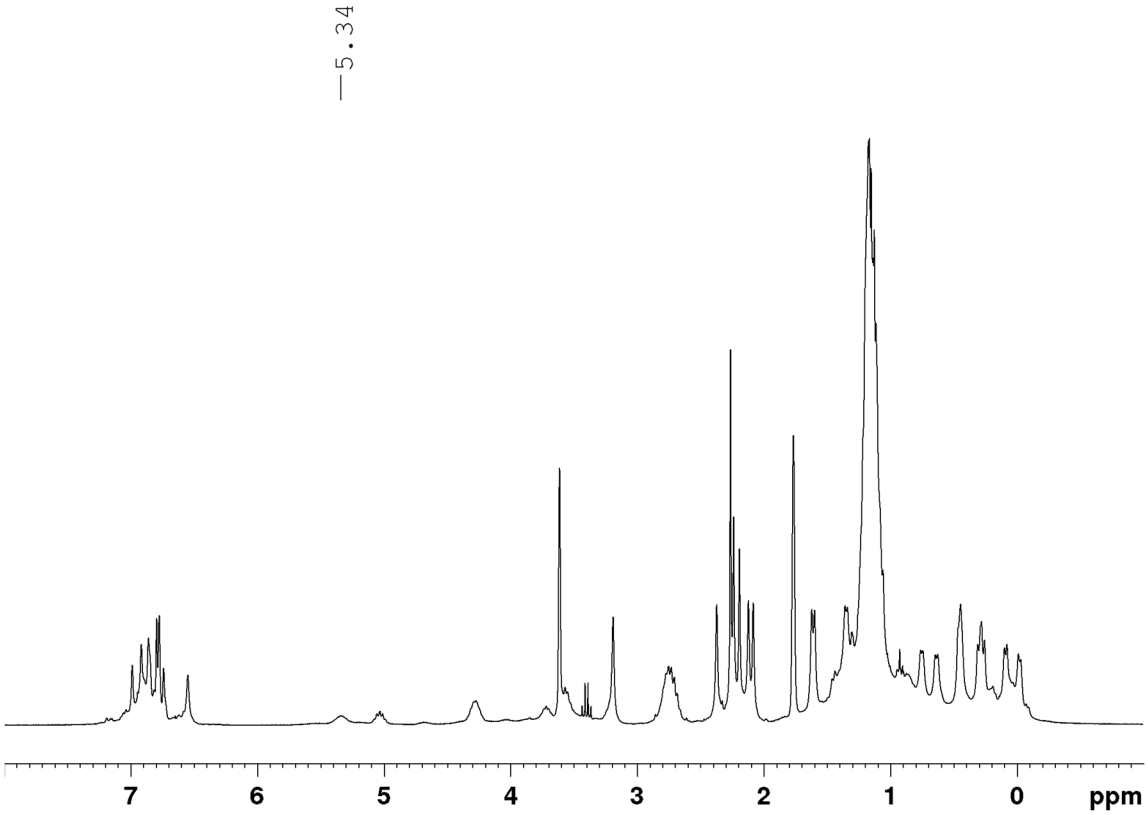

Figure 19. ^{1}H NMR spectrum of the reaction mixture of **104** with MesLi at −60 °C in thf-d_8.

Upon warming the reaction mixture to room temperature, three resonances in the ^{29}Si NMR spectrum are observed at δ = 4.71 ppm (starting material **104**) and two highfield shifts at δ = −58.34 and −80.71 ppm, which are almost identical to those reported for the heavier NHC-stabilized cyclopropene analogue **124a** (Figure 20).[146]

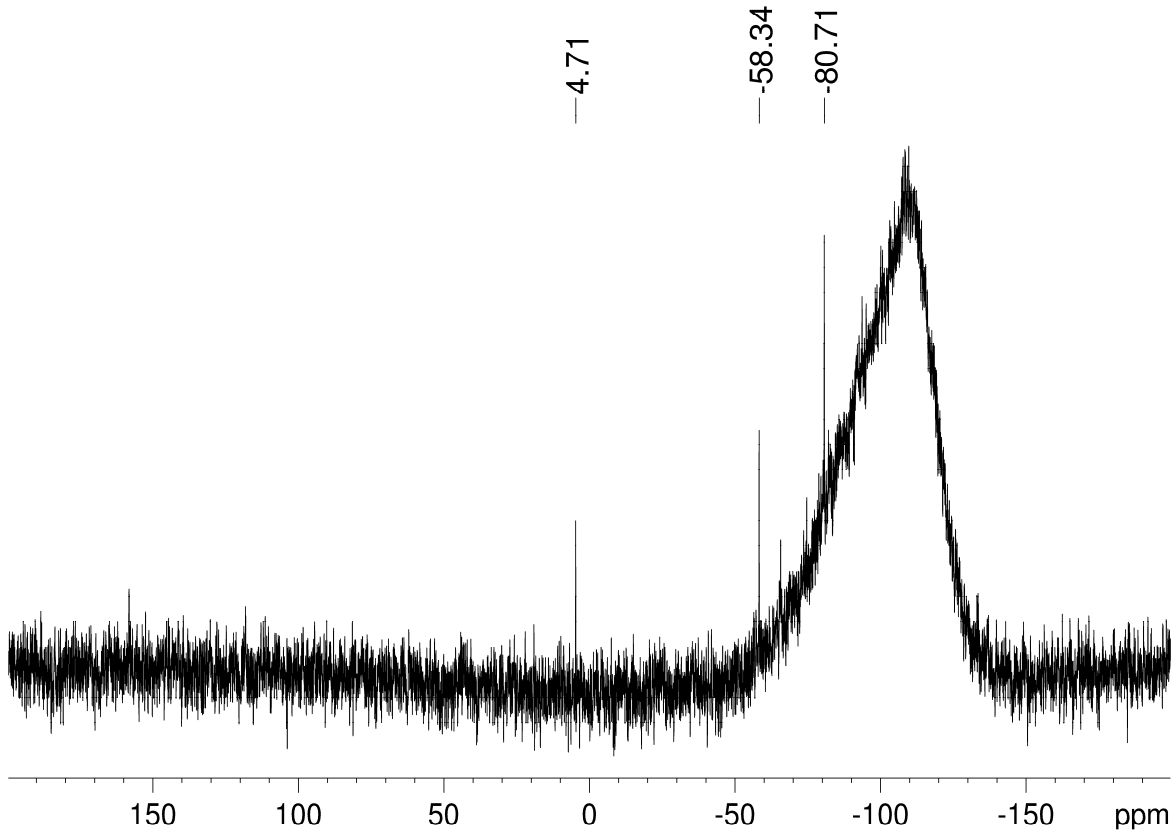

Figure 20. ^{29}Si NMR spectrum of the reaction mixture of **104** with MesLi at 27 °C in thf-d_8.

The ^{13}C NMR spectrum shows a signal at δ = 161.13 ppm (Figure 21), which is close to the value of the carbenic C-atom of the heavier cyclopropene analogue **124a** (δ = 164.53 ppm, **123a**: δ = 173.47 ppm) confirming our suggestion that isomer **124a** was formed as major product (besides residual starting material **104**). The initial formation of mesityl-substituted disilenyl germylene **128d** is in line with the observations for the reactions of PhLi and MeLi with silagermenylidene **104** and led to the conclusion that initial nucleophilic attack at low temperature only occurred at the Ge(II)-center. In case of disilenyl germylene **128c**, the phenyl group is able to shift to the silicon center, which was not observed in case of **128a** or **128d**. As the heavier cyclopropylidene analogue **123a** was not observed in the reaction mixture under these conditions, unambiguously

proves that an initial attack of the mesityl-anion at the formal sp^2-silicon center is necessary for its formation.

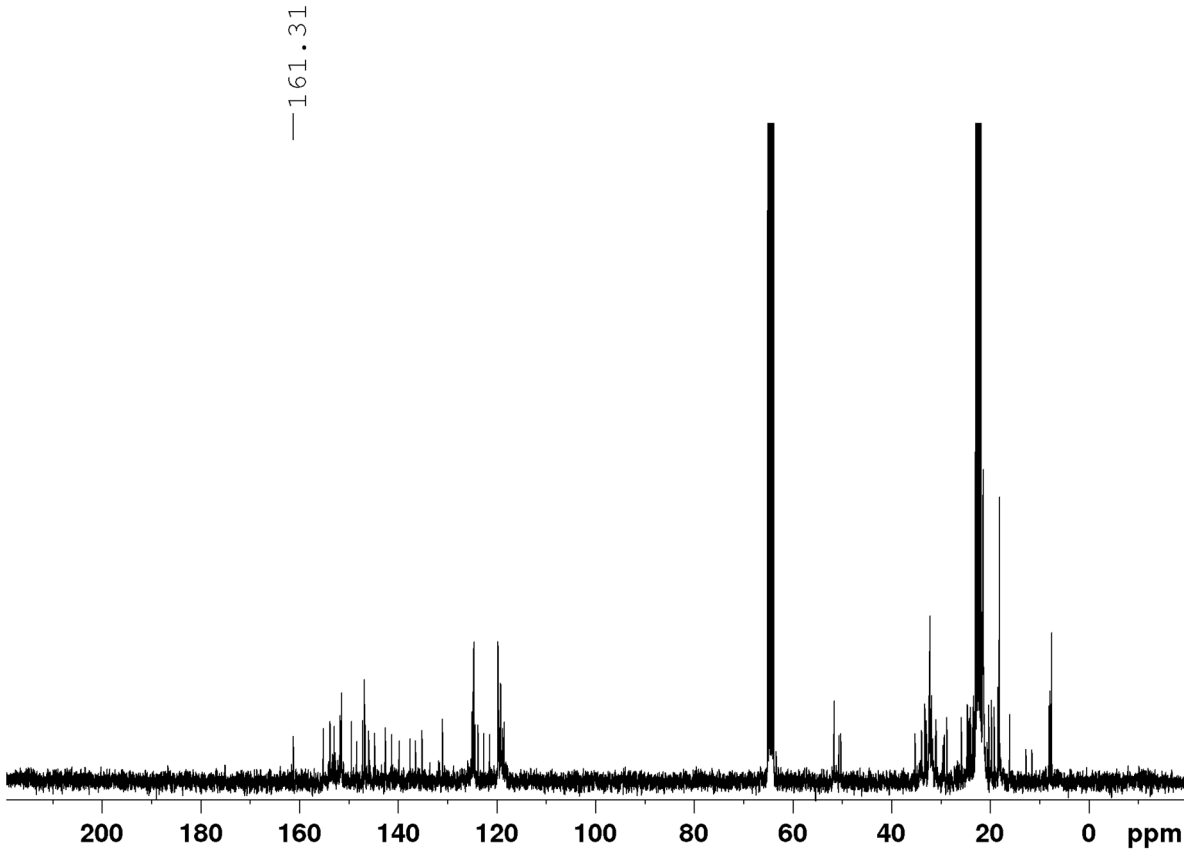

Figure 21. ^{13}C NMR spectrum of the reaction mixture of **104** with MesLi at 27 °C in thf-d_8.

The isolation of disilenyl germylene **128d** (X = Mes) in a preparative scale under the same conditions (thf, −78 °C) failed due to its thermal instability. In Table 1, all important NMR spectroscopic data are listed. The similarity of this data with those of the isolated disilenyl germylene **128c** (R = Ph) leaves no doubt about the NHC-stabilized disilenyl germylenes **128a** (R = Me) and **128d** (R = Mes) as the primary products at low temperature. It must therefore be assumed that the nucleophilic attack under these conditions takes place at the germanium center of silagermenylidene **104** initially. Most notably, the failure to interconvert between the two cyclic regioisomeric NHC-adducts of cyclopropylidene analogue **123a** and cyclopropene analogue **124a** was confirmed, providing further support for the assumption that the site of initial attack determines the regiochemistry of the final product.

Table 1. Summary of diagnostic NMR spectroscopic data of NHC-coordinated disilenyl germylenes **128a**, **128c** and **128d** (R = Tip).

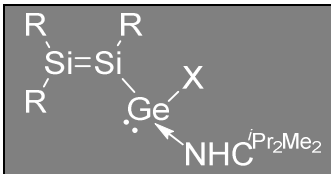	**128a** (X = Me, T = −20 °C)	**128c** (X = Ph, T = −20 °C)	**128d** (X = Mes, T = −60 °C)
^{29}Si NMR [ppm]	90.06	95.04	86.47
Si=Si moiety	85.72	74.40	83.92
^{13}C NMR [ppm]	175.29	172.38	172.54
Carbenic C-atom			

3.1.5. Reaction of Silagermenylidene 104 with ^{i}PrLi

In Chapter 3.1.3. and 3.1.4. evidence was presented that the initial attack of the anionic nucleophile R-Li in case of R = Mes and R = Ph occurs exclusively at the germanium center of silagermenylidene **104** at low temperature. Upon warming results in the uniform isomerization to the NHC-adduct of the heavier cyclopropene isomer **124a** (R = Mes) or the heavier cyclopropylidene analogue **123c** (R = Ph). The formation of the cyclopropylidene isomer **123a** at higher temperature can consequently only be due to an alternate reaction pathway, possibly the nucleophilic attack at the unsaturated silicon center. The reaction of **104** with ^{i}PrLi should shed light on the initial attack of organolithium nucleophiles (Scheme 67).

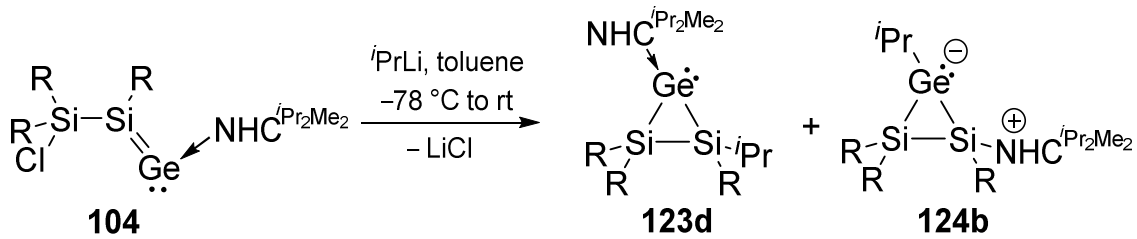

Scheme 67. Reaction of **104** with ^{i}PrLi resulting in isomers **123d** and **124b** (R = Tip).

As in case of EtLi, the reaction of **104** with ^{i}PrLi (0.7 M in *n*-pentane) at −78 °C in toluene resulted in a color change from pale red to deep red upon warming to room temperature. The ^{29}Si NMR spectrum at room temperature shows two sets of signals at δ = −62.26 and −72.66 ppm and δ = −69.06 and −78.04 ppm, which indicates the formation of two isomers (Figure 22). This reiterates the findings in case of the MesLi reaction with silagermenylidene **104** at 0 °C that was reported to afford the two cyclic

Si_2Ge-isomers **123a** and **124a** (**123a**: δ = −63.43 and −71.91 ppm, **124a**: δ = −56.08 and −78.10 ppm, Scheme 64, page 48).[146]

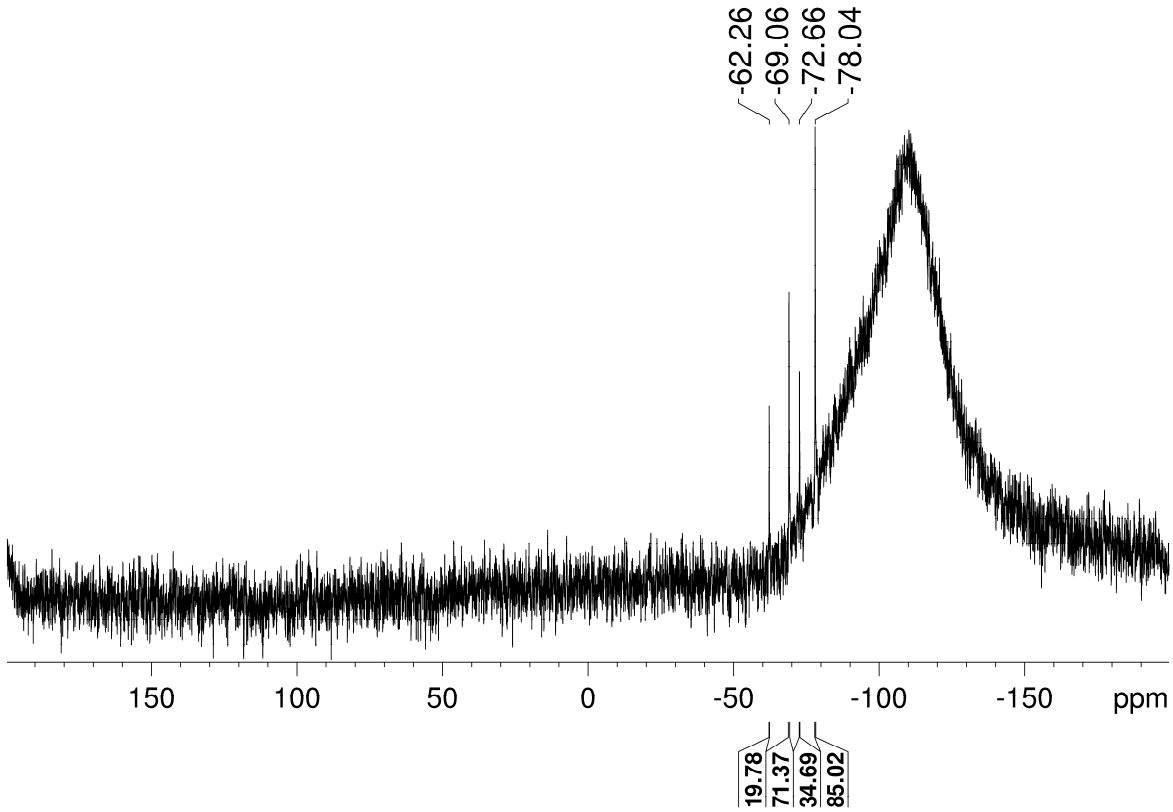

Figure 22. ^{29}Si NMR spectrum of the reaction mixture of **104** with ^{i}PrLi.

The ^{13}C NMR spectrum reveals one resonance for a carbenic C-atom at δ = 164.59 ppm (Figure 23, **124a**: δ = 161.13 ppm) which supports the suggestion that the heavier NHC-coordinated cyclopropene analogue **124b** has been formed as the major product (ca. 70% based on the integration of ^{29}Si NMR-signals). The signal for the carbenic C-atom of the minor product, the heavier NHC-coordinated cyclopropylidene **123d**, could not be identified presumably due to the general broadening of such signals.

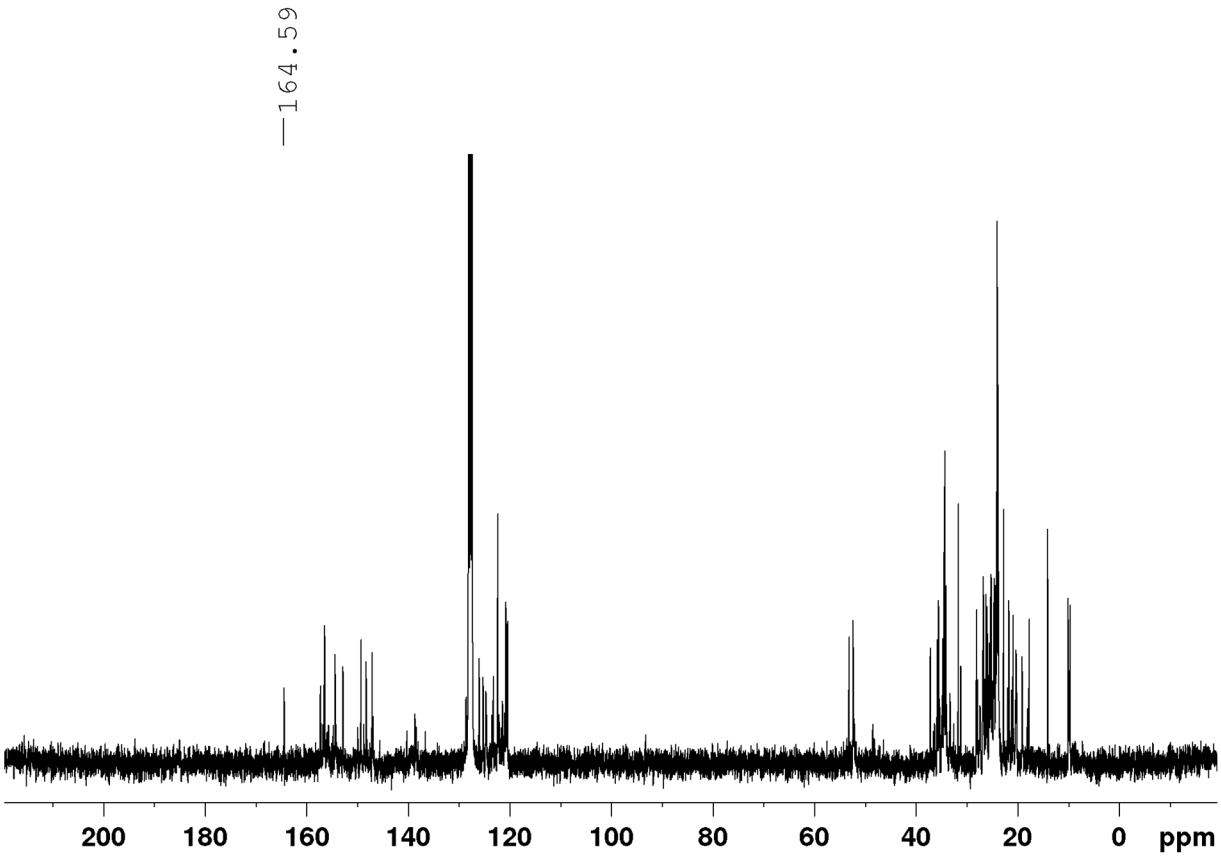

Figure 23. ^{13}C NMR spectrum of the reaction mixture of **104** with ^{i}PrLi.

Crystallization from a saturated toluene solution afforded orange crystals suitable for X-ray diffraction. The analysis confirmed the structure deduced from the NMR spectroscopic data. The NHC-coordinated cyclosilagermene **124b** (Figure 24) is structurally related to **124a**. The Si1-C4 bond length is with 1.950(2) Å slightly shorter than in **124a** (1.979 Å). The Ge-Si (Ge-Si1 2.3937(7) Å and Ge-Si2 2.4226(7) Å) and Si-Si bond lengths (Si1-Si2 2.4242(9) Å) of **124b** are in good agreement with those of **124a** (Ge1-Si1 2.4387 Å, Ge1-Si2 2.4399 Å and Si1-Si2 2.4127 Å).[146] The molecular structure in the solid state of heavier NHC-stabilized cyclopropylidene isomer **123d** could not be determined by X-ray diffraction. A mechanical separation of both isomers was impossible in this case and hence clean NMR spectra of **124b** could not be obtained either.

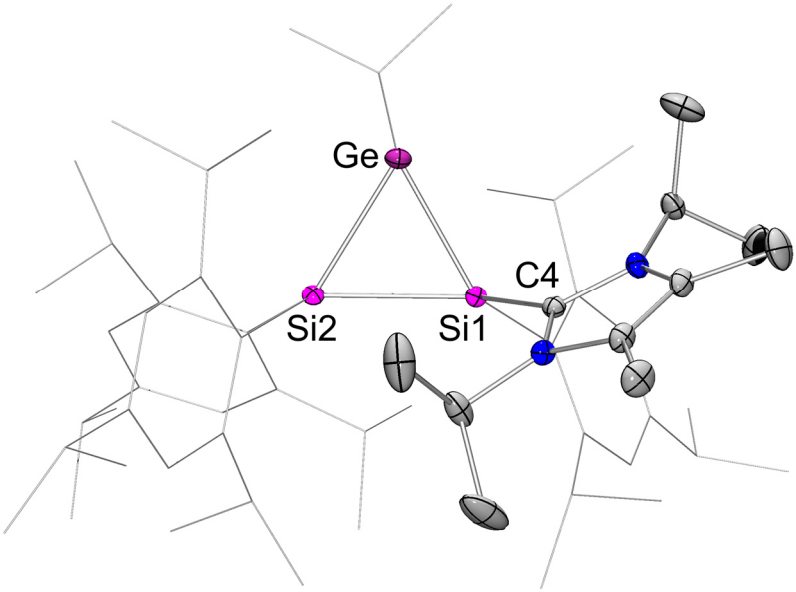

Figure 24. Molecular structure of **124b** in the solid state (thermal ellipsoids at 30%, H atoms and co-crystallized toluene omitted for clarity). Selected bond lengths [Å]: Si1-C4 1.950(2), Ge-Si1 2.3937(7), Ge-Si2 2.4226(7), Si1-Si2 2.4242(9).

3.1.6. Reaction of Silagermenylidene 104 with ^{s}BuLi and ^{t}BuLi

The reaction of silagermenylidene **104** with sterically demanding alkyl substituents was the last investigation in this study of anionic nucleophiles. ^{s}BuLi and ^{t}BuLi were chosen as suitable nucleophiles.

The addition of ^{s}BuLi (1.4 M in cyclohexane) at −78 °C to a toluene solution of **104** induced a change in color from pale red to deep red as observed for EtLi or ^{i}PrLi (Scheme 68).

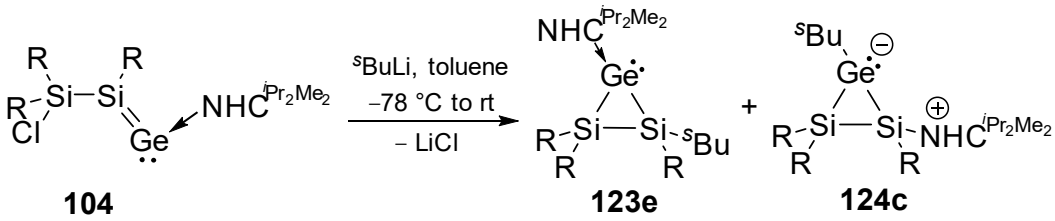

Scheme 68. Reaction of **104** with ^{s}BuLi resulting in Si_2Ge-isomers **123e** and **124c** (R = Tip).

A ^{29}Si NMR spectrum at room temperature shows two broadened signals at δ = −68.25 and −77.47 ppm as well as at δ = −61.87 and −72.10 ppm (Figure 25) similar to the reaction of **104** with ^{i}PrLi (**123d**: δ = −62.26 and −72.66 ppm, **124b**: δ = −69.06 and −78.04 ppm, Scheme 67, page 57). The ^{13}C NMR spectrum reveals one resonance at δ = 164.61 ppm typical for the coordination of an NHC to the silicon center already

observed in the case of cyclosilagermene **124a** with mesityl (δ= 161.13 ppm) and isomer **124b** with ^{i}PrLi (δ = 164.59 ppm) strongly suggesting that **124c** was formed as major product beside isomeric heavier cyclopropylidene **123e** (Figure 26). However, all attempts to isolate **124c** failed. The reaction of **104** with ^{t}BuLi (1.7 M in hexane) led only to a mixture of unidentified products.

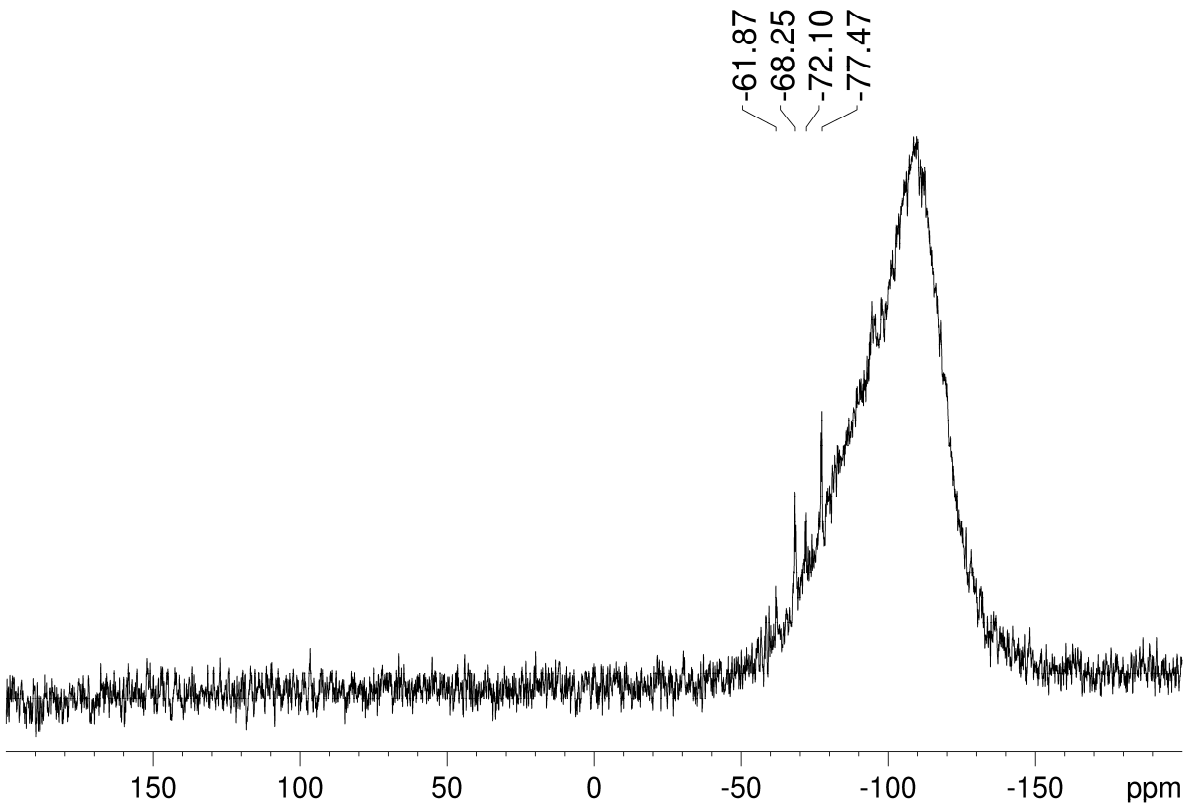

Figure 25. ^{29}Si NMR spectrum of the reaction mixture of silagermenylidene **104** with ^{s}BuLi.

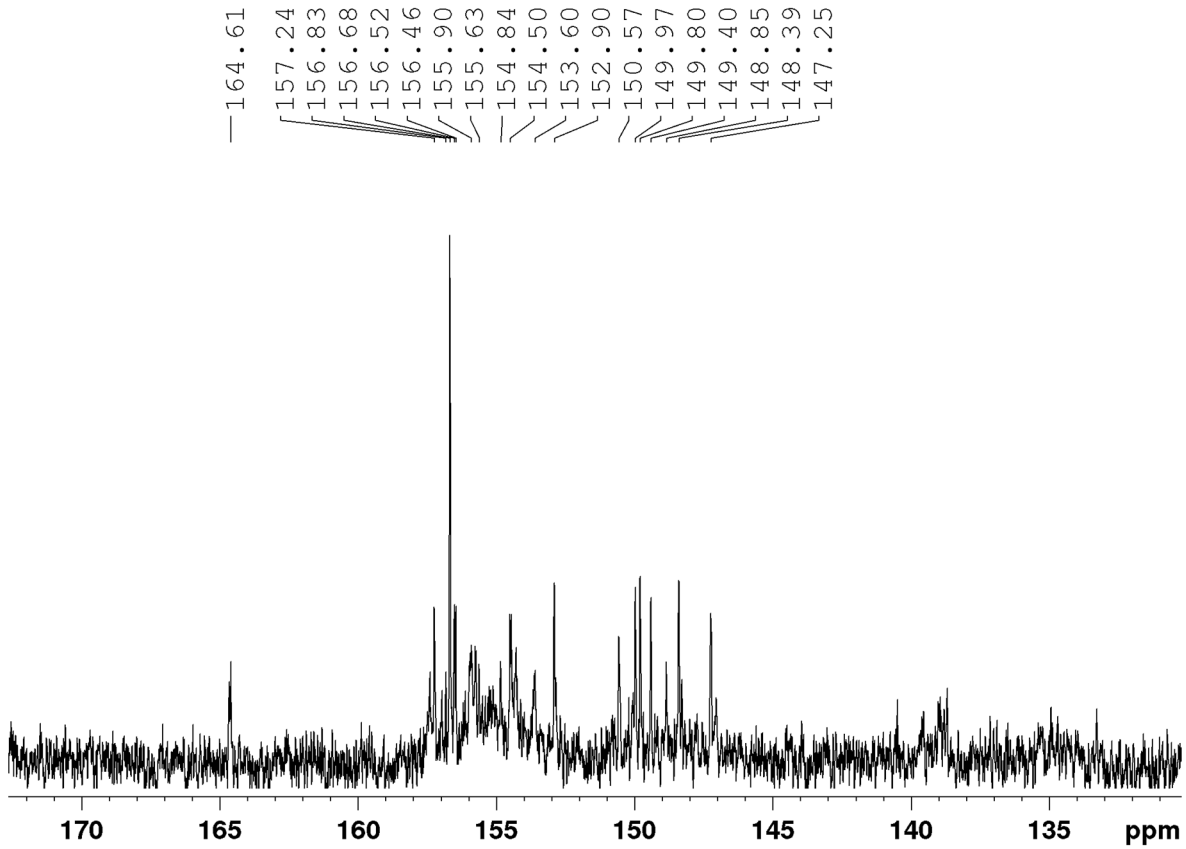

Figure 26. Excerpt of the aryl-region of the ^{13}C NMR spectrum of the reaction mixture of silagermenylidene **104** with $^{s}BuLi$.

3.2. Regiodiscriminating Reactivity of Disilenyl Germylene 128c and Its Isomeric Heavier Cyclopropylidene Analogue 123c toward Phenylacetylene and Xylyl Isocyanide

3.2.1. Synthesis of NHC-Coordinated Heavier Cyclopentenylidene Derivative 133

As described in Chapter 3.1.3., reaction of silagermenylidene **104** with PhLi led to the formation of persistent disilenyl germylene **128c** with subsequent rearrangement to its isomeric heavier cyclopropylidene analogue **123c**. The unprecedented opportunity that with **128c** and **123c** both the open-chained and cyclic germylene isomers of the net composition were isolated allows for a systematic comparison of their reactivity (Scheme 69).

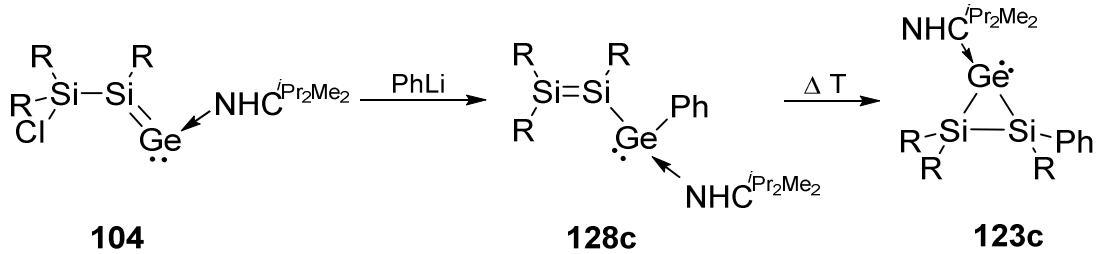

Scheme 69. Reaction of NHC-coordinated silagermenylidene **104** with PhLi leading to disilenyl germylene **128c** and heavier cyclopropylidene analogue **123c** (R = Tip).

The potential of **128c** and **123c** for further manipulations is based on the simultaneous presence of the base-stabilized Ge(II)-center and a further degree of unsaturation, either manifest as a reactive Si=Si moiety (**128c**) or a strained three-membered ring (**123c**). Disilenyl germylene **128c** was treated with one equivalent of phenylacetylene in toluene at −40 °C (Scheme 70). While slowly reaching room temperature, a color change from deep to pale red was observed. In the ^{29}Si NMR spectrum two new signals at δ = −1.51 and −15.39 ppm indicated the consumption of the Si=Si moiety. In contrast, the characteristic ^{13}C NMR resonance at δ = 169.45 ppm suggested that NHC^{i}Pr$_2$Me$_2$ still coordinates to the germanium(II)-center.[163]

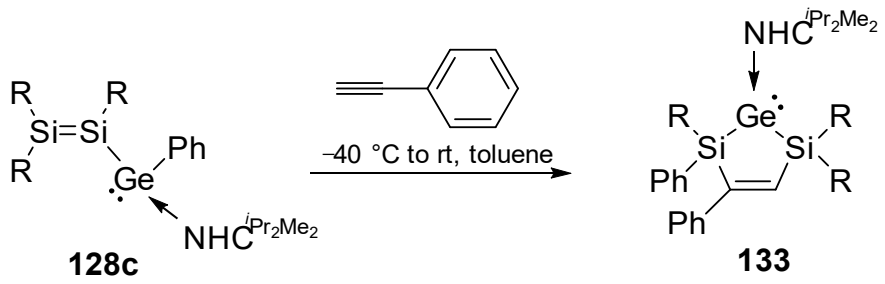

Scheme 70. Reaction of **128c** with phenylacetylene resulting in regioisomeric NHC-coordinated heavier cyclopentenylidene derivative **133** (R = Tip).

Yellow single crystals were obtained from a saturated toluene solution after three days at ambient temperature. The X-ray structure analysis (Figure 27) confirmed the structure of a five-membered ring **133** with an NHC-coordinated Ge(II)-center and two tetracoordinate Si-atoms in accordance with the NMR spectroscopic data.

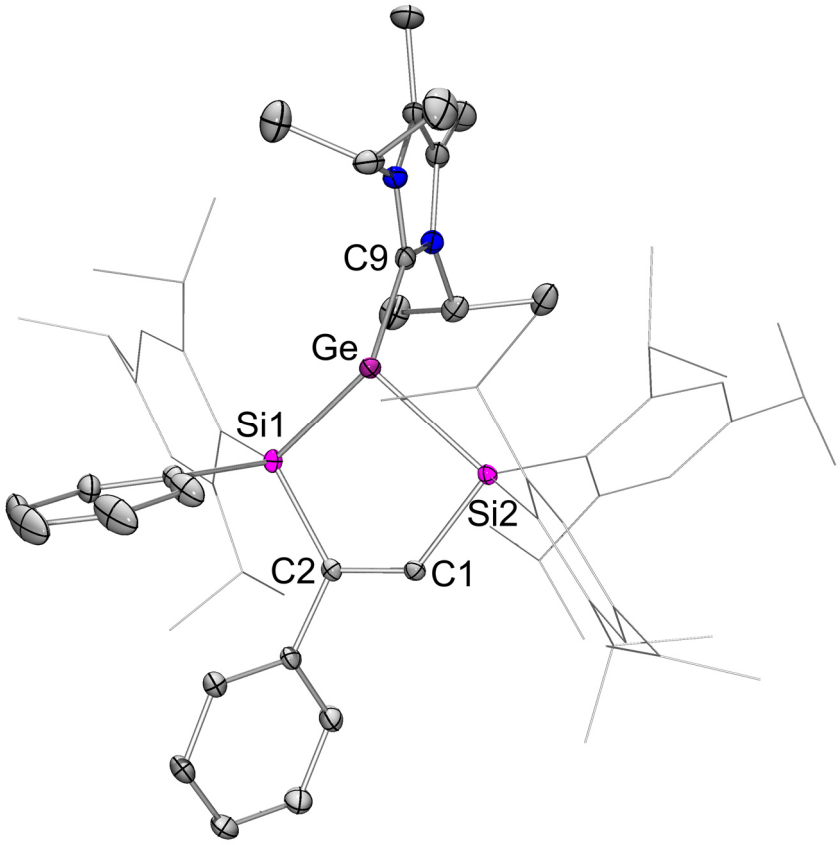

Figure 27. Molecular structure of **133** in the solid state (thermal ellipsoids at 30%, H atoms omitted for clarity). Selected bond lengths [Å] and angles [°]: Ge-C9 2.0496(16), Ge-Si2 2.4189(4), Ge-Si1 2.4236(4), Si2-C1 1.8923(15), Si1-C2 1.9312(16), C1-C2 1.354(2); C9-Ge-Si2 110.73(5), C9-Ge-Si1 114.43(4), Si2-Ge-Si1 92.34(14).

Surprisingly, the connectivity of the SiSiGe-moiety in **133** with both silicon atoms directly adjacent to germanium has changed in comparison with **128c**. In addition, the phenyl group in **133** has migrated from germanium to the neighboring silicon center.

The distance between Ge and the carbenic carbon atom (Ge-C9 2.0496(16) Å) is relatively short in comparison to Marschner's five-membered NHC^{Me4}-coordinated cyclic germylenes (2.070 and 2.076 Å).[163] In the absence of air and moisture, **133** is stable for months in the solid state and for several weeks in benzene solution. The yellow color of **133** is due to the longest wavelength absorption in the UV/vis spectrum at λ_{max} = 348 nm (ε = 8800 Lmol^{-1}cm^{-1}) and blue-shifted in comparison to heavier cyclopropylidene analogue **123c** (λ_{max} = 438 nm, ε = 6400 Lmol^{-1}cm^{-1}) or similar compounds.[169]

3.2.2. Synthesis of NHC-Coordinated Heavier Cyclopentenylidene Analogue 134

According to naïve expectation, the cyclopentenylidene derivative **133** obtained from treatment of the disilenyl germylene **128c** (see previous chapter) could have arisen from the insertion of the C-C triple bond of phenylacetylene into the Si-Si single bond of isomeric three-membered ring **123c**. In order to check this possibility, **123c** was treated with one equivalent of phenylacetylene at room temperature, but even after 24 h no discernible reaction took place thus ruling out the intermediacy of **123c** in the generation of **133** from disilenyl germylene **128c** (Scheme 71).

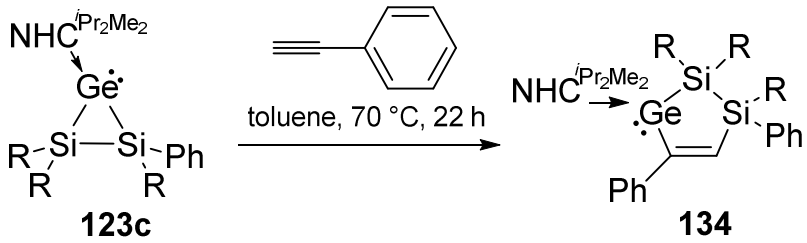

Scheme 71. Reaction of **123c** with phenylacetylene resulting in regioisomeric NHC-coordinated heavier cyclopentenylidene derivative **134** (R = Tip).

After heating to 70 °C for 22 h, however, a single product is detected alongside about 50% of unreacted **123c**. Addition of one further equivalent of phenylacetylene completes conversion at 70 °C after another 22 h. The single product features ^{29}Si NMR signals at δ = −1.10 and −19.16 ppm, in the typical range of tetracoordinate Si-atoms, but distinctly different from those of **133**. It is well-known that aryl acetylenes tend to polymerize under similar reaction conditions,[169,170] which explains the excess of phenylacetylene required for complete conversion of **123c** to the new product. Alongside the diagnostic signal at δ = 172.01 ppm for the carbenic carbon of Ge-

coordinated NHC, the ^{13}C NMR spectrum of the product reveals another downfield signal at δ = 187.94 ppm (not observed in **133**). It is known that C=*C*Ph moieties attached to germanium give rise to ^{13}C NMR resonances between δ = 173 and 192 ppm in the ^{13}C NMR.[163,169,171]

Red single crystals were obtained from a saturated pentane solution after 18 hours at room temperature. The analysis by X-ray diffraction determines the constitution of the new product as the NHC-adduct of five-membered cyclic germylene **134**, which – in contrast to the regioisomeric **133** – features the C-C double bond as directly attached to the Ge(II)-center (Figure 28). The bond length between germanium and the carbenic carbon atom in **134** is with 2.094(2) Å significant longer than that of **133** (2.0496(16) Å).

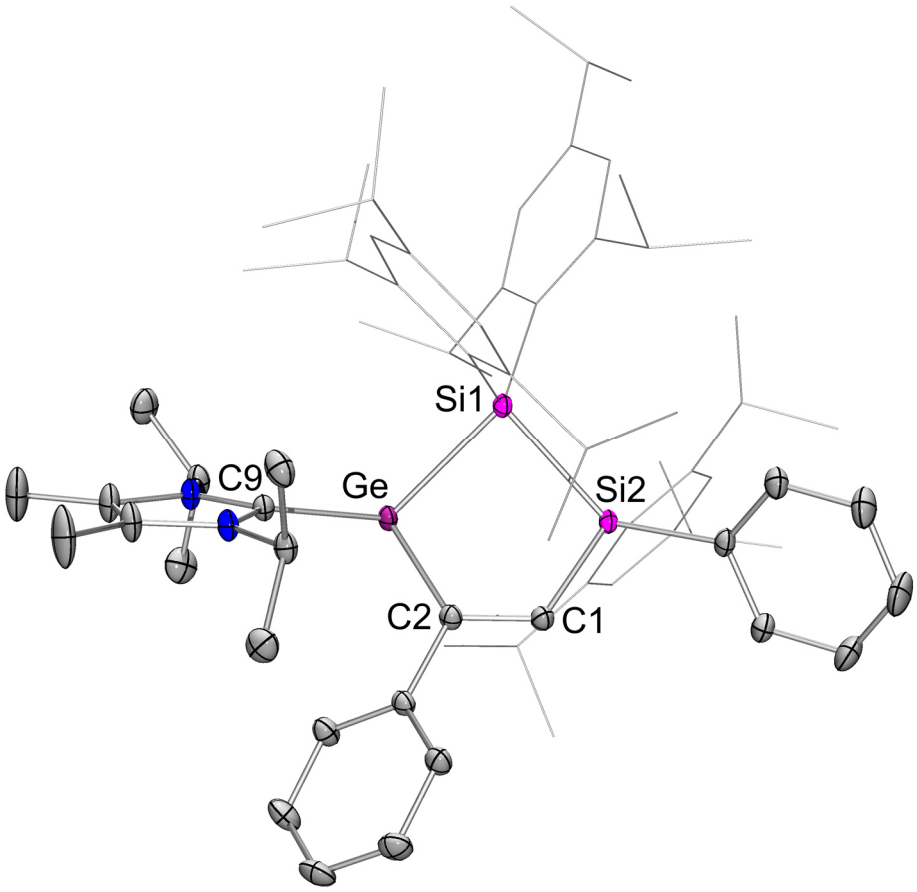

Figure 28. Molecular structure of **134** in the solid state (thermal ellipsoids at 30%, H atoms omitted for clarity). Selected bond lengths [Å] and angles [°]: Ge-C9 2.094(2), Ge-Si1 2.5174(7), Si1-Si2 2.4040(9), Si2-C1 1.861(3), Ge-C2 2.004(2), C1-C2 1.359(3).

The red color of **134** is due to the longest wavelength absorption in the UV/vis spectrum at λ_{max} = 425 nm (ε = 5500 $Lmol^{-1}cm^{-1}$), which is strongly red-shifted in comparison to **133** (λ_{max} = 348 nm, ε = 8800 $Lmol^{-1}cm^{-1}$).

3.2.3. Mechanistic Details for the Formation of 133 and 134

The formation mechanism of **134** would be readily explained by invoking the intermediacy of open-chained isomer **128c**: The disilenyl germylene could plausibly react in a [2 + 3] cycloaddition reaction, which, however, can virtually be excluded based on the diametrically opposing regioselectivity during the reaction of isolated **128c** (yielding **133** exclusively). In order to clarify the mechanism of the generation of **133** and **134**, DFT calculations were carried out by Dr. Cem B. Yildiz (now Aksaray University, Turkey) on simplified model systems (Me instead of Tip, Ph, and ^{i}Pr; for details see Chapter 5.4.) at the B3LYP/6-31G(d,p) level of theory. In view of the detailed studies by Baines and co-workers on the reaction of alkynes with disilenes,[172] we anticipated that the formal cycloaddition of phenylacetylene to the Si=Si moiety of disilenyl germylene **128c** would be favorable. Indeed, a stepwise, presumably ionic pathway to the [2 + 2] cycloadduct featuring an exocyclic germylene functionality **[135-Me]** was identified for the model reaction of methylacetylene with **128c-Me** (Scheme 72). The highest barrier of $\Delta G^{\neq}$ = 13.0 kcal mol^{-1} is well in line with a reaction occurring at room temperature (for details see Figure 98 in Chapter 7.2.). An alternative pathway *via* a CH addition of methylacetylene to the Si=Si moiety can be excluded on the basis of the high activation barriers of up to 34.8 kcal mol^{-1} (for details see Figure 101 in Chapter 7.2.).

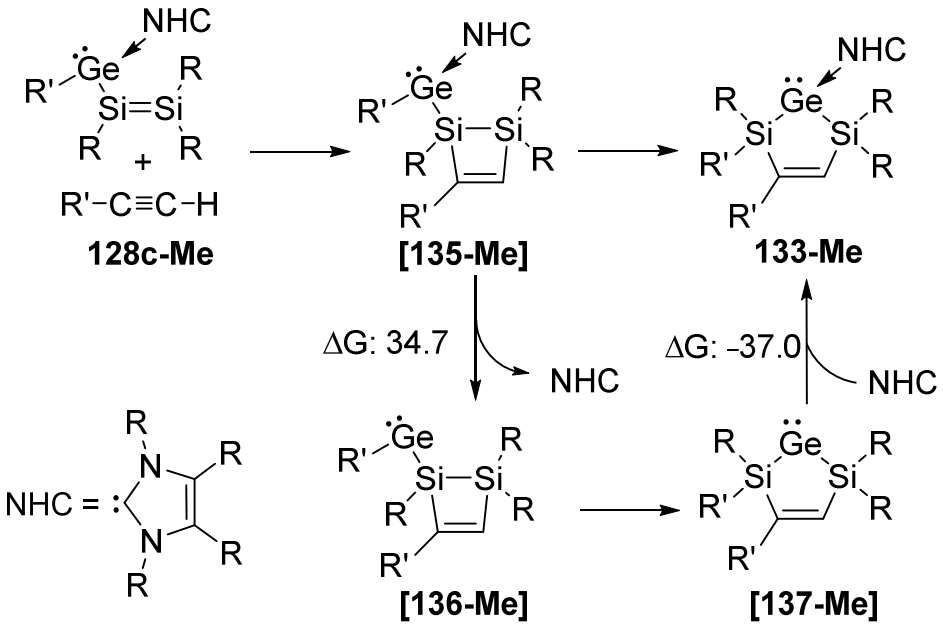

Scheme 72. Plausible mechanism for the formation of **133-Me** (R = R' = Me).

After formation of the intermediate **[135-Me]**, two competitive pathways can be considered to obtain product **133-Me**: The reaction may either proceed with or without dissociation of the NHC (Scheme 72). The highest barrier for the pathway without NHC-dissociation amounts to 31.5 kcal mol^{-1} (for details see Figure 99 in Chapter 7.2.), a value that is likely even higher in the experimental case due to the bulkier substituents and thus incompatible with a reaction readily proceeding at room temperature. In light of the often facile NHC-dissociation in unsaturated heavier main group systems,[147,155,173,174] the dissociative pathway to **133-Me** is a viable alternative (for details see Figure 100 in Chapter 7.2.). Although the liberation of NHC from **[135-Me]** to afford **[136-Me]** is with ΔG = 34.7 kcal mol^{-1} quite endergonic it can reasonably be expected that the steric bulk in the experimental case will lower this value drastically and thus exert the opposite effect compared to the pathway without NHC-dissociation. Indeed, the calculations with inclusion of the bulky substituents (R = Tip; R' = Ph in Scheme 72) decrease the energy difference between **[135]** and **[136]** to ΔE = 16.0 kcal mol^{-1} (optimization only). After the likely rate-determining dissociation of NHC the ring expansion of **[136-Me]** to **[137-Me]** proceeds smoothly with a much smaller barrier of $\Delta G^{\neq}$ = 13.5 kcal mol^{-1} for the required migration of one methyl group from the germanium center to the adjacent silicon atom as the rate-determining step. The reassociation of NHC with **[137-Me]** to give **133-Me** is strongly exergonic with ΔG = −37.0 kcal mol^{-1} so that the overall pathway is also decidedly exergonic (ΔG = −22.8 kcal mol^{-1}, Figure 100 in Chapter 7.2.). In order to gauge the influence of the phenyl group in the experimentally employed acetylene derivative, we have also investigated the mechanisms for the formation of **[135-Ph]** and **133-Ph** (R = Me; R' = Ph). Except for the appearance of two new intermediates (for details see: **254-Ph** in Figure 104 and **255-Ph** in Figure 105 in Chapter 7.2.), only minor differences compared to the methyl model were observed in pathways and energetics of the reactions with phenylacetylene (for details see Figure 104, Figure 105 and Figure 106 in Chapter 7.2.).

The formation mechanism of **134** was also investigated with a simplified model system at the B3LYP/6-31G(d,p) level of theory. As discussed previously, regiomer **134** could plausibly formed by [2 + 3] cycloaddition of open-chained **128c** to phenylacetylene. This pathway, however, exhibits very high energy barriers with up to 65.0 kcal mol^{-1} (for details see Figure 102 in Chapter 7.2.) thus confirming the exclusion of this option based on the experiment.

Conversely, the insertion of methylacetylene to Si-Ge single bond of **123c-Me** results in **134-Me** in a straightforward manner and the required energy barrier of $\Delta G^{\neq}$ = 29.7 kcal mol^{-1} is entirely compatible with the reaction conditions of the experimental case, i.e. heating to 70 °C for 48 h (Scheme 73). Overall, the reaction is strongly exergonic by ΔG = −39.1 kcal mol^{-1} (Figure 103).[168]

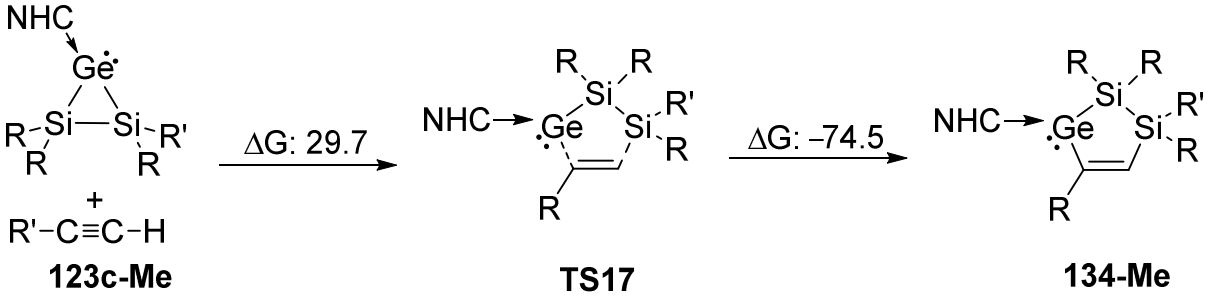

Scheme 73. Mechanistic scenario calculated by DFT calculations for the formation of **134-Me** (R = R' = Me; NHC = 1,3,4,5-tetramethylimidazol-2-ylidene).

3.2.4. Synthesis of Cyclic Germylene 138

In view of the unexpected reactivity of disilenyl germylene **128c** and its cyclic isomer **123c** toward phenylacetylene (see Chapter 3.2.1. and 3.2.2.), we sought to clarify whether the observed regiospecific additions to the C-C triple bond can also be observed in case of isocyanides (Scheme 74).

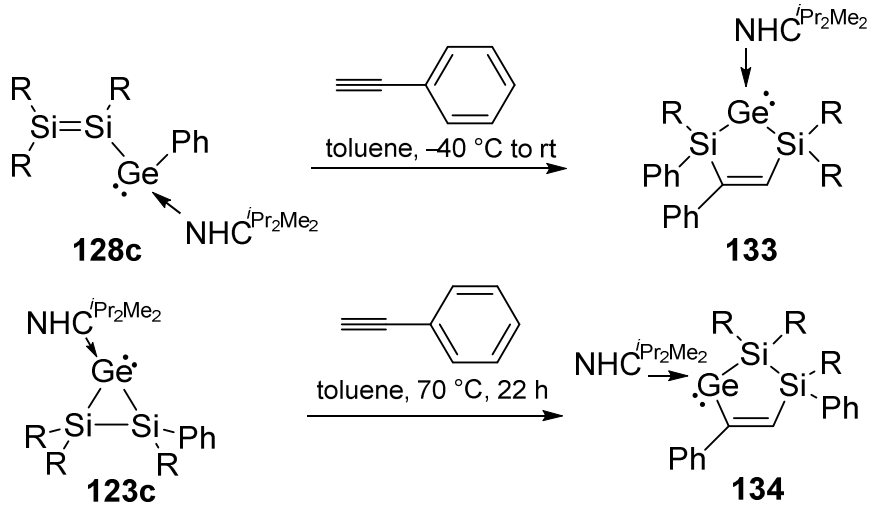

Scheme 74. Reaction of **128c** and **123c** with phenylacetylene resulting in regioisomeric NHC-coordinated heavier cyclopentenylidene derivatives **133** and **134** (R = Tip).

On the one hand isocyanides spontaneously insert into strained heavier Group 14 cycles,[147,175–177] on the other hand they readily react with Si-Si double bonds.[178–180] As in the case of the reactions with phenylacetylene, treatment of **128c** with one equivalent of xylyl isocyanide led to selective conversion to a new product **138** in 2 hours at room temperature (Scheme 75).

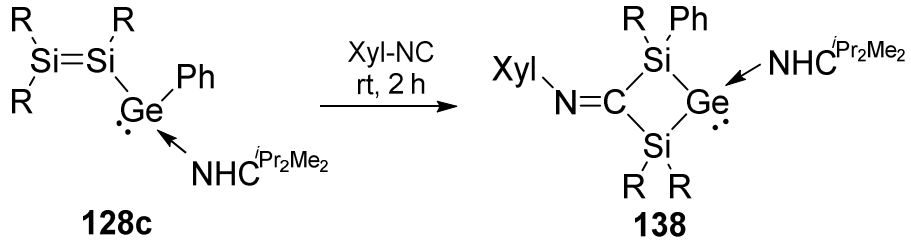

Scheme 75. Reaction of **128c** with xylyl isocyanide resulting in NHC-coordinated heavier cyclic germylene **138** (R = Tip).

Two ^{29}Si NMR signals in the typical region of tetracoordinate silicon atom are observed at δ = −1.74 and −3.92 ppm as well as one ^{13}C NMR resonance at δ = 169.33 ppm confirming the coordination of the NHC to the germanium(II)-center. Single crystals suitable for X-ray diffraction were obtained from a saturated toluene solution at room temperature after 12 hours. The X-ray analysis confirms the four-membered ring connectivity, which exactly reiterates the counter-intuitive regioselectivity observed in the case of the reaction of **128c** with phenylacetylene (Figure 29). The exocyclic imino functionality of **138** is situated between the two silicon atoms. The Ge-C10 bond length is with 2.020(3) Å longer than observed for cyclic germylene **139** (1.986 Å, Scheme 76).

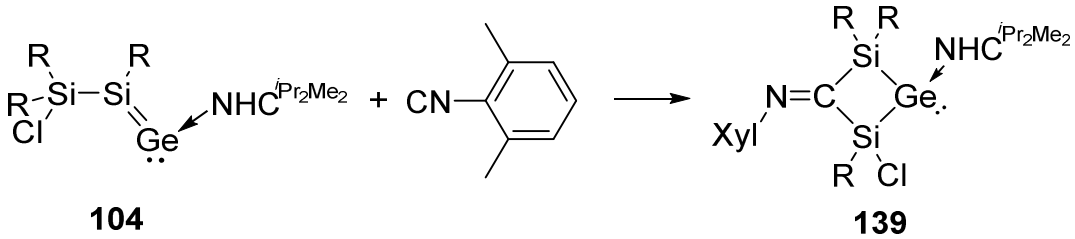

Scheme 76. Reaction of silagermenylidene **104** with xylyl isocyanide resulting in cyclic germylene **139** (R = Tip).

The Si-Ge and Si-C bond lengths of **138** are nearly the same as those in germylene **139**.[147]

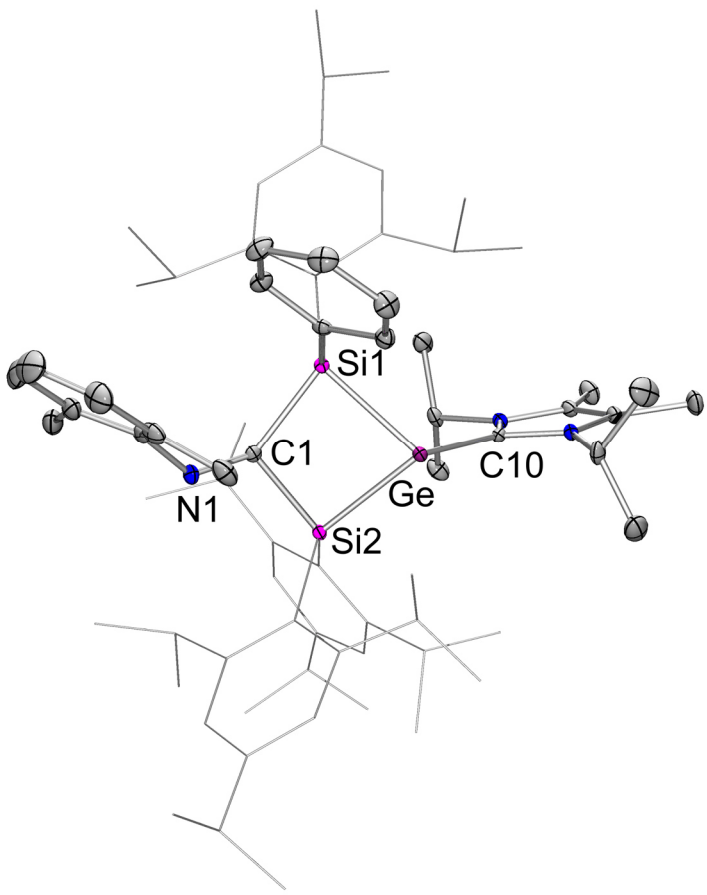

Figure 29. Molecular structure of **138** in the solid state (thermal ellipsoids at 30%, H atoms omitted for clarity). Selected bond lengths in [Å]: Ge-C10 2.020(3), Ge-Si1 2.3862(8), Ge-Si2 2.4018(7), Si1-C1 2.020(3), Si2-C1 1.965(3), C1-N1 1.286(3).

In order to clarify whether similar mechanistic pathways as in the phenylacetylene case are active in the reaction of **128c** with xylyl isocyanide, the formation of **138** was also addressed by DFT computations (Dr. Cem B. Yildiz, Aksaray University). We assumed the intermediacy of the germylene functionalized iminodisilirane **[140-Ph]** and indeed the largest energy barrier to its formation in a formal [1 + 2] cycloaddition is calculated to $\Delta G\neq$ = +6.3 kcal mol^{-1} (Scheme 77). After formation of intermediate **[140-Ph]**, the reaction undergoes a cyclization step to form **138-Ph** in a stepwise fashion including the necessary migration of one methyl group from the germanium to the silicon atom. The overall pathway is found to be strongly exergonic by the ΔG = −44.2 kcal mol^{-1} (for details see Figure 108 in Chapter 7.2.).

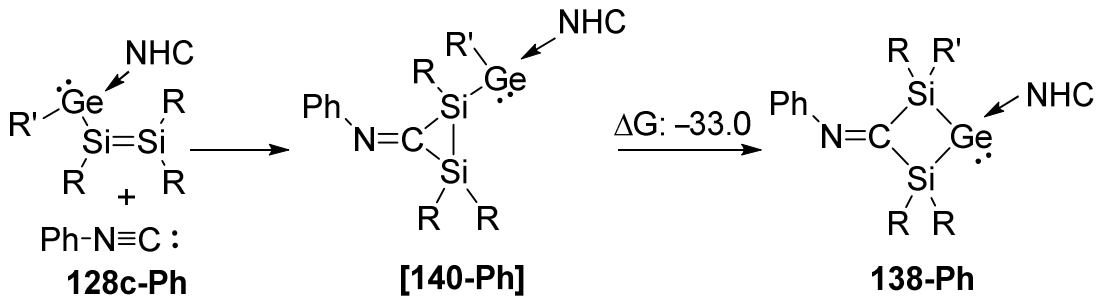

Scheme 77. Calculated mechanism for the reaction of **128c-Ph** to **138-Ph** (R = R' = Me).

Despite its carbene-like character, xylyl isocyanide reiterates the reactivity of the C-C triple bond of phenylacetylene toward **128c** perfectly.

3.2.5. NHC-Abstraction from 138 with BPh_3

In the case of germylene **139**, it was reported that the NHC can be abstracted with BPh_3 as Lewis-Acid to yield digermene **141a** (Scheme 78), which eluded spectroscopic characterization due to its near-insoluble nature.[147]

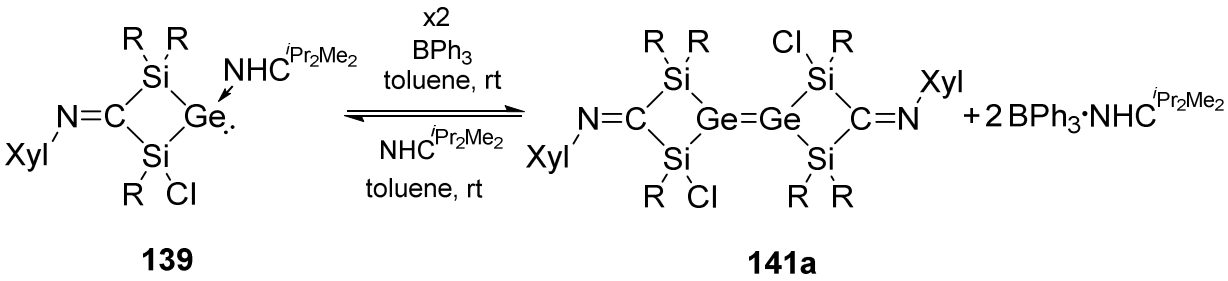

Scheme 78. NHC-abstraction from germylene **139** resulting in digermene **141a** (R = Tip).

The prospect to gain access to a similarly extended system **141b** without chlorine-functionality encouraged us to investigate the behavior of the chlorine-free **138** toward BPh_3. It was anticipated that the absence of a polar Si-Cl bond may result in a more soluble derivative **141b** (Scheme 79).

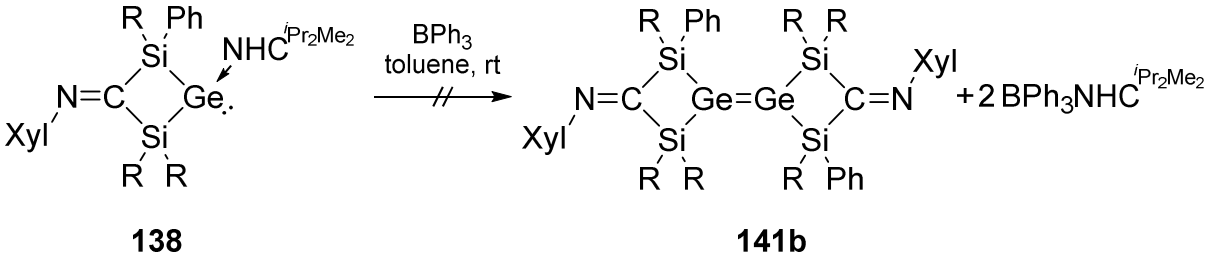

Scheme 79. Proposed synthetic pathway for the NHC-abstraction from germylene **138** leading to digermene **141b** (R = Tip).

Germylene **138** was dissolved in toluene and added to a solution of BPh_3 in toluene and stirred for 2 days at ambient temperature. The ^{29}Si NMR spectrum reveals a downfield shift at δ = 103.12 ppm and a resonance at δ = −4.14 ppm (Figure 30), which indicates the formation of an unsaturated silicon atom, a finding most likely incompatible with the formation of digermene **141b**.

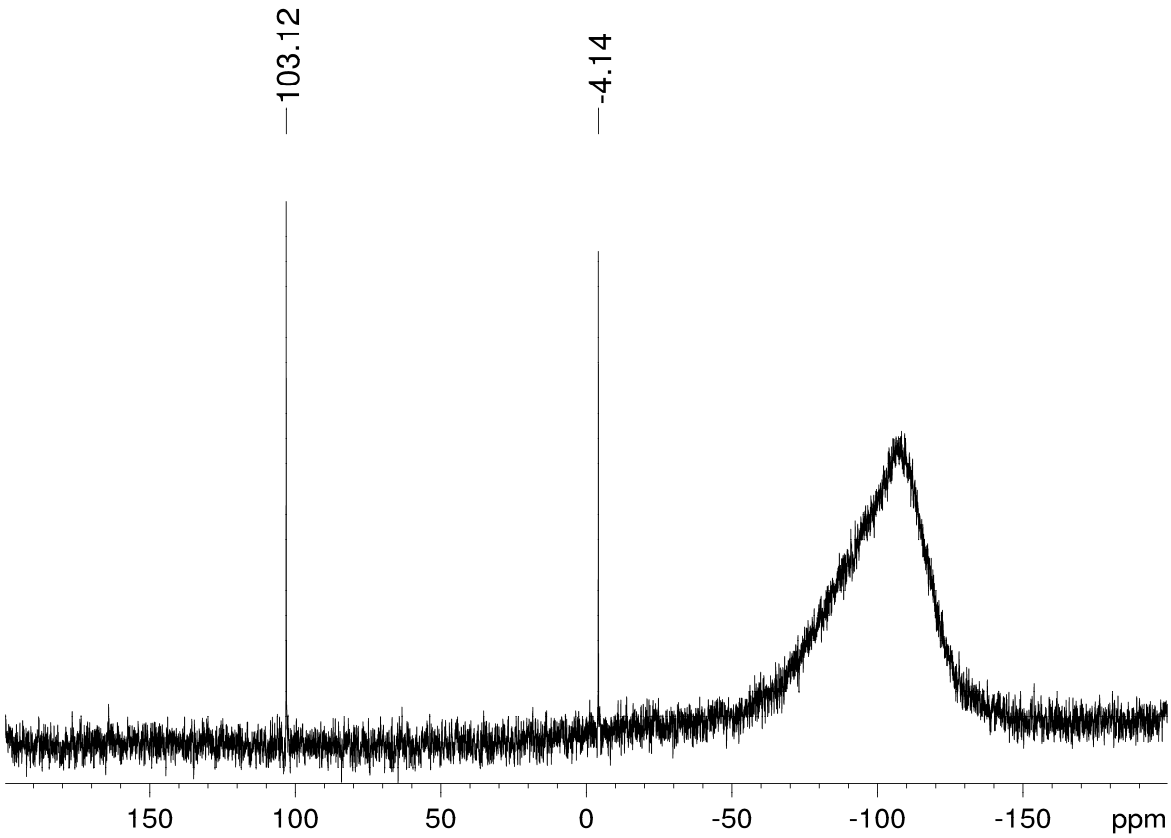

Figure 30. ^{29}Si NMR spectrum of the reaction mixture of the NHC-abstraction from cyclic germylene **138** resulting in heavier cyclobutene analogue **142**.

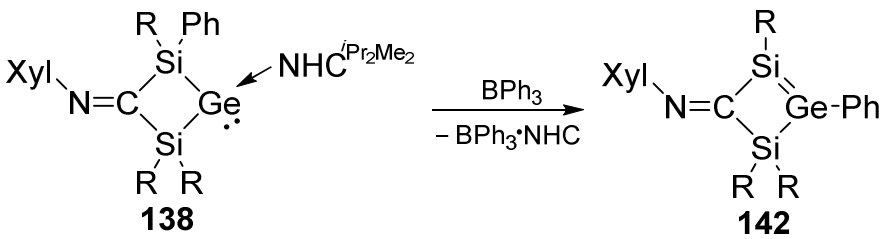

Scheme 80. NHC-abstraction from germylene **138** leading to cyclobutene isomer **142** (R = Tip).

The ^{1}H NMR spectrum shows the formation of $BPh_3{\cdot}NHC^{iPr_2Me_2}$ (for complete NMR spectroscopic data see Chapter 5.7.4., Figure 31). The typical resonance for the carbenic C-atom coordinated to the Ge(II)-center in germylene **138** at δ = 169.33 ppm was not detected anymore in the ^{13}C NMR spectrum of **142**. The ^{13}C NMR downfield shift at δ = 207.62 ppm is attributed to the C-atom of the imino-moiety (Figure 32).

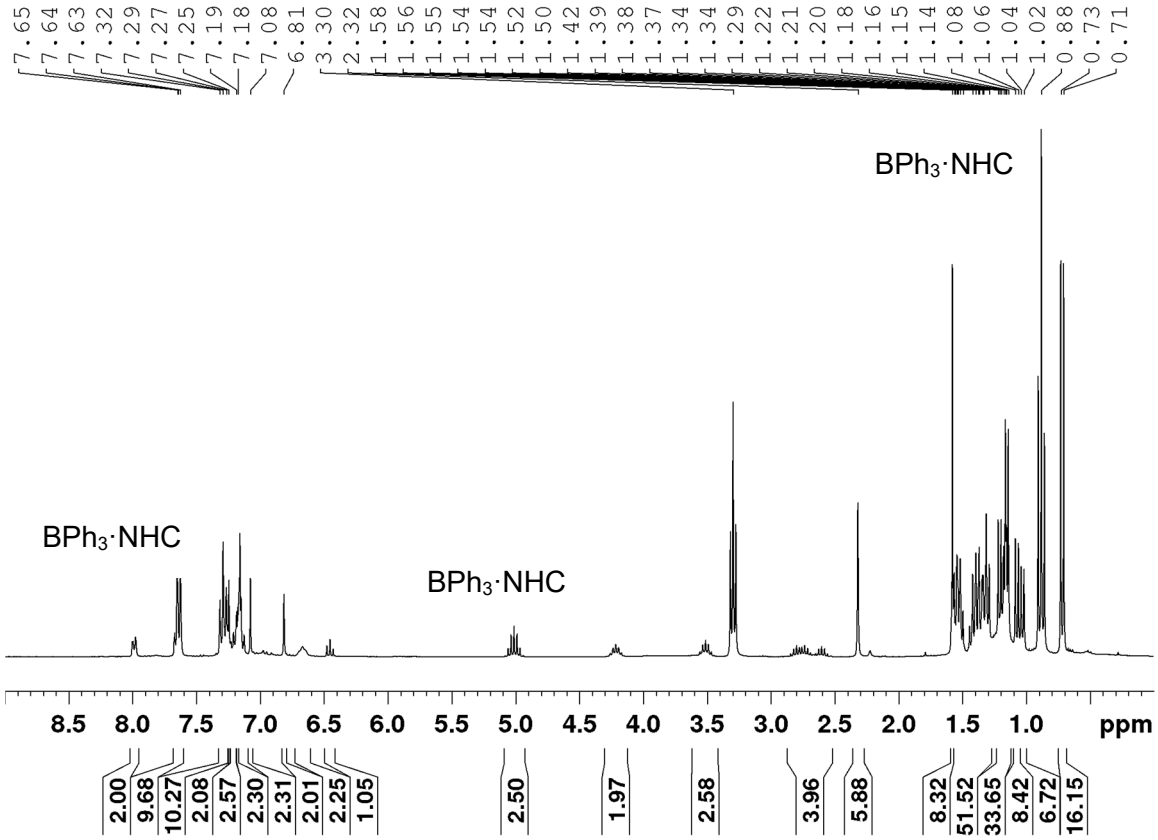

Figure 31. ^{1}H NMR spectrum of the reaction mixture of the NHC-abstraction from cyclic germylene **138** resulting in heavier cyclobutene analogue **142**.

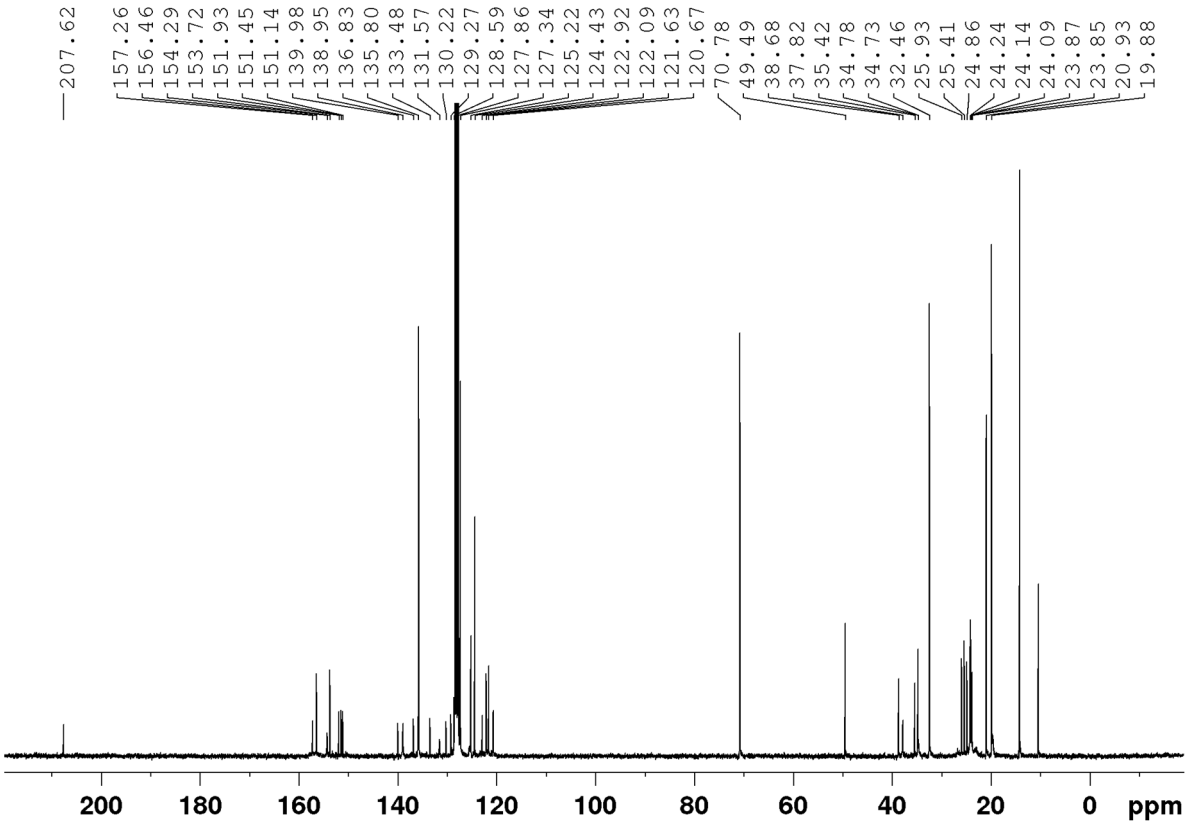

Figure 32. ^{13}C NMR spectrum of the reaction mixture of the NHC-abstraction from cyclic germylene **138** resulting in heavier cyclobutene analogue **142**.

These observations led us to the conclusion that no dimerization process to digermene **141b** displayed in Scheme 79 has taken place. Instead of the formation of the heavier cyclobutene analogue **142** is proposed as reaction product (Scheme 80). The phenyl group has most likely shifted back to the germanium-atom.

The predicted structure could not be confirmed in the solid state because only the byproduct $BPh_3{\cdot}NHC^{iPr2Me2}$ crystallized from the reaction mixture. Cyclobutene analogue **142** is not stable in solution and after 2 days at −26 °C, **142** decomposes to several unidentified products.

3.2.6. Synthesis of Cyclic Germylene 143

To clarify whether the regiospecific reaction observed for heavier cyclopropylidene analogue **123c** and phenylacetylene, can be transferred to the reaction of **123c** and xylyl isocyanide, a 1:1 reaction was carried out at room temperature. Again no reaction was observed for 24 hours at ambient temperature and heating to 75 °C for 6 hours was necessary to complete the reaction to afford cyclic germylene **143** (Scheme 81). Similar to the synthesis of NHC-coordinated cyclopentenylidene analogue **134**, an 1.5-

fold excess of xylyl isocyanide was necessary for full conversion due to the tendency of isocyanides to polymerize at higher temperatures.[181]

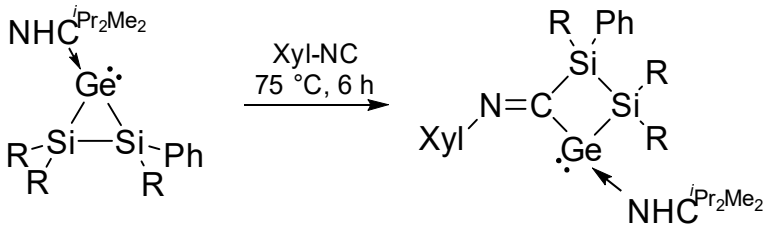

123c **143**

Scheme 81. Reaction of **123c** with xylyl isocyanide resulting in NHC-coordinated heavier cyclic germylene **143** (R = Tip).

Red single crystals of **143** suitable for X-ray diffraction were obtained from a saturated pentane solution at room temperature after 16 hours. Again regioselective formation of a four-membered ring **143** was observed where the exocyclic imino functionality is directly adjacent to the NHC-coordinated Ge(II)-center (Figure 33).

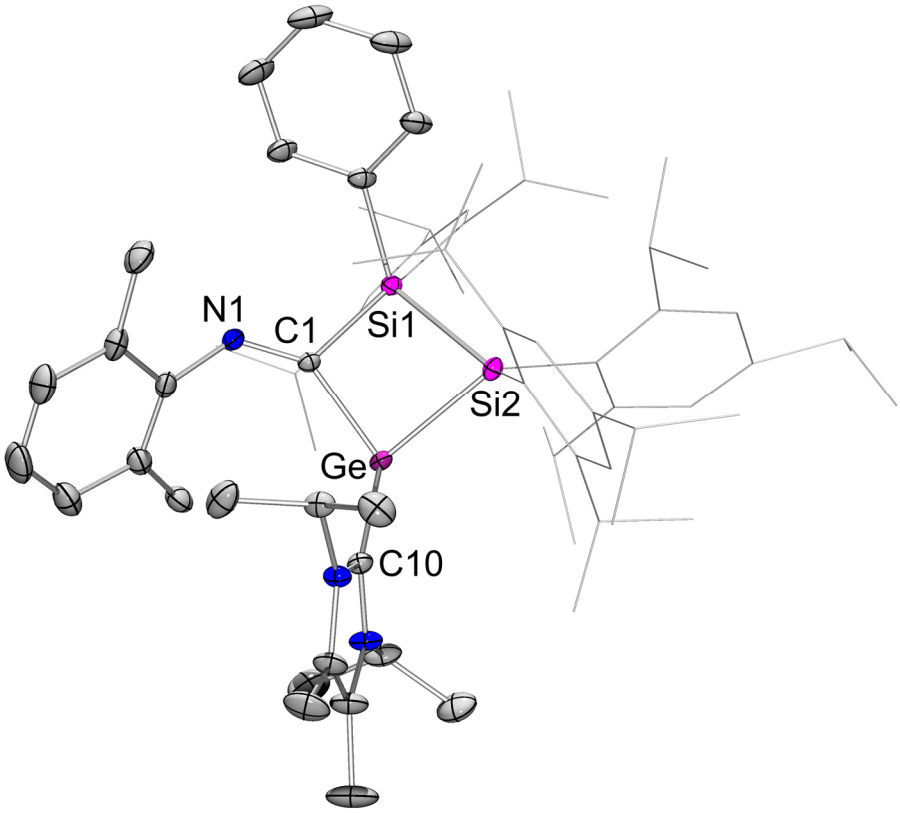

Figure 33. Molecular structure of **143** in the solid state (thermal ellipsoids at 30%, H atoms omitted for clarity). Selected bond lengths in [Å]: Ge-C10 2.0446(19), Ge-C1 2.0019(18), Ge-Si2 2.4350(6), Si1-Si2 2.4089(7), Si1-C1 1.9438(19), C1-N1 1.289(2).

The Ge-C10 bond length is with 2.0446(19) Å longer than observed for cyclic germylene **139** (1.986 Å)[147] and germylene **138** (2.020 Å) obtained in the reaction of disilenyl germylene **128c** and xylyl isocyanide.

In line with more pronounced conjugative effects, the longest wavelength in the UV/vis absorption spectrum of red **143** is bathochromically shifted to λ_{max} = 522 nm (ε = 3200 $Lmol^{-1}cm^{-1}$) in comparison to germylene **138** (λ_{max} = 290-320 nm, broad shoulder). Despite its carbene-like character, xylyl isocyanide reiterates the reactivity of the C-C triple bond of phenylacetylene toward **123c** perfectly and a similar mechanistic scenario is proposed.

In conclusion, the NHC-coordinated disilenyl germylene **128c** and its rearrangement product **123c**, a heavier cyclopropylidene analogue, were isolated and crystallographically analyzed. They show an unexpected regioselectivity in their reactions with either phenylacetylene or xylyl isocyanide. While the open-chained disilenyl germylene **128c** rapidly reacts even below room temperature, the three-membered ring isomer **123c** requires prolonged heating to about 70 °C in order to generate the regiomeric products with near perfect selectivity. The counter-intuitive connectivities of five-membered cyclic germylenes **133** and **134** (phenylacetylene reactions) and four-membered cyclic germylenes **138** and **143** (xylyl isocyanide) are rationalized on the basis of DFT calculations on model species for **133** and **134**. The behavior of **128c** is governed by an initial fast reaction at the Si=Si moiety but subsequently requires dissociation of the NHC as the rate-determining step to form **133**. Conversely, the formation of **134** plausibly proceeds in a concerted manner *via* the insertion of the C−C triple bond of phenylacetylene into the Si−Ge single bond of three-membered ring **123c**.

The selective access to isomeric heterocycles which incorporate germanium(II)-centers with simple unsaturated organic reagents offers significant opportunities for the incorporation of these cycles as building blocks of extended systems. Moreover, in the light of the current interest in main group catalysis, this study adds to the understanding of viable (possibly competing) reaction pathways that may be active in alkyne activation.

3.3. Reactivity of Silagermenylidenes 101 and 104, Disilenyl Germylene 128c and Its Cyclic Isomer 123c toward Bis-Functionalized Organic Substrates

3.3.1. Reactivity of Silagermenylidenes 101 and 104, Disilenyl Germylene 128c and Its Cyclic Isomer 123c toward Bis-Alkynes

3.3.1.1. Reactivity of Silagermenylidene 101 toward Bis-Alkynes

As already reported,[144] silagermenylidene **101** reacts with phenylacetylene to cyclic germylene **102** demonstrating the potential of the Si-Ge double bond of heavier vinylidenes for formal [2 + 2] cycloadditions. The reactivity of acetylenes toward heavier double bonds and carbene analogues is well-known.[182–185] While in organic chemistry thermal [2 + 2] cycloadditions are considered to be symmetry-forbidden (although in a strict sense this is only true for concerted reactions), such reactions are fairly common place in the case of disilenes or digermenes (Scheme 82).[144,172]

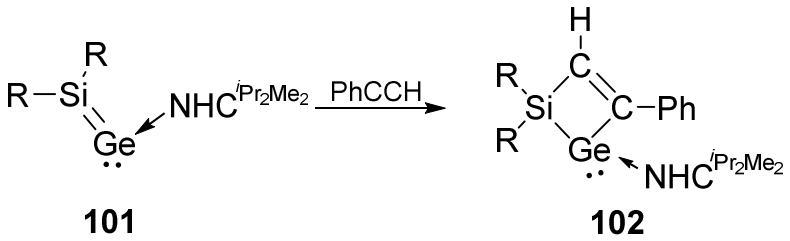

Scheme 82. Reaction of **101** with phenylacetylene leading to cyclic germylene **102** (R = Tip).

Through the use of bridged bis(alkynes) the application of the reaction principle illustrated in Scheme 82 could grant access to bis(germylenes). If the cleavage of the coordinating NHC by an appropriate scavenging reagent could be effectuated such bis(germylenes) would be ideal precursors for (possibly conjugated) materials incorporating unsaturated germanium centers.

In order to test this hypothesis, silagermenylidene **101** was reacted with half an equivalent of 1,4-diethynylbenzene at room temperature (Scheme 83).

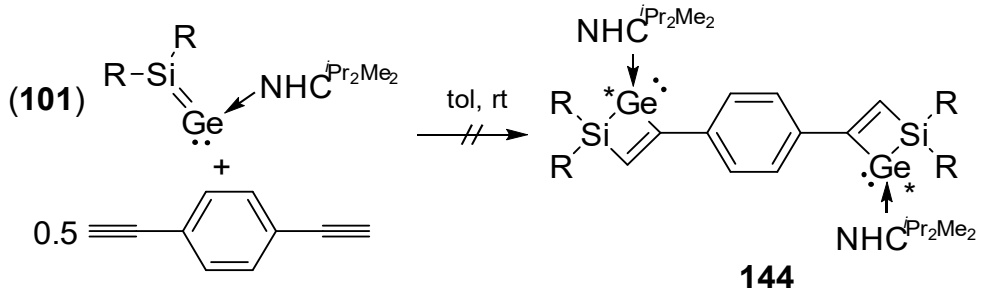

Scheme 83. Reaction of silagermenylidene **33** with 1,4-diethynylbenzene (R = Tip).

The ^{1}H NMR spectrum after 24 hours at room temperature shows several signals in the typical regions of vinylic protons from δ = 8.58 to 8.25 ppm (cyclic germylene **102**: δ = 8.57 ppm) suggesting a mixture of diastereomers (Figure 34).[144] However, in the ^{29}Si NMR spectrum no resonance could be observed.

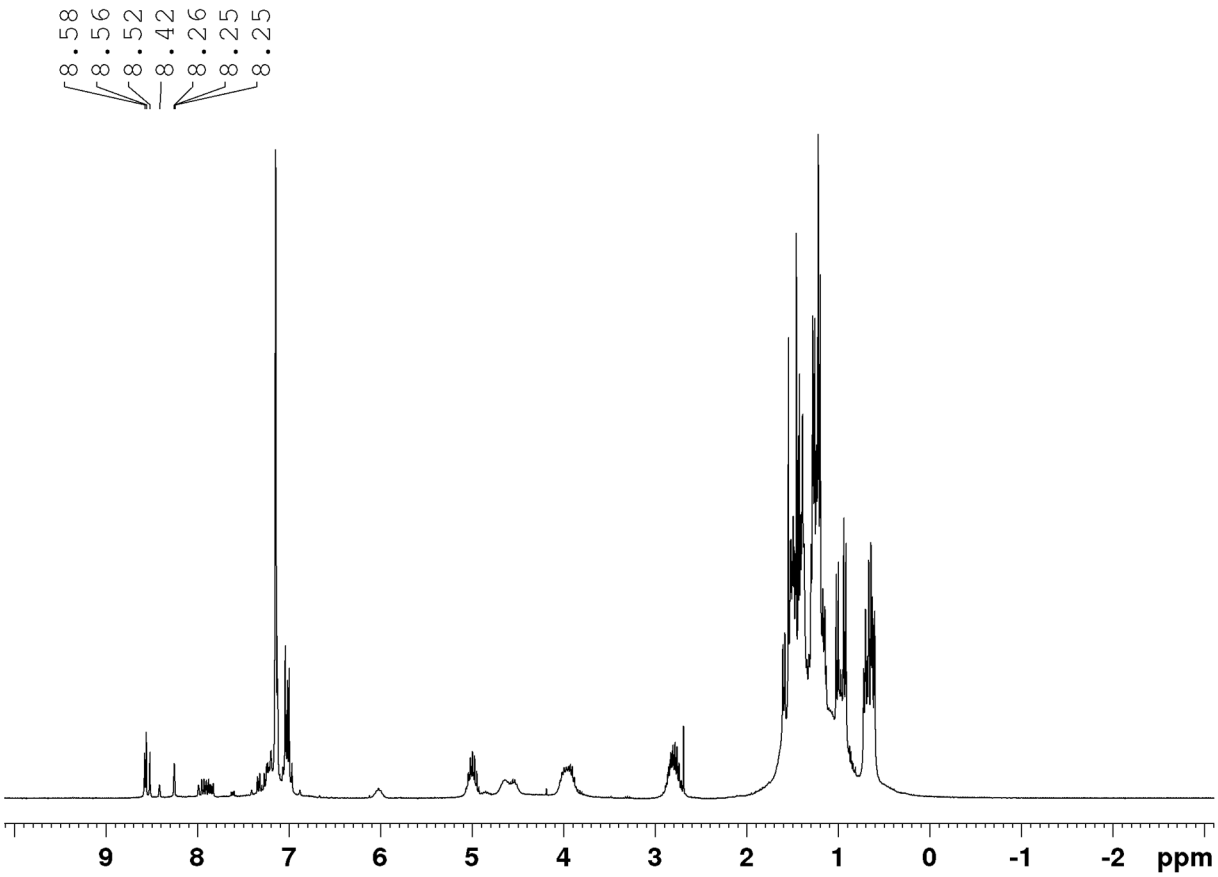

Figure 34. ^{1}H NMR spectrum of the reaction mixture of silagermenylidene **101** with 1,4-diethynylbenzene.

In an attempt to form a *meta*-phenylene-bridged bis-germylene, the heavier vinylidene analogue **33** was reacted with half an equivalent of 1,3-diethynylbenzene at room

temperature in toluene solution (Scheme 84). After 16 hours, the ^{29}Si NMR spectrum shows two resonances at δ = −38.92 (br) and −39.16 ppm (Figure 35), which on grounds of the similarity of chemical shifts suggests the presence of cyclic germylenes akin to **102** (δ = −39.12 ppm).[144]

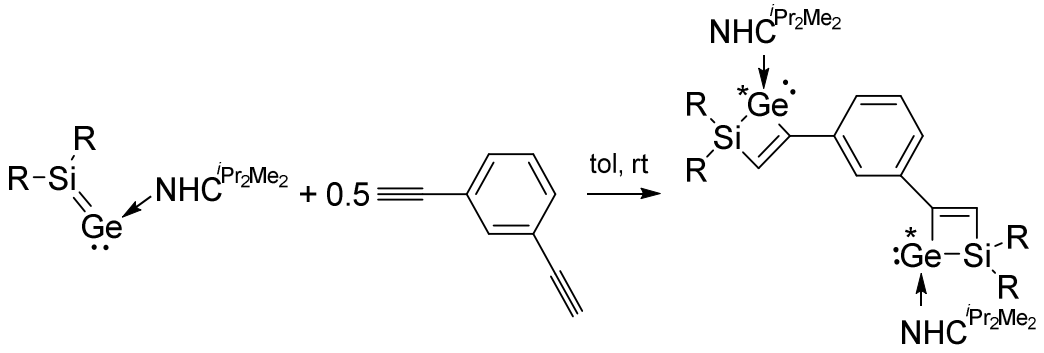

101 **145**

Scheme 84. Reaction of **101** with 1,3-diethynylbenzene (R = Tip).

Again a product mixture of diastereomers of **145** is the likely explanation for the presence of two signals (formation because of two chiral Ge(II)-atoms). The mediocre signal-noise ratio is due to the poor solubility of **145** in C_6D_6.

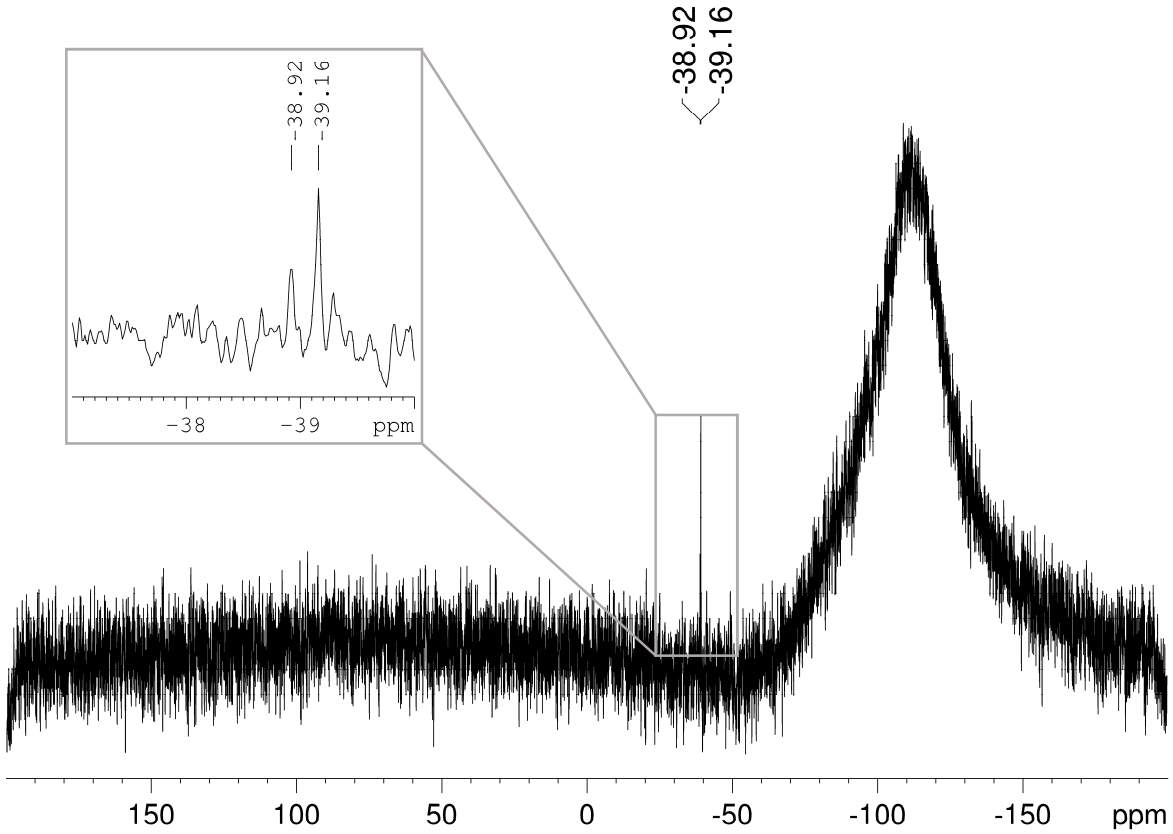

Figure 35. ^{29}Si NMR spectrum of the reaction mixture of silagermenylidene **101** with 1,3-diethynylbenzene. The excerpt shows the region of proposed diastereomers of **145**.

3.3.1.2. Reactivity of Silagermenylidene 104 toward Bis-Alkynes

In order to explore whether the Si=Ge-bond of α-chloro-silyl substituted silagermenylidene **104** shows a similar reaction behavior as observed for silagermenylidene **101**, reactions with bis-acetylenes were studied in view of extended (possibly conjugated) systems (Scheme 85).

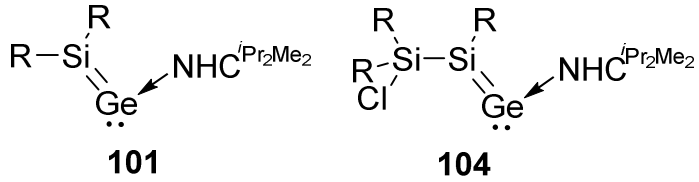

Scheme 85. Silagermenylidene **101** and silyl-functionalized silagermenylidene **104** (R = Tip).

The 1:0.5 reaction of silagermenylidene **104** with 1,4-diethynylbenzene in toluene at 60 °C induced a change in color from red to deep purple (Scheme 86). The ^{1}H NMR spectrum shows complete consumption of the bis-alkyne with ca 50% of starting material **104** remaining after 3 hours, which could be explained by polymerization processes of alkynes at similar temperature.[170]

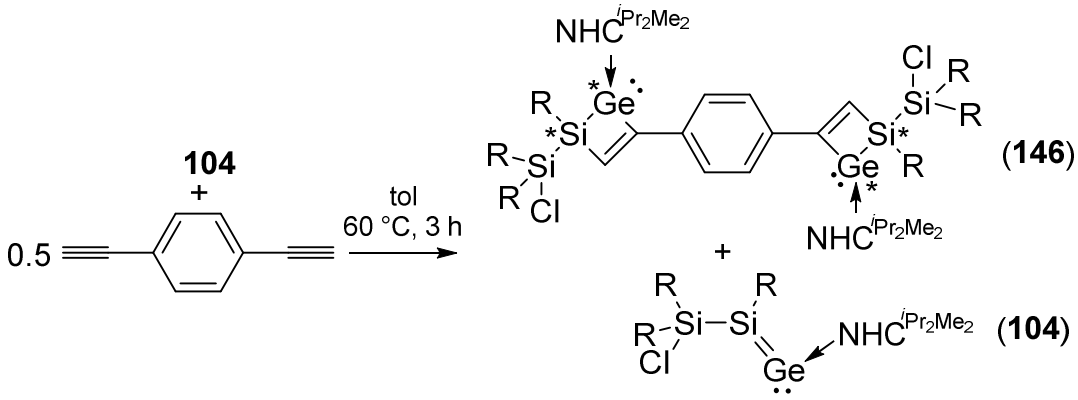

Scheme 86. Reaction of **104** with 1,4-diethynylbenzene resulting in **146** together with starting material **104** (R = Tip).

The ^{29}Si NMR spectrum shows two new resonances at δ = 3.82 and −43.90 ppm together with starting material **104** (δ = 7.34 ppm, downfield shift δ = 162.50 ppm not visible, Figure 36). The ^{29}Si NMR resonance of the highfield shifted silicon atom δ = −43.90 ppm is comparable to the signal of cyclic germylene **102** (δ = −39.12 ppm, page 78, Scheme 82), which led to the suggestion that a similar heavier cyclobutene ring with an extra silyl group had been formed (Scheme 86, compound **146**).

The ^{13}C NMR spectrum displays a resonance for the carbenic C-atom of **104** at δ = 178.37 ppm and an additional signal for the carbenic C-atom of the proposed phenylene-bridged cyclic germylene **146** at δ = 171.54 ppm.[145] In the alkenyl- and alkyne-region, four signals are observed at δ = 129.15, 128.38, 125.51 and 121.93 ppm which are not comparable to those of cyclic germylene **102** (δ = 173.50 (Ph*C*=C) and 154.87 ppm (C=*C*H)). An exact assignment of these signals to the corresponding carbon-atoms was not possible (Figure 37). Unfortunately, it was also not possible to bring the reaction to completeness and to obtain a pure sample of **146**, which could be, as described above, due to polymerization processes of alkynes under similar conditions (excess of bis-alkyne leads to decomposition of **104** at 60 °C).[170]

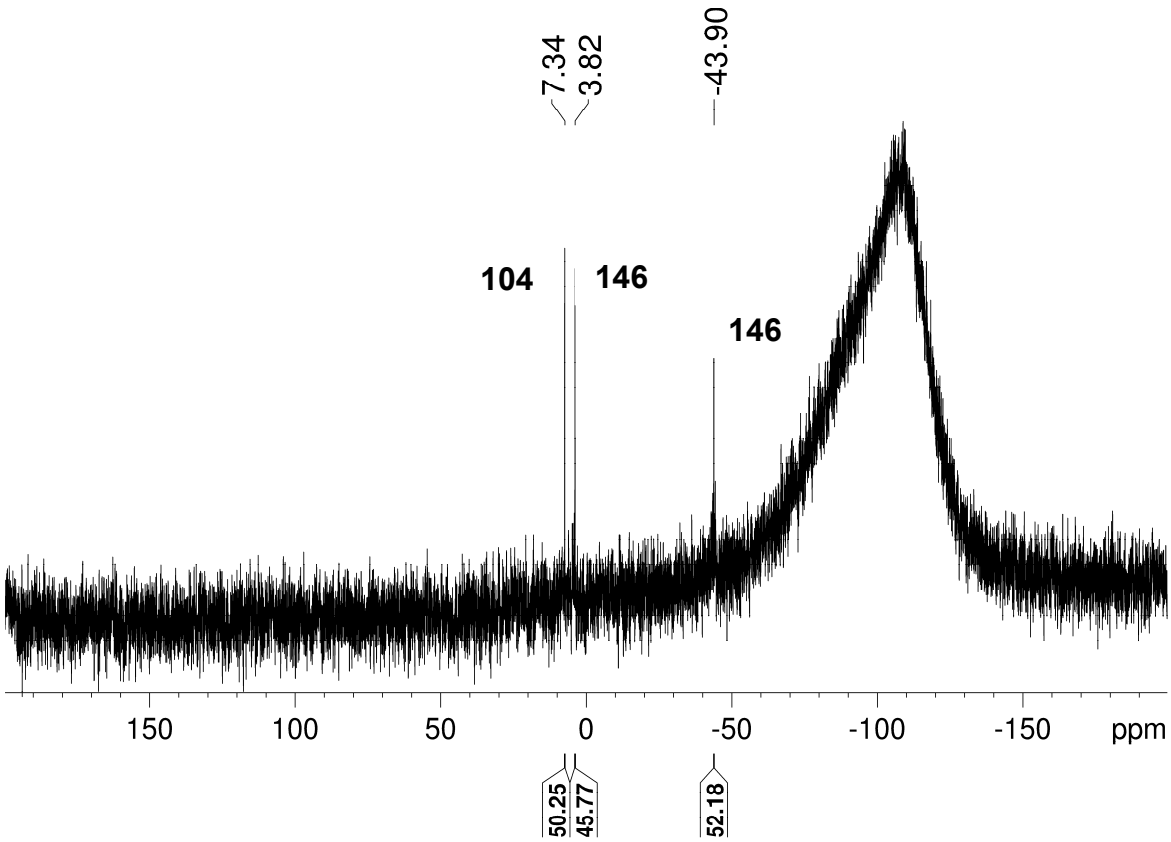

Figure 36. ^{29}Si NMR spectrum of the reaction mixture of silagermenylidene **104** and bis-alkyne.

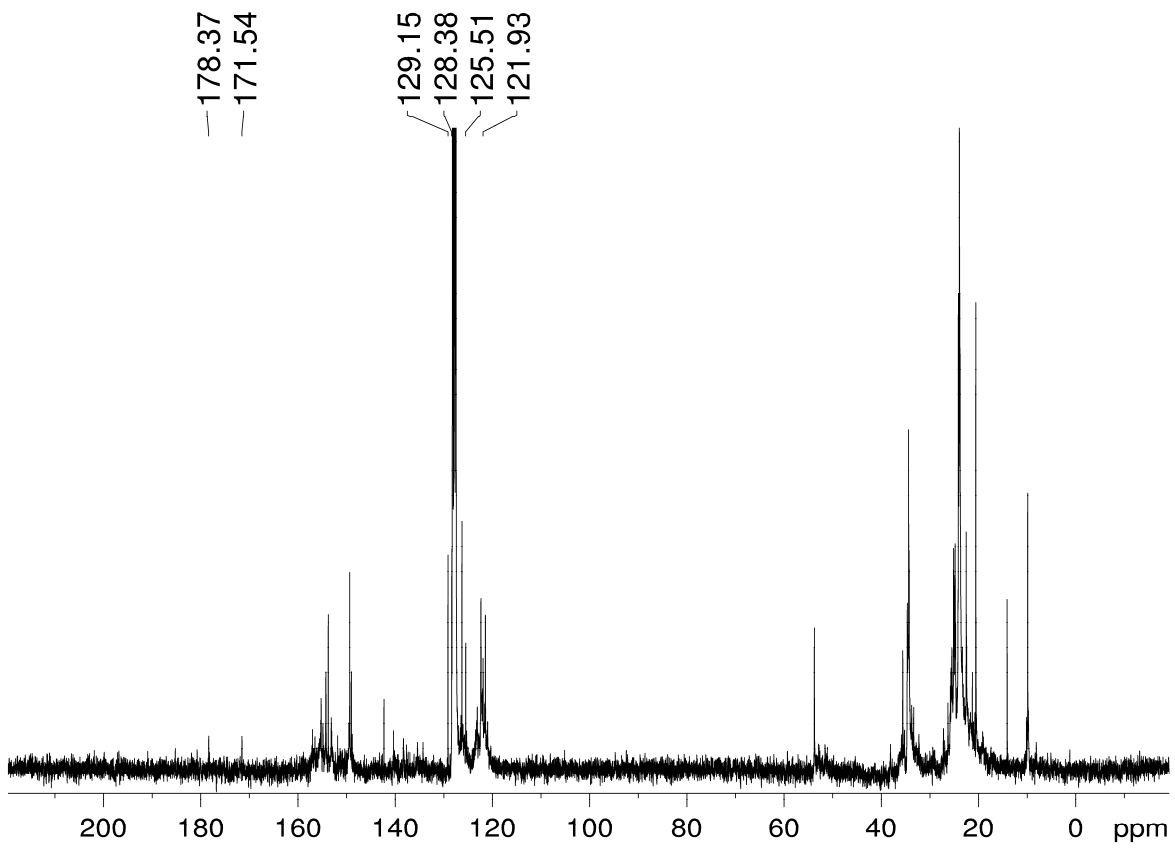

Figure 37. ^{13}C NMR spectrum of the reaction mixture of silagermenylidene **104** and bis-alkyne.

In another experiment the reaction was stopped after 50% (determined by ^{1}H NMR spectroscopy) of **104** had been consumed in the reaction with 1,4-diethynylbenzene. The solvent was evaporated and the reaction mixture filtered from pentane. A concentrated solution was stored at room temperature, which afforded small purple crystals suitable for X-ray diffraction of **146** (Figure 38) together with a precipitate of the heavier vinylidene analogue **104**.

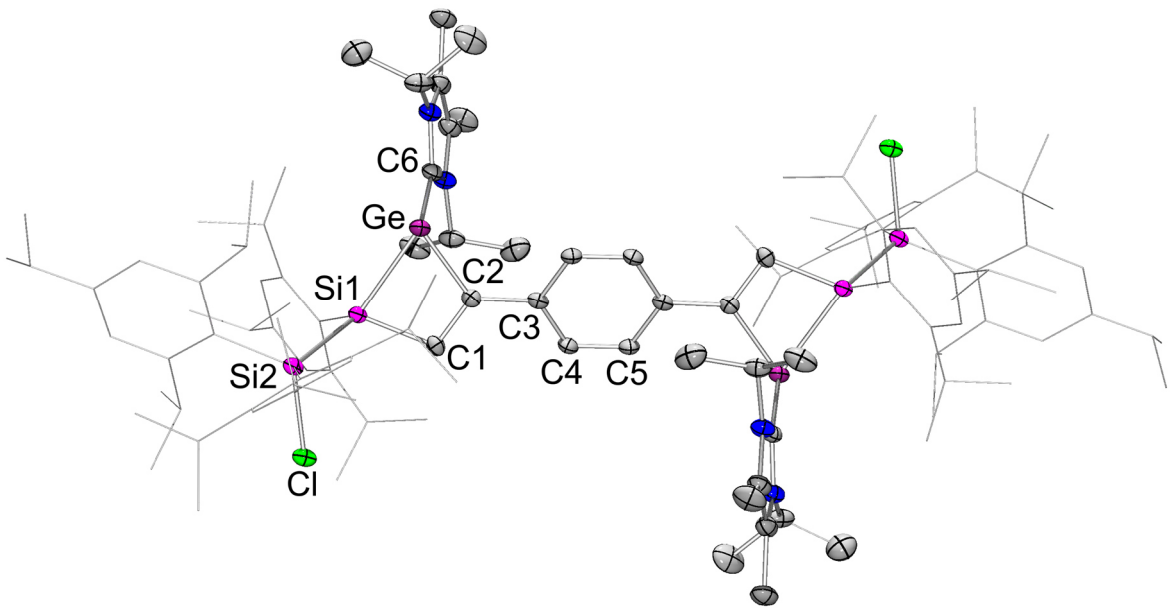

Figure 38. Molecular structure of racemic mixture of **146** in the solid state (thermal ellipsoids at 30%, H atoms and co-crystallized pentane omitted for clarity). Selected bond lengths [Å]: Ge-C6 2.078(8), Ge-Si1 2.4959(19), Si1-Si2 2.403(3), Si2-Cl 2.124 (2), C1-C2 1.351(9).

The molecular structure of **146** revealed the proposed structure of two cyclic germylenes with an exocyclic chloro silyl-group linked by a phenyl group. Bis-germylene **146** crystallizes as the *meso* form exclusively, which is most likely due to steric reasons (relative configuration 1*S**, 2*R**). The two chloro silyl-groups attached to each of the Si_2GeC_2-units are pointing in opposite directions as well as the NHCs at the Ge(II)-center and thus minimize the steric interactions. The germanium-carbon bond length involving the NHC is 2.078(8) Å and thus in the typical range of an NHC coordinated to a Ge(II)-center (2.061 to 2.106 Å).[61,145]

3.3.1.3. Reaction of Disilenyl Germylene 128c and Its Cyclic Isomer 123c with 1,3-Diethynylbenzene and 1,4-Diethynylbenzene

Disilenyl germylene **128c** was also reacted with 1,3-diethynylbenzene and 1,4-diethynylbenzene with the aim of generating extended conjugated systems with either ferro- or antiferromagnetic linking unit. The reactions of **128c** at room temperature in benzene solution or at low temperature in toluene (−78 °C to rt) resulted in the formation of a complex mixture (multiple ^{29}Si NMR resonances, Scheme 87).

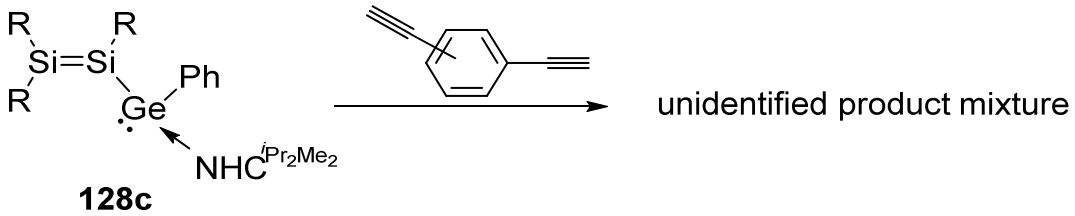

Scheme 87. Reaction of **128c** with 1,3-diethynylbenzene and 1,4-diethynylbenzene (R = Tip).

Furthermore, the heavier cyclopropylidene analogue **123c** showed no discernable reaction with 1,3-diethynylbenzene and 1,4-diethynylbenzene in benzene solution, even after heating for 8 hours to 70 °C (Scheme 88), which led to a slow decomposition of **123c**. The bis-alkynes again (see Chapter 3.3.1.2.) disappeared suggesting a polymerization reaction under these reaction conditions.[170]

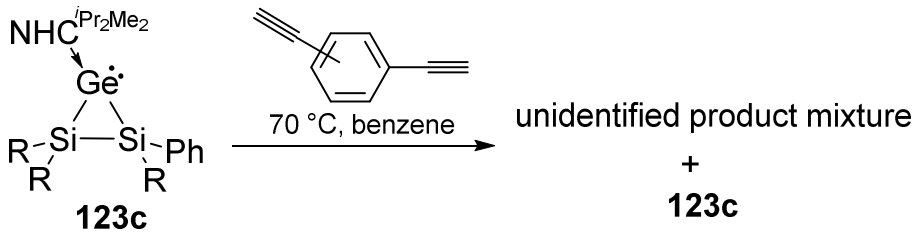

Scheme 88. Reaction of **123c** with 1,3-diethynylbenzene and 1,4-diethynylbenzene (R = Tip).

3.3.2. Reactivity of Silagermenylidene 104, Disilenyl Germylene 128c and Its Heavier Cyclopropylidene Analogue 123c toward Bis-Isocyanides 147-149

3.3.2.1. Reactivity of Silagermenylidene 104 toward Durylene Bis-Isocyanide 147

Recently, our group reported the generation of germylene **139** under mild conditions.[147]

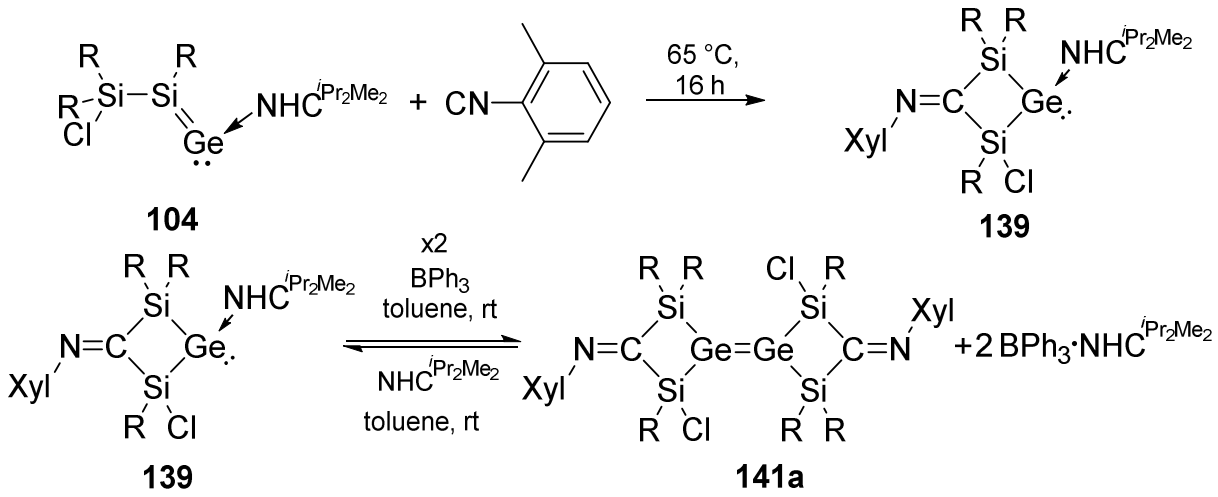

Scheme 89. Reaction of silagermenylidene **104** with xylyl isocyanide leading to germylene **139** and abstraction of NHC with BPh_3 resulting in digermene **141a** (R = Tip).

As the abstraction of the coordinating NHC from germylene **139** by BPh_3 led to the extensively conjugated dimerization product **141a** with a Ge-Ge-double bond (Scheme 89),[147] an investigation of the behavior of **104** toward bis(isocyanides) was prompted. In order to obtain extended (possibly conjugated) systems **150-152**, silagermenylidene **104** was treated with the bis-isocyanides of the conjugated linking unit **147-149** (Scheme 90).

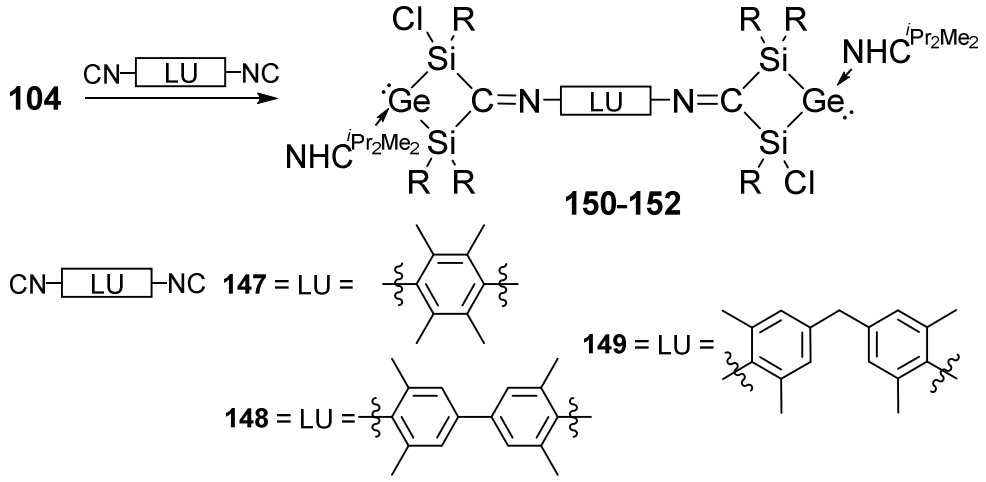

Scheme 90. Proposed reaction pathway for the formation of bis-germylenes **150-152** formed in the reaction of **104** with bis-isocyanides of **147-149** (R = Tip).

Therefore, the 1:0.5 reaction of heavier vinylidene analogue **104** with durylene bis-isocyanide **147** was investigated because of its close structural similarity to xylyl isocyanide (Scheme 91).

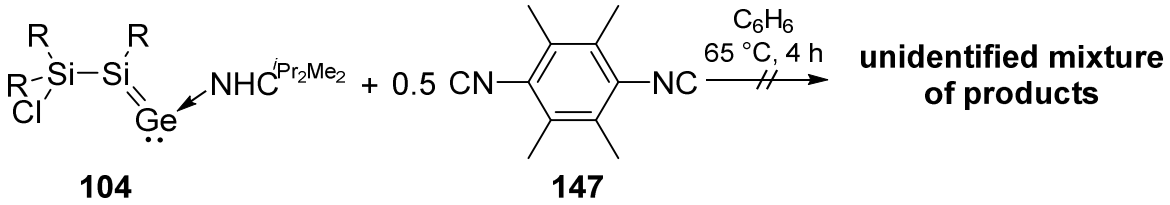

Scheme 91. Reaction of **104** with durylene bis-isocyanide leading to an unidentified mixture of products (R = Tip).

At room temperature no reaction was observed after 24 hours in benzene solution and the reaction mixture needs to be heated to 65 °C for 4 hours. The ^{29}Si NMR spectrum of the reaction mixture shows four resonances at δ = 119.91, 80.82, 37.38 and −6.56 ppm (Figure 39), which are significantly differing from the ^{29}Si NMR resonances of germylene **139** (δ = 5.6 and −13.5 ppm).[147] This observation led to the conclusion that the steric demand in the sphere of the durylene-substituent is probably too high preventing the formation of the targeted bis-germylene **150**. The ^{13}C NMR spectrum reveals many unidentified resonances, while no signal for a carbenic carbon-atom was observed (Figure 40).

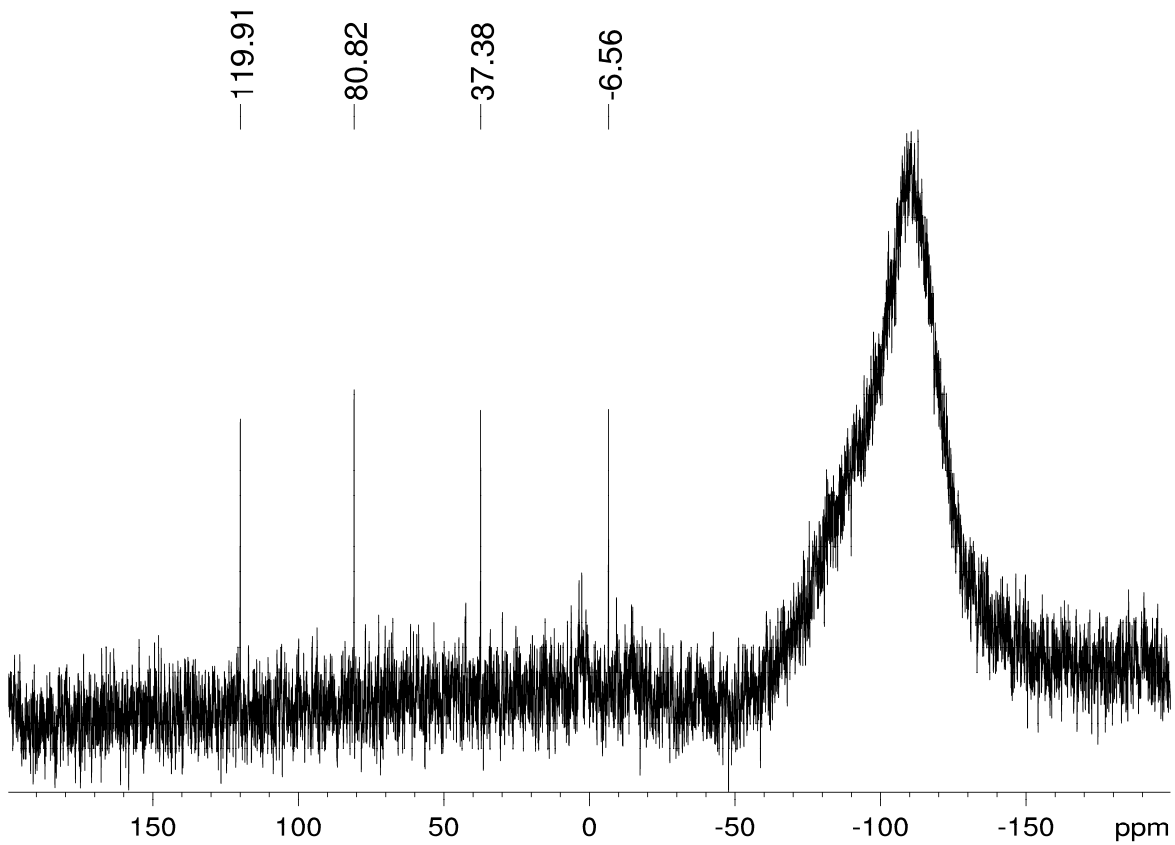

Figure 39. ^{29}Si NMR spectrum of the reaction mixture of **104** with durylene bis-isocyanide **147**.

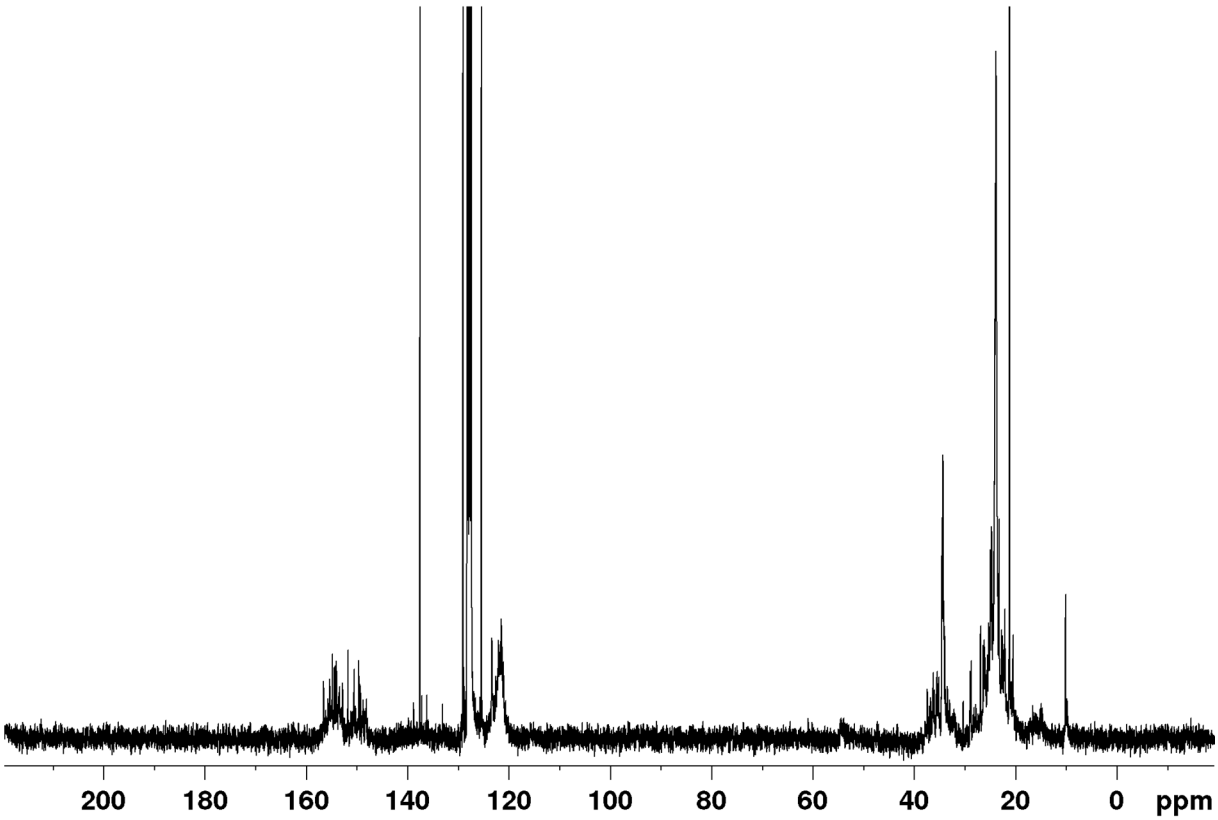

Figure 40. ^{13}C NMR spectrum of the reaction mixture of **104** with durylene bis-isocyanide **147**.

3.3.2.2. Reactivity of Silagermenylidene 104 toward 4,4'-Diisocyano-3,3',5,5'-tetramethyl-1,1'-biphenyl 148

In order investigate if an additional phenylene-group in the linking unit would lead to a sufficient decrease in steric strain in order to allow for the formation of a biphenylene-bridged bis-germylene **151**, silagermenylidene **104** was reacted with 0.5 eq of the bis-isocyanide **148** in benzene solution (Scheme 92).

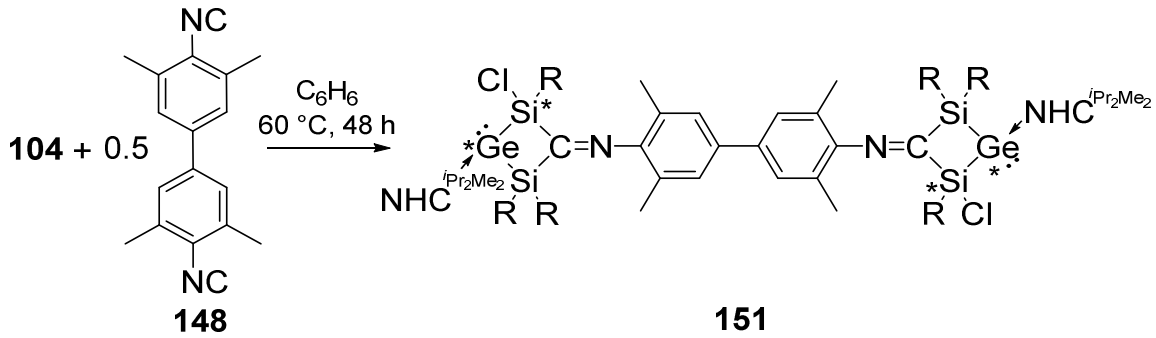

Scheme 92. Reaction of **104** with biphenyl-bis-isocyanide **148** (R = Tip).

As in the previous cases, the reaction needed prolonged heating to 60 °C for two days to reach full conversion to a new product. The color changed from red to deep purple, which was taken as a first indication for the presence of a conjugated system. The ^{29}Si NMR spectrum shows broadened resonances (probably more than one set of signals due to the general possibility of the formation of diastereomers of **151** or polymerization/oligomerization processes of the proposed product **151** with itself) at δ = 3.74 and −14.96 ppm (Figure 41) which are coincide with the ^{29}Si NMR signals of cyclic germylene **139** (δ = 5.6 and −13.5 ppm).

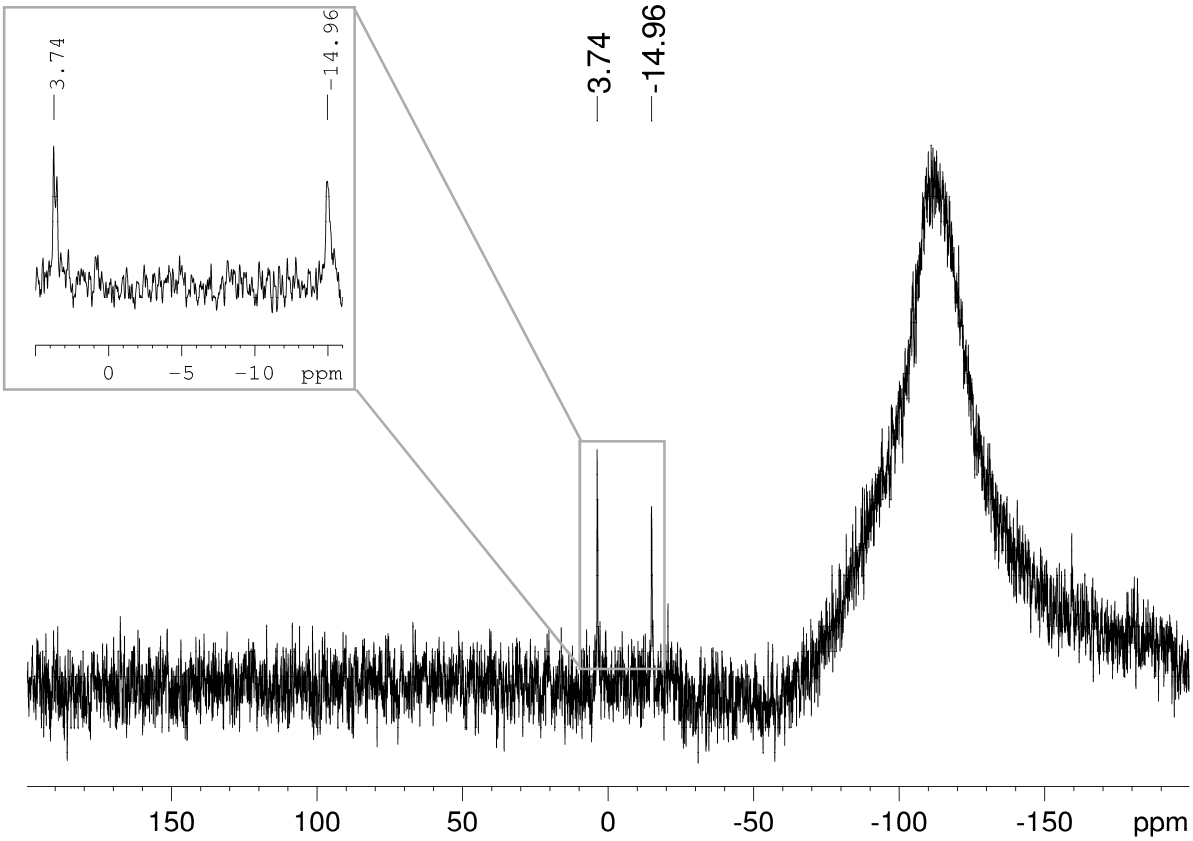

Figure 41. ^{29}Si NMR spectrum of the reaction mixture of **104** with biphenyl bis-isocyanide **148**. The excerpt shows the enlarged area for the resonances of the proposed product **151**.

Furthermore, by simple comparison of the ^{1}H NMR spectra of the crude reaction mixture of silagermenylidene **104** and biphenyl bis-isocyanide **148** with a pure sample of cyclic germylene **139** allowed us to disclose certain similarities in the ^{1}H NMR spectra (Figure 42). The methine protons of the NHC are in the same range for both products (between δ = 5.3 and 6 ppm) as well as the CH_3-groups at the phenyl group (**139**: δ = 2.6 ppm, **151**: δ = 2.7 ppm). The signals in the ^{1}H NMR spectrum of proposed bis-germylene **151** (Figure 42a) are somewhat broadened possibly due to the overlap of several diastereomers in the proposed NHC-coordinated bis-germylene **151**. A further explanation could be the formation of a polymeric or oligomeric system due to the higher temperature for a longer period of time (60 °C for 2 days).

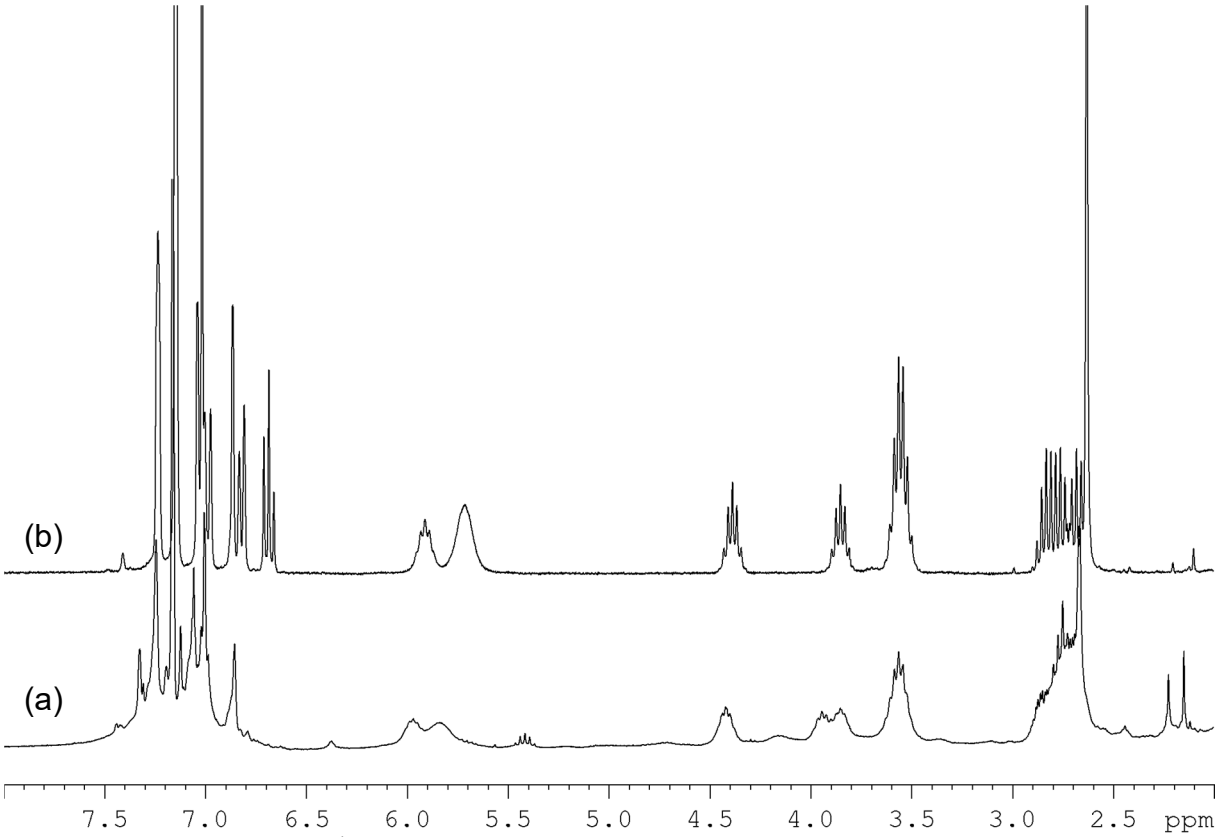

Figure 42. Excerpts of ^{1}H NMR spectra: (a) reaction mixture of **104** with biphenyl bis-isocyanide **148**, (b) pure sample of cyclic germylene **139**.

Due to the general broadening of the ^{13}C signals of the carbenic C-atoms coordinated to the Ge(II)-center it is not surprising that these signals were not detected in the ^{13}C NMR spectrum (typical region from δ = 165 to 175 ppm, Figure 43).[63,144,147]

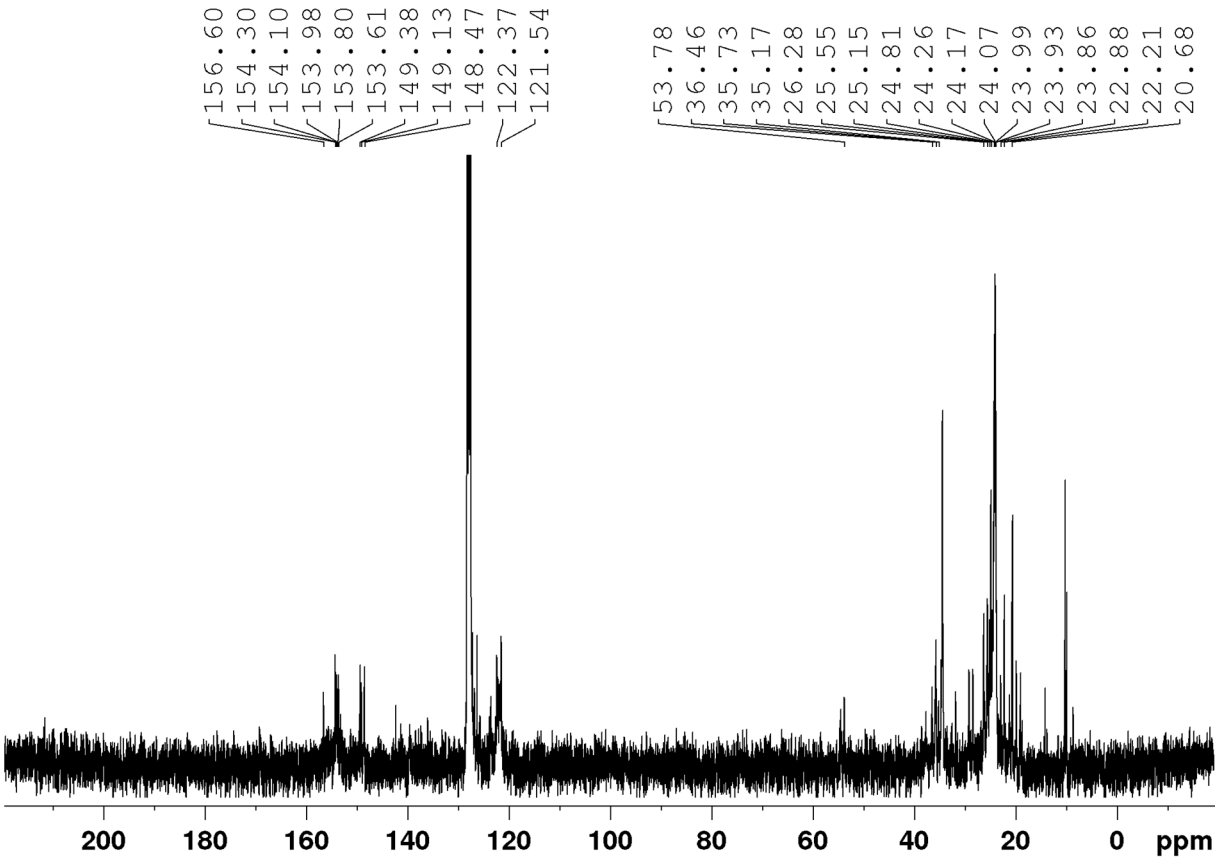

Figure 43. ^{13}C NMR spectrum of the reaction mixture of **104** with biphenyl bis-isocyanide **148**.

A further problem is the formation of the imidazolium chloride salt **153** (proven by ^{1}H NMR spectroscopy and X-ray diffraction, Scheme 93), which is produced immediately after workup and thus attempts to isolate a product out of the reaction mixture failed (workup at −20 °C).

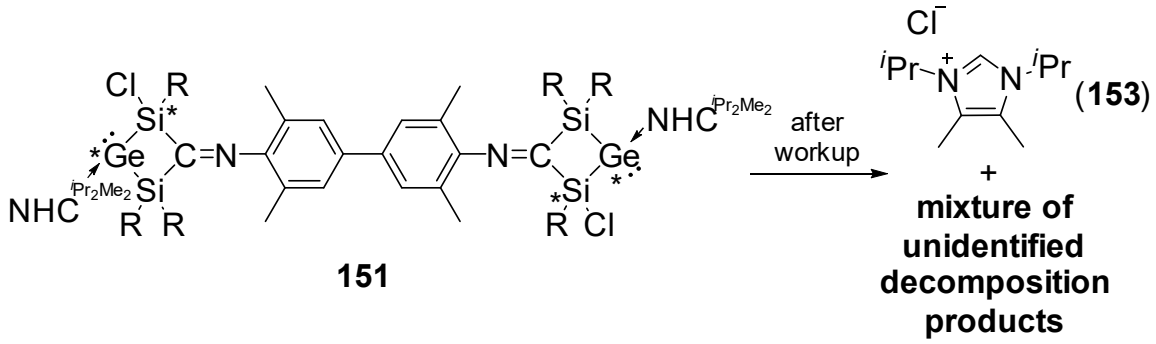

Scheme 93. Formation of imidazolium chloride **153** from the mixture of diastereomers of **151** (R = Tip).

3.3.2.3. Reactivity of Silagermenylidene 104 toward Bis-(4-Isocyano-3,5-dimethylphenyl)methane 149

The conjugation between the two initially formed germylene-fragments in the reaction of biphenyl bis-isocyanide **148** with silagermenylidene **104** might be the reason for the instability of the diastereomers of **151**. The conjugation of the cyclic germylene-fragments was deliberately interrupted by the introduction of a methylene-group between the two bridging phenylene-groups of bis-isocyanide **148** (Scheme 94).

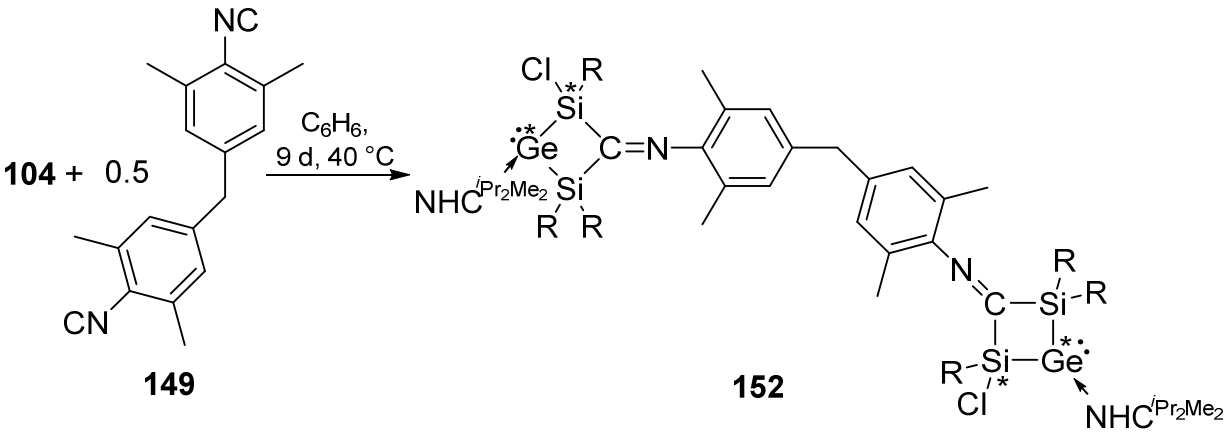

Scheme 94. Reaction of **104** with methylene bridged bis-isocyanide **149** (R = Tip).

Heating the heavier vinylidene analogue **104** and bis-isocyanide **149** to 60 °C in benzene solution yielded an unidentified mixture of products. However, cautious heating to 40 °C for 9 days resulted in the formation of a single product.

The ^{29}Si NMR spectrum reveals two broadened resonances (possibly more than one set of signals due to diastereomer formation of **152**) at δ = 4.05 and −14.53 ppm (Figure 44) well in line with the resonances of germylene **139** and bis-germylene **151** (**151**: δ = 3.74 and −14.96 ppm, **139**: δ = 5.6 and −13.5 ppm).

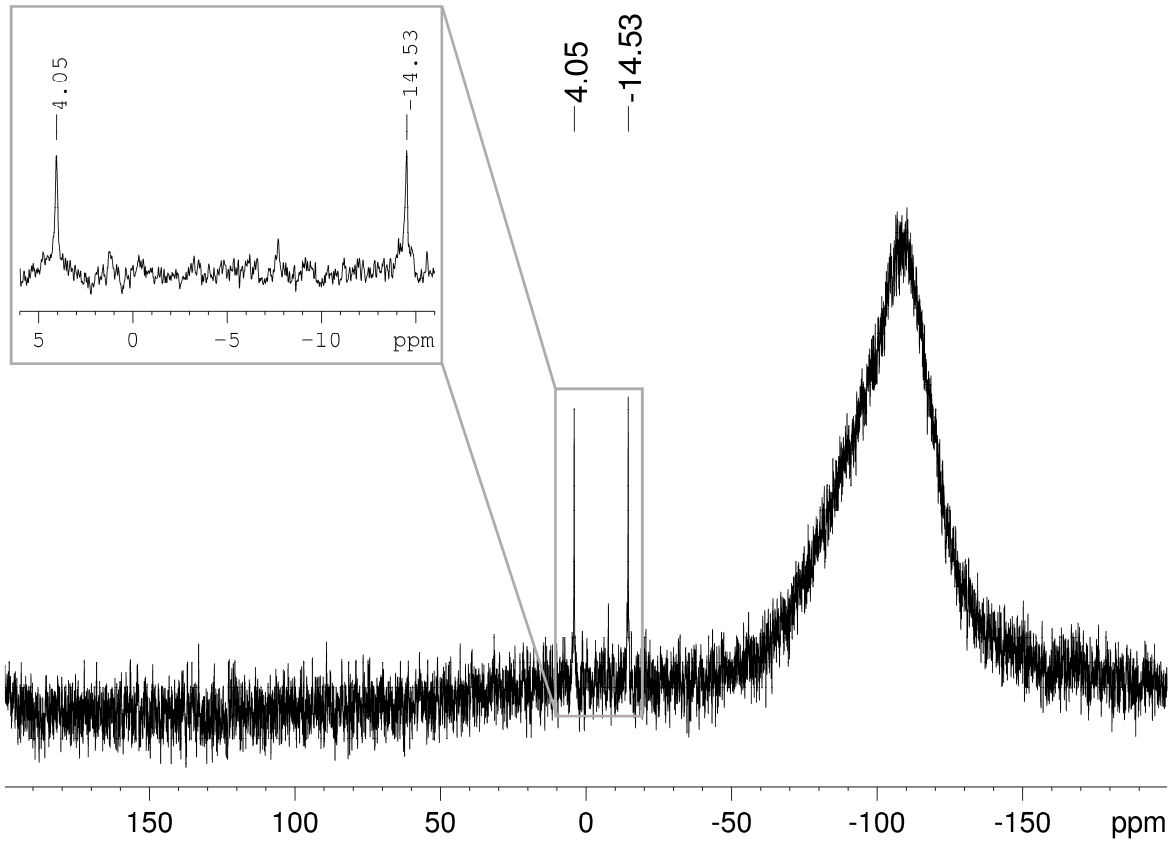

Figure 44. ^{29}Si NMR spectrum of the reaction mixture of **104** with methylene-bridged bis-isocyanide **149**. The excerpt shows the enlarged are for the resonances of the proposed product **152**.

Once more, the ^{1}H NMR spectrum shows similarities to the cyclic germylene **139** (Figure 45). The general broadening of the ^{1}H NMR spectrum can be attributed to the formation of a mixture of diastereomers of **152**. It is speculated (see the reaction of **104** with bis-isocyanide **148**, page 89, Scheme 92) that a mixture of diastereomers of methylene-bridged cyclic bis-germylene **152** was obtained. Another possibility could be the formation of isocyanide-based polymers, because of the general tendency of such bigger aggregates to oligomerize/polymerize under similar conditions (prolonged heating for 9 days).[181]

It was not possible to isolate a product from the reaction mixture. The imidazolium chloride **153** was again formed after 2 days at −26 °C together with a mixture of unidentified decomposition products. The chlorine-atom at the silicon-atom is most likely the reason for the instability of the phenylene-bridged systems **151** and **152**.

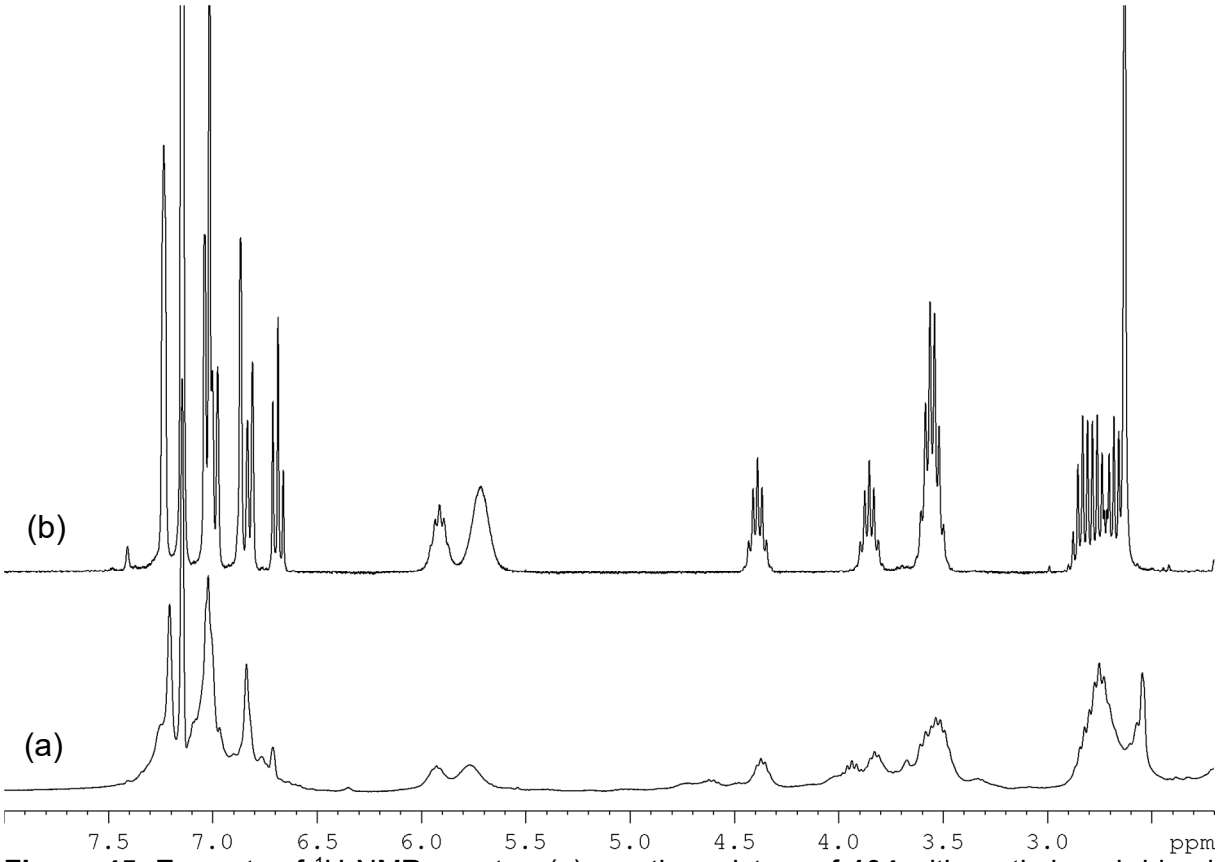

Figure 45. Excerpts of ^{1}H NMR spectra: (a) reaction mixture of **104** with methylene-bridged bis-isocyanide **149**, (b) pure sample of cyclic germylene **139**.

3.3.2.4. Reaction of Disilenyl Germylene 128c with Bis-(4-Isocyano-3,5-dimethylphenyl)methane 149

In Chapter 3.3.2.2. and 3.3.2.3., it was proposed that the chlorine functionality as well as high reaction temperatures might be the key to the instability of the mixture of diastereomers of phenylene-bridged bis-germylenes **151** and **152**. The NHC-stabilized disilenyl germylene **128c** was shown to react with xylyl isocyanide to give cyclic germylene **138** under much milder conditions than both the silagermenylidene **104** and the cyclic isomer **123c**. The assumption seemed justified that the milder reaction conditions thus possible might prevent side reactions such as polymerization.

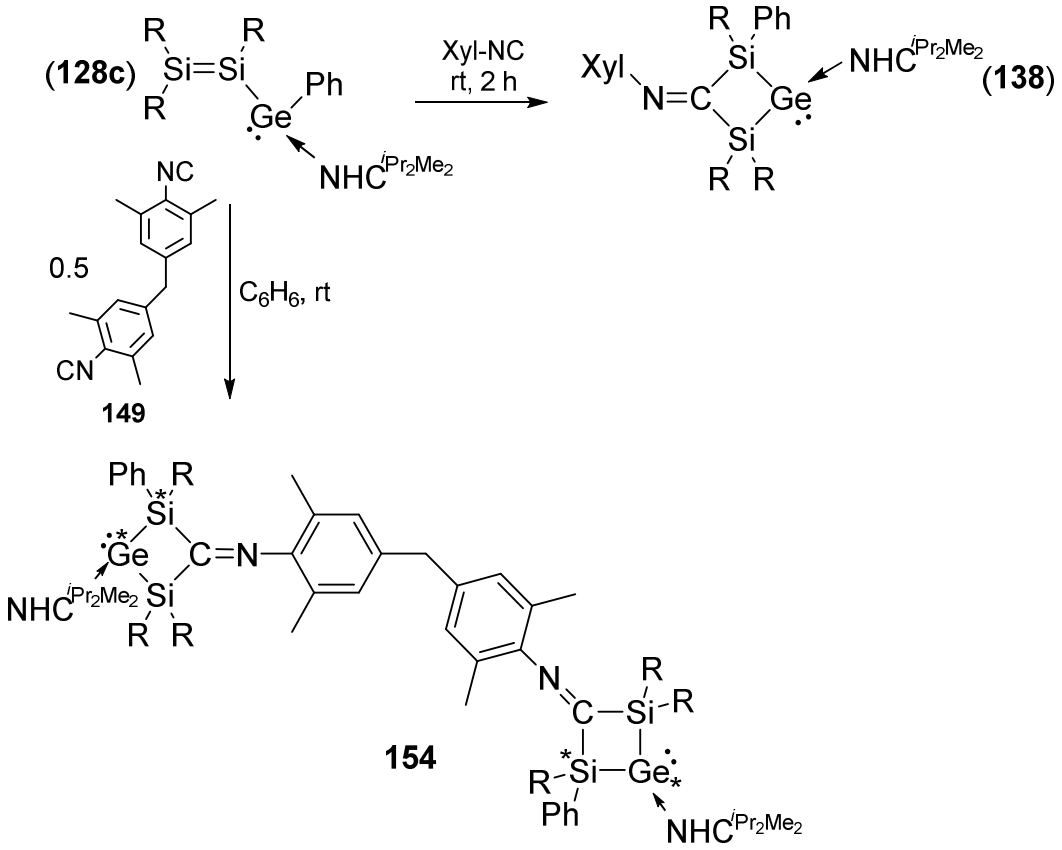

Scheme 95. Reaction of **128c** with xylyl isocyanide and methylene-bridged bis-isocyanide **149** resulting in germylene **138** and mixture of diastereomers of **154** (R = Tip).

Indeed, the reaction of disilenyl germylene **128c** with the methylene-bridged bis-isocyanide **149** at room temperature in benzene results in an immediate change in color from red to deep purple (Scheme 95). A ^{29}Si NMR spectrum indicates four broadened resonances at δ = −2.03, −2.22, −4.22 and −4.28 ppm (cyclic germlyene **138**: δ = −1.74 and −3.92 ppm, Scheme 95) suggesting a formation of a mixture of diastereomers of **154** (Figure 46).

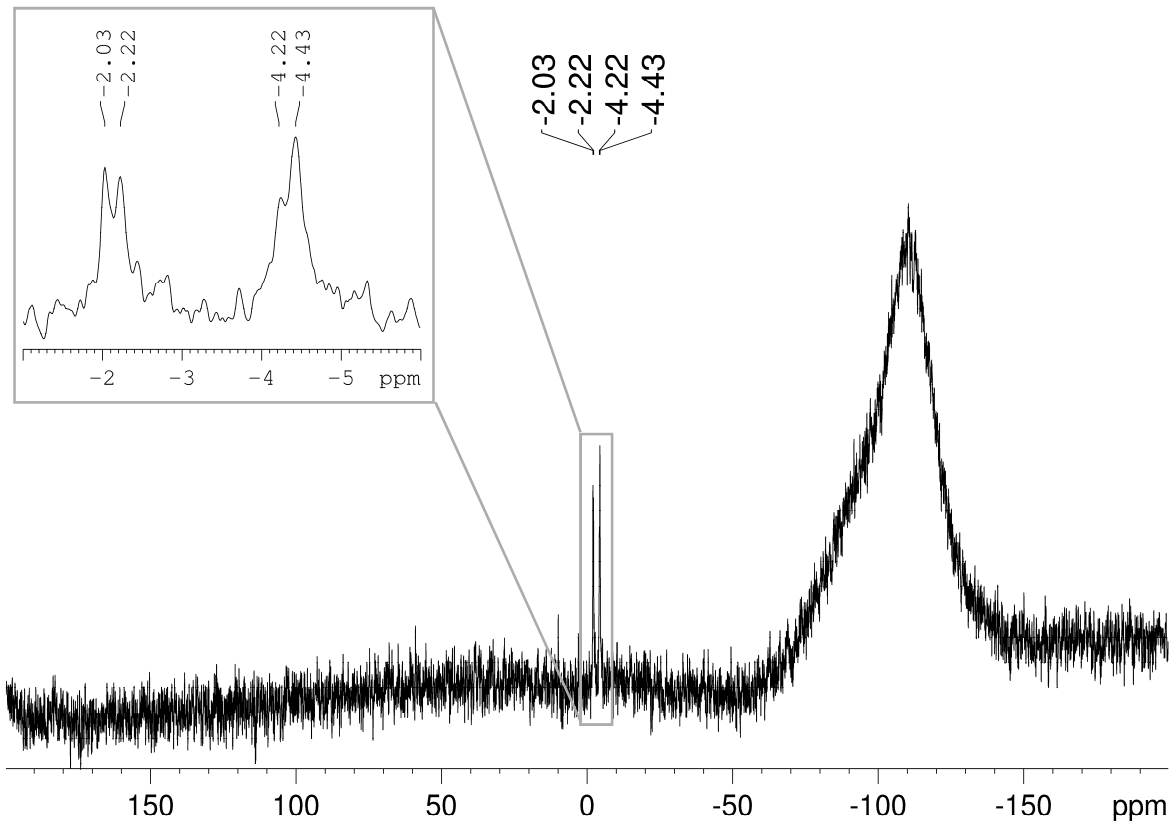

Figure 46. ^{29}Si NMR spectrum of the reaction mixture of **128c** with methylene-bridged bis-isocyanide **149**. The excerpt shows the enlarged region for the resonances of the proposed product **154**.

The ^{1}H NMR spectrum shows a typical resonance at δ = 5.16 ppm for the coordination of an NHC to the Ge(II)-center (cyclic germylene **138**: δ = 5.42 ppm, Figure 47).

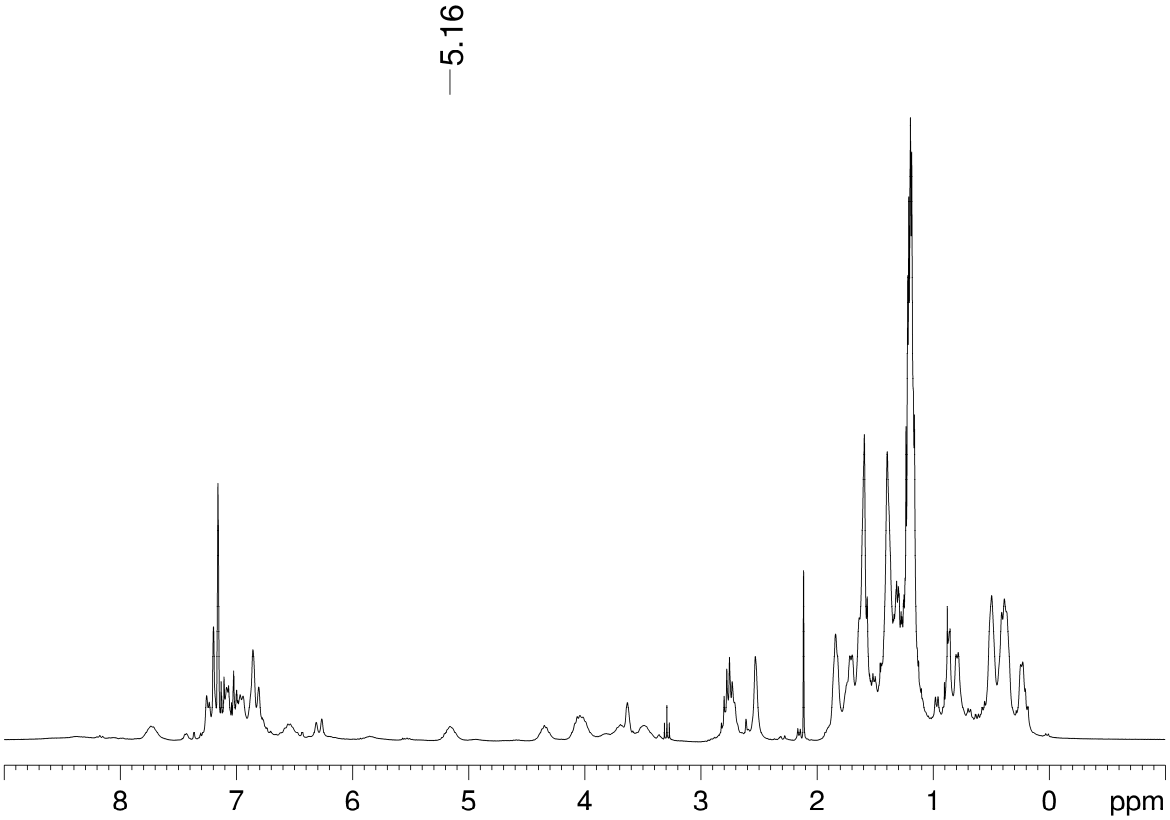

Figure 47. ^{1}H NMR spectrum of the reaction mixture of **128c** with methylene-bridged bis-isocyanide **149**.

The ^{13}C NMR spectrum reveals a resonance for a carbenic carbon-atom coordinated to a Ge(II)-center at δ = 169.48 ppm (Figure 48) comparable to those of the reaction of disilenyl germlyene **128c** with xylyl isocyanide (δ = 169.33 ppm, Scheme 95, page 96). Unfortunately, the crystallization attempt from a concentrated hexane solution at −26 °C did not afford any crystalline material.

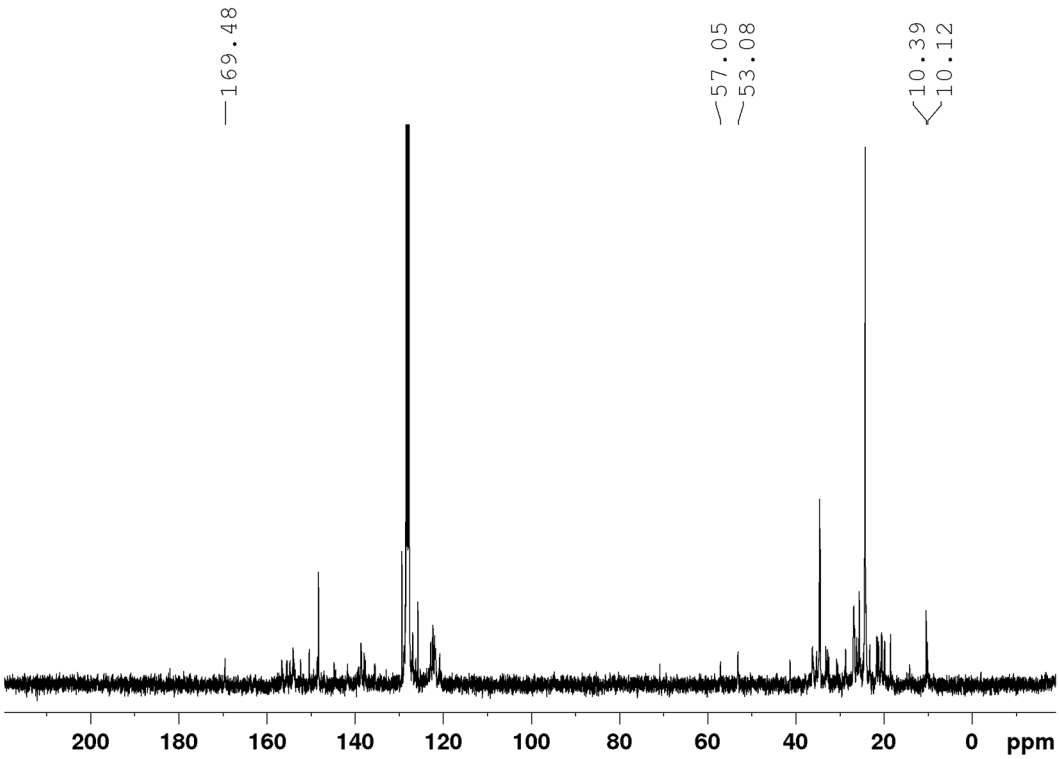

Figure 48. ^{13}C NMR spectrum of the reaction mixture of **128c** with methylene-bridged bis-isocyanide **149** (labelled: signals of coordinated NHC).

3.3.2.5. NHC-Abstraction from the Mixture of Diastereomers of Bis-Germylene 154 with BPh_3

Although no crystalline material of **154** was obtained, **154** is stable in hexane solution for at least 48 hours, most likely because of the phenyl group instead of the chlorine functionality at the chiral Si-atom. This allowed us to abstract the NHC from the proposed mixture of diastereomers of **154** (Scheme 96).

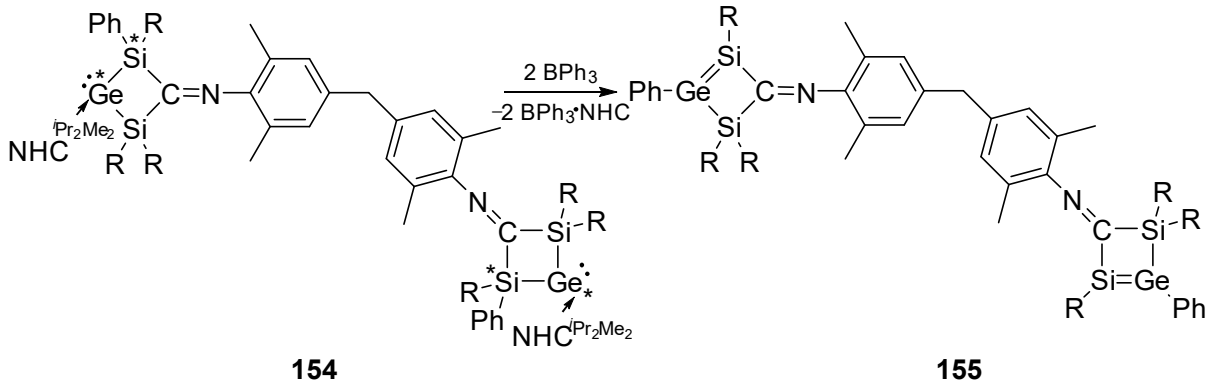

Scheme 96. NHC-abstraction from **154** with BPh_3 resulting in proposed heavier bis-cyclobutene **155** (R = Tip).

The ^{29}Si NMR spectrum reveals two new sharp main resonances at δ = 103.38 and −4.34 ppm together with an impurity at δ = −11.92 ppm (Figure 49). The ^{29}Si NMR data are similar to those of the proposed product of the NHC-abstraction from cyclic germylene **138** (δ = 103.12 and −4.14 ppm, Scheme 97).

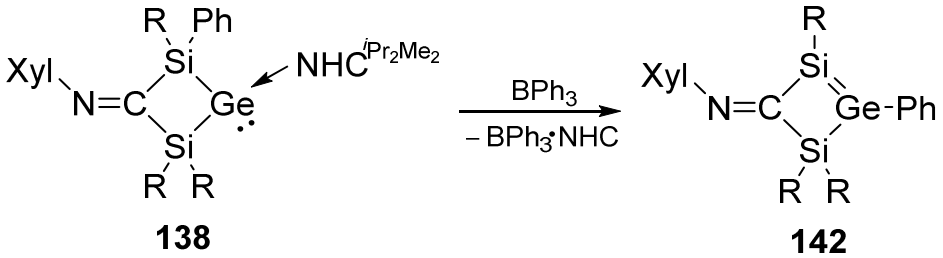

Scheme 97. Formation of heavier cyclobutene analogue **142** by NHC-abstraction from **138** (R = Tip).

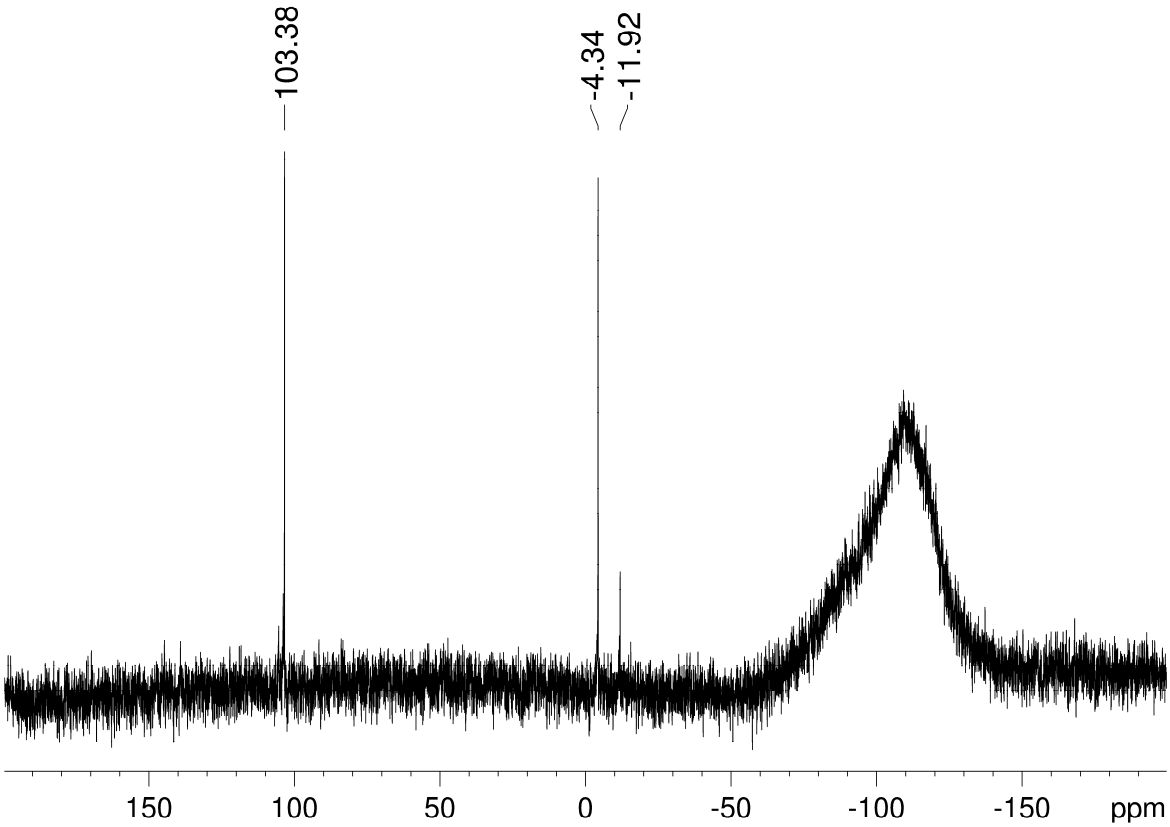

Figure 49. ^{29}Si NMR spectrum of the reaction mixture of the NHC-abstraction from phenylene-bridged cyclic bis-germylene **154** resulting in heavier phenylene-bridged bis-cyclobutene analogue **155**.

The ^{1}H NMR spectrum indicates the formation of BPh_3·NHC-adduct (see Figure 50).[174]

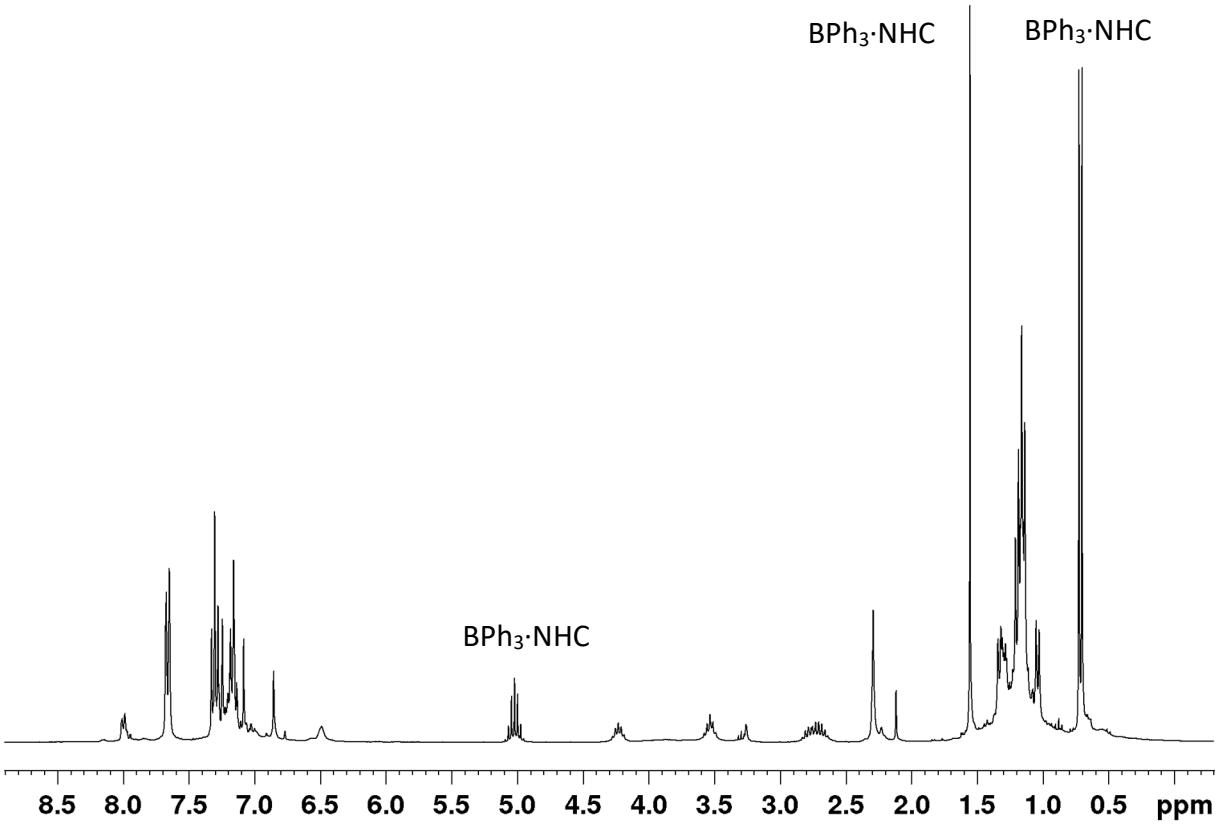

Figure 50. ^{1}H NMR spectrum of the reaction mixture of the NHC-abstraction from phenylene-bridged cyclic bis-germylene **154** resulting in heavier phenylene bridged bis-cyclobutene analogue **155**.

The ^{13}C NMR spectrum shows no more resonance for the carbenic carbon-atom at δ = 169.48 ppm observed in **154**. It is again proposed that the phenyl-group shifted back to the germanium-atom thus forming a Si=Ge-bond, which would explain only two resonances in the ^{29}Si NMR spectrum in contrast to the signal sets of diastereomers of starting material **154** (no more stereocenters in bis-cyclobutene analogue **155**). This observation provides some support for the above proposed theory of diastereomer formation for **151** and **152**. Another important factor are polymerization processes of the formed products or the bis-isocyanides with themselves at higher temperatures.[181] Unfortunately, single crystals to confirm this hypothesis could not be obtained.

3.3.2.6. Reaction of Heavier Cyclopropylidene 123c with Durylene Bis-Isocyanide 147

The similar reactivity of disilenyl germylene **128c** and its isomeric heavier cyclopropylidene analogue **123c** toward xylyl isocyanide encouraged us to also investigate reactions of **123c** with bis-isocyanides.

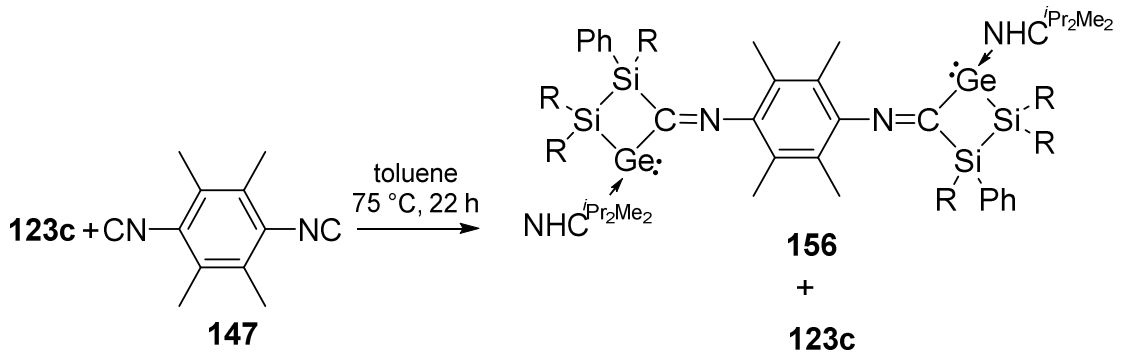

Scheme 98. Reaction of **123c** with durylene bis-isocyanide **147** (R = Tip).

The reaction of cyclopropylidene analogue **123c** with 0.5 eq of durylene bis-isocyanide **147** afforded a change in color from yellow to deep red after heating for 22 hours to 75 °C. The ^{13}C NMR spectrum reveals two new resonances in the range for the coordination of an NHC to a Ge(II)-center at δ = 168.85 and 168.71 ppm.[61,63,144,145] Bis-isocyanide **147** was completely consumed but starting material **123c** (δ = −62.74 and −68.83 ppm) was still detected in the ^{29}Si NMR spectrum in addition to two new resonances at δ = −7.09 and −45.91 ppm (Figure 52) comparable to those of the reaction of **123c** with xylyl isocyanide (δ = −7.06 and δ = −45.21 ppm, Scheme 81, page 76). A second half of an equivalent of bis-isocyanide **147** was added and again heated to 75 °C were the reaction stopped. It was not possible to bring the reaction to completeness by additionally heating for 20 hours to 75 °C, only bis-isocyanide **147** disappeared which could be due to polymerization processes at this temperature.[181]

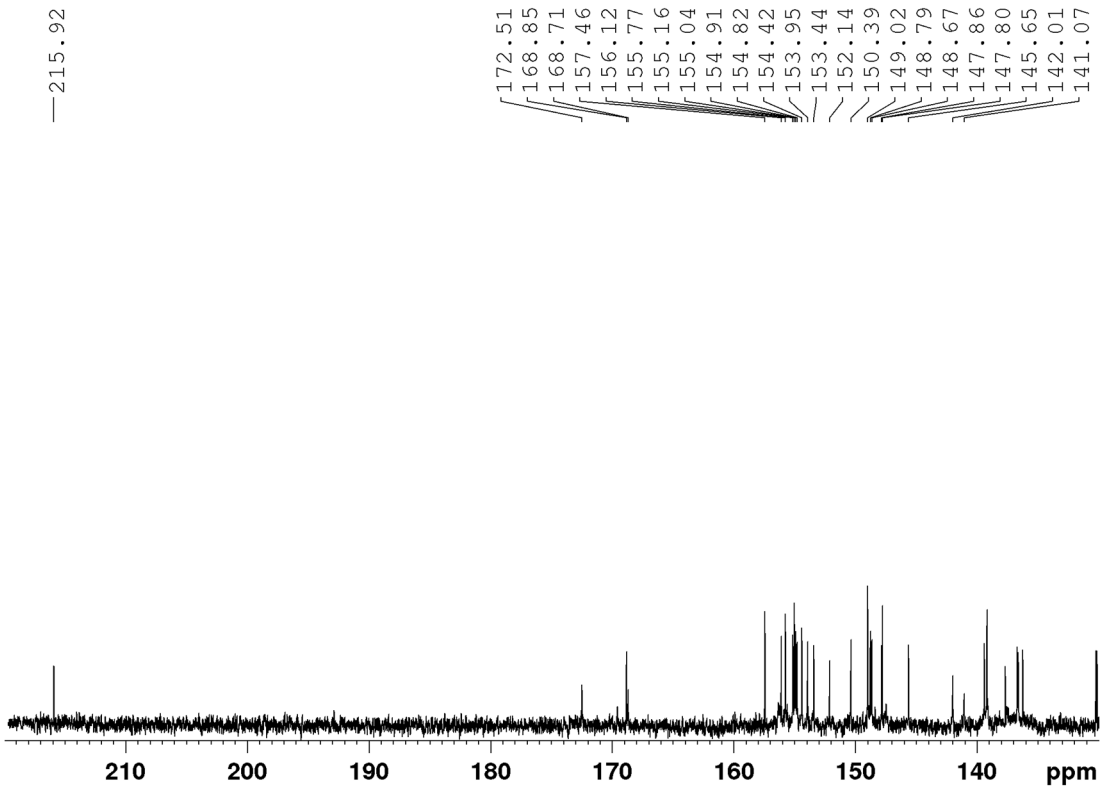

Figure 51. Excerpt of the ^{13}C NMR spectrum of the reaction mixture of **123c** with bis-isocyanide **147**.

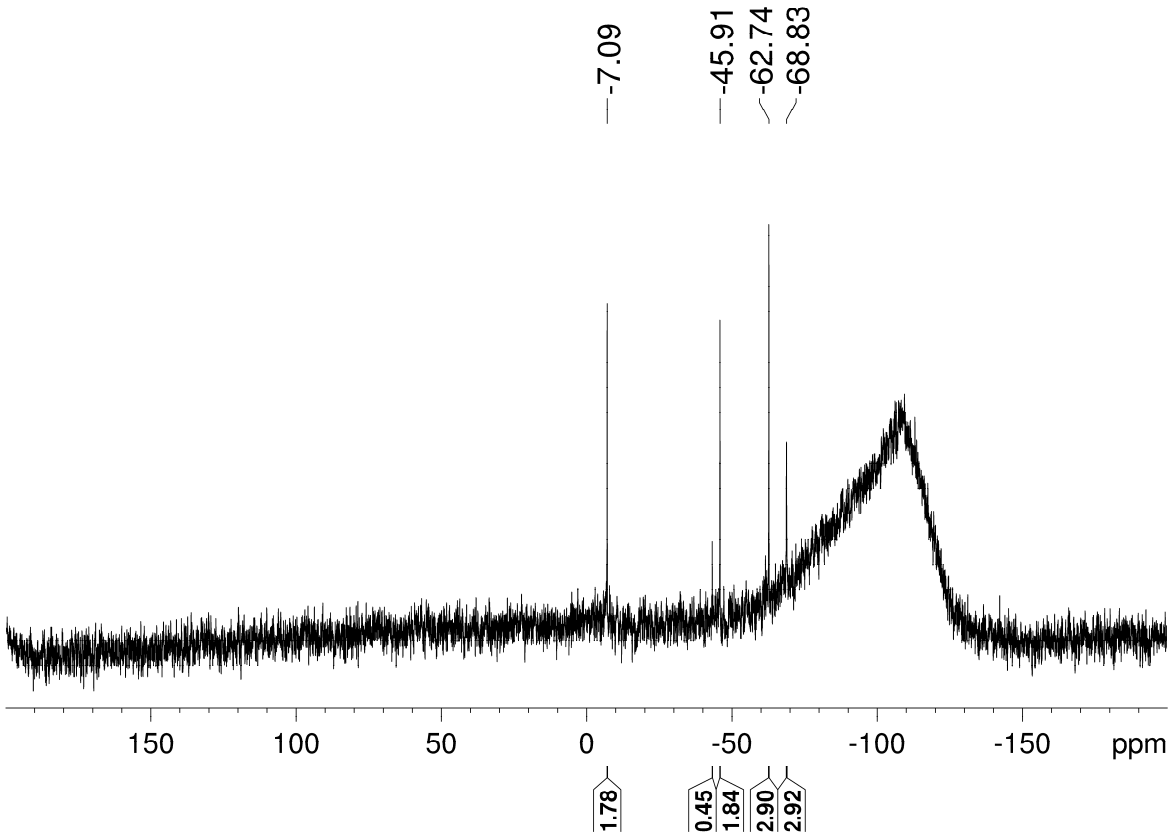

Figure 52. ^{29}Si NMR spectrum of the reaction mixture of **123c** with bis-isocyanide **147**.

3.3.2.7. Reaction of Heavier Cyclopropylidene 123c with Bis-(4-Isocyano-3,5-dimethylphenyl)methane 149

Because the reaction of durylene bis-isocyanide **147** and NHC-coordinated cyclopropylidene analogue **123c** was incomplete, **123c** was reacted with 0.5 eq of methylene-bridged bis-isocyanide **149** and heated the mixture up to 75 °C (Scheme 99). After 22 hours the bis-isocyanide **149** was consumed and remaining starting material detected.

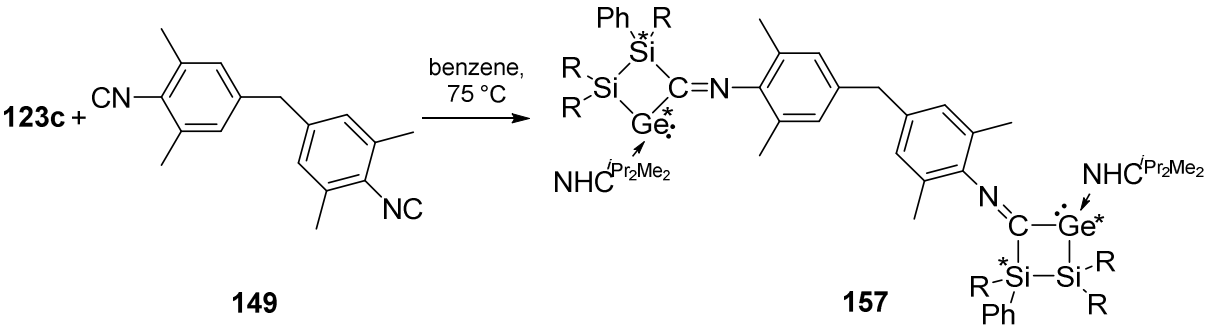

Scheme 99. Reaction of methylene bridged bis-isocyanide **149** with cyclopropylidene analogue **123c** (R = Tip).

Adding another half equivalent of bis-isocyanide **149** resulted most likely in a mixture of diastereomers of **157** with ^{29}Si NMR resonances at δ = −6.72, −7.28, −45.05, −45.30, −45.58 and −45.75 ppm which are comparable to the reaction of heavier cyclopropylidene analogue **123c** and xylyl isocyanide (δ = −7.06 and −45.21 ppm, Scheme 81, page 76). The ^{29}Si NMR resonances at δ = −62.74 and −68.80 ppm can be assigned to starting material **123c** (Figure 53).

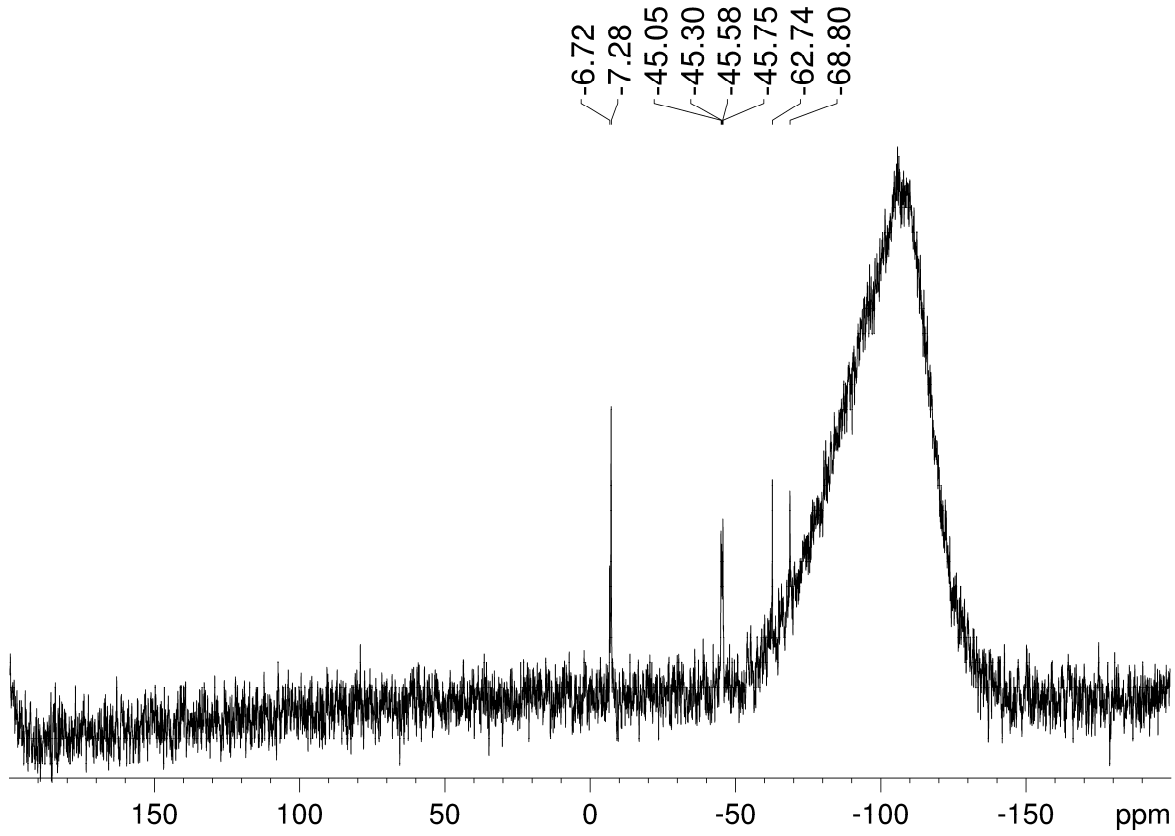

Figure 53. ^{29}Si NMR spectrum of the reaction mixture of **123c** with phenylene-bridged bis-isocyanide **149**.

3.4. Reactions of Arylsilanes with NHCs

3.4.1. Attempts to Synthesize NHC-Stabilized Diaryl Silylenes *vs.* Backbone Activation of NHCs

Since the isolation of the first crystalline NHC, the chemistry of functionalized NHCs is a rapidly evolving topic across the whole fields of chemistry.[46,48] Several NHCs with silyl-functionalities at the backbone have been reported,[47,186–191] e.g. Robinson's trimethylsilyl functionalized NHC **159** which was synthesized by a salt elimination reaction of anionic NHC **158** with Me_3SiCl (Scheme 100).[190] A different route which gave access to silyl functionalized NHC **160** was reported by the group of Roesky starting from NHC-stabilized dichloro silylene **35** (Scheme 100).[186] An example for a phosphino functionalized NHC **161** was reported by Bertrand *et al.* in 2010 also starting from NHC **158**.[188]

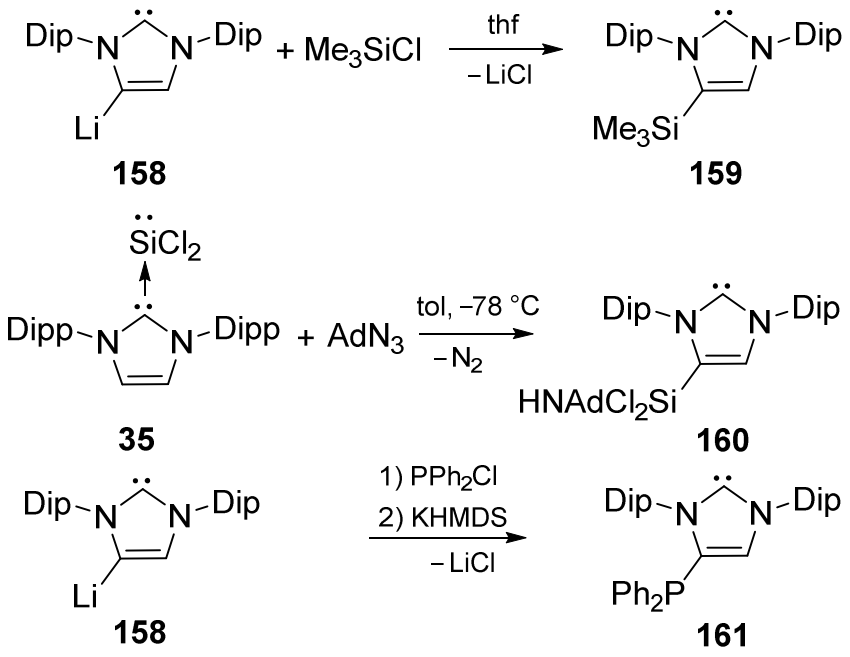

Scheme 100. Examples for backbone functionalized NHCs **159** to **161** reported by the groups of Robinson, Roesky and Bertrand.

All these modifications were possible when the C-C-double bond of the NHC possesses two protons. Functionalization at the backbone is still unknown when the C=C-bond is substituted with two methyl-groups.

Examples of NHC-stabilized arylhalo silylenes were reported by the groups of Filippou and Tokitoh using different approaches (Scheme 101). Filippou and co-workers reacted chloro silanes **162a**,**b** with NHC^{Me4} to obtain NHC-coordinated silylenes **163a**,**b**.[68] Tokitoh *et al.* were able to cleave the double bond of 1,2-dibromodisilene **84** with NHC^{Me4} and identified arylbromo silylene **165** by NMR spectroscopy.[192]

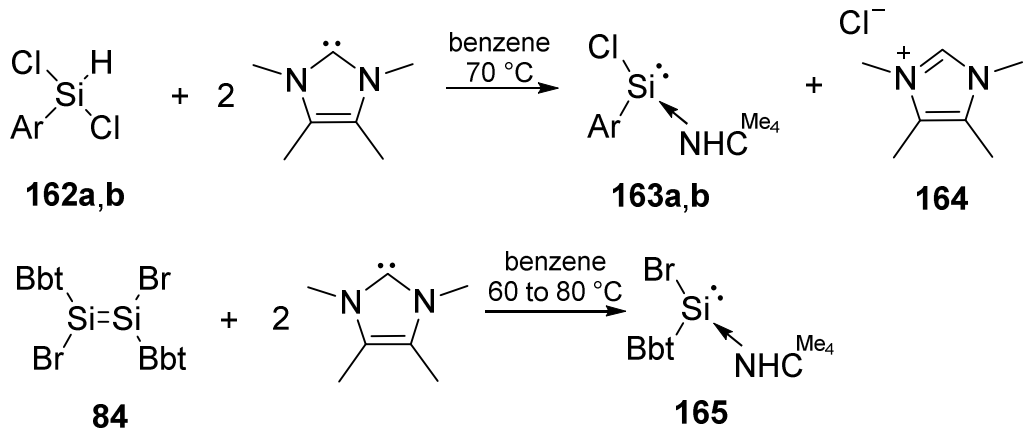

Scheme 101. Synthesis of Filippou's NHC-stabilized arylchloro silylenes **163a**,**b** (**a**: Ar = C_6H_3-2,6-Mes_2, **b**: Ar = C_6H_3-2,6-$Trip_2$) and Tokitoh's NHC-coordinated arylbromo silylene **165** (Bbt = 2,6-$[(Me_3Si)_2CH]_2$-4-$[(Me_3Si)_3C]$-C_6H_2).

While an NHC-coordinated disilyl silylene **167** was reported by the group of Sekiguchi in 2012, the related diaryl silylenes still remain unknown (Scheme 102).[193]

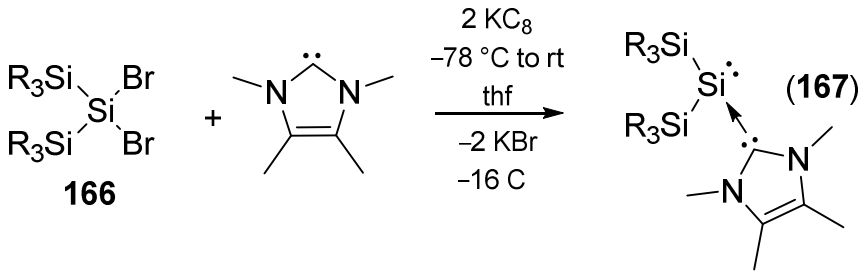

Scheme 102. Synthesis of NHC-coordinated disilyl silylene **167** by the group of Sekiguchi (R = ^{t}Bu).

In 2014, the group of Inoue reported the synthesis of an NHC-stabilized silyliumylidene in reaction of $TerSiHCl_2$ (Ter = 2,6-Mes_2-C_6H_3) and 3 eq of $NHC^{iPr2Me2}$.[194]

This chapter should shed a light on the reactions of different arylchloro silanes with different NHCs. It was expected that abstraction of chlorine or protons from silanes of type **XVI** with NHCs as bases could lead to diaryl silylenes **XVIII** or in case of NHC activation to functionalized NHC derivatives (**XVII**, Scheme 103).

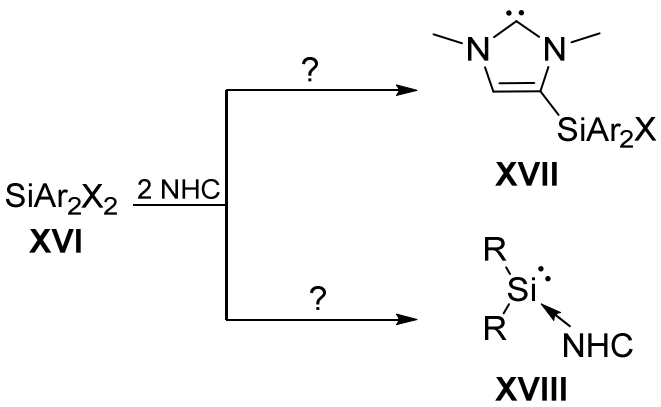

Scheme 103. Reactions of different $SiAr_2X_2$ **XVI** with NHCs: formation of NHC-coordinated silylene **XVIII** *vs.* functionalization of NHCs **XVII** (R = aryl group, X = H or Cl).

3.4.1.1. Reaction of Tip_2SiCl_2 64 with $NHC^{iPr2Me2}$

Silagermenylidene **101** was formed in a reductive dehalogenation of Tip_2SiCl_2 **64** and $GeCl_2{\cdot}NHC^{iPr2Me2}$ **8** with 4 eq Li/naphthalene in thf, which led not only to the targeted heavier vinylidene analogue **101**, but also to the symmetrical disilene **65** and free $NHC^{iPr2Me2}$ as unwanted side products (Scheme 104).[70,103,144]

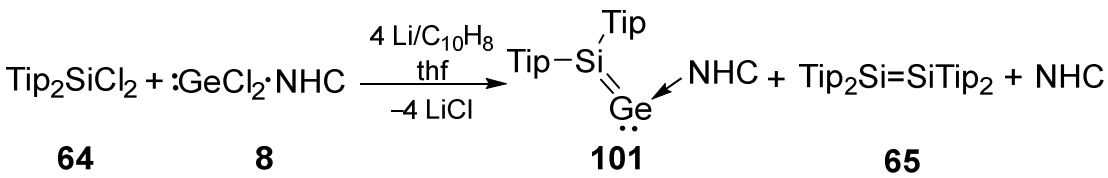

Scheme 104. Synthesis of heavier vinylidene analogue **101** with side products **65** and NHC (NHC = $NHC^{iPr2Me2}$ = 1,3-diisopropyl-4,5-dimethylimidazol-2-ylidene).

In order to avoid the unselective and harsh reduction conditions in the synthesis of silagermenylidene **101**, an alternative route was conceived with NHC-stabilized diaryl silylenes as suitable precursors. The reaction of a hitherto unknown diaryl silylene such as **117** with $GeCl_2{\cdot}$dioxane could lead to an NHC-stabilized chlorosilyl germylene **118** by a 1,2-shift of a chlorine atom from the Ge(II)-center to the adjacent silicon. In a next step, a reduction of the formed Si-Ge-scaffold **118** could afford silagermenylidenes in a more selective way (Scheme 105).

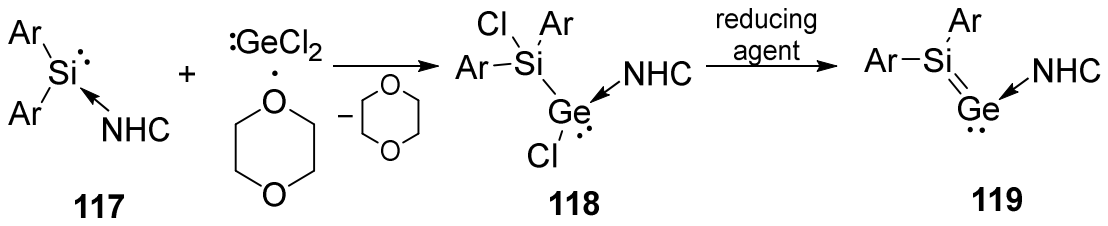

Scheme 105. Proposed reaction pathway as alternative for the synthesis of silagermenylidenes (Ar = aryl group).

In order to synthesize NHC-stabilized diaryl silylene **168** the bulky dichloro silane **64** was reacted with two equivalents of NHC^{iPr_2Me_2} in benzene solution in the hope of abstraction of the two chlorine atoms (Scheme 106).

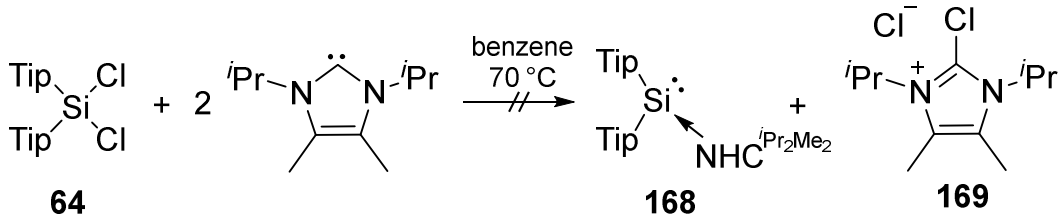

Scheme 106. Reaction of Tip_2SiCl_2 **64** with 2 eq NHC^{iPr_2Me_2}.

Since no reaction was observed at room temperature after 3 hours the sample was heated to 75 °C. After 3 days at this temperature the reaction mixture remained unchanged which leads to the conclusion that the steric demand of the NHC^{iPr_2Me_2} and the bulky aryl substituents at the silane **64** effectively prevents the abstraction of the chlorine atoms by the NHC. Consequently, the steric demand of the NHC was reduced in the subsequent experiment.

3.4.1.2. Reaction of Tip_2SiCl_2 64 with NHC^{Me_4}

In a further attempt to obtain NHC-coordinated diaryl silylene **170**, Tip_2SiCl_2 **64** was reacted with two equivalents of the sterically less demanding NHC^{Me_4} in toluene solution starting at −78 °C (Scheme 107).

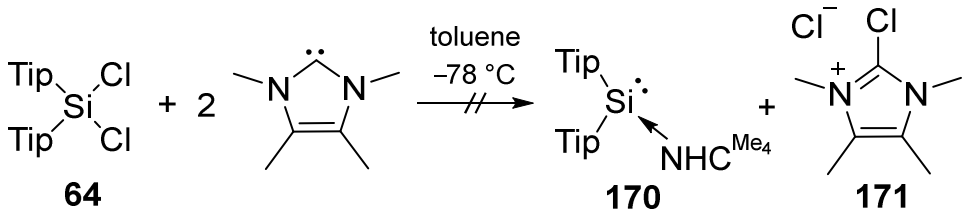

Scheme 107. Reaction of Tip_2SiCl_2 **64** with 2 eq NHC^{Me_4}.

After warming up to room temperature, no reaction was observed and stirring was continued for 14 hours at room temperature and the color turned from colorless into red in the course of warming to room temperature. Recording a ^{29}Si NMR spectrum of the reaction mixture displays seven resonances between δ = 1.98 and −49.04 ppm. All attempts to isolate a product from the reaction mixture by crystallization from a concentrated toluene solution failed.

3.4.1.3. Reduction of Tip_2SiCl_2 64 with $NHC^{iPr2Me2}$

The reduction of Tip_2SiCl_2 **64** with 2 eq of Li/naphthalene in the presence of the σ-donating $NHC^{iPr2Me2}$ should in principle be a possibility to trap a transient diaryl silylene $SiTip_2$ as NHC adduct **168** (Scheme 108).

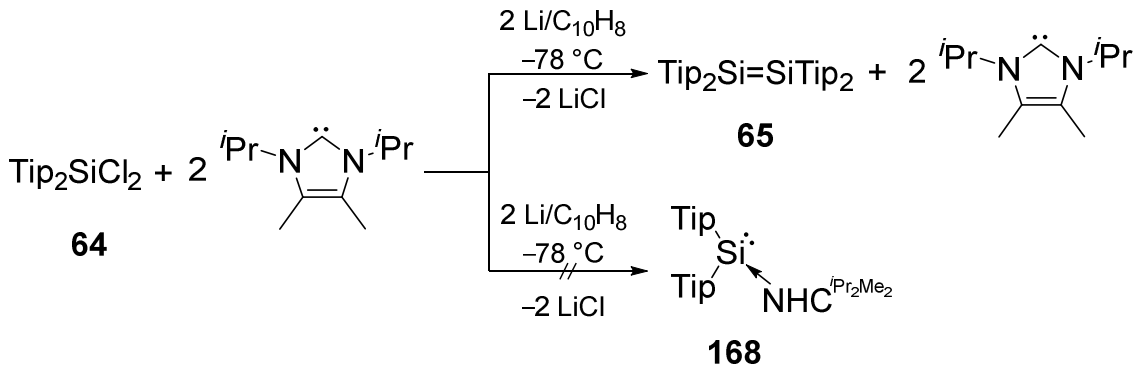

Scheme 108. Reduction of Tip_2SiCl_2 **64** with 2 eq $Li/C_{10}H_8$ in the presence of 2 eq $NHC^{iPr2Me2}$ resulting in **65** and free $NHC^{iPr2Me2}$.

The reduction was carried out at −78 °C in thf and upon warming to room temperature a ^{1}H NMR sample indicates the selective conversion into symmetrical disilene **65** (^{29}Si NMR shift at δ = 52.87 ppm), while the $NHC^{iPr2Me2}$ remained unaffected by the reduction conditions confirming that the attempted synthesis of NHC-stabilized diaryl silylene **168** failed under these conditions.

3.4.1.4. Reaction of Tip_2SiHCl 172 with $NHC^{iPr2Me2}$

Attempts to abstract two chlorine atoms from Tip_2SiCl_2 **64** with $NHC^{iPr2Me2}$ and NHC^{Me4} were unsuccessful (Chapter 3.4.1.1. and 3.4.1.2.). The abstraction of two chlorine atoms is usually realized under reductive conditions. Roesky *et al.* and the group of Filippou utilized 2 eq of NHC to abstract HCl from chloro silane precursors (Scheme

101, page 107).[68,80] Following their example, Tip_2SiHCl **172** was treated with 2 eq of $NHC^{iPr2Me2}$ as base.

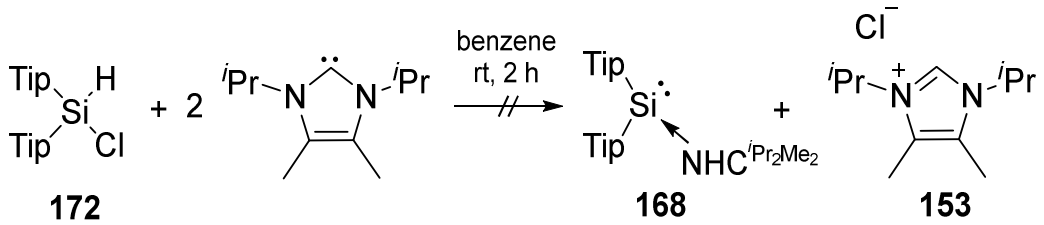

Scheme 109. Reaction of Tip_2SiHCl **172** with 2 eq of $NHC^{iPr2Me2}$.

Indeed, when Tip_2SiHCl **172** was reacted with 2 eq of $NHC^{iPr2Me2}$ in benzene solution the color turned orange, indicating that in contrast to the lack of conversion of Tip_2SiCl_2 **64** with 2 eq of $NHC^{iPr2Me2}$, a reaction had taken place (Scheme 109). An ^1H NMR spectrum after two hours stirring at room temperature shows residual free $NHC^{iPr2Me2}$ strongly suggesting that the proposed ratio of 2:1 was inadequate. The ^{29}Si NMR spectrum reveals a mixture of at least four products with chemical shifts at δ = −22.02, −28.52, −36.72 and −48.22 ppm, which are very roughly in the range expected for the targeted NHC-stabilized silylene (^{29}Si NMR resonance of NHC^{Me4}-coordinated $Si(Si(^tBu_3))_2$ at δ = −128.9 ppm, NHC^{Dip}-stabilized dihalo silylene complexes SiX_2 (δ = 19.1 ppm [X = Cl], δ = 10.1 ppm [X = Br]), NHC^{Me4}-coordinated arylchloro silylenes **163a**,**b** (δ = 1.34 ppm, **a**: Ar = C_6H_3-2,6-Mes_2; δ = 0.77 ppm, **b**: Ar = C_6H_3-2,6-$Trip_2$).[68,80,81,193] The ^{29}Si NMR chemical shift at δ = −22.02 ppm can be assigned to arylchloro silane **172**. However, no signal for a carbenic C-atom of an NHC-stabilized silylene is observed in the ^{13}C NMR spectrum (typical ^{13}C NMR chemical shifts for the carbenic C-atom to Si(II)-centers: NHC^{Me4}-coordinated $Si(Si(^tBu_3))_2$ **167** at δ = 172.6 ppm, NHC^{Me4}-coordinated arylchloro silylenes **163a**,**b** (δ = 165.2 ppm, **a**: Ar = C_6H_3-2,6-Mes_2, δ = 166.7 ppm, **b**: Ar = C_6H_3-2,6-$Trip_2$).[68,193] Attempts to isolate any of the products from the reaction mixture failed.

3.4.1.5. Reaction of Mes_2SiHCl 173 with $NHC^{iPr2Me2}$

In case of Tip_2SiHCl **172**, the abstraction of HCl with 2 eq of $NHC^{iPr2Me2}$ as base failed which might be attributed to the presence of the bulky Tip-substituents. Therefore, the sterically less congested Mes_2SiHCl **173** was treated with an excess of the $NHC^{iPr2Me2}$ (2.2 eq) in benzene solution (Scheme 110).

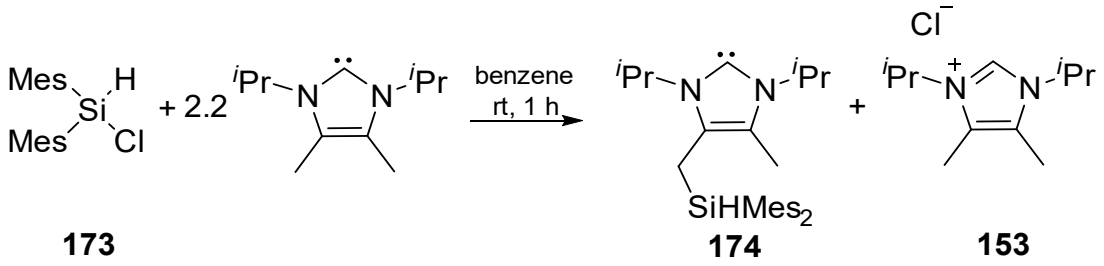

Scheme 110. Reaction of Mes_2SiHCl **173** with 2.2 eq of $NHC^{iPr_2Me_2}$.

After one hour at room temperature the reaction was complete and a white precipitate formed. Aside from signals for excess $NHC^{iPr_2Me_2}$, a ^1H NMR sample shows a triplet at δ = 5.27 ppm ($^3J_{H,H}$ = 5 Hz, $^1J_{Si,H}$ = 98 Hz), which is in the typical range for protons attached to the silicon-center (Figure 54).

The uniform ^1H NMR spectroscopic data with well-defined ratio of integrals is indicative of the presence of a single product.[195] Furthermore, the white precipitate is soluble in $CDCl_3$ and identified as the imidazolium chloride **153** (^1H NMR chemical shift of proton between 9 and 10 ppm; Figure 55).[196]

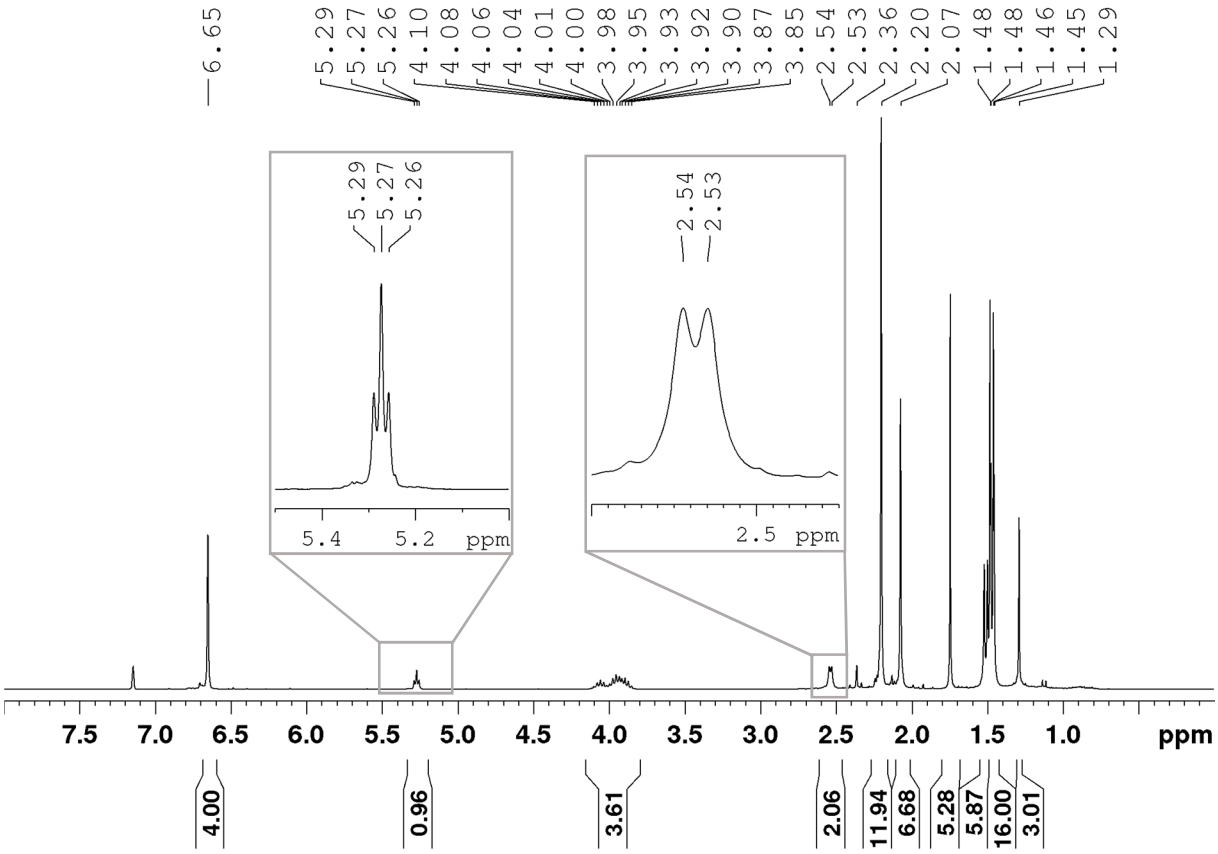

Figure 54. ^1H NMR spectrum of the reaction mixture of Mes_2SiHCl **173** with 2.2 eq of $NHC^{iPr_2Me_2}$. The excerpts show the Si*H* resonance at δ = 5.27 ppm and the CH_2-group at δ = 2.54 ppm.

The ^{29}Si NMR spectrum reveals a resonance at δ = −33.72 ppm (Figure 56) which confirms the formation of a single product beside the systematically formed imidazolium chloride **153** (identified by ^{1}H NMR spectroscopy, Figure 55) and excess of NHC^{i}Pr$_2$Me$_2$.

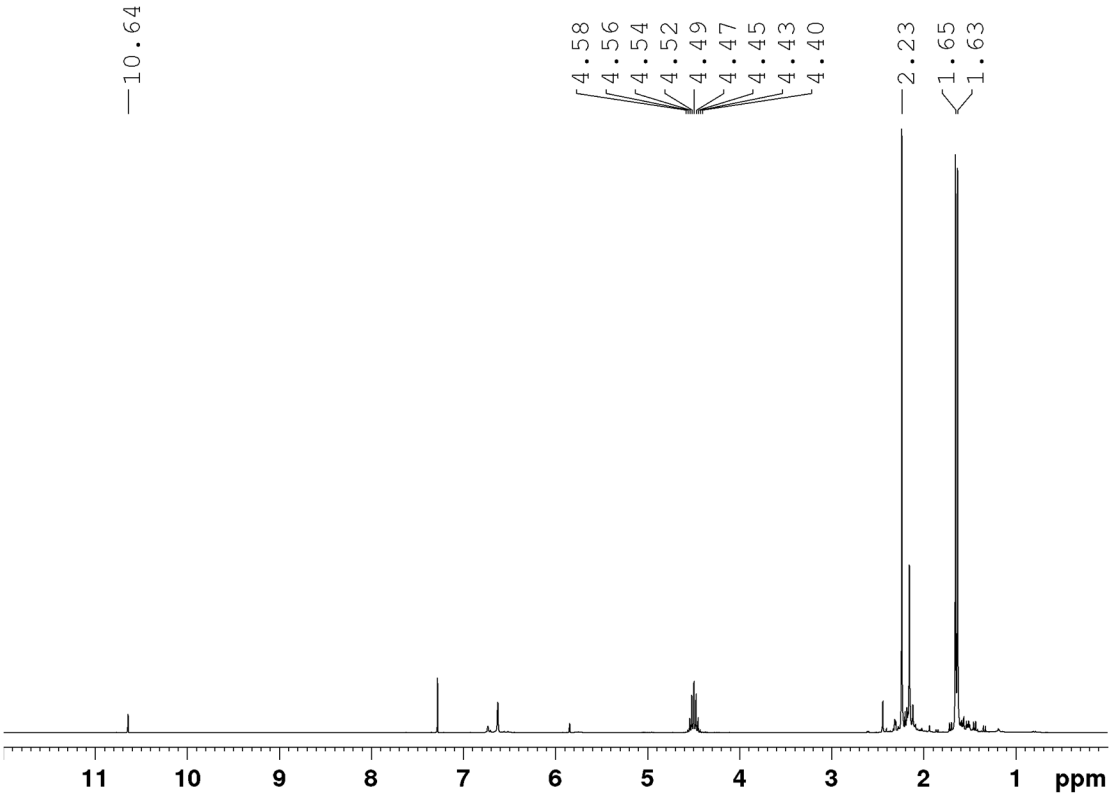

Figure 55. ^{1}H NMR spectrum of the reaction mixture of the white precipitate formed in the reaction of Mes$_2$SiHCl **173** with 2.2 eq of NHC^{i}Pr$_2$Me$_2$.

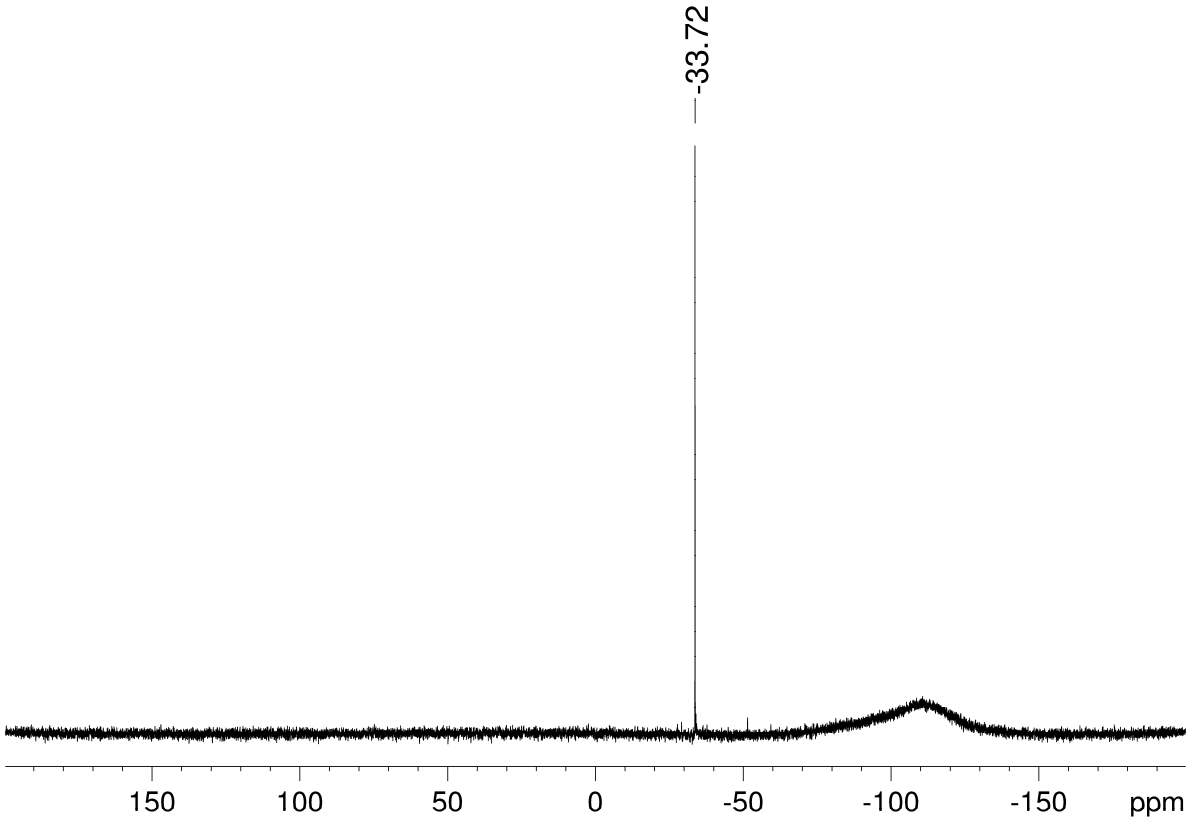

Figure 56. ^{29}Si NMR spectrum of the reaction mixture of Mes_2SiHCl **173** with 2.2 eq of $NHC^{iPr_2Me_2}$.

The ^{13}C NMR spectrum shows carbenic C-atom resonances at δ = 207.63 and 207.50 ppm (Figure 57). The signal at δ = 207.50 ppm is due to the excess of $NHC^{iPr_2Me_2}$. The lowfield ^{13}C NMR chemical shift of the second signal at δ = 207.63 ppm strongly suggests that the formation of an uncoordinated NHC as resonances of coordinated carbenic carbon atoms of NHCs are typically observed between δ = 165 and 173 ppm.[68,193]

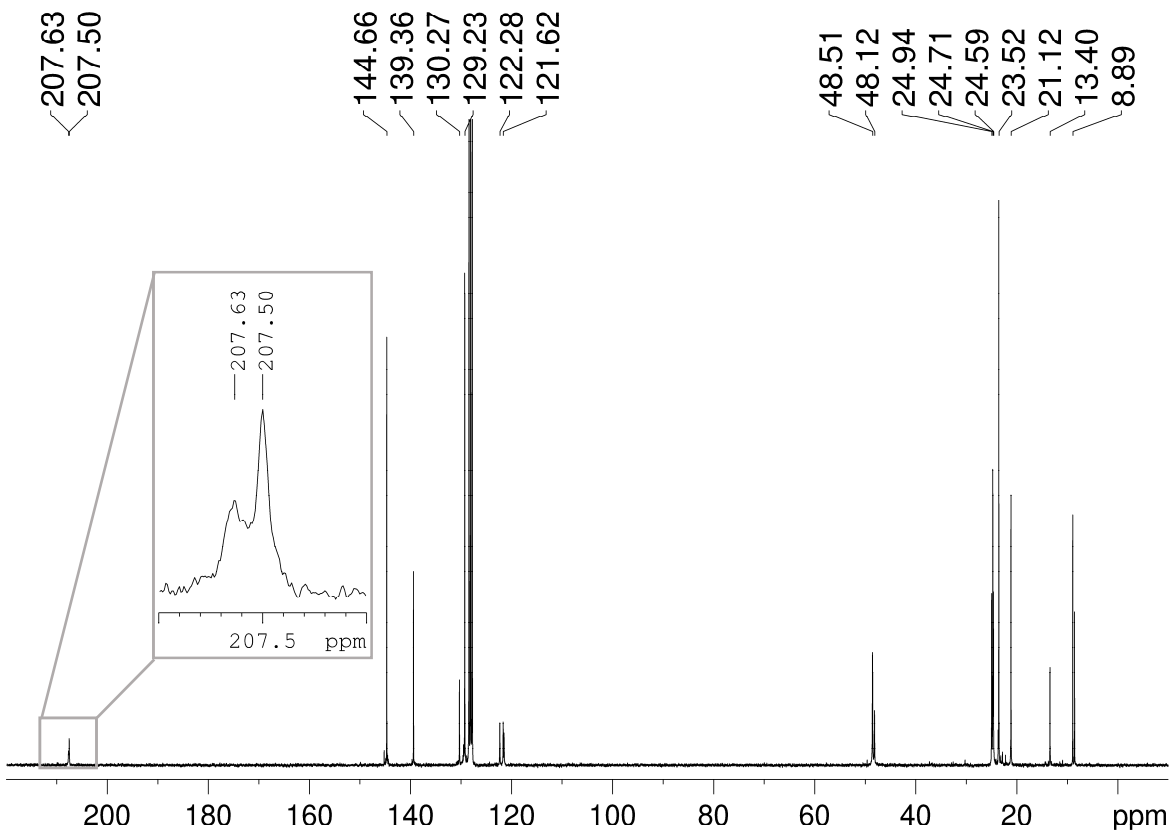

Figure 57. ^{13}C NMR spectrum of the reaction mixture of Mes_2SiHCl **173** with 2.2 eq of $NHC^{iPr_2Me_2}$. The excerpt shows the signals of the carbenic C-atoms of **173** and $NHC^{iPr_2Me_2}$.

The ^{13}C DEPT 135 NMR spectrum clearly shows a negative resonance at δ = 13.40 ppm indicating the presence of a CH_2-group at the C-C-double bond (value for the CH_3-groups in $NHC^{iPr_2Me_2}$ at δ = 8.89 ppm in ^{13}C NMR spectroscopy) in the product (Figure 58). This signal correlates in the 2D $^{13}C/^{1}H$ HMQC spectrum with the doublet (integrated 2H) at δ = 2.54 ppm in the ^{1}H NMR spectrum, which corroborates the assignment of this signal to the CH_2-group (Figure 59). The 2D $^{29}Si/^{1}H$ NMR correlation spectra show a clear cross signal between the resonance at δ = −33.72 ppm and the CH_2-group at δ = 2.54 ppm in the ^{1}H NMR spectrum, which proves the bonding of the methylene-fragment to the silicon-atom (Figure 60).

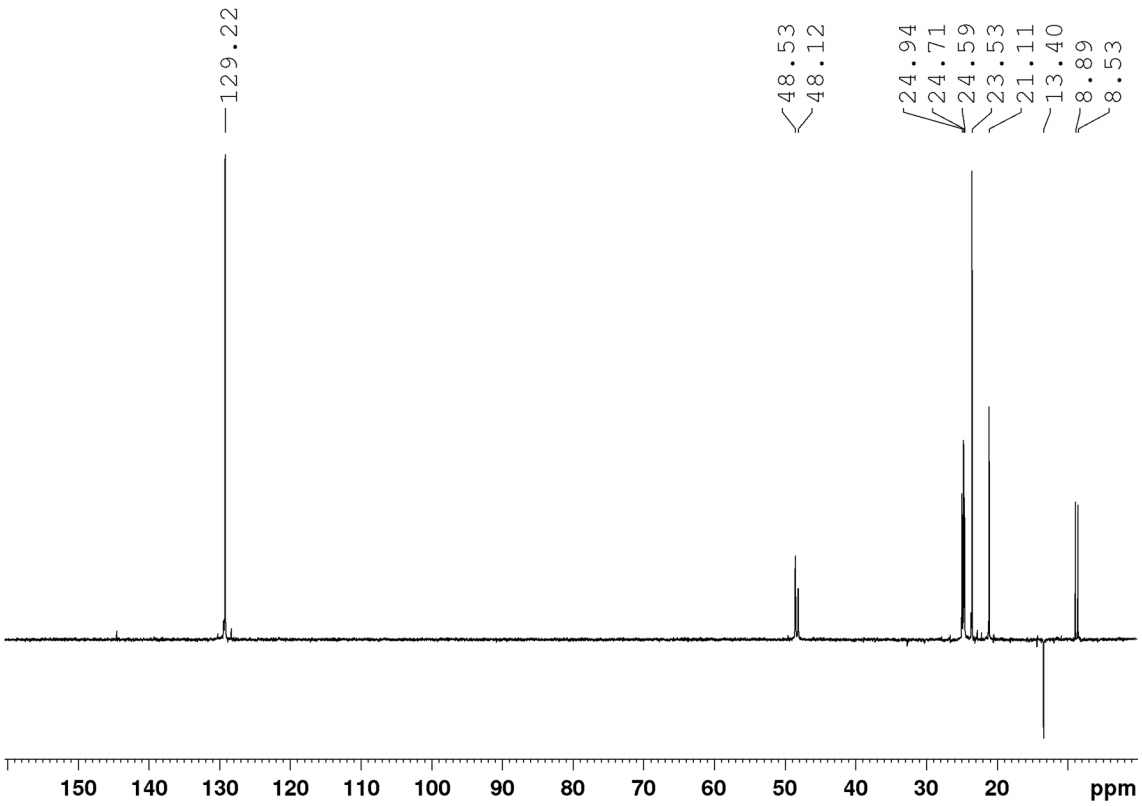

Figure 58. ^{13}C DEPT 135 NMR spectrum of the reaction mixture of Mes_2SiHCl **173** with 2.2 eq of $NHC^{iPr2Me2}$.

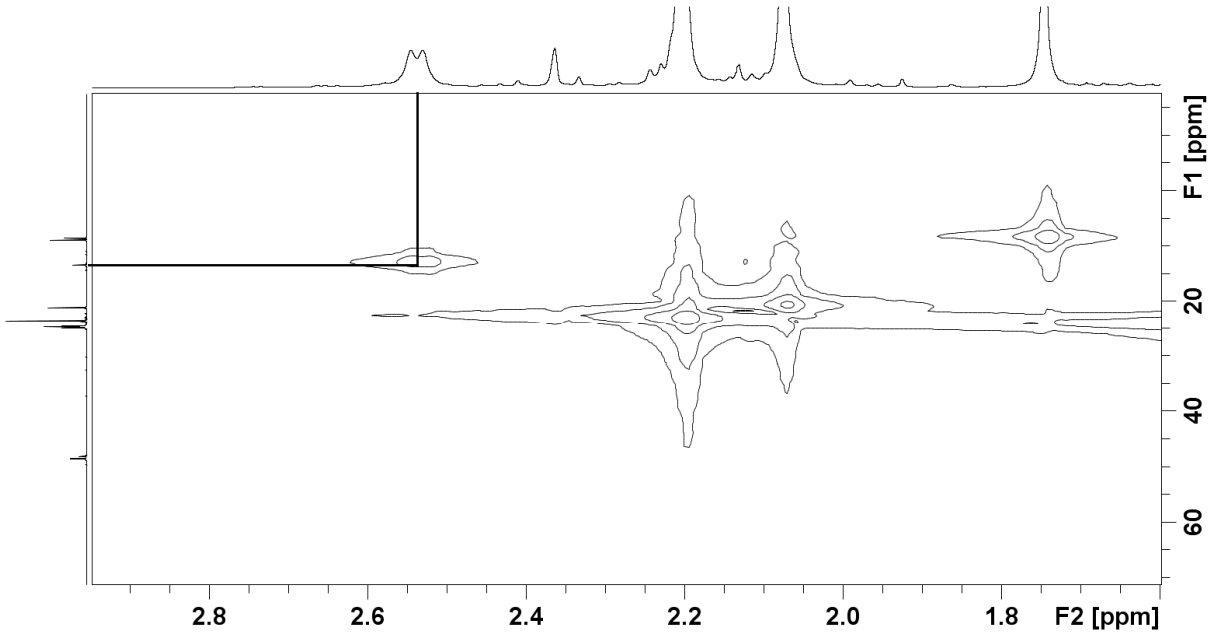

Figure 59. Selected area of the 2D $^{13}C/^{1}H$ HMQC correlation spectra of the reaction mixture of Mes_2SiHCl **173** with 2.2 eq of $NHC^{iPr2Me2}$.

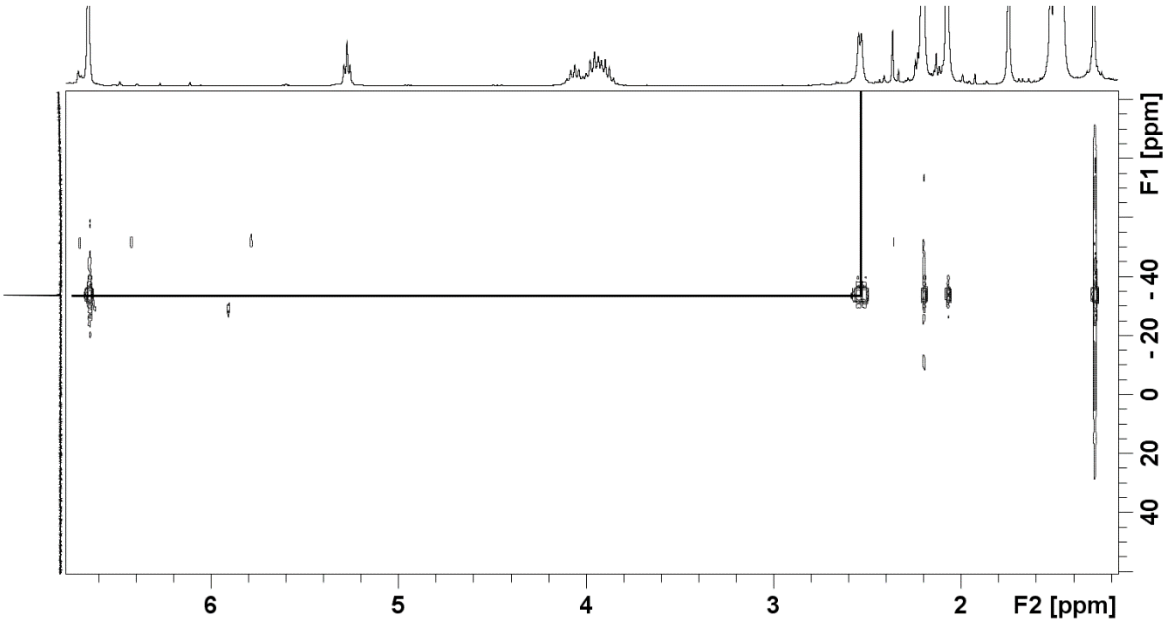

Figure 60. Selected area of the 2D NMR $^{29}Si/^{1}H$ correlation spectra of the reaction mixture of Mes_2SiHCl **173** with 2.2 eq of $NHC^{iPr2Me2}$.

Taking all information gained from the different types of NMR spectra into account led us to the suggestion that the backbone modified carbene **174** is the product of the reaction by activation of a methyl-group at the C-C-double-bond of the $NHC^{iPr2Me2}$. Unfortunately all attempts to crystallize the product failed, even when the reaction was carried out in the correct stoichiometric ratio of 2:1.

3.4.1.6. Reaction of Mes_2SiHCl 173 with NHC^{Mes2}

According to the NMR spectroscopic data, the reaction of Mes_2SiHCl **173** with 2.2 eq of $NHC^{iPr2Me2}$ led most likely to the activation of the methyl-group at the backbone of $NHC^{iPr2Me2}$ and resulted finally in the functionalized NHC **174** (Scheme 110, page 112). In order to explore whether a sterically more demanding NHC would avoid this activation, Mes_2SiHCl **173** was reacted with 2.2 eq of NHC^{Mes2} in benzene solution at room temperature (Scheme 111). As observed for all reactions of this type an immediate change in color from colorless to orange takes place.

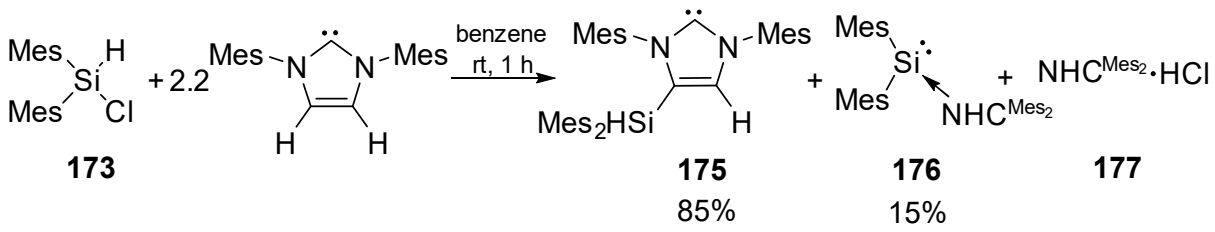

Scheme 111. Reaction of Mes_2SiHCl **173** with 2.2 eq of NHC^{Mes2}.

After one hour at room temperature the reaction was completed and the ^1H NMR spectrum shows a singlet at δ = 5.63 ppm, which was taken as a first hint for the formation of a backbone modified NHC **175** (Figure 61).

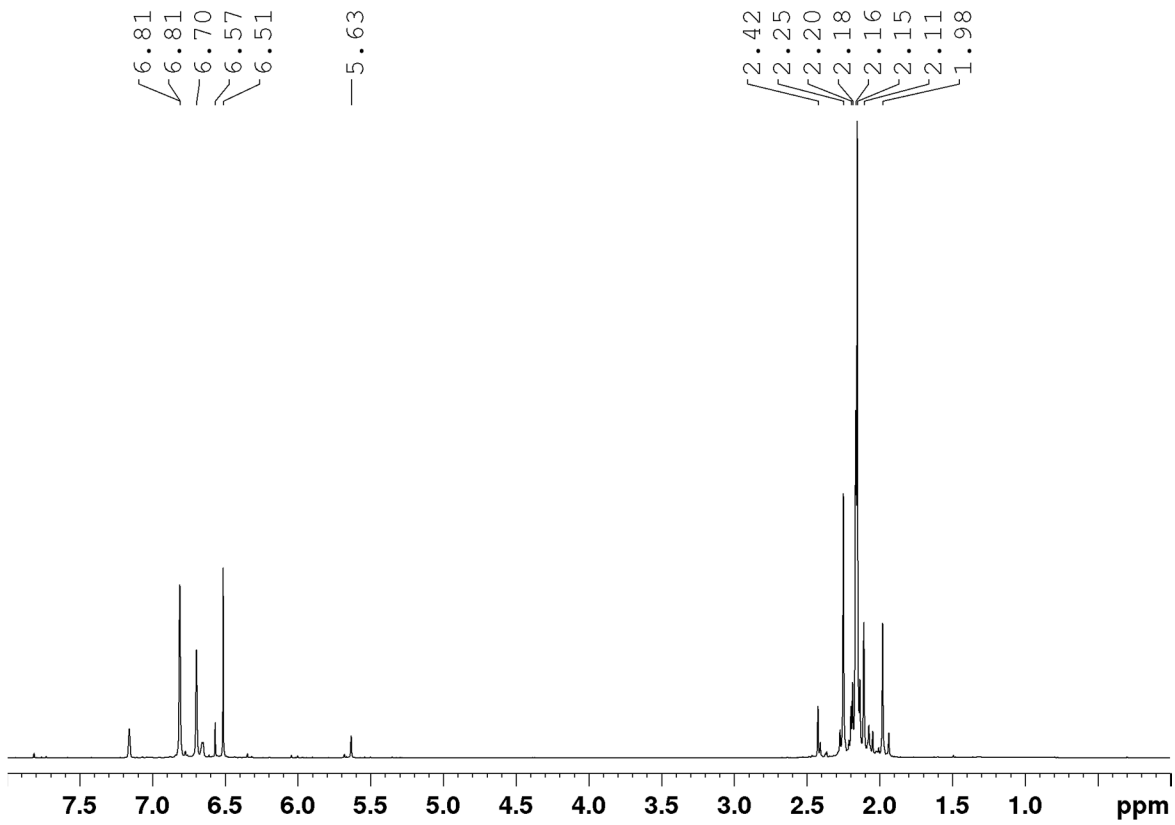

Figure 61. ^1H NMR spectrum of the reaction mixture of Mes_2SiHCl **173** with 2.2 eq of NHC^{Mes2}.

The ^{29}Si NMR spectrum reveals two new resonances at δ = −24.05 and −50.95 ppm (Mes_2SiHCl **173**: δ = −19.24 ppm) in a ratio of 19:81 (Figure 62).

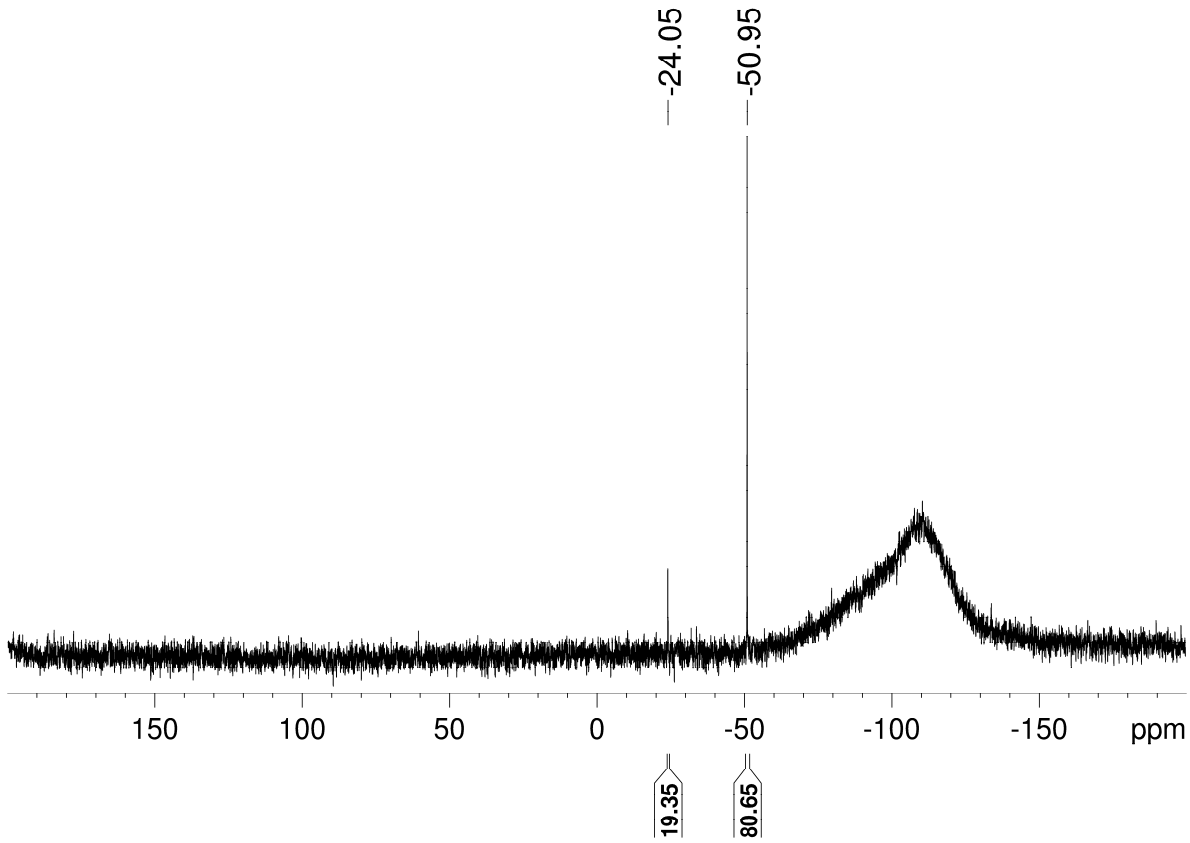

Figure 62. ^{29}Si NMR spectrum of the reaction mixture of Mes_2SiHCl **173** with 2.2 eq of NHC^{Mes2}.

The ^{13}C NMR spectrum displays a resonance at δ = 158.19 ppm, which might be attributed to a carbenic C-atom of an NHC-stabilized diaryl silylene **176** because the downfield shifts of the quaternary aryl signals of the precursors Mes_2SiHCl **173** and NHC^{Mes2} are with δ = 139.9 ppm and 144.3 ppm (greatest downfield shift in the ^{13}C NMR spectrum for both compounds) far away from this value (Figure 63).[197,198] Furthermore there is no cross signal of the resonance at δ = 158.19 ppm in the 2D ^{13}C/^{1}H HMQC or HMBC correlation spectra. The 2D ^{29}Si/^{1}H NMR correlation spectrum clearly indicates that the signal at δ = −50.95 ppm correlates with the signal at δ = 5.63 ppm in the ^{1}H NMR spectrum and therefore belongs most likely to the backbone modified NHC **175** (Figure 64).

In conclusion the reaction of Mes_2SiHCl **173** with 2.2 eq of NHC^{Mes2} led to the backbone modified NHC **175** to about 81%. The other 19% could reasonable be attributed to an NHC-stabilized silylene **176**, but unambiguous confirmation for its formation could not be obtained.

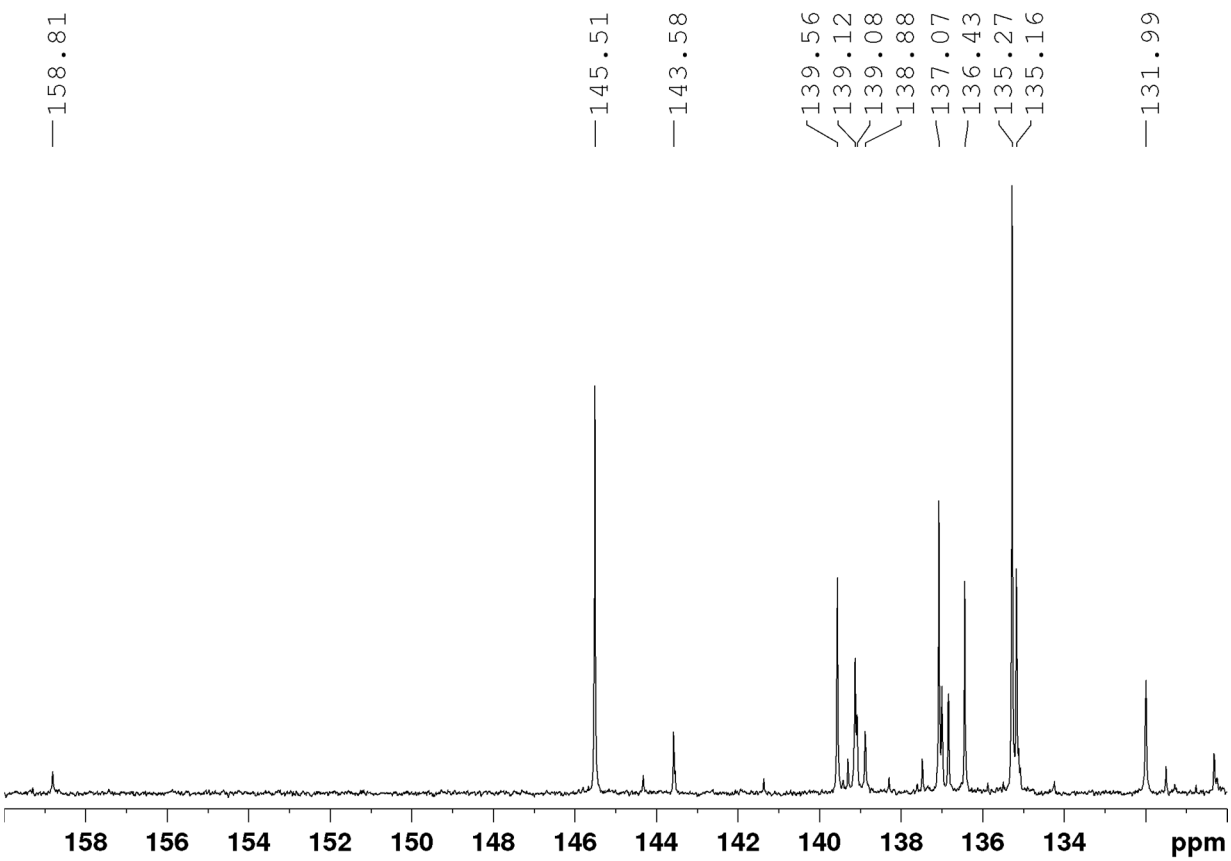

Figure 63. Excerpt of the aryl-region in the ^{13}C NMR spectrum of the reaction mixture of Mes_2SiHCl **173** with 2.2 eq of NHC^{Mes2}.

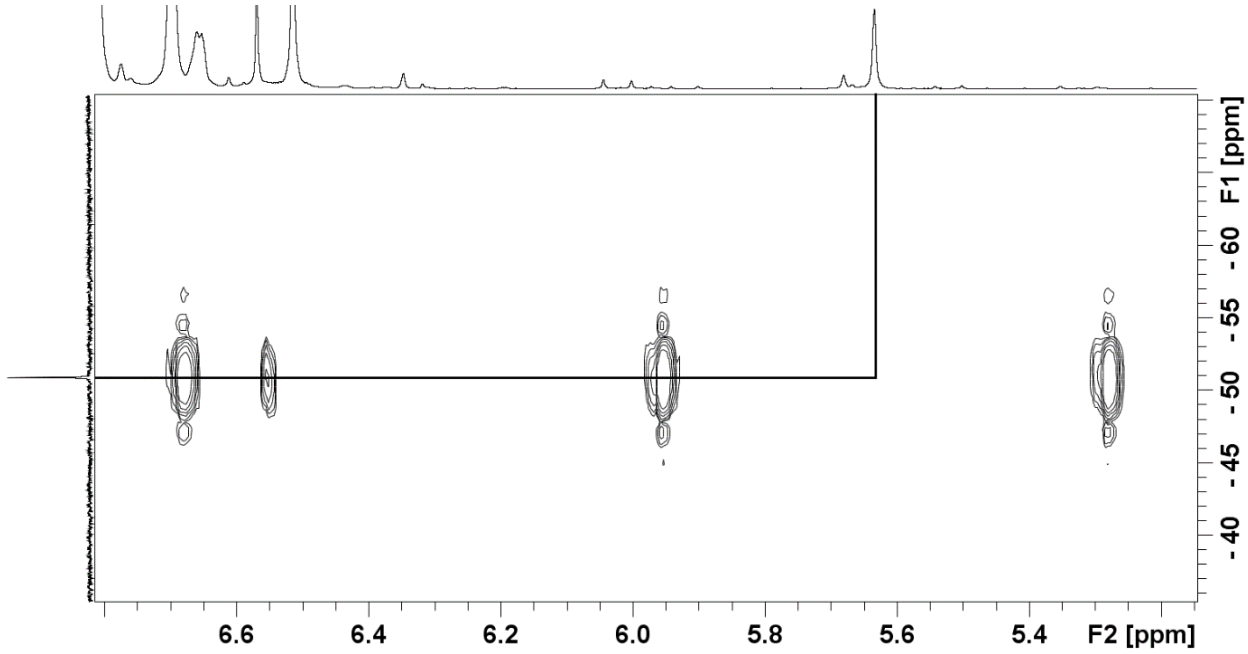

Figure 64. Selected area of the 2D $^{29}Si/^{1}H$ NMR correlation spectra of the reaction mixture of Mes_2SiHCl **173** with 2.2 eq of NHC^{Mes2}.

3.4.2. Attempts to Synthesize NHC-Stabilized Arylchloro Silylenes *vs.* Backbone Activation of NHCs

3.4.2.1. Reaction of $TipSiCl_3$ 178 with NHC^{Mes2}

The reaction of $TipSiCl_3$ **178** with 2 eq of NHC^{Mes2} could in principle lead to the NHC-coordinated arylchloro silylene **180** or could form the backbone functionalized NHC **179** (Scheme 112).

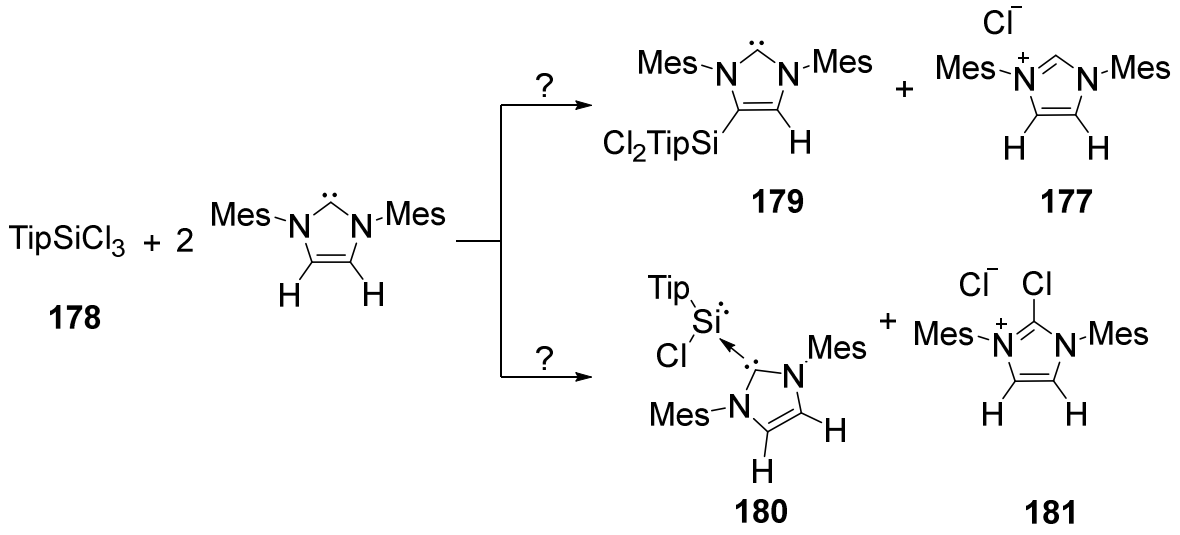

Scheme 112. Proposed reaction pathways for the reaction of $TipSiCl_3$ **178** with 2 eq of NHC^{Mes2}.

The addition of the colorless benzene solution of the trichloroaryl silane **178** to a suspension of 2 eq of the NHC^{Mes2} in benzene solution induced an immediate change in color to deep red with concomitant formation of a precipitate (Scheme 113).

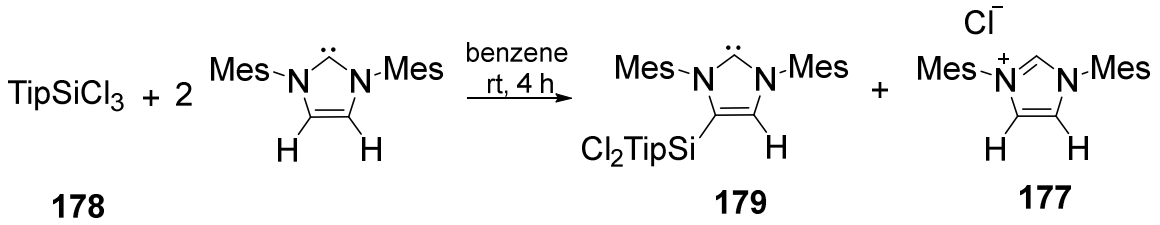

Scheme 113. Reaction of $TipSiCl_3$ **178** with 2 eq of NHC^{Mes2} leading to functionalized NHC **179**.

Complete conversion in a new product was observed after four hours at room temperature. The aryl-protons of the Tip-group are located at δ = 7.11 ppm in the ^1H NMR spectrum (Figure 65). Only one signal for a proton at a C-C-double bond is observed at δ = 7.08 ppm suggesting backbone substituted carbene **179** as product,

which is highfield shifted in contrast to the silyl-functionalized NHC **160** reported by Roesky *et al.* (δ = 7.45 ppm) or Ghadwal's silyl functionalized NHC **182** (δ = 7.25-7.44 ppm).[186,191,196,198]

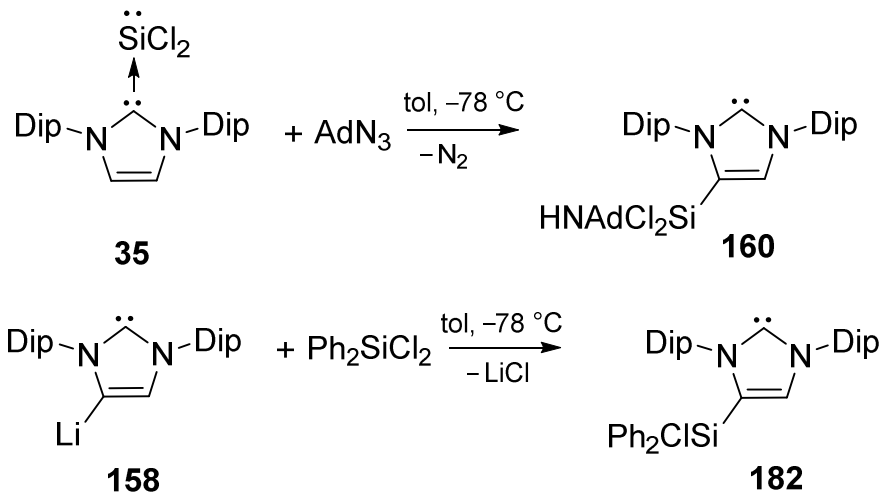

Scheme 114. Silyl-substituted NHC **160** reported by Roesky *et al.* (Ad = adamantly, Dip = 2,6-$^{i}Pr_2C_6H_3$) and silyl functionalized NHC **182** synthesized by the group of Ghadwal.

The aryl protons for the two mesityl-groups are also chemical inequivalent and result in two resonances at δ = 6.84 and 6.74 ppm in the integrated ratio of 1:1. Furthermore the resonances of the methine protons at the Tip-group reveal the expected sets of two septets at δ = 3.81 and 2.70 ppm in a ratio of 2:1. The CH_3-groups of the mesityl-substituents at the nitrogen atoms of the functionalized carbene **179** display different chemical shifts between δ = 2.25 and 2.10 ppm in the ^{1}H NMR spectrum, which is most likely due to the silyl-group in the backbone (Figure 65).

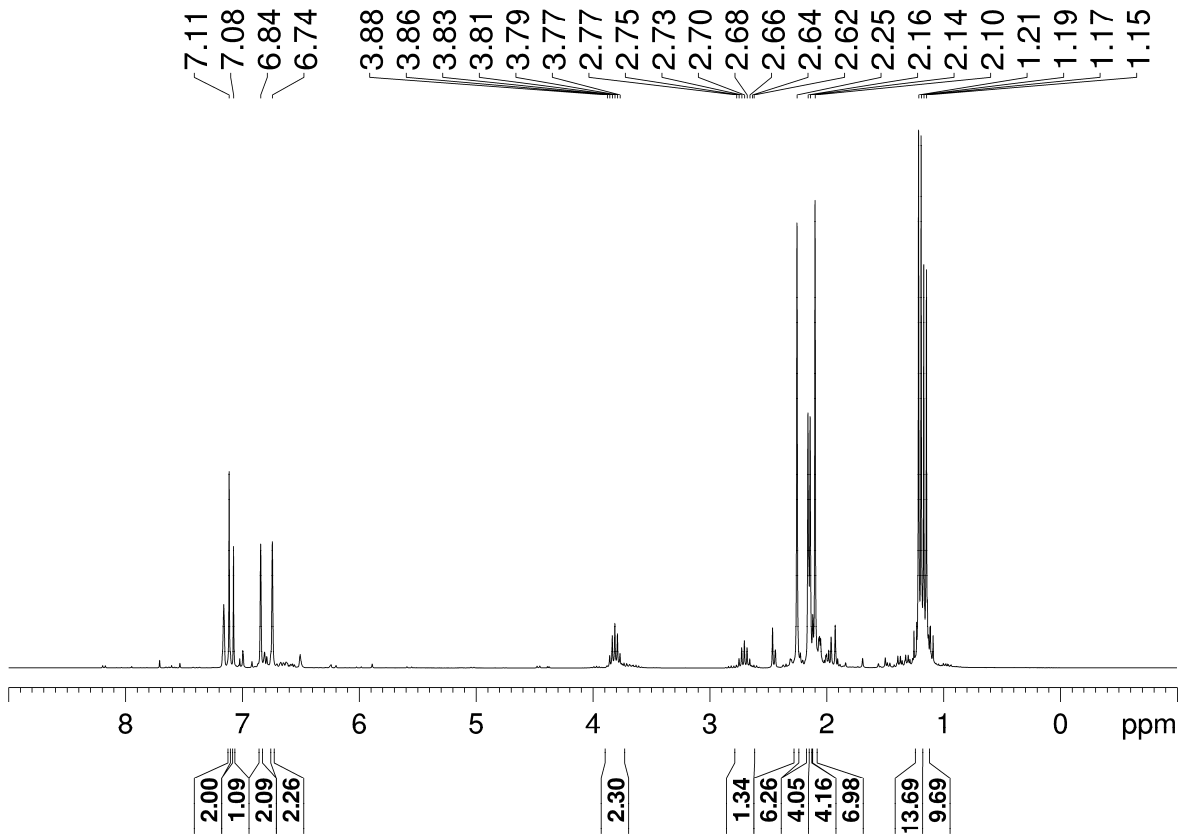

Figure 65. ^{1}H NMR spectrum of the reaction mixture of $TipSiCl_3$ **178** with 2 eq of NHC^{Mes2}.

The ^{29}Si NMR spectrum shows one new resonance at δ = −10.19 ppm ($TipSiCl_3$ **178**: ^{29}Si NMR: δ = −4.09 ppm, NHC **160**: δ = −30.01 ppm, NHC **182**: δ = −9.19 ppm) indicative for a tetracoordinate silicon atom (Figure 66).[186,191,199] An excerpt of the 2D ^{29}Si/^{1}H NMR correlation spectra show a cross signal between the ^{29}Si NMR resonance at δ = −10.19 ppm and the proton of the C-C-double bond at δ = 7.08 ppm, which supports the structure suggestion as backbone modified NHC **179** (Figure 67).

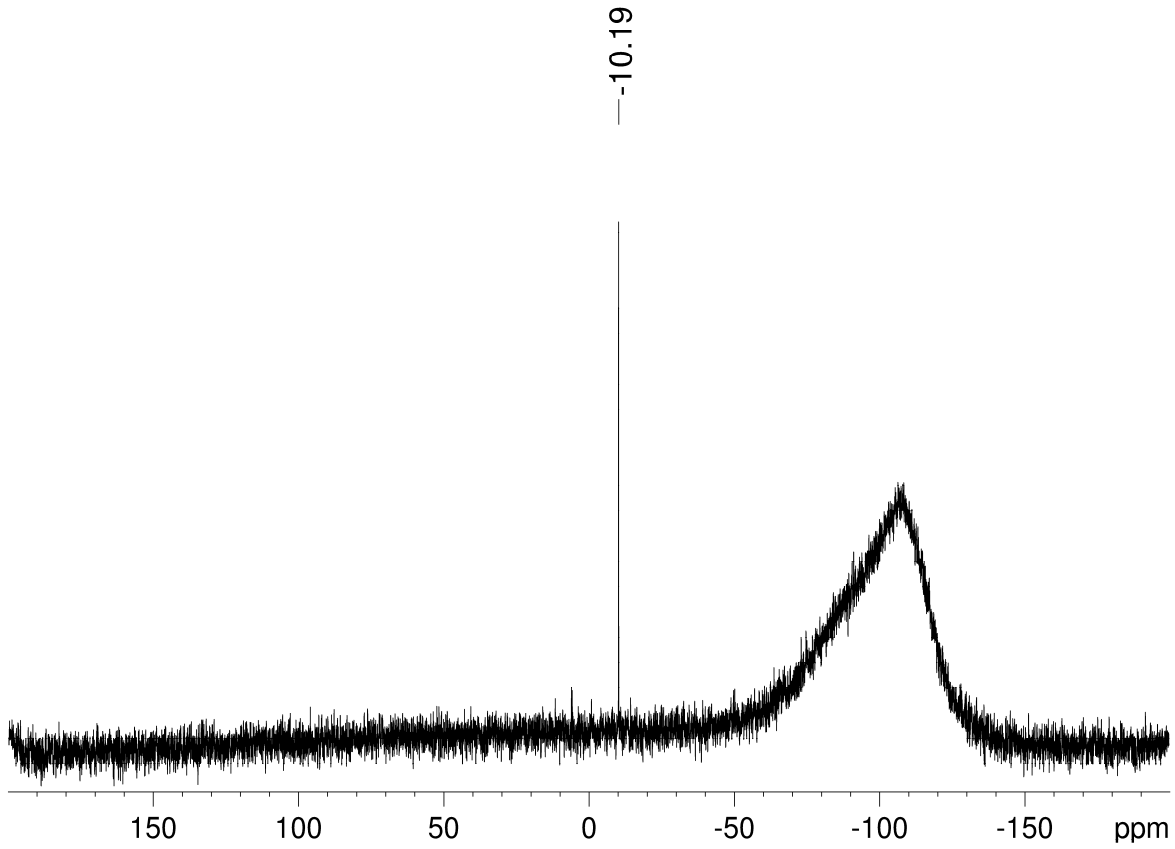

Figure 66. ^{29}Si NMR spectrum of the reaction mixture of $TipSiCl_3$ **178** with 2 eq of NHC^{Mes2}.

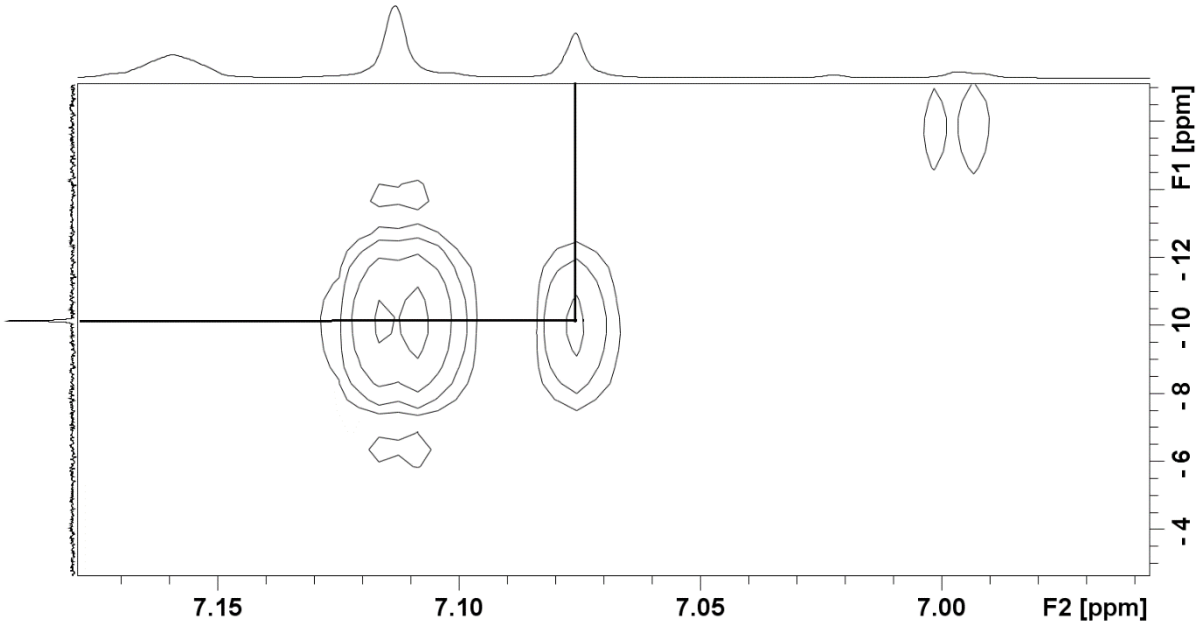

Figure 67. Selected area of the 2D ^{29}Si/^{1}H NMR correlation spectra of the reaction mixture of $TipSiCl_3$ **178** with 2 eq of NHC^{Mes2}.

A resonance that could be attributed to the carbenic C-atom was not observed in the ^{13}C NMR spectrum (Figure 68) most likely due to the measured range which is not sufficient to detect the NCN resonance (measured only up to 220 ppm, NCN for **160**: 224.21 ppm, NCN for **182**: 225.12 ppm).

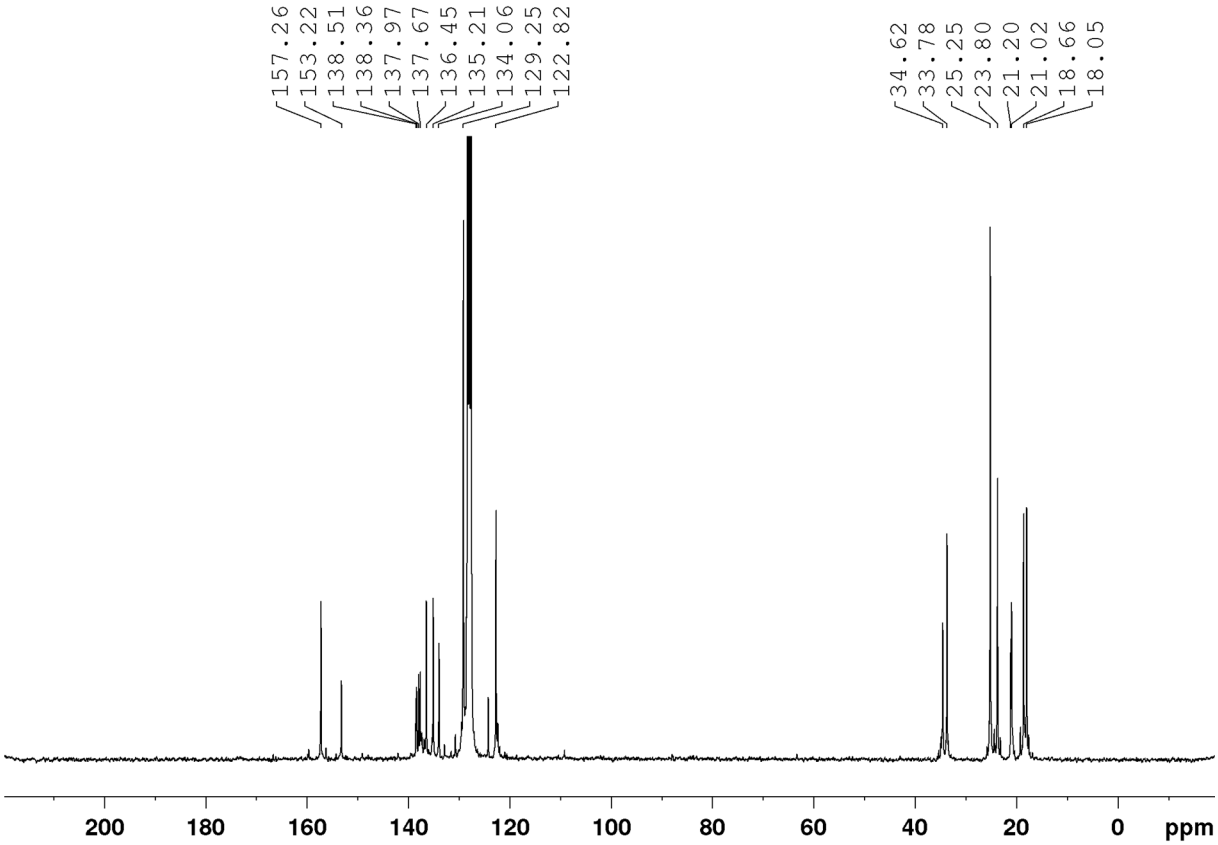

Figure 68. ^{13}C NMR spectrum of the reaction mixture of $TipSiCl_3$ **178** with 2 eq of NHC^{Mes2}.

3.4.2.2. Reaction of TipSiCl$_3$ 178 with NHC^{iPr2Me2}

In the context for the targeted synthesis of an NHC-stabilized arylchloro silylene the reaction of TipSiCl$_3$ **178** with NHC^{iPr2Me2} should clarify the question if an activation of the methyl-group in the backbone of the NHC is preferred, leading to **183** or if an NHC-stabilized silylene **184** can be obtained (Scheme 115).

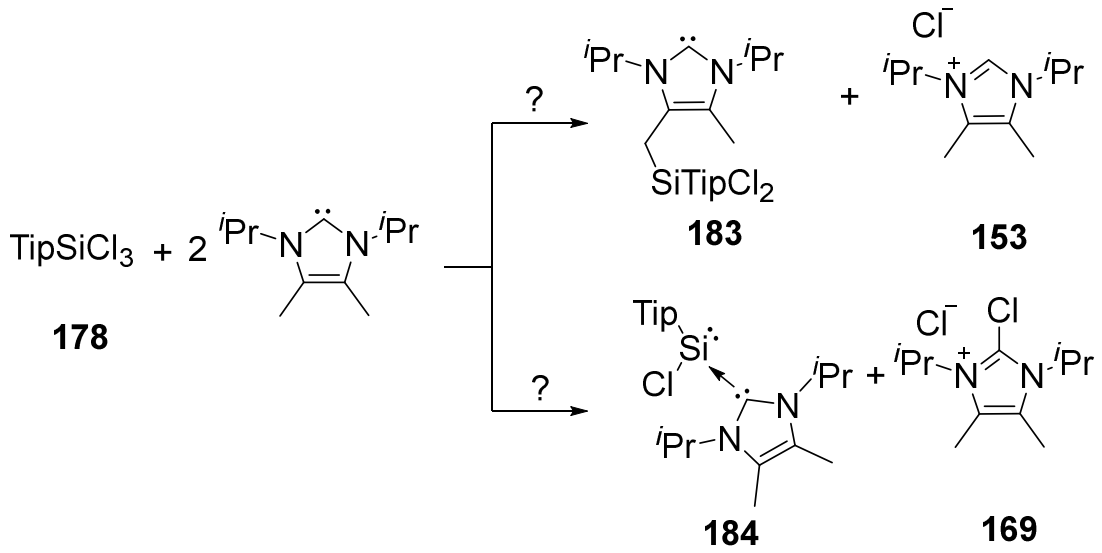

Scheme 115. Proposed reaction pathways for the reaction of TipSiCl$_3$ **178** with 2 eq NHC^{iPr2Me2}: backbone activation of NHC^{iPr2Me2} *vs.* chlorine abstraction.

The treatment of TipSiCl$_3$ **178** with two equivalents of NHC^{iPr2Me2} in benzene induced a change in color from colorless to deep red after 10 min at room temperature (Scheme 116).

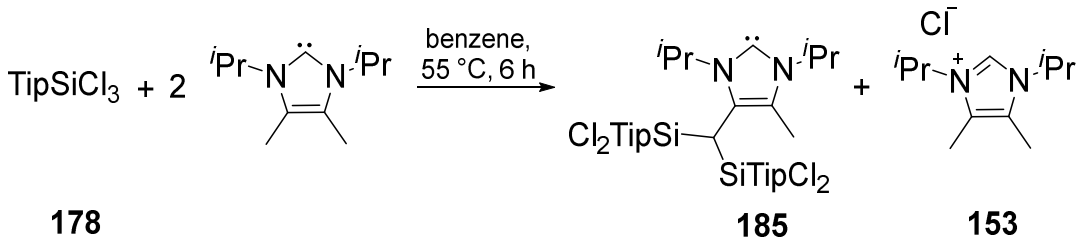

Scheme 116. Synthesis of disilyl carbene **185**.

The ^{29}Si NMR spectrum reveals the formation of a single product at δ = 7.42 ppm. The sample was heated for 6 hours to 55 °C to complete the reaction. The formation of the imidazolium chloride **153** was observed together with free NHC^{iPr2Me2}, which excluded the formation of an NHC-coordinated arylchloro silylene **184** simply by stoichiometric considerations.

Furthermore, a second resonance for a carbenic carbon-atom at δ = 211.01 ppm beside the signal of the free NHC^{i}Pr2Me2 is detected, which gave hints for the formation of a backbone modified NHC. The ^{13}C DEPT 135 NMR spectrum displays no negative signal, excluding the presence of a methylene-group in the formed molecule. The excess of NHC^{i}Pr2Me2 was sublimed under reduced pressure and the red residue dissolved in hexane. After filtration from warm hexane, the mother liquor was concentrated and stored at −26 °C for one week affording red crystals suitable for X-ray diffraction analysis. Surprisingly, the molecular structure disclosed the unprecedented NHC **185** with two SiTipCl$_2$-units at one methyl-group in the backbone (Figure 69).

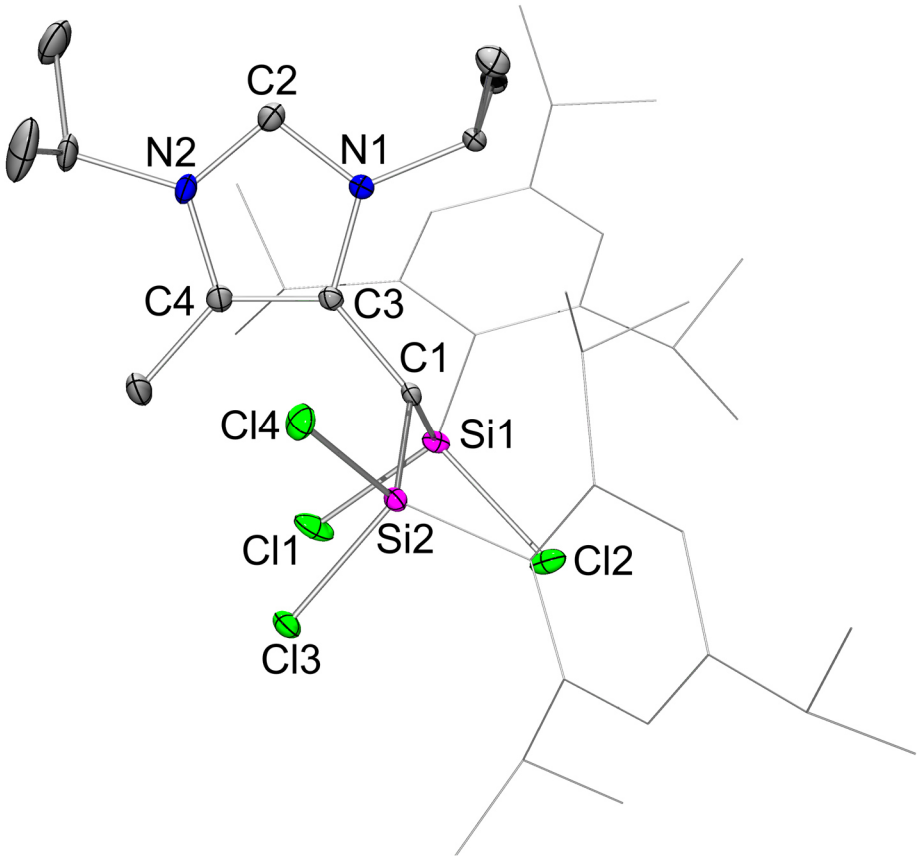

Figure 69. Molecular structure of **185** in the solid state (ellipsoids are at 30%, hydrogen atoms omitted for clarity). Selected bond lengths [Å]: N1-C2 1.370(2), N2-C2 1.355(3), N1-C3 1.413(3), N2-C4 1.391(3), C1-C3 1.513(3), Si1-C1 1.884(2), Si2-C1 1.904(2), Si1-Cl1 2.0559(7), Si1-Cl2 2.0680(7), Si2-Cl3 2.0548(7), Si2-Cl4 2.0668(7), C3-C4 1.353(3).

The N1-C2 bond distance of **185** is slightly longer (1.370(2) Å) than the N2-C2 bond distance (1.355(3) Å) most likely due to the steric requirements of the two silyl groups at the C1 position. The N2-C2 bond length is the same when compared to the N1-C1

bond in free NHC^{iPr2Me2} (1.355 Å). The double bond between C4-C3 is with 1.353(3) Å in good agreement with the double bond in free NHC^{iPr2Me2} (1.351 Å). The C1-C3 bond is with 1.513(3) Å longer than in the case of the free carbene (1.491 Å), which can be attributed to the silicon atoms at the C1 carbon atom.[200] In the UV/vis absorption spectrum of **185** a broad shoulder is observed (between λ = 480 and 420 nm). A second absorption band is detected at λ_{max} = 278 nm (ε = 4700 $Lmol^{-1}cm^{-1}$). Silyl functionalization at the C=C-bond of NHC^{Dipp_2} are literature known, whereas disilyl modified NHC **185** is the first example for a silyl functionalization at the methyl-group of the backbone.[186,191]

If the reaction is carried out in the right stoichiometry ($TipSiCl_3$: NHC^{iPr2Me2} 2:3), the reaction proceeds slower and prolonged heating for 4 days at 60 °C was necessary to obtain a conversion of about 85% (determined by ^1H NMR spectrum). The mechanism of the reaction could be rationalized by a first formation of the pentacoordinated NHC^{iPr2Me2}-$TipSiCl_3$ complex **[186]**, which are already known for NHCs and cAACs (cyclic alkyl amino carbenes) with SiR_4 (R = Cl, Br or I).[146,196,201] In a second step a molecule of free NHC^{iPr2Me2} would abstract a proton of a methyl-group in the backbone of the activated NHC-complex **[186]** (Scheme 117). The formed carbanion in intermediate **[187]** at the CH_2-unit could now attack the silicon-center at a $TipSiCl_3$-molecule leading to intermediate **[188]** with elimination of the imidazolium chloride **153**. In a next step the needed excess of free NHC^{iPr2Me2} could again abstract a proton from the substituted methyl-group in the backbone of the NHC-complex **[188]** forming the carbanion complex **[189]**. The fact that no free $TipSiCl_3$ is left in the reaction mixture would allow complex **[189]** to eliminate $TipSiCl_3$, which thus could be attacked by the carbanion of formed silyl functionalized NHC **[190]** finally resulting in the disilyl functionalized NHC **185** by elimination of **153**.

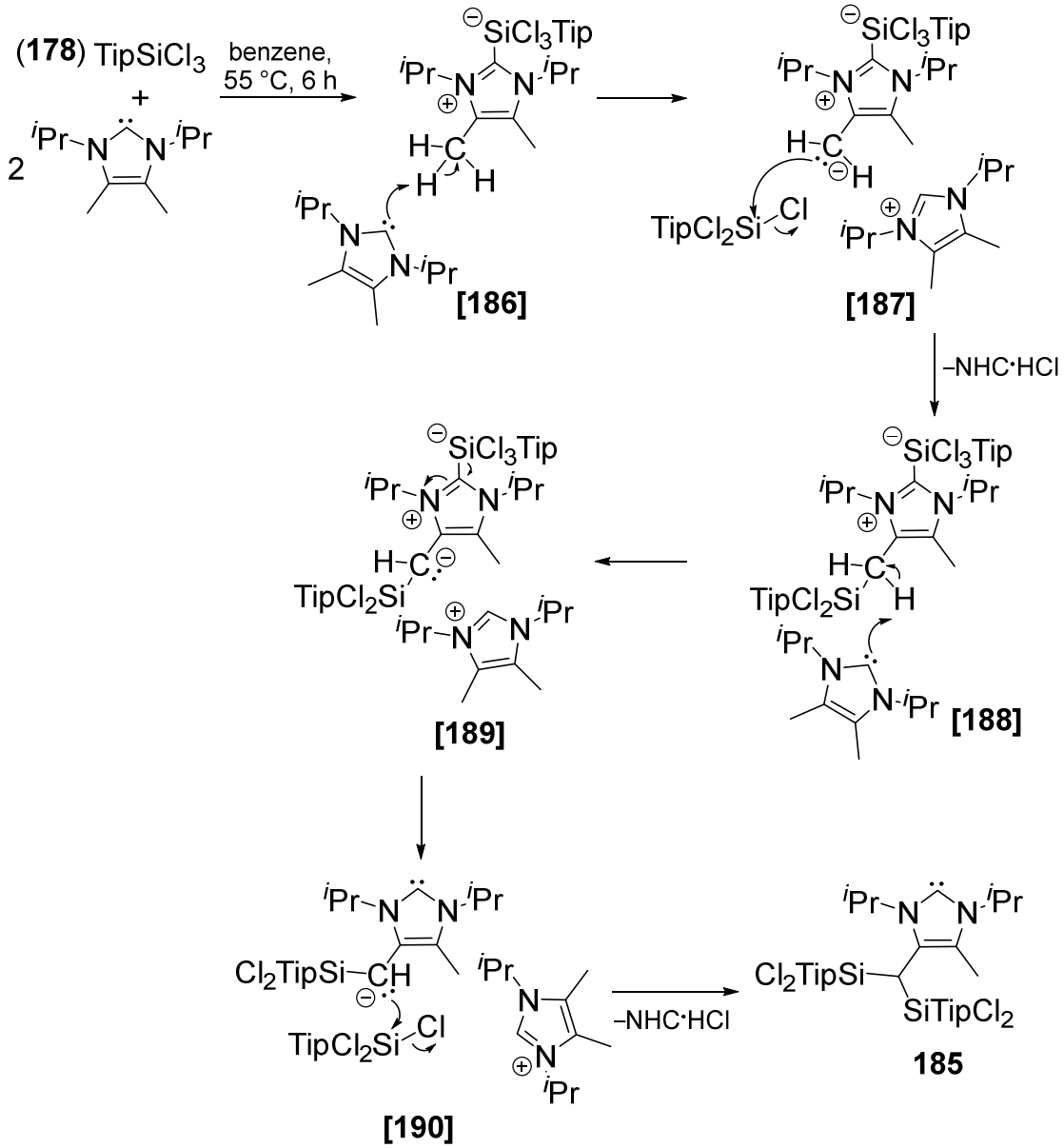

Scheme 117. Proposed mechanistic scenario for the formation of disilyl functionalized NHC **185**.

3.4.3. Reactivity of Disilyl Carbene 185

3.4.3.1. Reduction Attempt of Disilyl Carbene 185 with 2 eq KC_8

The unprecedented formation of the doubly backbone chlorosilyl functionalized NHC **185** offers the opportunity for reduction attempts with the aim to obtain bis-carbene **193** or silirene functionalized carbene **194**. These functionalized NHCs could be either obtained by step wise reduction over **191** and **192** or by reductive dehalogenation of **185** (Scheme 118).

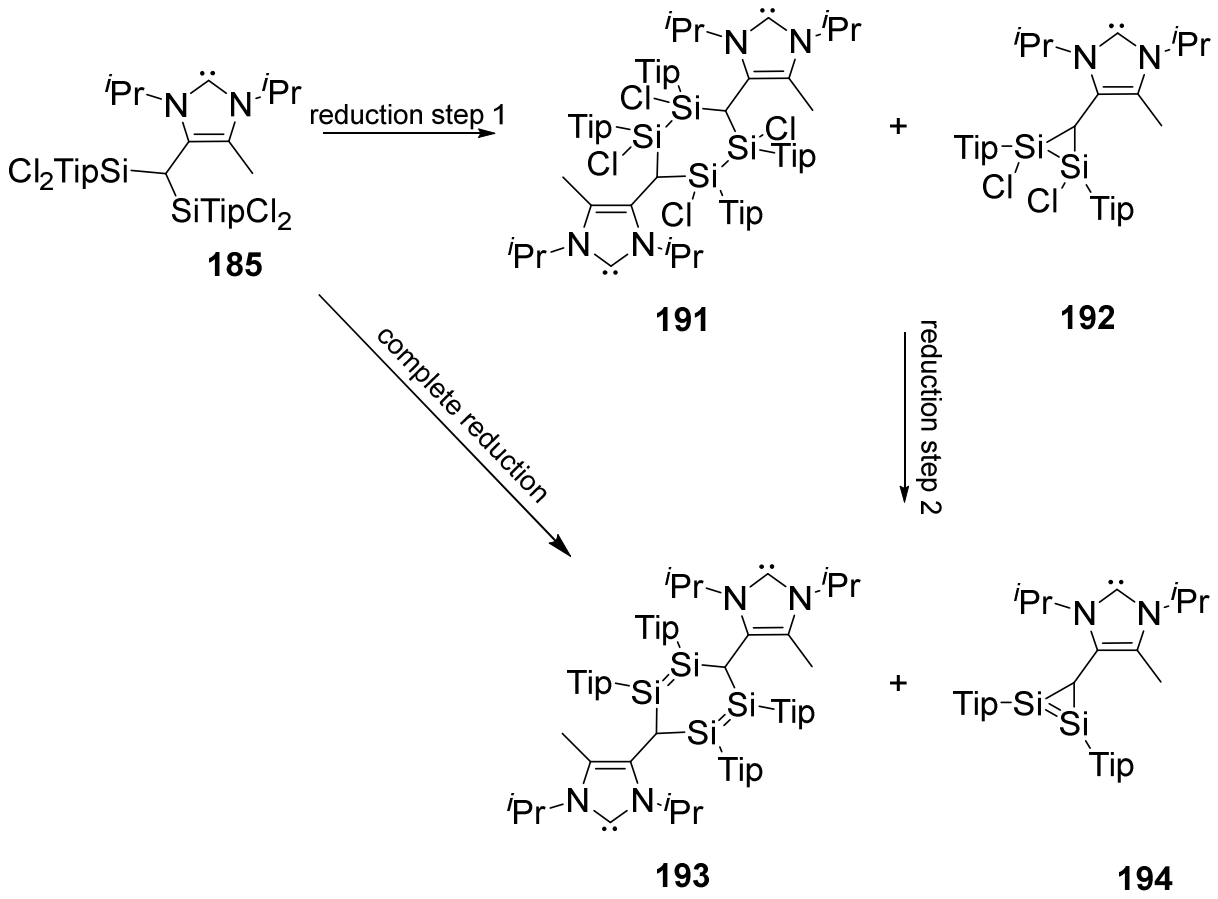

Scheme 118. Proposed reduction products of disilyl carbene **185**.

To gain a first impression of the reduction behavior of disilyl carbene **185**, the reduction with 2 eq of KC_8 at −50 °C in thf was investigated (Scheme 119). The reaction mixture was slowly allowed to warm to room temperature.

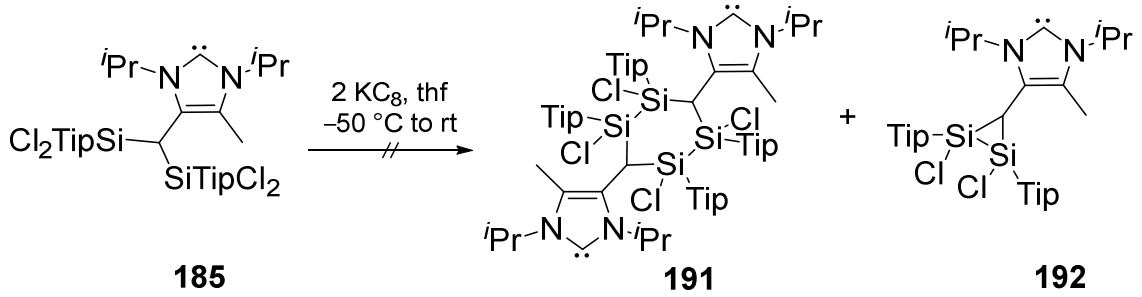

Scheme 119. Reduction of disilyl functionalized carbene **185** with 2 eq KC_8.

The ^{29}Si NMR spectrum shows four resonances at δ = −10.49, −15.87, −28.36 and −31.28 ppm, which are in the typical region of tetracoordinate silicon-atoms (Figure 70).

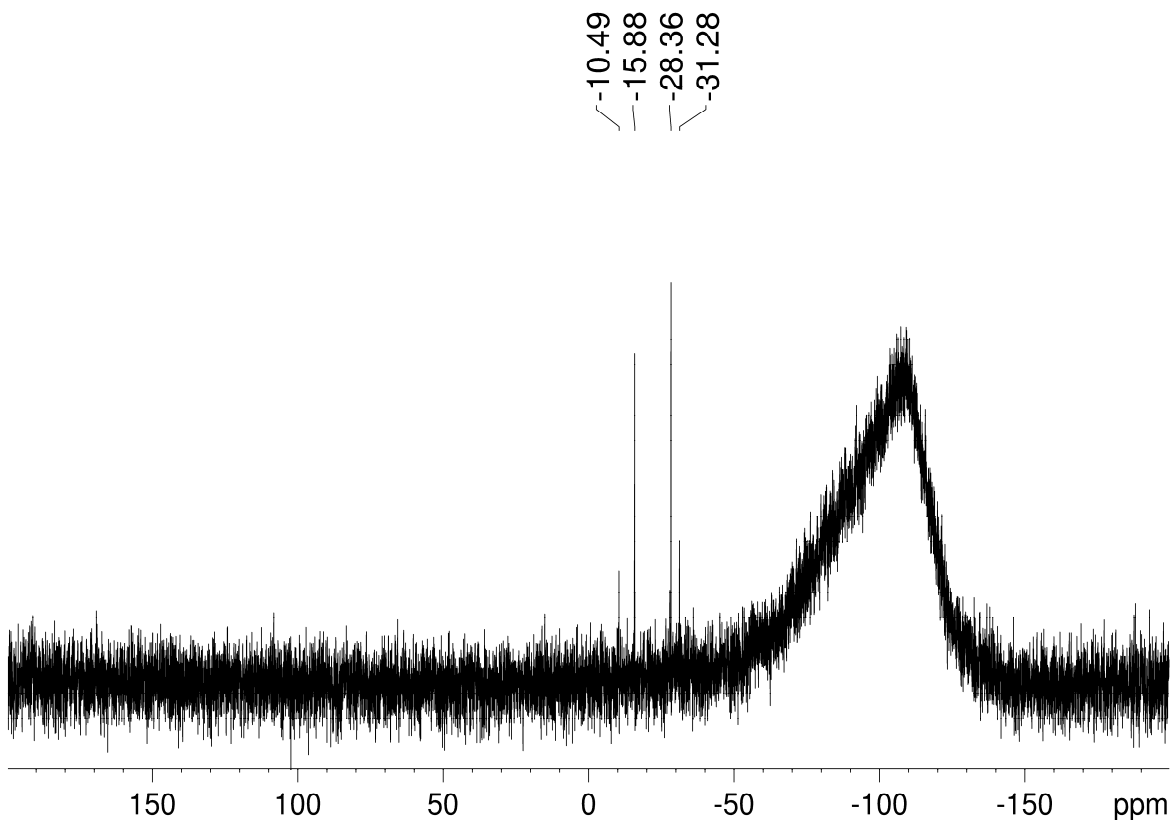

Figure 70. ^{29}Si NMR spectrum of the reaction mixture of the reduction of **185** with 2 eq KC_8.

The ^{1}H NMR spectrum reveals a mixture of products indicating a series of signals in the aryl-region, as well in the alkyl region. The ^{13}C NMR spectrum confirms these observations showing numerous of aryl resonances at δ = 130-140 ppm. The carbenic C-atom was not detected which is an indication that the two proposed reduction products **191** and **192** had not been formed. Unfortunately it was not possible to separate and analyze any one of the formed products.

3.4.3.2. Reduction Attempt of Disilyl Carbene 185 with Na/K

The fact that the stepwise reduction of functionalized NHC **185** with 2 eq of KC_8 was not possible, we investigated a complete reductive dehalogenation with an excess Na/K in thf/toluene solution which directly could lead to the proposed bis-carbene **193** or silirene functionalized NHC **194** (Scheme 120).

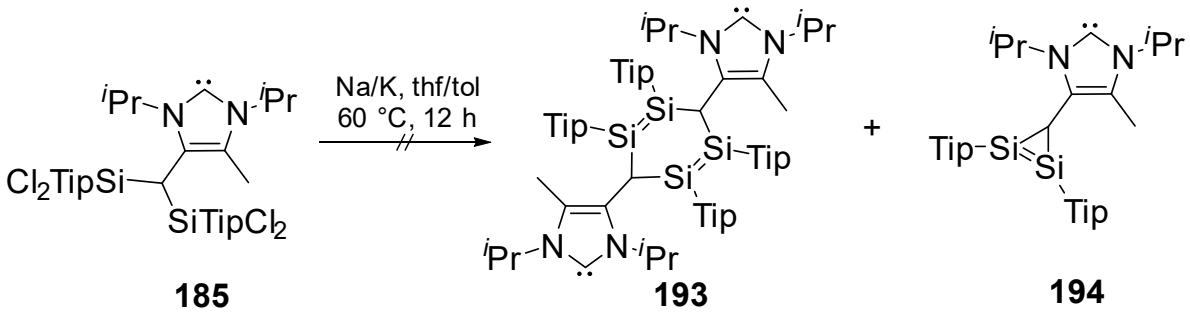

Scheme 120. Reduction of disilyl functionalized carbene **185** with Na/K.

Since there was no reaction after 2 hours at room temperature, the reaction mixture was heated up to 60 °C for 12 hours. The ^{1}H NMR spectrum reveals only one small signal in the aryl region at δ = 7.00 ppm indicating a decomposition of functionalized NHC **185** (Figure 71).

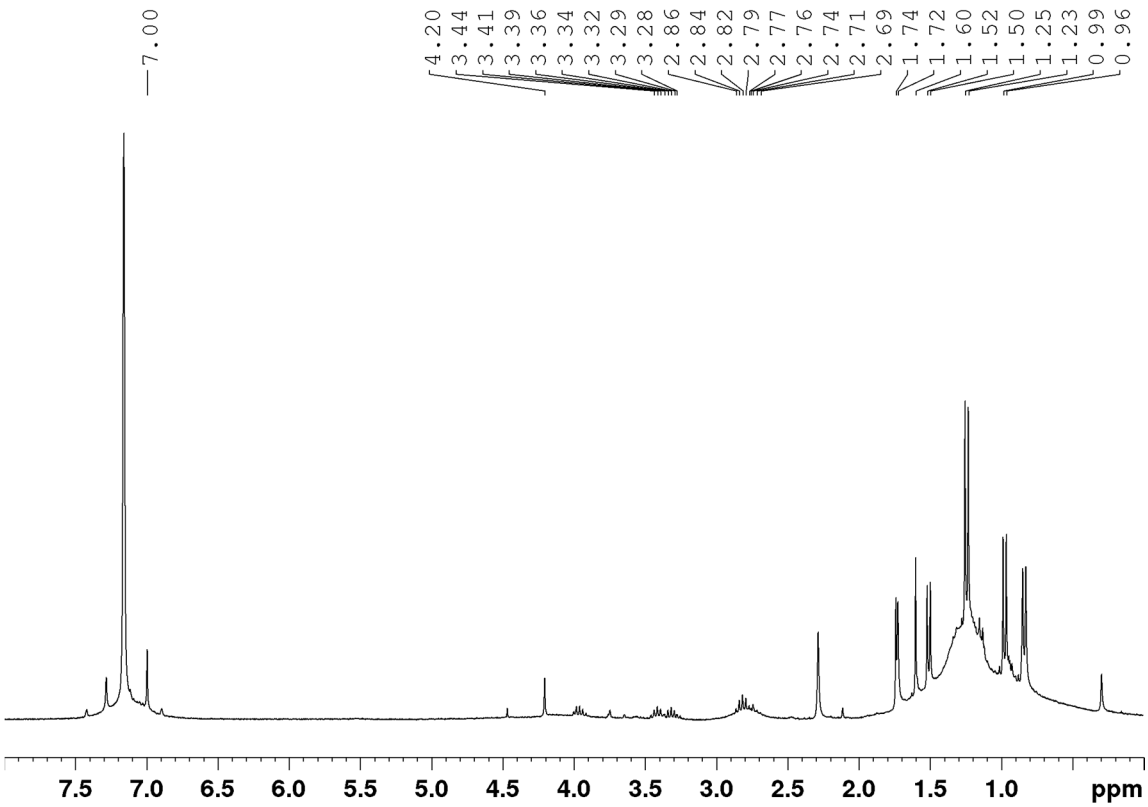

Figure 71. ^{1}H NMR spectrum of the reaction mixture of disilyl functionalized carbene **185** with Na/K.

The ^{13}C NMR spectrum shows some broadened signals, whereas the ^{29}Si NMR spectrum only reveals one resonance at δ = −68.58 ppm (Figure 72). These observations excluded the formation of the desired dimerization product **193** or the functionalized NHC **194**. It was not possible to separate a product from the reaction mixture by crystallization form a concentrated hexane solution at room temperature.

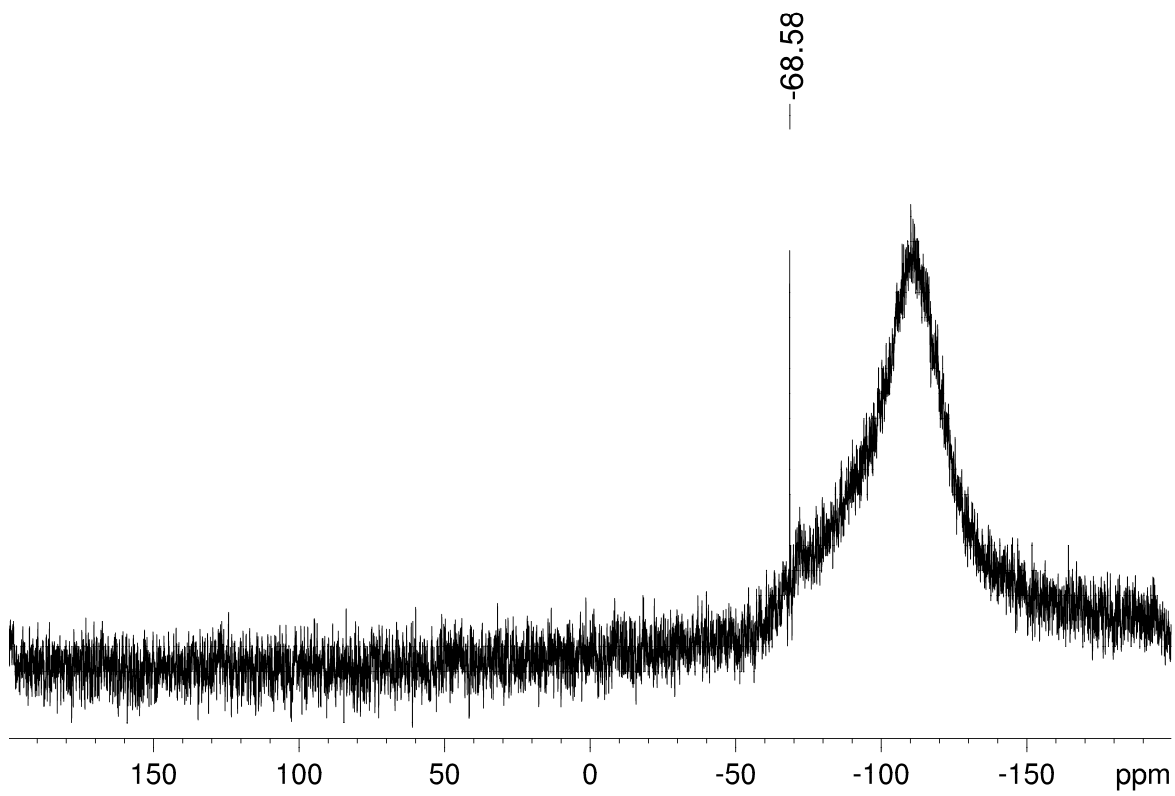

Figure 72. ^{29}Si NMR spectrum of the reaction mixture of disilyl functionalized carbene **185** with Na/K.

Attempts to synthesize one of the proposed reduction products **191-194** with the reducing agents Li/naphthalene (2 and 4 eq), KC_8 (4 eq), Mg-powder, Li-powder and Jones Mg(0)[72] failed and led to an unidentified mixture of products (Scheme 121). No further investigations on reductions attempts were carried out.

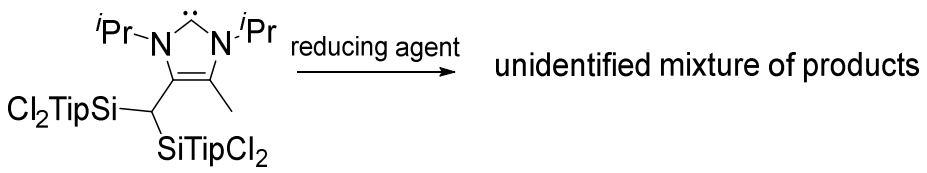

185

Scheme 121. Reduction attempts of disilyl carbene **185** with different reducing agents (Li/naphthalene (2 and 4 eq), KC_8 (4 eq), Mg-powder, Li-powder and Jones Mg(0)) leading to a complex mixture of products.

3.4.3.3. Reaction of Disilyl Carbene 185 with $BH_3 \cdot SMe_2$

To see if the functionalized NHC **185** can be utilized as a complexation reagent, it was treated with $BH_3 \cdot SMe_2$ in toluene at room temperature which resulted in the conversion into a single product (Scheme 122). After workup, a concentrated hexane solution was stored at room temperature to afford colorless crystals which were analyzed by NMR-spectroscopy in order to exclude the formation of imidazolium chloride **153**.

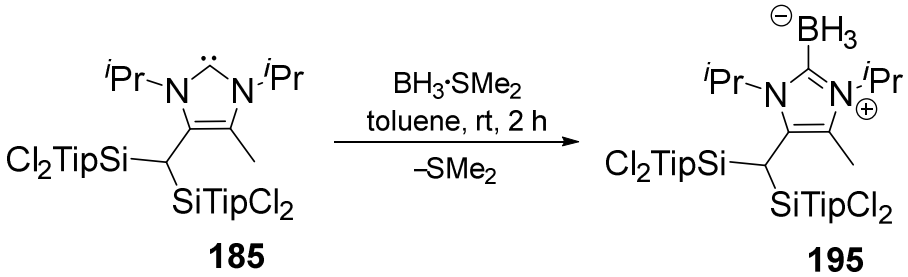

Scheme 122. Reaction of disilyl carbene **185** with $BH_3 \cdot SMe_2$.

The ^{29}Si NMR spectrum shows one resonance at δ = 7.46 ppm (Figure 73) nearly identical when compared to disilyl backbone functionalized carbene **185** (δ = 7.42 ppm).

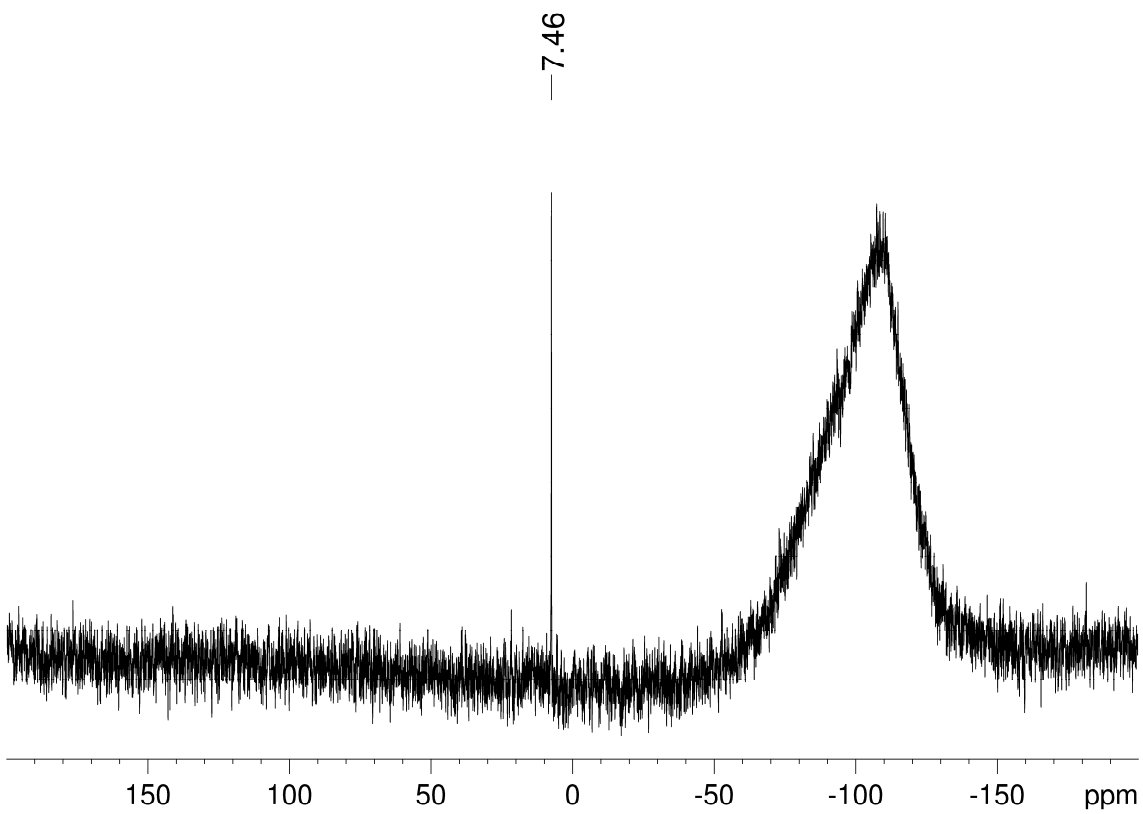

Figure 73. ^{29}Si NMR spectrum of the colorless crystals of disilyl carbene **185** with $BH_3 \cdot SMe_2$.

In the ^{13}C NMR spectrum the resonance of the carbenic C-atom disappeared in line with the formation of the Lewis-acid-base complex **195** (Figure 74). The two resonances at δ = 49.81 and 49.51 ppm can be attributed to the *C*H-atoms of the *iso*-propyl groups of carbene **195**. However, the signal of the C2-atom attached to the boron-center could not be detected in the ^{13}C NMR spectrum due to coupling of this C-atom to the quadrupolar ^{11}B nucleus (Figure 74).

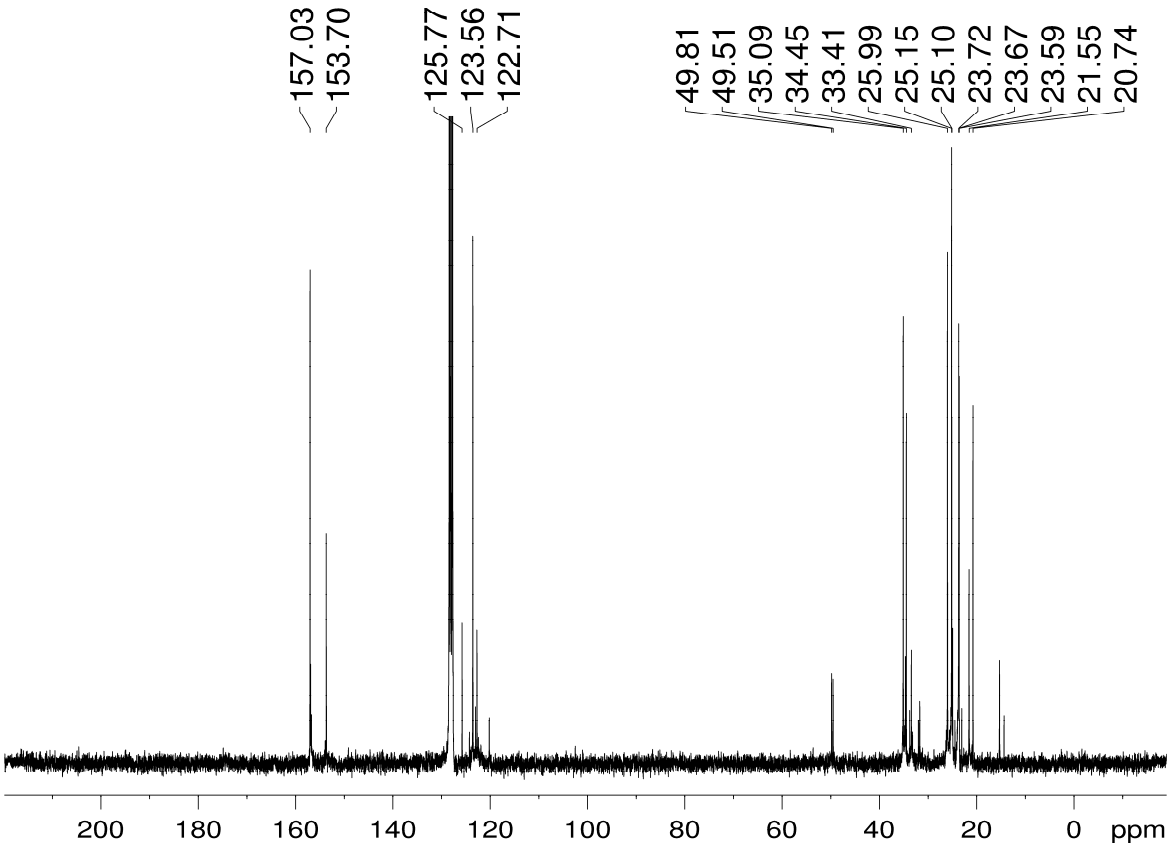

Figure 74. ^{13}C NMR spectrum of the colorless crystals of disilyl carbene **185** with $BH_3 \cdot SMe_2$. The excerpt shows the alkyl-region.

The ^{11}B NMR spectrum shows not the expected quartet for the BH_3-group, instead of a single broadened resonance at δ = −32.79 ppm (Figure 75) is observed which is in good agreement with the NHC^{iPr2Me2}·BH_3-complex **196** reported by Kuhn *et al.* (^{11}B NMR: δ = −34.12 ppm, Scheme 123).[202]

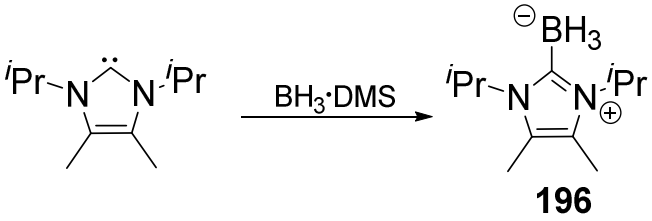

Scheme 123. Synthesis of NHC-BH_3 complex **196** reported by Kuhn *et al*.[202]

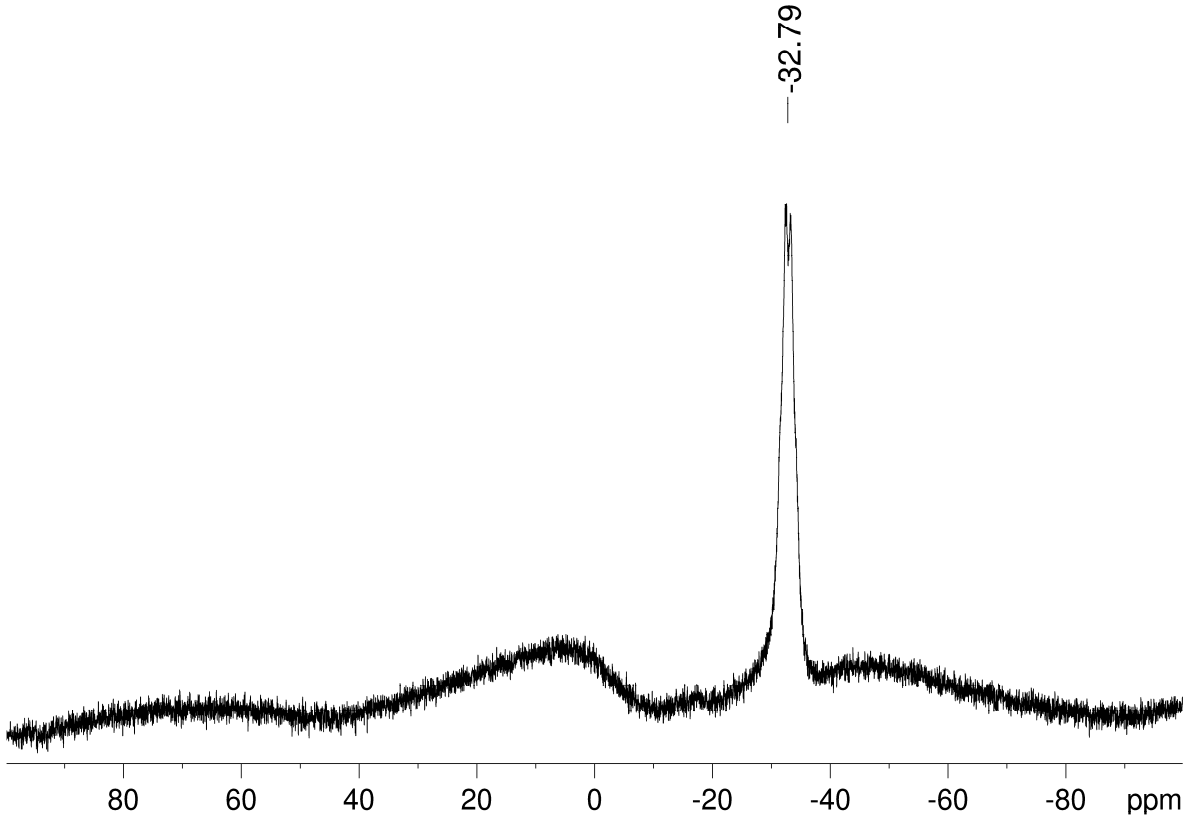

Figure 75. ^{11}B NMR spectrum of the colorless crystals of disilyl carbene **185** with $BH_3 \cdot SMe_2$.

3.4.4. Synthesis of NHC-Coordinated Disilyl Germylene 200

In order to synthesize a suitable precursor for the efficient and mild formation of silagermenyildene **199** the synthesis of silyl chloro germylene **198** was targeted. As a precursor silyl anion **197** was synthesized upon reduction of silane **173** with 10 eq of Li-powder in thf at 0 °C according to a literature procedure (Scheme 124).[203] In the next step, a solution of silyl anion **197** in thf at −70 °C was added to a −70 °C cold suspension of $GeCl_2{\cdot}NHC^{iPr_2Me_2}$ **8** in thf and an immediate color change from colorless to orange was observed.

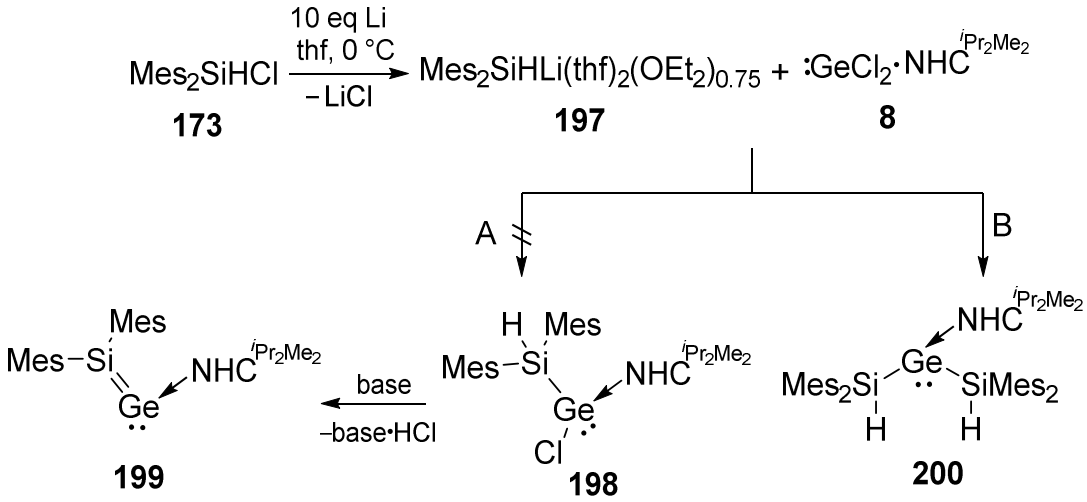

Scheme 124. Synthesis of silyl anion **197** and proposed reaction pathway of silyl anion **197** with $GeCl_2{\cdot}NHC^{iPr_2Me_2}$ **8** to precursor **198** and subsequent elimination of HCl with a base resulting in silagermenylidene **199** (pathway A) and obtained disilyl germylene **200** (pathway B).

After work up a ^{29}Si NMR spectrum indicates a mixture of products with one major signal at δ = −38.07 ppm (Figure 76), which would be in good agreement with the targeted NHC-stabilized silyl chloro germylene **198** (Scheme 124). The ^{13}C NMR spectrum shows one resonance at δ = 172.55 ppm typical for the coordination of an NHC to a Ge(II)-center.[61]

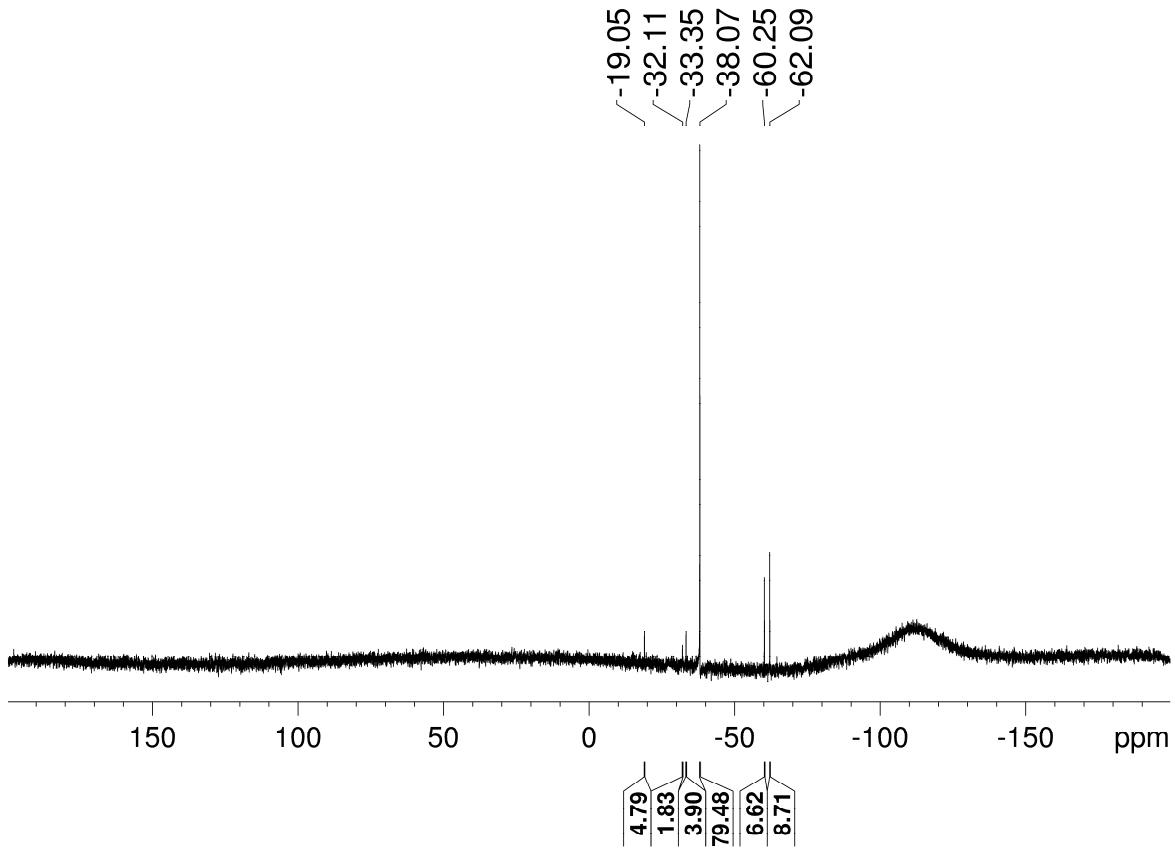

Figure 76. ^{29}Si NMR spectrum of the reaction mixture of silyl anion **197** with $GeCl_2{\cdot}NHC^{iPr_2Me_2}$ **8**.

The ^{1}H NMR spectrum reveals a typical septet for an NHC coordinated to a Ge(II)-center at δ = 6.09 ppm and a singlet for a Si*H* at δ = 6.37 ppm in an integrated ratio of 2:2 excluding the formation of the proposed product **198** (Scheme 124), which otherwise should be in an integrated ratio of 2:1. This led to the conclusion that a reaction in a 2:1 ratio had taken place and a disilyl germylene **200** stabilized by an NHC was formed. Yellow single crystals suitable for X-ray diffraction were obtained from a saturated toluene solution after three days at room temperature. The molecular structure reveals the connectivity of the expected NHC-coordinated bis-silyl germlyene **200** (Figure 77).

To prove the formation of germylene **200**, the reaction was repeated in the right stoichiometry (2:1) which afforded germylene **200** in 61% yield (Scheme 125).

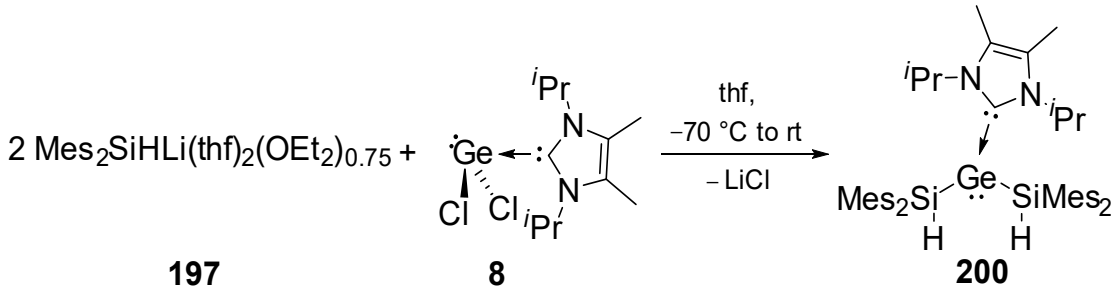

Scheme 125. Synthesis of NHC-stabilized bis-silyl germylene **200**.

The ^{29}Si NMR spectrum of a pure sample of bis-silyl germylene **200** shows a resonance at δ = −38.07 ppm, which means that germylene **200** is formed as major product (ca. 80%, determined by ^{29}Si NMR spectroscopy) in the reaction of silyl anion **197** with $GeCl_2 \cdot NHC^{iPr2Me2}$ **8** in a ratio of 1:1 (Figure 76).

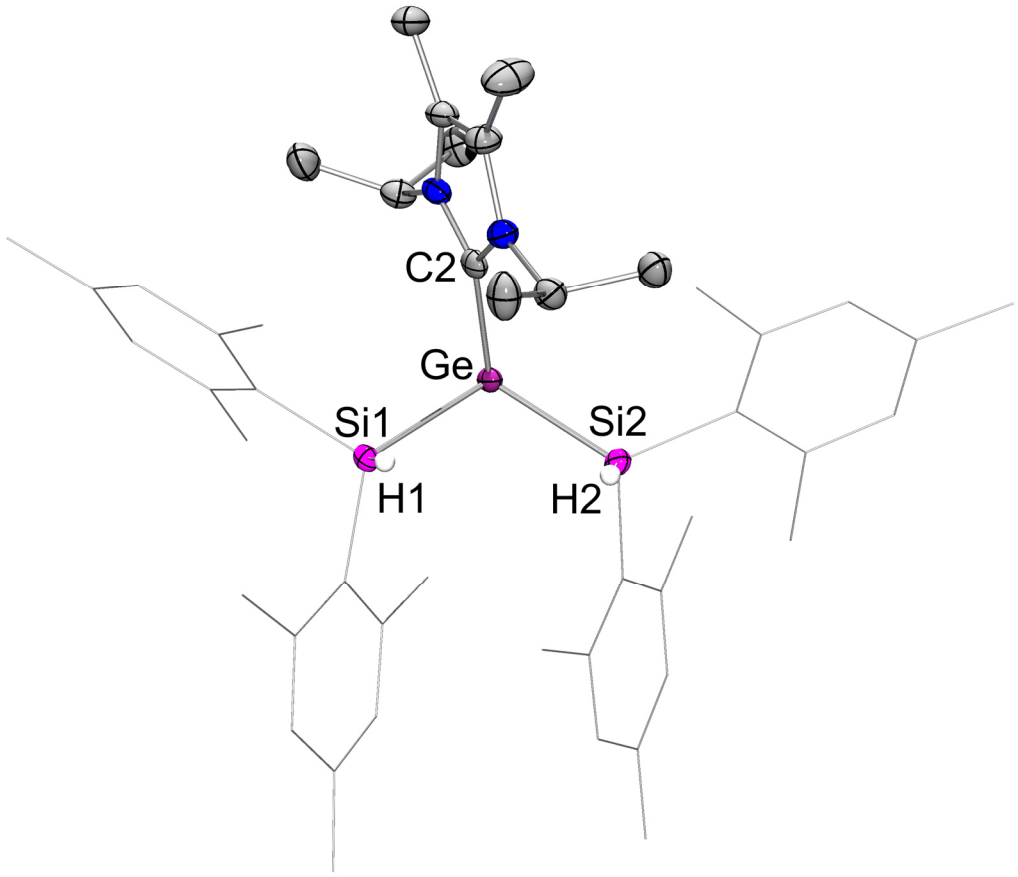

Figure 77. Molecular structure of **200** in the solid state (ellipsoids are at 30%, hydrogen atoms omitted for clarity). Selected bond lengths [Å]: Ge-C2 2.101(3), Ge-Si1 2.4380(8), Ge-Si2 2.4590(9), Si1-H1 1.40(2), Si2-H2 1.35(3).

All attempts to synthesize the NHC-coordinated silyl germylene **198** by this route failed (different addition of reagents, reaction at room temperature, comproportionation reaction with $GeCl_2 \cdot NHC^{iPr_2Me_2}$).

The Ge-C2 distance is with 2.101(3) Å at the longer end for the coordination of an NHC to the Ge(II)-center (2.061-2.106 Å)[61,145] and longer than in Marschner's bis-silyl germylene **221** (2.089 Å, Scheme 126).[204] The Ge-Si bond lengths are with 2.4380(8) Å and 2.4590(9) Å shorter when compared to Marschner's bis-silyl germylene **221** (2.484 and 2.502 Å), which could be attributed to the less steric congestion imposed by the silyl groups (only two mesityl groups and one proton) attached to the germanium(II)-center.

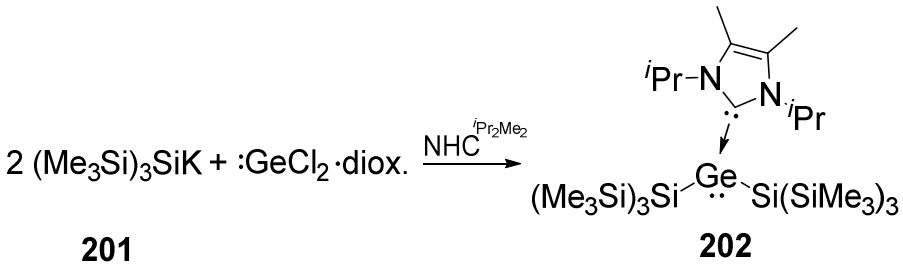

Scheme 126. Synthesis of Marschner's NHC-stabilized bis-silyl germylene **202**.

Germylene **200** is thermally stable at 80 °C for 3 days before an unselective decomposition was observed. In the UV/vis absorption spectrum of **200** a broad shoulder is observed (between λ = 420-300 nm).

3.4.4.1. Abstraction of the NHC from Bis-Silyl Germylene 200

The abstractions of the $NHC^{iPr_2Me_2}$ from low-valent Group 14 centers with BPh_3 as Lewis-acid have been demonstrated by Cui *et al.* or recently by our group (Scheme 127).[147,174]

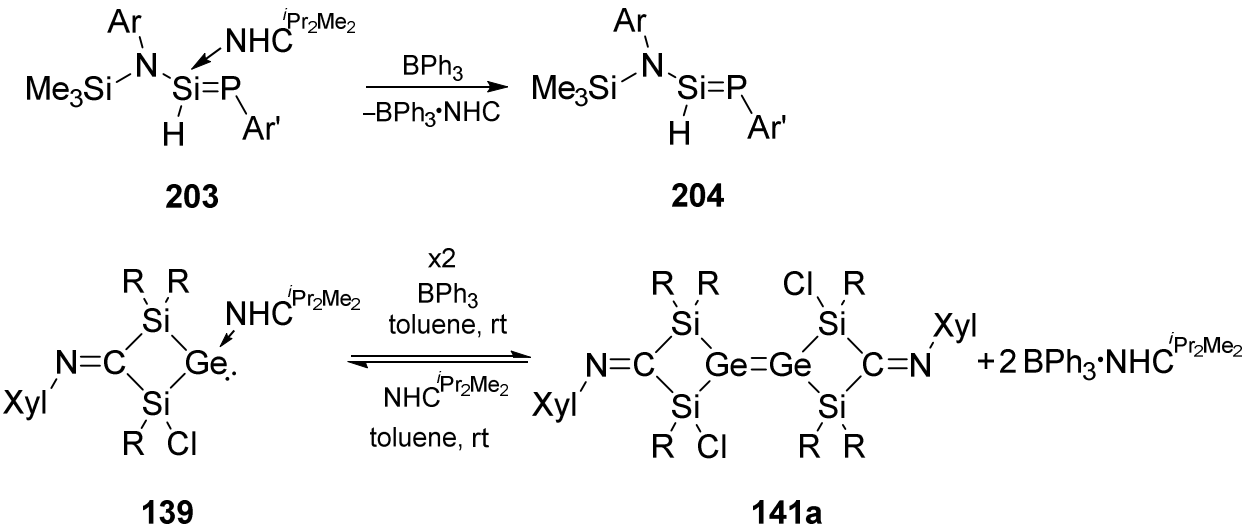

Scheme 127. Abstraction of NHC from NHC-stabilized phosphasilene **203** with BPh_3 resulting in **204** and from cyclic germylene **139** leading to digermene **141a** (Ar = 2,6-$^{i}Pr_2C_6H_3$, Ar' = 2,6-$Mes_2C_6H_3$, R = Tip).

In view of the comparatively weak bond between the carbenic C-atom and germanium (2.101(3) Å), **200** was treated with 1 eq of BPh_3 in toluene aiming at digermene **205** (Scheme 128). Since there was no reaction after heating to 70 °C for 2 hours, a repeat reaction of **200** with the stronger Lewis-acid $B(C_6F_5)_3$ in benzene solution was investigated (Scheme 128). The bis-silyl germylene **200** was completely consumed after 30 min at room temperature.

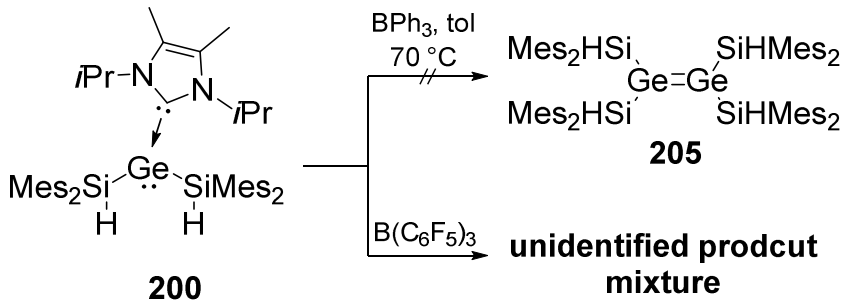

Scheme 128. Abstraction of NHC^{iPr_2Me_2} from **200** with BPh_3 and $B(C_6F_5)_3$ resulting in a unidentified product mixture.

The ^{29}Si NMR spectrum shows five resonances in the range of δ = −7.66 and −47.32 ppm. The ^{13}C NMR resonance for the carbenic C-atom has disappeared and the formation of the $B(C_6F_5)_3$·NHC-adduct is observed. Attempts to isolate any of the products by crystallization failed.

„Hat man es nun im Germanium an sich schon mit einem sehr merkwürdigen Elemente zu thun, dessen Studium hohen Genuss gewährt, so bildet die Ergründung seiner Eigenschaften noch insofern eine ungewöhnlich fesselnde Aufgabe, als sie thatsächlich zum Prüfstein des menschlichen Scharfsinns wird.“

Clemens Winkler, "Mittheilungen über des Germanium. Zweite Abhandlung", *J. Prak. Chem.* **1887**, *36*, 177–209.

3.5. Isolation of a Digerma Analogue of a Vinyl Anion

3.5.1. Synthesis and Characterization of Digermenide 90

As detailed in the introductory Chapter 1.6.1. “Digermenides and Disilenides”, a digerma analogue of a vinyl anion has not yet been fully characterized. Especially an X-ray structure of a digermenide remains to date unknown. The lighter congeners, the disilenides, are prominent building blocks in modern Group 14 chemistry for a variety of molecules in which the unsaturated Si=Si moiety remains intact or is converted into another low-valent functionality.[126,136,137]

In 1989 Masamune *et al.* isolated a red microcrystalline material, which was proposed to be digermenide **88**, on the basis of ^{1}H NMR data and a quenching reaction with MeOH.[92] About a decade later, Weidenbruch and co-workers proposed digermenide **90** as an unisolated intermediate on the way to tetragermabutadiene **92** (Scheme 129).[128]

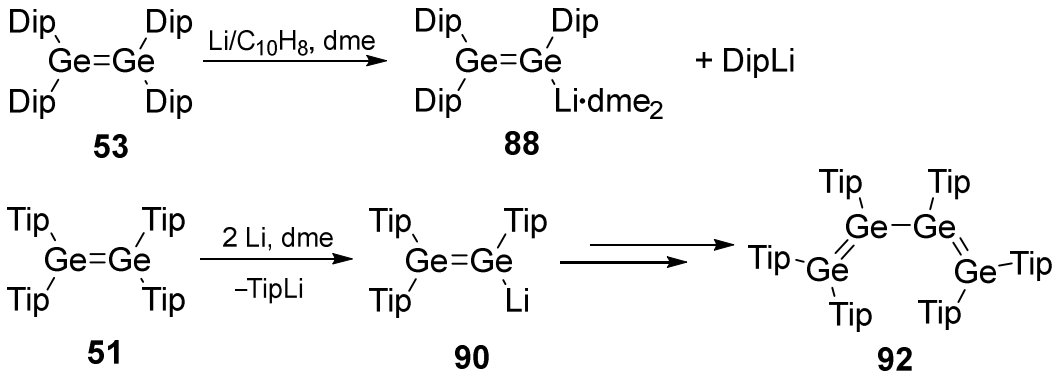

Scheme 129. Proposed digermenide **88** by Masamune *et al.* and digermenide **90** by the group of Weidenbruch.

In order to fully characterize a digermenide, the major focus in this part of the thesis laid on the development of a reproducible synthesis for lithium digermenide **90**. In analogy to disilenide **93**, lithium digermenide **90** could be an equally potent building block for the synthesis of heavier vinylidene analogues or multiple unsaturated heavier Group 14 scaffolds. Consequently, the synthetic approach was inspired by the synthesis of disilenide **93** by Scheschkewitz.[132] Tip_2GeX_2 **206** and Tip_2GeCl_2 **50** were synthesized as potential reduction precursors (Scheme 130).

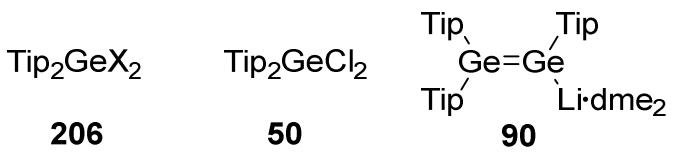

Scheme 130. Dihalo germane precursors **206** (X = Cl, Br), **50** and digermenide **90**.

3.5.1.1. Synthesis of Reduction Precursors Tip_2GeX_2 206 and Tip_2GeCl_2 50

In contrast to the synthesis of Tip_2SiCl_2 **64**, TipLi and $GeCl_4$ cannot be converted straightforward into Tip_2GeCl_2 **50** (Scheme 131). A plausible reason could be the high reduction potential of the organolithium compound, which would incorporate redox processes into the reaction sequence leading to side products.

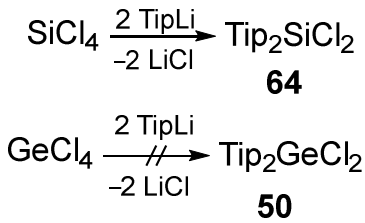

Scheme 131. Reaction of $SiCl_4$ and $GeCl_4$ with TipLi.

Instead, the Grignard reagent TipMgBr was synthesized in a reaction of TipBr with Mg-shavings in thf. TipMgBr (2.2 eq) was added to a solution of $GeCl_4$ in benzene at room temperature, which resulted in a mixture of dihalo germanes **206**.[93] Additional heating for 10 hours to reflux completed the reaction to Tip_2GeX_2 **206** (Tip_2GeCl_2, $Tip_2GeClBr$ and Tip_2GeBr_2) together with the formation of TipH and TipBr (Scheme 132).[205]

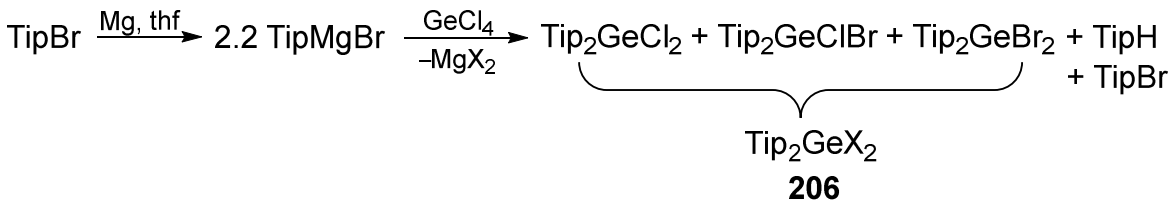

Scheme 132. Synthesis of Tip_2GeX_2 **206** (Tip_2GeCl_2, $Tip_2GeClBr$ and Tip_2GeBr_2).

TipH and TipBr were distilled off in high vacuum. The residue contained a mixture of Tip_2GeCl_2:$Tip_2GeClBr$:Tip_2GeBr_2 in an approximate ratio of 3:44:53 (determined by ^1H NMR spectroscopy, Figure 78). Hydration of Tip_2GeX_2 **206** with $LiAlH_4$ in thf afforded Tip_2GeH_2 **207**, which was subsequently chlorinated by CCl_4 with a catalytic amount of AIBN to afford Tip_2GeCl_2 **50** following a literature protocol (Scheme 133).[92,93]

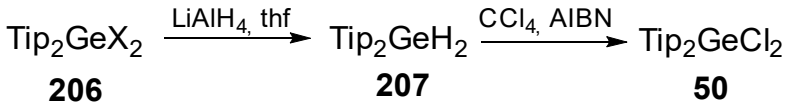

Scheme 133. Hydration of Tip_2GeX_2 **206** (X = Cl, Br) to **207** with subsequent chlorination to Tip_2GeCl_2 **50**.

Diaryldichloro germane **50** was additionally purified by Kugelrohr-distillation (150-160 °C, 4.5*10^{-2} mbar) to obtain 70% of pure **50**.[92]

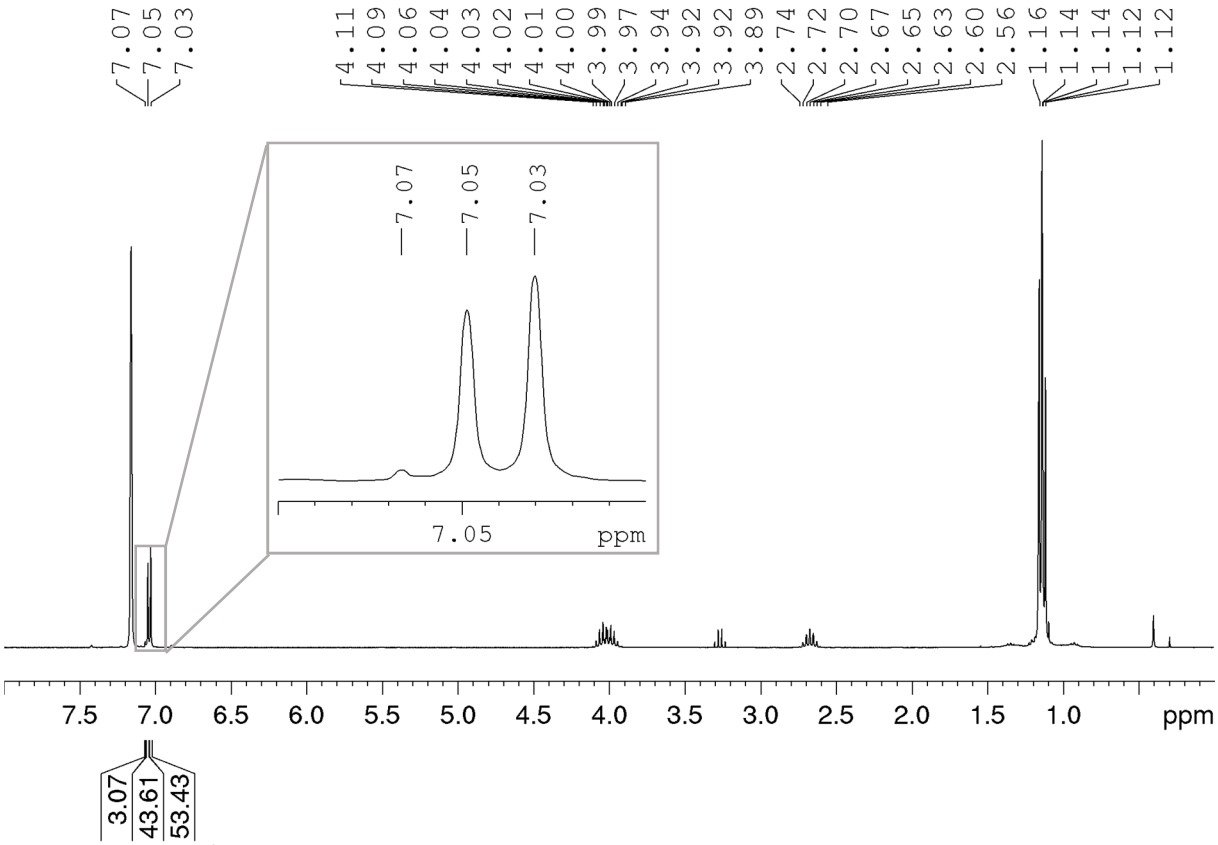

Figure 78. ^{1}H NMR spectrum of the reaction mixture of Tip_2GeX_2 **206** (Tip_2GeCl_2:$Tip_2GeClBr$:Tip_2GeBr_2 3:44:53). The excerpt shows the aryl protons of the mixture of diaryldihalo species **206**.

3.5.1.2. Reduction of Tip_2GeX_2 206 with Li

In a first reduction attempt the mixture of Tip_2GeX_2 **206** (additionally purified by crystallization from diethyl ether at −78 °C) was treated with 3.5 equivalents of Li-powder in dme at 0 °C (Scheme 134).

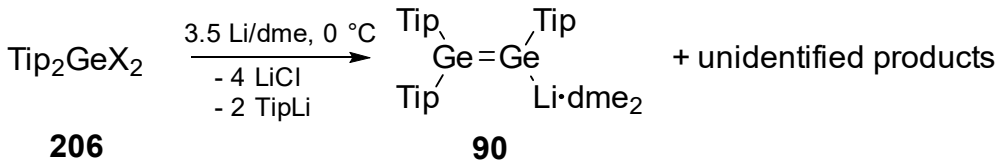

Scheme 134. Reduction of Tip_2GeX_2 **206** (X = Cl, Br) with 3.5 eq Li-powder in dme.

The ^{1}H NMR spectrum (Figure 79) indicates a mixture of products, containing TipLi (δ = 6.99 (s), 2.84 (sept), 1.24 (d) ppm) and Ge*H*-species (δ = 6.02 (s), 6.26 (s), 6.48 (s) ppm), as well as signals of coordinated dme molecules to a likely anionic reaction product (δ = 3.10 (s), 3.06 (s) ppm).

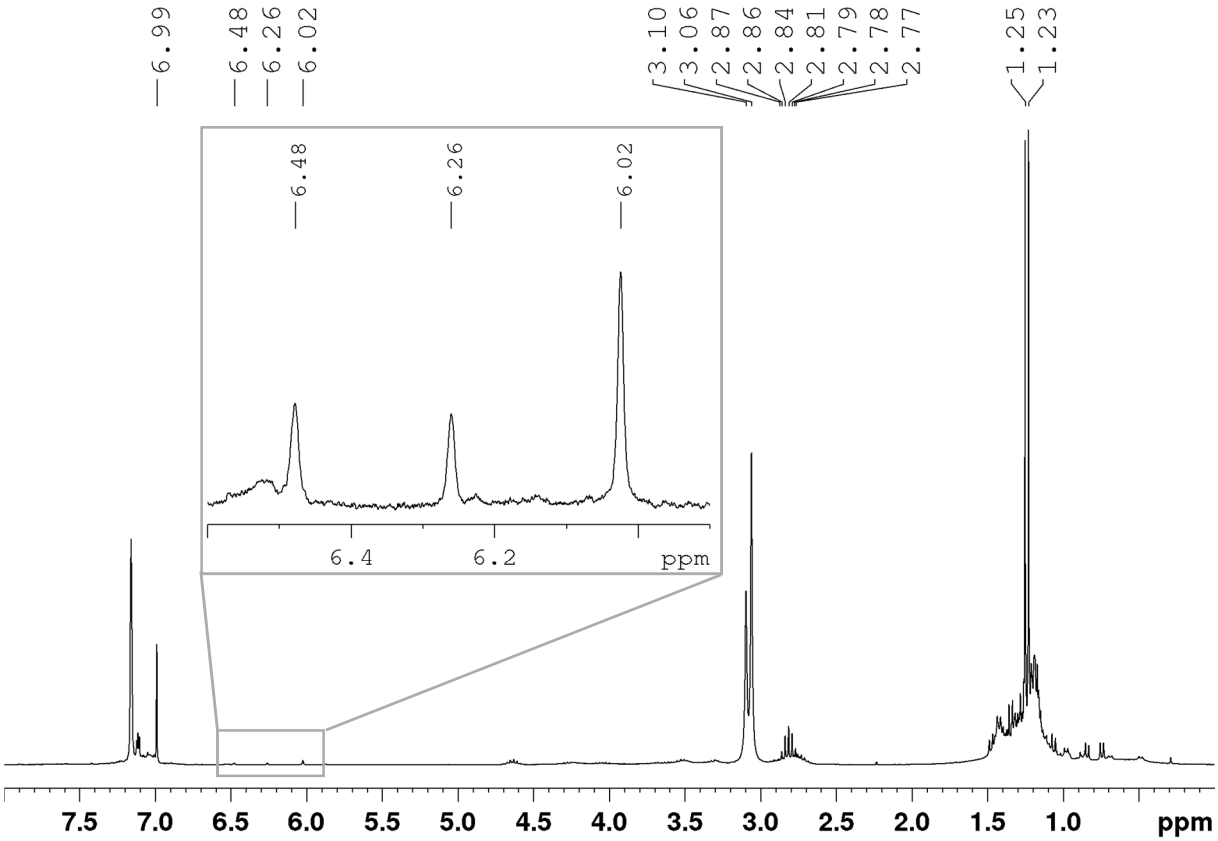

Figure 79. ^{1}H NMR spectrum of the crude reaction mixture from the reduction of Tip_2GeX_2 **206** with 3.5 eq Li. The excerpt shows different Ge*H*-species.

After filtration from pentane, the reaction mixture was frozen in liquid nitrogen and upon warming to room temperature the formation of a red microcrystalline precipitate was observed. The ^{1}H NMR spectrum of the red precipitate (Figure 80a) displays a strong similarity to the ^{1}H NMR spectrum of disilenide **93** (Figure 80b). Both ^{1}H NMR spectra show three signals in a ratio of 1:1:1 in the aryl region. Furthermore, the signals of the

two coordinated dme-molecules are nearly identical to those of disilenide **93**. Therefore, it is suggested that digermenide **90** had been formed, although in a poor yield of 2%. Attempts to grow single crystals from hexane at room temperature failed and led to unidentified decomposition products.

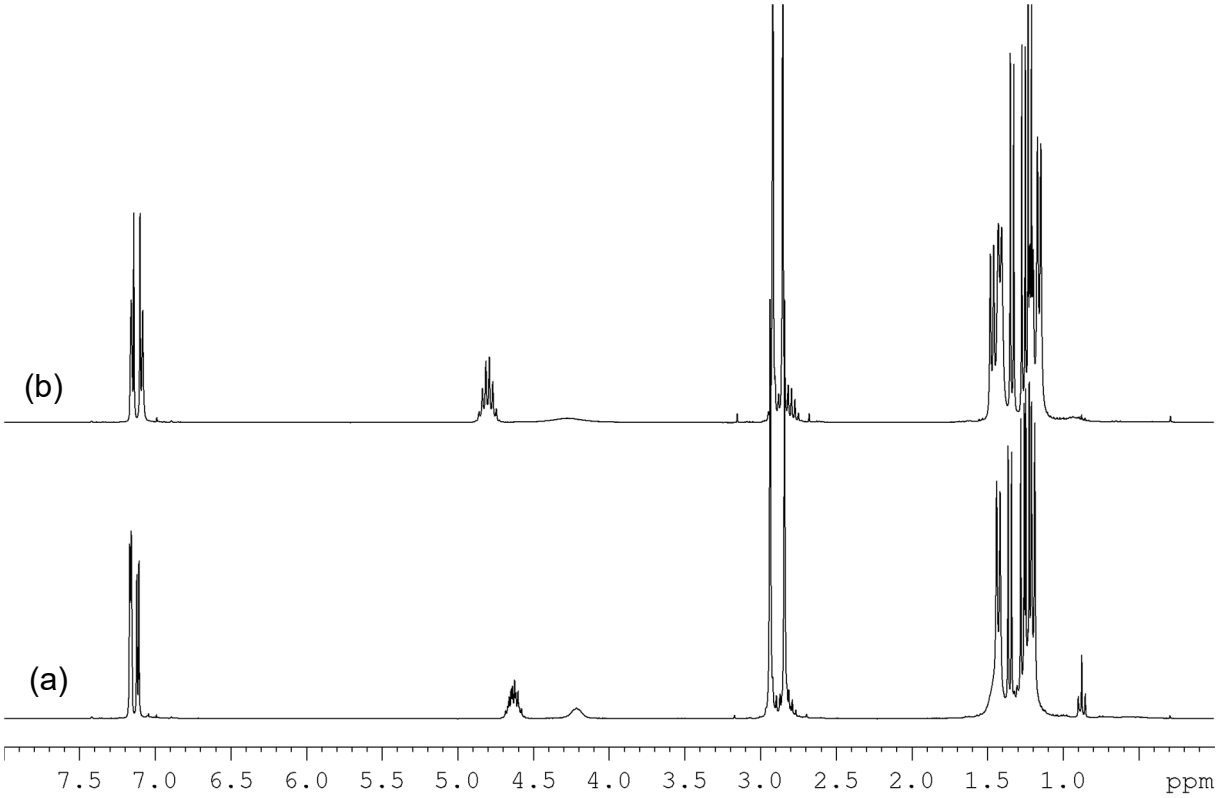

Figure 80. Comparison of ^{1}H NMR spectra: (a) red precipitate from reduction of Tip_2GeX_2 **206** with 3.5 eq Li-powder, (b) disilenide **93**.

3.5.1.3. Reduction of Tip_2GeCl_2 50 with Li

In a further reduction attempt, pure Tip_2GeCl_2 **50** (4.5 mmol) was reduced with 4 eq of Li-powder in dme at 0 °C according to the literature synthesis of disilenide **93**. In the process of warming to room temperature a heat development was observed and the ^{1}H NMR spectrum shows the same set of signals as displayed in Figure 80a together with TipLi and a second anionic product (Scheme 135).

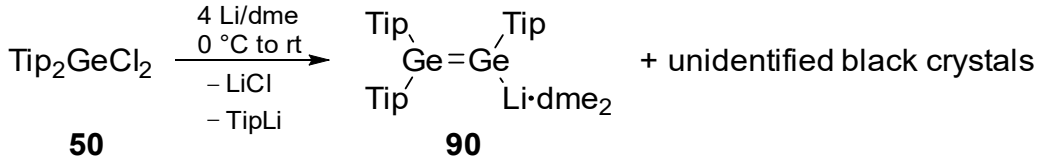

Scheme 135. Reduction of Tip_2GeCl_2 **50** with 4 eq of Li-powder affording digermenide **90** and unidentified black crystals.

After filtration from pentane and storing a concentrated pentane solution at −26 °C for 14 hours afforded a small amount of red crystals beside a large amount of almost black crystals.

The ^{1}H NMR spectrum reveals again the signals of proposed digermenide **90** displayed in Figure 80b together with the signals which were assigned to the unidentified black crystals (Figure 81).

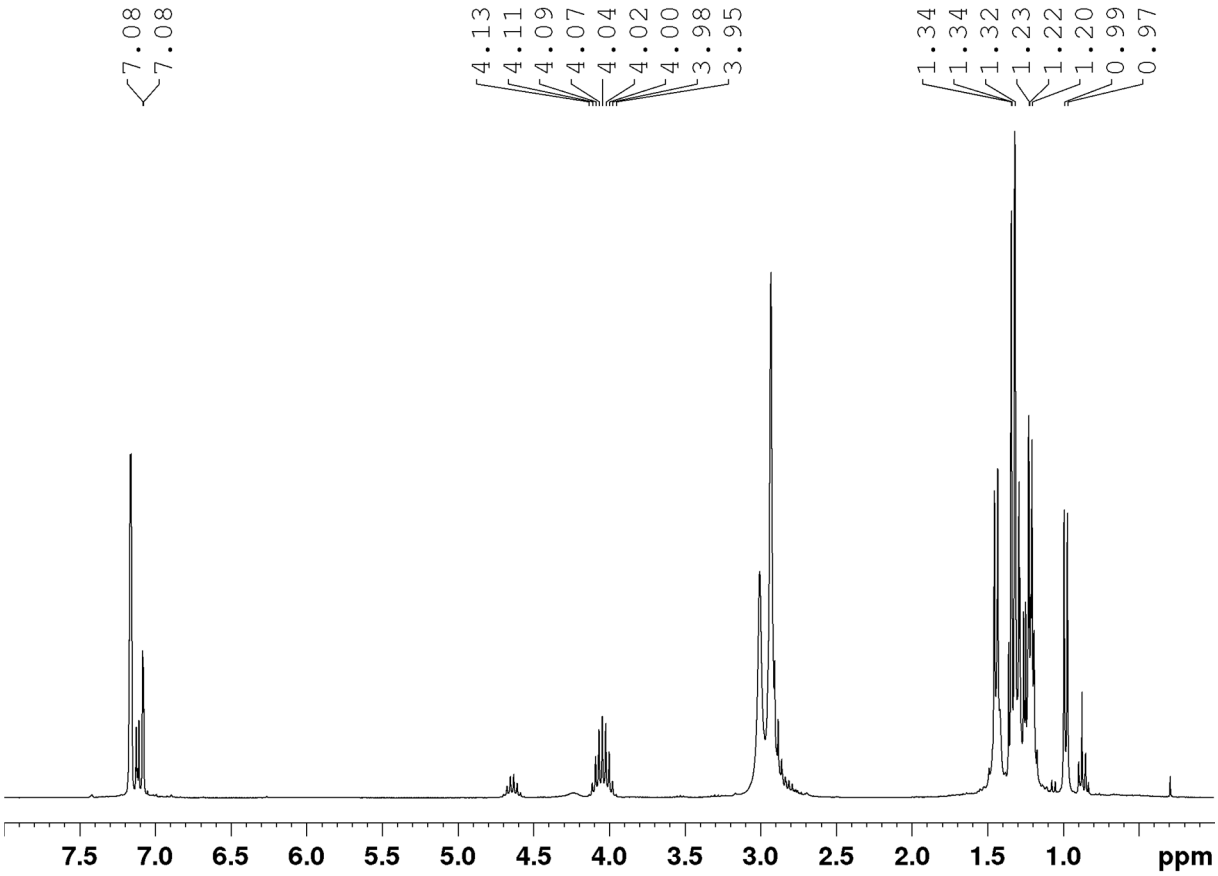

Figure 81. ^{1}H NMR spectrum of the crystals from the reduction of Tip_2GeCl_2 **50** with 4 eq Li (labelled: unidentified black crystals).

Unfortunately both types of crystals were not suitable for X-ray diffraction. At room temperature the crystals were unstable in solution and after three weeks of storing the mixture of both species at ambient temperature afforded orange block-like crystals. Surprisingly, the result of the X-ray analysis revealed the steric congested $GeTip_3H$ **209** (Scheme 136, Figure 82). The ^{1}H NMR spectrum of **209** shows a typical resonance for a Ge*H* at δ = 6.27 ppm.[93]

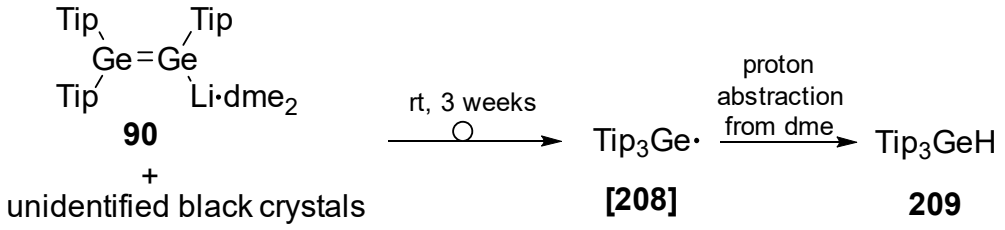

Scheme 136. Rearrangement of digermenide **90** and unidentified black crystals to form triaryl germane **209**.

The formation of the triaryl germane **209** is most likely a rearrangement product of digermenide **90** and the unidentified black crystals over the long period of time in solution (Scheme 136). An initial formed $GeTip_3$-radical **[208]** could have abstracted a proton from dme molecules to finally afford **209**.

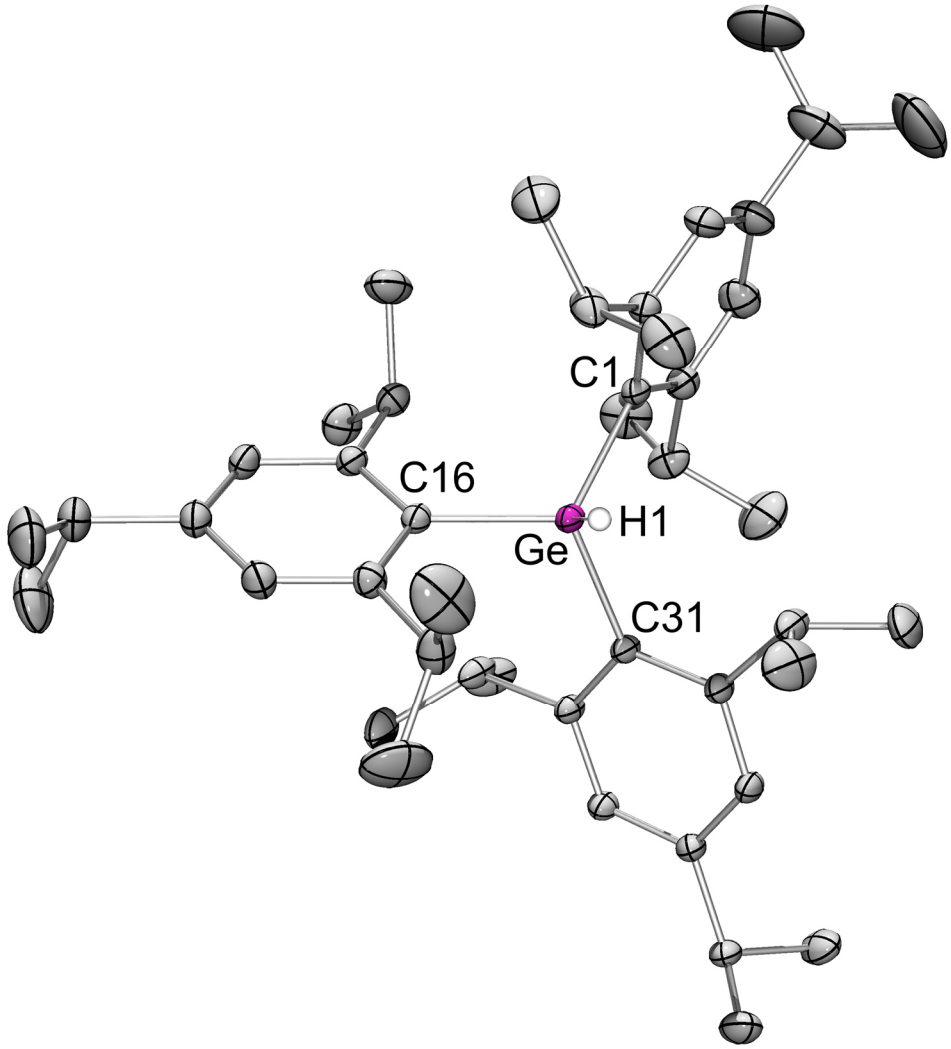

Figure 82. Molecular structure of **209** in the solid state (ellipsoids are at 30%, hydrogen atoms omitted for clarity). Selected bond lengths [Å]: Ge-H1 1.68(4), Ge-C1 1.9745(18), Ge-C16 1.9599(19), Ge-C31 1.9714(17).

The sum of angles at the germanium center of 348° indicates a significantly more planar coordination environment than expected for a tetracoordinate species, which could be interpreted as support for the absence of a fourth substituent and therefore would suggest that **209** was actually a radical species. However, the very fact that a ^{1}H NMR spectrum with the ordinary chemical shift range can be obtained clearly proves the absence of unpaired electrons. Moreover, the ^{1}H NMR reveals a characteristic signal for a germanium-bonded hydrogen at δ = 6.27 ppm. The Ge-C bond distances of **209** are with 1.9599(19) to 1.9745(18) Å shortened in comparison to $GeMes_3H$ **211** (Scheme 137) of Lambert *et al.* (2.031-2.06 Å).[206] Significant shorter is the Ge-H bond length with 1.68(4) Å when compared to $GeMes_3H$ **211** (2.047 Å), which could be rationalized by the more electron donating effects of the Tip-substituents.

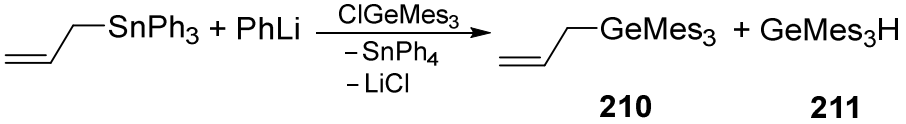

Scheme 137. Synthesis of $GeMes_3H$ **211** as byproduct in the synthesis of allyltrimesityl germane **210**.

The orange color of **209** is due to the longest wavelength absorption in the UV/vis spectrum at λ_{max} = 437 nm (ε = 1800 $Lmol^{-1}cm^{-1}$) and unusual colorful when compared to the colorless trimesityl silane or trimesityl germane.[206,207] Conversely, when the same reaction was carried out in a smaller scale (1 mmol), only $Tip_2Ge{=}GeTip_2$ **51** beside a small amount of proposed digermenide **90** was observed, even when the reaction mixture was stirred for 4 days at room temperature (Scheme 138).[208]

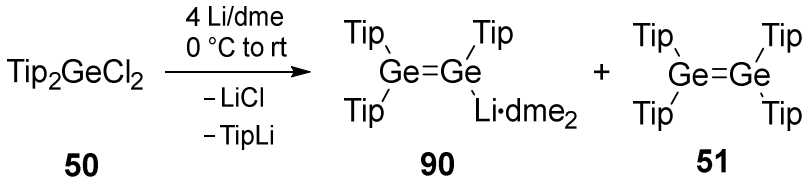

Scheme 138. Reduction of Tip_2GeCl_2 **50** with 4 eq of Li-powder affording proposed digermenide **90** and digermene **51** (1 mmol scale).

3.5.1.4. Synthesis of Digermenyllithium 90

In both reductions, described in Chapter 3.5.1.2. (Scheme 134, page 146) and Chapter 3.5.1.3. (Scheme 135, page 147), the formation of digermenide **90** was strongly supported by ^{1}H NMR spectroscopic data, although isolation in a good yield as well as growing single crystals of **90** to confirm the molecular structure by X-ray diffraction analysis failed.

In order to avoid the heat generation, observed during the reduction of Tip_2GeCl_2 **50** with 4 equivalents of Li in dme (Scheme 135), **50** was reacted at −78 °C with 3.3 equivalents of Li-powder in dme in presence of a catalytic amount naphthalene (0.004 mol%) to initiate the reduction at lower temperature (Scheme 139).

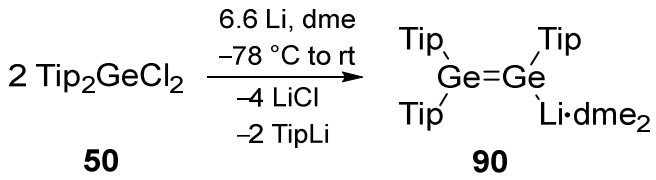

Scheme 139. Synthesis of digermenide **90** upon reduction of diaryldichloro germane **50** with 3.3 eq Li and cat. amount of naphthalene.

Upon warming to room temperature, a ^{1}H NMR sample indicates the clean conversion into proposed digermenide **90**, also isolated in Chapter 3.5.1.2. (Figure 80a, page 147), beside TipLi and LiCl. Excess dme was evaporated in high vacuum and filtered from pentane. The ^{7}Li NMR spectrum shows one resonance at δ = −0.22 ppm. A diluted pentane solution was stored at −26 °C for 14 hours to afford red crystals suitable for X-ray diffraction analysis. The X-ray analysis confirmed the predicted molecular structure as digermenyllithium **90** (Figure 83). The Li-atom is coordinated by two dme molecules in the same fashion as observed for disilenide **93**. The Ge=Ge moiety in **90** is slightly more twisted (τ = 19.9°) than in $Tip_2Ge{=}GeTip_2$ **51** (τ = 14°) and the *trans*-bent angles (θ, $GeTip_2$ = 7.1°; θ, GeTipLi = 12.8°) are comparable to those of $Tip_2Ge{=}GeTip_2$ **51** (θ, $GeTip_2$ = 12°) but only slightly *trans*-bent in comparison to $Mes_2Ge{=}GeMes_2$ **14** (θ, $GeMes_2$ = 33°).[97,208] The Ge1-Ge2 double bond length is with 2.284(6) Å nearly the same as in $Mes_2Ge{=}GeMes_2$ **14** (2.286 Å) and significant longer when compared to $Tip_2Ge{=}GeTip_2$ **51** (2.213 Å).[97,208] The distances between

germanium and carbon (1.986(3)-2.031(4) Å) are slightly shorter when compared to Power's Ge-dianion **78** (2.060 Å, Scheme 140).[209]

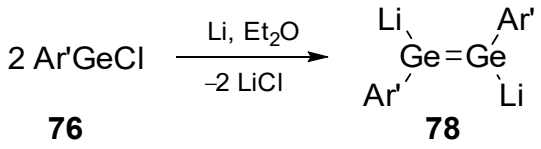

Scheme 140. Synthesis of dianion **78** (Ar' = 2,6-Dip_2-C_6H_3, Dip = 2,6-$^iPr_2$-C_6H_3).

The Ge-Li bond length is with 2.842(7) Å in the typical range (average Ge-Li bonds: 2.55-2.91 Å).[209–211]

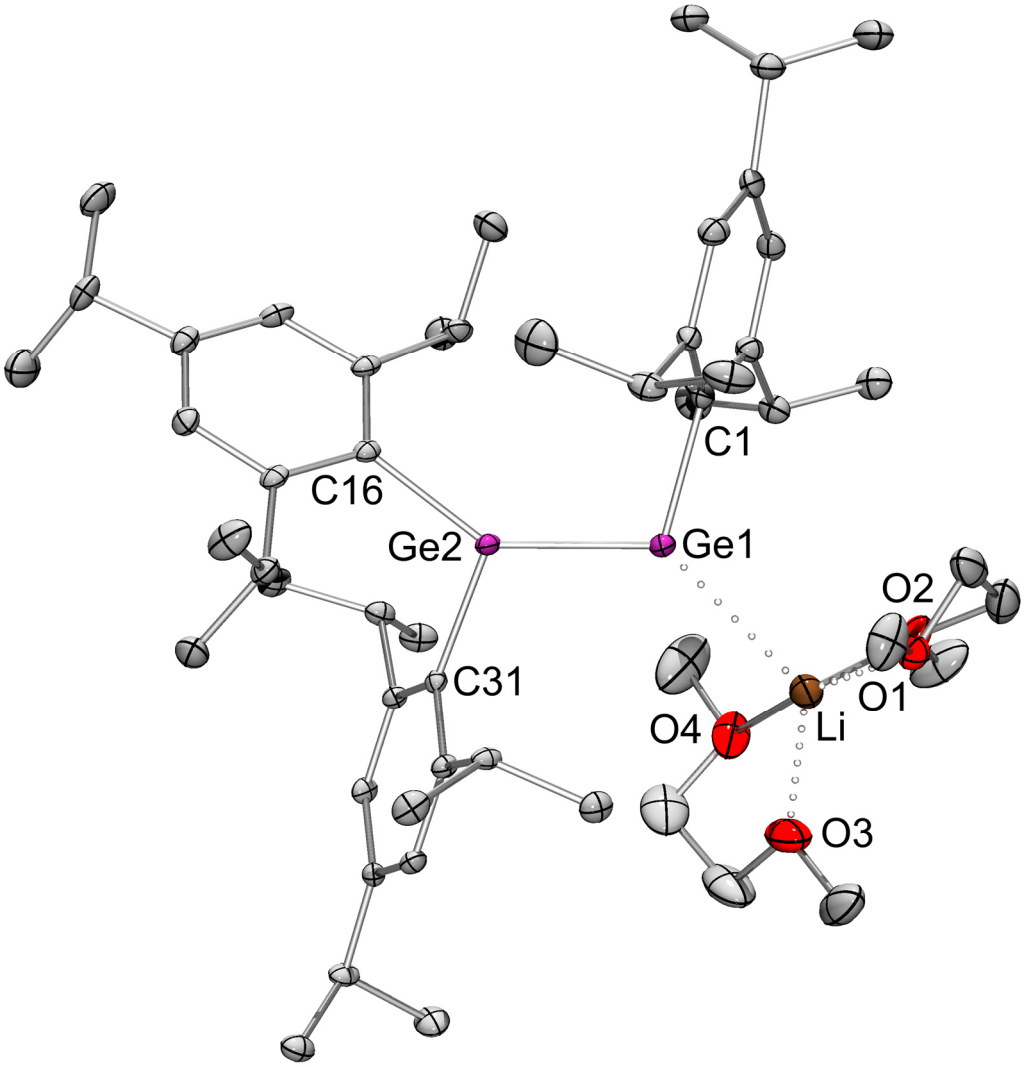

Figure 83. Molecular structure of digermenyllithium **90**·2 dme in the solid state (ellipsoids are at 30%, hydrogen atoms omitted for clarity). Selected bond lengths [Å]: Ge1-Ge2 2.2840(6), Ge1-C1 2.031(4), Ge1-Li 2.842(7), Ge2-C16 2.003(3), Ge2-C31 1.986(3).

The red color of digermenide **90** is due to the longest wavelength absorption in the UV/vis spectrum at λ_{max} = 435 nm (ε = 11800 $Lmol^{-1}cm^{-1}$) and slightly blue-shifted when compared to $Dip_2Ge{=}GeDip(Li)$ **88** reported by Masamune *et al.* (λ_{max} = 458 nm (ε = 4000 $Lmol^{-1}cm^{-1}$).[92] Digermenide **90** melts at 135-138 °C under conversion into $Tip_2Ge{=}GeTip_2$ **51** together with a mixture of unidentified decomposition products. The synthesis is reproducible in a scale from 1 to 6 mmol of Tip_2GeCl_2 **50** (average yield of **90**: 36-48%).

3.5.1.5. Reduction of Tip_2GeX_2 206 with Li and Cat. Amount of Naphthalene

With the reproducible synthesis of digermenide **90** in hand, reduction of Tip_2GeX_2 **206** under the same conditions as reported in Chapter 3.5.1.4. was investigated to circumvent the hydration and chlorination step of Tip_2GeX_2 **206** to Tip_2GeCl_2 **50**.

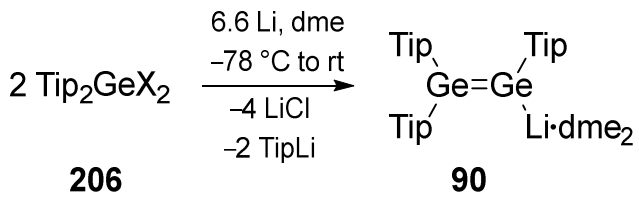

Scheme 141. Reduction of **206** with Li in the presence of cat. amount of naphthalene (X = Cl, Br).

Unfortunately, this synthetic pathway (Scheme 141) indicated a mixture of products. The heavier vinyllithium analogue **90** was isolated only in poor yields of 5%, suggesting that the chlorinated species Tip_2GeCl_2 **50** in presence of Li/cat. naphthalene is crucial for the targeted digermenyllithium **90**.

3.5.2. Reactivity of Digermenide 90

3.5.2.1. Reaction of Digermenide 90 with PhX (X = Cl, Br, I)

In order to gain a first impression of the reaction behavior of heavier vinyllithium analogue **90**, the reaction with PhI was carried out (Scheme 142), which yielded in case of disilenide **93** the unsymmetrically substituted disilene **213** (Scheme 143).[212]

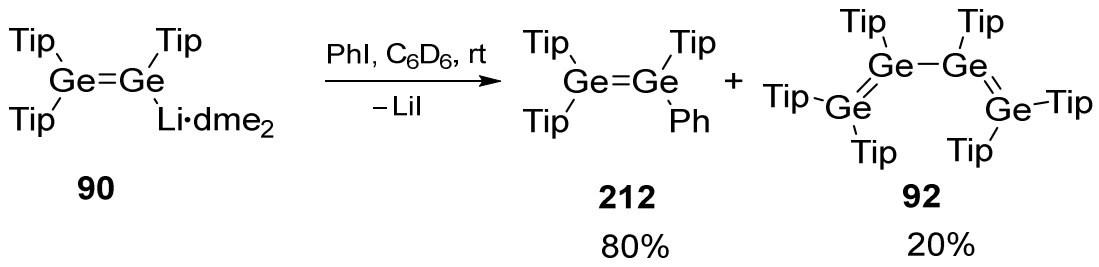

Scheme 142. Reaction of **90** with PhI leading to $Tip_2Ge{=}GeTipPh$ **212** and tetragermabutadiene **92**.

When PhI was added at room temperature to an NMR tube containing digermenide **90**, the major product (80%, determined by ^1H NMR spectroscopy) was the unsymmetrically substituted digermene **212**, beside the oxidation product of digermenide **90**, tetragermabutadiene **92** (Figure 84).

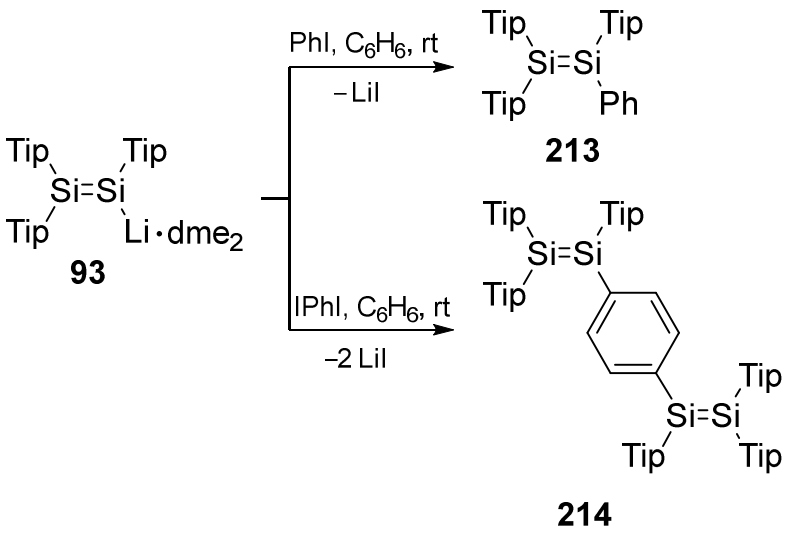

Scheme 143. Reaction of **93** with PhI to $Tip_2Si{=}SiTipPh$ **213** and reaction of **93** to phenylene-bridged tetrasilabutadiene **214**.

The reaction was repeated in a larger scale, which again yielded tetragermabutadiene **92** as major product, which prevented the isolation of **212**.

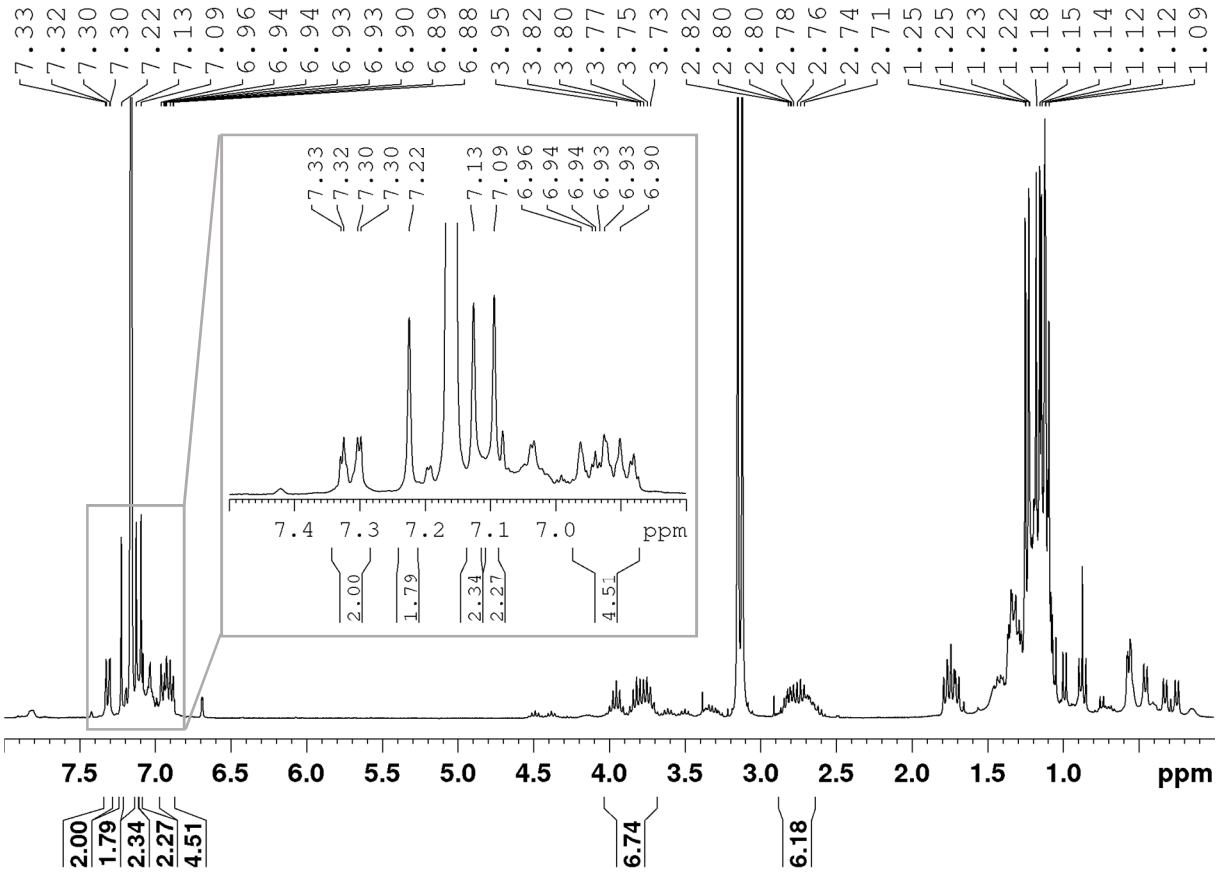

Figure 84. ^{1}H NMR spectrum of an NMR-scale reaction of digermenide **90** with PhI leading to Tip_2Ge=GeTipPh **212** and tetragermabutadiene **92** (integrated: signals of **212**). The excerpt shows the aryl-protons of compound **212**.

A plausible mechanism could start with a halogenation of digermenide **90** leading to intermediate Tip_2Ge=GeTipX **215**, which than reacted with a further equivalent of digermenide **90** to finally obtain tetragermabutadiene **92** (Scheme 144). Weidenbruch *et al.* already proposed this mechanistic scenario in the synthesis of tetragermabutdiene **92**.[128] More likely, a radical mechanism can be considered in which an electron is transferred from digermenide to the aromatic system. In a subsequent step two digermenyl-radicals would combine to tetragermabutadiene **92**. The reaction of digermenide **90** was also repeated with PhCl and PhBr which selectively led to the oxidation product **92**.

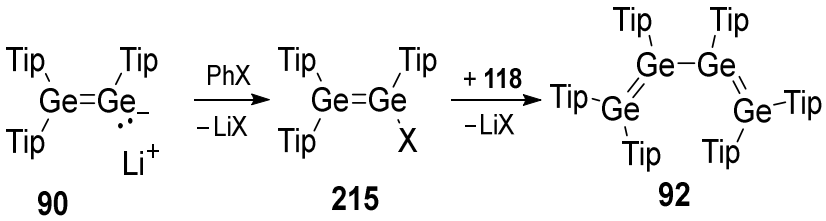

Scheme 144. Proposed mechanism for the formation of tetragermabutadiene **92** in the reaction of **90** with PhX *via* intermediate **215** (X = Cl, Br or I).

3.5.2.2. Synthesis of Phenylene-Bridged Tetragermabutdiene 216

The reaction of disilenide **93** with 1,4-diiodobenzene had reportedly afforded *para*-phenylene-bridged tetrasilabutadiene **214** selectively (Scheme 143).[212] In case of germanium, tetragermabutadiene **92** was the hitherto only known system with conjugated Ge-Ge-double bonds.[128] With regards to expanded and conjugated systems, digermenide **90** was reacted with 0.5 equivalents of 1,4-diiodobenzene in benzene at room temperature. The oxidation product **92** was once more observed as side product, albeit the major product was identified as the desired phenylene-bridged tetragermabutdiene **216** in this case (Scheme 145). The ^{1}H NMR spectrum of **216** is nearly identical when compared to the ^{1}H NMR spectrum of the phenylene-bridged tetrasilabutadiene **214**.[212] The similarity of the ^{1}H NMR spectra in this reaction is in line with the previous observed trend that the germanium systems display similar splitting patterns as the corresponding silicon-species.

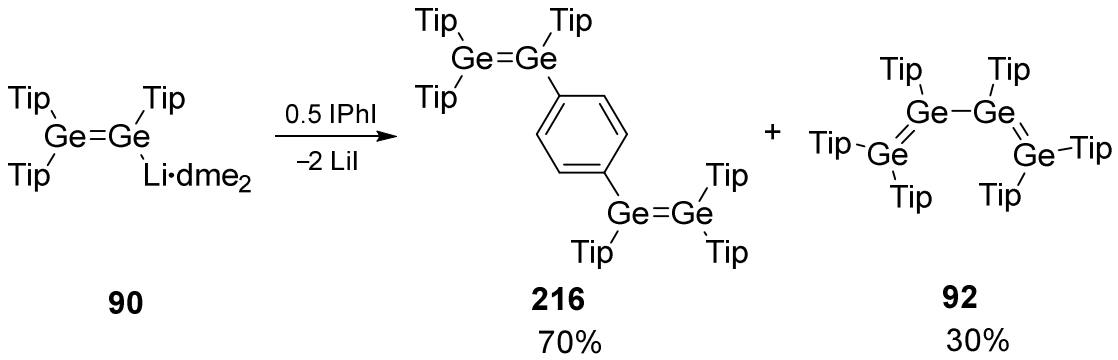

Scheme 145. Synthesis of *para*-phenylene-bridged tetragermabutadiene **216** beside oxidation product **92**.

In a repeat reaction intensely red colored single crystals suitable for X-ray diffraction were obtained from a saturated pentane solution at room temperature, confirming the proposed structure of *para*-phenylene-bridged tetragermabutadiene **216**. Co-crystallized tetragermabutadiene **92** was separated mechanically. The Ge=Ge moiety in **216** is slightly twisted (τ = 10.8°) and strongly *trans*-bent (θ, $GeTip_2$ = 33.5°; θ, GeTipPh = 43.3°) and comparable to tetragermabutadiene **92** (θ, $GeTip_2$ = 31.1° and 35.4°).[128] The Ge1-Ge2 double bond length is with 2.3132(4) Å longer than the Ge1-Ge2 distance in digermenide **90** (2.284(6) Å) and in $Tip_2Ge{=}GeTip_2$ **51** (2.213 Å), but shorter than observed for tetragermabutadiene **92** (2.344 and 2.357 Å).[128,208] The red color of **216** is due to the longest wavelength absorption in the UV/vis spectrum at λ_{max} = 480 nm (ε = 41300 $Lmol^{-1}cm^{-1}$) and blue-shifted when compared to heavier butadiene analogue **92** (λ_{max} = 560 nm (ε = 12800 $Lmol^{-1}cm^{-1}$) or the phenylene-bridged tetrasilabutadiene **214** (λ_{max} = 508 nm (ε = 28200 $Lmol^{-1}cm^{-1}$)). Compound **216** decomposes slowly in benzene solution at room temperature over the period of 16 hours to an unidentified product mixture. Melting of **216** at 207-210 °C afforded a mixture of decomposition products.

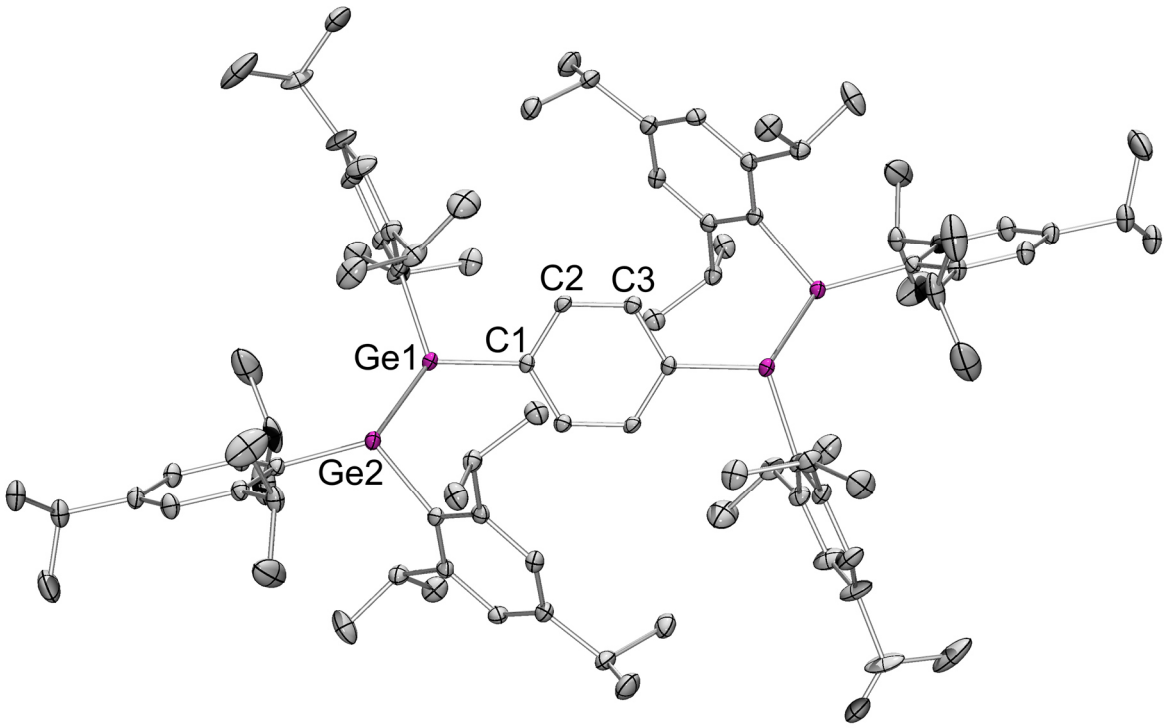

Figure 85. Molecular structure of phenylene-bridged tetragermabutdiene **216** in the solid state (ellipsoids are at 30%, hydrogen atoms omitted for clarity). Selected bond lengths [Å]: Ge1-Ge2 2.3132(4), Ge1-C1 1.948(2), C1-C2 1.401(3), C2-C3 1.386(3).

3.5.2.3. Reaction of Digermenide 90 with $GeCl_2{\cdot}NHC^{iPr_2Me_2}$ 8 and $GeCl_2$·dioxane

Silagermenylidene **104** was formed in a reaction of disilenide **93** with $GeCl_2{\cdot}NHC^{iPr_2Me_2}$ **8** and is a remarkable precursor for several multiple functionalized Si and Ge containing compounds.[145–147] Digermenide **90** represents a potential building block for the synthesis of a homonulcear heavier vinylidene analogue **120** (Scheme 146).

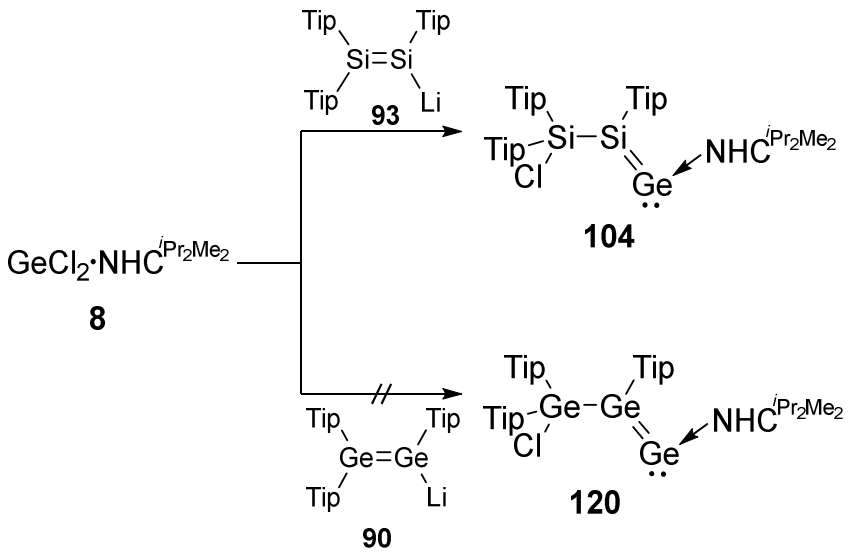

Scheme 146. Synthesis of silagermenylidene **104** and attempted synthesis of homonuclear heavier analogue **120**.

The 1:1 reaction of digermenide **90** and $GeCl_2{\cdot}NHC^{iPr_2Me_2}$ **8** at −78 °C in toluene afforded a complex product mixture which was not further followed due to the limited NMR active species involved in the reaction.

Given the fact that heavier vinylidene analogue **120** could not be obtained *via* the synthetic route described in Scheme 146, $GeCl_2$·dioxane was reacted in a 1:1 ratio with digermenide **90** at −78 °C in toluene to target the base-free vinylidene analogue **217** (Scheme 147).

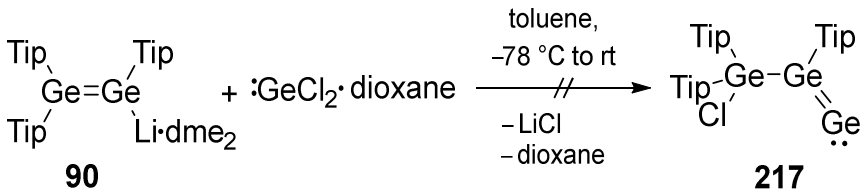

Scheme 147. Reaction of **90** with $GeCl_2$·dioxane.

As the reaction in Scheme 146, germyl digermavinylidene **217** could not be obtained. Instead of the selective formation of tetragermabutadiene **92** was observed. A base-free digermavinylidene **113** was recently reported by the group of Aldridge (Scheme 148).[151]

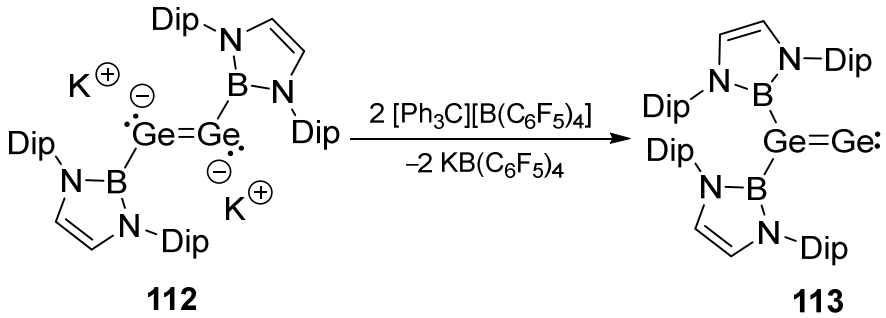

Scheme 148. Synthesis of recently reported base-free digermavinylidene **113** by Aldridge *et al*. (Dip = 2,6-^{i}Pr$_2$-C$_6$H$_3$).

3.5.2.4. Reaction of Digermenide 90 with $GeCl_4$

1,1,2-Trichlorocyclotrisilane is the key precursor on the way to a dismutational hexasilabenzene isomer.[213] An analogous reaction was carried out with digermenide **90** and $GeCl_4$ to target cyclotrigermane **218** (Scheme 149), which could be a starting material for the synthesis of hexagermabenzene analogues.

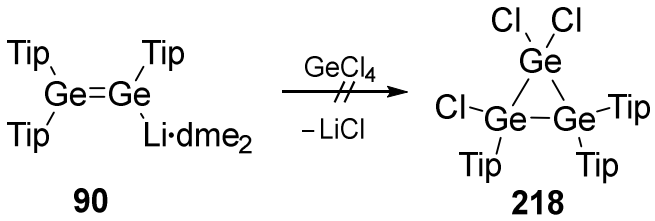

Scheme 149. Reaction of $GeCl_4$ with digermenide **90.**

In analogy to the synthesis of 1,1,2-trichlorocyclotrisilane, five equivalents of $GeCl_4$ were added to a solution of digermenyllithium **90** in hexane at room temperature. The ^{1}H NMR spectrum indicates a mixture of unidentified products. Changing the solvent to toluene as well as the use of 1 eq $GeCl_4$ also afforded a reaction mixture, even when the reaction was done at −78 °C. Notably, the default oxidation product of digermenide **90**, the tetragermabutadiene **92**, was not observed in these reactions.

3.5.2.5. Reaction of Digermenide 90 with $BH_3 \cdot SMe_2$

To further shed a light on the general reaction behavior of digermenide **90**, the 1:1 reaction was carried out with $BH_3 \cdot SMe_2$ at room temperature in benzene solution (Scheme 150). The color turned immediately to pale yellow.

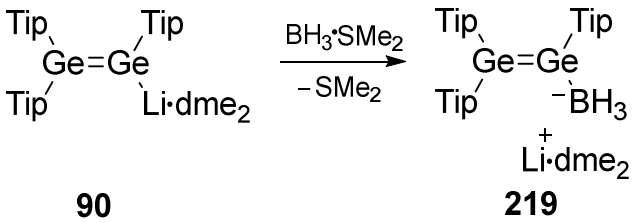

Scheme 150. Reaction of digermenyllithium **90** with $BH_3 \cdot SMe_2$ leading to open-chained product **219**.

A ^{1}H NMR spectrum indicates free SMe_2. The ^{11}B NMR spectrum shows a broad signal at $\delta = -32.99$ ppm and the ^{7}Li NMR spectrum a resonance at $\delta = -0.59$ ppm (**90**: $\delta = -0.22$ ppm) indicating the formation of a single product. After filtration, a concentrated pentane solution is stored at −26 °C for 14 hours to afford orange/yellow single crystals suitable for X-ray diffraction. The analysis revealed the molecular structure of the first example of a digermenyl borate **219** (Figure 86). The Ge=Ge moiety in **219** is slightly twisted (τ = 9.8°) and moderate *trans*-bent (θ, $GeTip_2$ = 27.1°; θ, $GeTipBH_3$ = 28.8°) and comparable to $Mes_2Ge{=}GeMes_2$ **14** (θ, $GeMes_2$ = 33°). The Ge1-Ge2 double bond length is with 2.285(3) Å close to the Ge1-Ge2 distance in digermenide **90** (2.284(6) Å) and shorter when compared to phenylene-bridged tetragermabutadiene **216** (2.3132(4) Å). The Ge-B bond length is with 2.074(4) Å shorter when compared to the saturated germyl borate **221** reported by Mochida *et al.* (2.138-2.145 Å, Scheme 151).[214]

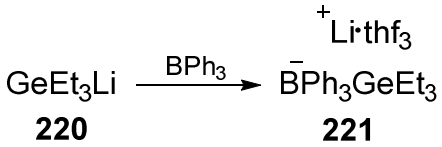

Scheme 151. Synthesis of germyl borate **221** reported by Mochida and co-workers.

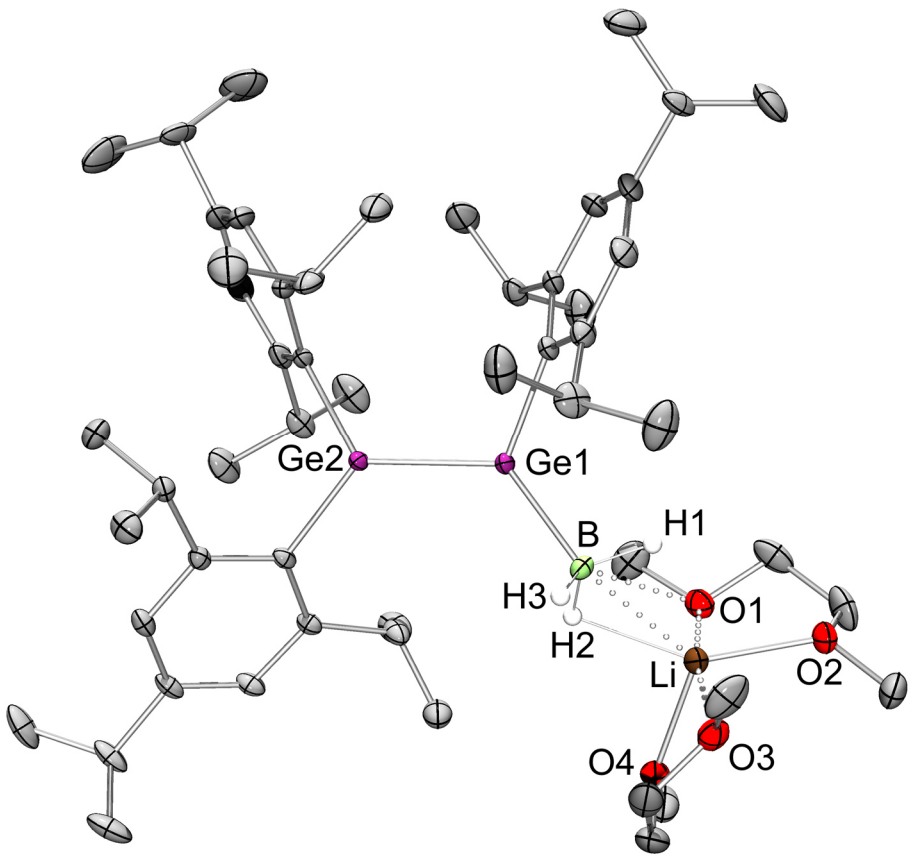

Figure 86. Molecular structure of digermenyl borate **219** in the solid state (ellipsoids are at 30%, hydrogen atoms omitted for clarity). Selected bond lengths [Å]: Ge1-Ge2 2.285(3), Ge1-B 2.074(2), B-H1 1.15(3), B-Li 2.503(4).

Digermenyl borate **219** is unstable in pentane solution at room temperature and decomposes over the period of 8 hours to unidentified Ge*H*-species. Melting of **219** at 125-127 °C afforded, as observed for digermenide **90**, $Tip_2Ge{=}GeTip_2$ **51** beside unidentified decomposition products.

The orange color of digermenyl borate **219** is due to the longest wavelength absorption in the UV/vis spectrum at λ_{max} = 438 nm (ε = 8900 $Lmol^{-1}cm^{-1}$) and nearly identical to that of digermenide **90** (λ_{max} = 435 nm (ε = 11800 $Lmol^{-1}cm^{-1}$)).

3.5.2.6. Reaction of Digermenide 90 with Ph_2NBCl_2

The reaction of Ph_2NBCl_2 and digermenyllithium **90**, should in principle form boryl digermene **222** with an additional chlorine functionality allowing for further manipulation (Scheme 152).

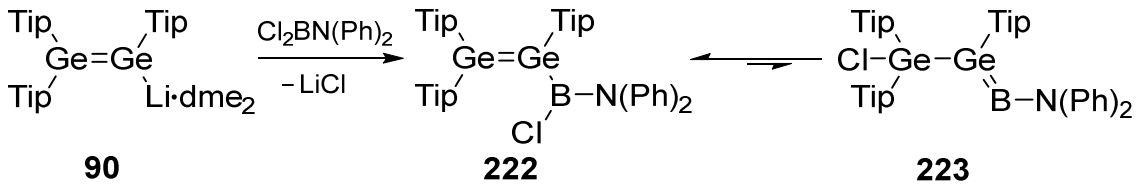

Scheme 152. Reaction of digermenide **90** with Ph_2NBCl_2 resulting in boryl digermene **222** in equilibrium with germyl boragermene **223**.

The 1:1 reaction of digermenide **90** with Ph_2NBCl_2 in benzene solution at room temperature shows a uniform conversion into a new product (as determined by ^1H NMR spectroscopy, Figure 87).

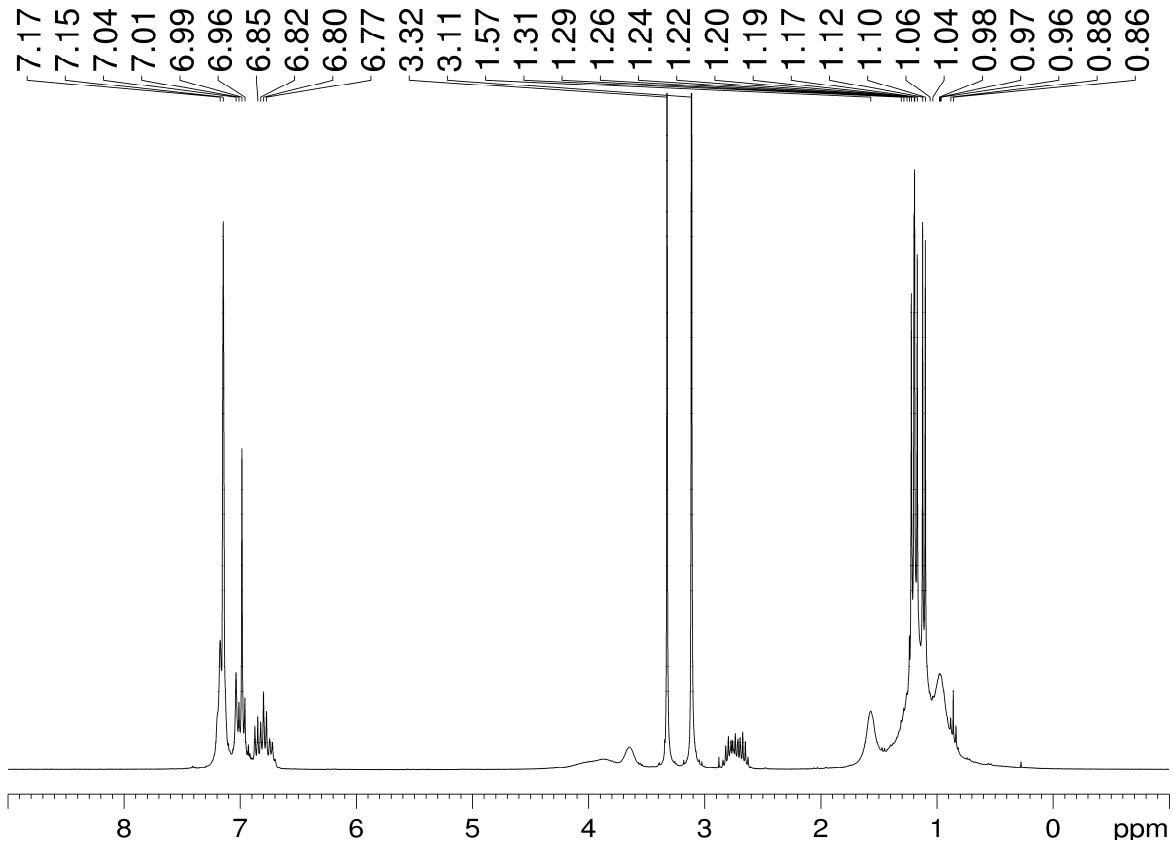

Figure 87. ^1H NMR spectrum of the crude reaction mixture of digermenide **90** with Ph_2NBCl_2 after 5 min at room temperature.

Filtration from pentane and storing a concentrated solution at room temperature afforded yellow single crystals suitable for X-ray diffraction (Figure 88).

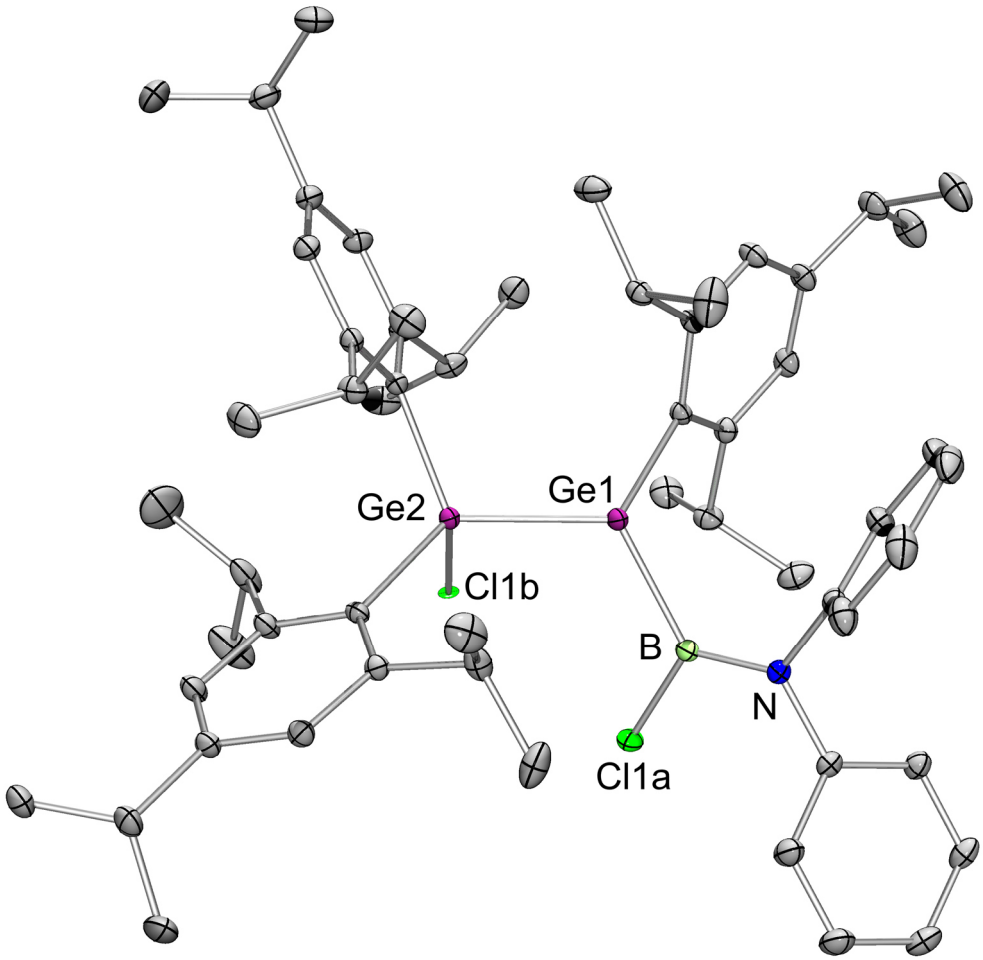

Figure 88. Molecular structure of 90% **222** and 10% of **223** in the solid state (ellipsoids are at 30%, hydrogen atoms omitted for clarity). Selected bond lengths [Å]: Ge1-Ge2 2.301(2), Ge1-B 2.059(16), Ge2-Cl1b 2.225(3), B-Cl1a 1.786(3), B-N 1.399(2).

Despite crystals of apparently high quality, the refinement resulted in appreciable residual electron density near Ge2 in approximately 2.2 Å distance and thus in line with a typical Ge-Cl single bond.[61,62,67] This may indicate the superposition of two isomeric species **222** and **223** in the solid state resulting from a 1,3-chlorine shift, which would be reminiscent of the irreversible 1,3-amino shift suggested for a plausible phosphino-substituted disilene intermediate **[224]** to lead to the phosphasilene **225**-*E*/*Z* (Scheme 153).[215]

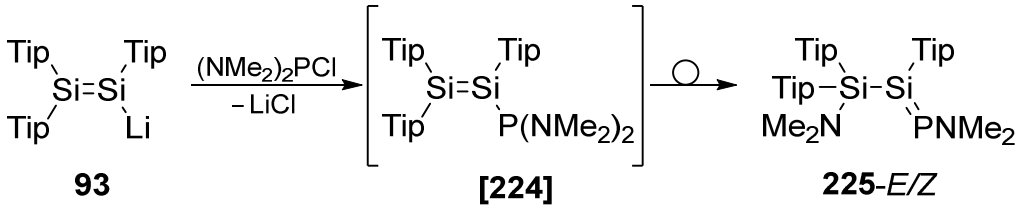

Scheme 153. Reaction of **93** with $(Me_2N)_2PCl$ resulting in phosphasilene **225**-*E*/*Z*.

In Figure 88 the chlorine atom Cl1a from the proposed boragermene **223** is displayed, whereas the second component of the smaller boron atom could not be detected. On the basis of the refined occupation numbers for Cl1a and Cl1b, the functionalized aminochloroboryl digermene **222** is present to 90% and the germyl boragermene **223** would account for the remaining 10%.

After dissolving the crystalline material of **222** and **223** in C_6D_6 the ^{1}H NMR spectrum is nearly identical to the spectrum of the crude reaction mixture (Figure 89). In order to resolve the suspected equilibrium of the species **222** and **223**, a low-temperature NMR was recorded. As had been the case at room temperature, no ^{11}B NMR signal could be detected at −50 °C either. In the ^{1}H NMR spectrum at −50 °C the broad signals present at room temperature are resolved better, especially in the region of the CH signals of the isopropyl groups (Figure 90). Although this ^{1}H NMR spectrum appears to indicate the presence of a major and a minor species, the ratio between them could not be determined due to severe overlap of the signals and therefore no correlation be established to the one deduced from the occupation numbers found in the solid state by X-ray diffraction analysis.

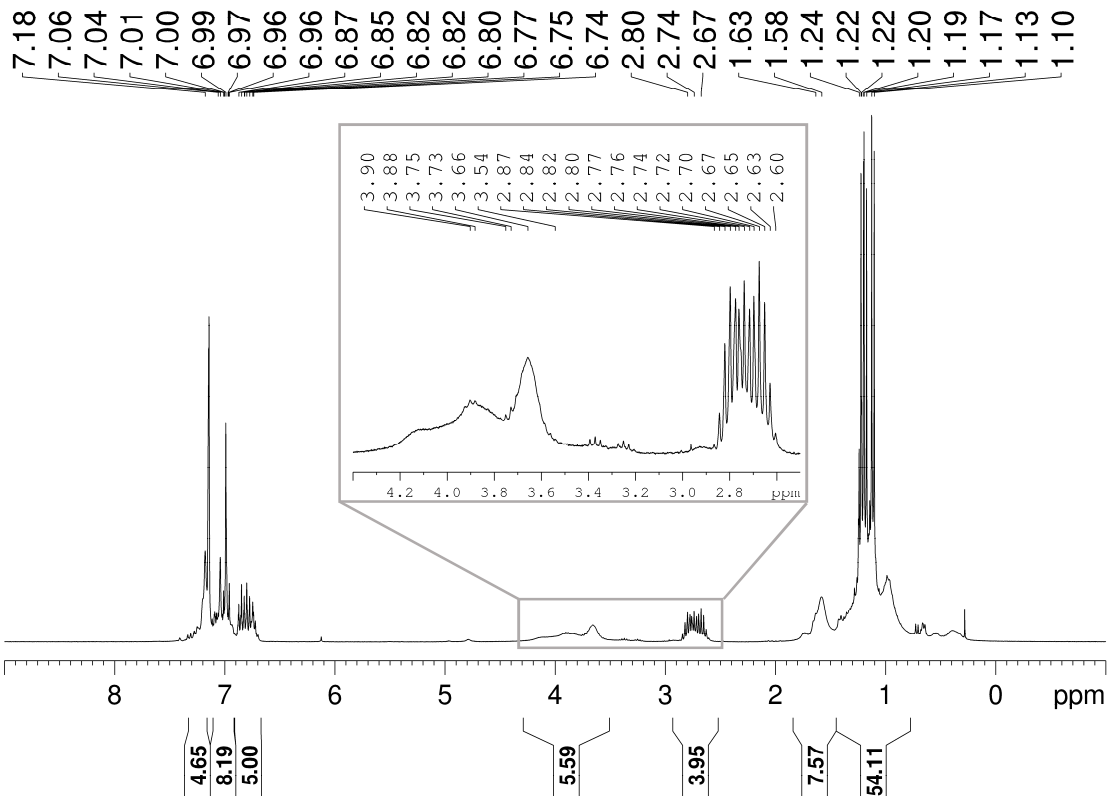

Figure 89. ^{1}H NMR spectrum of the crystalline material of **222** and **223**. The excerpt shows the signals of a C*H* at the isopropyl-groups of the Tip-substituents.

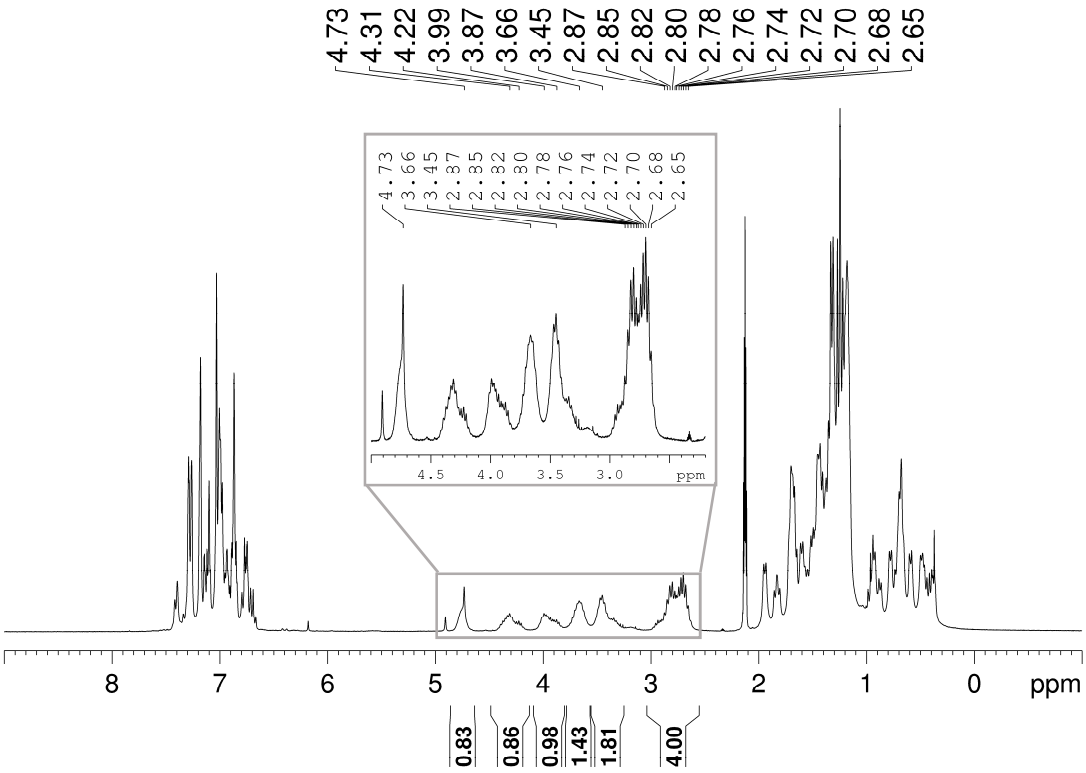

Figure 90. ^{1}H NMR spectrum of the crystalline material of **222** and **223** at (−50 °C in toluene-d_8). The excerpt shows the signals of a C*H* at the isopropyl-groups of the Tip-substituents.

It is not possible to thermally convert **222** to **223**. Heating a sample of **222** and **223** to 80 °C for 3 days indicated nearly the same ^{1}H NMR resonances together with some decomposition products.

3.5.2.7. Reaction of Digermenide 90 with (^{i}Pr$_2$N)$_2$PCl

The investigations concerning the reactivity of digermenide **90** toward Group 13 and Group 14 reagents have been described in the last chapters. The reactions of disilenide **93** with diamino chloro phosphines led to a variety of phosphino disilenes or phosphasilenes depending on the size of the substituent at the amino-groups.[215–217] Therefore, the reaction of **90** with (^{i}Pr$_2$N)$_2$PCl was investigated to target phosphino digermene **226** and possibly related species (Scheme 154).

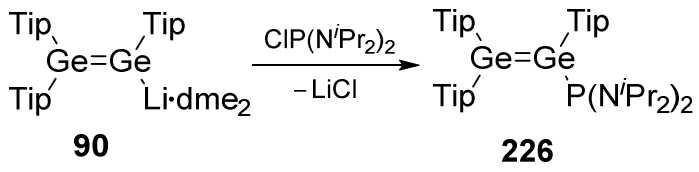

Scheme 154. Reaction of digermenide **90** with (^{i}Pr$_2$N)$_2$PCl to phosphino digermene **226**.

In a first attempt, digermenyllithium **90** was treated with one equivalent of (^{i}Pr$_2$N)$_2$PCl in benzene at room temperature. The ^{31}P NMR spectrum shows three main signals at δ = 134.7, 83.6 and 81.00 ppm (Figure 91). The signal at δ = 134.7 can be assigned to a slight excess of the starting material (^{i}Pr$_2$N)$_2$PCl and the major signal in the ^{31}P resonance at δ = 81.00 ppm was a hint for the formation of phosphino digermene **226**. While alkyl and aryl substituted phosphino disilenes reported by Scheschkewitz *et al.* can be found in the range of δ = 8.9 to −45.7 ppm in the ^{31}P NMR spectrum,[216] the ^{31}P signals of amino-substituted phosphino disilenes were more deshielded (^{31}P NMR: Tip$_2$Si=SiTipP(NPh$_2$)$_2$: δ = 104.5 ppm; Tip$_2$Si=SiTipP(N^{i}Pr$_2$)$_2$: δ = 58.4 ppm).[215,217] Due to the fact that these reactions are unprecedented only a theoretical study about phosphino digermenes were investigated by Li and Su in 2012.[218] Unfortunately, it was not possible to obtain single crystals for structural confirmation in the solid state.

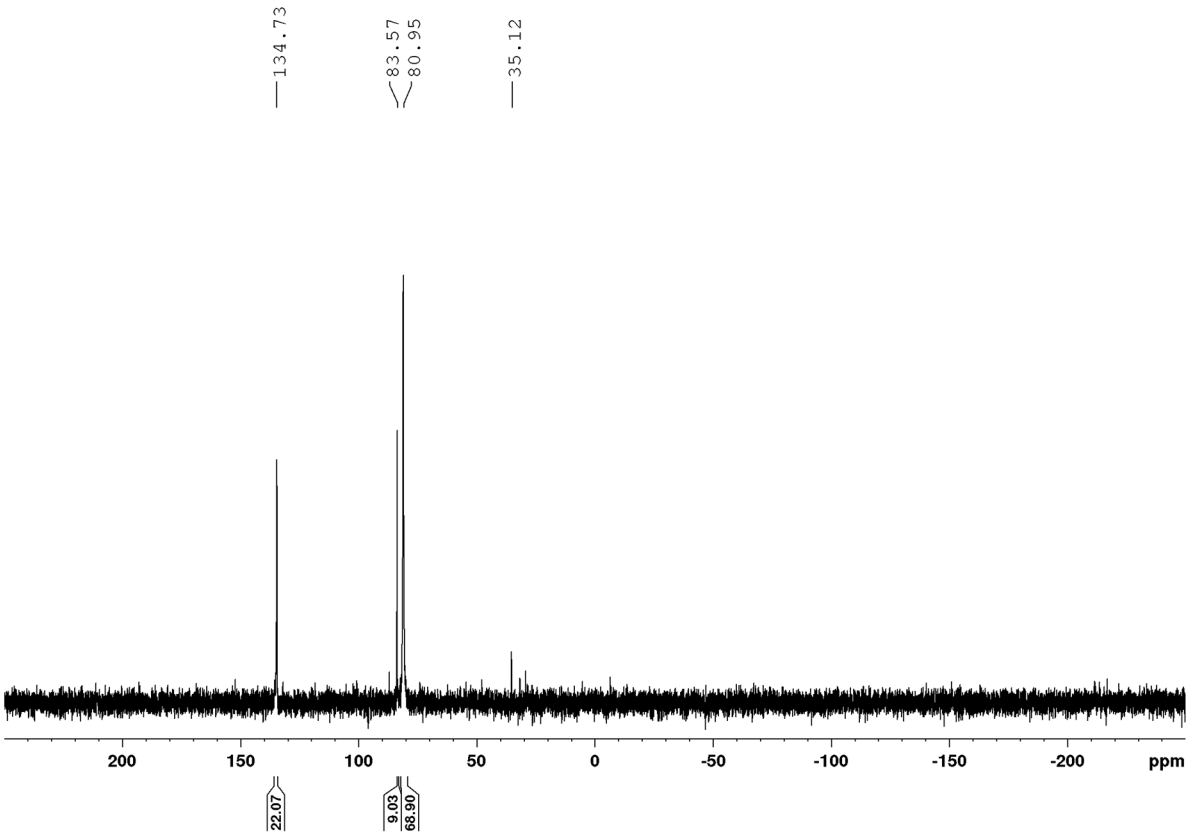

Figure 91. ^{31}P NMR spectrum of the reaction mixture of **90** with $(^{i}Pr_2N)_2PCl$.

3.5.2.8. Reaction of Digermenide 90 with $(Me_2N)_2PCl$

Phosphasilene **225** was obtained when disilenide **93** was reacted with $(Me_2N)_2PCl$. The analogous reaction in case of digermenyllithium **90** was expected to afford the corresponding phosphagermene (Scheme 155).

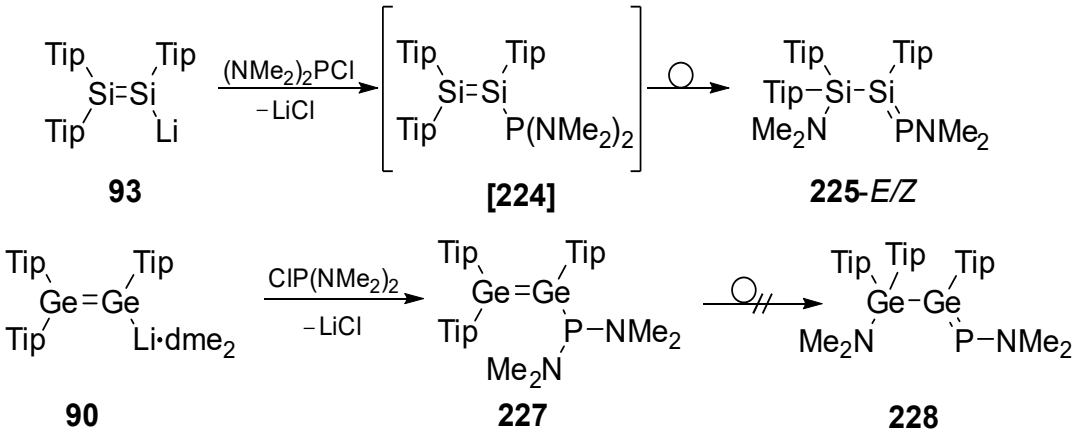

Scheme 155. Reaction of **90** with $(Me_2N)_2PCl$ resulting in phosphino digermene **227**.

The 1:1 reaction of **90** with $(Me_2N)_2PCl$ in C_6D_6 at room temperature shows one major signal in the ^{31}P NMR spectrum at δ = 112.5 ppm beside some smaller amounts of byproducts (Figure 92), which is an indication for the formation of an amino substituted phosphino digermene **227** (Scheme 155). In this case the amino group apparently remained attached to the phosphorus atom and was thus not shifted to the β-Ge-atom as had been observed in case of the formation of phosphasilene **225** reported by Scheschkewtiz and co-workers.[215] While polarized phosphasilenes (^{31}P NMR shift for **225**-*E*/*Z* at δ = 344.8 and 336.2 ppm) typically show ^{31}P NMR signals in the range from δ = 336.2 to 389.3 ppm, a phosphagermene reported by Sekiguchi *et al.* gave rise to an even more deshielded ^{31}P resonance at δ = 416.3 ppm (Figure 92). The observed ^{31}P NMR shift at relatively highfield therefore excludes the formation of phosphagermene **228**.[215,219]

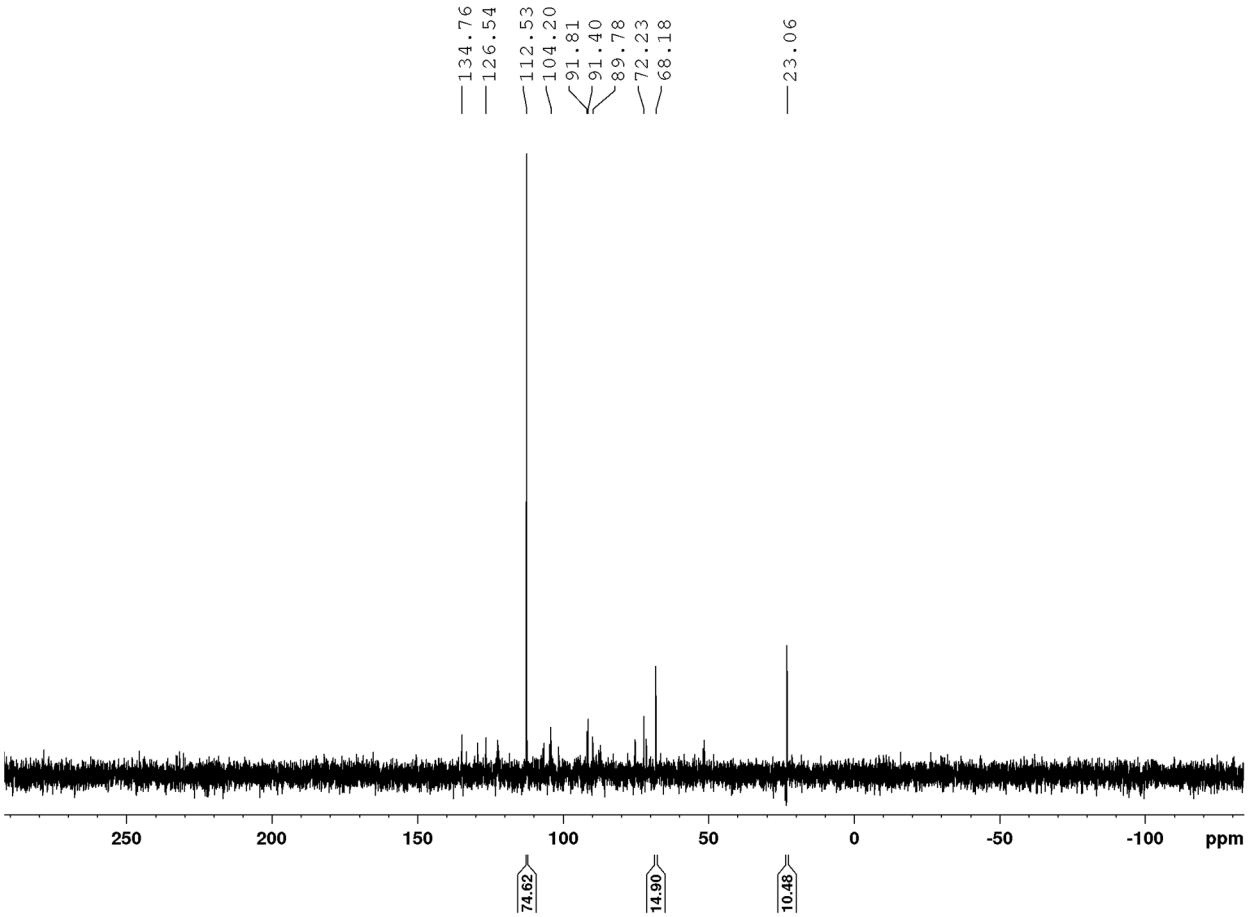

Figure 92. ^{31}P NMR spectrum of the reaction mixture of digermenide **90** with $(Me_2N)_2PCl$.

Unfortunately, no single crystals for X-ray diffraction analysis could be obtained in order to confirm the molecular structure of **227** in the solid state.

3.5.2.9. Reaction of Digermenide 90 with $P(NHC^{iPr_2Me_2})_2BPh_4$

In case of disilenide **93** the reaction with $P(NHC^{iPr_2Me_2})_2BPh_4$ led to cyclic phosphasilene **230** with the $NHC^{iPr_2Me_2}$ coordinated to the silicon-center (Scheme 156).[220] The reaction of digermenide **90** with $P(NHC^{iPr_2Me_2})_2BPh_4$ could therefore in principle result in a similar three-membered ring with the $NHC^{iPr_2Me_2}$ located at the phosphorous (**231**) or the germanium-center (**232**) after the reaction (Scheme 156).

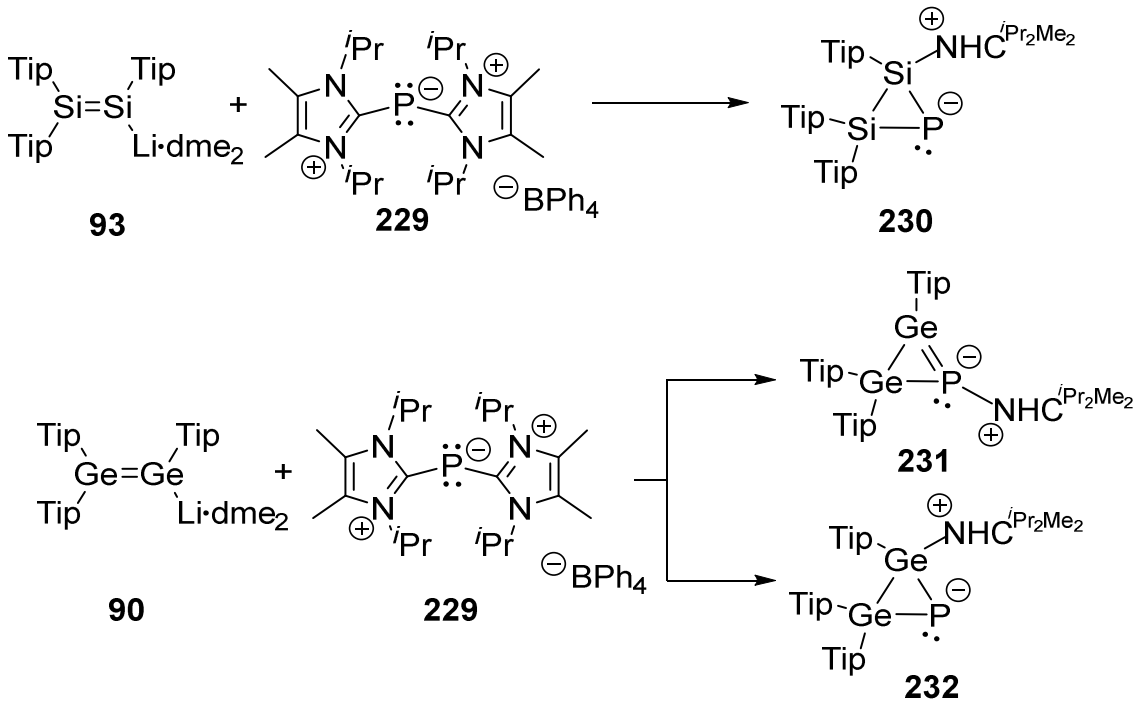

Scheme 156. Proposed reaction of digermenide **90** with $P(NHC^{iPr_2Me_2})_2BPh_4$ and reaction of disilenide **93** with $P(NHC^{iPr_2Me_2})_2BPh_4$ resulting in **230**.

The reaction of digermenyllithium **90** and $P(NHC^{iPr_2Me_2})_2BPh_4$ in toluene at room temperature indeed led to a change in color from deep red to orange. The ^{31}P NMR spectrum reveals a new resonance at $\delta = -187.5$ ppm (Figure 93), which is downfield shifted in contrast to the silicon-species **230** (^{31}P NMR resonances at $\delta = -252.2$ and -267.9 ppm). However, the ^{1}H NMR spectra of **230** and the proposed cyclic products **231** and **232** are completely different from each other (Figure 94). The splitting pattern of compound **230** (Figure 94b) differs significantly in the region of C*H* protons at the isopropyl groups of the NHC and Tip-substituents (Figure 94a).[221] A white precipitate formed, which was identified by ^{1}H NMR spectroscopy as $LiBPh_4$. In the ^{1}H and ^{13}C

NMR spectrum no free NHC^{i}Pr2Me2 is detected, but an exact assignment was not possible due to signal overlaps. After one day at room temperature, a slow decomposition of the product was apparent from new resonances in the ^{31}P NMR spectrum growing in at δ = −289 to 292 ppm. Unfortunately, despite repeated attempts, crystallization of the product from a saturated pentane solution at −26 °C failed.

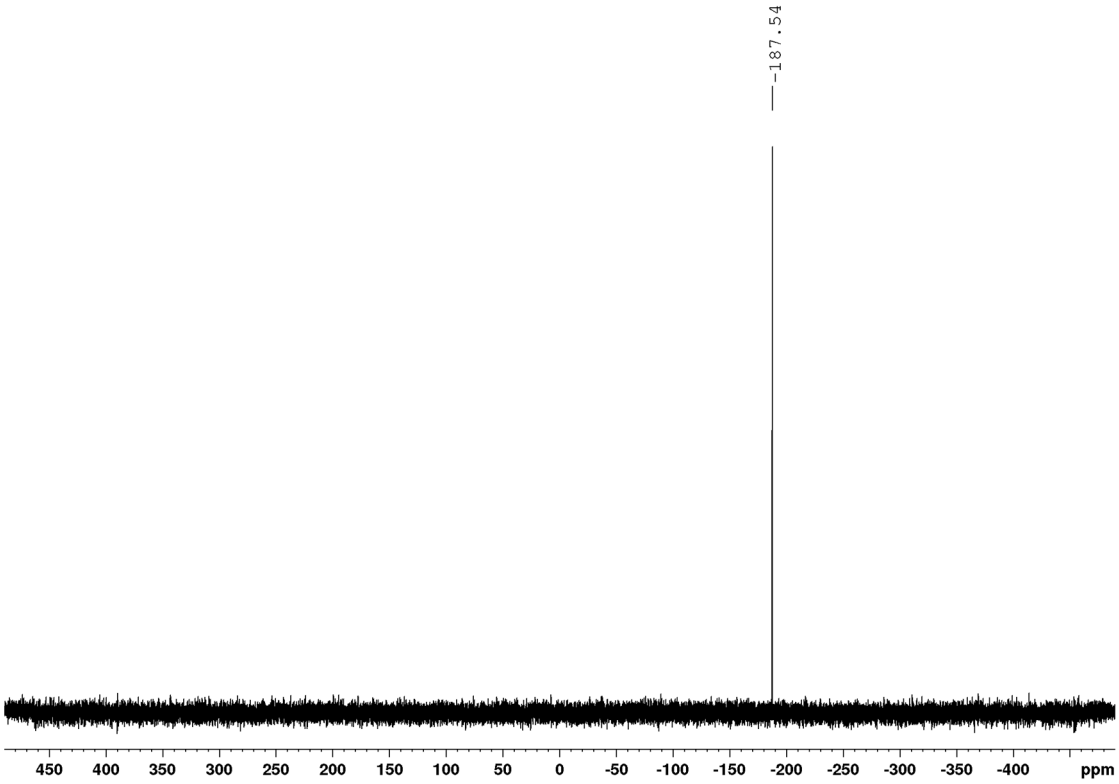

Figure 93. ^{31}P NMR spectrum of the reaction mixture of digermenide **90** with P(NHC^{i}Pr2Me2)$_2$BPh$_4$.

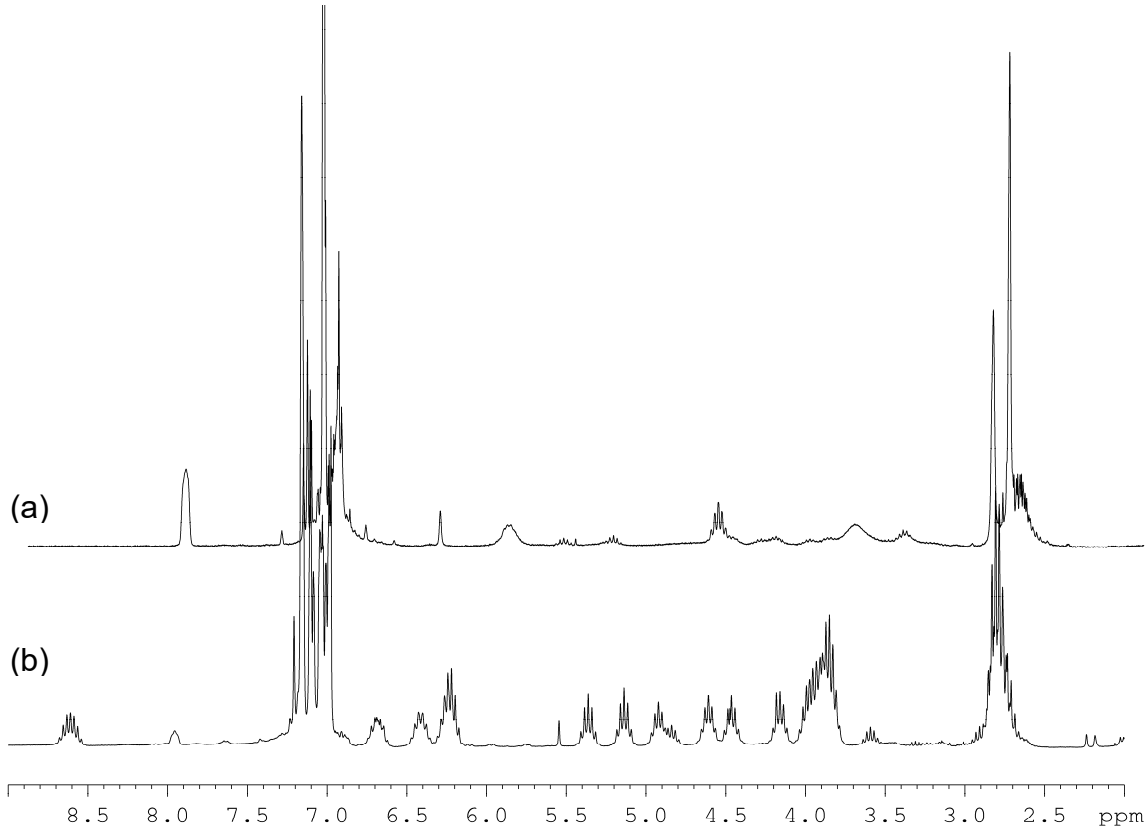

Figure 94. Comparison of ^{1}H NMR spectra excerpts (without alkyl region): (a) reaction mixture of digermenide **90** with $P(NHC^{iPr2Me2})_2BPh_4$, (b) pure sample of NHC-stabilized cyclic phosphasilene **230**.

3.5.2.10. Reaction of Digermenide 90 with NHC^{iPr2Me2}

In 2007 Baines *et al.* reported the cleavage of the Ge-Ge-double bond of the symmetrical tetramesityl digermene **14** with 2 eq of NHC^{iPr2Me2}, which led to the formation of two NHC-coordinated germylenes **15** (Scheme 157).[65]

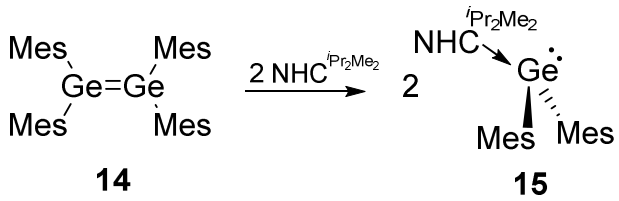

Scheme 157. Cleavage of symmetrical digermene **14** by 2 eq NHC^{iPr2Me2} resulting in 2 eq of NHC^{iPr2Me2}-coordinated diaryl germylenes **15**.

Encouraged by these results, digermenyllithium **90** was treated with 2 eq of NHC^{iPr2Me2} in C_6D_6 at room temperature with the aim to obtain unprecedented lithio germylene as NHC complex **233** alongside diaryl germylene/NHC adduct **234** (Scheme 158). In the ^{1}H NMR spectrum, however, no discernible change in the splitting pattern of the

structure motive of digermenide **90** was observed after the addition, except of the typical signal set of the NHC^{iPr_2Me_2} (Figure 95). For the proposed NHC-stabilized germylenes **233** and **234** two distinguishable multiplets for the methine protons of the coordinated NHCs are expected due to the different substituents at both Ge(II)-centers. The coordination of NHC^{iPr_2Me_2} to a Ge(II)-center can almost be excluded displaying only one multiplet for the methine protons of the NHC at δ = 4.34 ppm (5H), which is not in the typical range for a NHC-stabilized germylene in the ^{1}H NMR spectrum (typical chemical shifts for methine protons of a NHC^{iPr_2Me_2}-coordinated to Ge(II)-center in the ^{1}H NMR spectrum: δ = 5-6 ppm[62,63,65,144,145,147], for NHC-stabilized germylene **15**: δ = 5.73 ppm[65]).

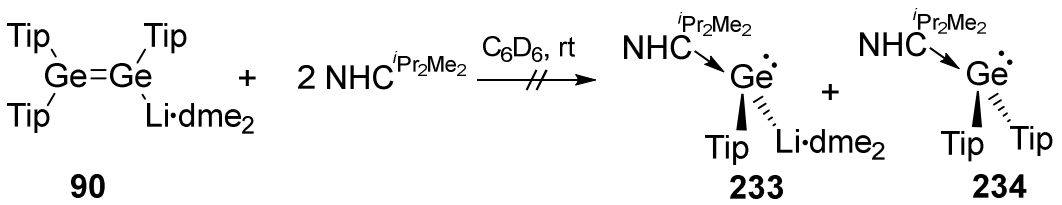

Scheme 158. Proposed synthetic pathway for the cleavage of the Ge=Ge-bond in **90** with 2 eq of NHC^{iPr_2Me_2} resulting in **233** and **234**.

Furthermore, three resonances for the aryl-protons of the Tip-substituents were observed at δ = 7.10, 7.09 and 7.08 ppm in the integrated ratio of 2:2:2 (Figure 95), suggesting that NHC-coordinated lithio germylene **233** and diaryl germylene **234** had not been formed (expected integrated ratio for the aryl-protons of **233** and **234** should be 2:4). In contrast, the signals of dme at δ = 3.22 and 3.09 ppm suggest the at least partial liberation of dme from the lithium cation (free dme δ = 3.33 and 3.12 ppm, dme coordinated to the Li-center in digermenide **90**: δ = 2.93 and 2.84 ppm). Apparently, a rapid exchange of NHC and dme in the coordination sphere of the Li-countercation of digermenide **90** takes place.* It is literature known that NHCs can coordinate to Li-centers.[222,223]

*NMR at variable temperature to back this assertion could not be carried out at the time of these experiments due to technical difficulties as well as the imminent move to new laboratories.

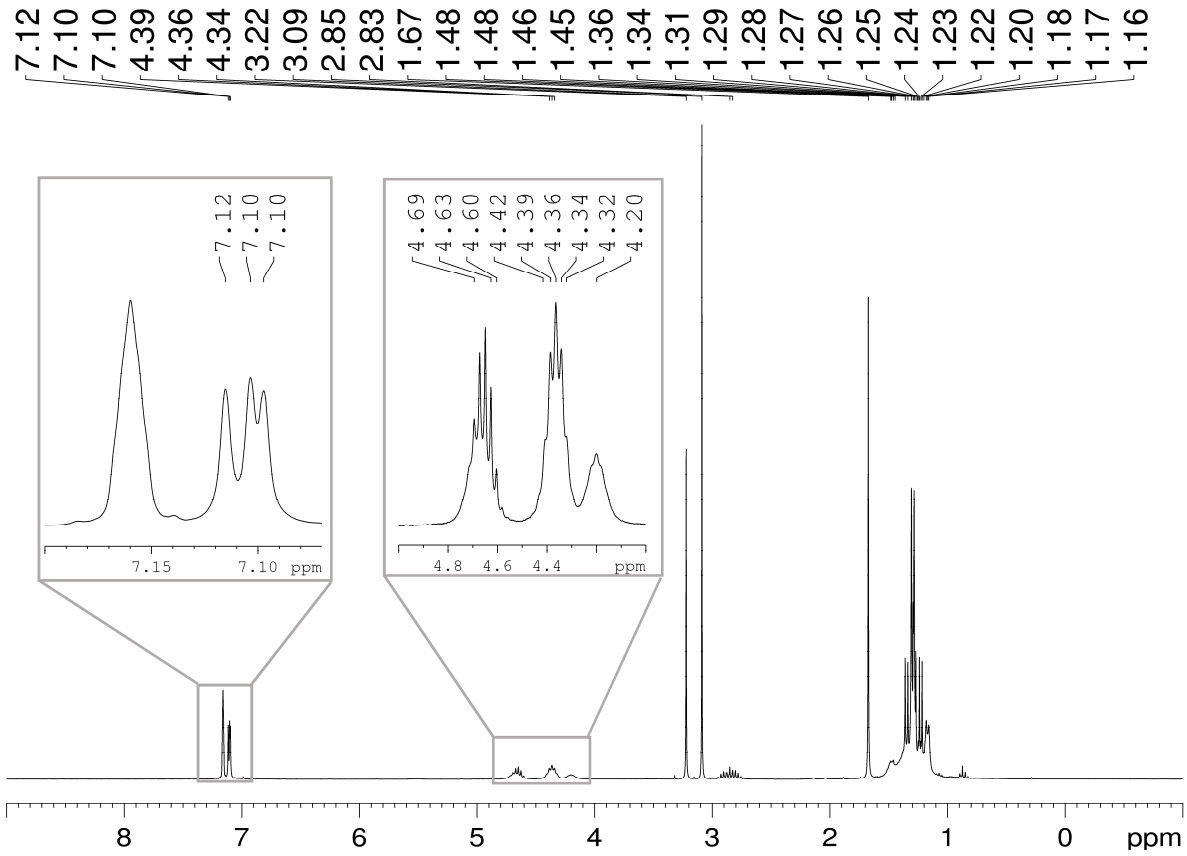

Figure 95. ^{1}H NMR spectrum of the reaction mixture of digermenide **90** with 2 eq of of NHC^{i}Pr2Me2. The excerpts show the aryl-region and signals of the methine protons for the NHC and of the Tip-groups.

To prove if an excess of NHC^{i}Pr2Me2 could cleave the Ge=Ge-bond, two further equivalents NHC^{i}Pr2Me2 were added to the reaction mixture of digermenide **90** and NHC^{i}Pr2Me2 at room temperature. After addition the mulitplet of the methine proton of the NHC^{i}Pr2Me2 has shifted from δ = 4.34 ppm to δ = 4.18 ppm and the dme signals shifted from δ = 3.22 and 3.09 ppm to δ = 3.28 and 3.10 ppm in the ^{1}H NMR spectrum (Figure 96c) and thus even close to the chemical shifts of free dme. The aryl region, however, still shows three signals for the aromatic protons of the Tip-substituents that the changed ration of NHC^{i}Pr2Me2 allows for probing, which of these species is more strongly coordinated to the Li-center.

Indeed, after evaporation of the solvent, the signals of dme had almost completely disappeared and a broad signal for the methine protons of the NHC^{i}Pr2Me2 is detected at δ = 4.14 ppm in the ^{1}H NMR spectrum (Figure 96d). Additionally, the aryl protons of the Tip-group are not observed in the previous ratio of 2:2:2, instead two sharp signals are observed at δ = 7.15 and 7.09 ppm in the integrated ratio of 2:4. The ^{7}Li NMR

spectrum shows one resonance at δ = 2.50 ppm (^{7}Li NMR spectrum of digermenide **90**: δ = –0.18 ppm). This could be taken as indication for the formation of NHC-stabilized diaryl germylene **234** and NHC-stabilized lithio germylene **235** with 2 eq of NHC^{iPr2Me2} coordinated to the Li-atom instead of two dme molecules (Scheme 159).

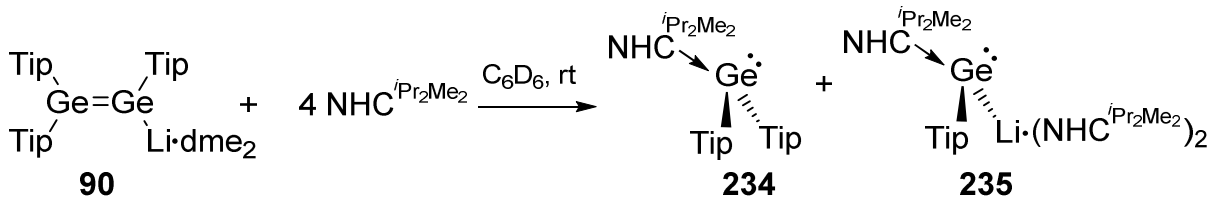

Scheme 159. Reaction of digermenide **90** with 4 eq of of NHC^{iPr2Me2} resulting in proposed NHC-stabilized germylenes **234** and **235**.

The broad resonance of the methine protons of the NHC could be due to a fast exchange of the coordinated NHC-species.

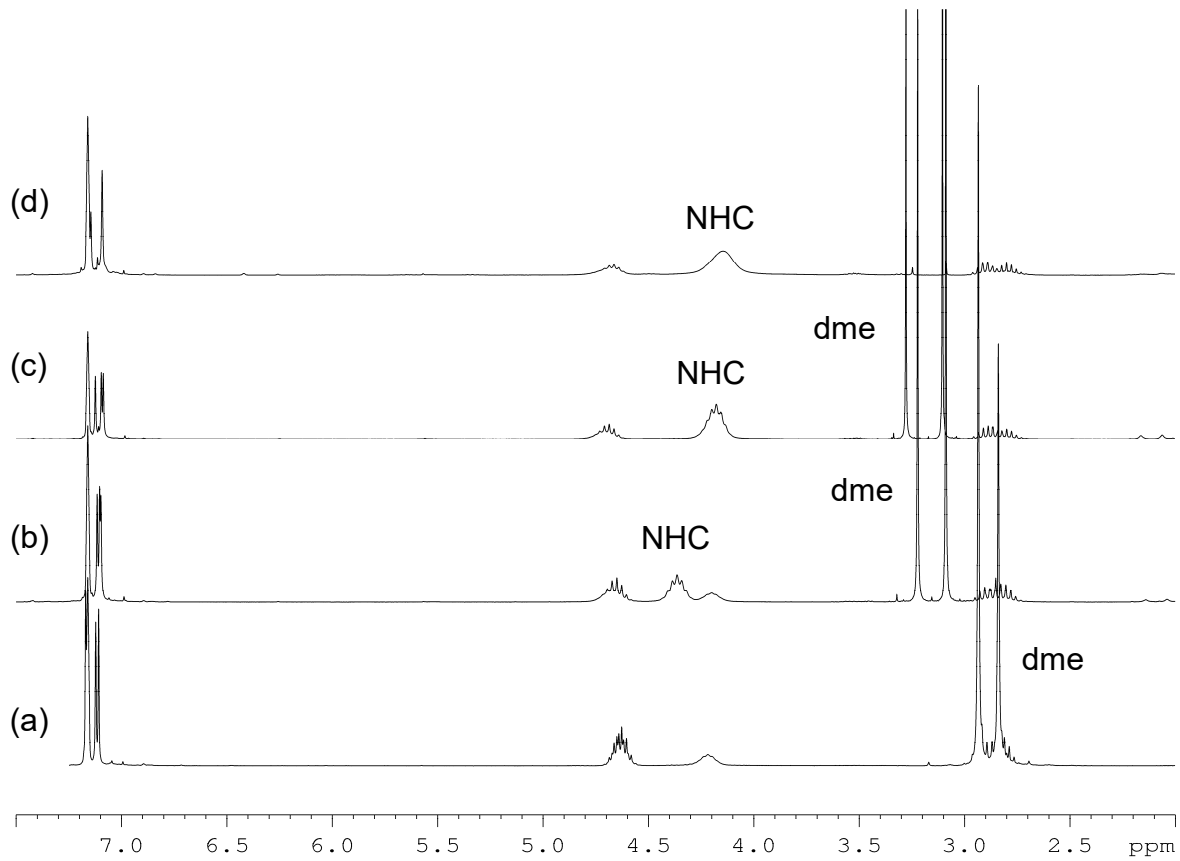

Figure 96. Excerpts of ^{1}H NMR spectra: (a) digermenide **90**, (b) **90** + 2 eq NHC^{iPr2Me2}, (c) after addition of to 2 further eq NHC^{iPr2Me2} to (b), (d) after evaporation of dme from the reaction mixture in (c) resulting most likely in NHC-stabilized germylenes **234** and **235**.

To further study the behavior of the proposed mixture of NHC-stabilized germylenes **234** and **235** toward additional NHC^{iPr2Me2}, the addition of two more equivalents was carried out (6 eq added overall). In the ^{1}H NMR spectrum, the methine protons of the NHC are shifted from δ = 4.14 ppm to δ = 4.05 ppm approaching the signal for free NHC^{iPr2Me2} at δ = 4.00 ppm. In the aryl region again three signals in the ratio 2:2:2 are observed for the aromatic protons of the Tip-groups at δ = 7.14, 7.11 and 7.09 ppm, which corresponds to the pattern typically observed for the digermenide precursor **90**. These observations may indicate that the digermenide scaffold has reassembled, which might be explained by the formation of a solvent-separated ion pair **236** by the excess of NHC (Figure 97b). The phosphinidene-like anionic fragment **236** would be expected to highly reactive so that a reassociation with the GeR_2 counterpart **234** might be favorable (Scheme 160).

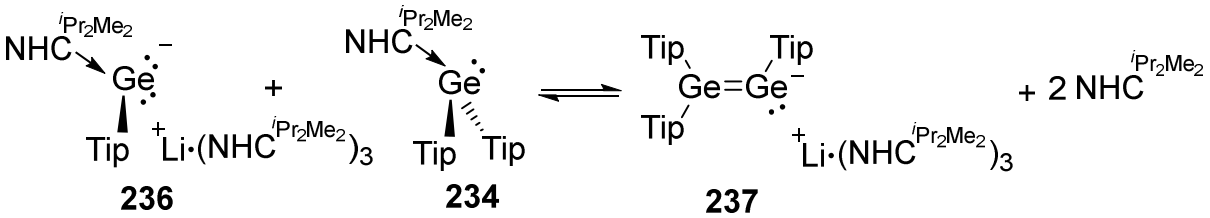

Scheme 160. Proposed reassociation for digermenide **237** by solvent-separated ion pair **236** and $GeTip_2$-fragment **234**.

Recently, during her Master Thesis Yvonne Kaiser isolated the anionic Ge_4-compound **238** in which three equivalents of NHC^{iPr2Me2} effectuate complete separation of a Li^+-cation from the counteranion (Scheme 161).[224]

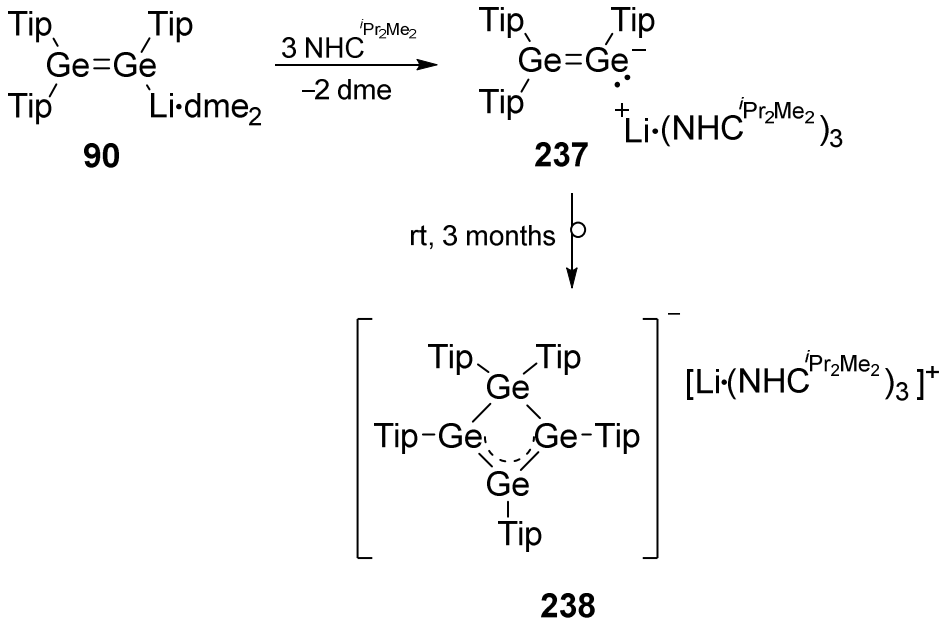

Scheme 161. Rearrangement of digermenide **90** to Ge_4-anion **238**.

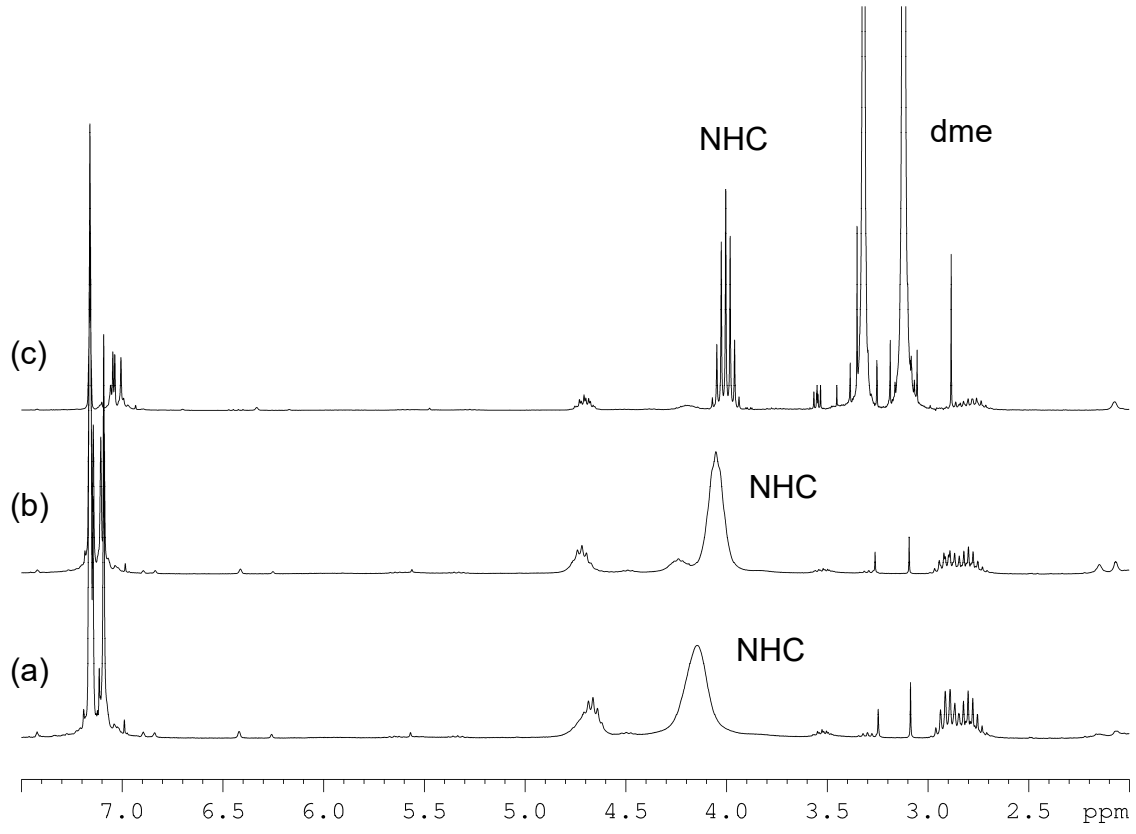

Figure 97. Excerpts of ^{1}H NMR spectra: (a) mixture of proposed NHC-coordinated germylenes **234** and **235**, (b) after addition of to 2 further eq NHC^{iPr_2Me_2} to the mixture of **234** and **235**, (c) after addition of excess dme to the reaction mixture of (b).

To prove whether the proposed NHC-coordination to the Li-center is reversible an excess of dme was added to the mixture. The ^{1}H NMR spectrum shows the formation of free NHC^{iPr_2Me_2} (methine proton of C*H*Me$_2$-group at δ = 4.00) together with dme at δ = 3.31 and 3.12 ppm which are close to the values of free dme (δ = 3.33 and 3.12 ppm). This observation confirms the suggestion that dme and the NHC^{iPr_2Me_2} compete with each other about the coordination sphere around the Li-center (Figure 97c).

A repeat reaction of digermenide **90** and 3 equivalents of NHC^{iPr_2Me_2} was carried out in benzene at room temperature to isolate the solvent separated ion pair **237**. A concentrated pentane solution was stored at room temperature. Unfortunately no crystals could be obtained to determine the structure in the solid state.

Analogous observations were made for the smaller NHC^{Me_4} and digermenyllithium **90**. As mentioned above, a low temperature NMR study could shed a light on the presence of NHC-stabilized germylene **234** and lithio germylene **235**, so that a definite conclusion of the suitability of NHCs for the dissociation of digermenide **90** cannot be drawn at this point. An alternative pathway for the cleavage of the Ge-Ge-double bond could be reactions of digermenide **90** with other types of carbenes, e.g. cyclic alkyl amino carbenes (cAACs), which are stronger σ-donors and weaker π-acceptors compared to NHCs.[225]

4. Summary and Outlook

Vinylidene is the only electron precise isomer of acetylene, but so far derivatives have only been observed in cold matrices and as ligands in transition metal complexes.[138–143] Recently, our group reported on the synthesis of the first two isolable heavier versions of vinylidene as donor-acceptor complexes with an *N*-heterocyclic carbene.[144,145] In particular, α-chlorosilyl-substituted silagermenylidene **104** is a versatile precursor due to the high degree of functionalization.[146,147]

On ground of this preceding studies, silagermenylidene **104** was reacted with different types of anionic nucleophiles. Reaction of **104** with MeLi led to the formation of Ge_2Si_4 dimeric aggregates **131** and **132** with saturated scaffolds that structurally resemble the recently reported unsaturated Ge_2Si_4-systems.[156] Initial attack of the sterically innocent methyl anion equivalent at the Ge(II)-center results in formation of an NHC-stabilized disilenyl germylene **128a**, followed by ring-closure to an NHC-adduct of a heavier cyclopropene **129**. Addition of an excess of NHC stabilizes the both intermediates and demonstrates the reversibility of rate-determining initial equilibria involving NHC dissociation (Scheme 162).

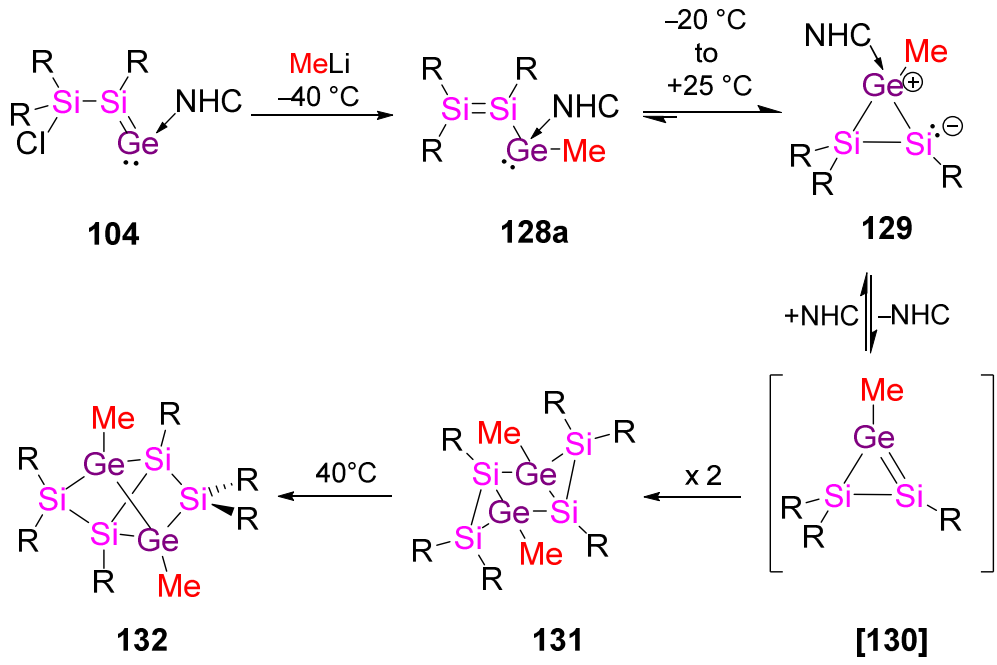

Scheme 162. Reaction of silagermenylidene **104** with MeLi resulting in Ge_2Si_4-isomers **131** and **132** *via* spectroscopically observed intermediates **128a** and **129** (R = Tip = 2,4,6-^{i}Pr$_3$-C$_6$H$_2$, NHC = 1,3-diisopropyl-4,5-dimethylimidazol-2-ylidene).

In contrast to the small Me-group, it was anticipated that a sterically more demanding substituent could provide sufficient inertness to a disilenyl germylene to allow for its isolation and full characterization. Indeed, reaction of **104** with PhLi afforded selectively NHC-coordinated disilenyl germylene **128c** which rearranges at higher temperatures to heavier cyclopropylidene analogue **123c**. Both isomers were isolated and crystallographically analyzed. Furthermore, it was possible to spectroscopically characterize disilenyl germylene **128d** at low temperatures by change of the reaction conditions of **104** with the steric bulky nucleophile MesLi.

On grounds of the reactivity of **104** with xylyl isocyanide, the isomeric compounds **128c** and **123c** were reacted with organic substrates.[147] Both isomers show an unexpected regioselectivity in their reactions with either phenylacetylene or xylyl isocyanide. While the open-chained disilenyl germylene **128c** rapidly reacts even below room temperature, the three-membered ring isomer **123c** requires prolonged heating to about 70 °C in order to generate the regiomeric products with perfect selectivity. The counter-intuitive connectivities of five-membered cyclic germylenes **133** and **134** (phenylacetylene reactions) and four-membered cyclic germylenes **138** and **143** (xylyl isocyanide) are rationalized on the basis of DFT-calculations on model species for **133** and **134**. The behavior of **128c** is governed by an initial fast reaction at the Si=Si moiety, but subsequently requires dissociation of the NHC as the rate determining step to form **133**. Conversely, the formation of **134** plausibly proceeds in a concerted manner via the insertion of the C-C triple bond of phenylacetylene into the Si-Ge single bond of three-membered ring **123c** (Scheme 163).

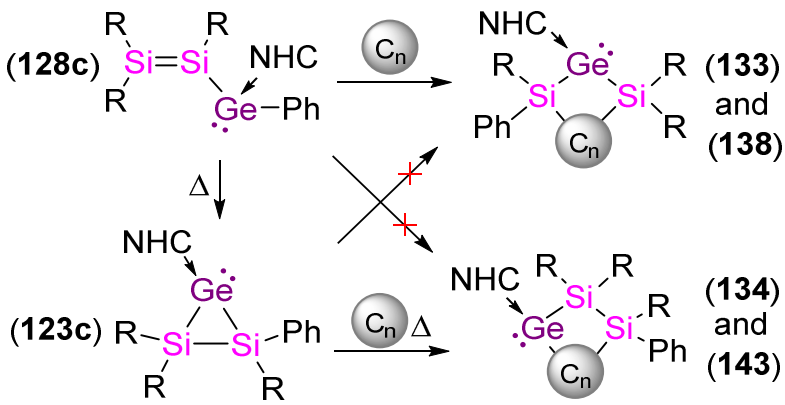

Scheme 163. Reactivity of isomer Si_2Ge-compounds **128c** and **123c** toward phenylacetlyene and xylyl isocyanide resulting in five- and four-membered ring systems **133, 134** and **138** and **143** (C_n = PhCCH, XylNC, R = Tip = 2,4,6-^{i}Pr$_3$-C$_6$H$_2$, NHC = 1,3-diisopropyl-4,5-dimethylimidazol-2-ylidene).

The selective access to isomeric heterocycles which incorporate Ge(II)-centers with simple unsaturated organic reagents offers significant opportunities for the incorporation of these cycles as building blocks of extended systems. The incorporation of these low-valent compounds into doubly-functionalized organic moieties was therefore investigated. Silagermenylidene **104** was reacted with xylyl isocyanide resulting in cyclic NHC-stabilized germylene.[147] Durylene bis-isocyanide was reacted with **104** while structurally closely related to xylyl isocyanide. Unfortunately a mixture of unidentified products was obtained. The expansion of the linking-unit was therefore investigated using bis-isocyanide **148** with an additional phenylene-group between the two CN-moieties and with **149** in which the conjugation of the system is interrupted by a CH_2-group (Scheme 164). Both reactions resulted, when cautiously heated, most likely in a mixture of diastereomeric products, which could unfortunately not be isolated as pure compounds.

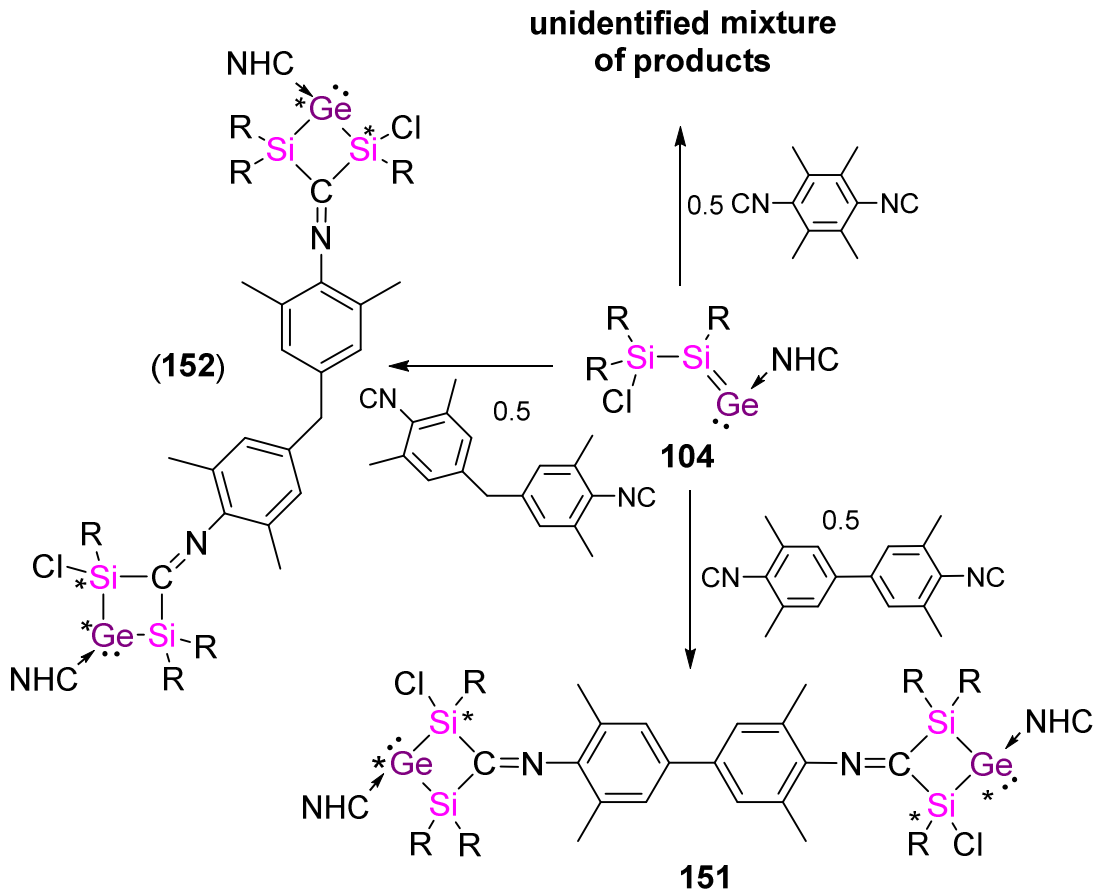

Scheme 164. Reaction of **104** with bis-isocyanides (R = Tip, NHC = 1,3-diisopropyl-4,5-dimethylimidazol-2-ylidene).

The same bis-isocyanides were utilized for the reaction of disilenyl germylene **128c** and its cyclic isomer **123c**. Also in this case no crystalline material was obtained to confirm the suggested molecular structures in the solid state.

In order to synthesize unknown NHC-coordinated diaryl substituted silylenes as precursors for low-valent Group 14 systems, different chlorosilanes were reacted with differently sized NHCs. The outcome of these reactions gave hints for the backbone activation of the NHCs by NMR-spectroscopy. In the reaction of $TipSiCl_3$ and 2 NHCs an unprecedented double activation of a methyl-group at the backbone of the NHC occurred resulting in disilyl functionalized NHC **185**. Furthermore, **185** was reduced with different reducing agents which only led to the formation of an unidentified product mixture.

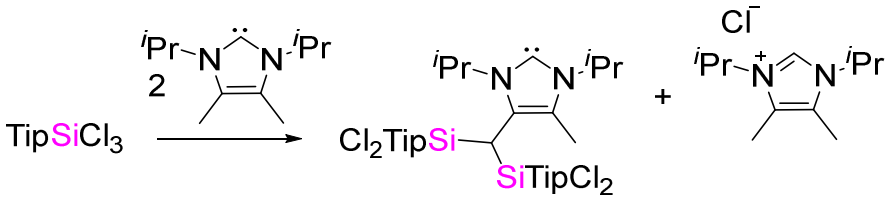

Scheme 165. Synthesis of unique doubly-backbone functionalized NHC **185**.

As stated in Chapter 1.6.1. heavier versions of disilenides have not been isolated to date.[92,128] Due to this fact, a part of this work focused on the synthesis and full characterization of a digermenide. As starting point Scheschkewitz's approach for the synthesis of disilenide **93**[132] was adopted: Tip_2GeCl_2 **50** was reduced with 3.3 equivalents of Li-powder at low temperatures with a catalytic amount of naphthalene which selectively formed digermenide **90** in ca. 50% yield as red crystalline material. Digermenyllithium **90** was characterized by X-ray diffraction which is line with the ^1H NMR data unambiguously proving the formation of the heavier Group 14 vinyllithium analogue **90** (Scheme 166).

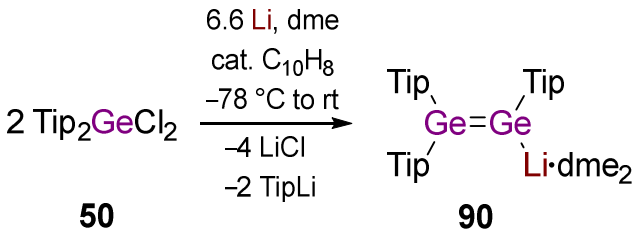

Scheme 166. Synthesis of the first isolated and fully characterized digermenide **90**.

The reactivity of **90** was investigated toward different organic and inorganic substrates. The reaction of **90** with PhI led to the formation of the oxidation product tetragermabutadiene **92** isolated by Weidenbruch and co-workers as major compound.[128] Conversely, in case of the doubly functionalized 1,4-diiodobenzene the main product of the reaction was the first example of a phenylene-bridged tetragermabutadiene **216** in analogy to the phenylene-bridged silicon analogue **214** synthesized by our group in 2007.[212] Furthermore, digermenyl borate **219** could be isolated. Reactions of **90** with $GeCl_4$ or $GeCl_2$·NHC **8** gave an unidentified mixture of products (Scheme 167). Within the timeframe of this thesis, it was also not possible to homolytically cleave the Ge-Ge-double bond of digermenide **90** in two NHC-stabilized germylene fragments with NHCs adopting the procedure reported by the Baines group.[65] In future experiments maybe a stronger σ-donor could be utilized to cleave the double bond in **90**, for instance cAACs.[225]

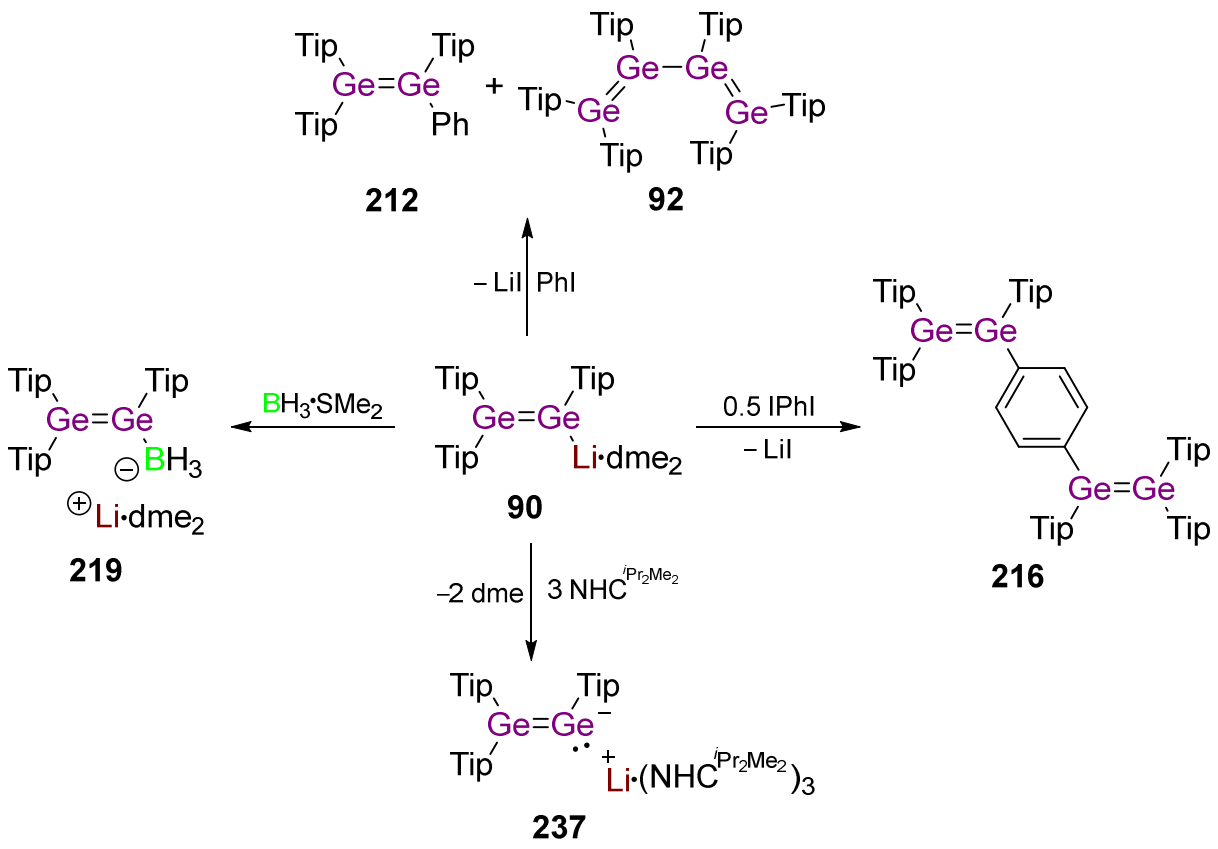

Scheme 167. Reactivity of digermenyllithium **90** toward different organic and inorganic substrates.

In conclusion, the solid state structure of digermenide **90** has been confirmed and the reactivity was studied toward different organic and inorganic substrates leading to unprecedented structure motives with intact Ge=Ge-bonds.

„Selbst heute, nachdem, allerdings unter namhaften Verlusten, wohl an hundert Gramm Germanium durch meine Hände gegangen sind, vermag ich dieses Element noch nicht vollkommen zu beherrschen…“

Clemens Winkler, "Mittheilungen über des Germanium. Erste Abhandlung", *J. Prak. Chem.* **1886**, *34*, 177–229.

5. Experimental Section

5.1. General

All experiments were carried out under a protective atmosphere of argon (5.0 supplied by PraxAir) applying standard Schlenk or glove-box techniques. All glassware was cleaned with KOH/isopropanol/H_2O bath, neutralized and kept in a drying oven at 120 °C prior to use. All setups were evacuated and purged with argon three times. The high vacuum was generated with a slide vane rotary vacuum pump RZ 6 by Vacuubrand.

5.2. Solvent purification

Solvents were refluxed over sodium/benzophenone (diethyl ether, tetrahydrofuran, 1,2-dimethoxyethane) or sodium/benzophenone/tetra(ethylene glycol)dimethyl ether (hexane, benzene, toluene) distilled and stored under argon or taken directly from a solvent purification system (Innovative Technology PureSolv MD7). C_6D_6, toluene-d_8, thf-d_8 were dried over potassium, refluxed and distilled under argon.

5.3. Analytical Methods

NMR analysis: NMR-spectra were recorded on a Bruker Avance III 300 spectrometer. ^{1}H and ^{13}C NMR spectra were referenced to external $SiMe_4$ using the residual signals of the deuterated solvent (^{1}H) or the solvent itself (^{13}C). ^{29}Si{^{1}H} NMR spectra were referenced to external $SiMe_4$. All chemical shifts are reported in parts per million (ppm). Coupling constants are reported in Hertz (Hz) and are given in the usual notation that $^nJ_{X-Y}$ means a coupling of nucleus X over n bonds with nucleus Y. Coupling constants are determined from satellite signals. The multiplicity and shape of the observed signals are given as s = singlet, d = doublet, t = triplet, quart = quartet, sept. = septet, m = multiplet, br = broad signal.

CHN analyses were performed on an Elementar Vario Micro Cube.

UV/vis absorption spectra were measured at a Perkin-Elmer Lambda 35 spectrometer using quartz cells with a path length of 0.1 cm.

Melting points were determined under argon in sealed NMR tubes and are uncorrected.

5.4. Computational Details

All theoretical calculations were carried out using the Gaussian09 suite of programs.[226] The proposed mechanisms and intermediates for the formation of **133-Me**, **134-Me** and **143-Ph** were calculated using simplified model system with methyl groups instead of Tip, Ph, and ^{i}Pr groups (Figure 98-Figure 108). The B3LYP/6-

31G(d,p) was chosen as level of theory due to dramatic raise in the computational costs with higher level of theories. Frequency analyses were performed to determine the character of optimized structures as minima or transition states. The relative Gibbs free energies are given in kcal/mol. The chemical reaction channels have been checked by the intrinsic reaction coordinate (IRC) method to verify the energy profiles at the B3LYP/6-31G(d,p) level of theory for the processes from transition states to intermediates, by using the second-order Gonzalez-Schlegel method.[227,228] The electronic absorption spectrum for **133-Me**, **134-Me**, **138-Me**, and **143-Me** was predicted with using the optimized geometry at time-dependent density functional theory (TD-DFT) method in solution (heptane) at B3LYP/6-31+G(d,p) level of theory. The GaussView 5.0 program was employed for visualization of the final geometries of the optimized structures.[229]

5.5. Starting Materials

5.5.1. General Starting Materials

General abbreviations for substituent's:

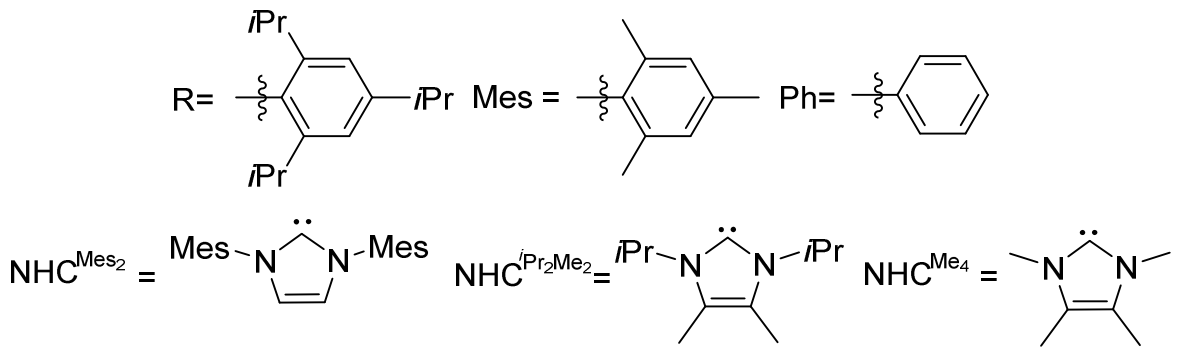

Commercially purchased chemicals

- *used without further purification:* PhLi (1.9 M in *n*-dibutyl ether), MeLi (1.6 M in Et_2O), MeLi (3.1 M in diethoxymethane), EtLi (0.5 M in benzene/cyclohexane), *i*PrLi (0.7 M in *n*-pentane), *t*BuLi (1.7 M in hexane), *s*BuLi (1.4 M in cyclohexane), xylyl isocyanide, $LiAlH_4$, 1,3-diethynylbenzene, 1,4-diethynylbenzene, 1,3-diisopropyl-2-thiourea, acetoin, 1-hexanol, potassium, sodium, lithium (granules, rod. diam. 12.7 mm, 99.9% trace metal basis), tributyltinhydrid, ethanol, Mg-shavings, $BH_3{\cdot}SMe_2$ (all Sigma-Aldrich), 3,3',5,5'-tetramethyl-[1,1'-biphenyl]-4,4'-diamine, 4,4'-methylenebis(2,6-dimethylaniline) (Alfa Aesar)

- *purified prior to use:* Phenylacetylene, 1,4-dioxane, $SiCl_4$, $GeCl_4$ and CCl_4, PhI were purchased from Sigma Aldrich, distilled and stored under argon until use. Naphthalene and 1,4-diiodobenzene were sublimed prior to use.

Starting materials supplied by the group:

TipBr, MesLi, Tip_2SiHCl, $TipSiCl_3$, Mes_2SiHCl, NHC^{Me4}, NHC^{Mes2}, AIBN, $ZnCl_2$, BPh_3, Fe_2CO_9, Li-powder, $Pd(PPh_3)_4$, $BPh_4P(NHC^{iPr2Me2})_2$, bis[dimethylamino]chlorophosphane, dichloro(*N*,*N*-diphenylamino)borane, bis[diisopropylamino]chlorophosphane, 1,2-bis(isocyano)-2,3,4,5-tetramethylbenzene

5.5.2. Synthesis of 1,3-Diisopropyl-4,5-dimethylimidazole-2(3H)-thione

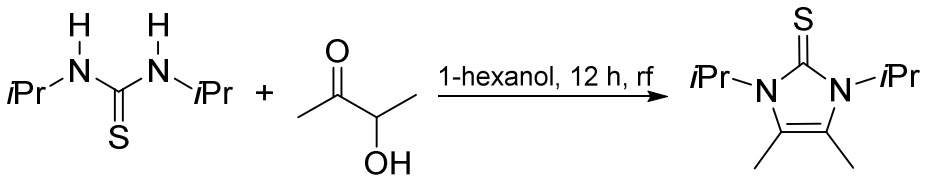

$C_7H_{16}N_2S$ 160.28 g mol^{-1} | $C_4H_8O_2$ 88.11 g mol^{-1} | $C_{11}H_{20}N_2S$ 212.36 g mol^{-1}

1,3-Diisopropyl-4,5-dimethylimidazole-2(3H)-thione was prepared following a procedure of Kuhn and Kratz.[230] To a solution of 31.66 g of 1,3-diisopropylthiourea (200 mmol) in 500 mL of 1-hexanol 17.45 mL of 3-hydroxybutan-2-one (17.62 g, 200 mmol) are added by a funnel in one go. The reaction mixture is heated to reflux for 12 h applying a water separator for the collection of reaction water. A 1:1 mixture of H_2O:ethanol (ca. 200 mL) causing a white solid to precipitate. The precipitate is re-crystallized to afford white needles of the thione. After filtration, the needles are washed with H_2O (3*50 mL) to yield 20.48 g (50%) of pure thione.

^{1}H NMR (300.13 MHz, $CDCl_3$, 300 K): δ = 5.64 (br, 2H, C*H*$(CH_3)_2$ of NHCS), 2.20 (s, 6H, C*H*$_3$ of NHCS), 1.46 (d, 12H, CH(C*H*$_3$)$_2$ of NHCS) ppm.

5.5.3. Synthesis of 1,3-Diisopropyl-4,5-dimethylimidazole-2-ylidene

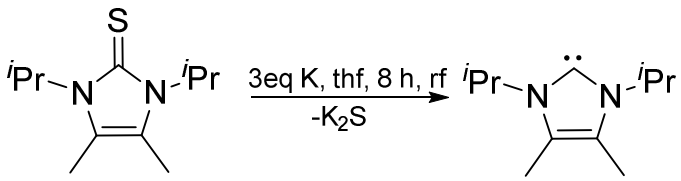

$C_{11}H_{20}N_2S$ 212.36 g mol^{-1} | K 39.10 g mol^{-1} | $C_{11}H_{20}N_2$ 180.30 g mol^{-1}

$NHC^{iPr2Me2}$ was prepared following a procedure of Kuhn and Kratz.[230] K (12.62 g, 321 mmol, 3 eq) is transferred to a Schlenk-flask (1 L) and 600 mL of thf are added by cannula. The reaction mixture is heated for 8 hours to reflux during which the color turns turquoise. After cooling to r.t. the suspension is cannulated over a big glass frit

with a 5 cm layer of celite. After filtration (ca. 8 h), the thf is evaporated and the colorless solid dried in high vacuum (1h, 2*10^{-2} mbar) to yield 17.26 g (90%) of pure NHC^{iPr2Me2}.

^{1}H NMR (300.13 MHz, C_6D_6, 300 K): δ = 3.96 (sept, 2H, C*H*(CH_3)$_2$ of NHC), 1.74 (s, 6H, C*H*$_3$ of NHC), 1.51 (d, 12H, CH(C*H*$_3$)$_2$ of NHC) ppm.

5.5.4. Synthesis of Germanium(II)chloride·dioxane Complex (1:1)

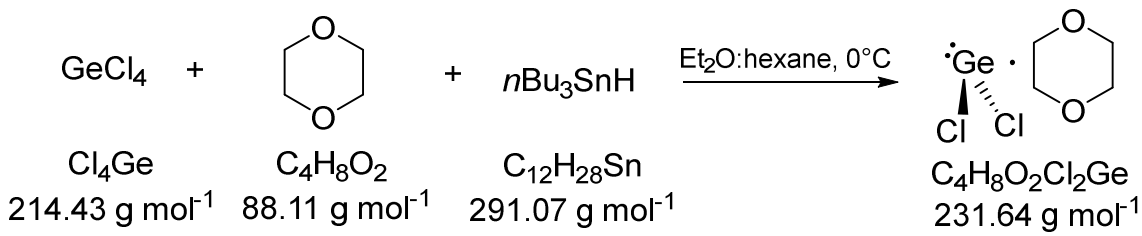

$GeCl_2$·dioxane was prepared following a procedure of the Lappert's group.[58] To a 1:1 solution of 100 mL diethyl ether and 100 mL *n*-hexane 36.88 g $GeCl_4$ (0.172 mol, 19.62 mL) and 19.96 g 1,4-dioxane (0.34 mol, 29 mL) were added and cooled with an ice-bath. Dropwise addition of 46 mL ^{n}Bu$_3$SnH (50 g, 0.172 mol) to the mixture results in formation of a white precipitate. After stirring for 30 min the solvent was decanted by cannula. The white (or sometimes pale yellow) powder was washed with *n*-hexane (2*30 mL) to afford pure $GeCl_2$·dioxane. The mother liquor can be stored at ambient temperature to afford colorless needles of $GeCl_2$·dioxane after three weeks. Yield: overall 28.74 g (73%).

^{1}H NMR (300.13 MHz, C_6D_6, 300 K): δ = 3.18 (s, 6H, dioxane) ppm.

5.5.5. Synthesis of Ge(II)chloride·NHC Complex 8 (1:1)

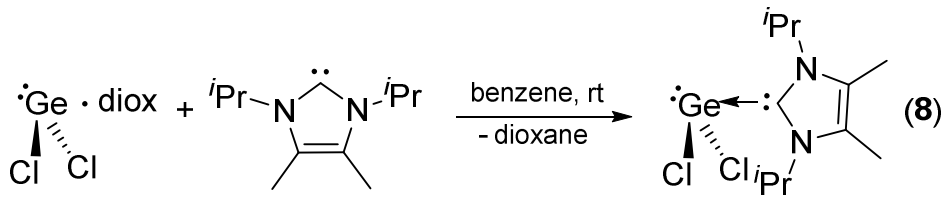

$GeCl_2$·NHC^{iPr2Me2} **8** was prepared following a procedure of Baines and co-workers.[61] To a suspension of 6.89 g $GeCl_2$·dioxane (30 mmol) in 10 mL benzene a solution of 5.3 g NHC^{iPr2Me2} (30 mmol) in 20 mL benzene is added by cannula. During stirring of the clear, light orange solution for 30 min at ambient temperature a white precipitate formed. The addition of 200 mL of hexane completes the precipitation. After filtration

the white solid is washed with pentane (2*30 mL) and dried in high vacuum (2 h, $2*10^{-2}$ mbar) to afford 8.6 g (93%) of pure $GeCl_2 \cdot NHC^{iPr2Me2}$.

^{1}H NMR (300.13 MHz, C_6D_6, 300 K): δ = 5.47 (br, 2H, C*H*$(CH_3)_2$ of NHC), 1.55 (s, 6H, C*H*$_3$ of NHC), 1.18 (d, 12H, CH(C*H*$_3$)$_2$ of NHC) ppm.

5.5.6. Synthesis of Dichlorobis(2,4,6-triisopropylphenyl)silane 64

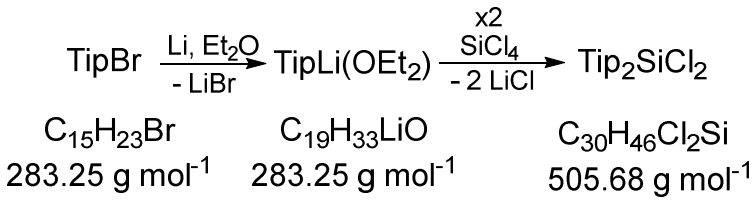

TipLi and Tip_2SiCl_2 were prepared following a modified literature procedure by Smit and Bickelhaupt.[199] Li-granules (19.2 g, 3.9 eq) are stirred intensely in a 2 L Schlenk-flask at r.t and 1.6 L Et_2O is added and again intensely stirred. To the suspension of Li-granules in Et_2O, 202.38 g degassed TipBr (180 mL, 0.71 mol) are added slowly at room temperature. After the addition of ca. 50 mL of TipBr the Et_2O begins slightly to boil and is therefore shortly cooled (ca. 5 min, not cooled to r.t.) with an ice bath. The color changes to greenish-brown and after complete addition the mixture is stirred overnight under argon. A hydrolyzed sample indicates 87 % (TipH/TipBr) conversion. The mixture is filtered *via* a big reverse frit to yield an orange solution. The solvent is evaporated in high vacuum and the residue is dried carefully until an off-white solid is obtained (ca. 20 h at $2*10^{-3}$ mbar), which is used without further purification. 1.2 L of toluene is added to the dried TipLi (contains 13% TipBr). To the beige suspension 30 mL of $SiCl_4$ (0.45 eq) are added dropwise within 45 min under ice-cooling (important, first substitution generates heat) and stirring is continued for two additional days at r.t. The toluene is removed under reduced pressure. The 13% TipBr are distilled off under reduced pressure ($2*10^{-2}$ mbar, 160 °C). The crude yield is 131.47 g (95%) of Tip_2SiCl_2. The solid is digested with 530 mL of pentane to obtain a pale yellow solution, which is filtered over a thin layer of celite with filter paper. Crystallization from pentane at −80 °C (14 h) yields 70 g (53%) Tip_2SiCl_2 which contains small impurities. A second crystallization from pentane (4 mL pentane/g Tip_2SiCl_2) at −80 °C yields 60 g of pure Tip_2SiCl_2 (44%).

^{1}H NMR (300.13 MHz, $CDCl_3$, 300 K): δ = 6.99 (s, 4H, Tip*H*), 3.68 (sept, 4H, C*H*$(CH_3)_2$ of Tip), 2.85 (sept, 2H, C*H*$(CH_3)_2$ of Tip), 1.21 (d, 12H, CH(C*H*$_3$)$_2$ of Tip), 1.02 (d, 24H, CH(C*H*$_3$)$_2$ of Tip) ppm.

5.5.7. Synthesis of Silyl Anion 197

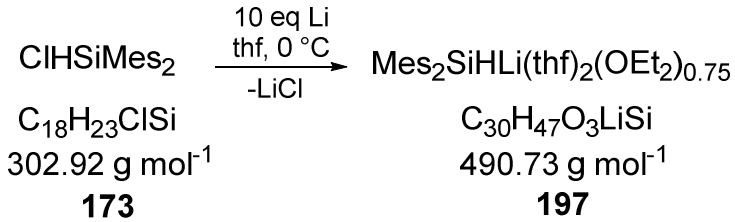

$Mes_2SiHLi(thf)_2(OEt_2)_{0.75}$ was synthesized according to a modified literature procedure.[203] A precooled (0 °C) solution of 10.83 g of Mes_2SiHCl (0.0358 mol) in 50 mL of thf was added through a dropping funnel over 30 min to the suspension of 2.48 g Li-powder (0.358 mol, 10 eq) in 12 mL of thf and cooled down to 0 °C. The reaction mixture turned green and was stirred for 1h 30 min while acquiring a brownish tone. The thf was evaporated at 0 °C and dried in high vacuum (2 h, $2*10^{-2}$ mbar). The black residue was dissolved in 50 mL toluene and filtered. The toluene was evaporated and the black solid washed with pentane (5*40 mL). The almost black powder was dissolved in 60 mL of diethyl ether. The light orange solution was stored at −80 °C to obtain 10.24 g (60%) of **197** as an off-white powder.

^{1}H NMR (300.13 MHz, C_6D_6, 300 K): δ = 6.92 (s, 4H, Mes-*H*), 4.73 (s, 1H, Si-*H*), 3.39-3.35 (m, 8H, C*H*$_2$O of coordinated thf), 3.21 (q, 3H, C*H*$_2$ of coordinated Et_2O), 2.69 (s, 12H, *o*-C*H*$_3$), 2.27 (s, 6H, *p*-C*H*$_3$), 1.27-1.18 (m, 8H, C*H*$_2$ of coordinated thf), 1.03 (t, 4H, C*H*$_3$ of coordinated Et_2O) ppm. **^{13}C NMR** (125.76 MHz, C_6D_6, 300 K): δ = 146.01, 143.94 (Mes*C*$_{quart}$), 133.99, 127.99 (Mes*C*H), 68.44 (*C*H$_2$O of coordinated thf), 65.92 (*C*H$_2$ of coordinated Et_2O), 25.76, 25.36 (*C*H$_3$ of Mes), 21.33 (*C*H$_3$ of coordinated thf), 15.28 (*C*H$_3$ of coordinated Et_2O) ppm. **^{29}Si NMR** (125.76 MHz, C_6D_6, 300 K): δ = −72.20 ppm.

5.5.8. Synthesis of 1,1,2-Tris(2,4,6-triisopropylphenyl)disilenyllithium 93

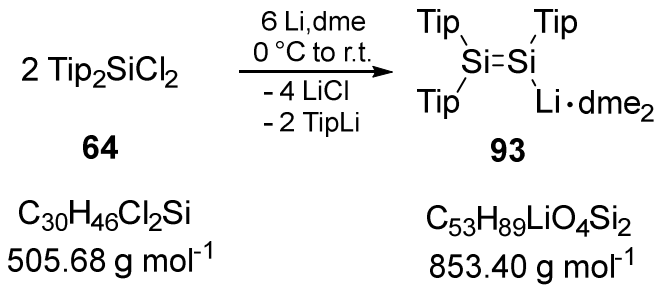

Disilenide **93** was prepared following a modified procedure of Scheschkewitz.[132] Tip_2SiCl_2 (60 g, 0.12 mol) is mixed with 3.54 g Li-powder (0.52 mol, 4.3 eq) and 400 mL dme are added quickly under intense stirring and ice-cooling. After stirring for 14 hours, the dme is removed under reduced pressure and dried carefully (2 h, $2*10^{-2}$ mbar). The red solid is dissolved in 600 mL of hexane and filtered from hot hexane (ca.

50 °C). The clear intense red solution is stored at r.t. (no concentration of the hexane). After 16 hours at ambient temperature red crystals of disilenide **93** are obtained in 25 g (48%) yield.

^{1}H NMR (300.13 MHz, C_6D_6, 300 K, TMS): δ = 7.14 (s, 2H, *m*-Tip*H*), 7.10 (s, 2H, *m*-Tip*H*), 7.08 (s, 2H, *m*-Tip*H*), 4.86-4.75 (m, 4H, C*H*$(CH_3)_2$ of Tip), 4.28 (br, 2H, C*H*$(CH_3)_2$ of Tip), 2.92 (s, 12H, dme), 2.85 (s, 8H, dme), 2.88-2.72 (m, 3H, C*H*$(CH_3)_2$ of Tip), 1.47 (d, 16H, CH(C*H*$_3)_2$ of Tip), 1.42 (d, 6H, CH(C*H*$_3)_2$ of Tip), 1.33 (d, 6H, CH(C*H*$_3)_2$ of Tip) 1.26, 1.22, 1.16 (each d, overall 32H, CH(C*H*$_3)_2$ of Tip) ppm.

5.5.9. Synthesis of Silagermenylidene 101

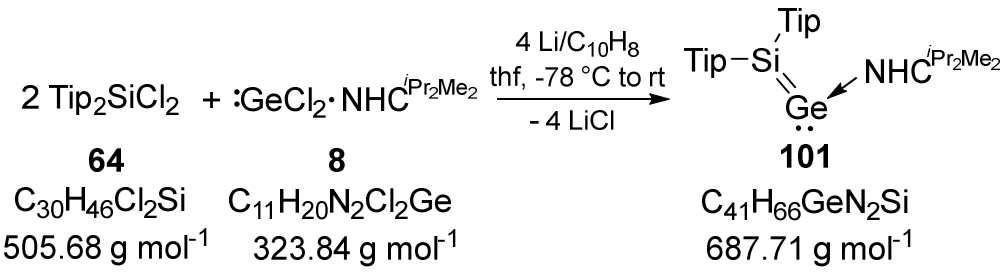

Silagermenylidene **101** was prepared following a literature procedure of Scheschkewitz and co-workers.[144] A solution of Li/naphthalene (freshly prepared from 221 mg Li-granules (31.84 mmol) and 4.90 g $C_{10}H_8$ (38.25 mmol) in 65 mL thf) is added dropwise to a solution of 4.04 g Tip_2SiCl_2 (7.96 mmol) and 2.56 g of $GeCl_2{\cdot}NHC^{iPr2Me2}$ (7.96 mmol) in 100 mL of thf at −80 °C. The red reaction mixture is slowly allowed to warm to r.t. and stirred for 12 hours at ambient temperature. All volatiles are removed under reduced pressure at 70°C and the residue is dissolved in 200 mL of hexane. After filtration the solution is stored −80 °C overnight. The mother liquor is separated from an oily precipitate and concentrated to about 30 mL. After 20 hours at −26 °C yellow crystals of $Tip_2Si{=}SiTip_2$[103] are formed from which the mother liquor is separated again and stored at −80°C. After 16 hours a red precipitate is formed and separated from the mother liquor to afford 420 mg of silagermenylidene **101** (8%).

^{1}H NMR (300.13 MHz, C_6D_6, 300 K): δ = 7.21 (br, 2H, Tip*H*), 7.05 (br, 2H, Tip*H*), 6.03 (br, 2H, C*H*$(CH_3)_2$ of NHC), 5.20-3.80 (br, 4H, C*H*$(CH_3)_2$ of Tip), 2.91-2.70 (m, 2H, C*H*$(CH_3)_2$ of Tip), 1.62 (br, 6H, CH(C*H*$_3)_2$ of Tip), 1.55 (s, 6H, C*H*$_3$ of NHC), 1.27 (d, 6H, CH(C*H*$_3)_2$ of Tip), 1.21 (d, 6H, CH(C*H*$_3)_2$ of Tip), 1.31-0.91 (m, 30H, CH(C*H*$_3)_2$ of Tip and CH(C*H*$_3)_2$ of NHC) ppm.

5.5.10. Synthesis of Silagermenylidene 104

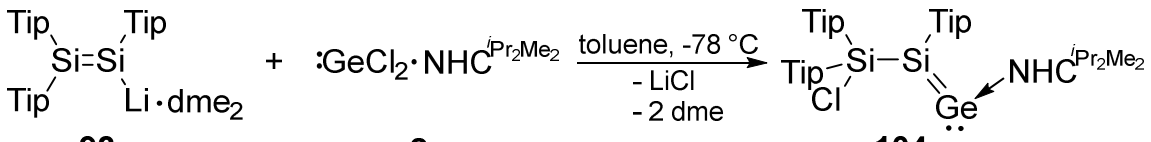

93	**8**	**104**
$C_{53}H_{89}LiO_4Si_2$	$C_{11}H_{20}N_2Cl_2Ge$	$C_{56}H_{89}ClGeN_2Si_2$
853.40 g mol^{-1}	323.84 g mol^{-1}	954.59 g mol^{-1}

Silagermenylidene **104** was prepared following a literature procedure of the group of Scheschkewitz.[145] $Tip_2Si{=}SiTipLi{\cdot}dme_2$ **93** (6.79 g, 7.96 mmol) is dissolved in 40 mL of toluene and cooled to −78 °C (an immersed thermometer is recommended to check the actual temperature). In the same manner, 2.58 g $GeCl_2{\cdot}NHC^{iPr_2Me_2}$ (27.96 mmol) are dissolved in 20 mL of toluene and also cooled to −78 °C. The red colored solution of $Tip_2Si{=}SiTipLi{\cdot}dme_2$ **93** is added by cannula to the suspension of $GeCl_2{\cdot}NHC^{iPr_2Me_2}$. The color changed immediately from pale red to dark red. The reaction mixture is allowed to slowly warm to room temperature (ca. 3 hours) and stirred for additional 12 hours. The toluene is distilled off in vacuum and dried (2 h, $2{*}10^{-2}$ mbar). The pale red solid is diluted with 200 mL of *n*-hexane and filtered. Upon reduction of the volume of *n*-hexane to about half a red solid begins to precipitate. At this point the evaporation of *n*-hexane is stopped and the flask is kept at room temperature for 14 hours. The mother liquor is decanted with a cannula and the red solid is washed with *n*-pentane (2*15 mL). The solid is dried in high vacuum for 2 hours to afford 4.9 g (65%) of silagermenylidene **104**. The volume of the mother liquor (including the 30 mL of pentane) is reduced to a third and the flask is kept at −26 °C for 24 hours to afford red crystalline needles in 20% (1.5 g) yield (purification see first crystallization step). Overall yield: 6.4 g of **104** (85%).

^{1}H NMR (300 MHz, C_6D_6, 300 K, TMS): δ = 7.08 (s, 4H, Tip-*H*), 7.03 (s, 2H, Tip-*H*), 5.38 (sept, 2H, C*H*$(CH_3)_2$ of NHC), 4.47-3.96 (m and br, altogether 6H, C*H*$(CH_3)_2$ of Tip) 2.83-2.65 (m, 3H, C*H*$(CH_3)_2$ of Tip), 1.52 (s, 6H, C*H*$_3$ of NHC), 1.33-1.11 (br and m, altogether 48H, CH(C*H*$_3$)$_2$ of Tip), 1.01 (d, 6H, CH(C*H*$_3$)$_2$ of Tip), 0.85 (d, 12H, CH(C*H*$_3$)$_2$ of NHC).

5.5.11. Durylene-bis-Isocyanide

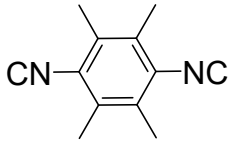

147

$C_{12}H_{12}N_2$

184.24 g mol^{-1}

Durylene-bis-isocyanide[231,232] **147** was supplied by the group, which was contaminated by traces of diisopropylamine and recrystallized from a saturated CH_2Cl_2 solution at −26 °C for 14 hours. The crystalline material was additionally purified by sublimation on a cooling finger (2.6*10^{-2} mbar, 50 °C, 3 h).

^{1}H NMR (300 MHz, C_6D_6, 300 K, TMS): δ = 1.91 (s, 12H, PhC*H*$_3$) ppm.

5.5.12. Synthesis of 4,4'-Diisocyano-3,3',5,5'-tetramethyl-1,1'-biphenyl 148

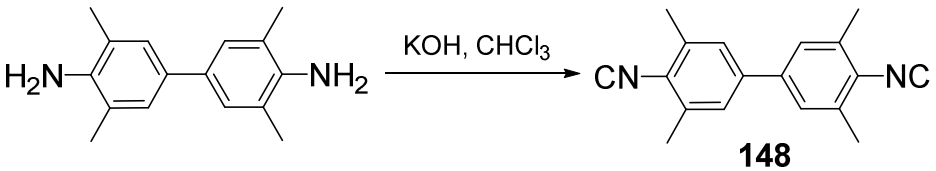

$C_{16}H_{20}N_2$ 240.35 g mol^{-1}

148 $C_{18}H_{16}N_2$ 260.34 g mol^{-1}

4,4'-diisocyano-3,3',5,5'-tetramethyl-1,1'-biphenyl **148** was synthesized according to a modified literature procedure of Scott and co-workers.[233] 3,3',5,5'-tetramethyl-[1,1'-biphenyl]-4,4'-diamine (3.0 g, 12.5 mmol) is dissolved in 200 mL of CH_2Cl_2 and a 45% aqueous KOH solution (200 ml) is added. A two-phase-system formed, with the organic layer on top. Butyl-triethyl-ammonium chloride (14.7 mg, 61.5 µmol) and 13.4 mL of chloroform (20.0 g, 0.17 mol) are added and the reaction is refluxed at 45 °C for 72 hours. The mixture is diluted with 400 mL of distilled water, washed twice with distilled water and once with aqueous saturated NaCl solution. The remaining organic phase is dried under vacuum. The yellow residue is purified by crystallization at −80 °C from CH_2Cl_2 giving yellow crystals. The crude product is further purified by sublimation in high vacuum (5*10^{-3} mbar, 140 °C, 5 h) on a cooling finger (−78 °C) to obtain 0.49 g (15% yield) of **148** as white crystalline powder.

^{1}H NMR (300 MHz, C_6D_6, 300 K, TMS): δ = 6.82 (br s, 4H, Xyl-*H*), 2.14 (s, 12H, Me-H) ppm.

5.5.13. Synthesis of Bis(4-Isocyano-3,5-dimethylphenyl)methane 149

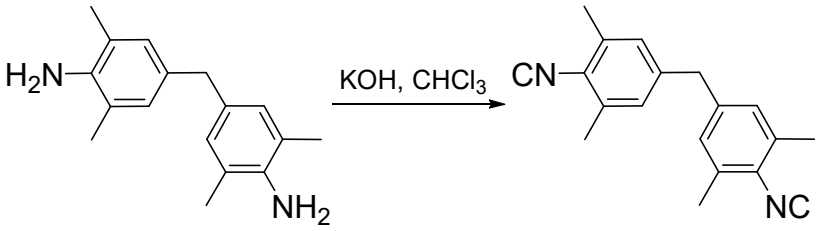

	149
$C_{17}H_{22}N_2$	$C_{19}H_{18}N_2$
254.38 g mol^{-1}	274.37 g mol^{-1}

Bis(4-isocyano-3,5-dimethylphenyl)methane **149** was synthesized according to a modified literature procedure of the group of Villinger.[234] 4,4'-methylene-bis(2,6-dimethylaniline) (750 mg, 2.95 mmol) and 50 mg $BuEt_3NCl$ (0.22 mmol) are dissolved in 725 mg of $CHCl_3$ (6.07 mmol) and 25 mL of CH_2Cl_2. The mixture is heated to reflux for 6 hours. After cooling down to r.t. 250 mL of H_2O are added and the organic phase is separated. The aqueous phase is extracted three times with CH_2Cl_2 (40 mL). The combined organic phases are dried over $MgSO_4$ and filtered over celite. The solvent is evaporated and the brownish residue dissolved in 5 mL of CH_2Cl_2 by slight warming. The solution is stored at −26 °C to afford colorless crystals of **149** in 18% (133 mg) yield.

^{1}H NMR (300 MHz, $CDCl_3$, 300 K, TMS): δ = 6.87 (s, 4H, Xyl-*H*), 3.82 (s, 2H, -C*H*$_2$-), 2.38 (s, 12H, CH_3 of Xyl) ppm.

5.6. Versatile Reactivity of Silagermenylidene 104 toward Anionic Nucleophiles

5.6.1. Reaction of Silagermenylidene 104 with MeLi: Synthesis of Tricyclic Si_4Ge_2 Chair-Isomer 131 and Doubly-Bridged Si_4Ge_2 Tetrahedral Isomer 132

Exp. 1:

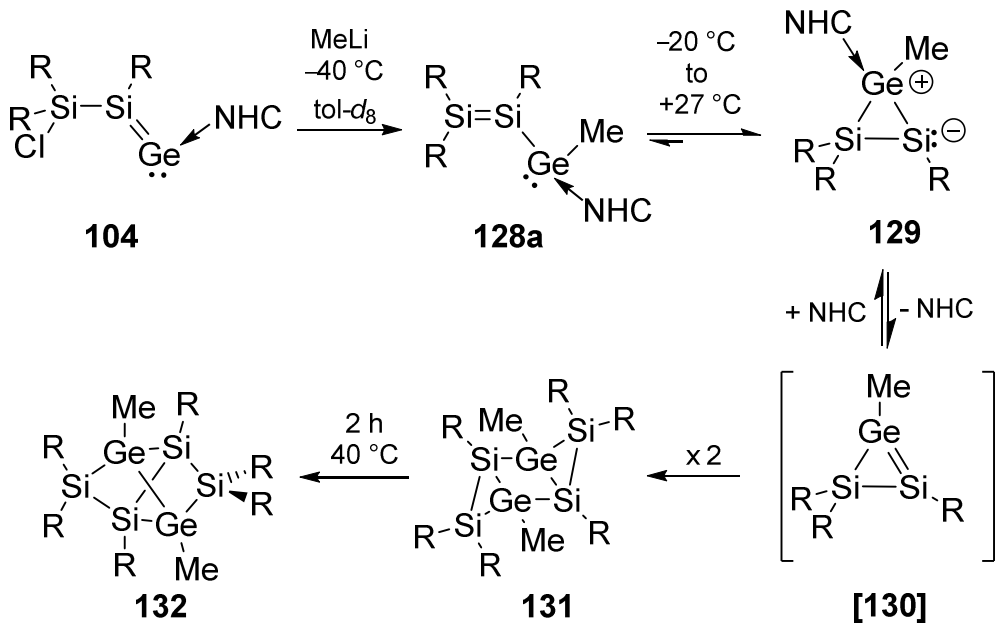

A solution of MeLi (1.6 M in Et_2O, 0.76 mL, 1.216 mmol, 1 eq) is added slowly (2 min) to a cold toluene solution (5 mL, −78 °C) of silagermenylidene **104** (1.16 g, 1.215 mmol). The reaction mixture is allowed to warm to room temperature and the solvent is immediately evaporated. The red solid is dried in high vacuum for one hour and dissolved in *n*-pentane (20 mL). After filtration with a reverse frit, all volatiles were removed again and free $NHC^{iPr2Me2}$ is sublimed from the crude product at $5x10^{-6}$ mbar for 12 hours at ambient temperature. The residue is dissolved in toluene and a very concentrated solution is stored at −26 °C. A few pale red crystals of compound **131** and a large amount of colorless crystals of **132** suitable for X-ray diffraction are obtained after three days alongside an unidentified impurity with a SiH bond.
Due to its instability in solution, we were unable to obtain a pure sample of **131** despite repeated attempts. Conversely, a pure sample of **132** can be obtained by heating the reaction mixture of **131** and **132** to 40 °C for 2 hours. Crystallization from a saturated toluene solution at room temperature for one day affords colorless crystals of **132**. The total yield (3 crops) of **132** is 0.60 g (63%).

Selected data of chair-like isomer **131** (extracted from spectra of mixtures with **132** and an unknown CH insertion product)

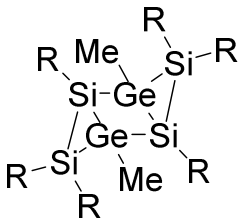

131

^{1}H NMR (300.13 MHz, C_6D_6, 300 K): δ = 5.57 (1H, Si*H* of unknown CH insertion product, $^{1}J_{HSi}$ = 96 Hz) ppm. **^{13}C NMR** (75.56 MHz, C_6D_6, 300 K): δ = 157.35, 157.08, 156.33, 155.89, 155.82, 155.12 155.04, 151.02, 149.98, 149.65, 149.44, 135.37, 133.53, 131.13, 122.69, 121.46, 120.60 (Ar*C*), 121.22 (N*C*(CH_3)=*C*(CH_3)N of free NHC), 49.84 (*C*H(CH_3)$_2$ of free NHC), 36.98, 36.50, 34.97, 34.88, 34.81, 34.73, 34.37, 31.33 (*C*H(CH_3)$_2$ of Tip), 29.04, 27.87, 26.62, 26.01, 25.86, 24.84, 24.49, 23.51 (CH(*C*H_3)$_2$ of Tip), 24.64 (CH(*C*H_3)$_2$ of free NHC), 8.39 (*C*H_3 of free NHC), 5.89 (Ge*C*H_3) ppm. **^{29}Si NMR** (59.62 MHz, C_6D_6, 300 K): δ = −82.55 (**131**), −96.42 (**131**) and −65.94 (unknown CH insertion product; SiH, $^{1}J_{SiH}$ = 96 Hz) ppm. *Note:* Due to considerable overlap of the occasionally broad signals of **131** with those of **132** the ^{1}H NMR is beyond interpretation.

Data of doubly edge-capped tetrahedral isomer **132** (obtained from a pure crystalline sample)

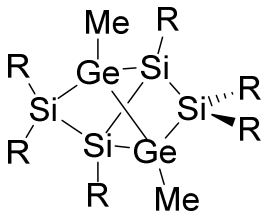

132

MP: > 225°C. **^{1}H NMR** (300.13 MHz, C_6D_6, 300 K): δ = 7.13 (m, toluene), 7.11 (br, 5H, Tip*H*), 7.06 (br, 4H, Tip*H*), 7.02 (m, toluene), 6.92 (s, 3H, Tip*H*), 4.43 (br, 3H, C*H*(CH_3)$_2$ of Tip), 3.87-3.79 (m, 6H, C*H*(CH_3)$_2$ of Tip), 3.20 (br, 4H, C*H*(CH_3)$_2$ of Tip), 2.90-2.62 (m, 8H, C*H*(CH_3)$_2$ of Tip), 2.11 (s, toluene), 1.46-1.30 (m, 42H, CH(C*H*$_3$)$_2$ of Tip), 1.24-1.14 (m, 64H, CH(C*H*$_3$)$_2$ of Tip), 0.35 (br, 12H, CH(C*H*$_3$)$_2$ of Tip and GeC*H*$_3$) ppm. **^{13}C NMR** (75.56 MHz, C_6D_6, 300 K): δ = 156.66 (br), 154.73 (br), 154.25, 149.51, 149.38, 149.27, 139.12 (br), 135.32 (br) (Ar*C*$_{quart}$), 128.17 (masked by C_6D_6), 123.95, 123.72, 123.12, 122.83, 121.66 (br) (Ar*C*H), 37.87 (br), 35.71, 35.62, 34.57, 34.48, 30.48 (*C*H(CH_3)$_2$ of Tip), 28.70, 25.47, 25.19 (br), 24.95, 24.64, 24.14, 24.10, 23.96 (CH(*C*H_3)$_2$ of Tip), 0.35 (Ge*C*H_3) ppm. **^{29}Si NMR** (59.62 MHz, C_6D_6, 300 K): δ = 21.97, −37.74 ppm. *Note:* Due to the broadness of the signals the ^{29}Si NMR signals cannot be assigned by a ^{29}Si-HMBC correlation. **Element. anal.:** Calcd. for $C_{92}H_{144}Ge_2Si_4 \cdot 1.5\ C_7H_8$: C, 74.80; H, 9.55. Found: C, 73.86; H, 9.79.

Exp. 2: Low temperature NMR study of the reaction of **104** with MeLi and preparation of a solution of NHC adduct of disilenyl germylene **128a**

MeLi (3.0 M in DEM, 106 µL, 0.318 mmol, 1 eq) was added to a cold solution (−78 °C) of **104** (303 mg, 0.317 mmol) in toluene-d_8 (2 mL) in a Schlenk-flask. One third of the solution was transferred via a pre-cooled glass pipette into a pre-cooled NMR-tube at −78 °C (the remainder was stored at −78°C for use in experiments 3 and 4, see below).

The following distinct ^{29}Si NMR spectra were obtained in the process of warming the sample to ambient temperature:

- at 213 K only starting material **104** with signals at δ = 163.47 and 8.37 ppm is observed.
- at 253 K two new resonances at δ = 90.07 and 85.40 ppm appeared in the ^{29}Si NMR which correspond to disilenyl germylene **128a**.
- after 30 h at room temperature the signals of **6** had completely disappeared and only resonances of **129** at δ = −64.92 and −66.51 ppm and **131** at δ = −82.55 and −96.42 ppm could be detected.

Data of disilenyl germylene **128a**

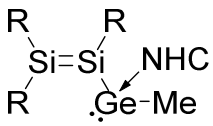

128a

^{1}H NMR (300.13 MHz, toluene-d_8, 253 K, TMS): δ = 7.12-6.95 (m, 6H, overlap with toluene-d_8, Tip*H*), 5.70 (m, 2H, C*H*(CH_3)$_2$ of NHC), 4.54 (s, 2H, OCH_2O, dem), 4.12-3.91 (m, 5H, C*H*(CH_3)$_2$ of Tip), 3.46 (q, 4H, OC$H_2$$CH_3$, dem), 2.82-2.62 (m, 4H, C*H*(CH_3)$_2$ of Tip), 1.65 (br, 3H, GeCH_3) 1.51 (s, 6H, CH_3 of NHC), 1.37-1.13 (m, 44H, CH(CH_3)$_2$ of Tip and CH(CH_3)$_2$ of NHC, overlap with dem: t, 6H, CH_3), 0.96-0.92 (m, 6H, CH(CH_3)$_2$ of Tip), 0.84-0.70 (m, 18H, CH(CH_3)$_2$ of Tip) ppm. **^{13}C NMR** (75.56 MHz, toluene-d_8, 253 K, TMS): δ = 174.88 (N*C*N), 155.03, 154.39, 153.77, 153.50, 149.24, 148.91, 148.21, 138.92, 138.82, 137.98, 125.94, 122.26, 121.77, 121.40, 121.30, 121.06 (Aryl*C* of Tip and N*C*(CH_3)=*C*(CH_3)N of NHC), 94.94 (O*C*H_2O, dem), 62.91 (O*C*$H_2$$CH_3$, dem), 52.09 (*C*H($CH_3$)$_2$ of NHC), 37.42, 37.02, 36.65, 34.92, 34.66, 34.47, 28.26, 26.13, 25.02, 24.55, 24.43, 24.34, 24.26, 24.19, 24.11, 21.54, 21.19, 20.06 (*C*H(*C*H_3)$_2$ of Tip and *C*H(*C*H_3)$_2$ of NHC), 15.43 (OCH_2*C*H_3, dem), 9.91 (NC(*C*H_3)=C(*C*H_3)N of NHC), 4.07 (Ge*C*H_3) ppm. **^{29}Si NMR** (59.62 MHz, toluene-d_8, 253 K, TMS): δ = 90.11, 85.29 ppm.

Exp. 3: Heating of a mixture of **128a**, **129** and **131** to 323K in the absence of additional NHC

The following distinct ^{29}Si NMR spectra were obtained in the process of warming the sample from 300 K to 323 K:

- warming of the sample to 300 K showed after 50 min three sets of signals in the ^{29}Si NMR: δ = 90.07 and 85.40 ppm (**128a**), δ = −64.92 and −66.51 ppm (**129**) and δ = −82.55 and −96.42 ppm (**131**).
- the temperature is increased to 323 K and two sets of signals were observed at δ = −64.92 and −66.51 ppm (**129**) and δ = −82.55 and −96.42 ppm (**131**).
- after 2 hours at 323 K only resonances at δ = −64.92 and −66.51 ppm (**129**) and δ = 21.97, –37.74 ppm (**132**) were observed.

Exp. 4: NMR study of **128a** with 3.8 equivalents of additional NHC and synthesis of intermediate **129** (NHC adduct of germadisilacyclopropene **[130]**)

A cold solution of **128a** (−48 °C) is added via syringe in a NMR tube containing NHC (3.8 eq) at room temperature:

- a ^{29}Si NMR of the mixture of **128a** and the free NHC was recorded at 300 K and only the signals of **128a** were observed even after 50 min at ambient temperature.
- the temperature was raised to 323 K and a nearly full conversion of **6** was reached after 1 hour at this temperature. The ^{29}Si NMR indicated that the mixture predominantly contained **129**.
- a ^{1}H NMR clearly shows that neither of compounds **131** and **132** are formed, even if the mixture is heated for 5 hours to 323 K. Without additional NHC, **128a** rearranges after 1h at 323 K to **129** and **131**.

Data of NHC adduct **129** of germadisilacyclopropene

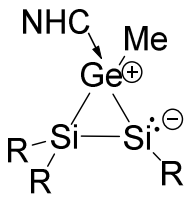

129

^{1}H NMR (300.13 MHz, toluene-d_8, 323 K, TMS): δ = 5.66 (sept, C*H*(CH$_3$)$_2$ of NHC), 1.75 (s, CH(C*H*$_3$)$_2$ of NHC) ppm. **^{13}C NMR** (75.56 MHz, toluene-d_8, 323 K, TMS): δ = 175.90 (N*C*N), 156.65, 154.71, 154.45, 154.19, 149.41, 149.27, 149.15, 148.79, 147.72, 140.44, 135.53, 126.36, 123.82, 123.60, 122.75, 122.32, 122.00 (Aryl*C* of Tip and N*C*(CH$_3$)=*C*(CH$_3$)N of NHC), 53.24 (*C*H(CH$_3$)$_2$ of NHC), 36.54, 35.61, 35.52, 34.59, 34.36, 28.57, 25.49, 25.34, 25.16, 24.97, 24.83, 24.05, 23.92 (*C*H(*C*H$_3$)$_2$ of Tip and *C*H(*C*H$_3$)$_2$ of NHC), 10.66 (NC(*C*H$_3$)=C(*C*H$_3$)N of NHC), 1.68 (Ge*C*H$_3$) ppm. *Note:*

The ^{1}H and ^{13}C NMR spectra of a relatively pure sample of **129** are dominated by the excess NHC used for the stabilization of this species. Therefore, only characteristic resonances of compound **129** are given due to significant overlaps with the dominating NHC and dem signals. **^{29}Si NMR** (59.62 MHz, toluene-d_8, 323 K, TMS): δ = −64.73, −66.49 ppm.

5.6.2. Reaction of Silagermenylidene 104 with EtLi

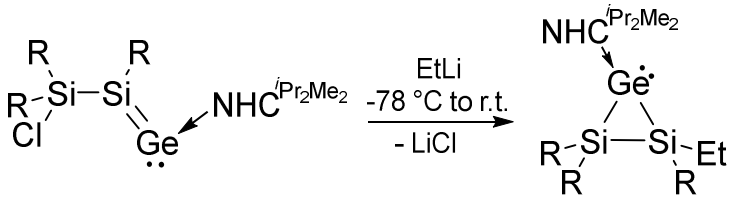

104 **123b**

A solution of EtLi (0.5 M in benzene/cyclohexane, 0.355 mL, 0.18 mmol, 1 eq) is added to a solution of 170 mg **104** (0.18 mmol) in 2 mL of toluene at −78 °C. The color turned in the process of warming to r.t. from pale red to orange/yellow. The solvent is evaporated in high vacuum and filtered from 10 mL of hexane. All crystallization attempts failed (r.t. or –26 °C in pentane or toluene).

^{29}Si NMR (59.62 MHz, C_6D_6, 300 K, TMS): δ = −61.52 (*Si*Tip$_2$), −70.09 (*Si*Tip) ppm.

5.6.3. Synthesis of Disilenyl Germylene 128c

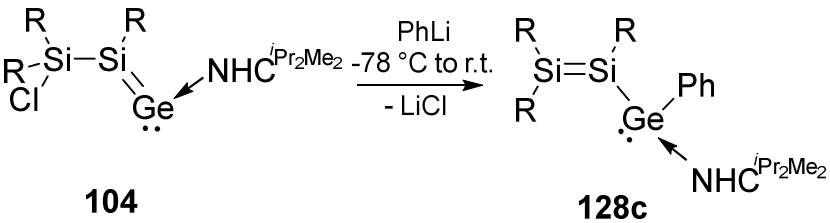

104 **128c**

$C_{56}H_{89}ClGeN_2Si_2$ 954.59 g mol^{-1} $C_{62}H_{93}GeN_2Si_2$ 995.24 g mol^{-1}

A solution of PhLi (1.9 M in *n*Butyl$_2$O, 0.605 mL, 1.15 mmol, 1 eq) is added quickly to a −78 °C cold solution of 1.10 g **104** (1.15 mmol) in 5 mL of toluene. At −40 °C the color of the pale red solution turned into deep red. A ^{1}H NMR spectrum indicates a full conversion into a new product. The reaction mixture is allowed to warm to −10 °C and the solvent is removed immediately. The red solid is dried for 2 hours in high vacuum ($2*10^{-2}$ mbar) and afterwards diluted in 100 mL of pentane. After filtration of the deep red solution at ca. −20 °C, the pentane is evaporated to approximately a third of volume and stored at −26 °C. After two days at this temperature, an orange microcrystalline precipitate of **128c** is formed in 768 mg (67%) yield. Red single crystals of **128c** suitable for X-Ray diffraction are obtained from a concentrated toluene or mesitylene solution after three days at −26 °C.

MP: 128-131°C (full conversion into **123c**). **^{1}H NMR** (300.13 MHz, toluene-d_8, 300 K, TMS): δ = 7.97 (br, 2H, Ph*H*), 7.17-6.93 (m, 9H, overlap with toluene-d_8, Tip*H* and Ph*H*), 5.69 (br, 2H, C*H*(CH_3)$_2$ of NHC), 4.88-4.79 (m, 1H, C*H*(CH_3)$_2$ of Tip), 4.43 (br, 1H, C*H*(CH_3)$_2$ of Tip), 4.05-3.82 (m, 4H, C*H*(CH_3)$_2$ of Tip), 2.78-2.64 (m, 3H, C*H*(CH_3)$_2$ of Tip), 1.57-1.53 (m, 9H, CH(C*H*$_3$)$_2$ of Tip and C*H*$_3$ of NHC), 1.37-1.29 (m, 18H, CH(C*H*$_3$)$_2$ of Tip and CH(C*H*$_3$)$_2$ of NHC), 1.20-1.13 (m, 24H, CH(C*H*$_3$)$_2$ of Tip and of CH(C*H*$_3$)$_2$ of NHC), 0.90-0.84 (m, 6H, CH(C*H*$_3$)$_2$ of Tip and of C*H*$_3$ of NHC), 0.76-0.65 (m, 16H, CH(C*H*$_3$)$_2$ of Tip), 0.50 (d, 6H, CH(C*H*$_3$)$_2$ of Tip) ppm. **^{1}H NMR** (300.13 MHz, toluene-d_8, 253K, TMS): δ = 8.13 (br, 2H, Ph*H*), 7.24-6.87 (m, 9H, overlap with toluene-d_8, Tip*H* and Ph*H*), 5.76 (br, 2H, C*H*(CH_3)$_2$ of NHC), 4.99 (br, 1H, C*H*(CH_3)$_2$ of Tip), 4.53 (br, 1H, C*H*(CH_3)$_2$ of Tip), 4.06 (br, 2H, C*H*(CH_3)$_2$ of Tip), 3.83 (br, 2H, C*H*(CH_3)$_2$ of Tip), 2.76-2.65 (m, 3H, C*H*(CH_3)$_2$ of Tip), 1.64 (d, 3H, C*H*$_3$ of NHC), 1.47-1.38 (m, 22H, CH(C*H*$_3$)$_2$ of Tip and CH(C*H*$_3$)$_2$ of NHC), 1.23-1.15 (m, 22H, CH(C*H*$_3$)$_2$ of Tip and of CH(C*H*$_3$)$_2$ of NHC), 0.91-0.87 (m, 6H, CH(C*H*$_3$)$_2$ of Tip and of C*H*$_3$ of NHC), 0.62-0.48 (m, 22H, CH(C*H*$_3$)$_2$ of Tip) ppm. **^{13}C NMR** (75.56 MHz, toluene-d_8, 253 K, TMS): δ = 172.91 (br, N*C*N), 156.26, 155.16, 154.34, 154.10, 149.31, 149.21, 148.85, 139.53, 138.64, 138.01, 136.87 (Ar*C*$_{quart}$), 153.91 (N*C*C*N), 137.73, 129.28, 128.34, 127.64, 125.33 (masked by toluene-d_8), 126.43, 122.87, 121.85, 121.75, 121.21 (Ar*C*H), 54.14 (br, *C*H(CH_3)$_2$ of NHC), 38.56, 37.70, 37.21, 36.28, 35.04 (*C*H(CH_3)$_2$ of Tip), 27.74, 26.20, 24.97, 24.70, 24.55, 24.46, 24.30 (masked by toluene-d_8), 24.12, 23.88, 23.71, 21.29 (CH(*C*H$_3$)$_2$ of Tip and NHC), 20.35 (masked by toluene-d_8, CH(*C*H$_3$)$_2$ of Tip), 34.67, 23.00, 14.53 (*n*-pentane), 9.89 (*C*H$_3$ of NHC) ppm. **^{29}Si NMR** (59.62 MHz, toluene-d_8, 253 K, TMS): δ = 95.06 (*Si*Tip$_2$), 73.88 (*Si*Tip) ppm. **UV/vis** (hexane): λ_{max} = 452 nm (ε = 10900 Lmol^{-1}cm^{-1}), 373 nm (ε = 13900 Lmol^{-1}cm^{-1}), 308 nm (ε = 14200 Lmol^{-1}cm^{-1}). **Element. anal.:** Calcd. for $C_{62}H_{94}GeN_2Si_2 \cdot 0.25\ C_7H_8$ (1019.3): C, 75.12; H, 9.49; N, 2.75. Found: C, 74.66; H, 9.29; N, 2.65.

5.6.4. Synthesis of Heavier Cyclopropylidene Analogue 123c

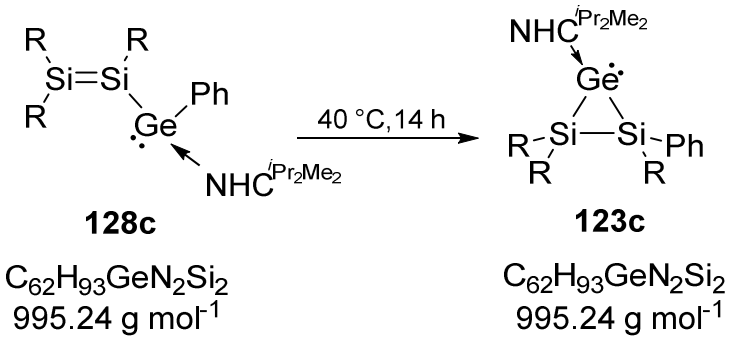

128c **123c**

$C_{62}H_{93}GeN_2Si_2$ $C_{62}H_{93}GeN_2Si_2$
995.24 g mol^{-1} 995.24 g mol^{-1}

A solution of 700 mg of **128c** (0.70 mmol) in 4 mL of toluene are heated for 14 hours to 40 °C (NMR study). The solvent was evaporated to dryness. After filtration of the yellow solid from 40 mL of hexane, the solvent is concentrated to the half of volume and a yellow microcrystalline precipitate of **123c** is obtained in 574 mg (82%) yield after three days at room temperature. The precipitate is separated from the mother liquor

and dissolved in 2 mL of toluene. Storing at room temperature for two days afforded orange crystals of **123c** suitable for X-Ray diffraction.

MP: 179-181 °C (decomposition). **^{1}H NMR** (300.13 MHz, C_6D_6, 300 K, TMS): δ = 7.70 (br, 2H, Ph*H*), 7.30 (br, 2H, Tip*H*), 7.24 (br, 1H, Ph*H*), 7.14-7.00 (m, 4H, Tip*H* and Ph*H* overlay with co-crystallized toluene), 6.87 (br, 3H, Tip*H*), 6.00-5.81 (m, 3H, C*H*$(CH_3)_2$ of Tip and C*H*$(CH_3)_2$ of NHC), 4.59 (sept, 1H, C*H*$(CH_3)_2$ of Tip), 4.33 (sept, 1H, C*H*$(CH_3)_2$ of Tip), 4.06-3.96 (m, 2H, C*H*$(CH_3)_2$ of Tip), 3.69 (sept, 1H, C*H*$(CH_3)_2$ of Tip), 2.99-2.73 (m, 3H, C*H*$(CH_3)_2$ of Tip), 2.12 (C*H*$_3$ of co-crystallized toluene), 1.83 (d, 3H, CH(C*H*$_3$)$_2$ of Tip), 1.68 (br, 3H, CH(C*H*$_3$)$_2$ of Tip), 1.58-1.52 (m, altogether 12H, 6H of CH(C*H*$_3$)$_2$ of Tip and 6H C*H*$_3$ of NHC), 1.40-1.19 (m, altogether 36H, 24H of CH(C*H*$_3$)$_2$ of Tip and 12H of CH(C*H*$_3$)$_2$ of NHC), 1.09 (br, 3H, CH(C*H*$_3$)$_2$ of Tip), 0.87 (d, 3H, CH(C*H*$_3$)$_2$ of Tip), 0.75 (br, 3H, CH(C*H*$_3$)$_2$ of Tip), 0.63-0.58 (br, 12H, CH(C*H*$_3$)$_2$ of Tip) ppm. **^{13}C NMR** (75.56 MHz, C_6D_6, 300 K, TMS): δ= 172.75 (N*C*N), 157.64, 155.97, 155.21, 154.62, 154.11, 149.24, 148.99, 148.02, 147.68 (br), 142.17, 141.26, (Ar*C*$_{quart}$), 156.54 (br, 2C, N*C*CN), 137.88, 129.33, 128.56, 125.69 (toluene), 136.79, 128.24, 127.91 (masked by C_6D_6), 126.64, 122.59, 122.37, 121.98, 121.48, 121.14, 121.03 (Ar*C*H and Ph*C*H), 54.05, 53.52 (br, *C*H$(CH_3)_2$ of NHC), 37.74, 36.29, 36.19, 34.94, 34.81, 34.73, 34.64, 34.57, 34.15 (*C*H$(CH_3)_2$ of Tip), 30.07, 28.38, 27.73, 27.43, 27.04, 25.59, 25.12, 24.74, 24.53, 24.45, 24.41, 24.38, 24.31, 24.22, 23.84, 23.46, 22.52, 22.23, 21.44, 20.15 (CH(*C*H$_3$)$_2$ of Tip and NHC), 10.85, 10.42 (br, *C*H$_3$ of NHC) ppm. **^{29}Si NMR** (59.62 MHz, C_6D_6, 300 K, TMS): δ = −62.74 (*Si*Tip$_2$), −68.81 (*Si*Tip) ppm. **UV/vis** (hexane): λ_{max} = 438 nm (ε = 6400 Lmol^{-1}cm^{-1}), 370 nm (ε = 11100 Lmol^{-1}cm^{-1}), 311 nm (ε = 14200 Lmol^{-1}cm^{-1}), 272 nm (ε = 21700 Lmol^{-1}cm^{-1}). **Element. anal.:** Calcd. for $C_{62}H_{94}GeN_2Si_2$·0.3 C_7H_8 (1023.9): C, 75.19; H, 9.49; N, 2.74. Found: C, 74.27; H, 9.47; N, 2.90.

5.6.5. Synthesis of Heavier Cyclopropylidene Derivative 123d and NHC-Coordinated Cyclosilagermene 124b

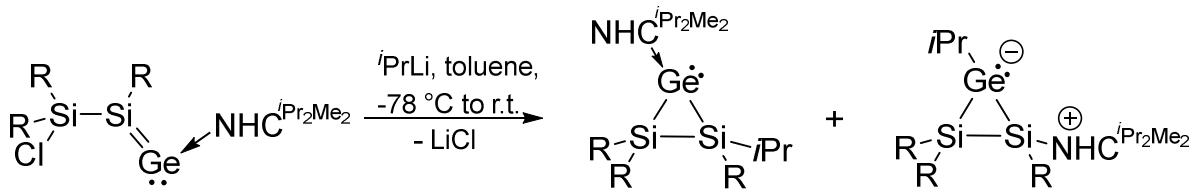

A solution of *i*PrLi (0.7 M in *n*-pentane, 1 mL, 0.7 mmol, 1 eq) is added in one go to 663 mg of **104** (0.7 mmol) in 5 mL of toluene at –78 °C. The reaction mixture is stirred in the thawing cooling bath until it reached room temperature and stirred at ambient temperature for 14 hours. The solvent is removed under reduced pressure and the red solid is dissolved in 20 mL of hexane. After filtration with a filter-tipped cannula, the hexane is concentrated to about 5 mL. The saturated solution is stored for one day at

room temperature affording crystals suitable for X-Ray diffraction of **124b**. The overall yield of the 1:1 mixture of **123d** and **124b** is 0.353 g (56%).

Note: A multinuclear NMR evaluation of the isomers is due to signal overlaps of both isomers not possible.

^{29}Si NMR (59.62 MHz, C_6D_6, 300 K, TMS): δ = −62.26, −69.06, −72.66, −78.04 ppm.

5.6.6. Low Temperature NMR Study of Silagermenylidene 104 with MesLi

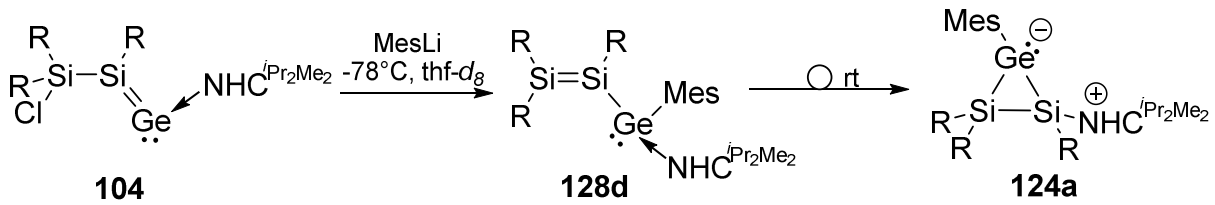

A −78 °C cold solution of 100 mg **104** (0.105 mmol) in 0.5 mL of thf-d_8 was added to a −78 °C cold solution of 14 mg of MesLi (0.105 mmol) in 1.5 mL thf-d_8 in a 10 mL round bottom flask under argon atmosphere. The mixture was stirred for 2 hours to guarantee a homogenous system. A part of the reaction mixture was transferred via a cold glass pipette into a cold NMR-tube (both −78 °C). A ^{29}Si NMR was recorded at 213 K and two new signals of **128d** appeared at δ = 86.47 and 83.92 ppm together with a small amount of **104** (only the downfield shift at 161.20 ppm is visible). The ^{13}C NMR as well as the ^{1}H NMR spectrum shows signals typical for the coordination of an NHC to the Ge(II)-center (^{13}C NMR: δ = 172.54 ppm, ^{1}H NMR: 5.34 ppm). At 253 K and 273 K no signals were detected in the ^{29}Si NMR. Warming the reaction mixture to room temperature shows three resonances: 4.71 ppm (starting material **104**) and two highfield shifts at −58.34 and −80.71 ppm which belong to compound **124a**. The ^{13}C NMR shows a signal at δ = 161.13 ppm which was assigned to the carbenic atom of **124a**.[146]

Note: Due to overlaps with starting material **104** and the broad resonances in ^{13}C NMR only characteristic signals for the coordination of the NHC of compound **124a** was evaluated.

^{1}H NMR (300.13 MHz, C_6D_6, 300 K, TMS): δ = 5.34 (br, 2H, C*H*$(CH_3)_2$ of NHC) ppm. **^{13}C NMR** (75.56 MHz, C_6D_6, 300 K, TMS): δ = 172.54 (s, N*C*N) ppm. **^{29}Si NMR** (59.62 MHz, C_6D_6, 300 K, TMS): δ = 86.47, 83.92 ppm.

5.6.7. Reaction of Silagermenylidene 104 with *sec*-BuLi

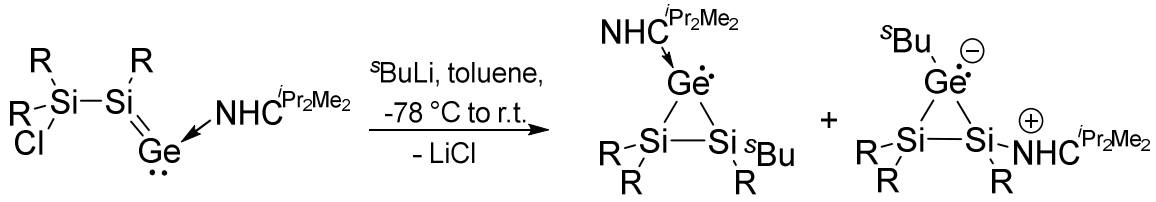

104 **123e** **124c**

A solution of *sec*-BuLi (1.4 M in cyclohexane, 0.16 mL, 0.22 mmol, 1 eq) was added to a −78 °C cold solution of 209 mg **104** (0.22 mmol) in 3 mL of toluene. The color changed during the warming process from pale red to orange/yellow. The solvent was evaporated in high vacuum and filtered from 10 mL of hexane. All crystallization attempts failed (r.t. or −26 °C in pentane or toluene).

^{29}Si NMR (59.62 MHz, C_6D_6, 300 K, TMS): δ = −68.25, −77.47 ppm and −61.87, −72.10 ppm.

5.6.8. Reaction of Silagermenylidene 104 with *tert*-BuLi

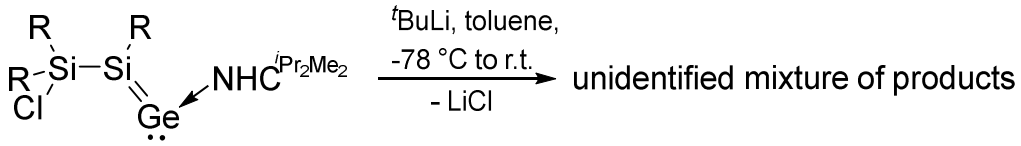

104

A solution of *tert*-BuLi (1.7 M in hexane, 0.16 mL, 0.27 mmol, 1 eq) was added to a −78 °C cold solution of 260 mg **104** (0.27 mmol) in 3 mL of toluene. The reaction mixture was slowly allowed to warm up to rt. The color changed at r.t. from pale red to orange/yellow. The solvent was evaporated in high vacuum and filtered from 10 mL of hexane. All crystallization attempts failed (r.t. or −26 °C in pentane or toluene).

^{29}Si NMR (59.62 MHz, C_6D_6, 300 K, TMS): δ = 7.73 (starting material), −72.45, −76.62 ppm.

5.7. Reactivity of Disilenyl Germylene 128c and Its Isomeric Heavier Cyclopropylidene Analogue 123c toward Phenylacetylene and Xylyl Isocyanide

5.7.1. Synthesis of Heavier Cyclopentenylidene Derivative 133

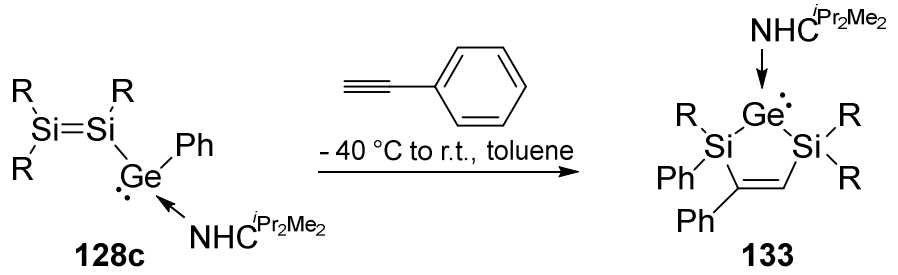

128c

$C_{62}H_{93}GeN_2Si_2$
995.24 g mol^{-1}

133

$C_{70}H_{100}GeN_2Si_2$
1098.38 g mol^{-1}

To a −20 °C cold solution of 855 mg of **128c** (0.896 mmol) in 4 mL of toluene, 98.5 μL phenylacetylene (92 mg, 0.902 mmol, 1 eq) are added by a microliter syringe. The reaction mixture is allowed to warm to room temperature and is stirred for 2 hours at ambient temperature. The solvent is evaporated to dryness and the residue is digested in 60 mL of hexane. After filtration, the hexane is concentrated to the half of volume and a yellow microcrystalline precipitate of **133** in 583 mg (59%) is obtained. Yellow single crystals of **133** suitable for X-ray diffraction are obtained from a saturated toluene solution after 3 days at room temperature.

MP: >220 °C (decomposition). **^{1}H NMR** (300.13 MHz, C_6D_6, 300 K, TMS): δ = 7.85 (s, 1H, PhC=C*H*), 7.63 (br, 1H, C*H*(CH_3)$_2$ of NHC), 7.36 (br, 1H, Ph*H*), 7.19 (br, 4H, Ar*H*), 7.16 (br, 2H, masked by C_6D_6, Ar*H*), 7.07-6.83 (m, 8H from Ph*H*, Tip*H* and 1H from C*H*(CH_3)$_2$ of Tip), 6.79 (br, 1H, Ph*H*), 5.03 (sept, 1H, C*H*(CH_3)$_2$ of NHC), 4.69 (sept, 1H, C*H*(CH_3)$_2$ of Tip), 3.87-3.61 (m, 4H, C*H*(CH_3)$_2$ of Tip), 2.92-2.67 (m, 3H, C*H*(CH_3)$_2$ of Tip), 1.80-1.74 (m, 9H, CH(C*H*$_3$)$_2$ of Tip), 1.61-1.38 (m, 16H, CH(C*H*$_3$)$_2$ of Tip and C*H*$_3$ and CH(C*H*$_3$)$_2$ of NHC), 1.31-1.19 (m, 26H, CH(C*H*$_3$)$_2$ of Tip), 0.90 (br, 3H, CH(C*H*$_3$)$_2$ of Tip), 0.68 (br, 3H, CH(C*H*$_3$)$_2$ of Tip), 0.60 (d, 3H, CH(C*H*$_3$)$_2$ of Tip), 0.51 (d, 3H, CH(C*H*$_3$)$_2$ of Tip), 0.46-0.42 (m, 6H, CH(C*H*$_3$)$_2$ of Tip), 0.30 (br, 3H, CH(C*H*$_3$)$_2$ of Tip), 0.16 (d, 3H, CH(C*H*$_3$)$_2$ of Tip) ppm. **^{13}C NMR** (75.56 MHz, C_6D_6, 300 K, TMS): δ = 169.45 (N*C*N), 166.17 (HC=*C*Ph), 162.50 (H*C*=CPh), 156.26, 156.02, 155.36, 154.92, 154.18, 152.76, 152.73, 148.75, 148.38, 148.31, 148.24, 142.36, 138.54, 137.71 (Ar*C*$_{quart}$), 128.60, 128.52, 128.18, 128.05, 127.97, 127.73, 127.67, 125.32 (Ar*C*H, 5C's masked by C_6D_6), 126.32 (br, 2C, N*CC*N), 122.97, 122.83 (br), 122.69, 122.47, 121.63, 120.91 (Ph*C*H), 56.78, 53.22 (*C*H(CH_3)$_2$ of NHC), 35.42, 35.28, 34.65, 34.49, 34.11, 33.41, 33.03 (*C*H(CH_3)$_2$ of Tip), 28.57, 27.59, 25.64, 25.50, 25.27, 25.11, 24.56, 24.47, 24.36, 24.32, 24.18, 23.77, 22.03, 21.33, 20.16 (CH(*C*H$_3$)$_2$ of Tip and NHC), 10.41, 10.01 (*C*H$_3$ of NHC) ppm. **^{29}Si NMR** (59.62 MHz, C_6D_6, 300 K, TMS): δ

= −1.51 (*Si*Tip$_2$), −15.39 (*Si*TipPh) ppm. **UV/vis** (hexane): λ_{max} = 348 nm (ε = 8800 Lmol^{-1}cm^{-1}). **Element. anal.:** Calcd. for $C_{70}H_{100}GeN_2Si_2$ (1098.7): C, 76.55; H, 9.18, N, 2.55. Found: C, 75.70; H, 9.32; N, 2.31.

5.7.2. Synthesis of Heavier Cyclopentenylidene Analogue 134

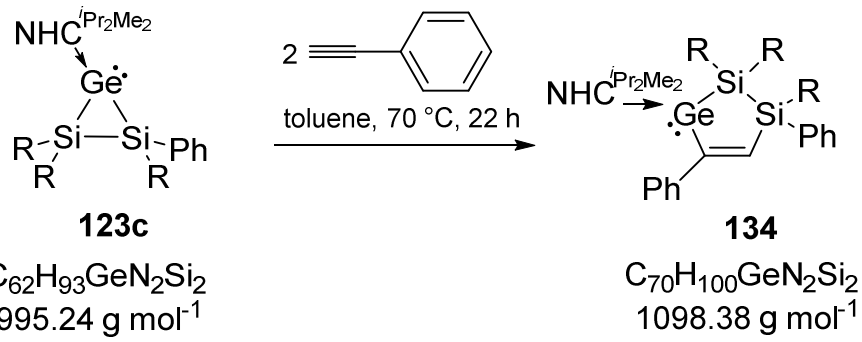

To a solution of 570 mg **123c** (0.572 mmol) in 4 mL of toluene 126 μL phenylacetylene (117 mg, 1.145 mmol, 2 eq) are added by a microliter syringe at room temperature. The reaction begins to proceed by heating to 70 °C (tested by NMR-study). After 22 hours at this temperature the reaction is completed. All volatiles are removed under reduced pressure and a pale red solid remains. The product is dissolved in 35 mL of warm hexane and filtered. Concentrating the solvent to approximately the third afforded a red precipitate. Separating the solid from the mother liquor and dissolving in 2.5 mL warm pentane afforded cubic red crystals suitable for X-Ray diffraction after 18 hours at room temperature. The total yield (3 crops) of **123c** is 492 mg (77%).

MP: 202-204 °C (decomposition). **^{1}H NMR** (300.13 MHz, C_6D_6, 300 K, TMS): δ = 8.13 (br, 2H, Ph*H*), 7.87 (s, 1H, PhC=C*H*), 7.49 (br, 2H, *H*-PhC=CH), 7.26 (br, 1H, Ph*H*), 7.24-7.19 (m, 2H, Tip*H* and Ph*H*), 7.15-6.92 (m, 8H, Tip*H*, Ph*H* and 1H, C*H*(CH$_3$)$_2$ of NHC), 6.86 (br, 1H, Ph*H*), 6.78 (br, 1H, Ph*H*), 5.29 (sept, 1H, C*H*(CH$_3$)$_2$ of Tip), 5.10 (sept, 1H, C*H*(CH$_3$)$_2$ of Tip), 4.33-4.13 (m, 2H, C*H*(CH$_3$)$_2$ of Tip and C*H*(CH$_3$)$_2$ of NHC), 3.72 (sept, 1H, C*H*(CH$_3$)$_2$ of Tip), 3.44 (sept, 1H, C*H*(CH$_3$)$_2$ of Tip), 3.00 (sept, 1H, C*H*(CH$_3$)$_2$ of Tip), 2.88-2.62 (m, 3H, C*H*(CH$_3$)$_2$ of Tip), 1.81 (d, 3H, CH(C*H*$_3$)$_2$ of NHC), 1.62-1.52 (m, 15H, CH(C*H*$_3$)$_2$ of Tip and C*H*$_3$ of NHC), 1.39-1.14 (m, 32H, CH(C*H*$_3$)$_2$ of Tip, C*H*$_3$ of NHC and co-crystallized pentane), 0.88 (co-crystallized pentane), 0.69 (d, 3H, CH(C*H*$_3$)$_2$ of Tip), 0.41-0.38 (m, 6H, CH(C*H*$_3$)$_2$ of Tip), 0.30-0.24 (m, 9H, CH(C*H*$_3$)$_2$ of Tip), 0.05 (d, 3H, CH(C*H*$_3$)$_2$ of NHC), 0.01 (d, 3H, CH(C*H*$_3$)$_2$ of NHC) ppm. **^{13}C NMR** (75.56 MHz, C_6D_6, 300 K, TMS): δ = 187.94 (HC=*C*Ph), 172.01 (N*C*N), 158.22, 156.50, 155.25, 154.84, 153.77, 152.47, 152.12, 149.05, 148.49, 147.50, 145.94, 139.97, 133.80 (Ar*C*$_{quart}$), 145.21 (H*C*=CPh), 145.50, 137.40, 128.34, 127.57, 127.32, 125.66 (Ar*C*H), 127.09, 126.23 (N*C*C*N*), 123.37, 123.14, 122.97, 122.57, 122.42, 122.22 (Ph*C*H), 54.16, 52.39 (*C*H(CH$_3$)$_2$ of NHC), 38.65, 36.59, 36.27, 35.98, 35.86, 34.72, 34.65, 31.13 (*C*H(CH$_3$)$_2$ of Tip), 28.51, 27.48, 26.69, 26.40, 26.26, 25.80, 25.41, 25.36, 24.68, 24.54, 24.21, 24.18, 24.13, 24.06, 24.04, 23.77, 23.52, 21.59, 21.19, 20.60 (CH(*C*H$_3$)$_2$ of Tip and NHC), 34.46, 22.72, 14.28 (*C*H$_3$ and *C*H$_2$ of co-crystallized pentane),10.59, 10.01 (*C*H$_3$ of NHC) ppm. **^{29}Si NMR** (59.62 MHz, C_6D_6, 300 K, TMS):

δ = −1.10 (*Si*Tip$_2$), −19.16 (*Si*TipPh) ppm. **UV/vis** (hexane): λ_{max} = 425 nm (ε = 5500 Lmol^{-1}cm^{-1}). **Element. anal.:** Calcd. for $C_{70}H_{100}GeN_2Si_2 \cdot 0.25\ C_5H_{12}$ (1116.4): C, 76.65; H, 9.3, N, 2.51. Found: C, 76.65; H, 8.93; N, 2.48.

5.7.3. Synthesis of Cyclic Germylene 138

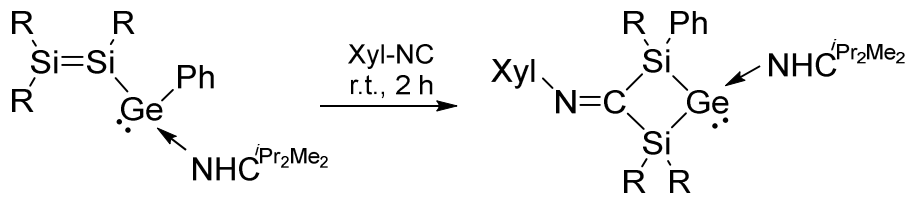

128c — $C_{62}H_{93}GeN_2Si_2$, 995.24 g mol^{-1}

138 — $C_{71}H_{103}GeN_3Si_2$, 1127.43 g mol^{-1}

To a −20 °C cold solution of 542 mg **128c** (0.568 mmol) in 3 mL of toluene, 75 mg of xylyl isocyanide (0.572 mmol, 1 eq) in 1 mL of toluene are added by syringe. The color changed immediately from deep red to deep purple. The reaction mixture is allowed to warm to room temperature and stirred for 1 hour at ambient temperature. The solvent is evaporated to dryness and the residue is diluted in 40 mL of hexane. After filtration, the hexane is concentrated to about 3 mL. The dark purple solution is frozen in liquid nitrogen and stored at room temperature. After one day purple needles of **138** are obtained (103 mg). Storing the mother liquor at room temperature for 2 days afforded again purple needles (157 mg). The total yield of **138** (2 crops) is 263 mg (41%). Dissolving the purple solid in toluene (concentrated solution, ca. 1.3 mL) afforded after one day at room temperature purple crystals of **138** suitable for X-ray diffraction.

MP: 163-165 °C (decomposition). **^{1}H NMR** (300.13 MHz, C_6D_6, 300 K, TMS): δ = 7.73 (br, 1H, C*H*(CH$_3$)$_2$ of NHC), 7.29-7.19 (m, 3H, Ph*H* and Tip*H*), 7.03-6.68 (m, 10H, Tip*H*, Ph*H* and Xyl*H*), 6.56 (br, 1H, C*H*(CH$_3$)$_2$ of Tip), 6.41 (d, 1H, ArH), 5.16 (br, 1H, C*H*(CH$_3$)$_2$ of NHC), 4.36 (br, 1H, C*H*(CH$_3$)$_2$ of Tip), 4.09-4.01 (m, 2H, C*H*(CH$_3$)$_2$ of Tip), 3.70 (br, 1H, C*H*(CH$_3$)$_2$ of Tip), 3.52 (br, 1H, C*H*(CH$_3$)$_2$ of Tip), 3.29 (impurity: t, *n*-dibutyl ether from **128c**), 2.86-2.66 (m, 4H, C*H*(CH$_3$)$_2$ of Tip), 2.60 (s, 3H, C*H*$_3$ of Xyl), 1.86-1.60 (m, 22H, CH(C*H*$_3$)$_2$ of Tip, C*H*(CH$_3$)$_2$ of NHC and C*H*$_3$ of NHC), 1.39-1.12 (m, 54H, CH(C*H*$_3$)$_2$ of Tip, CH(C*H*$_3$)$_2$ of NHC, C*H*$_3$ of NHC and co-crystallized *n*-hexane), 0.92-0.79 (m, 13H, CH(C*H*$_3$)$_2$ of Tip and co-crystallized *n*-hexane), 0.53-0.24 (m, 21H, CH(C*H*$_3$)$_2$ of Tip) ppm. **^{13}C NMR** (75.56 MHz, C_6D_6, 300 K, TMS): δ = 169.33 (N*C*N), 156.68, 155.63, 154.85, 153.68, 152.16 (br), 148.70, 148.46, 144.62, 141.49 (br), 139.18, 138.75 (Ar*C*$_{quart}$ and XylN=*C*), 128.44, 128.20, 122.90, 122.51, 121.93, 120.75 (Ar*C*H), 127.70 (N*CC*N), 127.01 (N*CC*N), 57.07, 53.13 (*C*H(CH$_3$)$_2$ of NHC), 36.14, 35.36, 34.60 (br), 34.44, 33.22, 32.78, 30.39 (*C*H(CH$_3$)$_2$ of Tip), 28.68, 26.78 (br), 25.57, 24.21 (br), 20.61, 18.61 (CH(*C*H$_3$)$_2$ of Tip and NHC), 21.19, 19.72 (CH$_3$ of Xyl), 31.97, 23.05, 14.35 (CH$_2$ and CH$_3$ of co-crystallized hexane), 10.36, 10.09 (*C*H$_3$ of NHC) ppm. **^{29}Si NMR** (59.62 MHz, C_6D_6, 300 K, TMS): δ = −1.74 (*Si*Tip$_2$), −3.92

(*Si*TipPh) ppm. **UV/vis** (hexane): λ_{max} = br sh from 290-320 nm. **Element. anal.:** Calcd. for $C_{71}H_{103}GeN_3Si_2 \cdot 0.25\ C_6H_{14}$ (1148.9): C, 75.79; H, 9.34; N, 3.66. Found: C, 75.41; H, 9.27; N, 3.63.

5.7.4. NHC-Abstraction from Cyclic Germylene 138

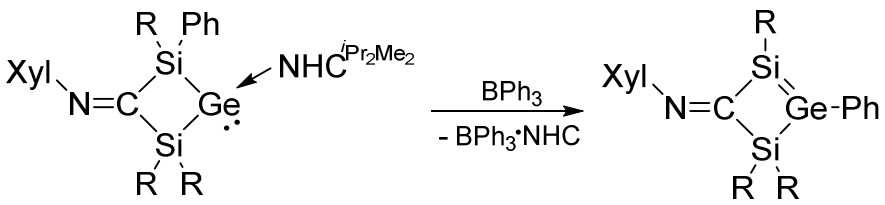

138 **142**

A solution of 93 mg BPh_3 (0.38 mmol, 1 eq) in 3 mL of toluene are added by syringe to 430 mg of **138** (0.38 mmol) in 3 mL of toluene and stirred for one day at room temperature. The color changed from light purple to dark green. After removing of the solvent in high vacuum, the green residue is filtered from 20 mL of hexane. The hexane is concentrated and stored at −26 °C for 3 days only affording $BPh_3 \cdot NHC^{iPr_2Me_2}$ adduct as colorless crystals. All crystallization attempts failed due to the instability of the formed product and co-crystallizing $BPh_3NHC^{iPr_2Me_2}$[174] adduct. Other attempts with $ZnCl_2$ instead of BPh_3 as Lewis-acid failed.

*Note: The NMR-spectra gets evaluated from an NMR-scale reaction (100 mg of **142**):*

^{1}H NMR (300.13 MHz, C_6D_6, 300 K, TMS): δ = 8.00-7.97 (m, 2H,Ph*H*), 7.25 (s, 2H, Tip*H*), 7.23-7.18 (m, 3H, Ph*H*), 7.08 (s, 2H, Tip*H*), 6.81 (s, 2H, Tip*H*), 6.67 (br, 2H, Xyl*H*), 6.45 (t, 1H, Xyl*H*), 4.21 (sept, 2H, C*H*$(CH_3)_2$ of Tip), 3.51 (sept, 3H, C*H*$(CH_3)_2$ of Tip), 3.29 (impurity: t, *n*-dibutyl ether), 2.87-2.56 (m, 4H, C*H*$(CH_3)_2$ of Tip), 2.32 (s, 3H, C*H*$_3$ of Xyl), 1.56-1.29 (m, 24H, CH(C*H*$_3$)$_2$ of Tip), 1.22-1.14 (m, 18H, CH(C*H*$_3$)$_2$ of Tip), 1.07 (d, 6H, CH(C*H*$_3$)$_2$ of Tip), 1.03 (d, 6H, CH(C*H*$_3$)$_2$ of Tip), 0.88 (impurity: t, *n*-dibutyl ether) ppm. **^{13}C NMR** (75.56 MHz, C_6D_6, 300 K, TMS): δ = 207.62 (XylN=*C*), 157.26, 156.46, 154.29, 153.72 (br), 151.93 , 151.45, 151.14, 139.98, 138.95 (br) (Ar*C*$_{quart}$), 136.83, 133.48, 131.57 (br), 130.22, 129.27, 128.44, 128.59, 127.86, 122.92, 122.09, 121.63, 120.67 (Ar*C*H), 70.78 (impurity: *n*-dibutyl ether), 36.68, 37.82 (br), 35.42, 34.78, 34.73 (*C*H$(CH_3)_2$ of Tip), 25.93, 25.41, 24.86, 24.24, 24.14 (CH(*C*H$_3$)$_2$ of Tip), 23.87, 23.85 (CH_3 of Xyl), 32.46, 19.88, 14.19 (impurity: *n*-dibutyl ether) ppm. **^{29}Si NMR** (59.62 MHz, C_6D_6, 300 K, TMS): δ = 103.12, −4.14 ppm.

$BPh_3 \cdot NHC^{iPr_2Me_2}$: ^{1}H NMR (300.13 MHz, C_6D_6, 300 K, TMS): δ = 7.67-7.62 (m, 6H, Ar*H*), 7.32-7.26 (m, 6H, Ar*H*), 7.18 (d, 3H, Ar*H*), 5.01 (sept, 2H, C*H*$(CH_3)_2$ of NHC), 1.57 (s, 6H, CH_3 of NHC), 0.72 (d, 12H, CH(C*H*$_3$)$_2$ of NHC) ppm. **^{13}C NMR** (75.56 MHz, C_6D_6, 300 K, TMS): δ = 135.80, 125.22, 124.43 (Ar*C*) 127.34 (N*CC*N), 49.49 (*C*H$(CH_3)_2$ of NHC), 20.93 (CH(*C*H$_3$)$_2$ of NHC), 10.42 (*C*H$_3$ of NHC) ppm.[174]

5.7.5. Synthesis of Cyclic Germylene 143

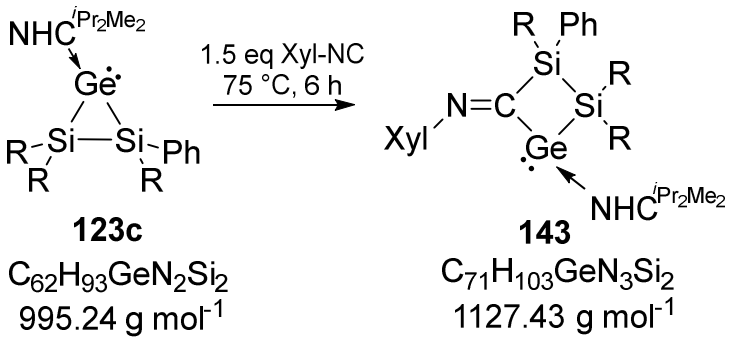

A solution of 503 mg **123c** (0.505 mmol) and 99 mg xylyl isocyanide (0.755 mmol, 1.5 eq) in 4 mL of toluene are heated to 75 °C (NMR-study). After 6 hours the reaction is completed. All volatiles are removed under reduced pressure and a red solid remains. The product is dissolved in 20 mL of hexane and filtered. The hexane is evaporated in vacuum and the red solid is dried in high vacuum (8 h, 6x10^{-6} mbar). Afterwards 1.5 mL of pentane is added to the red mortared solid and slightly warmed until everything is dissolved again. Red single crystals of **143** suitable for X-ray diffraction are obtained after 16 hours at room temperature. The yield is 212 mg (36 %).

MP: 145-148 °C (full conversion into starting material **123c**). **^{1}H NMR** (300.13 MHz, C_6D_6, 300 K, TMS): δ = 8.44 (br, 2H, Ph*H*), 7.34-7.29 (m, 3H, Tip*H*), 7.18-7.14 (br, 1H, Tip*H*, overlap with C_6D_6), 7.10-7.05 (m, 3H, Xyl*H*), 6.93-6.88 (m, 2H, Tip*H* and Ph*H*), 6.79-6.70 (m, 3H, Tip*H* and Ph*H*), 6.43 (sept, 1H, C*H*(CH_3)$_2$ of NHC), 5.68 (sept, 1H, C*H*(CH_3)$_2$ of Tip), 5.15 (sept, 1H, C*H*(CH_3)$_2$ of Tip), 4.31-4.19 (m, 2H, C*H*(CH_3)$_2$ of Tip and C*H*(CH_3)$_2$ of NHC), 3.84 (sept, 1H, C*H*(CH_3)$_2$ of Tip), 3.72 (sept, 1H, C*H*(CH_3)$_2$ of Tip), 3.47 (sept, 1H, C*H*(CH_3)$_2$ of Tip), 2.86-2.62 (m, 3H, C*H*(CH_3)$_2$ of Tip), 2.48 (s, 3H, C*H*$_3$ of Xyl), 2.16-2.15 (m, 4H, CH(C*H*$_3$)$_2$ of NHC and C*H*$_3$ of Xyl), 1.75 (d, 3H, CH(C*H*$_3$)$_2$ of Tip), 1.66-1.62 (m, 6H, CH(C*H*$_3$)$_2$ of Tip), 1.57 (d, 3H, CH(C*H*$_3$)$_2$ of Tip), 1.48 (s, 3H, C*H*$_3$ of NHC), 1.45 (d, 3H, CH(C*H*$_3$)$_2$ of Tip), 1.37 (d, 3H, CH(C*H*$_3$)$_2$ of NHC), 1.34 (s, 3H, C*H*$_3$ of NHC), 1.26-1.34 (m, 24H, CH(C*H*$_3$)$_2$ of NHC, CH(C*H*$_3$)$_2$ of Tip and C*H*$_2$ of co-crystallized pentane), 1.04 (d, 3H, CH(C*H*$_3$)$_2$ of Tip), 0.88 (C*H*$_3$ of co-crystallized pentane), 0.70 (d, 3H, CH(C*H*$_3$)$_2$ of Tip), 0.66 (d, 3H, CH(C*H*$_3$)$_2$ of Tip), 0.48-0.34 (m, 12H, CH(C*H*$_3$)$_2$ of Tip), 0.08-0.02 (m, 6H, CH(C*H*$_3$)$_2$ of NHC). **^{13}C NMR** (75.56 MHz, C_6D_6, 300 K, TMS): δ = 214.58 (XylN=*C*), 169.56 (N*C*N), 156.67, 155.37, 155.20, 155.16, 153.85, 151.78, 150.80, 149.02, 148.66, 147.90, 146.16, 139.76, 137.31, 136.65, 133.18, 123.44 (Ar*C*$_{quart}$), 139.55, 129.16, 128.36, 127.70, 127.38, 126.81 (Ar*C*H), 127.15 (N*C*CN), 126.96 (N*C*CN), 123.75, 123.21, 122.93, 122.61, 122.41, 122.36, 122.31 (Ar*C*H), 55.57, 52.51 (*C*H(CH_3)$_2$ of NHC), 38.95, 35.86, 35.48, 35.13, 34.66, 34.61, 33.84, 31.50 (*C*H(CH_3)$_2$ of Tip), 27.88, 27.79, 27.11, 26.26, 25.22, 25.06, 24.75, 24.61, 24.54, 24.44, 24.24, 24.21, 24.18, 24.05, 23.99, 23.55, 21.93, 21.33, 21.10, 20.78, 19.62, (CH(*C*H$_3$)$_2$ of Tip and NHC), 20.40 (CH$_3$ of Xyl), 34.43, 22.72, 14.28 (*C*H$_2$ and *C*H$_3$ of co-crystallized pentane),10.23, 9.94 (*C*H$_3$ of NHC) ppm. **^{29}Si NMR** (59.62 MHz, C_6D_6, 300 K, TMS): δ = −7.06 (*Si*Tip$_2$), −45.21 (*Si*TipPh) ppm.

UV/vis (hexane): λ_{max} = 347 nm (ε = 16400 $Lmol^{-1}cm^{-1}$), 442 nm (ε = 3400 $Lmol^{-1}cm^{-1}$), 522 nm (ε = 3200 $Lmol^{-1}cm^{-1}$). **Element. anal.:** Calcd. for $C_{71}H_{103}GeN_3Si_2 \cdot 0.25\ C_5H_{12}$ (1145.44): C, 75.87; H, 9.44; N, 3.61. Found: C, 75.49; H, 9.22; N, 3.62.

5.8. Reactivity of Silagermenylidenes 101 and 104, Disilenyl Germylene 128c and Its Cyclic Isomer 123c toward Bis-Functionalized Organic Substrates

5.8.1. Reaction of Silagermenylidene 101 with 1,4-Diethynylbenzene

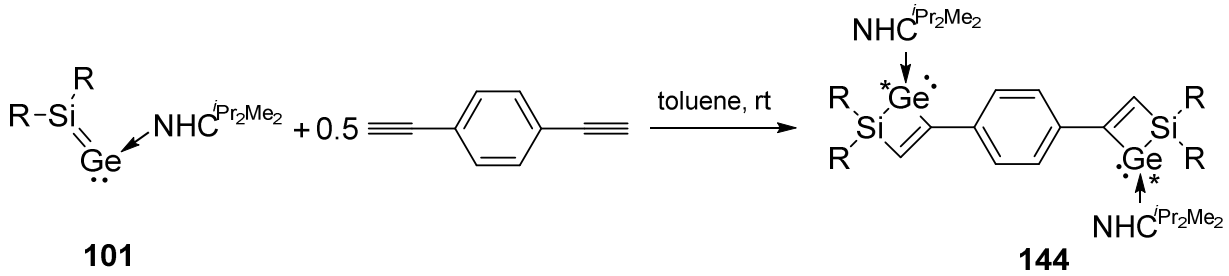

A solution of 28 mg of the bis-alkyne (0.228 mmol) in 2 mL toluene were quickly added at room temperature to a solution of 300 mg of **101** (0.435 mmol) in 5 mL toluene. After a few minutes the color changed from red to dark purple. The mixture was stirred for 1 day at ambient temperature. The solvent was evaporated and the solid dried in high vacuum (2 h at $8*10^{-3}$ mbar). The solid was digested in 30 mL of hexane and filtered. All crystallization attempts failed due to the formation of at least four products.

Note: In the ^{29}Si NMR no resonances were detected.

^{1}H NMR (300.13 MHz, C_6D_6, 300 K, TMS): δ = 8.63 (s, HC=CPhC=C*H*), 8.56 (s, *H*C=CPhC=CH), 7.98 (s, HC=CPhC=C*H*), 7.94 (s, *H*C=CPhC=CH) ppm.

5.8.2. Reaction of Silagermenylidene 101 with 1,3-Diethynylbenzene

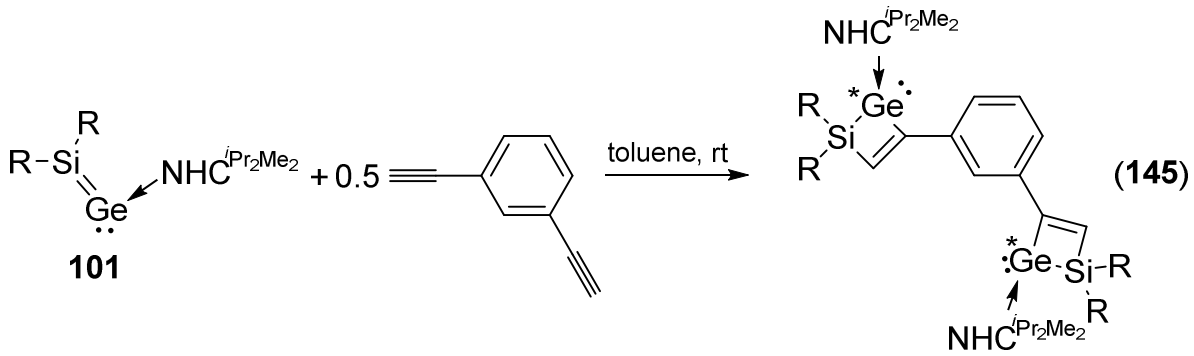

Silagermenylidene **101** (50 mg, 0.073 mmol) was dissolved in 1 mL toluene and 5 µL of the bis-alkyne (5 mg, 0.037 mmol) were added. After a few minutes the color changed from red to dark purple. The mixture was stirred for 1 hour at ambient

temperature. The solvent was evaporated and the NMR data showed a mixture of products.

^{1}H NMR (300.13 MHz, C_6D_6, 300 K, TMS): δ = 8.58 (s, HC=CPhC=C*H*), 8.52 (s, *H*C=CPhC=CH) ppm. **^{29}Si NMR** (59.62 MHz, C_6D_6, 300 K, TMS): δ = −38.92 (br), −39.16 ppm.

5.8.3. Reaction of Silagermenylidene 104 with 1,4-Diethynylbenzene

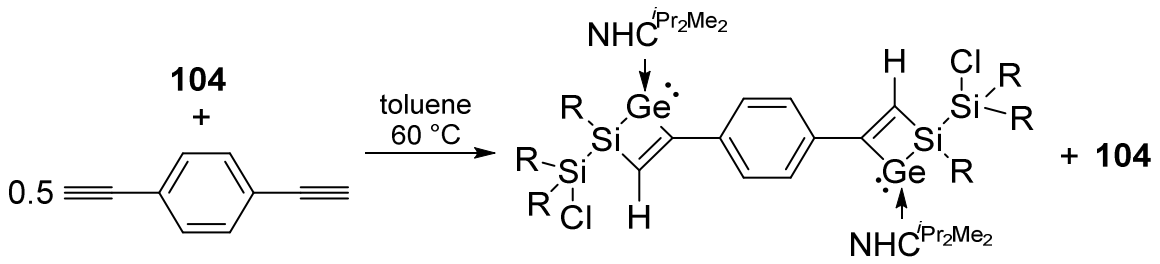

146

A solution of 27 mg of the bis-alkyne (0.217 mmol, 0.5 eq) in 3 mL of toluene are added *via* syringe to 415 mg of **104** (0.434 mmol) in 4 mL of toluene. The mixture is heated for 2 hours to 60 °C. A NMR sample showed a mixture of products (product and staring material). An excess of the bis-alkyne is added (54 mg, 1 eq) and the mixture is heated again for 3 hours to 60 °C. The solvent of the reaction mixture (containing starting material and product) is evaporated in high vacuum and filtered from 50 mL pentane. The pentane is concentrated and stored at room temperature to afford a few single crystals suitable for X-ray diffraction of **146** together with precipitated of **104** in a ratio of ca. 1:1.

In a further attempt to obtain a pure sample of **146**, a 3 fold excess (100 mg) of the bis-alkyne was reacted with 500 mg of silagermenylidene **104** (0.52 mmol) in 10 mL of toluene at 60 °C for 3 hours. After ca. 50% of silagermenylidene **104** was consumed the reaction stopped and it was not possible bring the reaction to completeness even by adding 3 eq of the bis-alkyne, because of the general tendency of acetylenes to polymerize under similar reaction conditions.

^{13}C NMR (75.56 MHz, C_6D_6, 300 K, TMS): δ = 178.37 (N*C*N), 171.54 (N*C*N) ppm. **^{29}Si NMR** (59.62 MHz, C_6D_6, 300 K, TMS): δ = 7.34 (starting material **104**), 3.82, −43.90 ppm.

5.8.4. Reaction of Silagermenylidene 104 with Durylene-bis-Isocyanide 147

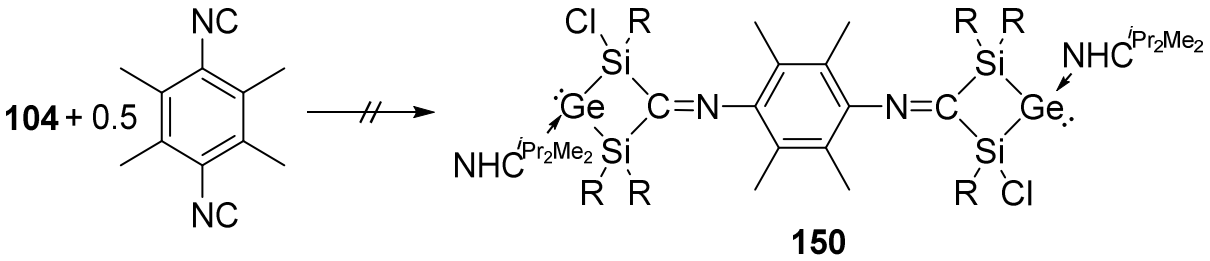

A solution of 535 mg **104** (0.56 mmol) and 52 mg durylene-bis-isocyanide (0.28 mmol, 0.5 eq) in 4 mL of benzene is heated to 65 °C for 4 hours. The color turned from red to brownish during the reaction process. An NMR sample showed an unidentified product mixture.

Note: ^{1}H NMR and ^{13}C NMR could not be evaluated due to signal overlaps.

^{29}Si NMR (300 MHz, C_6D_6, 300 K, TMS): δ = 119.91, 80.82, 37.38, −6.56 ppm.

5.8.5. Reaction of Silagermenylidene 104 with Bis-Isocyanide 148

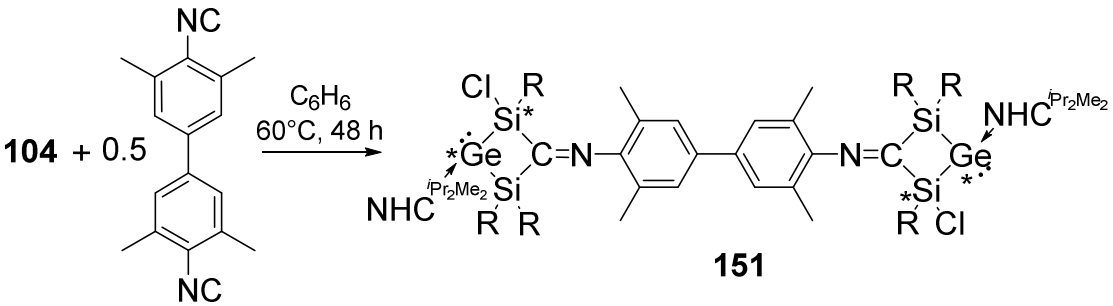

A solution of 960 mg **104** (1.00 mmol) and 131 mg bis-isocyanide **147** (0.5 mmol) in 10 mL of benzene are heated to 60 °C for 2 days. The color changed during the reaction process from red to intense purple. The solvent is evaporated in high vacuum and 150 mL of hexane are added to the purple solid. The solution is heated to 60 °C and filtered while hot. The solvent is concentrated to ca. 5 mL. All crystallization attempts failed (only colorless needles are obtained after 3 days at −26 °C, which are identified as 1,3-diisopropyl-4,5-dimethyl-1H-imidazol-3-ium chloride **153**).

NMR data of the purple solid:

^{1}H NMR (300 MHz, C_6D_6, 300 K, TMS): δ = 7.42-6.45 (m, altogether 14H, Tip*H* and Xyl-*H*), 5.91 (br, 1H, C*H*$(CH_3)_2$ of NHC), 5.77 (br, 1H, C*H*$(CH_3)_2$ of NHC), 4.36 (sept, 1H, C*H*$(CH_3)_2$ of Tip), 3.90-3.66 (m, 2H, C*H*$(CH_3)_2$ of NHC), 3.51 (sept, 4H, C*H*$(CH_3)_2$ of NHC), 2.89-2.44 (m, 9H, C*H*$(CH_3)_2$ of NHC and Xyl-C*H*$_3$), 2.17 (s, 1H, Xyl-C*H*$_3$), 2.09

(s, 1H, Xyl-C*H*$_3$), 1.80 (s, 1H, Xyl-C*H*$_3$), 1.76-1.39 (m, altogether 24H, CH(C*H*$_3$)$_2$ of Tip and C*H*$_3$ of NHC), 1.39-0.94 (m, 70H, CH(C*H*$_3$)$_2$ of Tip and C*H*$_3$ of NHC), 0.94-0.70 (m, 12H, CH(C*H*$_3$)$_2$ of Tip), 0.62 (d, 6H, CH(C*H*$_3$)$_2$ of Tip), 0.49 (d, 6H, CH(C*H*$_3$)$_2$ of Tip), 0.25 (d, 4H, CH(CH$_3$)$_2$ of Tip) ppm. **^{13}C NMR** spectrum is beyond interpretation. **^{29}Si NMR** (300 MHz, C_6D_6, 300 K, TMS): δ = 3.74 (br), −14.96 (br) ppm.

NMR data of 1,3-diisopropyl-4,5-dimethyl-1H-imidazol-3-ium chloride **153**:

^{1}H NMR (300 MHz, $CDCl_3$, 300 K, TMS): δ = 11.01 (s, 1H, N-C*H*-N), 4.56 (sept, 2H, C*H*(CH$_3$)$_2$), 2.29 (s, 6H, CH$_3$ of NHC), 1.76 (d, 12H, CH(C*H*$_3$)$_2$) ppm.

5.8.6. Reaction of Silagermenylidene 104 with Bis-Isocyanide 149

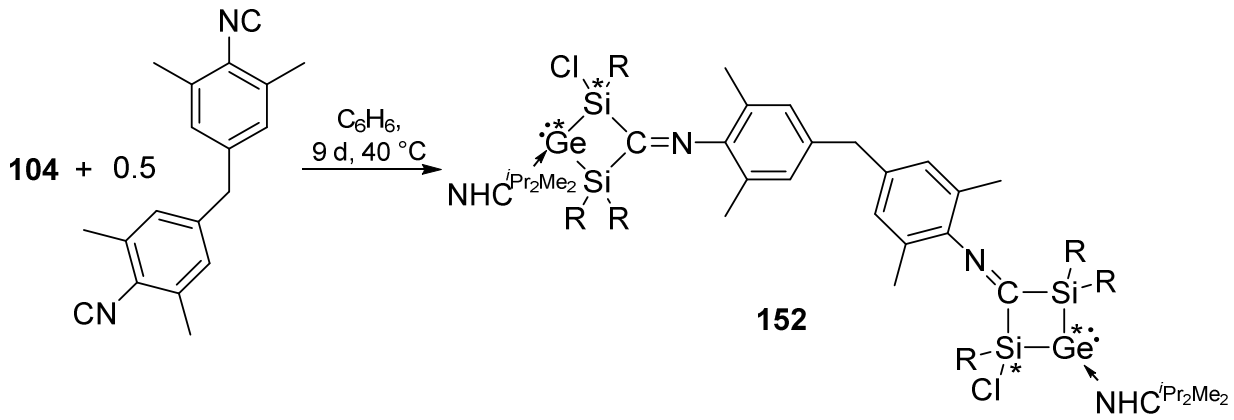

A solution of 506 mg **104** (0.53 mmol) and 74 mg of bis-isocyanide **149** (0.26 mmol) in 9 mL of toluene are heated to 40 °C for 9 days. The color changed during the process of reaction from red to intense purple. The solvent is evaporated in high vacuum and 100 mL of pentane are added to the purple solid. The solution is filtered while hot (40 °C). The solvent is concentrated to ca. 2 mL. All crystallization attempts failed (only colorless needles are obtained after 3 days at −26 °C, which are identified as imidazolium chloride **153**).

NMR data of the purple solid:

^{1}H NMR (300 MHz, C_6D_6, 300 K, TMS): δ = 7.42-6.45 (m, altogether 14H, Tip*H* and Xyl-*H*), 5.91 (br, 1H, C*H*(CH$_3$)$_2$ of NHC), 5.77 (br, 1H, C*H*(CH$_3$)$_2$ of NHC), 4.36 (sept, 1H, C*H*(CH$_3$)$_2$ of Tip), 3.90-3.66 (m, 2H, C*H*(CH$_3$)$_2$ of Tip), 3.51 (sept, 4H, C*H*(CH$_3$)$_2$ of Tip), 2.89-2.44 (m, altogether 9H, C*H*(CH$_3$)$_2$ of Tip and Xyl-C*H*$_3$), 2.09 (s, 3H, Xyl-CH$_3$), 1.80 (s, 3H, Xyl-CH$_3$), 1.76-1.39 (m, altogether 24H, CH(C*H*$_3$)$_2$ of Tip and C*H*$_3$ of NHC), 1.39-0.94 (m, 70H, CH(C*H*$_3$)$_2$ of Tip and C*H*$_3$ of NHC), 0.94-0.70 (m, 12H, CH(C*H*$_3$)$_2$ of Tip), 0.62 (d, 6H, CH(C*H*$_3$)$_2$ of Tip), 0.49 (d, 6H, CH(C*H*$_3$)$_2$ of Tip), 0.25 (d, 4H, CH(C*H*$_3$)$_2$ of Tip) ppm. **^{13}C NMR** spectrum is beyond interpretation. **^{29}Si NMR** (300 MHz, C_6D_6, 300 K, TMS): δ = 4.05 (br), −14.53 (br) ppm.

5.8.7. Reaction of Disilenyl Germylene 128c with Bis-Isocyanide 149

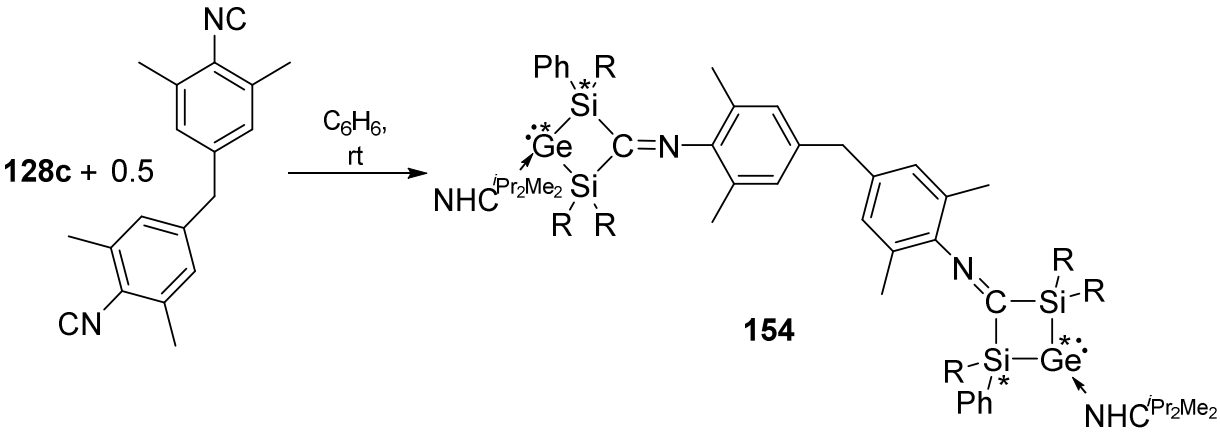

A solution of 22 mg methylene-bridged bis-isocyanide **149** (0.08 mmol, 0.5 eq) in 2 mL of benzene is added by syringe to a solution of 160 mg **128c** (0.16 mmol) in 2 mL of benzene at room temperature. The color changed immediately from deep red to deep purple and is stirred for 3 hours at ambient temperature. The solvent is evaporated to dryness and the purple residue dissolved in 15 ml of hexane. After filtration, the hexane is concentrated (ca. 2 mL). The solution is stored at −26 °C for 3 days without the formation of crystalline material.

Note: The NMR-spectra contains a mixture of diastereomers and therefore only characteristic resonances in the ^{1}H NMR (without integration) and the ^{13}C NMR of the mixture are listed due to signal overlaps:

^{1}H NMR (300.13 MHz, C_6D_6, 300 K, TMS): δ = 7.73 (br, Ph*H*), 7.26-6.56 (m, Tip*H*, Ph*H* and Xyl*H*), 5.16 (m, C*H*$(CH_3)_2$ of NHC), 4.35 (br, C*H*$(CH_3)_2$ of Tip), 4.04 (br, C*H*$(CH_3)_2$ of Tip), 2.82-2.80 (m, C*H*$(CH_3)_2$ of Tip), 2.53 (br s, C*H*$_3$ of Xyl), 1.83-0.25 (CH(C*H*$_3$)$_2$ of Tip, C*H*$(CH_3)_2$ of NHC and C*H*$_3$ of NHC) ppm. **^{13}C NMR** (75.56 MHz, C_6D_6, 300 K, TMS): δ = 169.49 (br, N*C*N), 57.07, 53.07 (*C*H$(CH_3)_2$ of NHC), 10.36, 10.39, 10.12 (*C*H$_3$ of NHC) ppm. **^{29}Si NMR** (59.62 MHz, C_6D_6, 300 K, TMS): δ = −2.03, −4.22 and −2.22, −4.28 (broad signals) ppm.

5.8.8. NHC-Abstraction from Cyclic Bis-Germylene 154

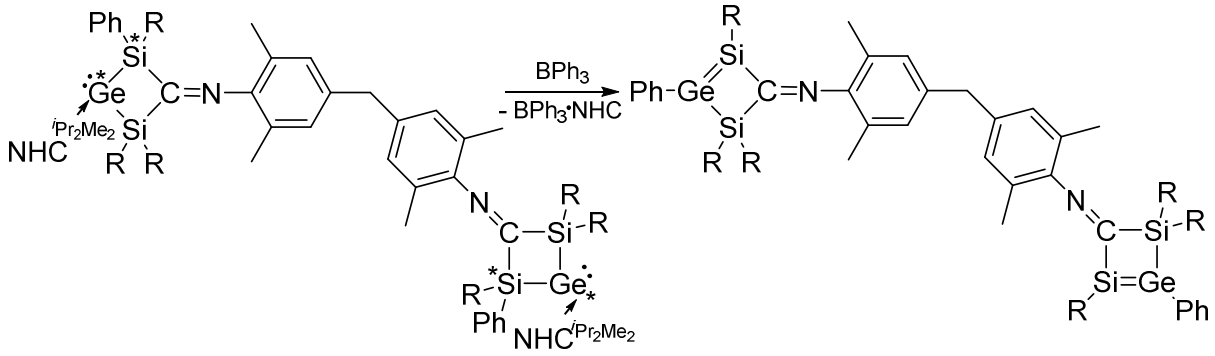

A solution of 21 mg BPh_3 (0.088 mmol) in 2 mL of benzene is added by syringe to a solution of 100 mg **154** (0.044 mmol) in 2 mL of benzene at room temperature. The color changed immediately from deep purple to green and is stirred for 1 hour at ambient temperature. A ^{1}H NMR indicated the formation of $BPh_3{\cdot}NHC^{iPr_2Me_2}$ and full conversion into a new product.

^{1}H NMR (300.13 MHz, C_6D_6, 300 K, TMS): δ = 8.01-7.98 (m, 4H, *o*-Ph*H*), 7.25 (s, 4H, Tip*H*), 7.23-7.13 (m, 6H, Ph*H*), 7.08 (s, 4H, Tip*H*), 6.85 (s, 4H, Tip*H*), 6.49 (br, 4H, Xyl*H*), 4.23 (sept, 4H, C*H*$(CH_3)_2$ of Tip), 3.53 (sept, 6H, C*H*$(CH_3)_2$ of Tip), 3.26 (s, 2H, C*H*$_2$ of Xyl$_2$), 2.85-2.58 (m, 8H, C*H*$(CH_3)_2$ of Tip), 2.29 (s, 9H, C*H*$_3$ of Xyl), 2.23 (s, 3H, C*H*$_3$ of Xyl), 1.34-1.03 (m, CH(C*H*$_3$)$_2$ of Tip) ppm. **^{29}Si NMR** (59.62 MHz, C_6D_6, 300 K, TMS): δ = 103.38, −4.34, −11.92 (impurity) ppm.

$BPh_3{\cdot}NHC^{iPr_2Me_2}$: **^{1}H NMR** (300.13 MHz, C_6D_6, 300 K, TMS): δ = 7.67-7.62 (m, 6H, Ar*H*), 7.32-7.26 (m, 6H, Ar*H*), 7.18 (d, 3H, Ar*H*), 5.01 (sept, 2H, C*H*$(CH_3)_2$ of NHC), 1.57 (s, 6H, CH_3 of NHC), 0.72 (d, 12H, CH(C*H*$_3$)$_2$ of NHC) ppm.[174]

5.8.9. Reaction of Heavier Cyclopropylidene 123c with Durylene-bis-Isocyanide 147

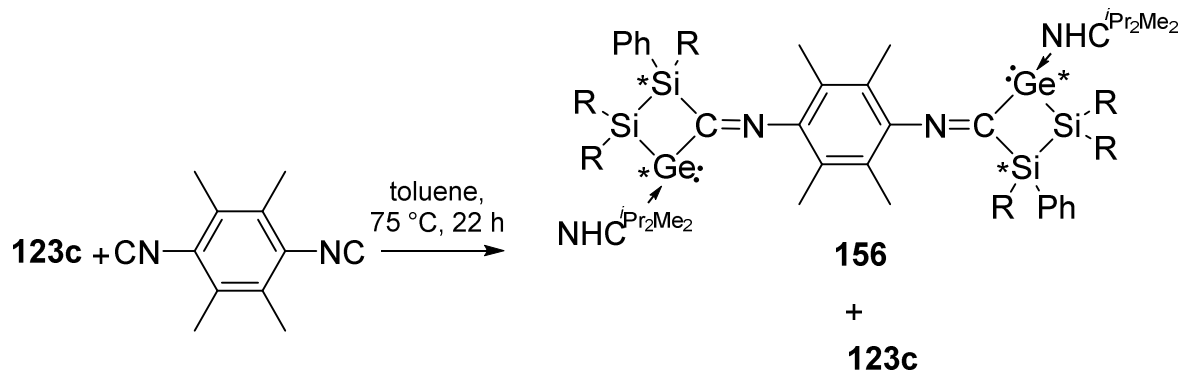

A solution of 87 mg **123c** (0.10 mmol) and 7 mg **147** (0.05 mmol, 0.5 eq) in 2 mL of toluene were heated to 75 °C (NMR-study). After 22 hours a second equivalent of **147** was added to the mixture due to the incompleteness of the reaction. Further warming for 2 days to 75 °C afforded a product mixture.

^{29}Si NMR (59.62 MHz, C_6D_6, 300 K, TMS): δ = −7.09 and −45.91, −62.73 and −68.83 (starting material **123c**) ppm.

5.8.10. Reaction of Heavier Cyclopropylidene 123c with Bis-Isocyanide 149

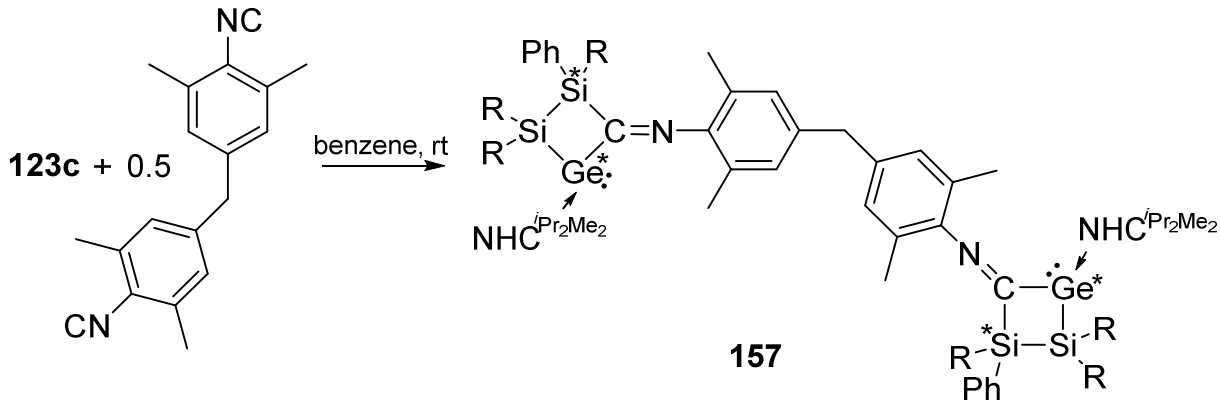

A solution of 100 mg **123c** (0.10 mmol) and 14 mg **149** (0.05 mmol, 0.5 eq) in 2 mL of toluene were heated to 75 °C (NMR-study). After 22 hours a second equivalent of **149** was added to the mixture due to the incompleteness of the reaction. Further warming for 2 days to 75° C afforded a product mixture.

^{29}Si NMR (59.62 MHz, C_6D_6, 300 K, TMS): δ = −6.72 (br), −7.28 (br), −45.05, −45.30, −45.58, −45.75, −62.74 and −68.80 (starting material **123c**) ppm.

5.9. Reactions of Arylsilanes with NHCs

5.9.1. Attempts to Synthesize an NHC-Stabilized Diaryl Silylene

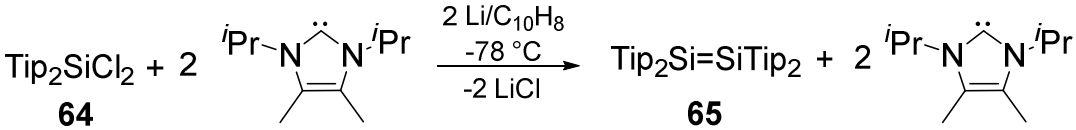

Tip_2SiCl_2 (419 mg, 0.83 mmol) and 150 mg $NHC^{iPr2Me2}$ (0.83 mmol) were dissolved in 10 mL Et_2O and cooled down to −78 °C. Freshly prepared $Li/C_{10}H_8$ (2 eq, 11.5 mg Li-granules and 260 mg $C_{10}H_8$) in 15 mL thf was added by cannula to the mixture. The mixture was slowly allowed to warm up to room temperature. A NMR sample indicated the formation of $Tip_2Si{=}SiTip_2$[103] while the $NHC^{iPr2Me2}$ was unaffected by the reduction conditions.

5.9.2. Attempts to Synthesize an NHC-Stabilized Diaryl Silylene 170

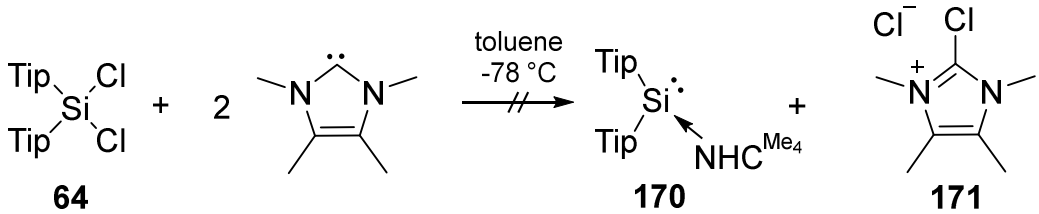

Tip_2SiCl_2 (400 mg, 0.79 mmol) was dissolved in 5 mL of toluene and added to a solution of 216 mg NHC^{Me4} (1.74 mmol, 2.2 eq) in 5 mL toluene at −78°C. The mixture was allowed to slowly warm up to room temperature and stirred for ca. 14 hours at room temperature. The color turned from colorless into red. A NMR sample indicated a product mixture.

^{29}Si NMR (59.62 MHz, C_6D_6, 300K, TMS): δ = 1.98, −0.55, −28.08, −37.68, −38.07, −40.66, −49.04 ppm.

5.9.3. Reaction of Mes_2SiHCl with $NHC^{iPr2Me2}$

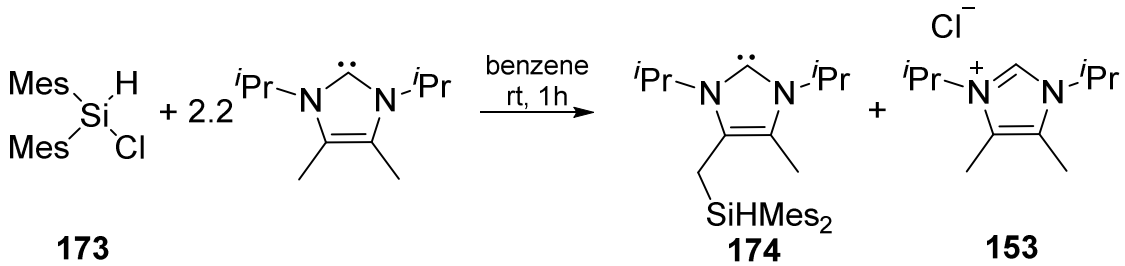

Mes_2SiHCl (1.00 g, 3.30 mmol) is dissolved in 10 mL of benzene and added to a solution of 1.31 g $NHC^{iPr2Me2}$ (7.26 mmol, 2.2 eq) in 10 mL benzene at room

temperature. After addition the color changed immediately from colorless to orange with concomitant formation of a white precipitate. The mixture is stirred for 1 hour while the orange color gets more intense. The benzene is evaporated in high vacuum and the excess of NHC^{iPr2Me2} sublimed at room temperature (2*10^{-3} mbar for 3 hours). The oily residue is dissolved in 50 mL of toluene and filtered. The white residue from the filtration is identified as imidazolium chloride **153**. The filtrate is concentrated to ca. 5 mL and stored at −26 °C for 4 days. No crystals are formed, only a white solid is obtained (rests of imidazolium salt). All crystallization attempts failed (conc. Et_2O, thf or flourobenzene solution from r.t. to −26 °C). It was also not possible to crystallize the product with a stoichiometry of 1:2.

^{1}H NMR (300.13 MHz, C_6D_6, 300 K, TMS): δ = 6.65 (s, 4H, Mes*H*), 5.27 (t, 1H, Si*H*, $^1J_{HSi}$ = 98 Hz), 3.91 (m, 2H, C*H*$(CH_3)_2$ and *H*C$(CH_3)_2$ [close to $SiMes_2H$] of NHC), 2.53 (d, 2H, CH_2SiMes2H of NHC), 2.20 (s, 12H, *o*-CH_3 of Mes), 2.07 (s, 6H, *p*-CH_3 of Mes), 1.48-1.45 (m, 12H, CH(CH_3)$_2$ of NHC), 1.29 (s, CH_3 of NHC) ppm. **^{13}C NMR** (75.56 MHz, C_6D_6, 300 K, TMS): δ = 207.63 (N*C*N), 144.66, 139.36, 130.27, (ArC_{quart}), 129.23 (Ar*C*H), 122.28 (NC*C*CH_3N), 121.62 (NH(SiClMes)C*C*CCH_3N), 48.51, 48.12 (*C*H$(CH_3)_2$ of NHC), 24.94, 24.59, 23.52, 21.12 (*C*H_3 of Mes), 13.40 (Mes_2HSi*C*H_2 of NHC), 8.53 (*C*H_3 of NHC) ppm. **^{29}Si NMR** (59.62 MHz, C_6D_6, 300 K, TMS): δ = −33.72 (H_2C*Si*Mes_2H) ppm.

Note: It was not possible to sublime out the complete excess of the NHC^{iPr2Me2}.

NMR data of the imidazolium chloride **153**:

^{1}H NMR (300 MHz, $CDCl_3$, 300 K, TMS): δ = 11.01 (s, 1H, N-C*H*-N), 4.56 (sept, 2H, C*H*$(CH_3)_2$), 2.29 (s, 6H, CH_3 of NHC), 1.76 (d, 12H, CH(CH_3)$_2$) ppm.

5.9.4. Reaction of Tip$_2$SiHCl with NHC^{iPr2Me2}

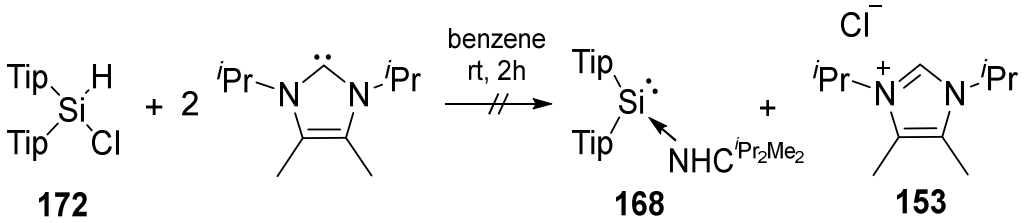

Tip_2SiHCl (305 mg, 0.63 mmol) was dissolved in 10 mL benzene and added to a solution of 234 mg NHC^{iPr2Me2} (1.29 mmol, 2.2 eq) in 10 mL benzene at room temperature. After addition the color changed immediately from colorless to deep orange with concomitant formation of a white precipitate. The mixture was stirred for 2 hours. The benzene was evaporated in high vacuum and the excess of NHC^{iPr2Me2} was sublimed-off at room temperature (5*10^{-3} mbar for 1 h). The NMR data showed a product mixture. The white precipitate was identified as a mixture of Tip_2SiHCl, imidazolium chloride **153** and the NHC^{iPr2Me2}.

^{29}Si NMR (59.62 MHz, C_6D_6, 300 K, TMS): δ = −22.02, −28.52, −36.72, −48.22 ppm.

5.9.5. Reaction of Mes_2SiHCl with NHC^{Mes_2}

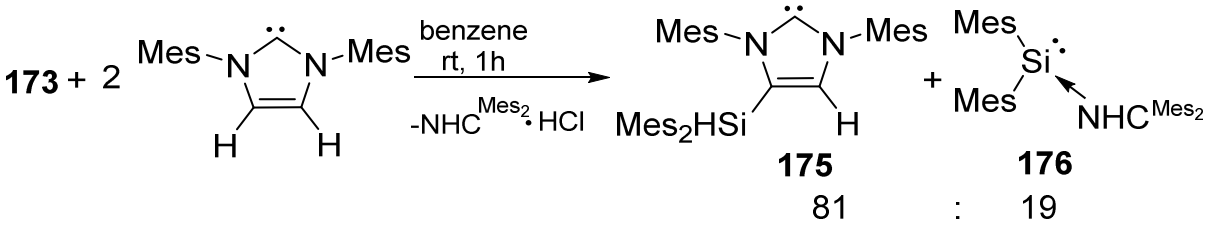

Mes_2SHiCl (50 mg, 0.17 mmol) was dissolved in 2 mL benzene and added to a solution of 100 mg NHC^{Mes2} (0.33 mmol, 2.2 eq) in 2 mL benzene at room temperature. After addition the color changed immediately from colorless to orange with concomitant formation of a white precipitate. The NMR data showed a product mixture.

^{13}C NMR (59.62 MHz, C_6D_6, 300 K, TMS): δ = 158.81 ppm.

^{29}Si NMR (59.62 MHz, C_6D_6, 300 K, TMS): δ = −24.04 (19%), −50.95 (81%) ppm.

5.9.6. Reaction of $TipSiCl_3$ with NHC^{Mes_2}

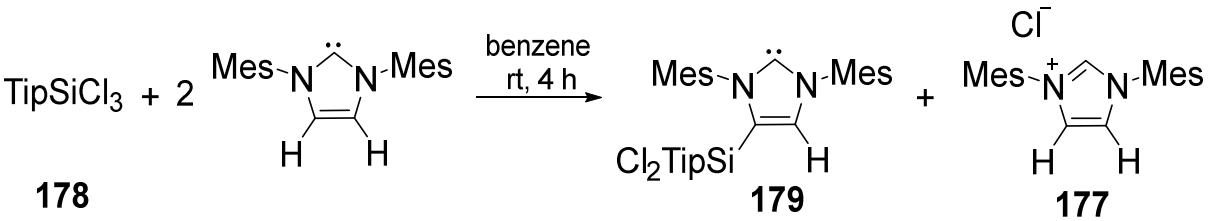

$TipSiCl_3$ (500 mg, 1.48 mmol) is dissolved in 6 mL of benzene and added to the off-white suspension of 897 mg NHC^{Mes2} (2.96 mmol, 2 eq) in 6 mL benzene at room temperature. After addition the color turned to dark red with concomitant formation of a precipitate. The mixture is stirred for 4 hours at ambient temperature. A NMR sample indicated full conversion into a new product. The benzene is evaporated in high vacuum ($5*10^{-3}$ mbar for 1 h). The residue is dissolved in 80 mL of hexane and filtered. All attempts to crystallize the product failed (conc. toluene, thf or diethyl ether solution from −26 °C to r.t.).

^{1}H NMR (300.13 MHz, C_6D_6, 300 K, TMS): δ = 7.11 (s, 2H, Tip*H*), 7.08 (s, 1H, $TipCl_2SiC{=}C$*H*), 6.84 (s, 2H, Mes*H*), 6.74 (s, 2H, Mes*H*), 3.81 (sept, 2H, *o*-C*H*$(CH_3)_2$ of Tip), 2.70 (sept, 1H, *p*-C*H*$(CH_3)_2$ of Tip), 2.25 (s, 6H, *o*-C*H*$_3$ of Mes), 2.16 (s, 3H, *p*-C*H*$_3$ of Mes), 2.14 (s, 3H, *p*-C*H*$_3$ of Mes), 2.10 (s, 6H, *o*-C*H*$_3$ of Mes),1.20 (d, 12H, *o*-CH(C*H*$_3$)$_2$ of Tip), 1.56 (d, 6H, *p*-CH(C*H*$_3$)$_2$ of Tip) ppm. **^{13}C NMR** (75.56 MHz, C_6D_6, 300 K, TMS): δ = N*C*N: not detected, 157.26, 153.22, 138.51, 138.36, 137.97, 137.67 (ArC_{quart}), 136.45, 135.21, 129.25 (Ar*C*H), 134.06 ($NTipCl_2SiC$*C*HN), 122.82 ($NTipCl_2Si$*C*CHN), 121.62, 34.62, 33.78 (*C*H$(CH_3)_2$ of Tip), 25.25, 23.80 (CH(*C*H$_3$)$_2$ of Tip), 21.20, 21.02, 18.67, 18.05 (*C*H$_3$ of Mes) ppm. **^{29}Si NMR** (59.62 MHz, C_6D_6, 300 K, TMS): δ = −10.19 ppm.

5.9.7. Synthesis of Disilyl Carbene 185

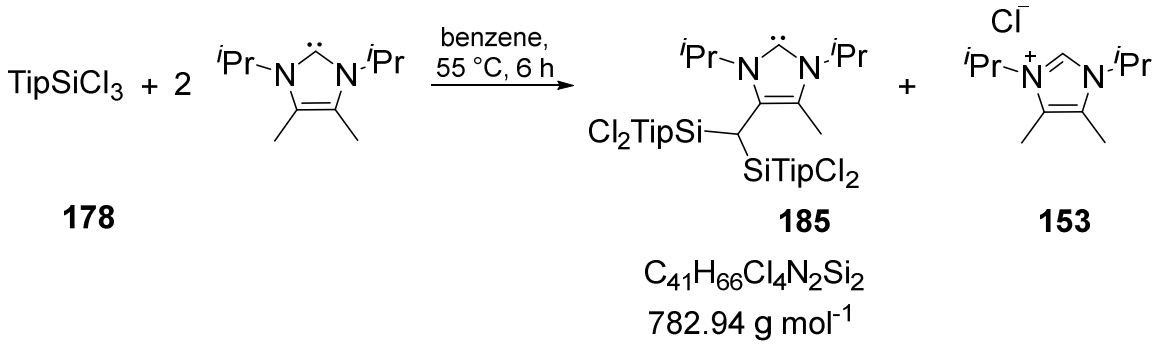

$TipSiCl_3$ (500 mg, 1.48 mmol) and 560 mg $NHC^{iPr2Me2}$ (3.11 mmol, 2.1 eq) are dissolved together in 3 mL of benzene and heated to 55 °C for 6 hours. In the course of the reaction the solution turned from colorless into dark red. The solvent is evaporated and the excess of $NHC^{iPr2Me2}$ sublimed-off in high vacuum ($2*10^{-2}$ mbar, 50 °C). The red solid is dissolved in 40 mL of hexane and filtered over reverse frit with a 5 cm layer of celite. Again the solvent is evaporated to dryness and the residue dissolved in 60 mL of hexane. The hexane is heated to approximately 50 °C and filtered while hot. The solution is concentrated to a third of volume. At this stage a red precipitated has formed. The solution is stored overnight at −26 °C. After 24 hours the mother liquor is separated from the red solid, which includes 450 mg of **185** (39%) together with small amounts of impurities. Red single crystals of **185** are obtained from a diluted hexane solution of the red solid after storing at −26 °C for one week. The crystalline yield is 177 mg (15%).

MP: 74-77°C (rearrangement to unknown SiH-insertion product). **^{1}H NMR** (300.13 MHz, C_6D_6, 300 K, TMS): δ = 7.11 (s, 4H, Tip*H*), 4.15 (sept, 1H, C*H*$(CH_3)_2$ of NHC), 3.91 (m, 2H, C*H*$(CH_3)_2$ of NHC and *H*C(($SiTipCl_2$))$_2$), 3.73 (sept, 4H, *o*-C*H*$(CH_3)_2$ of Tip), 2.66 (sept, 2H, *p*-C*H*$(CH_3)_2$ of Tip), 2.39 (s, 3H, C*H*$_3$ of NHC), 1.48 (d, 6H, CH(C*H*$_3$)$_2$ of NHC), 1.40 (d, 6H, CH(C*H*$_3$)$_2$ of NHC), 1.31 (d, 12H, *p*-CH(C*H*$_3$)$_2$ of Tip), 1.27 (d, 12H, *o*-CH(C*H*$_3$)$_2$ of Tip), 1.11 (d, 12H, *o*-CH(C*H*$_3$)$_2$ of Tip) ppm. **^{13}C NMR** (75.56 MHz, C_6D_6, 300 K, TMS): δ = 211.01 (N*C*N), 156.99, 153.15, 126.54, (Ar*C*$_{quart}$), 128.35 (masked by C_6D_6), 123.33 (Ar*C*H), 125.58 (NC*C*CH$_3$N), 117.07 (NH($SiCl_2$Tip)$_2$C*C*CCH$_3$N), 48.21, 47.36 (*C*H$(CH_3)_2$ of NHC), 31.08 (*C*H($SiCl_2$Tip)$_2$ of NHC), 35.00, 34.45 (*C*H$(CH_3)_2$ of Tip), 26.21, 25.93, 25.13, 24.52, 23.69, 23.64 (CH(*C*H$_3$)$_2$ of Tip), 12.85 (*C*H$_3$ of NHC) ppm. **^{29}Si NMR** (59.62 MHz, C_6D_6, 300 K, TMS): δ = 7.42 (*Si*TipCl_2) ppm. **UV/vis** (hexane): λ_{max} = 278 nm (ε = 4700 $Lmol^{-1}cm^{-1}$). **Element. anal.:** Combustion analysis did not yield satisfactory results presumably due to the oxygen sensitivity of **185**.

5.9.8. Reaction of Disilyl Carbene 185 with $BH_3 \cdot SMe_2$

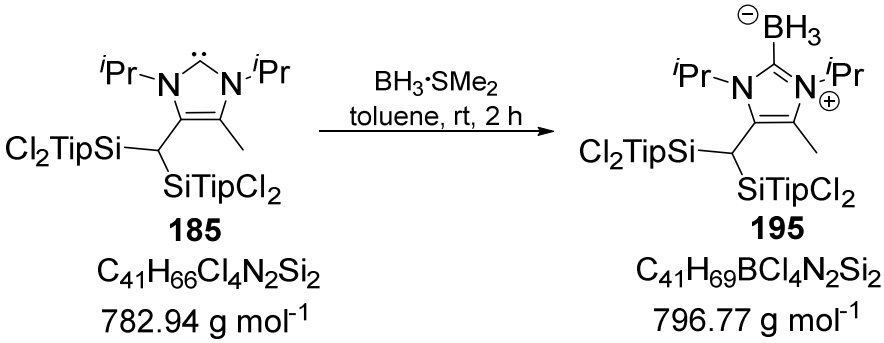

$BH_3 \cdot SMe_2$ (29 μL, 0.38 mmol) was added to a solution of 300 mg **185** (0.38 mmol) in 4 mL of toluene. The red color of the reaction mixture changed after 10 min to pale yellow and was stirred for an additional hour. The toluene was removed in high vacuum and the yellow foam was dried (1 h, $2*10^{-2}$ mbar). After adding 10 mL of hexane, a concentrated solution was stored at r.t. to afford colorless crystals of **195** after 4 days in 84 mg yield. Due to the small amount of crystals only a NMR-study could be carried out.

^{1}H NMR (300.13 MHz, C_6D_6, 300 K, TMS): δ = 7.10 (s, 4H, Tip*H*), 4.35-4.31 (m, 1H, C*H*$(CH_3)_2$ of NHC), 4.09-3.88 (m, 2H, C*H*$(CH_3)_2$ of NHC and *H*C(($SiTipCl_2$))$_2$), 3.61 (sept, 4H, *o*-C*H*$(CH_3)_2$ of Tip), 2.65 (sept, 2H, *p*-C*H*$(CH_3)_2$ of Tip), 2.35 (s, 3H, C*H*$_3$ of NHC), 1.68 (d, 6H, CH(C*H*$_3$)$_2$ of NHC), 1.26 (d, 12H, *o*-CH(C*H*$_3$)$_2$ of Tip), 1.25 (d, 12H, *p*-CH(C*H*$_3$)$_2$ of Tip), 1.21 (d, 6H, CH(C*H*$_3$)$_2$ of NHC), 1.10 (d, 12H, *o*-CH(C*H*$_3$)$_2$ of Tip) ppm. **^{11}B NMR** (96.29 MHz, C_6D_6, 300 K, TMS): δ = −32.94 (br, -BH_3) ppm. **^{13}C NMR** (75.56 MHz, C_6D_6, 300 K, TMS): δ = 157.03, 153.70, 127.44, (Ar*C*$_{quart}$), 128.19 (masked by C_6D_6), 123.56 (Ar*C*H), 125.78 (NC*C*CH$_3$N), 122.71 (NH($SiCl_2Tip$)$_2$C*C*CCH$_3$N), 49.81, 49.51 (*C*H$(CH_3)_2$ of NHC), 35.09 (*C*H($SiCl_2Tip$)$_2$ of NHC), 34.45, 33.41 (*C*H$(CH_3)_2$ of Tip), 26.00, 25.15, 25.10, 23.72, 23.67, 23.59 (CH(*C*H$_3$)$_2$ of Tip), 15.30 (*C*H$_3$ of NHC) ppm. **^{29}Si NMR** (59.62 MHz, C_6D_6, 300 K, TMS): δ = 7.46 (*Si*TipCl$_2$) ppm.

5.9.9. Reduction Attempts of Disilyl Carbene 185

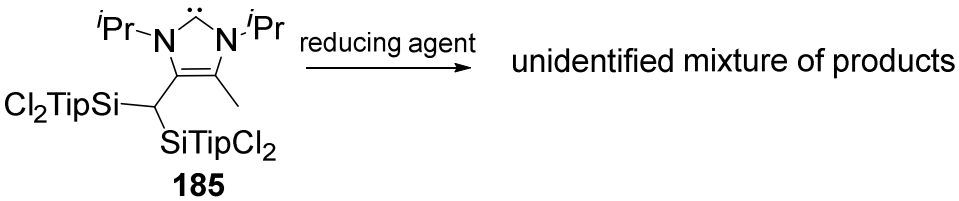

A −50 °C cold solution of 640 mg (0.82 mmol) of disilyl carbene **185** in 10 mL thf are added to a suspension of 464 mg of KC_8 (3.33 mmol, 4.4 eq) in 5 mL of thf at −50 °C. The reaction mixture is slowly allowed to warm to room temperature over a period of 6 hours. The color changed from pale red to intense red in process of warming. The

solvent is evaporated and the dark residue filtered from 40 mL hexane. The hexane is concentrated to a third of volume and stored at −26 °C. No crystals could be obtained.

Note: No NMR data can be evaluated: In the ^{29}Si NMR no resonance was detected, while the ^{1}H and ^{13}C NMR was broadened that no signal assignment was possible.

A series of reduction experiments were investigated with the following reducing agents: 2 and 4 eq $Li/C_{10}H_8$, 4 eq KC_8, 4 eq Na_2FeCO4, Mg-powder, Na, K, Jones Magnesium(I). All reductions showed the same outcome as described above.

5.9.10. Reduction Attempts of Disilyl Carbene 185 with 2 eq KC_8

A −50 °C cold solution of 530 mg (0.68 mmol) of disilyl carbene **185** in 5 mL thf were added to a suspension of 183 mg of KC_8 (1.35 mmol, 2 eq) in 5 mL of thf at −50 °C. The reaction mixture was slowly allowed to warm to room temperature over a period of 6 hours. The solvent was evaporated and residue filtered from 20 mL hexane. The ^{29}Si NMR indicated a mixture of several products. The hexane was concentrated to a third of volume and stored at room temperature. No crystals were obtained, not even from a very concentrated hexane solution at −26 °C.

^{29}Si NMR (59.62 MHz, C_6D_6, 300 K, TMS): δ = −10.49, −15.87, −28.36, −31.28 ppm.

5.9.11. Reduction Attempts of Disilyl Carbene 185 with Na/K

A solution of 250 mg (0.32 mmol) of NHC **185** and an excess of Na/K (48 mg/90 mg K, ca 6eq) were suspended in 4 mL of thf/toluene. The reaction mixture was heated to 60 °C for 12 hours. The solvent was evaporated in high vacuum and the remaining solid dissolved in hexane. After filtration a concentrated hexane solution was stored at room temperature which did not afford single crystals.

^{29}Si NMR (59.62 MHz, C_6D_6, 300 K, TMS): δ = −68.58 ppm.

5.9.12. Synthesis of Bis-Silyl Germylene 200

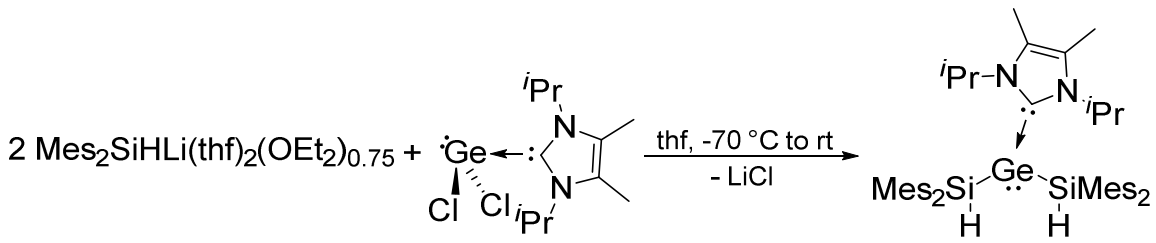

197	**8**	**200**
$C_{30}H_{47}O_3LiSi$	$C_{11}H_{20}N_2Cl_2Ge$	$C_{47}H_{66}N_2Si_2Ge$
490.73 g mol^{-1}	323.84 g mol^{-1}	787.85 g mol^{-1}

A precooled solution of 500 mg $Mes_2SiHLi(thf)_2(OEt_2)_{0.75}$ (1.05 mmol) in 10 mL of thf is added at −70 °C by cannula to a solution of 171 mg $GeCl_2{\cdot}NHC^{iPr_2Me_2}$ (0.53 mmol) in 20 mL of thf. The colorless solution immediately turned orange. At 0 °C the reaction is complete and the solvent is evaporated in high vacuum. The residue is dissolved in 40

mL of hexane. After filtration the solvent is reduced to a third of the volume to afford a yellow precipitate of **200**. Single crystals of **200** suitable for X-ray diffraction are obtained from a saturated toluene solution after three days at rt. Yield: 253 mg (61%).

MP: 217-220 °C (Formation of unidentified GeH-species). **^{1}H NMR** (300.13 MHz, C_6D_6, 300 K): δ = 6.71 (s, 8H, Mes-*H*), 6.37 (s, 2H, Si-*H*), 6.09 (hept, 2H, C*H*$(CH_3)_2$ of NHC), 2.52 (s, 24H, *o*-C*H*$_3$), 2.15 (s, 12H, *p*-C*H*$_3$), 1.53 (s, 6H, CH_3 of NHC) , 0.94 (d, 12H, CH(C*H*$_3$)$_2$ of NHC) ppm. **^{13}C NMR** (125.76 MHz, C_6D_6, 300 K): δ = 172.55 (N*C*N), 145.40, 137.09 (Ar*C*$_{quart}$), 128.94 (Ar*C*H), 126.63 (NC*C*CH$_3$N), 54.05 (*C*H$(CH_3)_2$ of NHC), 24.82, 21.41, 21.17 (*C*H$_3$ of Mes), 10.16 (*C*H$_3$ of NHC) ppm. **^{29}Si NMR** (125.76 MHz, C_6D_6, 300 K): δ = −38.06 ppm. **UV/vis** (thf): λ_{max} = 320 nm (ε = 5300 Lmol^{-1}cm^{-1}). **Element. anal.:** Calcd. for $C_{47}H_{66}N_2Si_2Ge$: C, 71.65; H, 8.44; N, 3.56. Found: C, 71.68; H, 8.39; N, 3.48.

5.9.13. Abstraction of NHC from Bis-Silyl Germylene 200

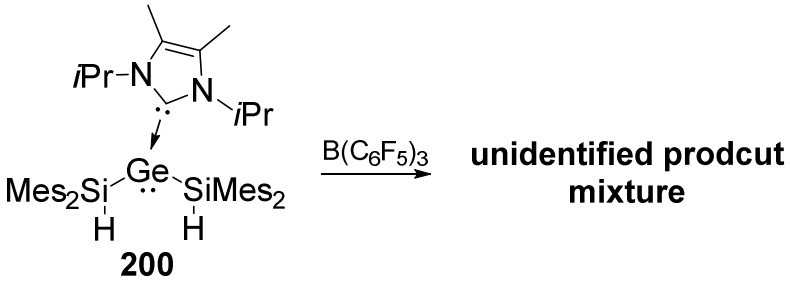

A solution of 230 mg (0.44 mmol) $B(C_6F_5)_3$ in 2 mL of benzene was added to solution of 350 mg (0.44 mmol) bis-germylene **200** in 3 mL of benzene at room temperature. The solvent was removed in high vacuum after 30 min stirring at room temperature. The residue was filtered from 20 mL of hexane and a concentrated solution was stored at room temperature. It was not possible to grow single crystals from the reaction mixture.

^{29}Si NMR (125.76 MHz, C_6D_6, 300 K): δ = −7.66, −12.49 −29.17, −42.56, −47.32 ppm.

5.10. Synthesis and Reactivity of Digermenide 90

5.10.1. Synthesis of Dihalodiaryl germanes 206

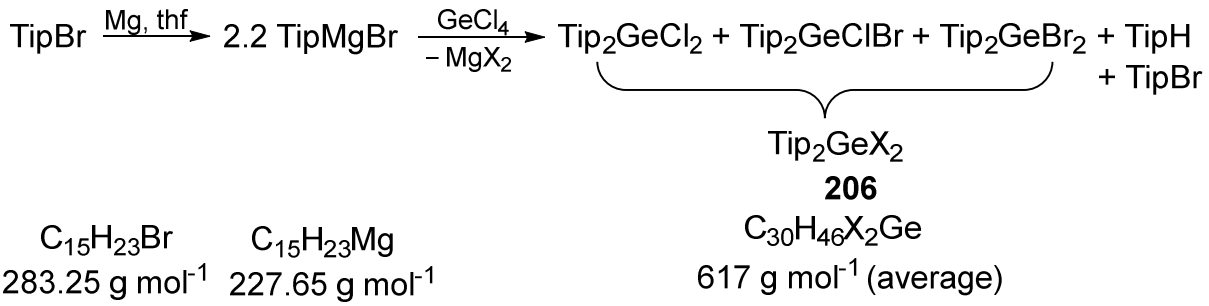

TipMgBr and Tip_2GeX_2 **206** were synthesized according to modified literature procedures.[93][205] Magnesium shavings (4.78 g, 0.2 mol, 1.2 eq) are treated with heat under reduced pressure and afterwards suspended in 200 mL of thf. A solution of 47 g degassed TipBr (0.17 mol) and 50 mL of thf are added slowly through a dropping funnel. After adding ca. 75% of the TipBr-solution, a heat development is observed and the mixture is heated for 2 hours to reflux to complete the reaction. After cooling down to rt, stirring is continued for 1 hour and a ^{1}H NMR spectrum of a hydrolyzed sample indicated full conversion into TipH.

Tip*H*: **^{1}H NMR** (300 MHz, C_6D_6, 300 K): δ = 7.00 (s, 3H, Ar*H*), 2.82 (sept, 3H, C*H*$(CH_3)_2$ of Tip), 1.24 (18H, CH(C*H*$_3$)$_2$ of Tip) ppm.

The yellow Grignard reagent solution (TipMgBr, 2.2 eq) in thf is slowly added to a solution of 8.8 mL $GeCl_4$ (16.56 g, 0.08 mol) in 100 mL of benzene. After heating to 80 °C for 17 hours and cooling down to r.t., a ^{1}H NMR spectrum indicated full conversion. The reaction mixture is quenched by addition of 50 mL of 10%-HCl-solution. The aqueous phase is extracted with diethyl ether (3 x 100 mL). The combined organic layers are dried over $MgSO_4$ and evaporation of the solvent afforded a yellow oily mass (Tip_2GeCl_2, $Tip_2GeClBr$, Tip_2GeBr_2, TipBr, TipH). TipBr and TipH are distilled of in high vacuum ($2*10^{-2}$ mbar, 160 °C). The residue contained a mixture of three *bis*-arylgermaniumdihalides in an approximately ratio of Tip_2GeCl_2:$Tip_2GeClBr$:Tip_2GeBr_2 (3:44:53) in a yield of 43 g (approximate average molar mass: 617 g*mol^{-1} based on the integration of TipH signals from a ^{1}H NMR spectrum; yield based on this mass: 88%, 0.07 mol).

Note: Due to signal overlaps of the mixture of dihalodiarylgermanes, only characteristic signals in the aromatic region are given.

Tip_2GeCl_2, $Tip_2GeClBr$, Tip_2GeBr_2: **^{1}H NMR** (300 MHz, C_6D_6, 300 K): δ = 7.07 (s, 4H, Tip*H* of Tip_2GeCl_2), 7.05 (s, 4H, Tip*H* of $Tip_2GeBrCl$), 7.03 (s, 4H, Tip*H* of Tip_2GeBr_2) ppm.

5.10.2. Synthesis of Bis(2,4,6-triisopropylphenyl)germane 207

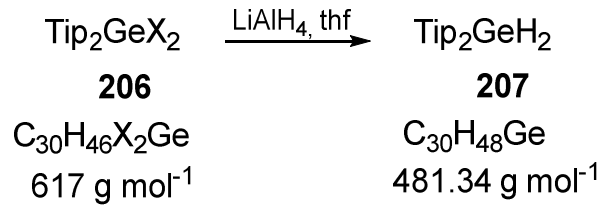

Tip_2GeH_2 was synthesized according to a modified literature procedure of Baines and co-workers.[205] A 0 °C cold solution of the diaryl-substituted germanium halides (43 g, 0.07 mol, Tip_2GeCl_2: $Tip_2GeClBr$: Tip_2GeBr_2 3:44:53) in 130 mL of thf is added to a 0 °C cooled suspension of 5.3 g $LiAlH_4$ (0.14 mol) in 50 mL of thf. After addition the cooling bath is replaced and the reaction mixture is heated for 4 hours to reflux to complete the reaction. Slow addition of ca. 200 mL of 10%-HCl solution quenched the excess of $LiAlH_4$. The organic phase is separated and the aqueous phase extracted three times with diethyl ether (3*100 mL). The combined organic phases are dried over $MgSO_4$. After distilling off the organic solvents, **207** is obtained as a pale yellow oil (with small amount of impurities) in 31.6 g (94%) yield.

^{1}H NMR (300 MHz, C_6D_6, 300 K): δ = 7.13 (s, 4H, Ar*H*), 5.58 (s, 2H, Ge*H*), 3.52 (sept, 4H, *o*-C*H*(CH_3)$_2$ of Tip), 2.78 (sept, 2H, *p*-C*H*(CH_3)$_2$ of Tip), 1.21 (d, 12H, *p*-CH(C*H*$_3$)$_2$ of Tip), 1.20 (d, 24H, *o*-CH(C*H*$_3$)$_2$ of Tip) ppm.

5.10.3. Synthesis of Diaryldichloro germane 50

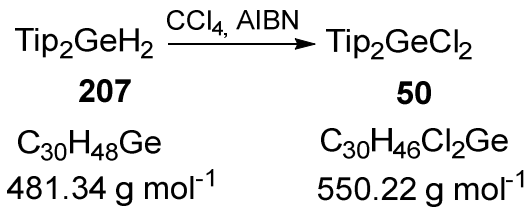

Tip_2GeCl_2 was synthesized according to modified literature procedures.[93][92] To a solution of 31.6 g Tip_2GeH_2 **207** (0.066 mol) in 150 mL of CCl_4 a small amount of AIBN is added. The reaction mixture is refluxed for 3 hours. After cooling down to r.t., a ^{1}H NMR spectrum indicated full conversion into a new product. Purification of the crude 34 g of Tip_2GeCl_2 (0.062 mol) by Kugelrohr-distillation (150–160 °C, 4.5*10^{-2} mbar) afforded 25.6 g (70%) of pure **50** (yield based on $GeCl_4$: 58%)

^{1}H NMR (300 MHz, C_6D_6, 300 K): δ = 7.07 (s, 4H, Ar*H*), 3.40 (sept, 4H, *o*-C*H*(CH_3)$_2$ of Tip), 2.68 (sept, 2H, *p*-C*H*(CH_3)$_2$ of Tip), 1.17-1.12 (m, 36H, CH(C*H*$_3$)$_2$ of Tip) ppm. **^{13}C NMR** (75 MHz, C_6D_6, 300 K): δ = 153.01, 152.23 (Tip*C*$_{quart}$), 136.21, 122.98 (Tip*C*H), 34.58, 33.77 (*C*H(CH_3)$_2$ of Tip), 24.49, 23.91 (CH(*C*H$_3$)$_2$ of Tip) ppm.

5.10.4. Synthesis of (2,4,6-Triisopropylphenyl)digermenyllithium

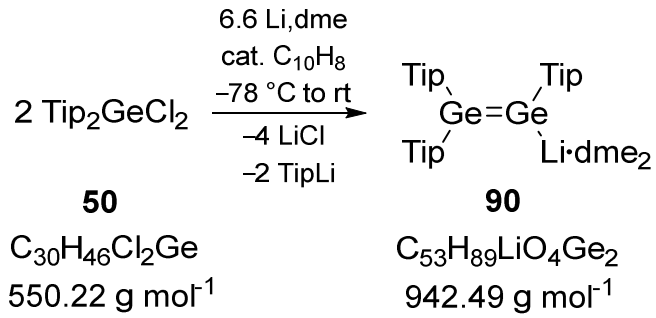

Dry, −70 °C cold viscous dme (8 mL) is added by cannula to a finely dispersed (stirred for 30 min in the cooling bath to homogenize the components) and −70 °C cold mixture of 1.036 g **50** (1.88 mmol), 1 mg naphthalene (cat. amount) and 43 mg of Li-powder (6.2 mmol, 3.3 eq). The off-white suspension is slowly allowed to warm up. At −58 °C the color turned to light green. In the further warming process the color changes to dark green (−46 °C) and finally turned into dark red (−23 °C). The reaction mixture is allowed to slowly warm up to r.t. and stirred for 30 min at ambient temperature. A ^{1}H NMR spectrum indicated a complete conversion into a new product. Insoluble parts are filtered off in a first filtration. Dme is evaporated to dryness and the sticky deep red residue is dried in high vacuum (ca. 1 hour at 7x10^{-2} mbar) until the residue turned into an orange solid. The solid is dissolved in 50 mL of pentane and the deep red solution is filtered again (to filter off TipLi and LiCl). The pentane is concentrated to ca. 40 mL and stored at −26 °C. After 14 hours red crystals of **90** are obtained in 45% (450 mg) yield.

Yield: 38%-45% (scale: 1-6 g)

MP: 135-138 °C (conversion into Tip$_2$Ge=GeTip$_2$ and unidentified product mixture)

^{1}H NMR (300.13 MHz, C_6D_6, 300 K, TMS): δ = 7.17 (s, 2H, *m*-Tip*H*), 7.12 (s, 2H, *m*-Tip*H*), 7.11 (s, 2H, *m*-Tip*H*), 4.71-4.56 (m, 4H, C*H*(CH$_3$)$_2$ of Tip), 4.22 (br, 2H, C*H*(CH$_3$)$_2$ of Tip), 2.93 (s, 12H, dme), 2.84 (s, 8H, dme), 2.96-2.76 (m, 3H, C*H*(CH$_3$)$_2$ of Tip), 1.42 (d, 16H, CH(C*H*$_3$)$_2$ of Tip), 1.35 (d, 6H, CH(C*H*$_3$)$_2$ of Tip), 1.35 (d, 6H, CH(C*H*$_3$)$_2$ of Tip) 1.27, 1.24, 1.20 (each d, overall 32H, CH(C*H*$_3$)$_2$ of Tip) 0.87 (tr, pentane) ppm. **^{7}Li NMR** (116.59 MHz, C_6D_6, 300 K, Li$^+$ aq): δ = −0.22 ppm. **^{13}C NMR** (75.56 MHz, C_6D_6, 300 K, TMS): δ = 155.40, 153.82, 153.69, 152.66 (br), 152.48, 152.08, 147.33, 146.7, 145.49 (Tip*C*$_{quart}$), 128.33 (masked by C_6D_6), 121.44, 120.63, 120.06 (Tip*C*H), 70.47 (*C*H$_2$ of dme), 59.17 (*C*H$_3$ of dme), 36.68, 36.17, 35.35, 35.03, 34.78, 34.66 (*C*H(CH$_3$)$_2$ of Tip), 26.52 (br), 25.21 (br), 24.90, 24.76, 24.63, 24.39 (CH(*C*H$_3$)$_2$ of Tip), 22.72 (pentane), 14.27 (pentane) ppm. **UV/vis** (hexane): λ_{max} = 435 nm (ε = 11800 Lmol^{-1}cm^{-1}), 356 nm (ε = 5600 Lmol^{-1}cm^{-1}). **Element. anal.:** Calcd. for $C_{53}H_{89}Ge_2LiO_4$ (942.5): C, 67.54; H, 9.52. Found: C, 67.56; H, 9.03.

5.10.5. Reaction of Tip_2GeX_2 206 with 4 eq Li-Powder with $C_{10}H_8$

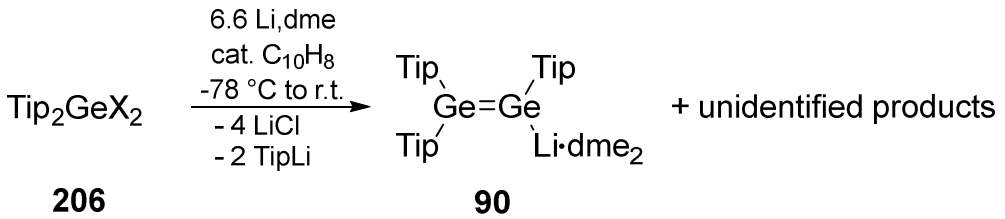

Tip_2GeX_2 (5.4 g, average molar mass: 617 g*mol^{-1}, 8.75 mmol) was mixed together with 200 mg of Li-powder (28.89 mmol, 3.3 eq) and 2 mg of naphthalene. The flask was cooled down to −70 °C and stirring was continued for 30 min. 40 mL of dry dme were also cooled down to −70 °C and transferred to Tip_2GeX_2, Li and naphthalene. In the process of warming the color changed to dark red. A ^{1}H NMR indicated the formation of digermenide beside unidentified by-products. After filtration from 200 mL of pentane, the solution was concentrated to a third of volume and stored at −26 °C. After 14 hours a red microcrystalline precipitate of digermenide **90** has been formed in 5 % (207 mg) yield.

5.10.6. Reaction of Tip_2GeX_2 206 with 3.5 eq Li-Powder

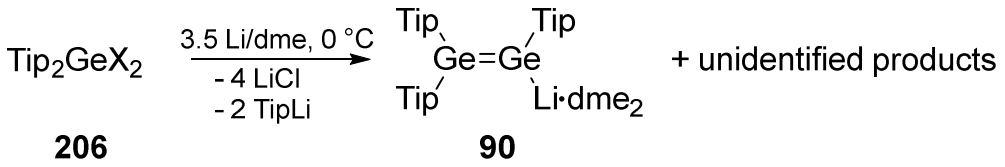

Tip_2GeX_2 (4.2 g, average molar mass: 617 g*mol^{-1}, 6.81 mmol) was mixed together with 165 mg of Li-powder (23.82 mmol, 3.5 eq). The reaction was cooled to 0 °C and 30 mL of dry dme were added. The color changed immediately to dark red. A ^{1}H NMR sample indicates a mixture of products. After filtration from 150 mL pentane the solution was concentrated to ca. 30 mL and is frozen in liquid nitrogen. In the process of warming to room temperature a red precipitate of digermenide **90** has been formed in 2% (64 mg) yield.

5.10.7. Reaction of Tip_2GeCl_2 50 with 4 eq Li-Powder without $C_{10}H_8$

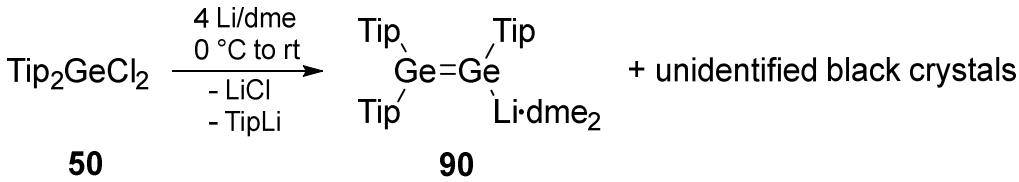

Tip_2GeCl_2 **50** (3 g, 4.54 mmol) and 151 mg of Li-powder (22 mmol, 4 eq) were finely dispersed in a Schlenk-flask and stirred for 30 min at r.t. Dry dme (15 mL) was added by cannula under ice cooling to **50** and Li-powder. The reaction mixture turned immediately to dark green. After stirring for 15 min under ice cooling, a heat development was observed while the mixture turned into dark red. Stirring was

continued for 30 min in the thawing ice bath. The solvent was removed in high vacuum and the remaining solid dried (2 h, 2*10^{-2} mbar). After filtration from 300 mL of pentane, a concentrated solution was stored at −26 °C which formed red and almost black crystals after 20 hours. The red crystals were assigned to digermenide **90** while the black crystals were an unidentified, anionic compound. When the mother liquor was stored at r.t. orange crystals of $GeTip_3H$ **209** were obtained after 3 weeks in % (67 mg) yield.

Note: only main signals of the black crystals are listed due to signal overlaps.

^{1}H NMR (300.13 MHz, C_6D_6, 300 K, TMS): δ = 7.08 (s, Tip*H*), 4.05 (sept, C*H*$(CH_3)_2$ of Tip), 0.98 (d, CH(C*H*$_3$)$_2$ of Tip).

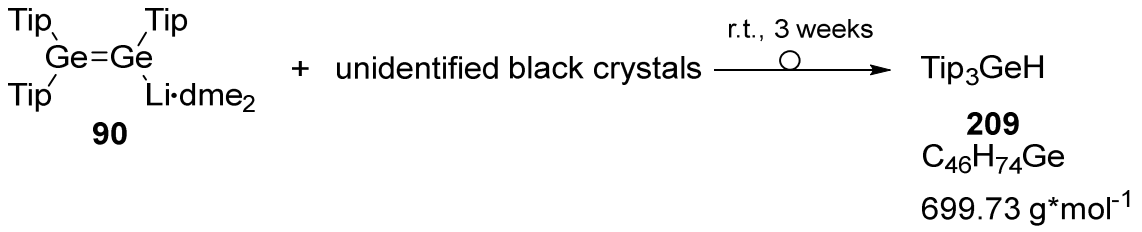

$GeTip_3H$ **209**:

MP: 180-183 °C (Decomposition). **^{1}H NMR** (300.13 MHz, C_6D_6, 300 K, TMS): δ = 7.12 (s, 6H, Tip*H*), 6.27 (s, 1H, Ge*H*), 3.53 (sept, 3H, C*H*$(CH_3)_2$ of Tip), 3.31 (sept, 3H, C*H*$(CH_3)_2$ of Tip), 2.76 (sept, 3H, C*H*$(CH_3)_2$ of Tip), 1.48 (d, 9H, CH(C*H*$_3$)$_2$ of NHC), 1.31 (d, 9H, CH(C*H*$_3$)$_2$ of NHC), 1.18 (d, 22H, CH(C*H*$_3$)$_2$ of Tip), 1.06 (d, 9H, CH(C*H*$_3$)$_2$ of Tip), 0.84 (d, 9H, CH(C*H*$_3$)$_2$ of Tip) ppm. **^{13}C NMR** (75.56 MHz, C_6D_6, 300 K, TMS): δ = 154.62, 154.49, 150.14, 135.94 (Ar*C*$_{quart}$), 128.35, 122.45, 121.66 (Ar*C*H), 35.85, 34.59, 33.91 (*C*H$(CH_3)_2$ of Tip), 25.80, 24.86, 24.57, 24.13 (CH(*C*H$_3$)$_2$ of Tip), 22.72 (pentane), 14.27 (pentane) ppm. **UV/vis** (hexane): λ_{max} = 349 nm (ε = 5200 Lmol^{-1}cm^{-1}), 437 nm (ε = 1800 Lmol^{-1}cm^{-1}). **Element. anal.:** Calcd. for $C_{46}H_{74}Ge$ (699.73 g/mol) : C, 78.96; H, 10.66. Found: C, 78.37; H, 10.24.

5.10.8. Reduction Attempt of Digermenide 90 with 2 eq Li-Powder

Dry, −50 °C cold dme (8 mL) was added by cannula to a finely dispersed and −50 °C cold mixture of 360 mg **50** (0.38 mmol), 3 mg naphthalene (cat. amount) and 6.4 mg of Li-powder (0.92 mmol, 2.4 eq). The red colored mixture was slowly allowed to warm to room temperature and stirring was continued for 14 hours. A 1H NMR spectrum indicates the formation of a product mixture. The solvent was evaporated and filtered from 20 mL pentane.

5.10.9. Reduction of Tip_2GeCl_2 50 with 4.4 eq of Li-Powder

Dry, −70 °C cold dme (20 mL) was added by cannula to a finely dispersed and −70 °C cold mixture of 1.12 g **50** (2.06 mmol), 10 mg naphthalene (cat. amount) and 62 mg of Li-powder (8.96 mmol, 4.4 eq). The mixture was slowly allowed to warm to room temperature. The color turned into dark red. The solvent was evaporated and the black solid filtered from 30 mL of pentane. The pentane solution was stored at −26 °C for 14 hours to obtain 250 mg (26%) of digermenide **90**.

5.10.10. Reaction of Digermenide 90 with $GeCl_2$·dioxane

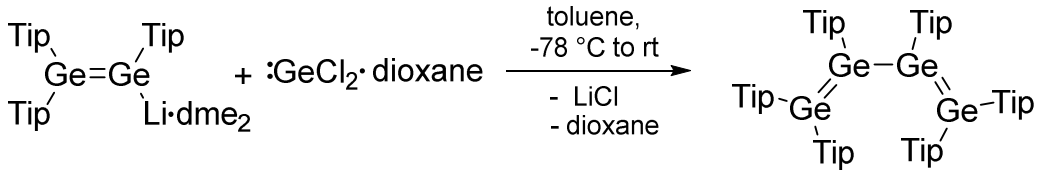

90 **92**

$C_{90}H_{138}Ge_4$
1510.61 g mol^{-1}

A solution of 156 mg **90** (0.17 mmol) in 3 mL of toluene is added to a solution of 38 mg $GeCl_2$·dioxane (0.17 mmol) in 3 mL of toluene. The color changed immediately from pale red to intensely green. After stirring for 30 min the solvent is evaporated to dryness and the nearly black solid is dissolved in 15 mL of pentane. After filtration, the pentane is concentrated to ca. 2 mL and the blue solution is stored at r.t. After 2 days at ambient temperature dark green crystals of tetragermabutadiene **92**[128] are obtained in 40 mg (15%) yield. When the reaction is repeated at low temperatures, the outcome stays the same.

^{1}H NMR (300.13 MHz, C_6D_6, 300 K, TMS): δ = 7.19, 7.04, 6.96, 6.92, 6.88, 6.69 (each d, each 2H, Tip*H*), 5.54-4.34 (m, 4H, C*H*$(CH_3)_2$ of Tip), 3.66-3.44 (m, 4H, C*H*$(CH_3)_2$ of Tip), 3.32 (sept, 4H, C*H*$(CH_3)_2$ of Tip), 2.74-2.55 (m, 6H, C*H*$(CH_3)_2$ of Tip), 1.79-1.69 (m, 12H, CH(C*H*$_3$)$_2$ of Tip), 1.37-1.29 (m, 20H, CH(C*H*$_3$)$_2$ of Tip), 1.18-1.05 (m, 38H, CH(C*H*$_3$)$_2$ of Tip and C*H*$_2$ of co-crystallized pentane), 0.87 (t, 6H, C*H*$_3$ of co-crystallized pentane) 0.57 (dd, 12H, CH(C*H*$_3$)$_2$ of Tip), 0.46 (d, 6H, CH(C*H*$_3$)$_2$ of Tip), 0.33 (d, 6H, CH(C*H*$_3$)$_2$ of Tip), 0.25 (d, 6H, CH(C*H*$_3$)$_2$ of Tip) ppm.

5.10.11. Synthesis of 1,4-Bis{1',2',2'-[tris(2,4,6-triisopropylphenyl)]}digermenylbenzene 216

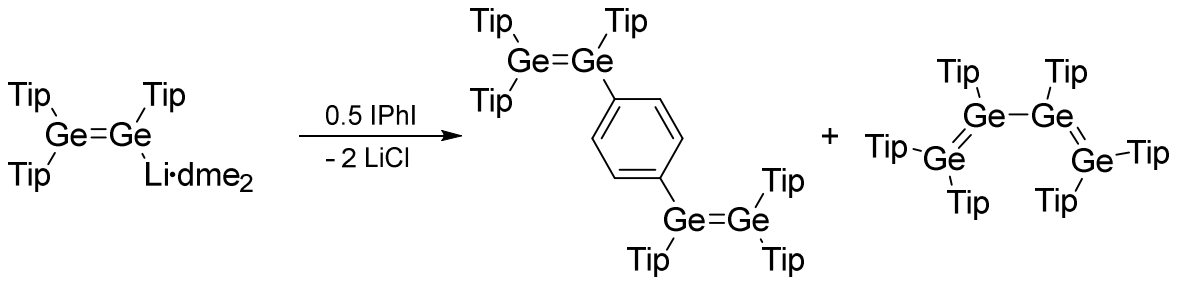

90 **216** **92**

$C_{96}H_{142}Ge_4$
1586.71 g*mol^{-1}

A solution of 584 mg **90** (0.62 mmol) in 3 mL of benzene is added to a solution of 102 mg 1,4-diiodobenze (0.31 mmol) in 3 mL of benzene. The color changed immediately from pale red to dark red. After stirring for 10 min the solvent is evaporated to dryness and the deep red residue is dissolved in 15 mL of pentane. After filtration, the pentane is concentrated to ca. 2 mL and the dark red solution is stored at r.t. After 14 hours at ambient temperature square like red crystals of **216** are obtained among of dark green crystals of tetragermabutadiene **92**.[128] The red crystals are separated mechanically to afford 36 mg (7%) of **216**.

MP: 207-210 °C (transformation into different GeH-species). **^{1}H NMR** (300.13 MHz, C_6D_6, 300 K, TMS): δ = 7.18, 7.08, 7.06 (each s, each 4H, Tip*H*), 6.95 (s, 4H, C_6H_4), 3.86 (sept, 4H, C*H*(CH_3)$_2$ of Tip), 3.80-3.63 (m, 8H, C*H*(CH_3)$_2$ of Tip), 2.90-2.61 (m, 6H, C*H*(CH_3)$_2$ of Tip), 1.34 (d, 12H, CH(C*H*$_3$)$_2$ of Tip), 1.27 (d, 16H, CH(C*H*$_3$)$_2$ of Tip), 1.21-1.10 (m, 88H, CH(C*H*$_3$)$_2$ of Tip and C*H*$_2$ of co-crystallized pentane), 0.87 (t, 6H, C*H*$_3$ of co-crystallized pentane) ppm. **^{13}C NMR** (75.56 MHz, C_6D_6, 300 K, TMS): δ = 154.32, 153.87, 152.61, 149.86, 147.36, 145.69, 141.88 (Tip*C*$_{quart}$ and Ph*C*$_{quart}$), 134.85, 128.39 (masked by C_6D_6), 122.70 (br), 122.44 (br), 122.16 (br, Tip*C*H and Ph*C*H), 38.35, 38.16, 34.84, 34.77, 34.64, (*C*H(CH_3)$_2$ of Tip), 25.96, 24.90 (br), 24.77, 24.69, 24.62, 24.34, 24.30, 24.20, 24.09 (CH(*C*H$_3$)$_2$ of Tip), 34.55, 22.72 (pentane), 14.27 (pentane) ppm. **UV/vis** (hexane): λ_{max} = 480 nm (ε = 41300 Lmol^{-1}cm^{-1}), 367 nm (ε = 8100 Lmol^{-1}cm^{-1}). **Element. anal.:** Combustion analysis did not yield satisfactory results presumably due to the oxygen sensitivity of **216**.

5.10.12. Synthesis of Boryl Digermene 222

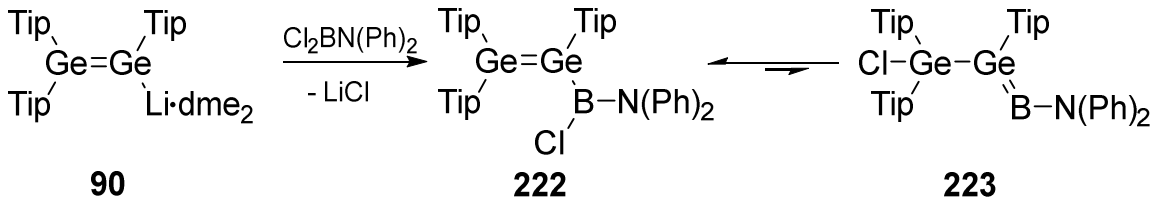

A solution of 80 mg dichloro(*N*,*N*-diphenylamino)borane (0.32 mmol) in 2.5 mL of benzene is added to a solution of 300 mg **90** (0.32 mmol) in 2.5 mL of benzene at room temperature. After addition the color changed immediately from red to orange. After stirring for 30 min at ambient temperature, the solvent is evaporated to dryness in high vacuum and dried for ca. 2 hours ($5*10^{-2}$ mbar). Filtration from 15 mL of pentane and storing a diluted solution (ca. 5 mL) at r.t. for 4 days afforded orange-yellow crystals of **222** suitable for X-ray diffraction in 45 mg (15%) yield. A second crop afforded 35 mg (11%) of **222** (overall yield 80 mg (26%)).

MP: 178-181 °C (conversion into $Tip_2Ge{=}GeTip_2$ and decomposition of $ClBNPh_2$-group). **^{1}H NMR** (300.13 MHz, C_6D_6, 300 K, TMS): δ = 7.38-7.19 (m, 4H, Tip*H* and N(Ph*H*)$_2$), 7.16-6.71 (m, 12H, Tip*H* and N(Ph*H*)$_2$, overlap with C_6D_6), 4.26-3.55 (br, 5H, C*H*(CH$_3$)$_2$ of Tip), 2.88-2.62 (m, 4H, C*H*(CH$_3$)$_2$ of Tip), 1.74-0.40 (m, 54H, CH(C*H*$_3$)$_2$ of Tip) ppm. **^{13}C NMR** (75.56 MHz, C_6D_6, 300 K, TMS): δ = 154.06 (br), 152.61, 150.28, 149.95, 149.81, 148.56 (br), 147.45 (Tip*C*$_{quart}$), 140.65, 137.36, 129.34, 129.27, 128.36, 127.91, 127.83, 127.64, 127.37, 127.04 (masked by C_6D_6), 126.56, 126.41, 122.17 (br), 121.68 (br), (Ph*C*H and Tip*C*H), 38.53 (br), 38.17 (br), 36.91, 34.69(br), 34.57 (br) (*C*H(CH$_3$)$_2$ of Tip), 24.51 (br), 24.23 (br), 24.07 (br) (CH(*C*H$_3$)$_2$ of Tip) ppm. **Element. anal.:** Calcd. for $C_{57}H_{79}Ge_2BCl$ (969.8): C, 70.59; H, 8.21; N, 1.44. Found: C, 70.38; H, 8.32; N, 1.29.
Note: Due to the broadness of the ^{11}B resonance because of equilibrium effects no signal was detected.

5.10.13. Synthesis of Digermenyl Borate 219

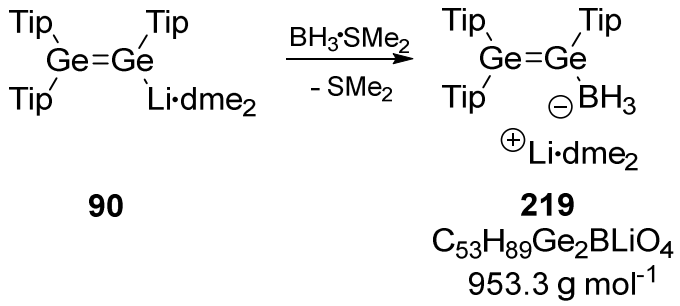

To a solution of 258 mg **90** (0.27 mmol) in 4 mL of benzene, 26 µL BH_3·DMS (20.5 mg, 0.27 mmol) were added via a microliter syringe at r.t. The reaction mixture turned immediately from red to yellow and was stirred for 5 min at ambient temperature. The solvent was evaporated to dryness in high vacuum and dried for 30 min ($3*10^{-2}$ mbar).

Filtration from 25 mL of pentane and storing a diluted solution (ca. 5 mL) at −26 °C for 1 day afforded yellow crystals of **219** suitable for X-ray diffraction in 54 mg (20%) yield.

MP: 125-127 °C (decomposition). **^{1}H NMR** (300.13 MHz, C_6D_6, 300 K, TMS): δ = 7.11 (s, 4H, Tip*H*), 7.08(m, 2H, Tip*H*), 4.30-4.27 (br, 4H, C*H*(CH_3)$_2$ of Tip), 4.03 (sept, 2H, C*H*(CH_3)$_2$ of Tip), 2.92 (s, 12H, dme), 2.83 (s, 8H, dme), 2.86-2.68 (m, 3H, C*H*(CH_3)$_2$ of Tip), 1.36-1.09 (m, 72, CH(C*H*$_3$)$_2$ of Tip and C*H*$_2$ of co-crystallized pentane), 0.87 (t, 6H, C*H*$_3$ of co-crystallized pentane) ppm. **^{7}Li NMR** (116.59 MHz, C_6D_6, 300 K, Li^+ aq): δ = −0.59 ppm. **^{11}B NMR** (96.29 MHz, C_6D_6, 300 K, TMS): δ = −32.99 (br q) ppm. **^{13}C NMR** (75.56 MHz, C_6D_6, 300 K, TMS): δ = 153.89 (br), 153.36, 152.84, 148.26, 148.08, 147.97 (br), 145.85 (Tip*C*$_{quart}$), 135.94, 128.27 (masked by C_6D_6), 121.77 (br), 121.32 (br), 120.69 (br, Tip*C*H), 70.25 (*C*H$_2$ of dme), 59.02 (*C*H$_3$ of dme), 37.19 (br), 36.88 (br), 36.74, 34.91(br), 34.74 (br), 34.61 (*C*H(CH_3)$_2$ of Tip), 25.28 (br), 25.02 (br), 24.69, 24.52, 24.29 (CH(*C*H$_3$)$_2$ of Tip) ppm. **UV/vis** (hexane): λ_{max} = 438 nm (ε = 8900 $Lmol^{-1}cm^{-1}$). **Element. anal.:** Calcd. for $C_{53}H_{89}Ge_2BLiO_4$ (953.3): C, 66.78; H, 9.41. Found: C, 66.10; H, 9.38.

5.10.14. Reaction of Digermenide 90 with PhI

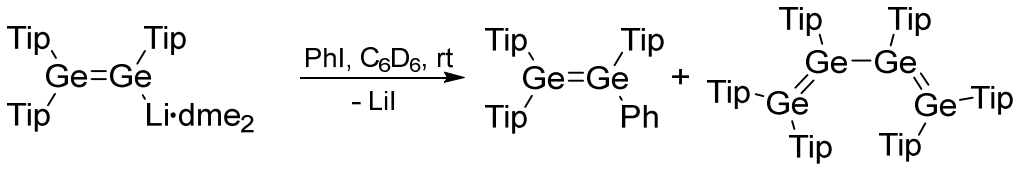

90 **212** **92**

To a solution of 21.5 mg **90** (0.023 mmol) in 0.5 mL of C_6D_6 in a NMR-tube, 2.55 μL PhI (0.023 mmol) were added by microliter syringe. The color changed immediately from pale red to yellow/green. After 10 min a ^{1}H NMR sample indicated a mixture of tetragermabutadiene **92** and digermene **212** in an approximate ratio about 20:80 (NMR). A repeat reaction in a larger scale under the same conditions (0.157 mmol) led to a mixture of unidentified products and tetragermabutadiene **92** as main product.

^{1}H NMR (300.13 MHz, C_6D_6, 300 K, TMS): δ = 7.33-7.30 (m, 2H, *o*-Ph*H*), 7.22 (s, 2H, Tip*H*), 7.13 (s, 2H, Tip*H*), 7.09 (s, 2H, Tip*H*), 6.96-6.88 (m, 3H, *m*-Ph*H* and *p*-Ph*H*), 4.01-3.63 (m, 6H, C*H*(CH_3)$_2$ of Tip), 2.84-2.62 (m, 3H, C*H*(CH_3)$_2$ of Tip), 1.25-1.09 (m, 54H, CH(C*H*$_3$)$_2$ of Tip) ppm.

5.10.15. Reaction of Digermenide 90 with PhX (X=Cl, Br)

General procedure: Digermenide **90** (100 mg, 0.053 mmol) and the corresponding haloarenes (0.053 mmol) are each dissolved in benzene (3 mL). The benzene solution of **90** is transferred by syringe to the benzene solution of the haloarenes. The color changed immediately from pale red to dark green, indicating the formation of tetragermabutadiene **92** (NMR: approximate ratio 9:1).[128]

5.10.16. Reaction of Digermenide 90 with $GeCl_4$

To a −78 °C cold solution of 150 mg **90** (0.16 mmol) in 3 mL of toluene, 91 μL $GeCl_4$ (0.8 mmol) was added via microliter syringe. The reaction mixture was slowly allowed to warm to room temperature (ca. 5 hours). In the course of warming the color changed from intense red to orange. After stirring at room temperature for 12 hours the solvent was evaporated and dried (2 h, $3*10^{-2}$ mbar). A NMR sample indicated a mixture of unidentified products.

Note: ^{1}H and ^{13}C NMR data were due to signal overlaps beyond interpretation.

5.10.17. Reaction of Digermenide 90 with P(I)-Source 229

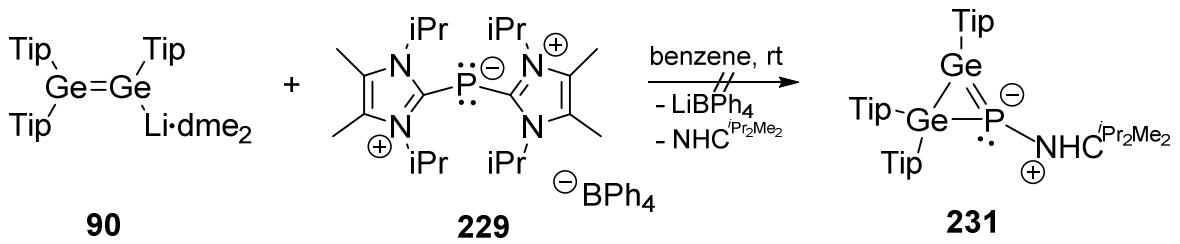

A solution of 248 mg **90** (0.26 mmol) in 4 mL of benzene was transferred to a suspension of 187 mg $BPh_4P(NHC^{iPr_2Me_2})_2$ (0.26 mmol) in 4 mL of benzene at room temperature. The color changed immediately from pale red to orange and a white precipitate was formed ($LiBPh_4$). After stirring for 30 min at ambient temperature, the solvent was evaporated to dryness and an orange foam retained which was dissolved in 25 mL of pentane. After filtration, the pentane was concentrated to ca. 2 mL and the solution was stored at r.t. No crystals were obtained after 4 days at rt. Storing the concentrated pentane solution at −26 °C for 3 days also afforded no crystalline material.

Note: ^{1}H and ^{13}C NMR data are due to signal overlaps beyond interpretation.

^{31}P NMR (121.5 MHz, C_6D_6, 300 K, TMS): δ = −187.54 ppm.

5.10.18. Reaction of Digermenide 90 with $(Me_2N)_2PCl$

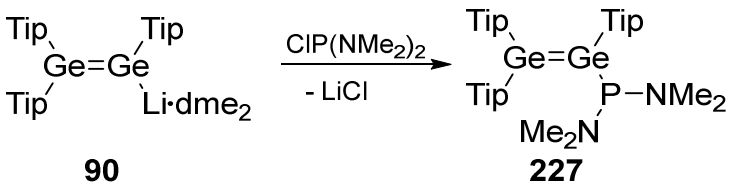

To a solution of 22 mg **90** (0.023 mmol) in 1 mL of benzene 3.4 μL bis[dimethylamino]chlorophosphane (0.023 mmol) were added by microliter syringe at room temperature. The color changed immediately from pale red to dark red. After 10 min of stirring at ambient temperature the color changed again from dark red to orange. The solvent was evaporated and the sample dried in high vacuum.

Note: ^{1}H and ^{13}C NMR data are due to signal overlaps beyond interpretation.

^{31}P NMR (121.5 MHz, C_6D_6, 300 K, TMS): δ = 112.53 (main signal), number of unidentified side products in the range from 104-23 ppm.

5.10.19. Reaction of Digermenide 90 with (^{i}Pr$_2$N)$_2$PCl

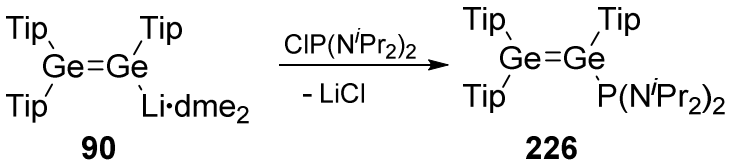

A solution of 5 mg bis[diisopropylamino]chlorophosphane (0.018 mmol) in 0.25 mL of C_6D_6 were added to a solution of 17 mg of **90** (0.018 mmol) in 0.25 mL of C_6D_6. The phosphane was added to **90**. The color changed immediately from pale red to dark red.

Note: ^{1}H and ^{13}C NMR data are due to signal overlaps beyond interpretation.

^{31}P NMR (121.5 MHz, C_6D_6, 300 K, TMS): δ = 134.73, 83.57, 80.95 ppm.

5.10.20. Reaction of Digermenide 90 with 2-6 eq of NHC^{i}Pr$_2$Me$_2$

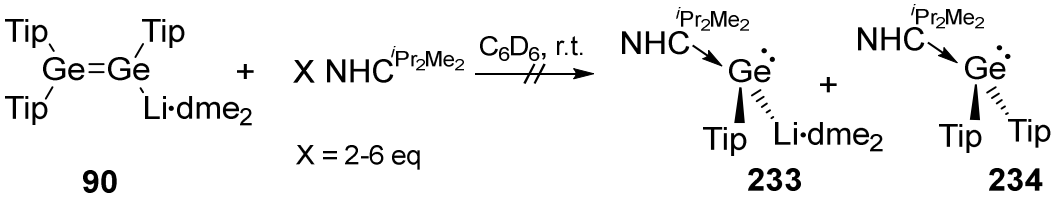

A solution of 30 mg of digermenide **90** (0.032 mmol) in 0.5 mL C_6D_6 (0.5 mL) was added to 11.5 mg of NHC^{i}Pr$_2$Me$_2$ (0.064 mmol, 2eq). There was no change in color observed, even after heating for 12 hours at 60 °C.

^{1}H NMR (300.13 MHz, C_6D_6, 300 K, TMS): δ = 7.12 (s, 2H, *m*-Tip*H*), 7.10 (s, 2H, *m*-Tip*H*), 7.10 (s, 2H, *m*-Tip*H*), 4.69-4.58 (m, 4H, C*H*(CH$_3$)$_2$ of Tip), 4.42-4.32 (m, 4H, C*H*(CH$_3$)$_2$ of NHC), 4.20 (br, 2H, C*H*(CH$_3$)$_2$ of Tip), 3.22 (s, 8H, dme), 3.01 (s, 12H, dme), 2.95-2.71 (m, 3H, C*H*(CH$_3$)$_2$ of Tip), 1.67 (s, 12H, C*H*$_3$ of NHC), 1.48-1.45 (m, 12H, CH(C*H*$_3$)$_2$ of Tip), 1.35 (d, 14H, CH(C*H*$_3$)$_2$ of Tip), 1.30-1.16 (m, 66H, CH(C*H*$_3$)$_2$ of Tip and CH(C*H*$_3$)$_2$ of NHC) ppm. **^{7}Li NMR** (116.59 MHz, C_6D_6, 300 K, Li^+ aq): δ = 2.06 ppm.

2 further equivalents of NHC^{i}Pr$_2$Me$_2$ were added to the same sample which results in a slight shift of the ^{1}H NMR signals.

^{1}H NMR (300.13 MHz, C_6D_6, 300 K, TMS): δ = 7.12 (s, 2H, *m*-Tip*H*), 7.10 (s, 2H, *m*-Tip*H*), 7.09 (s, 2H, *m*-Tip*H*), 4.73-4.64 (m, 4H, C*H*(CH$_3$)$_2$ of Tip), 4.20-4.16 (m, 10H, C*H*(CH$_3$)$_2$ of NHC and Tip), 3.28 (s, 8H, dme), 3.10 (s, 12H, dme), 2.96-2.73 (m, 3H, C*H*(CH$_3$)$_2$ of Tip), 1.72 (s, 24H, C*H*$_3$ of NHC), 1.38 (br, 74H, CH(C*H*$_3$)$_2$ of Tip and NHC),

1.29 (d, 12H, CH(C*H*$_3$)$_2$ of Tip), 1.22 (d, 12H, CH(C*H*$_3$)$_2$ of Tip) ppm. **^{7}Li NMR** (116.59 MHz, C_6D_6, 300 K, Li^+ aq): δ = 2.50 ppm.

The C_6D_6 was evaporated and dried in high vacuum for 3 hours at $3*10^{-3}$ mbar resulting in a small change of the chemical shifts.

^{1}H NMR (300.13 MHz, C_6D_6, 300 K, TMS): δ = 7.14 (s, 2H, *m*-Tip*H*), 7.09 (s, 4H, *m*-Tip*H*), 4.71-4.62 (m, 4H, C*H*(CH$_3$)$_2$ of Tip), 4.14 (br, 10H, C*H*(CH$_3$)$_2$ of NHC and Tip), 2.98-2.71 (m, 3H, C*H*(CH$_3$)$_2$ of Tip), 1.67 (s, 24H, C*H*$_3$ of NHC), 1.39-1.38 (m, 86H, CH(C*H*$_3$)$_2$ of Tip and NHC), 1.31 (d, 14H, CH(C*H*$_3$)$_2$ of Tip), 1.22 (d, 14H, CH(C*H*$_3$)$_2$ of Tip) ppm. **^{7}Li NMR** (116.59 MHz, C_6D_6, 300 K, Li^+ aq): δ = 2.90 ppm.

Again 2 further equivalents of NHC^{iPr2Me2} (6 eq overall) were added to the same sample which results in a slight shift of the ^{1}H NMR signals.

^{1}H NMR (300.13 MHz, C_6D_6, 300 K, TMS): δ = 7.14 (s, 2H, *m*-Tip*H*), 7.11 (s, 2H, *m*-Tip*H*), 7.09 (s, 2H, *m*-Tip*H*), 4.74-4.67 (m, 4H, C*H*(CH$_3$)$_2$ of Tip), 4.21 (br, 2H, C*H*(CH$_3$)$_2$ of Tip), 4.05 (br, 14H, C*H*(CH$_3$)$_2$ of NHC and Tip), 2.99-2.73 (m, 3H, C*H*(CH$_3$)$_2$ of Tip), 1.67 (s, 42H, C*H*$_3$ of NHC), 1.44-1.40 (m, 112H, CH(C*H*$_3$)$_2$ of Tip and NHC), 1.31 (d, 14H, CH(C*H*$_3$)$_2$ of Tip), 1.22 (d, 14H, CH(C*H*$_3$)$_2$ of Tip) ppm. **^{7}Li NMR** (116.59 MHz, C_6D_6, 300 K, Li^+ aq): δ = 2.76 (br) ppm.

To the sample with 6 eq of NHC^{iPr2Me2} 0.1 mL dme were added to result in a different set of NMR data (Note: ^{1}H NMR evaluated without integration).

^{1}H NMR (300.13 MHz, C_6D_6, 300 K, TMS): δ = 7.05 (s, *m*-Tip*H*), 7.04 (s, *m*-Tip*H*), 7.01 (s, *m*-Tip*H*), 4.75-4.66 (m, C*H*(CH$_3$)$_2$ of Tip), 4.20 (br, C*H*(CH$_3$)$_2$ of Tip), 4.00 (sept, C*H*(CH$_3$)$_2$ of NHC), 3.32 (s, dme), 3.12 (s, dme), 2.86-2.71 (m, C*H*(CH$_3$)$_2$ of Tip), 1.76 (s, C*H*$_3$ of NHC), 1.43 (d, CH(C*H*$_3$)$_2$ of NHC), 1.34, 1.30, 1.23, 1.18, 1.08 (each d CH(C*H*$_3$)$_2$ of Tip) ppm. **^{7}Li NMR** (116.59 MHz, C_6D_6, 300 K, Li^+ aq): δ = 0.98 ppm.

5.10.21. Reaction of Digermenide 90 with 3 eq of NHC^{iPr2Me2}

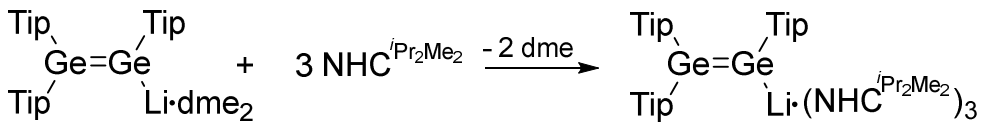

90 **237**

A solution of 500 mg of digermenide **90** (0.53 mmol) in 10 mL C_6H_6 was added to a solution of 286 mg NHC^{iPr2Me2} (1.59 mmol, 3 eq) in 5 mL C_6H_6. The solvent is evaporated in high vacuum and filtered from 30 mL of pentane. Unfortunately no crystalline material could be obtained after storing at room temperature from a concentrated pentane solution.

^{1}H NMR (300.13 MHz, C_6D_6, 300 K, TMS): δ = 7.12 (s, 2H, *m*-Tip*H*), 7.10 (s, 2H, *m*-Tip*H*), 7.09 (s, 2H, *m*-Tip*H*), 4.73-4.64 (m, 4H, C*H*(CH$_3$)$_2$ of Tip), 4.20-4.16 (m, 10H,

C*H*(CH_3)$_2$ of NHC and Tip), 2.96-2.73 (m, 3H, C*H*(CH_3)$_2$ of Tip), 1.72 (s, 24H, C*H*$_3$ of NHC), 1.38 (br, 74H, CH(C*H*$_3$)$_2$ of Tip and NHC), 1.29 (d, 12H, CH(C*H*$_3$)$_2$ of Tip), 1.22 (d, 12H, CH(C*H*$_3$)$_2$ of Tip) ppm. **^{7}Li NMR** (116.59 MHz, C_6D_6, 300 K, Li^+ aq): δ = 2.90 ppm.

5.10.22. Reaction of Digermenide 90 with 2-6 eq of NHC^{Me4}

A solution of 40 mg **90** (0.042 mmol) in 0.5 mL C_6D_6 was added to 13 mg of NHC^{Me4} (0.084 mmol, 2eq). There was no change in color observed, even after heating for 12 hours at 60 °C.

^{1}H NMR (300.13 MHz, C_6D_6, 300 K, TMS): δ = 7.14 (s, 2H, *m*-Tip*H*), 7.13 (s, 2H, *m*-Tip*H*), 7.12 (s, 2H, *m*-Tip*H*), 4.78 (sept, 4H, C*H*(CH_3)$_2$ of Tip), 4.23 (br, 2H, C*H*(CH_3)$_2$ of Tip), 3.29 (s, 8H, dme), 3.22 (s, 12H, C*H*$_3$=C of NHC), 3.10 (s, 12H, dme), 2.98-2.73 (m, 3H, C*H*(CH_3)$_2$ of Tip), 1.46 (s, 12H, C*H*$_3$N of NHC), 1.38 (br, 10 H, CH(C*H*$_3$)$_2$ of Tip), 1.34, 1.30, 1.24, 1.19 (each d, 12H, CH(C*H*$_3$)$_2$ of Tip) ppm. **^{7}Li NMR** (116.59 MHz, C_6D_6, 300 K, Li^+ aq): δ = 2.89 ppm.

Two further equivalents of NHC^{Me4} were added to the same sample which results in a slight shift of the ^{1}H NMR signals.

^{1}H NMR (300.13 MHz, C_6D_6, 300 K, TMS): δ = 7.16 (s, 2H, *m*-Tip*H*, masked by C_6D_6), 7.12 (s, 2H, *m*-Tip*H*), 7.10 (s, 2H, *m*-Tip*H*), 4.98-4.83 (m, 4H, C*H*(CH_3)$_2$ of Tip), 4.40 (br, 2H, C*H*(CH_3)$_2$ of Tip), 3.33 (s, 8H, dme), 3.32 (br s, 24H, C*H*$_3$=C of NHC), 3.12 (s, 12H, dme), 2.98-2.75 (m, 3H, C*H*(CH_3)$_2$ of Tip), 1.60 (s, 24H, C*H*$_3$N of NHC), 1.38 (d, 18 H, CH(C*H*$_3$)$_2$ of Tip), 1.34, 1.24, 1.21 (each d, 12H, CH(C*H*$_3$)$_2$ of Tip) ppm. **^{7}Li NMR** (116.59 MHz, C_6D_6, 300 K, Li^+ aq): δ = 2.33 ppm.

Again 1 further equivalent of NHC^{Me4} (5 eq overall) was added to the same sample which results in a slight shift of the ^{1}H NMR signals.

^{1}H NMR (300.13 MHz, C_6D_6, 300 K, TMS): δ = 7.15 (s, 2H, *m*-Tip*H*), 7.10 (s, 2H, *m*-Tip*H*), 7.08 (s, 2H, *m*-Tip*H*), 5.02-4.86 (m, 4H, C*H*(CH_3)$_2$ of Tip), 4.44 (br, 2H, C*H*(CH_3)$_2$ of Tip), 3.34 (br s, 40H, C*H*$_3$=C of NHC), 3.32 (s, 8H, dme), 3.11 (s, 12H, dme), 2.98-2.81 (m, 3H, C*H*(CH_3)$_2$ of Tip), 1.61 (s, 40H, C*H*$_3$N of NHC), 1.46-1.18 (m, 70 H, CH(C*H*$_3$)$_2$ of Tip) ppm. **^{7}Li NMR** (116.59 MHz, C_6D_6, 300 K, Li^+ aq): δ = 1.90 ppm.

Heating of the sample to 60 °C with 5 eq of NHC^{Me4} resulted in unknown decomposition products.

6. References

[1] R. Höll, M. Kling, E. Schroll, *Ore Geol. Rev.* **2007**, *30*, 145–180.

[2] G. Roewer, in *Strateg. Rohstoffe-Risikovorsorge*, **2011**, pp. 233–259.

[3] R. R. Moskalyk, *Miner. Eng.* **2004**, *17*, 393–402.

[4] C. Winkler, *Berichte der Dtsch. Chem. Gesellschaft* **1886**, *19*, 210–211.

[5] C. Winkler, *J. Prakt. Chem.* **1886**, *34*, 177–229.

[6] C. Winkler, *J. Prakt. Chem.* **1887**, *36*, 177–209.

[7] M. Kaji, *Bull. Hist. Chem.* **2002**, *27*, 4–16.

[8] R. Z. Hu, H. W. Qi, M. F. Zhou, W. C. Su, X. W. Bi, J. T. Peng, H. Zhong, *Ore Geol. Rev.* **2009**, *36*, 221–234.

[9] J. Bardeen, W. H. Brattain, *Phys. Rev.* **1948**, *74*, 230–231.

[10] U. K. Thiele, *Int. J. Polym. Mater. Polym. Biomater.* **2001**, *50*, 387–394.

[11] D. E. Goldberg, D. H. Harris, M. F. Lappert, K. M. Thomas, *J. Chem. Soc., Chem. Commun.* **1976**, 261–262.

[12] P. J. Davidson, D. H. Harris, M. F. Lappert, *J. Chem. Soc., Dalt. Trans.* **1976**, 2268–2274.

[13] P. B. Hitchcock, M. F. Lappert, S. J. Miles, A. J. Thorne, *J. Chem. Soc., Chem. Commun.* **1984**, 480–482.

[14] R. West, M. J. Fink, J. Michl, *Science* **1981**, *214*, 1343–1344.

[15] Y. Wang, G. H. Robinson, *Chem. Commun.* **2009**, *32*, 5201–5213.

[16] R. C. Fischer, P. P. Power, *Chem. Rev.* **2010**, *110*, 3877–3923.

[17] V. Y. Lee, *CheM* **2012**, *2*, 35–46.

[18] M. Kira, *Proc. Jpn. Acad., Ser. B* **2012**, *88*, 167–191.

[19] M. Weidenbruch, *Eur. J. Inorg. Chem.* **1999**, 373–381.

[20] Holeman-Wiberg, *Lehrb. der Anorg. Chemie, 102. Auflage, Gruyter* **2007**.

[21] D. Bourissou, O. Guerret, F. P. Gabbaï, G. Bertrand, *Chem. Rev.* **2000**, *100*, 39–91.

[22] G. Trinquier, *J.Am.Chem.Soc.* **1990**, *112*, 2130–2137.

[23] Y. Mizuhata, T. Sasamori, N. Tokitoh, *Chem. Rev.* **2009**, *109*, 3479–3511.

[24] E. Rivard, *Chem. Soc. Rev.* **2016**, *45*, 989–1003.

[25] P. P. Power, *J. Chem. Soc. Dalt. Trans.* **1998**, 2939–2951.

[26] Y. Apeloig, R. Pauncz, M. Karni, R. West, W. Steiner, D. Chapman, *Organometallics* **2003**, *22*, 3250–3256.

[27] M. Kira, T. Iwamoto, T. Maruyama, C. Kabuto, H. Sakurai, *Organometallics* **1996**, *15*, 3767–3769.

[28] M. Karni, Y. Apeloig, *J. Am. Chem. Soc.* **1990**, *112*, 8589–8590.

[29] G. Trinquier, J. P. Malrieu, *J. Phys. Chem.* **1990**, *94*, 6184–6196.

[30] G. Trinquier, J. P. Malrieu, *J. Am. Chem. Soc.* **1987**, *109*, 5303–5315.

[31] E. A. Carter, W. Goddard, *J. Phys. Chem.* **1986**, *90*, 998–1001.

[32] L. G. M. Pettersson, P. E. M. Siegbahn, *Chem. Phys.* **1986**, *105*, 355–360.

[33] K. Balasubramanian, *Chem. Phys. Lett.* **1986**, *127*, 585–589.

[34] M. S. Gordon, *Chem. Phys. Lett.* **1985**, *114*, 348–352.

[35] P. P. Power, *Acc. Chem. Res.* **2011**, *44*, 627–637.

[36] M. Kira, *Organometallics* **2011**, *30*, 4459–4465.

[37] G. Trinquier, J. P. Malrieu, P. Riviere, *J. Am. Chem. Soc.* **1982**, *104*, 4529–4533.

[38] R. A. Phillips, R. J. Buenker, R. Beardsworth, P. R. Bunker, P. Jensen, W. P. Kraemer, *Chem. Phys. Lett.* **1985**, *118*, 60–63.

[39] W. Carrier, W. Zheng, Y. Osamura, R. I. Kaiser, *Chem. Phys.* **2006**, *330*, 275–286.

[40] X. Wang, L. Andrews, G. P. Kushto, P. O. Box, V. Uni, V. Charlottes, *J. Phys. Chem. A* **2002**, *106*, 5809–5816.

[41] T. Fjeldberg, A. Haaland, M. F. Lappert, B. E. R. Schilling, R. Seip, A. J. Thorne, *J. Chem. Soc., Chem. Commun.* **1982**, 1407–1408.

[42] M. Asay, C. Jones, M. Driess, *Chem. Rev.* **2011**, *111*, 354–396.

[43] M. Driess, H. Grützmacher, *Angew. Chem. Int. Ed. Engl.* **1996**, *35*, 828–856.

[44] P. Jutzi, A. Becker, H. G. Stammler, B. Neumann, *Organometallics* **1991**, *10*, 1647–1648.

[45] M. Denk, R. Lennon, R. Hayashi, R. West, A. V. Belyakov, H. P. Verne, A. Haaland, M. Wagner, N. Metzler, *J. Am. Chem. Soc.* **1994**, *116*, 2691–2692.

[46] A. J. Arduengo, R. L. Harlow, M. Kline, *J. Am. Chem. Soc.* **1991**, *113*, 361–363.

[47] D. J. Nelson, S. P. Nolan, *Chem. Soc. Rev.* **2013**, *42*, 6723–6753.

[48] M. N. Hopkinson, C. Richter, M. Schedler, F. Glorius, *Nature* **2014**, *510*, 485–496.

[49] W. A. Herrmann, M. Elison, C. Kocher, G. R. J. Artus, *Angew. Chem. Int. Ed. Engl.* **1995**, *34*, 2371–2374.

[50] S. Diez-Gonzalez, N. Marion, S. P. Nolan, *Chem. Rev.* **2009**, *109*, 3612–3676.

[51] D. Enders, O. Niemeier, A. Henseler, *Chem. Rev.* **2007**, *107*, 5606–5655.

[52] F. E. Hahn, M. C. Jahnke, *Angew. Chem. Int. Ed.* **2008**, *47*, 3122–3172.

[53] Y. Wang, G. H. Robinson, *Inorg. Chem.* **2014**, *53*, 11815–11832.

[54] G. Prabusankar, A. Sathyanarayana, P. Suresh, C. Naga Babu, K. Srinivas, B. P. R. Metla, *Coord. Chem. Rev.* **2014**, *269*, 96–133.

[55] A. L. Allred, E. G. Rochow, *J. Inorg. Nucl. Chem.* **1958**, *5*, 264–268.

[56] A. L. Allred, E. G. Rochow, *J. Inorg. Nucl. Chem.* **1958**, *5*, 269–288.

[57] S. P. Kolesnikov, V. I. Shiryaev, O. M. Nefedov, *Izv. Akad. Nauk SSSR, Ser. Khim.* **1966**, *3*, 584.

[58] T. Fjeldberg, A. Haaland, B. E. R. Schilling, A. J. Thorne, M. F. Lappert, *J. Chem. Soc., Dalt. Trans.* **1986**, 1551–1556.

[59] B. Gehrhus, P. B. Hitchcock, M. F. Lappert, *J. Chem. Soc. Dalt. Trans.* **2000**, 3094–3099.

[60] A. J. Arduengo, H. V. R. Dias, J. C. Calabrese, F. Davidson, *Inorg. Chem.* **1993**, *32*, 1541–1542.

[61] P. A. Rupar, V. N. Staroverov, P. J. Ragogna, K. M. Baines, *J. Am. Chem. Soc.* **2007**, *129*, 15138–15139.

[62] P. A. Rupar, M. C. Jennings, K. M. Baines, *Organometallics* **2008**, *27*, 5043–5051.

[63] P. A. Rupar, V. N. Staroverov, K. M. Baines, *Organometallics* **2010**, *29*, 4871–4881.

[64] A. J. Ruddy, P. A. Rupar, K. J. Bladek, C. J. Allan, J. C. Avery, K. M. Baines, *Organometallics* **2010**, *29*, 1362–1367.

[65] P. A. Rupar, M. C. Jennings, P. J. Ragogna, K. M. Baines, *Organometallics* **2007**, 4109–4111.

[66] P. A. Rupar, V. N. Staroverov, K. M. Baines, *Science* **2008**, *322*, 1360–1363.

[67] A. Rit, R. Tirfoin, S. Aldridge, *Angew. Chem. Int. Ed.* **2016**, *55*, 378–382.

[68] A. C. Filippou, O. Chernov, B. Blom, K. W. Stumpf, G. Schnakenburg, *Chem. Eur. J.* **2010**, *16*, 2866–2872.

[69] L. Pu, M. M. Olmstead, P. P. Power, *Organometallics* **1998**, *17*, 5602–5606.

[70] A. Sidiropoulos, C. Jones, A. Stasch, S. Klein, G. Frenking, *Angew. Chem. Int. Ed.* **2009**, *48*, 9701–9704.

[71] S. P. Green, C. Jones, A. Stasch, *Science* **2007**, *318*, 1754–1757.

[72] S. J. Bonyhady, S. P. Green, C. Jones, S. Nembenna, A. Stasch, *Angew. Chem. Int. Ed.* **2009**, *48*, 2973–2977.

[73] S. J. Bonyhady, C. Jones, S. Nembenna, A. Stasch, A. J. Edwards, G. J. McIntyre, *Chem. Eur. J.* **2010**, *16*, 938–955.

[74] G. Frenking, *Angew. Chem. Int. Ed.* **2014**, *53*, 6040–6046.

[75] D. Himmel, I. Krossing, A. Schnepf, *Angew. Chem. Int. Ed.* **2014**, *53*, 370–374.

[76] A. Jana, V. Huch, H. S. Rzepa, D. Scheschkewitz, *Organometallics* **2015**, *34*, 2130–2133.

[77] M. El Ezzi, T. G. Kocsor, F. D'Accriscio, D. Madec, S. Mallet-Ladeira, A. Castel, *Organometallics* **2015**, *34*, 571–576.

[78] Y. Xiong, S. Yao, G. Tan, S. Inoue, M. Driess, *J. Am. Chem. Soc.* **2013**, *135*, 5004–5007.

[79] N. Kuhn, T. Kratz, D. Bläser, R. Boese, *Chem. Ber.* **1995**, *128*, 245–250.

[80] R. S. Ghadwal, H. W. Roesky, S. Merkel, J. Henn, D. Stalke, *Angew. Chem. Int. Ed.* **2009**, *48*, 5683–5686.

[81] A. C. Filippou, O. Chernov, G. Schnakenburg, *Angew. Chem. Int. Ed.* **2009**, *48*, 5687–5690.

[82] Y. Wang, Y. Xie, P. Wei, B. King, H. Schaefer, P. V. R. Schleyer, G. H. Robinson, *Science* **2008**, *321*, 1069–1071.

[83] Y. Wang, M. Chen, Y. Xie, P. Wei, H. F. Schaefer III, P. V. R. Schleyer, G. H. Robinson, *Nat. Chem.* **2015**, *7*, 509–513.

[84] M. I. Arz, M. Straßmann, A. Meyer, G. Schnakenburg, O. Schiemann, A. C. Filippou, *Chem. Eur. J.* **2015**, *21*, 12509–12516.

[85] M. I. Arz, D. Geiß, M. Straßmann, G. Schnakenburg, A. C. Filippou, *Chem. Sci.* **2015**, *6*, 6515–6524.

[86] M. I. Arz, M. Straßmann, D. Geiß, G. Schnakenburg, A. C. Filippou, *J. Am. Chem. Soc.* **2016**, *138*, 4589–4600.

[87] Y. Xiong, S. Yao, S. Inoue, J. D. Epping, M. Driess, *Angew. Chem. Int. Ed.* **2013**, *52*, 7147–7150.

[88] A. Burchert, S. Yao, R. Müller, C. Schattenberg, Y. Xiong, M. Kaupp, M. Driess, *Angew. Chem. Int. Ed.* **2017**, *56*, 1894–1897.

[89] J. Satgé, *Adv. Organomet. Chem.* **1982**, *21*, 241–287.

[90] S. Masamune, Y. Hanzawa, D. J. Williams, *J. Am. Chem. Soc.* **1982**, *104*, 6136–6137.

[91] J. T. Snow, S. Murakami, S. Masamune, D. J. Williams, *Tetrahedron Lett.* **1984**, *25*, 4191–4194.

[92] J. Park, S. A. Batcheller, S. Masamune, *J. Organomet. Chem.* **1989**, *367*, 39–45.

[93] W. Ando, H. Itoh, T. Tsumuraya, *Organometallics* **1989**, *8*, 2759–2766.

[94] H. Schäfer, W. Saak, M. Weidenbruch, *Organometallics* **1999**, *18*, 3159–3163.

[95] T. Tsumuraya, S. Sato, W. Ando, *Organometallics* **1988**, *7*, 2015–2019.

[96] W. Ando, T. Tsumuraya, *J. Chem. Soc., Chem.Commun.* **1989**, 770–772.

[97] K. L. Hurni, P. A. Rupar, N. C. Payne, K. M. Baines, *Organometallics* **2007**, *26*, 5569–5575.

[98] C. E. Dixon, H. W. Liu, C. M. VanderKant, K. M. Baines, *Organometallics* **1996**, *15*, 5701–5705.

[99] V. Y. Lee, K. McNeice, Y. Ito, A. Sekiguchi, *Chem. Commun.* **2011**, *47*, 3272–3274.

[100] K. K. Milnes, L. C. Pavelka, K. M. Baines, *Chem. Soc. Rev.* **2015**, *45*, 1019–1035.

[101] S. Masamune, Y. Eriyama, T. Kawase, *Angew. Chem. Int. Ed. Engl.* **1987**, *26*, 584–585.

[102] S. Masamune, Y. Hanzawa, S. Murakami, T. Bally, J. F. Blount, *J. Am. Chem. Soc.* **1982**, *104*, 1150–1153.

[103] H. Watanabe, K. Takeuchi, N. Fukawa, M. Kato, M. Goto, Y. Nagai, *Chem. Lett.* **1987**, *16*, 1341–1344.

[104] M. Kira, T. Maruyama, C. Kabuto, K. Ebata, H. Sakurai, *Angew. Chem. Int. Ed. Engl.* **1994**, *33*, 1489–1491.

[105] A. Sekiguchi, S. Inoue, M. Ichinohe, Y. Arai, *J. Am. Chem. Soc.* **2004**, *126*, 9626–9629.

[106] K. M. Baines, J. A. Cooke, *Organometallics* **1992**, *11*, 3487–3488.

[107] M. Chen, Z. Yang, H. Wu, X. Pan, X. Xie, C. Wu, *Heteroat. Chem.* **2008**, *19*, 649–653.

[108] M. Ichinohe, Y. Arai, A. Sekiguchi, N. Takagi, S. Nagase, *Organometallics* **2001**, *20*, 4141–4143.

[109] V. Y. Lee, A. Sekiguchi, *Organometallics* **2004**, *23*, 2822–2834.

[110] T. Iwamoto, J. Okita, N. Yoshida, M. Kira, *Silicon* **2011**, *2*, 209–216.

[111] L. Hintermann, A. Labonne, *Synthesis* **2007**, 1121–1150.

[112] G. Fang, X. Bi, *Chem. Soc. Rev.* **2015**, *44*, 8124–8173.

[113] R. Dorel, A. M. Echavarren, *Chem. Rev.* **2015**, *115*, 9028–9072.

[114] L. Pu, B. Twamley, P. P. Power, *J. Am. Chem. Soc.* **2000**, *122*, 3524–3525.

[115] M. Stender, A. D. Phillips, R. J. Wright, P. P. Power, *Angew. Chem. Int. Ed.* **2002**, *41*, 1785–1787.

[116] P. P. Power, *Appl. Organomet. Chem.* **2005**, *19*, 488–493.

[117] L. Pu, A. D. Phillips, A. F. Richards, M. Stender, R. S. Simons, M. M. Olmstead, P. P. Power, *J. Am. Chem. Soc.* **2003**, *125*, 11626–11636.

[118] Y. Sugiyama, T. Sasamori, Y. Hosoi, Y. Furukawa, N. Takagi, S. Nagase, N. Tokitoh, *J. Am. Chem. Soc.* **2006**, *128*, 1023–1031.

[119] J. Li, C. Schenk, C. Goedecke, G. Frenking, C. Jones, *J. Am. Chem. Soc.* **2011**, *133*, 18622–18625.

[120] T. J. Hadlington, M. Hermann, J. Li, G. Frenking, C. Jones, *Angew. Chem. Int. Ed.* **2013**, *52*, 10199–10203.

[121] A. Sekiguchi, R. Kinjo, M. Ichinohe, *Science* **2004**, *305*, 1755–1757.

[122] A. Sekiguchi, *Pure Appl. Chem.* **2008**, *80*, 447–457.

[123] T. Yamaguchi, A. Sekiguchi, M. Driess, *J. Am. Chem. Soc.* **2010**, *132*, 14061–14063.

[124] T. Sasamori, K. Hironaka, Y. Sugiyama, N. Takagi, S. Nagase, Y. Hosoi, Y. Furukawa, N. Tokitoh, *J. Am. Chem. Soc.* **2008**, *130*, 13856–13857.

[125] Y. Murata, M. Ichinohe, A. Sekiguchi, *J. Am. Chem. Soc.* **2010**, *132*, 16768–16770.

[126] C. Präsang, D. Scheschkewitz, *Chem. Soc. Rev.* **2016**, *45*, 900–921.

[127] L. Li, T. Matsuo, D. Hashizume, H. Fueno, K. Tanaka, K. Tamao, *J. Am. Chem. Soc.* **2015**, *137*, 15026–15035.

[128] H. Schäfer, W. Saak, M. Weidenbruch, *Angew. Chem. Int. Ed.* **2000**, *39*, 3703–3705.

[129] G. Ramaker, A. Schäfer, W. Saak, M. Weidenbruch, *Organometallics* **2003**, *22*, 1302–1304.

[130] G. Ramaker, W. Saak, D. Haase, M. Weidenbruch, *Organometallics* **2003**, *22*, 5212–5216.

[131] M. Weidenbruch, S. Willms, W. Saak, G. Henkel, *Angew. Chem. Int. Ed. Engl.* **1997**, *36*, 2503–2504.

[132] D. Scheschkewitz, *Angew. Chem. Int. Ed.* **2004**, *43*, 2965–2967.

[133] M. Ichinohe, K. Sanuki, S. Inoue, A. Sekiguchi, *Organometallics* **2004**, *230*, 3088–3090.

[134] T. Iwamoto, M. Kobayashi, K. Uchiyama, S. Sasaki, S. Nagendran, H. Isobe, M. Kira, *J. Am. Chem. Soc.* **2009**, *131*, 3156–3157.

[135] T. Kosai, S. Ishida, T. Iwamoto, *J. Am. Chem. Soc.* **2016**, *139*, 99–102.

[136] D. Scheschkewitz, *Chem. Eur. J.* **2009**, *15*, 2476–2485.

[137] D. Scheschkewitz, *Chem. Lett.* **2011**, *40*, 2–11.

[138] D. Sülze, H. Schwarz, *Chem. Phys. Lett.* **1989**, *156*, 397–400.

[139] R. P. Durin, V. T. Amorebieta, A. J. Colussi, *J. Am. Chem. Soc.* **1987**, *109*, 3154–3155.

[140] K. Zhurnal, S. Pharmacopoeia, *Chem. Phys. Lett.* **1981**, *79*, 412–415.

[141] M. I. Bruce, *Chem. Rev.* **1991**, *91*, 197–257.

[142] A. M. Lozano-Vila, S. Monsaert, A. Bajek, F. Verpoort, *Chem. Rev.* **2010**, *110*, 4865–4909.

[143] M. I. Bruce, *Chem. Rev.* **1998**, *98*, 2797–2858.

[144] A. Jana, V. Huch, D. Scheschkewitz, *Angew. Chem. Int. Ed.* **2013**, *52*, 12179–12182.

[145] A. Jana, M. Majumdar, V. Huch, M. Zimmer, D. Scheschkewitz, *Dalton Trans.* **2014**, *43*, 5175–5181.

[146] A. Jana, I. Omlor, V. Huch, H. S. Rzepa, D. Scheschkewitz, *Angew. Chem. Int. Ed.* **2014**, *53*, 9953–9956.

[147] A. Jana, V. Huch, H. S. Rzepa, D. Scheschkewitz, *Angew. Chem. Int. Ed.* **2015**, *54*, 289–292.

[148] D. Geiß, M. I. Arz, M. Straßmann, G. Schnakenburg, A. C. Filippou, *Angew. Chem. Int. Ed.* **2015**, *54*, 2739–2744.

[149] P. Ghana, M. I. Arz, U. Das, G. Schnakenburg, A. C. Filippou, *Angew. Chem. Int. Ed.* **2015**, *54*, 9980–9985.

[150] T. Yang, B. B. Dangi, R. I. Kaiser, K.-H. Chao, B.-J. Sun, A. H. H. Chang, T. L. Nguyen, J. F. Stanton, *Angew. Chem. Int. Ed.* **2017**, *56*, 1264–1268.

[151] A. Rit, J. Campos, H. Niu, S. Aldridge, *Nat. Chem.* **2016**, *8*, 1022–1026.

[152] D. Scheschkewitz, *Nat. Chem.* **2016**, *8*, 993–995.

[153] Y. Segawa, M. Yamashita, K. Nozaki, *Science* **2006**, *314*, 113–115.

[154] C. Cui, M. M. Olmstead, J. C. Fettinger, G. H. Spikes, P. P. Power, *J. Am. Chem. Soc.* **2005**, *127*, 17530–17541.

[155] M. J. Cowley, V. Huch, H. S. Rzepa, D. Scheschkewitz, *Nat. Chem.* **2013**, *5*, 876–879.

[156] A. Jana, V. Huch, M. Repisky, R. J. F. Berger, D. Scheschkewitz, *Angew. Chem. Int. Ed.* **2014**, *53*, 3514–3518.

[157] V. Y. Lee, H. Yasuda, A. Sekiguchi, *J. Am. Chem. Soc.* **2007**, *129*, 2436–2437.

[158] V. Y. Lee, H. Yasuda, M. Ichinohe, A. Sekiguchi, *Angew. Chem. Int. Ed.* **2005**, *44*, 6378–6381.

[159] V. Y. Lee, M. Ichinohe, A. Sekiguchi, *J. Am. Chem. Soc.* **2000**, *122*, 9034–9035.

[160] K. Abersfelder, D. Scheschkewitz, *J. Am. Chem. Soc.* **2008**, *130*, 4114–4121.

[161] M. Kosa, M. Karni, Y. Apeloig, *J. Am. Chem. Soc.* **2013**, *135*, 9032–9040.

[162] A. Sekiguchi, N. Fukaya, M. Ichinohe, *J. Am. Chem. Soc.* **1999**, *121*, 11587–11588.

[163] J. Hlina, J. Baumgartner, C. Marschner, L. Albers, T. Müller, *Organometallics* **2013**, *32*, 3404–3410.

[164] K. Abersfelder, A. J. P. White, R. J. F. Berger, H. S. Rzepa, D. Scheschkewitz, *Angew. Chem. Int. Ed.* **2011**, *50*, 7936–7939.

[165] Y. Kabe, M. Kuroda, Y. Honda, O. Yamashita, T. Kawase, S. Masamune, *Angew. Chem. Int. Ed. Engl.* **1988**, *27*, 1725–1727.

[166] T. Iwamoto, K. Uchiyama, C. Kabuto, K. Mitsuo, *Chem. Lett.* **2007**, *36*, 368–369.

[167] K. Abersfelder, A. Russell, H. S. Rzepa, A. J. P. White, P. R. Haycock, D. Scheschkewitz, *J. Am. Chem. Soc.* **2012**, *134*, 16008–16016.

[168] C. B. Yildiz, *Calculations*, Aksaray University, Turkey, **2016**.

[169] V. Y. Lee, M. Ichinohe, A. Sekiguchi, *J. Organomet. Chem.* **2001**, *636*, 41–48.

[170] M.-F. Grenier-Loustalot, *High Perform. Polym.* **1994**, *6*, 347–383.

[171] A. V Protchenko, M. P. Blake, A. D. Schwarz, C. Jones, P. Mountford, S. Aldridge, *Organometallics* **2015**, *34*, 2126–2129.

[172] K. K. Milnes, L. C. Pavelka, K. M. Baines, *Chem. Soc. Rev.* **2016**, *45*, 1019–1035.

[173] A. C. Filippou, O. Chernov, K. W. Stumpf, G. Schnakenburg, *Angew. Chem. Int. Ed.* **2010**, *49*, 3296–3300.

[174] H. Cui, J. Zhang, C. Cui, *Organometallics* **2013**, *32*, 1–4.

[175] M. Weidenbruch, J. Hamann, S. Pohl, W. Saak, *Chem. Ber.* **1992**, *125*, 1043–1046.

[176] M. Weidenbruch, J. Hamann, K. Peters, H. G. Von Schnering, H. Marsmann, *J. Organomet. Chem.* **1992**, *441*, 185–195.

[177] M. Weidenbruch, E. Kroke, K. Peters, G. Von Schnering, *J. Organomet. Chem.* **1993**, *461*, 35–38.

[178] M. Majumdar, V. Huch, I. Bejan, A. Meltzer, D. Scheschkewitz, *Angew. Chem. Int. Ed.* **2013**, *52*, 3516–20.

[179] T. Iwamoto, N. Ohnishi, N. Akasaka, K. Ohno, S. Ishida, *J. Am. Chem. Soc.* **2013**, *135*, 10606–10609.

[180] Y. Ohmori, M. Ichinohe, A. Sekiguchi, M. J. Cowley, V. Huch, D. Scheschkewitz, *Organometallics* **2013**, *32*, 1591–1594.

[181] F. Millich, *Chem. Rev.* **1972**, *72*, 101–113.

[182] K. L. Hurni, K. M. Baines, *Chem. Commun.* **2011**, *47*, 8382–8384.

[183] M. Driess, S. Yao, C. Van Wüllen, *Chem. Commun.* **2008**, 5393–5395.

[184] M. Walewska, B. Judith, C. Marschner, *Chem. Commun.* **2015**, *51*, 276–278.

[185] M. Majumdar, I. Bejan, V. Huch, A. J. P. White, G. R. Whittell, A. Schäfer, I. Manners, D. Scheschkewitz, *Chem. Eur. J.* **2014**, *20*, 9225–9229.

[186] R. S. Ghadwal, H. W. Roesky, M. Granitzka, D. Stalke, *J. Am. Chem. Soc.* **2010**, *132*, 10018–10020.

[187] H. Schneider, D. Schmidt, U. Radius, *Chem. Eur. J.* **2014**, *21*, 2793–2797.

[188] D. Mendoza-Espinosa, B. Donnadieu, G. Bertrand, *J. Am. Chem. Soc.* **2010**, *132*, 7264–7265.

[189] D. M. Khramov, V. M. Lynch, C. W. Bielawski, *Organometallics* **2007**, *26*, 6042–6049.

[190] Y. Wang, Y. Xie, M. Y. Abraham, P. Wei, H. F. Schaefer III, P. V. R. Schleyer, G. H. Robinson, *J. Am. Chem. Soc.* **2010**, *132*, 14370–14372.

[191] R. S. Ghadwal, S. O. Reichmann, E. Carl, R. Herbst-Irmer, *Dalt. Trans.* **2014**, *43*, 13704–13710.

[192] T. Agou, N. Hayakawa, T. Sasamori, T. Matsuo, D. Hashizume, N. Tokitoh, *Chem. Eur. J.* **2014**, *20*, 9246–9249.

[193] H. Tanaka, M. Ichinohe, A. Sekiguchi, *J. Am. Chem. Soc.* **2012**, *134*, 5540–5543.

[194] S. U. Ahmad, T. Szilvási, S. Inoue, *Chem. Commun.* **2014**, *50*, 12619–12622.

[195] H. J. Campbell-Ferguson, E. A. V Ebsworth, A. G. MacDiarmid, T. Yoshioka, *J. Phys. Chem.* **1967**, *71*, 723–726.

[196] A. J. Arduengo, R. Krafczyk, R. Schmutzler, H. a. Craig, J. R. Goerlich, W. J. Marshall, M. Unverzagt, *Tetrahedron* **1999**, *55*, 14523–14534.

[197] S. A. Powell, J. M. Tenenbaum, K. A. Woerpel, *J. Am. Chem. Soc.* **2002**, *124*, 12648–12649.

[198] T. Ramnial, S. A. Taylor, M. L. Bender, B. Gorodetsky, P. T. K. Lee, D. A. Dickie, B. M. McCollum, C. C. Pye, C. J. Walsby, J. A. C. Clyburne, *J. Org. Chem.* **2008**, *73*, 801–812.

[199] C. N. Smit, F. Bickelhaupt, *Organometallics* **1987**, *6*, 1156–1163.

[200] D. Bläser, R. Boese, M. Göhner, F. Herrmann, N. Kuhn, M. Ströbele, *Zeitschrift für Naturforschung, B Chem. Sci.* **2014**, *69*, 71–76.

[201] Y. Li, Y.-C. Chan, Y. Li, I. Purushothaman, S. De, P. Parameswaran, C.-W. So, *Inorg. Chem.* **2016**, *55*, 9091–9098.

[202] N. Kuhn, G. Henkel, T. Kratz, J. Kreutzberg, R. Boeseb, A. H. Maulitzb, *Chem. Ber.* **1993**, *126*, 2041–2045.

[203] D. M. Roddick, R. H. Heyn, T. D. Tilley, *Organometallics* **1989**, *8*, 324–330.

[204] M. Walewska, J. Baumgartner, C. Marschner, *Chem. Commun.* **2015**, *51*, 276–278.

[205] K. M. Baines, R. J. Groh, B. Joseph, U. R. Parshotam, *Organometallics* **1992**, *11*, 2176–2180.

[206] J. B. Lambert, C. L. Stern, Y. Zhao, W. C. Tse, C. E. Shawl, K. T. Lentz, L. Kania, *J. Organomet. Chem.* **1998**, *568*, 21–31.

[207] J. B. Lambert, Y. Zhao, *Angew. Chem. Int. Ed. Engl.* **1997**, *36*, 400–401.

[208] H. Schäfer, W. Saak, M. Weidenbruch, *Organometallics* **2004**, *18*, 3159–3162.

[209] L. Pu, A. D. Phillips, A. F. Richards, M. Stender, R. S. Simons, M. M. Olmstead, P. P. Power, *J. Am. Chem. Soc.* **2003**, *125*, 11626–11636.

[210] R. West, H. Sohn, D. R. Powell, T. Müller, Y. Apeloig, *Angew. Chem. Int. Ed. Engl.* **1996**, *35*, 1002–1004.

[211] M. Veith, O. Schütt, V. Huch, *Angew. Chem., Int. Ed.* **2000**, *39*, 601–604.

[212] I. Bejan, D. Scheschkewitz, *Angew. Chem. Int. Ed.* **2007**, *46*, 5783–5786.

[213] K. Abersfelder, A. J. P. White, H. S. Rzepa, D. Scheschkewitz, *Science* **2010**, *327*, 564–566.

[214] M. Nanjo, K. Matsudo, M. Kurihara, S. Nakamura, Y. Sakaguchi, H. Hayashi, K. Mochida, *Organometallics* **2006**, *25*, 832–838.

[215] P. Willmes, M. J. Cowley, M. Hartmann, M. Zimmer, V. Huch, D. Scheschkewitz, *Angew. Chem. Int. Ed.* **2014**, *53*, 2216–2220.

[216] M. Hartmann, A. Haji-Abdi, K. Abersfelder, P. R. Haycock, A. J. P. White, D. Scheschkewitz, *Dalton Trans.* **2010**, *39*, 9288–9295.

[217] P. Willmes, *Master Thesis* **2013**.

[218] B. Li, M. Su, *J. Phys. Chem. A* **2012**, *116*, 9412–9420.

[219] V. Y. Lee, M. Kawai, A. Sekiguchi, H. Ranaivonjatovo, J. Escudi, *Organometallics* **2009**, *28*, 4262–4265.

[220] B. D. Ellis, C. A. Dyker, A. Decken, C. L. B. Macdonald, *Chem. Commun.* **2005**, 1965–1967.

[221] P. Willmes, *PhD Thesis* **2016**.

[222] M. S. Hill, G. Kociok-Köhn, D. J. MacDougall, *Inorg. Chem.* **2011**, *50*, 5234–5241.

[223] S. Bellemin-Laponnaz, S. Dagorne, *Chem. Rev.* **2014**, *114*, 8747–8774.

[224] Y. Kaiser, *Master Thesis* **2016**.

[225] V. Lavallo, Y. Canac, C. Präsang, B. Donnadieu, G. Bertrand, *Angew. Chem. Int. Ed.* **2005**, *44*, 5705–5709.

[226] M. J. Frisch, G. W. Trucks, H. B. Schlegel, G. E. Scuseria, M. A. Robb, J. R. Cheeseman, G. Scalmani, V. Barone, B. Mennucci, G. A. Petersson, et al., *Gaussian, Inc., Wallingford, CT* **2009**, Revision A.02.

[227] K. Fukui, *Acc. Chem. Res.* **1981**, *14*, 363–368.

[228] C. Gonzalez, H. B. Schlegel, *J Chem Phys* **1991**, *95*, 5853–5860.

[229] R. Dennington, T. Keith, J. Millam, *Semichem Inc.* **2009**, Shawnee Mission, KS, GaussView, Version 5.

[230] N. Kuhn, T. Kratz, *Synthesis* **1993**, 561–562.

[231] J. Li, N. Wang, C. Li, X. Jia, *Chem. Eur. J.* **2012**, *18*, 9645–9650.

[232] Y. Yamamotoa, H. Suzuki, N. Tajima, K. Tatsumi, *Chem. Eur. J.* **2002**, *8*, 372–379.

[233] S. A. Swanson, R. Mcclain, K. S. Lovejoy, N. B. Alamdari, J. S. Hamilton, J. C. Scott, *Langmuir* **2005**, *21*, 5034–5039.

[234] A. Hinz, A. Schulz, A. Villinger, *J. Am. Chem. Soc.* **2015**, *137*, 9953–9962.

7. Appendix

7.1. Overview of Numbered Compounds

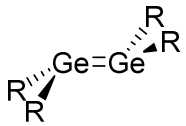

1: R = $CH(SiMe_3)_2$

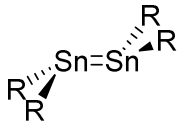

2: R = $CH(SiMe_3)_2$

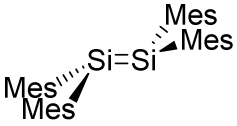

3

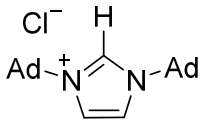

4

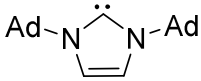

5

6

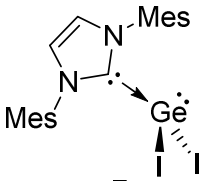

7

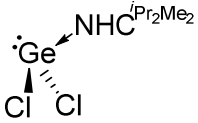

8

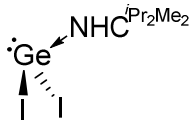

9

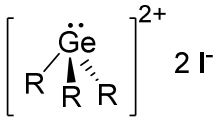

10: R = $NHC^{iPr_2Me_2}$

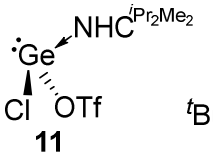

11

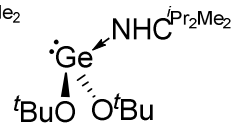

12

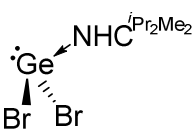

13

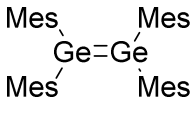

14

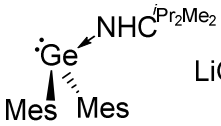

15

$LiGeMes_2Me$

16

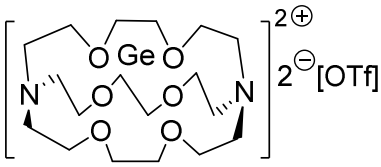

17

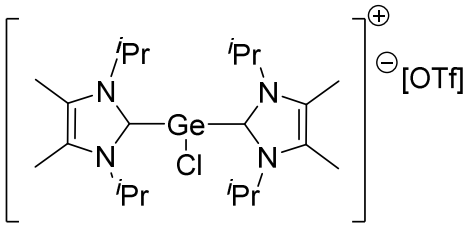

18

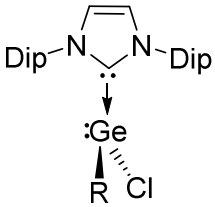

19: R = $CH(SiMe_3)_2$

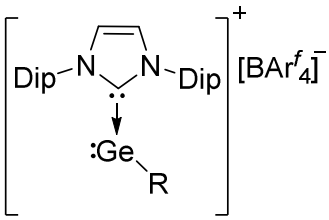

20: R = $CH(SiMe_3)_2$

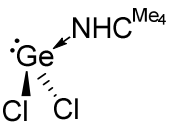

21

22

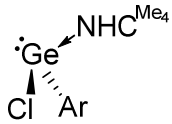

23a: Ar = 2,6-Mes_2-C_6H_3
23b: Ar = 2,6-Tip_2-C_6H_3

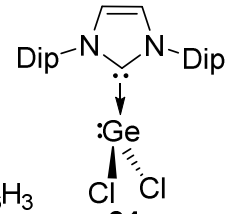

24

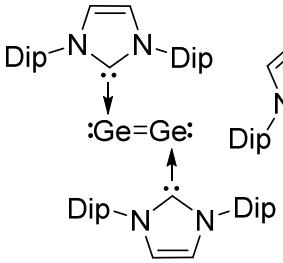

25

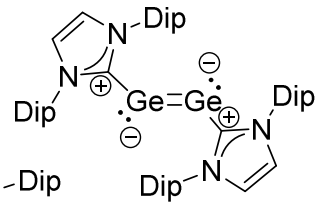

25'

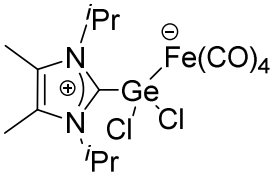

26

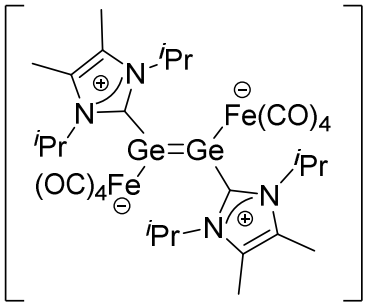

[27]

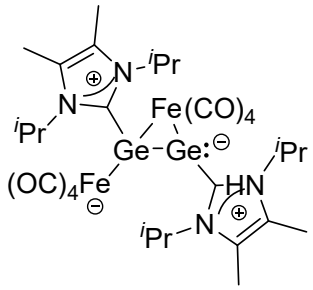

28

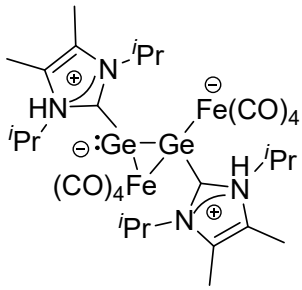

28'

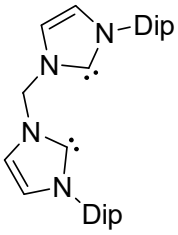

29

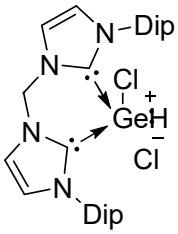

30

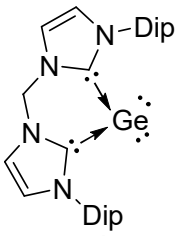

31

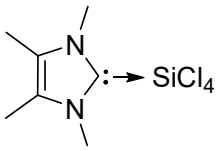

32

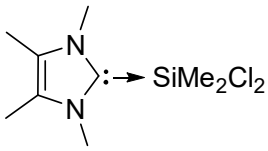

33

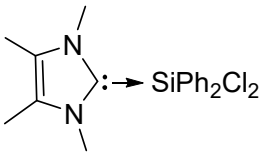

34

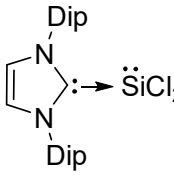

35

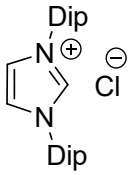

36

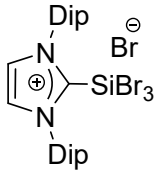

37

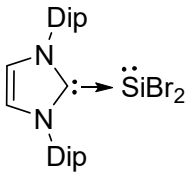

38

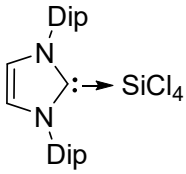

39

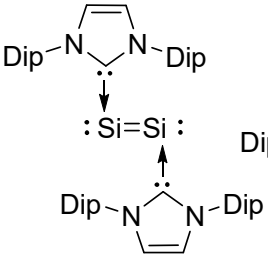

40

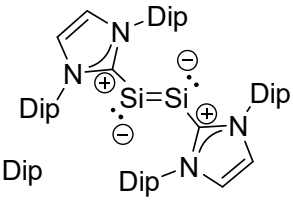

40'

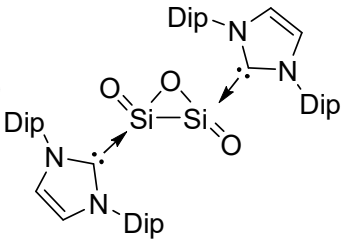

41

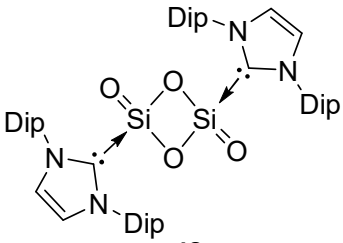

42

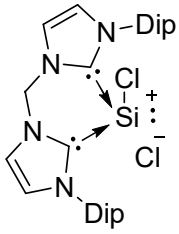

43

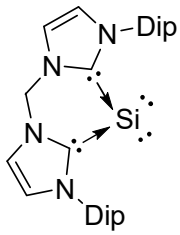

44

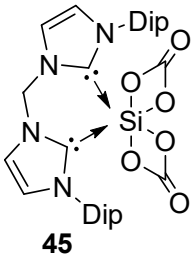

45

$Ge[N(SiMe_3)_2]_2$

46

47: R = $CH(SiMe_3)_2$

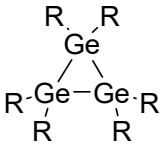

48

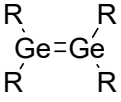

49

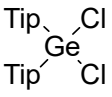

50

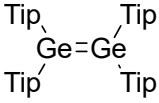

51

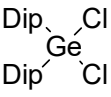

52

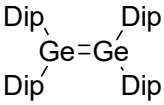

53

$Mes_2Ge(SiMe_3)_2$

54

R = 2,6-diethylphenyl

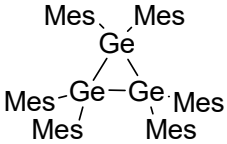

55

56

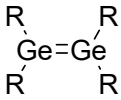

57

$Mes_2Si(SiMe_3)_2$ **58**

Ar_2SiCl_2 **59**

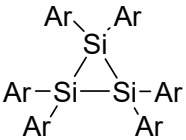

60

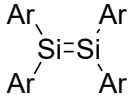

61

Ar = 2,6-Me_2-C_6H_3

R_2SiI_2 **62**

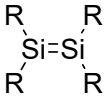

63

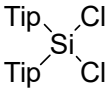

64

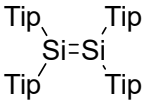

65

R = $(Me_3Si)_2CH$

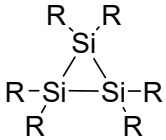

66: R = $SiMe_2{}^tBu$

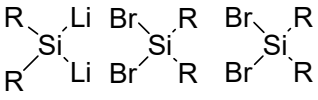

67, 68, 69: R = $SiMe^tBu_2$

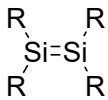

70a: R = $SiMe_2{}^tBu$, **70b:** R = $SiMe^tBu_2$

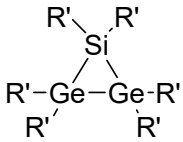

71: R' = Mes

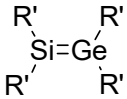

72: R' = Mes

73: R = $Si{}^tBu_3$

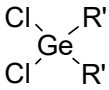

74: R' = Mes

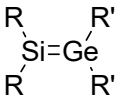

75: R = $Si{}^tBu_3$, R' = Mes

76,

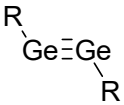

77,

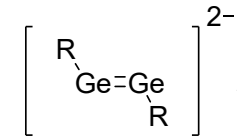

78: R = 2,6-Dip_2-C_6H_3

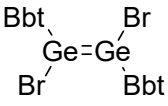

79

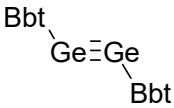

80

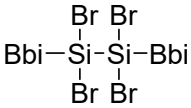

81

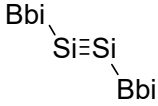

82

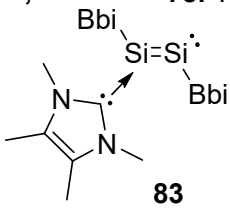

83

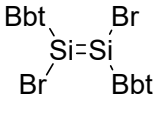

84

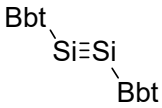

85

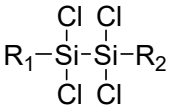

86

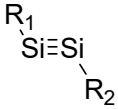

87

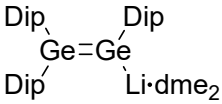

88

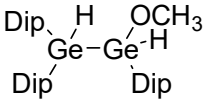

89

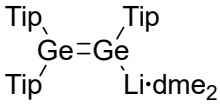

90

R_1 = $SiNpDsi_2$, R_2 = $Si{}^iPrDsi_2$

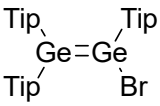

91

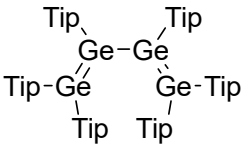

92

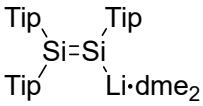

93

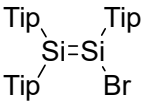

94

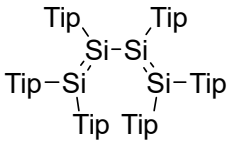

95

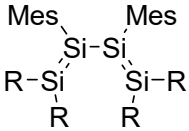

96: R = $^tBu_2MeSi$ **97:** R = $^tBu_2MeSi$

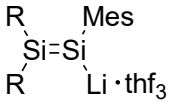

98

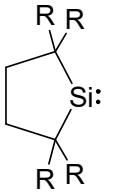

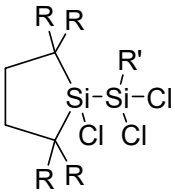

99a,b

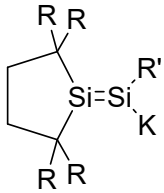

100a,b

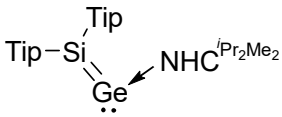

101

R = $SiMe_3$, **a:** R' = tBu, **b:** R' = Mes

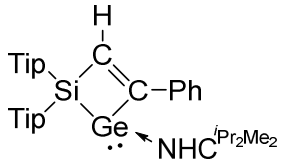

102

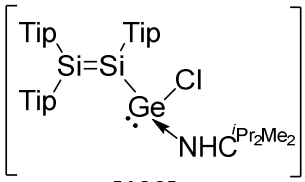

[103]

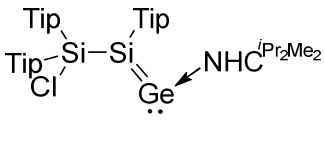

104

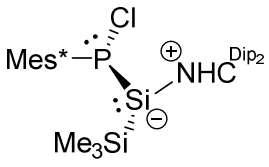

105

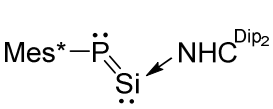

106

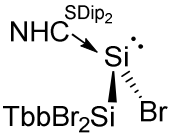

107

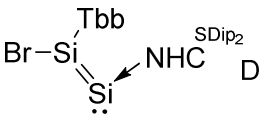

108

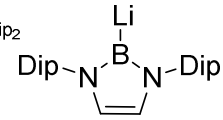

109

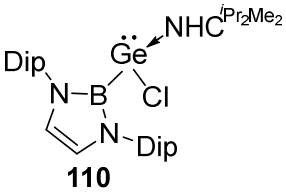

110

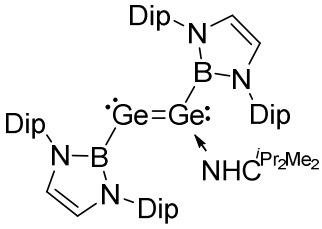

111

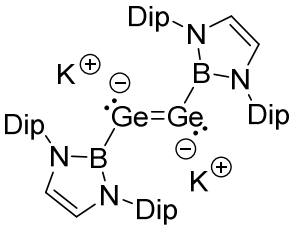

112

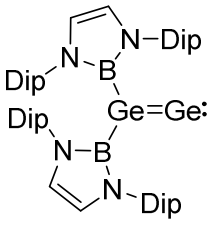

113

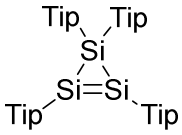

114

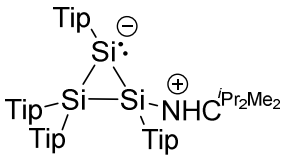

115

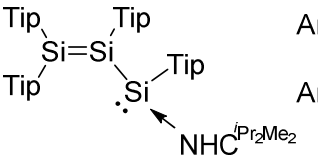

116

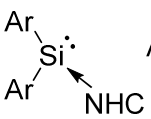

117

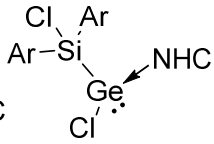

118

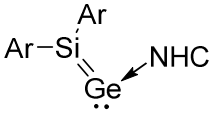

119

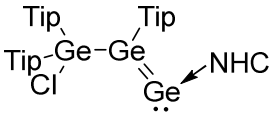

120

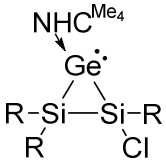

121

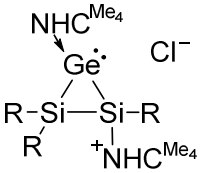

122

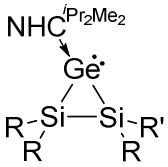

123a: R' = Mes
123b: R' = Et
123c: R' = Ph
123d: R' = *i*Pr
123e: R' = *s*Bu

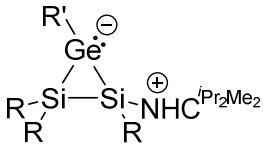

124a: R' = Mes
124b: R' = *i*Pr
124c: R' = *s*Bu

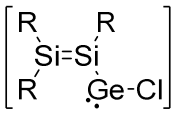

[125]

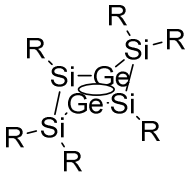

126

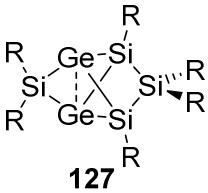

127

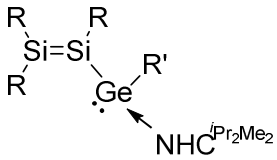

128a: R' = Me
[128b]: R' = Et
128c: R' = Ph
128d: R' = Mes

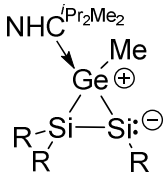

129

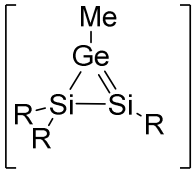

[130]

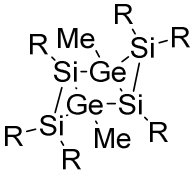

131

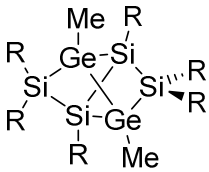

132

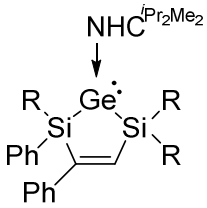

133

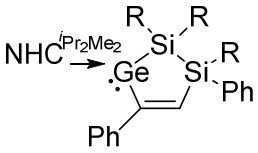

134

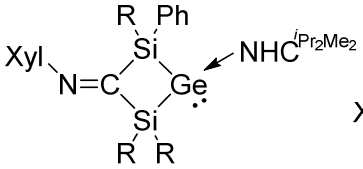

138

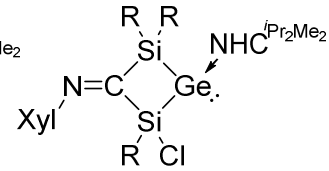

139

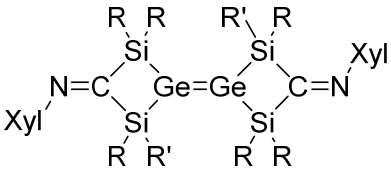

141a: R' = Cl **141b:** R' = Ph

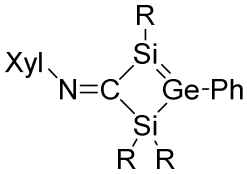

142

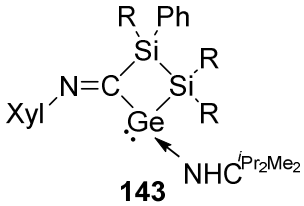

143

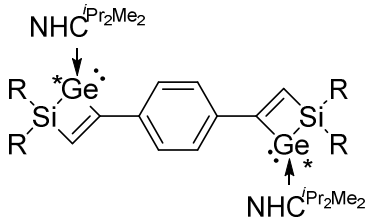

144

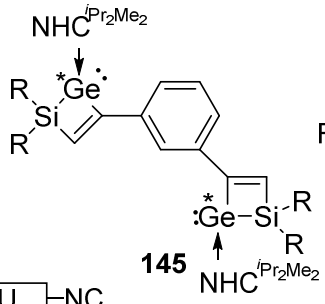

145

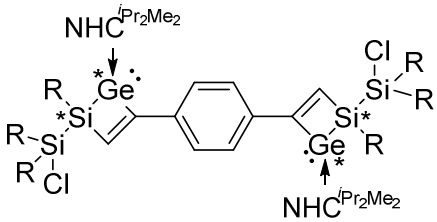

146

147 = LU =

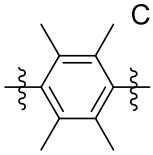

148 = LU =

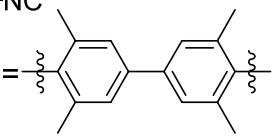

149 = LU =

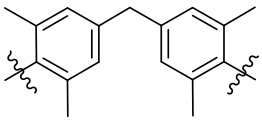

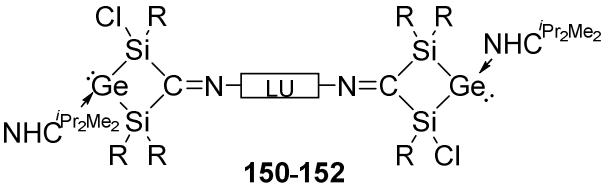

150-152

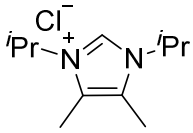

153

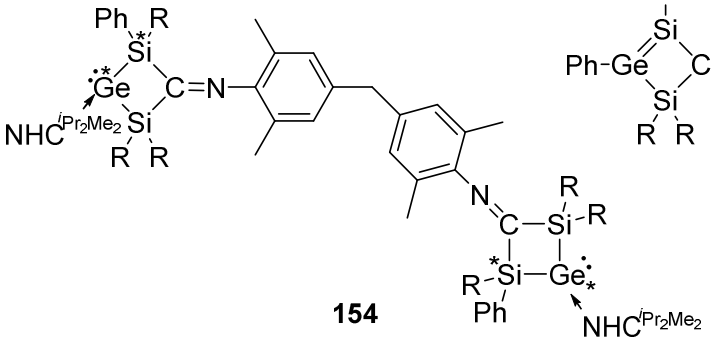

154

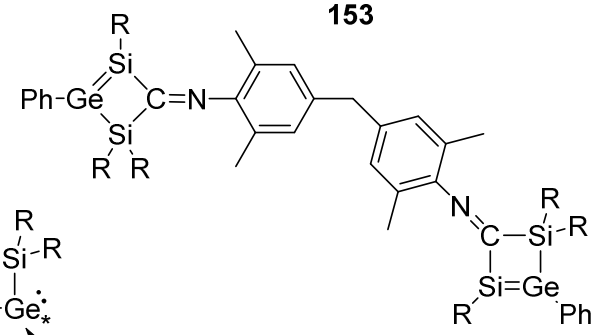

155

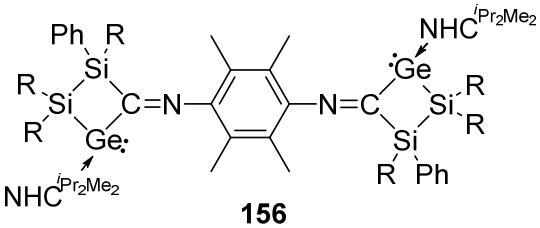

156

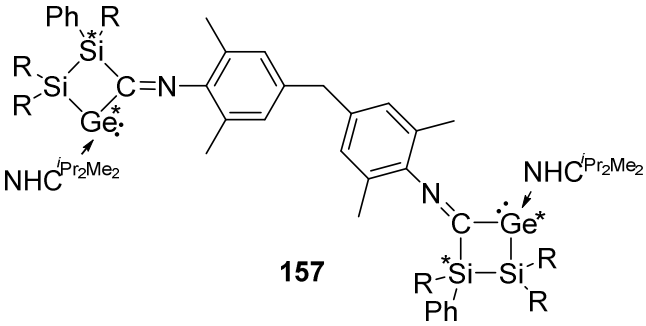

157

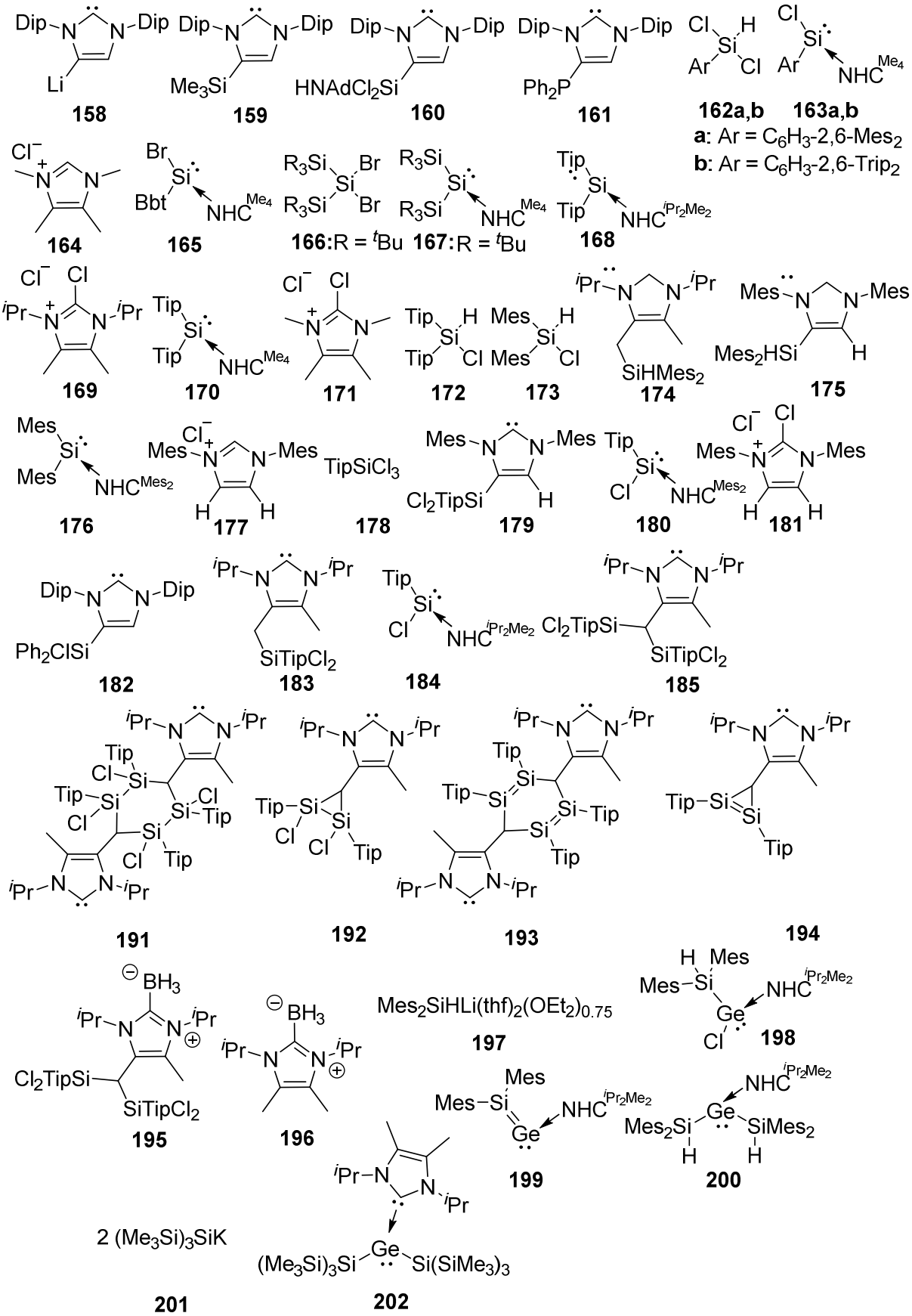
158
159
160
161
162a,b
163a,b
a: Ar = C6H3-2,6-Mes2
b: Ar = C6H3-2,6-Trip2
164
165
166:R = tBu
167:R = tBu
168
169
170
171
172
173
174
175
176
177
178
179
180
181
182
183
184
185
191
192
193
194
195
196
197
198
199
200
201
202

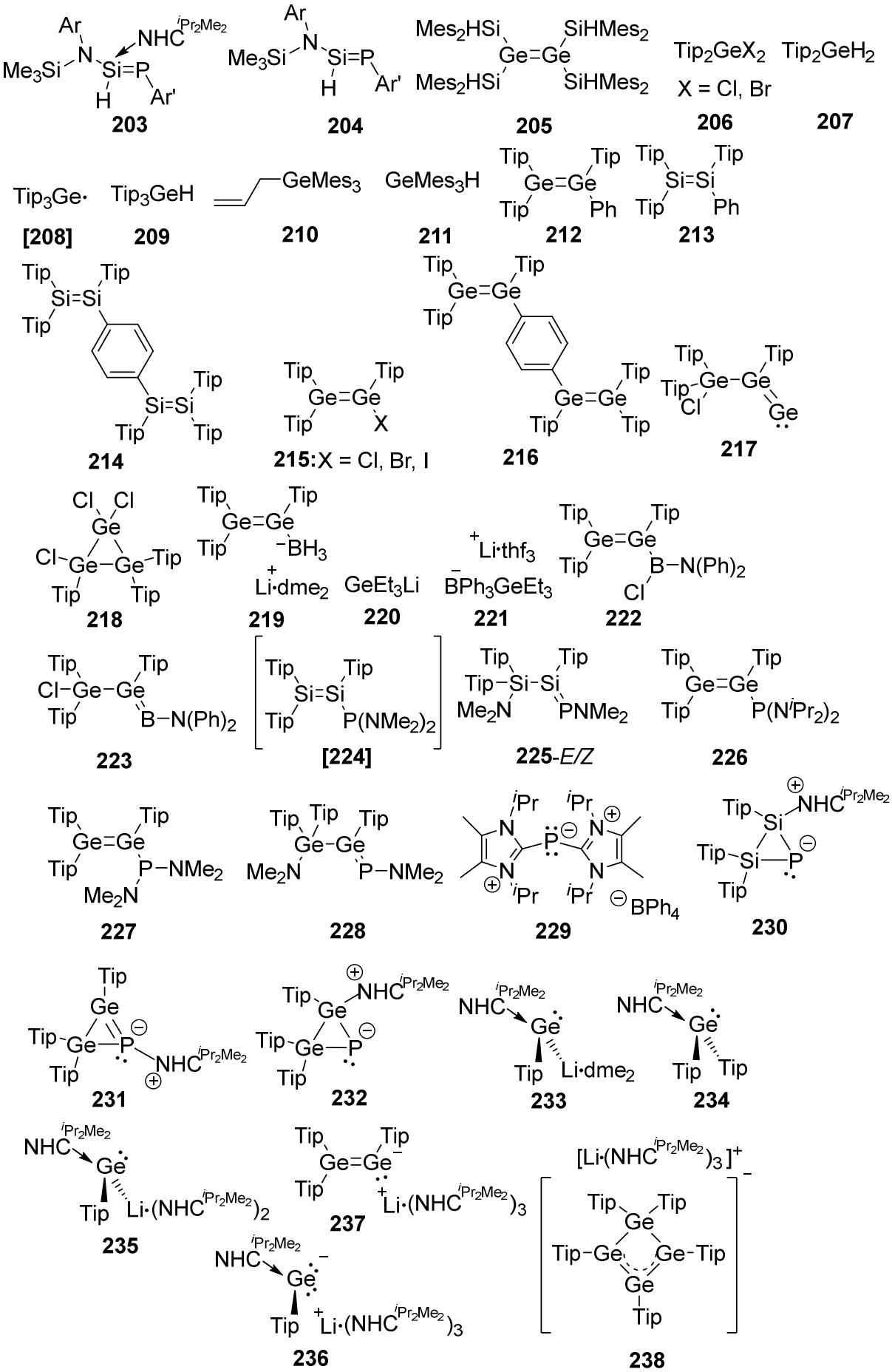
203
204
205
206
X = Cl, Br
207
[208]
209
210
211
212
213
214
215:X = Cl, Br, I
216
217
218
219
220
221
222
223
[224]
225-E/Z
226
227
228
229
230
231
232
233
234
235
237
236
238

7.2. Computational Details

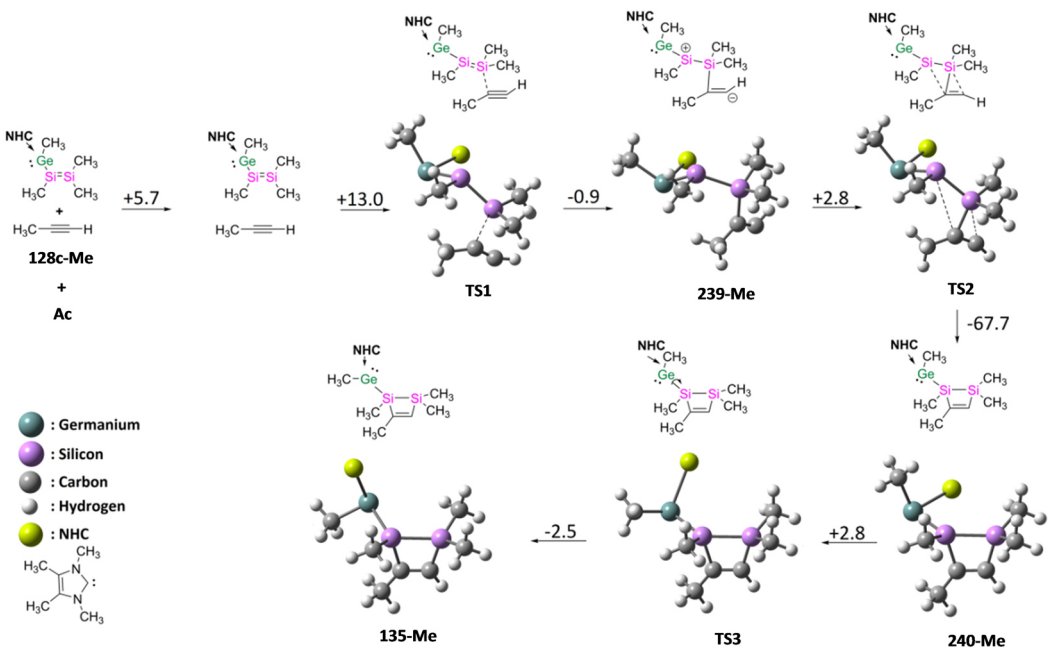

Figure 98. First proposed mechanism and intermediates for the formation of **135-Me** from **128c-Me + Ac** using simplified model system with methyl groups instead of Tip, Ph, and ^{i}Pr groups at B3LYP/6-31G(d,p) level of theory, respectively. ΔG energy values at 298 K are given in kcal mol^{-1}.

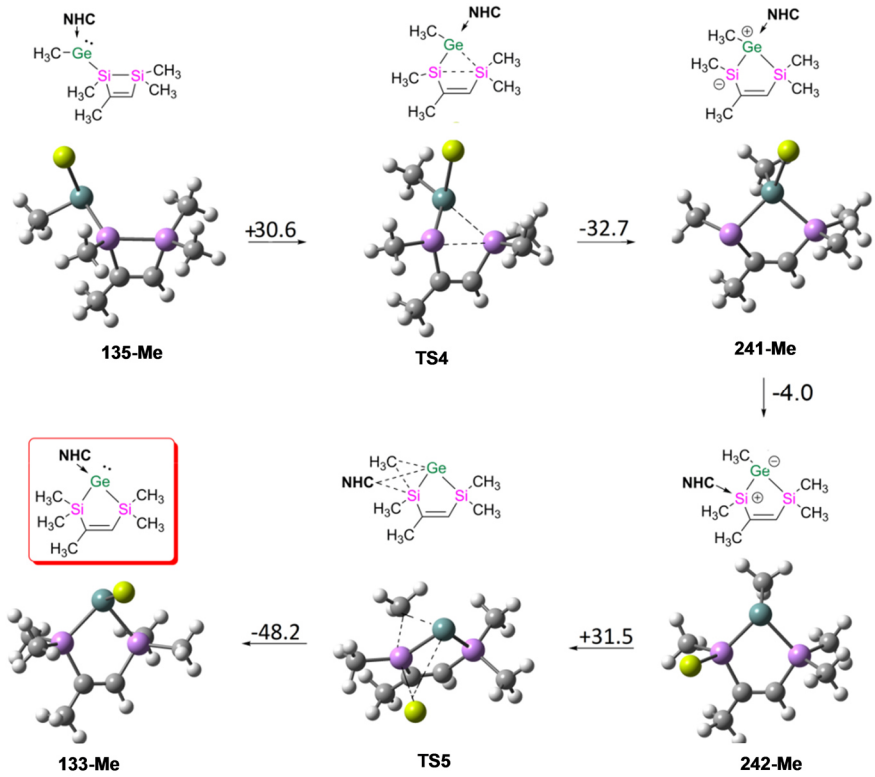

Figure 99. Proposed mechanism and intermediates for the formation of **133-Me** from NHC coordinated system using simplified model system with methyl groups instead of Tip, Ph, and ^{i}Pr groups at B3LYP/6-31G(d,p) level of theory, respectively. ΔG energy values at 298 K are given in kcal mol^{-1}.

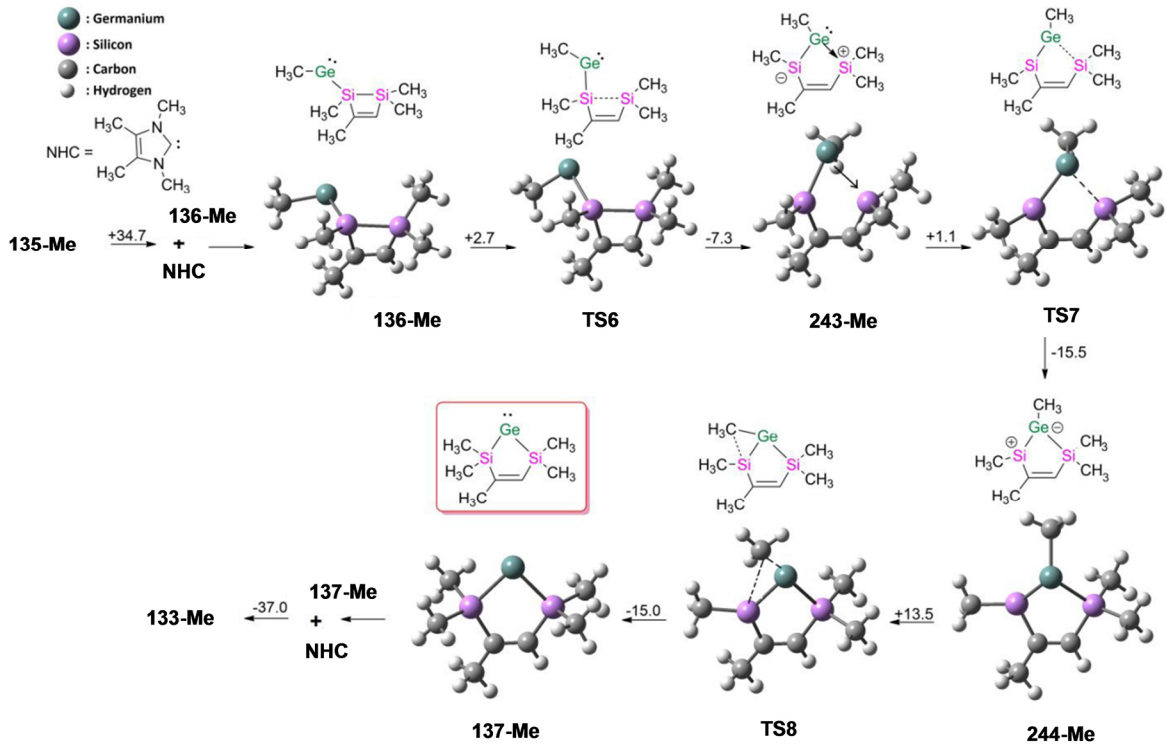

Figure 100. Proposed mechanism and intermediates for the formation of **133-Me** from NHC free system using simplified model system with methyl groups instead of Tip, Ph, and ^{i}Pr groups at B3LYP/6-31G(d,p) level of theory, respectively. ΔG energy values at 298 K are given in kcal mol^{-1}.

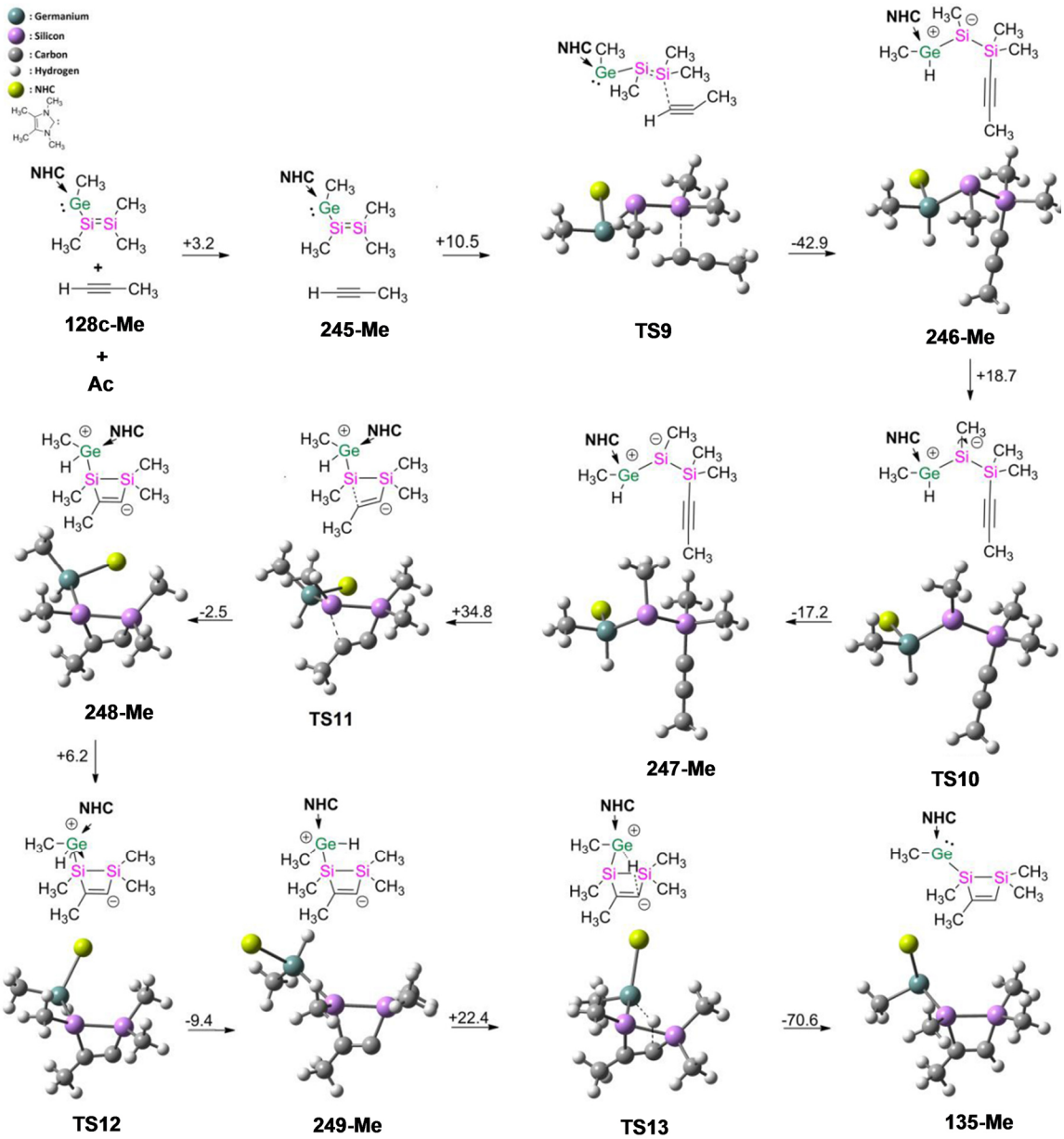

Figure 101. Alternative mechanism and intermediates for the formation of **135-Me** from **128c-Me + Ac** using simplified model system with methyl groups instead of Tip, Ph, and ^{i}Pr groups at B3LYP/6-31G(d,p) level of theory, respectively. ΔG energy values at 298 K are given in kcal mol^{-1}.

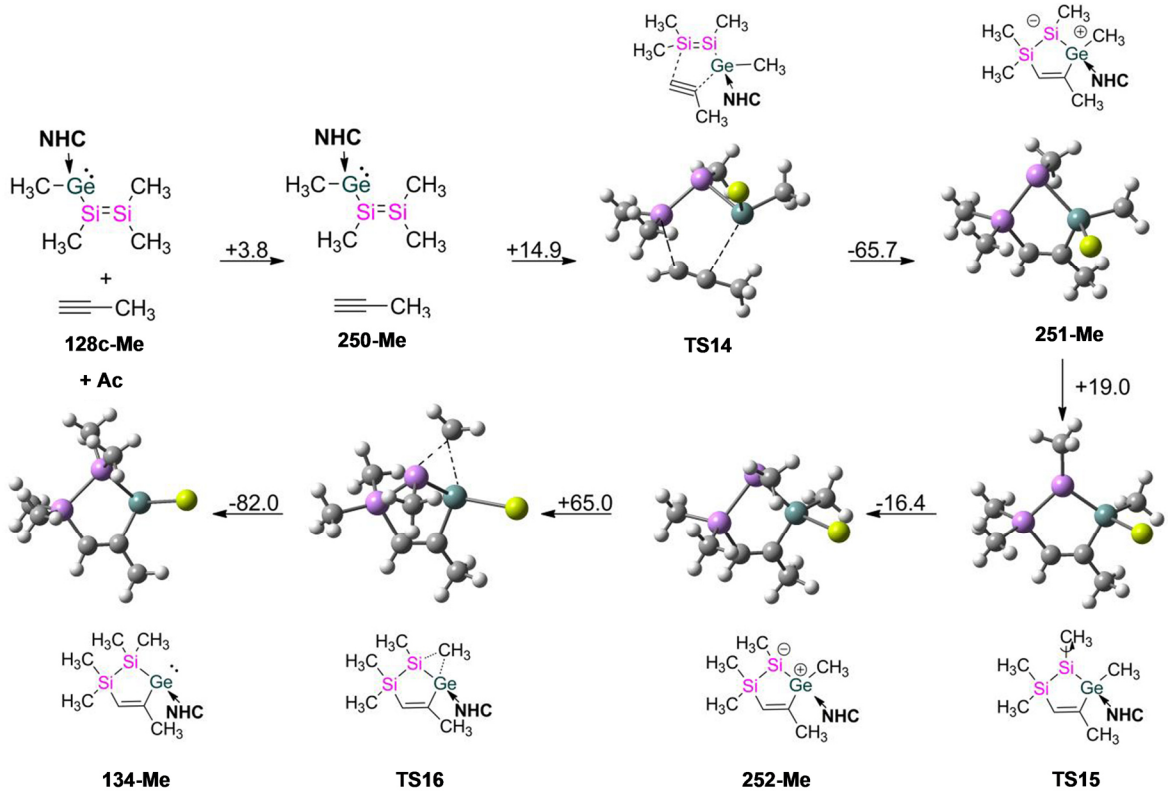

Figure 102. Unfavoured mechanism due to high energy barriers and intermediates for the formation of **134-Me** from [2 + 3] addition of **128c-Me + Ac** using simplified model system with methyl groups instead of Tip, Ph, and ^{i}Pr groups at B3LYP/6-31G(d,p) level of theory, respectively. ΔG energy values at 298 K are given in kcal mol^{-1}.

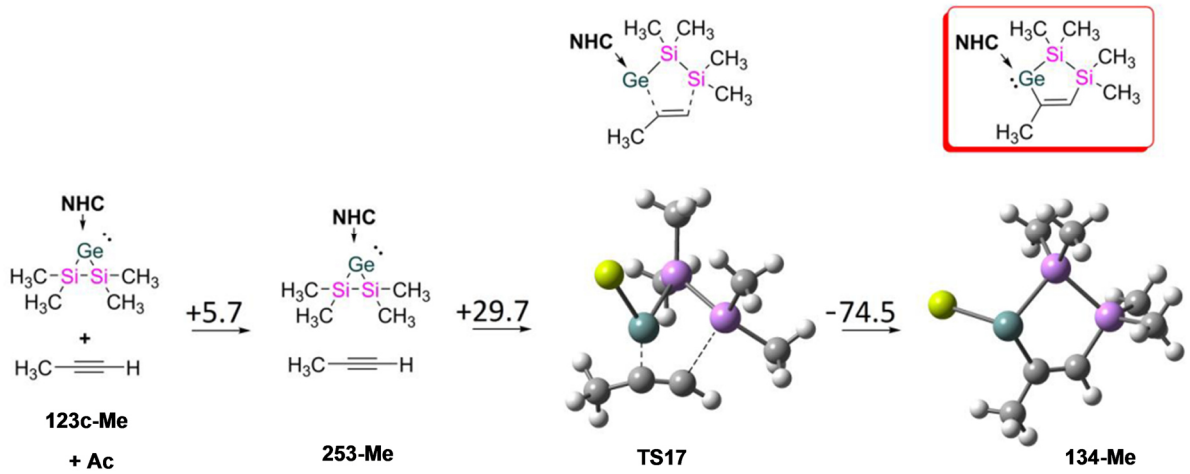

Figure 103. Proposed mechanism and intermediates for the formation of **134-Me** from insertion of **Ac** to Si-Ge single bond of **123c-Me** using simplified model system with methyl groups instead of Tip, Ph, and ^{i}Pr groups at B3LYP/6-31G(d,p) level of theory, respectively. ΔG energy values at 298 K are given in kcal mol^{-1}.

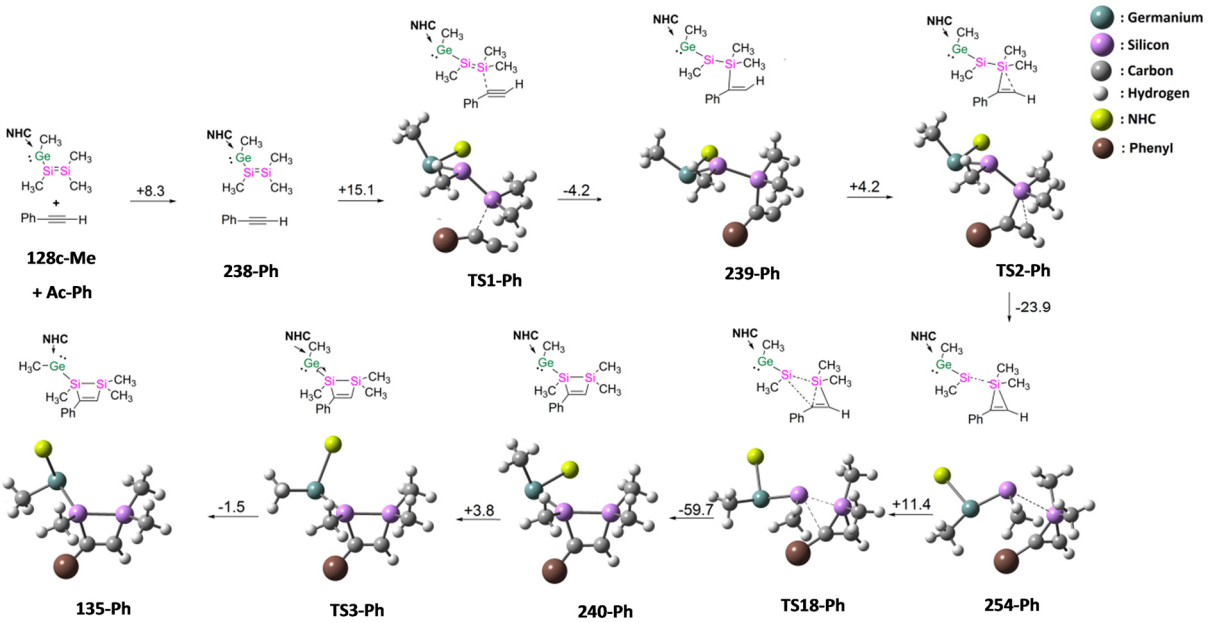

Figure 104. First proposed mechanism and intermediates for the formation of **135-Ph** from **128c-Me** + phenylacetylene using simplified model system with methyl groups instead of Tip, Ph, and ^{i}Pr groups at B3LYP/6-31G(d,p) level of theory, respectively. ΔG energy values at 298 K are given in kcal mol^{-1}.

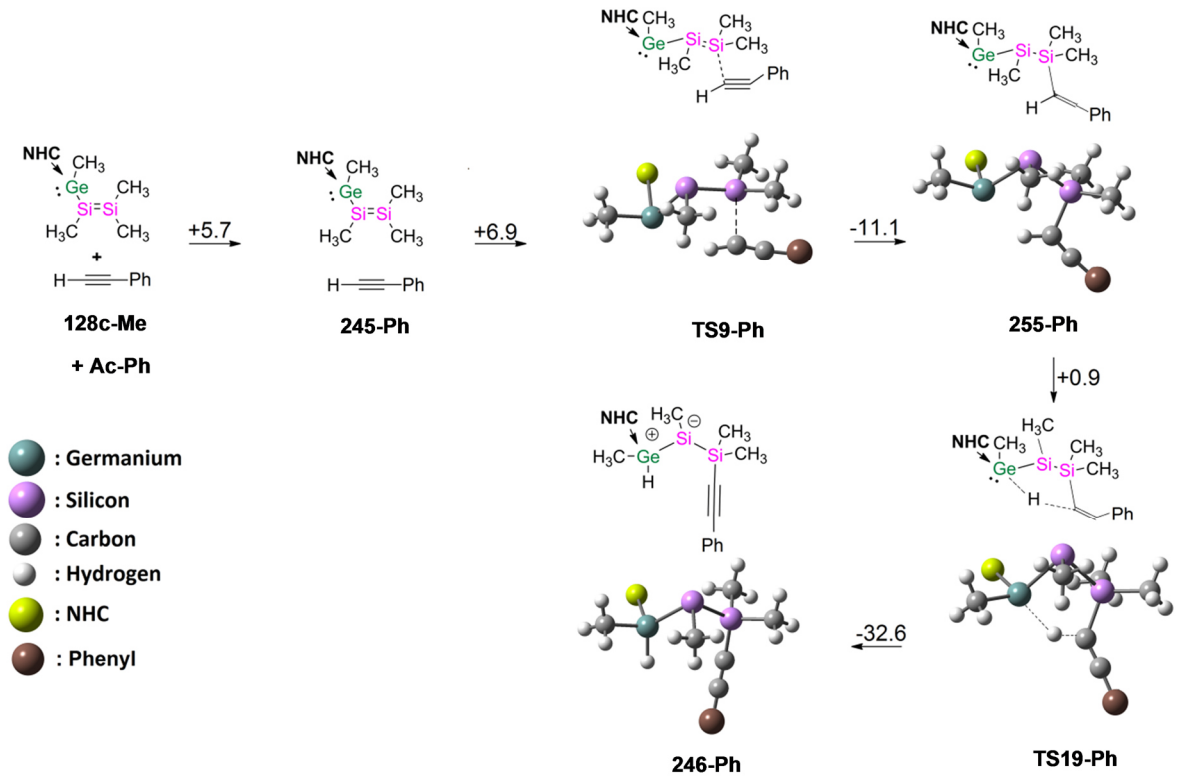

Figure 105. First two steps of the alternative mechanism for the formation of **135-Ph** from **128c-Me** + phenylacetylene using simplified model system with methyl groups instead of Tip, Ph, and ^{i}Pr groups at B3LYP/6-31G(d,p) level of theory, respectively. ΔG energy values at 298 K are given in kcal mol^{-1}.

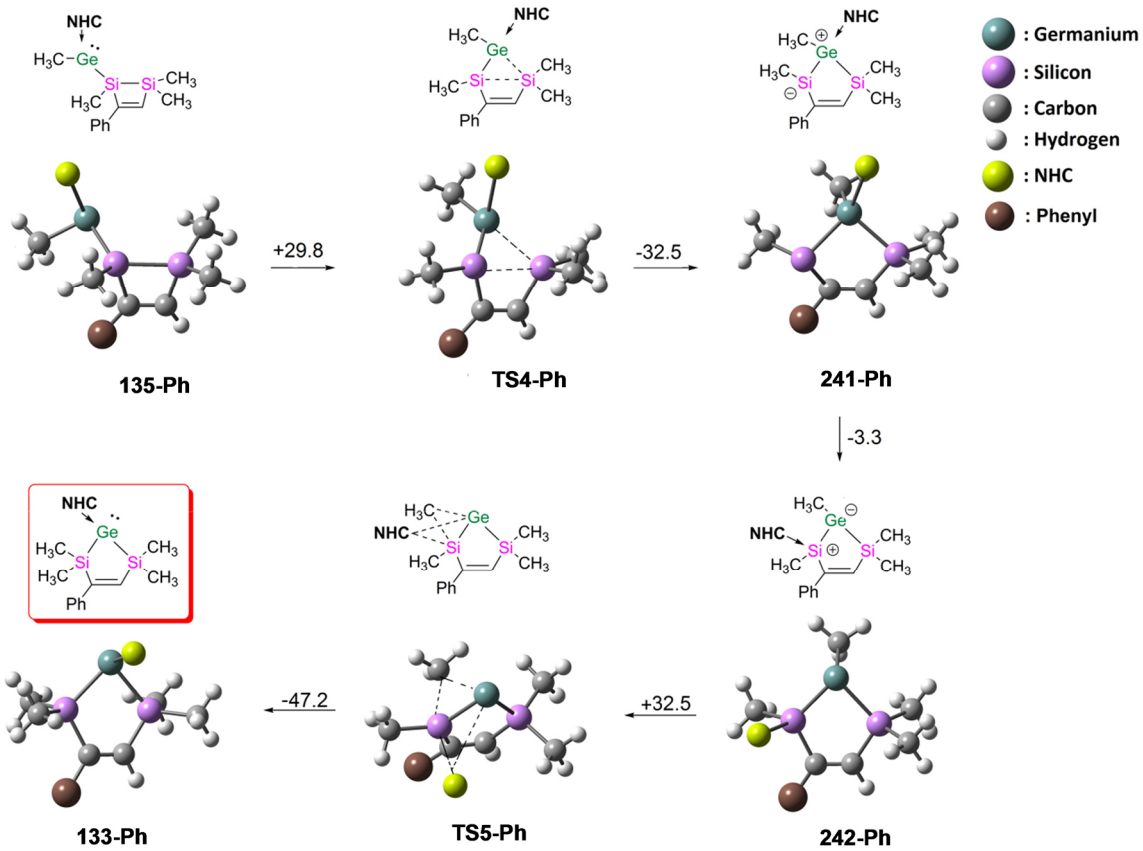

Figure 106. Proposed mechanism and intermediates for the formation of **133-Ph** from NHC coordinated system using simplified model system with methyl groups instead of Tip, Ph, and ^{i}Pr groups at B3LYP/6-31G(d,p) level of theory, respectively. ΔG energy values at 298 K are given in kcal mol^{-1}.

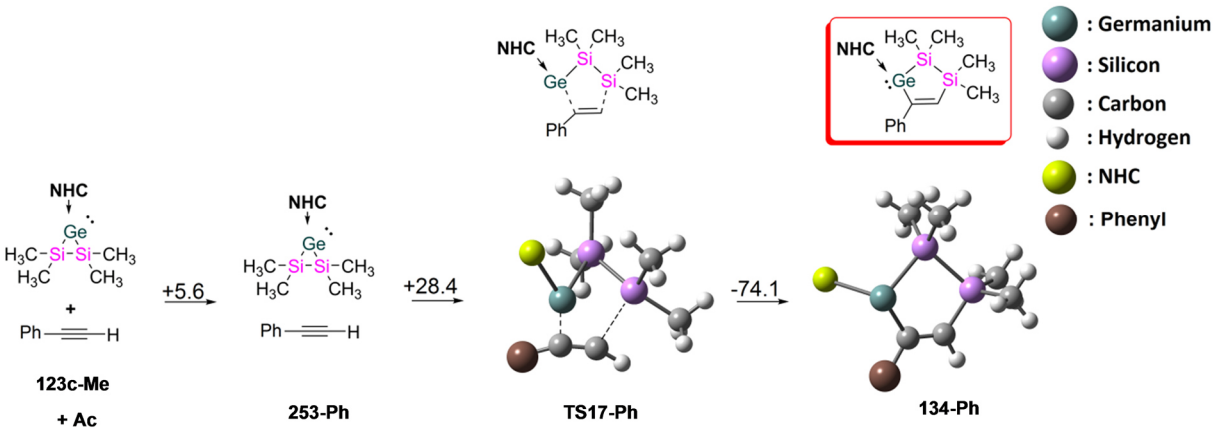

Figure 107. Proposed mechanism and intermediates for the formation of **134-Ph** from insertion of phenylacetylene to Si-Ge single bond of **123c-Me** using simplified model system with methyl groups instead of Tip, Ph, and ^{i}Pr groups at B3LYP/6-31G(d,p) level of theory, respectively. ΔG energy values at 298 K are given in kcal mol^{-1}.

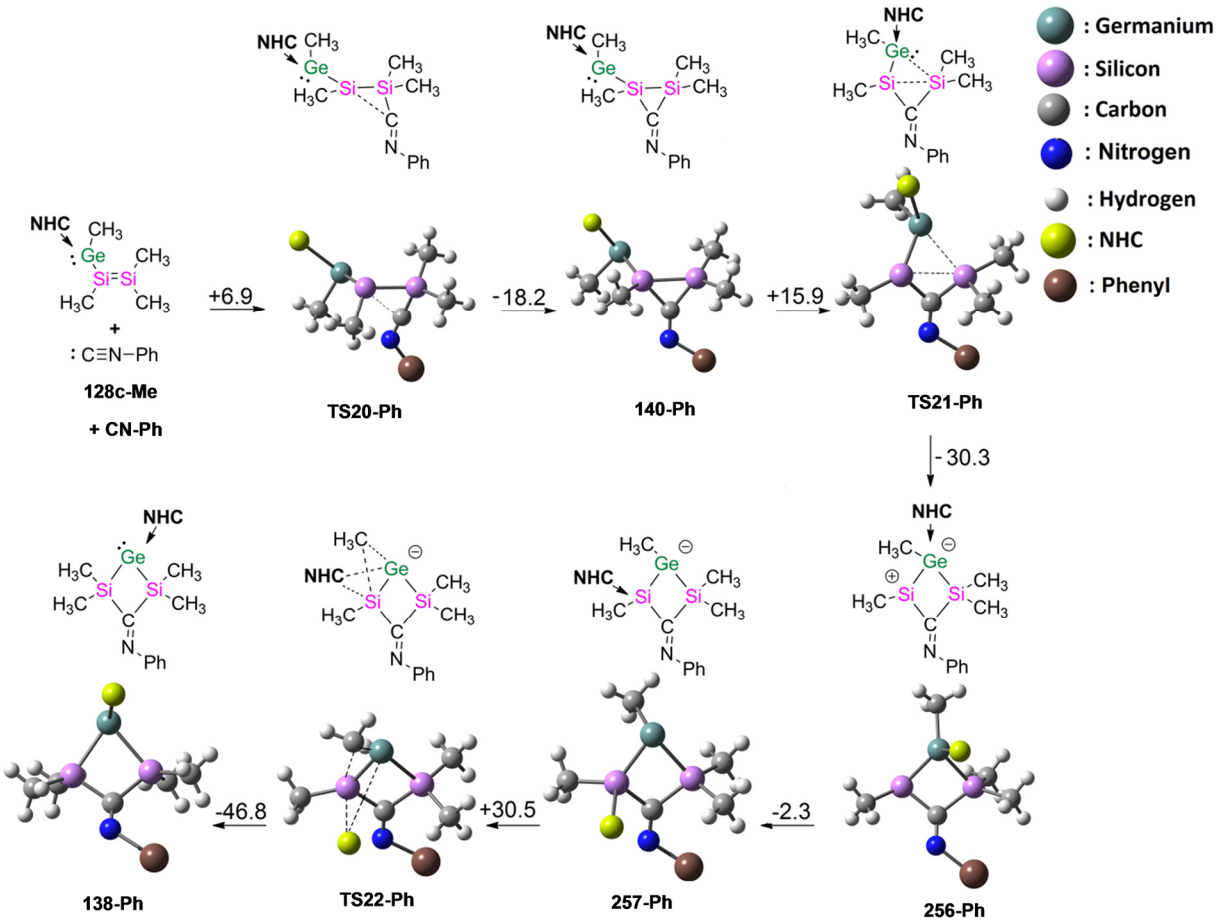

Figure 108. Proposed mechanism and intermediates for the formation of **138-Ph** from insertion of phenylacetylene to Si-Si double bond of **128c-Me** using simplified model system with methyl groups instead of Tip, Ph, and ^{i}Pr groups at B3LYP/6-31G(d,p) level of theory, respectively. ΔG energy values at 298 K are given in kcal mol^{-1}.

7.3. Absorption Spectra

7.3.1. UV/vis Spectra and Determination of ε for Disilenyl Germylene 128c

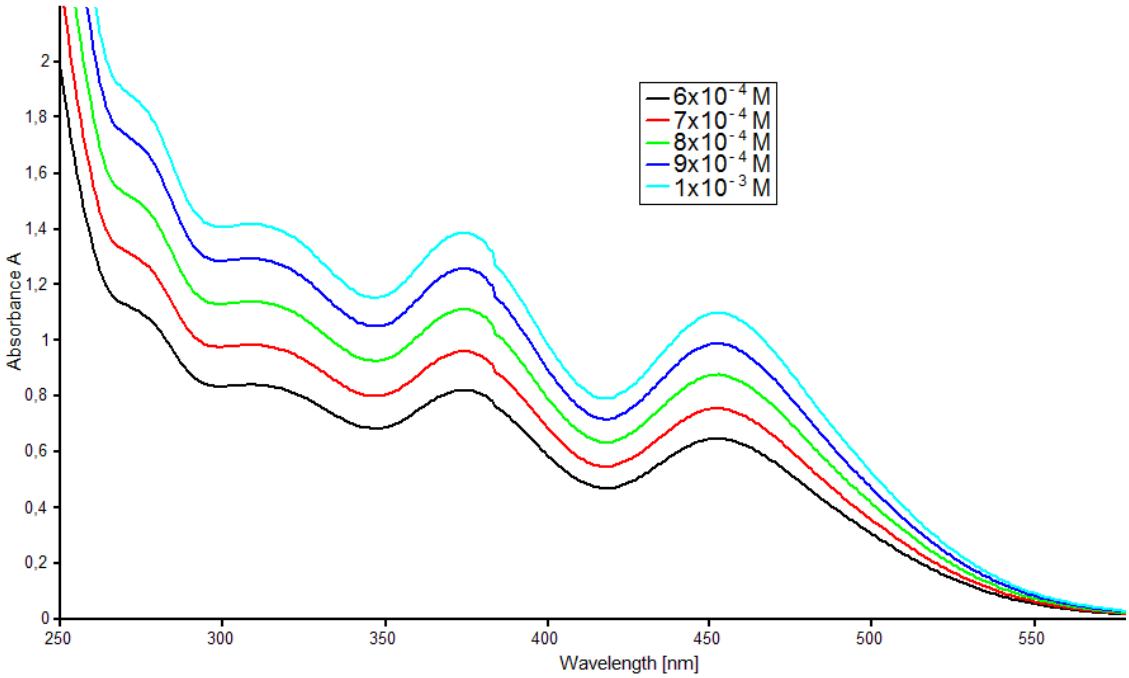

Figure 109. UV/vis spectra of disilenyl germylene **128c** in hexane at different concentrations ($6x10^{-4}$ – $1x10^{-3}$ mol/L).

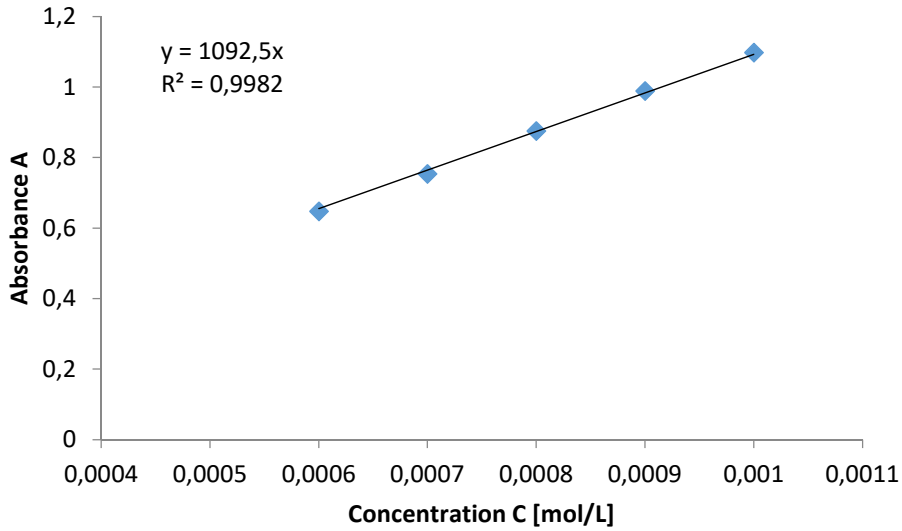

Figure 110. Determination of ε (10100 $M^{-1}cm^{-1}$) through a graphical draw of absorptions (λ = 452 nm) of **128c** against their concentrations.

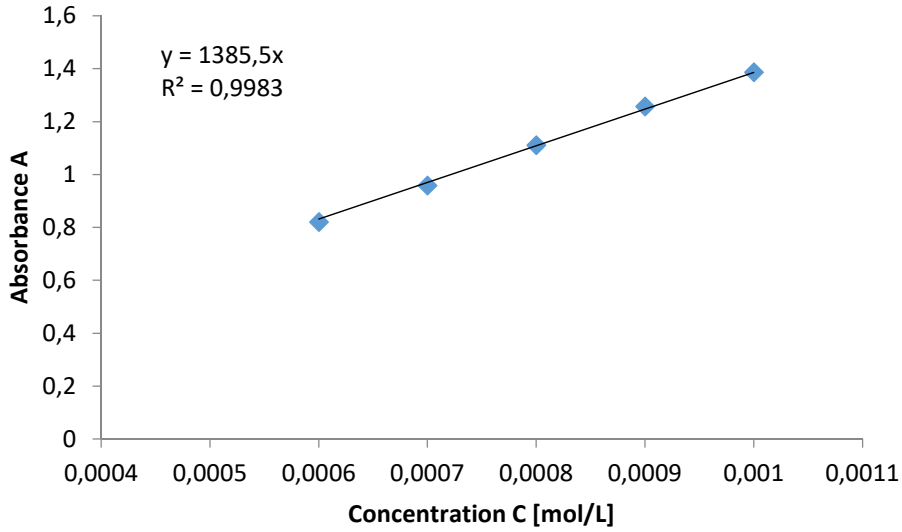

Figure 111. Determination of ε (13900 $M^{-1}cm^{-1}$) through a graphical draw of absorptions (λ = 373 nm) of **128c** against their concentrations.

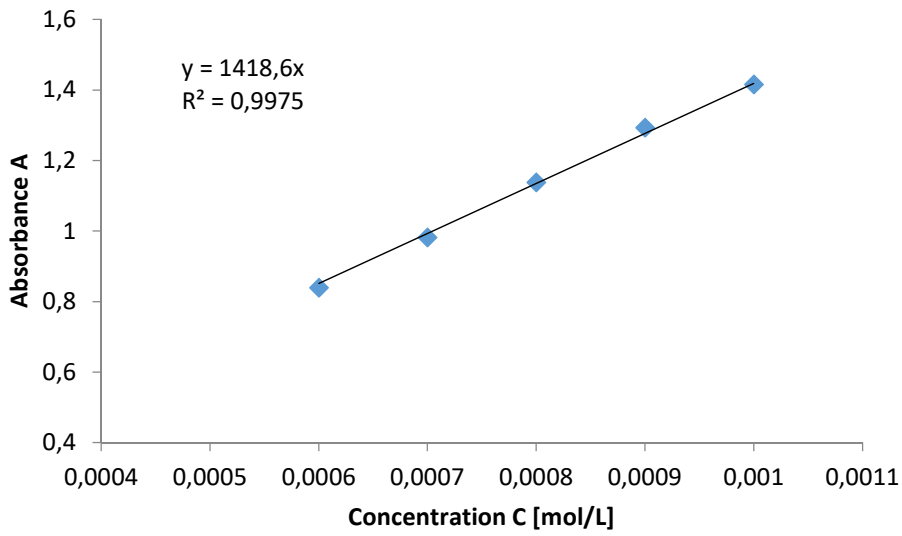

Figure 112. Determination of ε (14200 $M^{-1}cm^{-1}$) through a graphical draw of absorptions (λ = 308 nm) of **128c** against their concentrations.

7.3.2. UV/vis Spectra and Determination of ε for Heavier Cyclopropylidene Analogue 123c

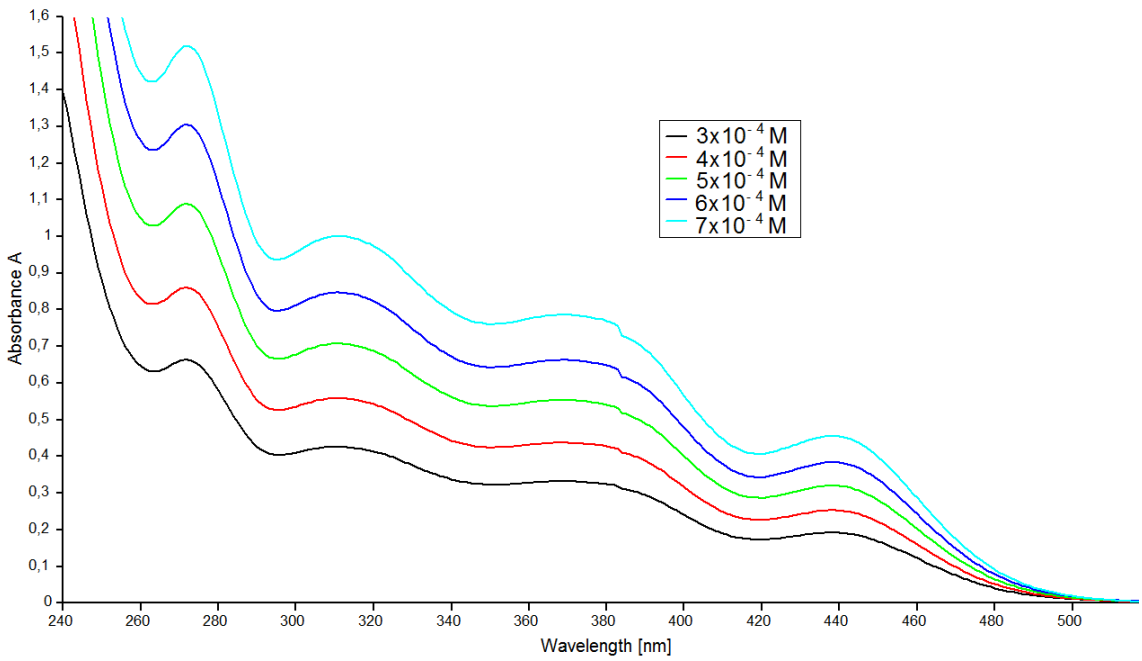

Figure 113. UV/vis spectra of cyclopropylidene **123c** in hexane at different concentrations ($3x10^{-4}$ – $7x10^{-4}$ mol/L).

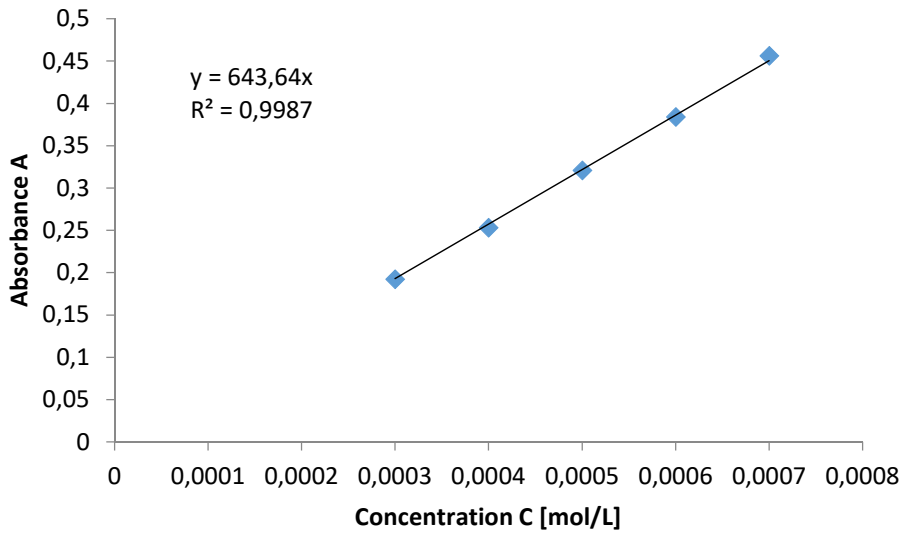

Figure 114. Determination of ε (6400 $M^{-1}cm^{-1}$) through a graphical draw of absorptions (λ = 438 nm) of **123c** against their concentrations.

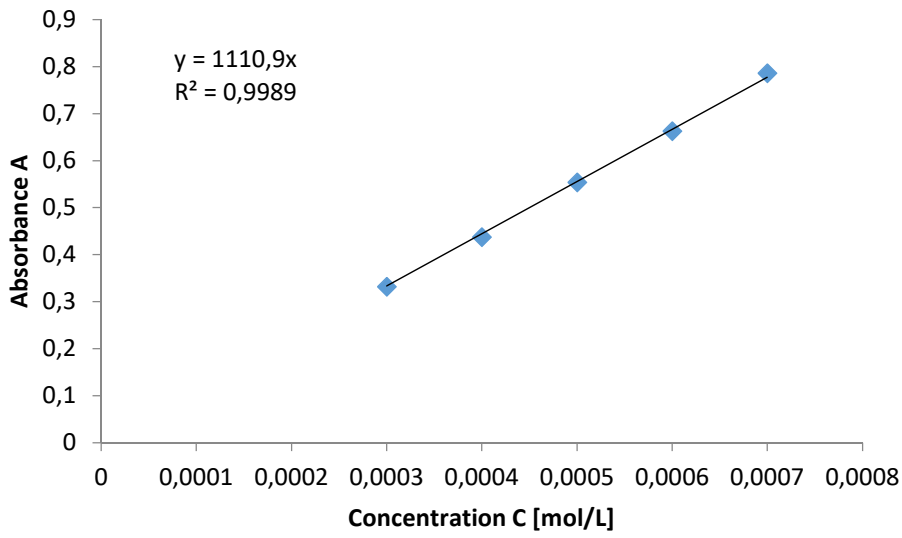

Figure 115. Determination of ε (11100 $M^{-1}cm^{-1}$) through a graphical draw of absorptions (λ = 370 nm) of **123c** against their concentrations.

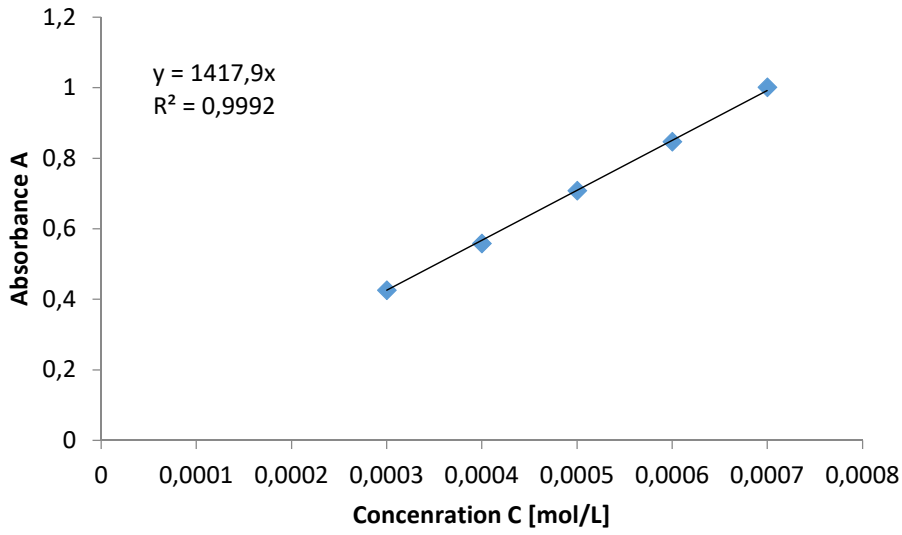

Figure 116. Determination of ε (14200 $M^{-1}cm^{-1}$) through a graphical draw of absorptions (λ = 311 nm) of **123c** against their concentrations.

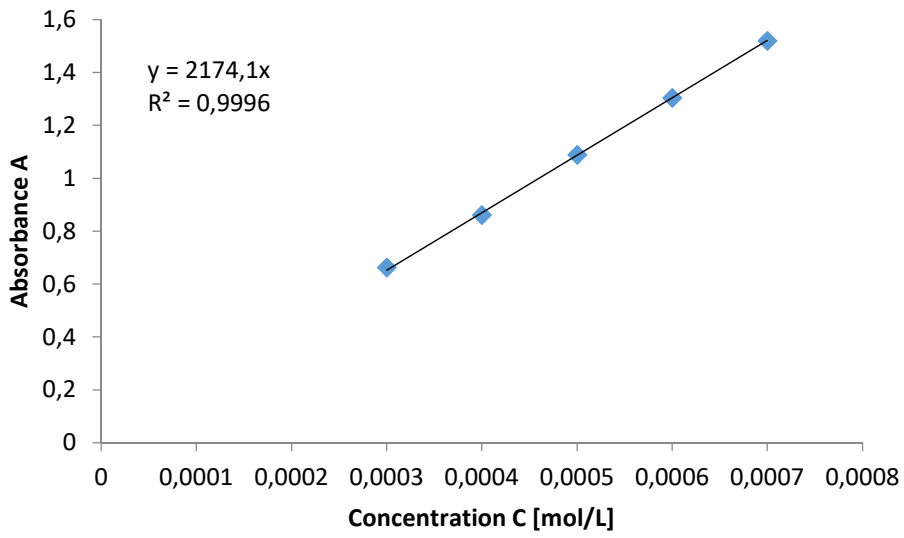

Figure 117. Determination of ε (21700 $M^{-1}cm^{-1}$) through a graphical draw of absorptions (λ = 272 nm) of **123c** against their concentrations.

7.3.3. UV/vis Spectra and Determination of ε for Heavier Cyclopentenylidene Derivative 133

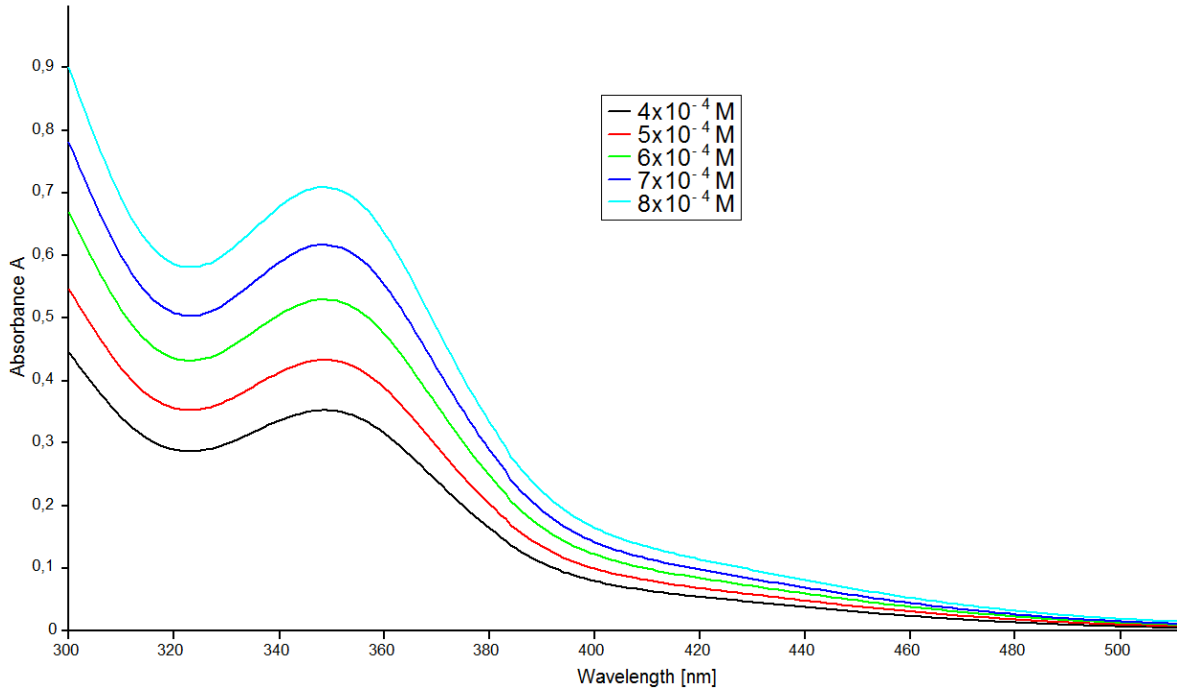

Figure 118. UV/vis spectra of **133** in hexane at different concentrations ($4x10^{-4}$ – $8x10^{-4}$ mol/L).

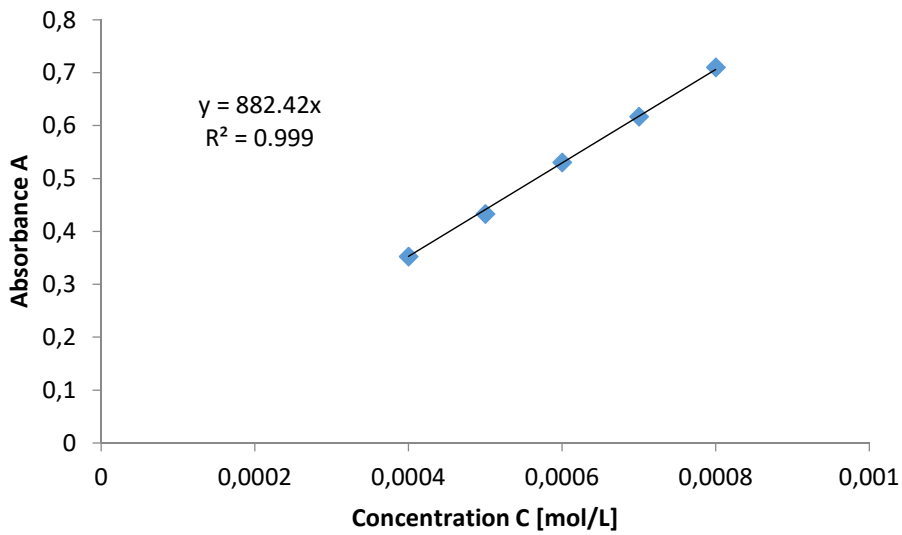

Figure 119. Determination of ε (8800 $M^{-1}cm^{-1}$) through a graphical draw of absorptions (λ = 348 nm) of **133** against their concentrations.

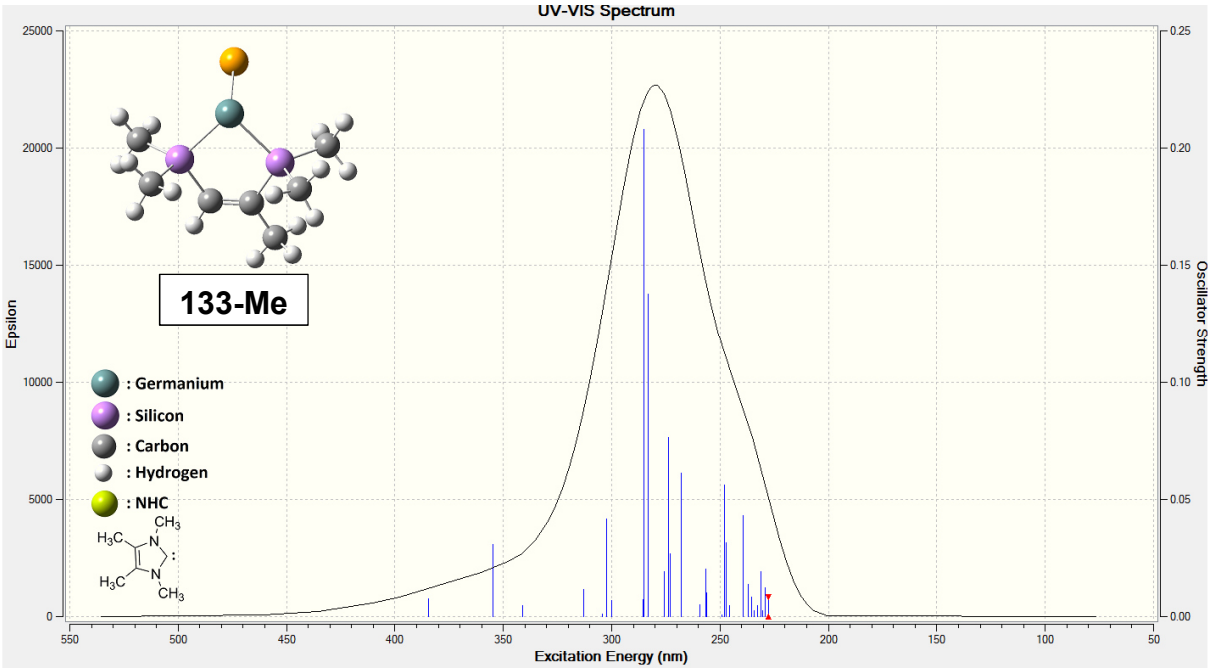

Figure 120. Calculated UV/vis spectrum of **133-Me** at B3LYP/6-31+G(d,p) level of theory (solvent = hexane); figure produced by Cem B. Yildiz, Aksaray University, Turkey.

7.3.4. UV/vis Spectra and Determination of ε for Heavier Cyclopentenylidene 134

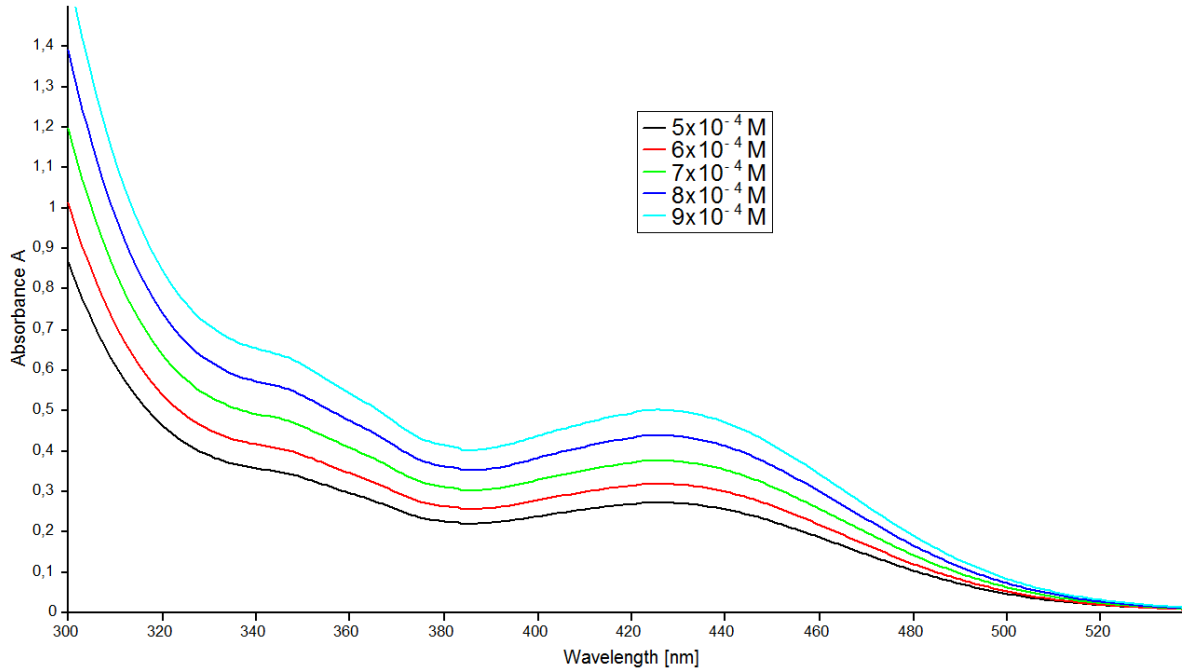

Figure 121. UV/vis spectra of **134** in hexane at different concentrations ($5x10^{-4}$ – $9x10^{-4}$ mol/L).

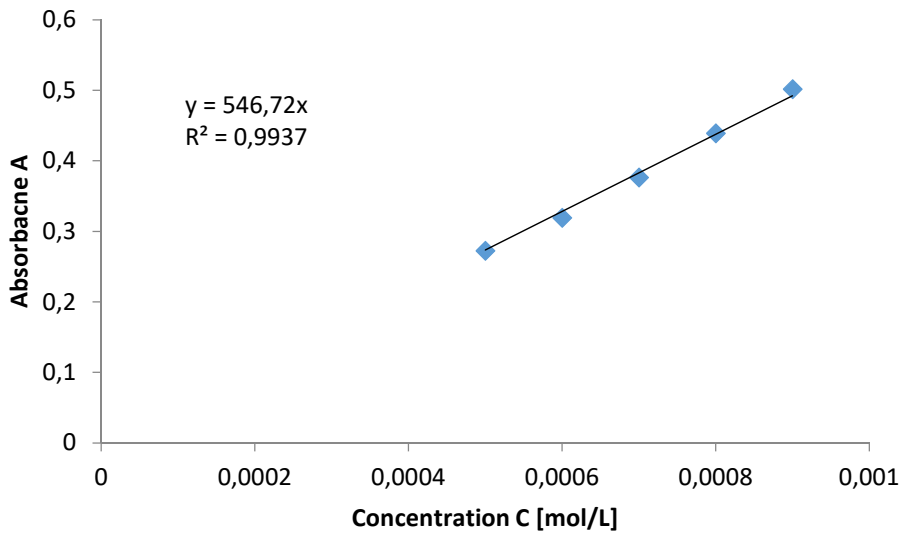

Figure 122. Determination of ε (5500 $M^{-1}cm^{-1}$) through a graphical draw of absorptions (λ = 425 nm) of **134** against their concentrations.

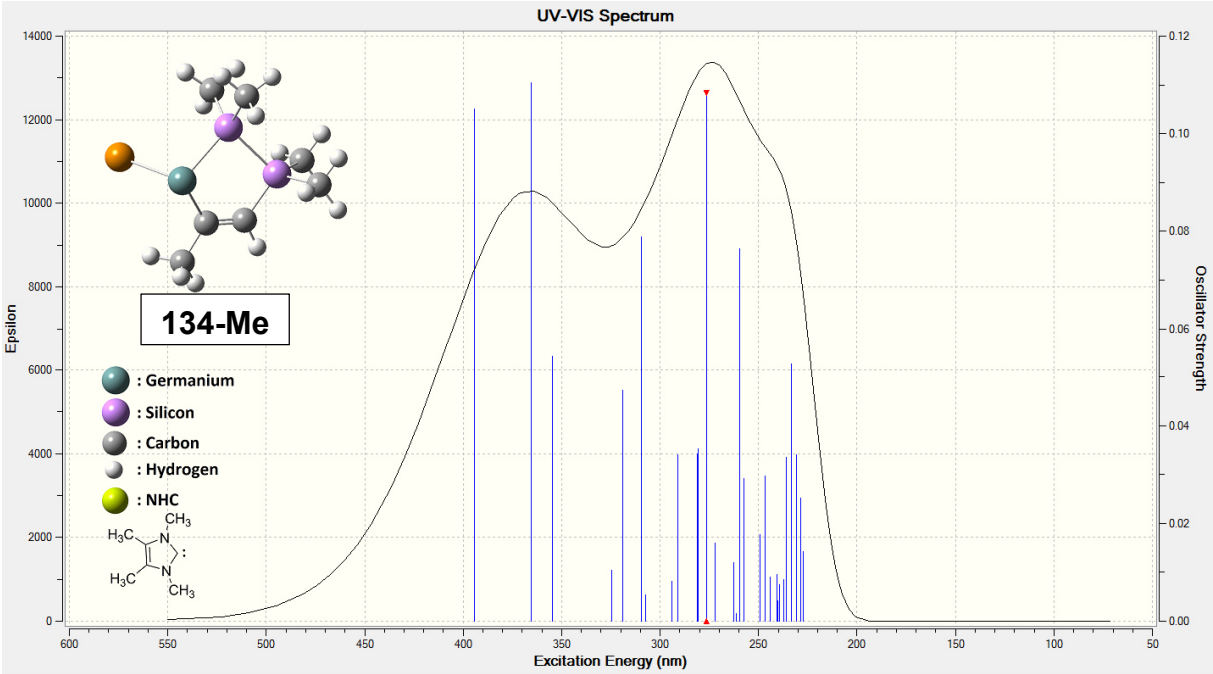

Figure 123. Calculated UV/vis of spectrum **134-Me** at B3LYP/6-31+G(d,p) level of theory (solvent = hexane); figure produced by Cem B. Yildiz, Aksaray University, Turkey

7.3.5. UV/vis Spectra and Determination of ε for Cyclic Germylene 138

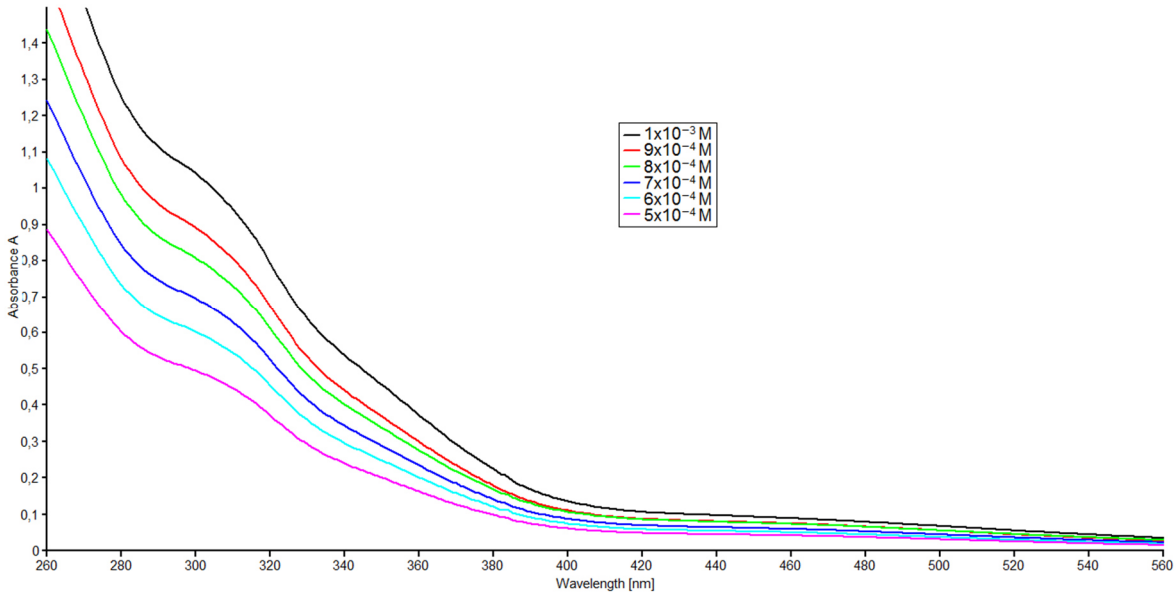

Figure 124. UV/vis spectra of **138** in hexane at different concentrations ($1x10^{-3}$ – $5x10^{-4}$ mol/L); λ_{max} = 290-320 (br sh) nm.

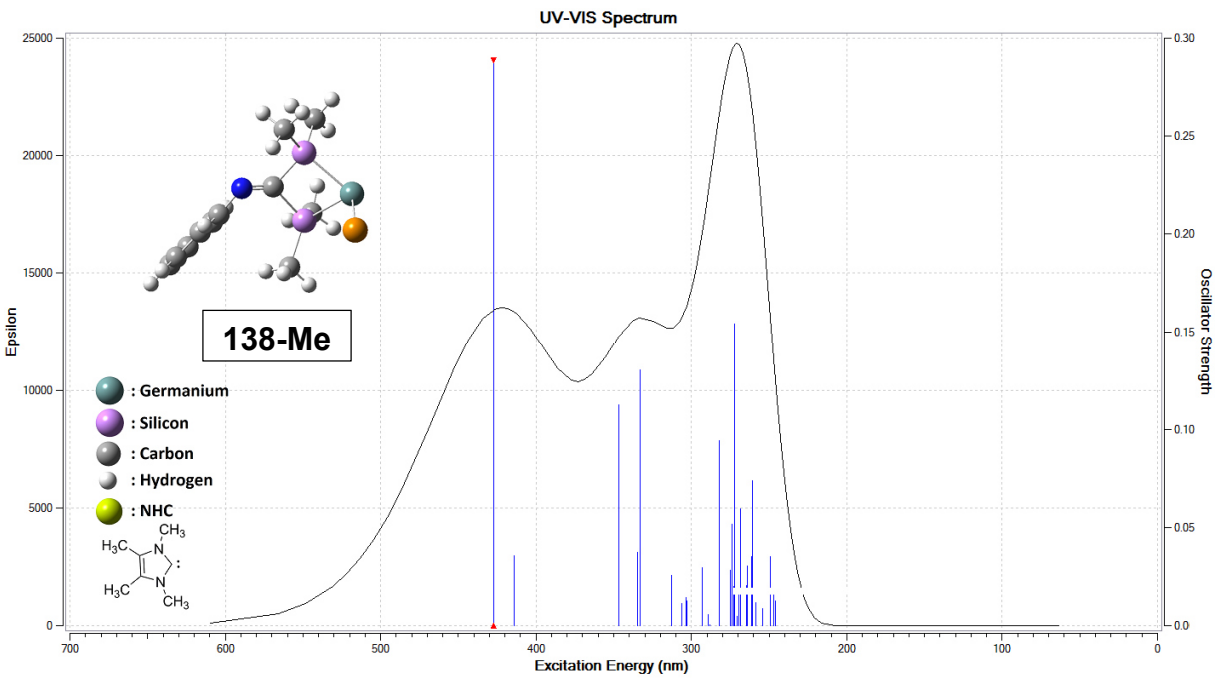

Figure 125. Calculated UV/vis spectrum of **138-Me** at B3LYP/6-31+G(d,p) level of theory (solvent = hexane); figure produced by Cem B. Yildiz, Aksaray University, Turkey.

7.3.6. UV/vis Spectra and Determination of ε for Cyclic Germylene 143

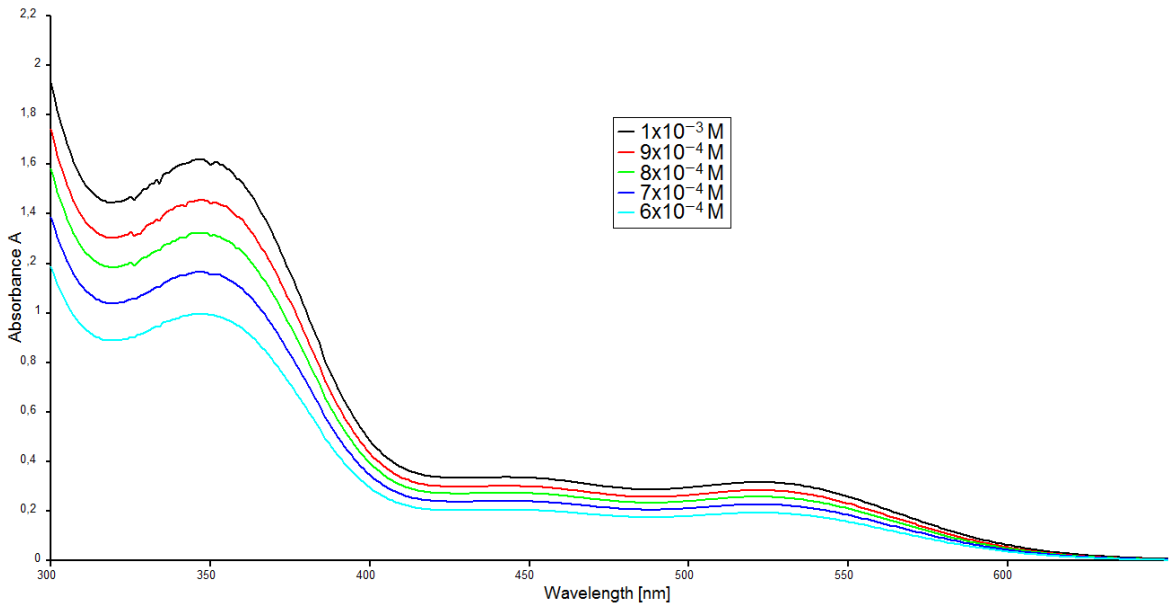

Figure 126. UV/vis spectra of **143** in hexane at different concentrations ($1x10^{-3}$ – $6x10^{-4}$ mol/L).

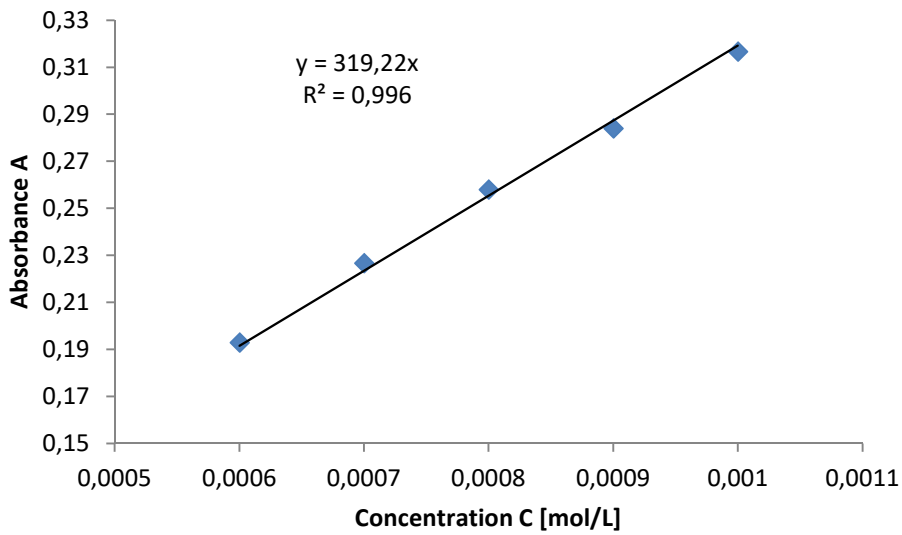

Figure 127. Determination of ε (3200 $M^{-1}cm^{-1}$) through a graphical draw of absorptions (λ = 522 nm) of **143** against their concentrations.

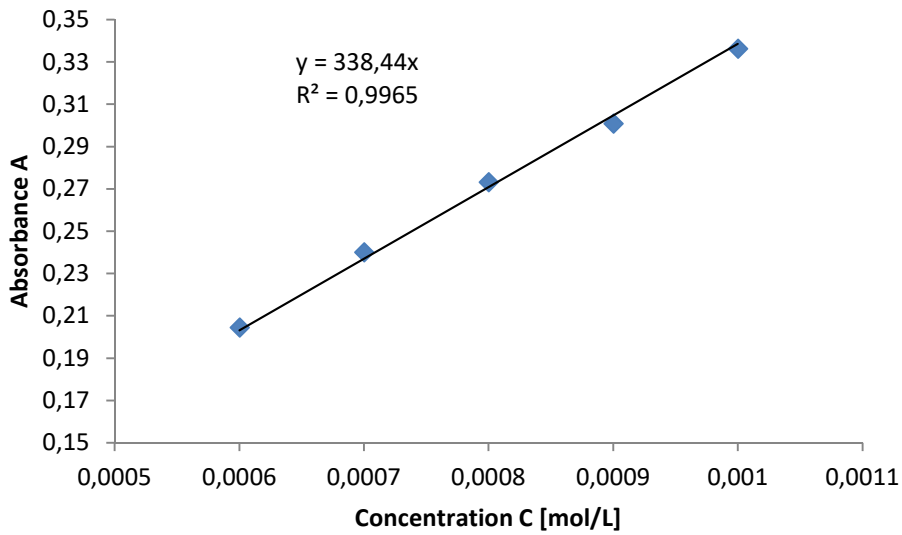

Figure 128. Determination of ε (3400 $M^{-1}cm^{-1}$) through a graphical draw of absorptions (λ = 442 nm) of **143** against their concentrations.

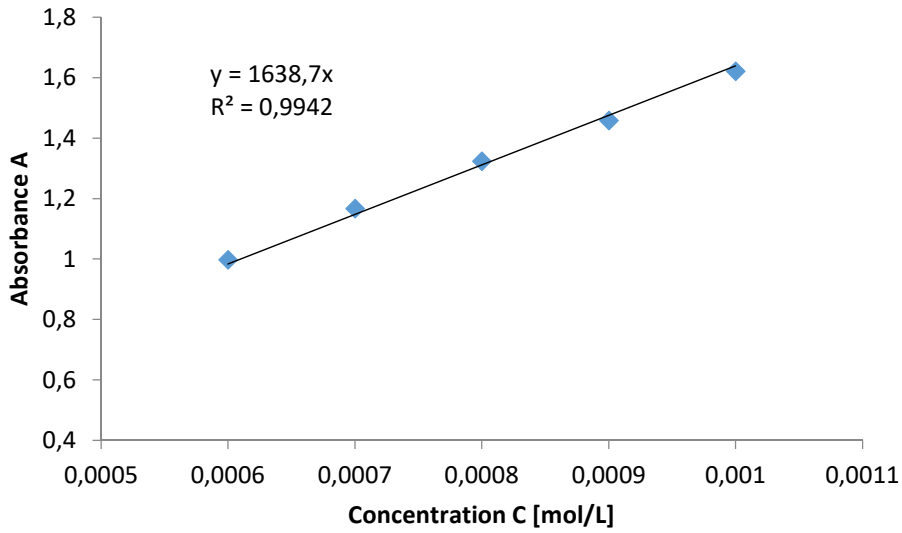

Figure 129. Determination of ε (16400 $M^{-1}cm^{-1}$) through a graphical draw of absorptions (λ = 347 nm) of **143** against their concentrations.

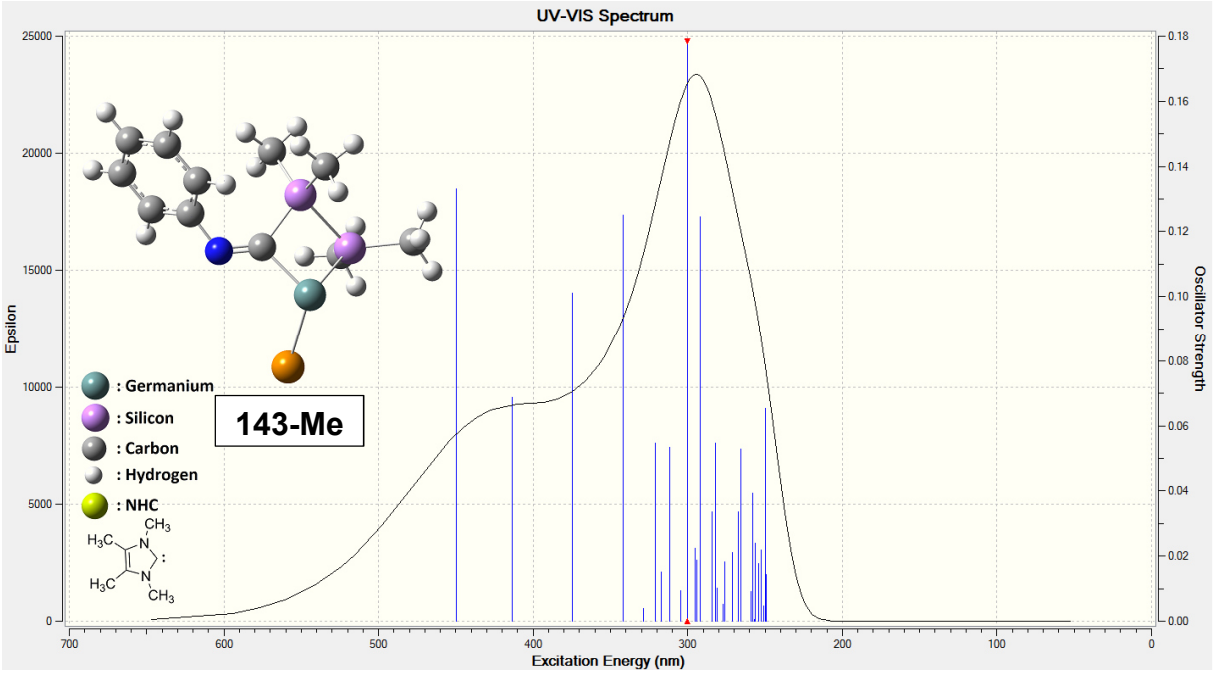

Figure 130. Calculated UV/vis spectrum of **143-Me** at B3LYP/6-31+G(d,p) level of theory (solvent = hexane); figure produced by Cem B. Yildiz, Aksaray University, Turkey.

7.3.7. UV/vis Spectra and Determination of ε for Disilyl Carbene 185

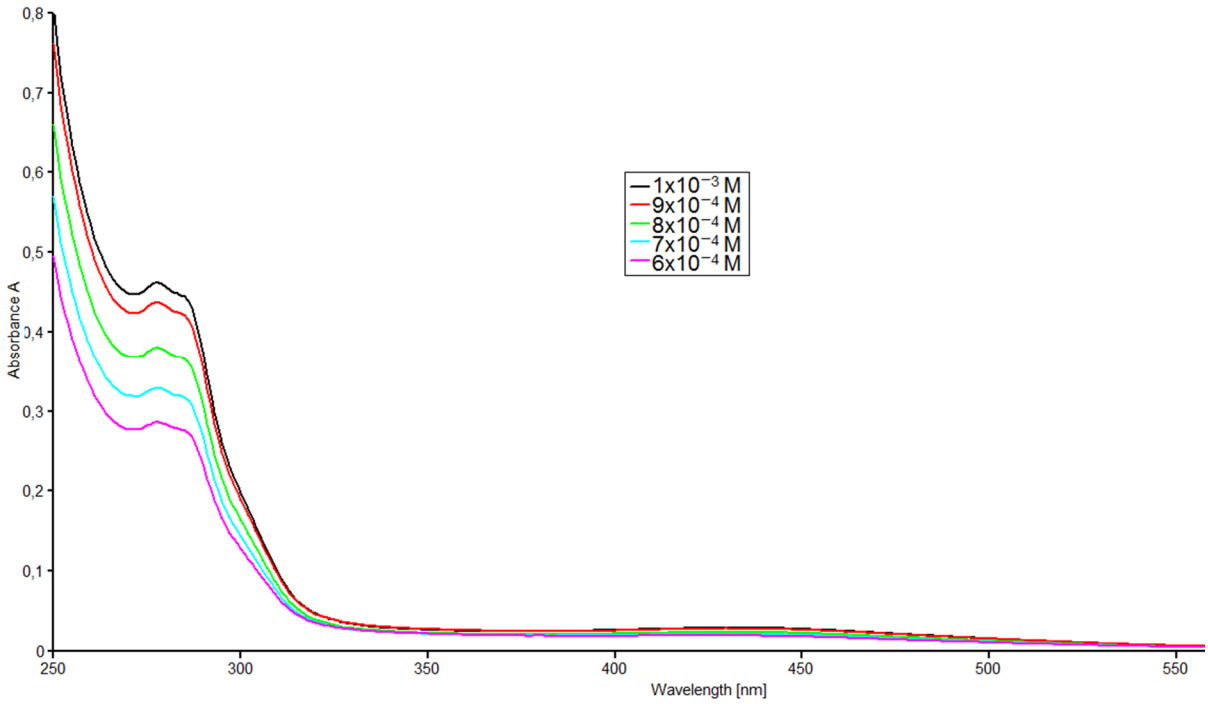

Figure 131. UV/vis spectra of **185** in hexane at different concentrations ($1x10^{-3}$ – $6x10^{-4}$ mol/L).

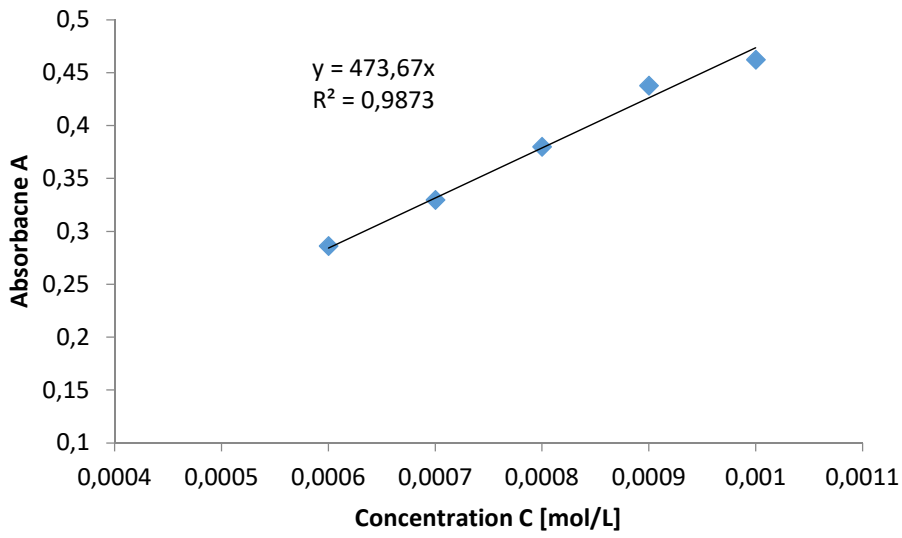

Figure 132. Determination of ε (4700 $M^{-1}cm^{-1}$) through a graphical draw of absorptions (λ = 278 nm) of **185** against their concentrations.

7.3.8. UV/vis Spectra and Determination of ε for Bis-Silyl Germylene 200

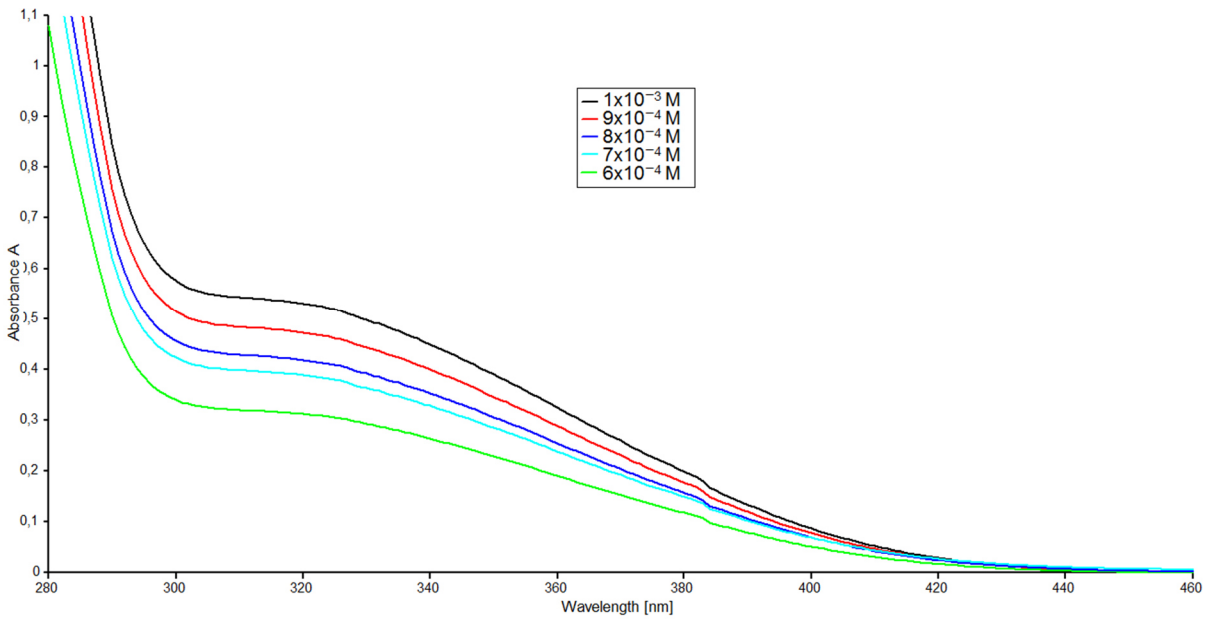

Figure 133. UV/vis spectra of **200** in thf at different concentrations ($1x10^{-3}$ – $6x10^{-4}$ mol/L).

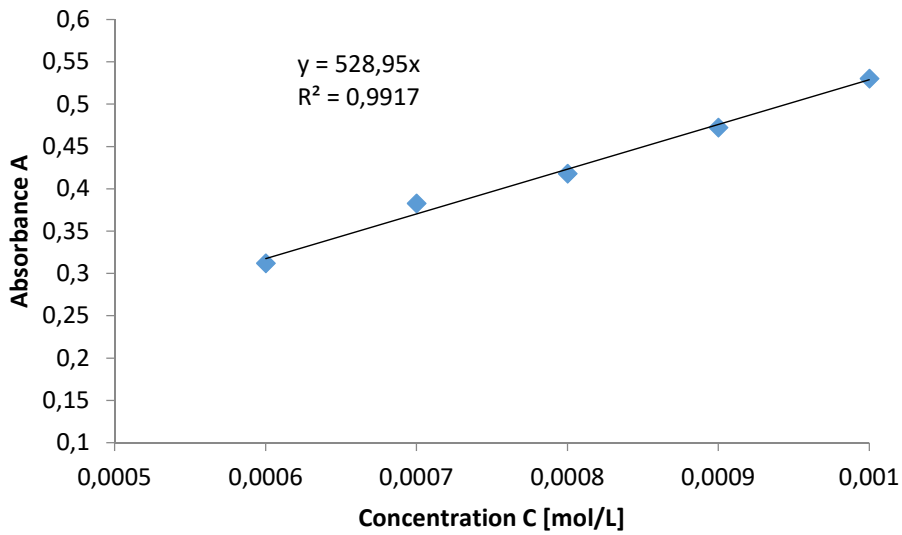

Figure 134. Determination of ε (5300 $M^{-1}cm^{-1}$) through a graphical draw of absorptions (λ = 320 nm) of **200** against their concentrations

7.3.9. UV/vis Spectra and Determination of ε for Triaryl Germane 209

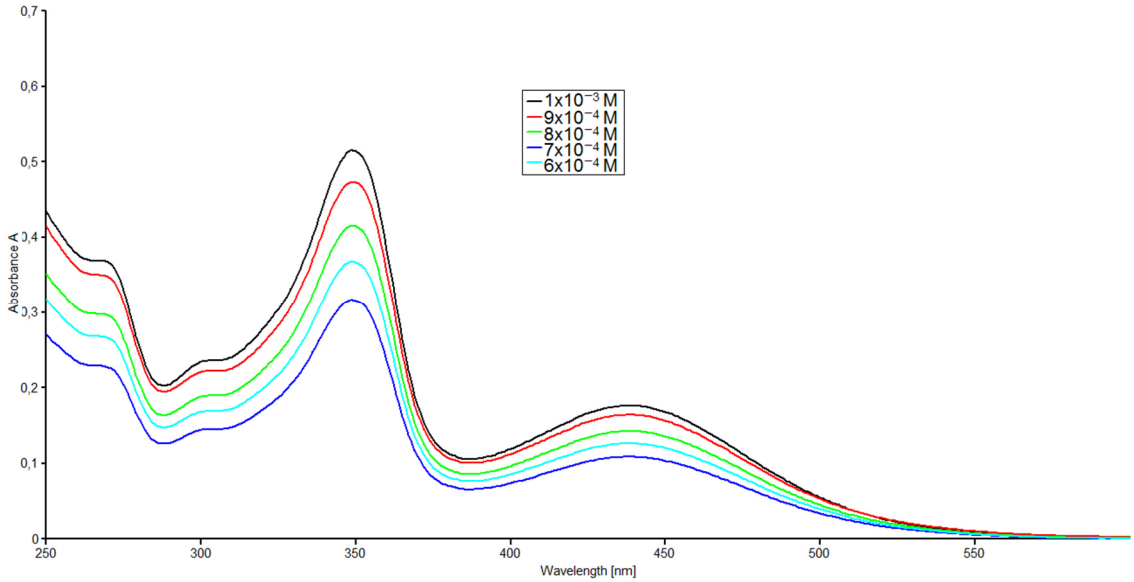

Figure 135. UV/vis spectra of **209** in hexane at different concentrations ($1x10^{-3}$ – $6x10^{-4}$ mol/L).

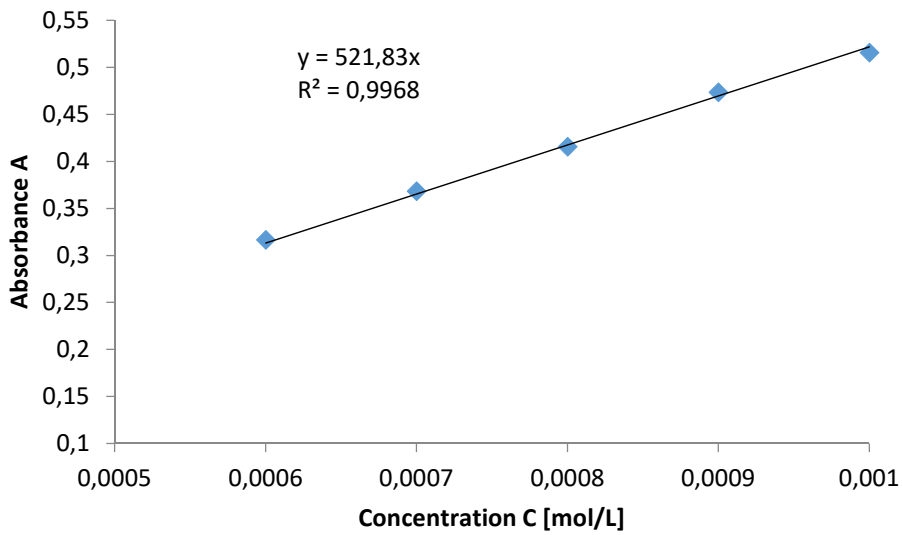

Figure 136. Determination of ε (5200 $M^{-1}cm^{-1}$) through a graphical draw of absorptions (λ = 349 nm) of **209** against their concentrations.

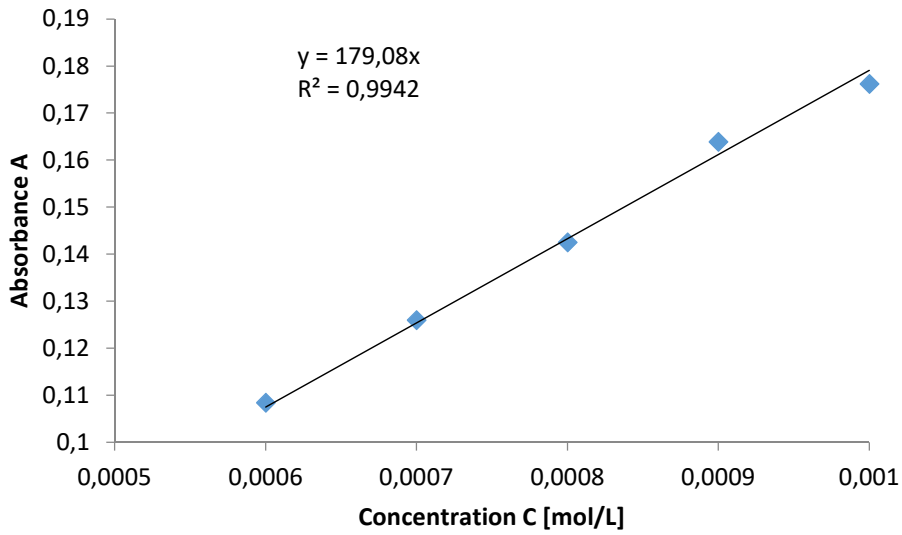

Figure 137. Determination of ε (1800 $M^{-1}cm^{-1}$) through a graphical draw of absorptions (λ = 437 nm) of **209** against their concentrations.

7.3.10. UV/vis Spectra and Determination of ε for Digermenide 90

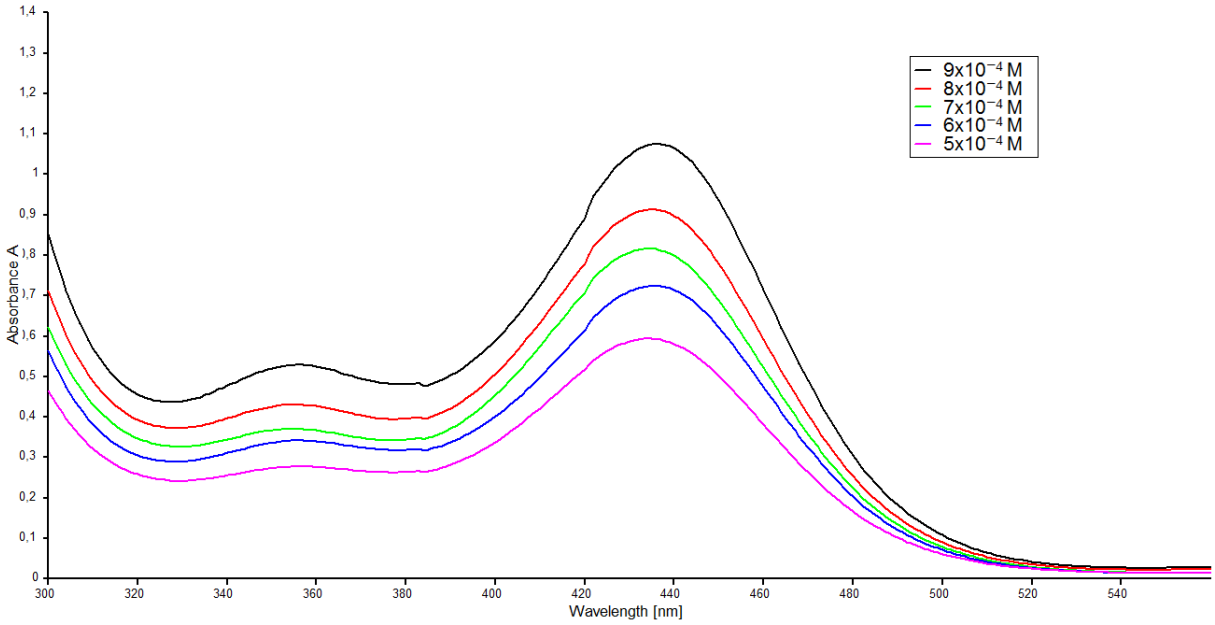

Figure 138. UV/vis spectra of **90** in hexane at different concentrations ($9x10^{-4}$ – $5x10^{-4}$ mol/L).

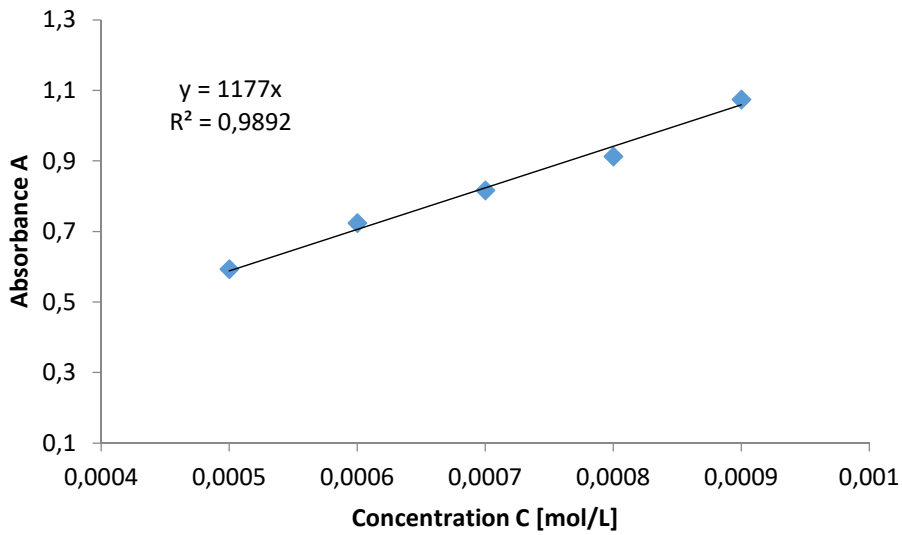

Figure 139. Determination of ε (11800 $M^{-1}cm^{-1}$) through a graphical draw of absorptions (λ = 435 nm) of **90** against their concentrations.

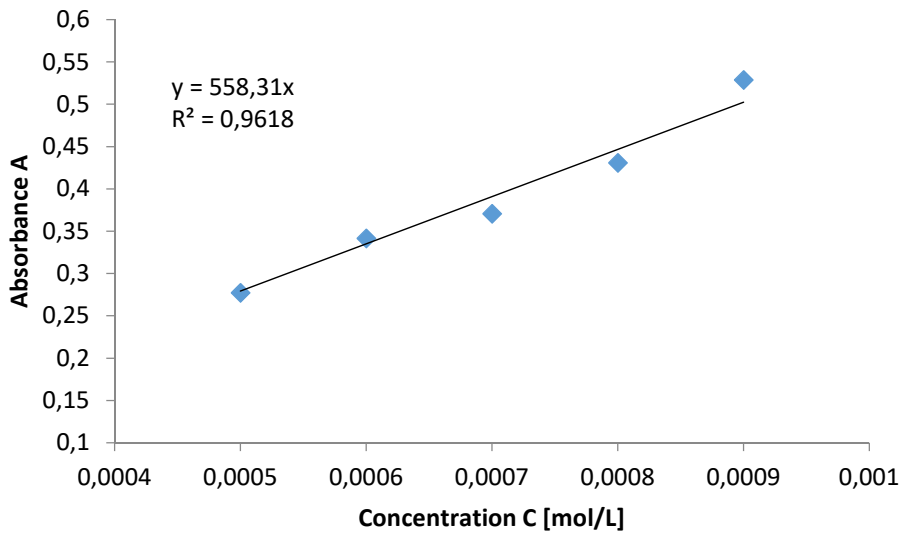

Figure 140. Determination of ε (5600 $M^{-1}cm^{-1}$) through a graphical draw of absorptions (λ = 356 nm) of **90** against their concentrations

7.3.11. UV/vis Spectra and Determination of ε for Phenylene-Bridged Tetragermabutadiene 216

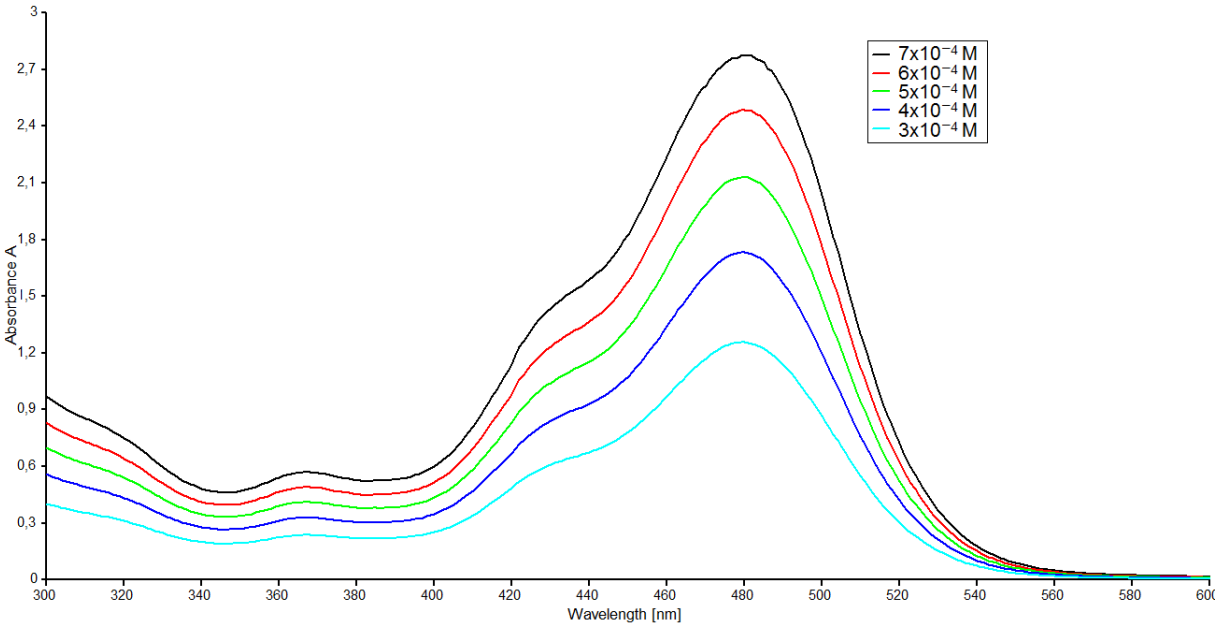

Figure 141. UV/vis spectra of **216** in hexane at different concentrations ($9x10^{-4}$ – $5x10^{-4}$ mol/L).

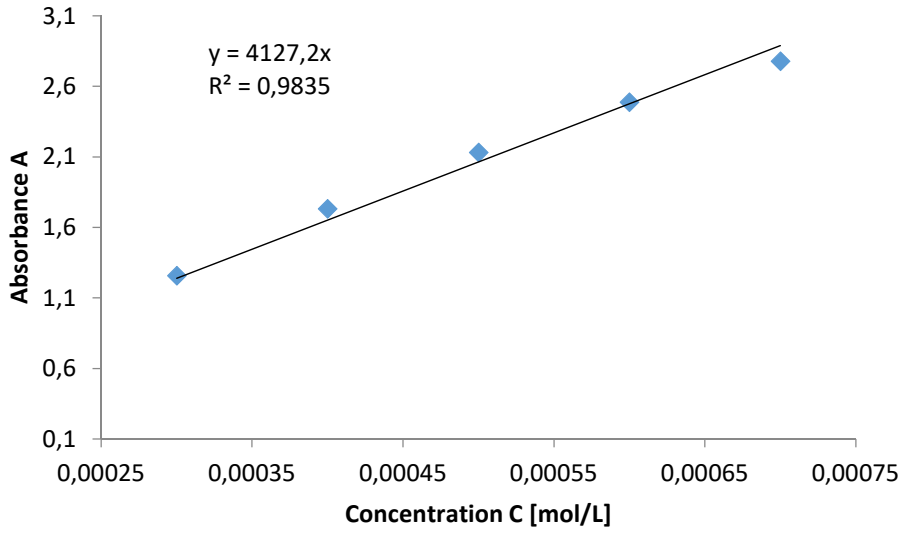

Figure 142. Determination of ε (41300 $M^{-1}cm^{-1}$) through a graphical draw of absorptions (λ = 480 nm) of **216** against their concentrations.

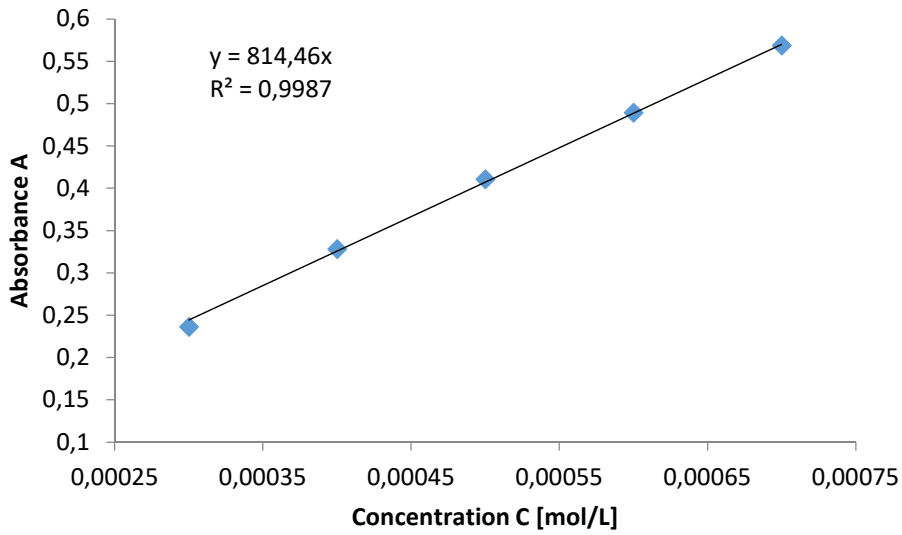

Figure 143. Determination of ε (8100 $M^{-1}cm^{-1}$) through a graphical draw of absorptions (λ = 367 nm) of **216** against their concentrations.

7.3.12. UV/vis Spectra and Determination of ε for Digermenyl Borate 219

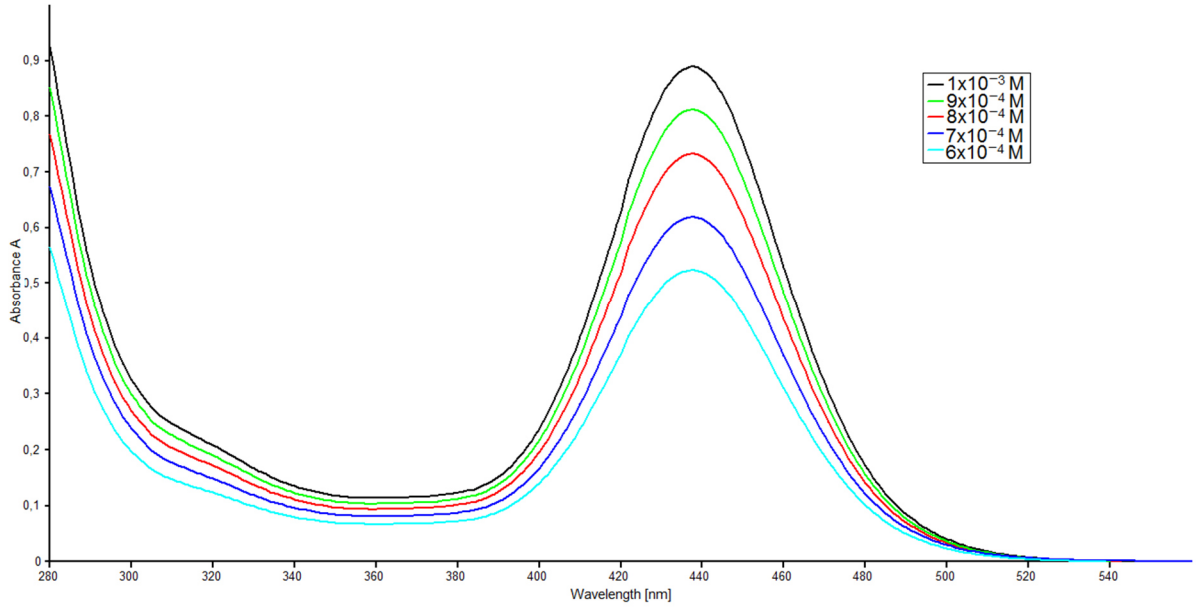

Figure 144. UV/vis spectra of **219** in hexane at different concentrations ($6x10^{-4}$ – $1x10^{-3}$ mol/L).

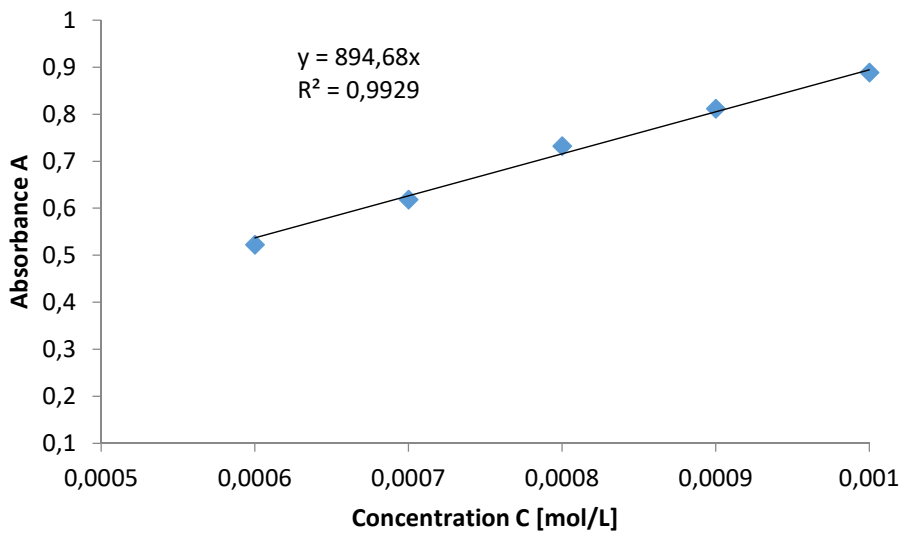

Figure 145. Determination of ε (8900 $M^{-1}cm^{-1}$) through a graphical draw of absorptions (λ = 438 nm) of **219** against their concentrations.

7.4. X-ray Structure Determination

7.4.1. Crystal Data and Structure Refinement for Chair-Isomer Si_4Ge_2 131

Identification code	sh3530
Empirical formula	C92 H144 Ge2 Si4, C7 H8
Formula weight	1599.74
Temperature	152(2) K
Wavelength	0.71073 Å
Crystal system	Triclinic
Space group	P-1
Unit cell dimensions	a = 16.3223(6) Å α = 71.4780(19)°.
	b = 17.6076(7) Å β = 77.6430(18)°.
	c = 18.3797(8) Å γ = 67.4580(17)°.
Volume	4600.3(3) $Å^3$
Z	2
Density (calculated)	1.155 Mg/m^3
Absorption coefficient	0.749 mm^{-1}
F(000)	1732
Crystal size	0.303 x 0.248 x 0.210 mm^3
Theta range for data collection	1.297 to 27.210°.
Index ranges	-20<=h<=20, -22<=k<=22, -23<=l<=23
Reflections collected	77965
Independent reflections	20276 [R(int) = 0.0508]
Completeness to theta = 25.242°	100.0 %
Absorption correction	Semi-empirical from equivalents
Max. and min. transmission	0.7455 and 0.7011
Refinement method	Full-matrix least-squares on F^2
Data / restraints / parameters	20276 / 49 / 1051
Goodness-of-fit on F^2	1.024
Final R indices [I>2sigma(I)]	R1 = 0.0488, wR2 = 0.1187
R indices (all data)	R1 = 0.0828, wR2 = 0.1344
Extinction coefficient	n/a
Largest diff. peak and hole	1.332 and -0.616 e.$Å^{-3}$

7.4.2. Crystal Data and Structure Refinement for Doubly-Bridged Tetrahedron Si_4Ge_2 132

Identification code	sh3557
Empirical formula	C92H144 Ge2 Si4 x 0.5 C7 H8
Formula weight	1557.70
Temperature	133(2) K
Wavelength	0.71073 Å
Crystal system	Monoclinic
Space group	C2/c
Unit cell dimensions	a = 33.8499(14) Å α = 90°.
	b = 26.2285(14) Å β = 97.911(2)°.
	c = 20.2919(8) Å γ = 90°.
Volume	17844.3(14) $Å^3$
Z	8
Density (calculated)	1.160 Mg/m^3
Absorption coefficient	0.771 mm^{-1}
F(000)	6760
Crystal size	0.389 x 0.230 x 0.046 mm^3
Theta range for data collection	1.215 to 26.502°.
Index ranges	-42<=h<=42, -32<=k<=32, -25<=l<=15
Reflections collected	136792
Independent reflections	18398 [R(int) = 0.0917]
Completeness to theta = 25.242°	99.9 %
Absorption correction	Semi-empirical from equivalents
Refinement method	Full-matrix least-squares on F^2
Data / restraints / parameters	18398 / 110 / 987
Goodness-of-fit on F^2	1.011
Final R indices [I>2sigma(I)]	R1 = 0.0463, wR2 = 0.0951
R indices (all data)	R1 = 0.0883, wR2 = 0.1105
Extinction coefficient	n/a
Largest diff. peak and hole	0.873 and -0.653 $e.Å^{-3}$

7.4.3. Crystal Data and Structure Refinement for Disilenyl Germylene 128c

Identification code	sh3676aa
Empirical formula	C62 H94 Ge N2 Si2 x C9 H12
Formula weight	1116.34
Temperature	122(2) K
Wavelength	0.71073 Å
Crystal system	Trigonal
Space group	R-3
Unit cell dimensions	a = 37.7343(15) Å α = 90°.
	b = 37.7343(15) Å β = 90°.
	c = 25.323(3) Å γ = 120°.
Volume	31226(4) $Å^3$
Z	18
Density (calculated)	1.069 Mg/m^3
Absorption coefficient	0.514 mm^{-1}
F(000)	10908
Crystal size	0.332 x 0.277 x 0.172 mm^3
Theta range for data collection	1.017 to 27.150°.
Index ranges	-48<=h<=48, -48<=k<=48, -32<=l<=32
Reflections collected	134431
Independent reflections	15353 [R(int) = 0.0592]
Completeness to theta = 25.242°	100.0 %
Absorption correction	Semi-empirical from equivalents
Max. and min. transmission	0.7455 and 0.7015
Refinement method	Full-matrix least-squares on F^2
Data / restraints / parameters	15353 / 9 / 723
Goodness-of-fit on F^2	1.078
Final R indices [I>2sigma(I)]	R1 = 0.0526, wR2 = 0.1180
R indices (all data)	R1 = 0.0814, wR2 = 0.1275
Extinction coefficient	n/a
Largest diff. peak and hole	0.719 and -0.604 e.$Å^{-3}$

7.4.4. Crystal Data and Structure Refinement for Heavier Cyclopropylidene Analogue 123c

Identification code	sh3540
Empirical formula	C62 H93 Ge N2 Si2 x 3 C7 H8
Formula weight	1271.55
Temperature	173(2) K
Wavelength	0.71073 Å
Crystal system	Triclinic
Space group	P-1
Unit cell dimensions	a = 15.9617(17) Å α = 114.148(5)°.
	b = 16.6009(18) Å β = 112.883(5)°.
	c = 17.9948(19) Å γ = 96.575(5)°.
Volume	3790.4(7) $Å^3$
Z	2
Density (calculated)	1.114 Mg/m^3
Absorption coefficient	0.478 mm^{-1}
F(000)	1378
Crystal size	1.451 x 0.723 x 0.354 mm^3
Theta range for data collection	1.414 to 30.504°.
Index ranges	-22<=h<=22, -23<=k<=23, -25<=l<=25
Reflections collected	81062
Independent reflections	22760 [R(int) = 0.0332]
Completeness to theta = 25.242°	100.0 %
Absorption correction	Semi-empirical from equivalents
Max. and min. transmission	0.7460 and 0.6433
Refinement method	Full-matrix least-squares on F^2
Data / restraints / parameters	22760 / 0 / 786
Goodness-of-fit on F^2	1.042
Final R indices [I>2sigma(I)]	R1 = 0.0493, wR2 = 0.1414
R indices (all data)	R1 = 0.0672, wR2 = 0.1525
Extinction coefficient	n/a
Largest diff. peak and hole	1.713 and -0.735 e.$Å^{-3}$

7.4.5. Crystal Data and Structure Refinement for Si_2Ge-Ring 124b

Identification code	sh3546	
Empirical formula	C74 H127 Ge N2 Si2	
Formula weight	1173.54	
Temperature	162(2) K	
Wavelength	0.71073 Å	
Crystal system	Monoclinic	
Space group	$P2_1/c$	
Unit cell dimensions	a = 13.6295(7) Å	α = 90°.
	b = 19.7334(10) Å	β = 97.980(3)°.
	c = 21.4547(10) Å	γ = 90°.
Volume	5714.5(5) $Å^3$	
Z	4	
Density (calculated)	1.364 Mg/m^3	
Absorption coefficient	0.628 mm^{-1}	
F(000)	2580	
Crystal size	0.643 x 0.298 x 0.084 mm^3	
Theta range for data collection	1.408 to 27.182°.	
Index ranges	-17<=h<=17, -23<=k<=25, -25<=l<=27	
Reflections collected	50447	
Independent reflections	12692 [R(int) = 0.0631]	
Completeness to theta = 25.242°	100.0 %	
Absorption correction	Semi-empirical from equivalents	
Max. and min. transmission	0.7455 and 0.6859	
Refinement method	Full-matrix least-squares on F^2	
Data / restraints / parameters	12692 / 0 / 629	
Goodness-of-fit on F^2	1.010	
Final R indices [I>2sigma(I)]	R1 = 0.0456, wR2 = 0.1020	
R indices (all data)	R1 = 0.0828, wR2 = 0.1160	
Extinction coefficient	n/a	
Largest diff. peak and hole	1.324 and -0.421 $e.Å^{-3}$	

7.4.6. Crystal Data and Structure Refinement for Heavier Cyclopentenylidene Derivative 133

Identification code	sh3548
Empirical formula	C77 H108 Ge N2 Si2
Formula weight	1190.42
Temperature	163(2) K
Wavelength	0.71073 Å
Crystal system	Triclinic
Space group	P-1
Unit cell dimensions	a = 11.4319(5) Å α= 100.5120(10)°.
	b = 14.6466(5) Å β= 92.0450(10)°.
	c = 21.5014(9) Å γ = 95.2650(10)°.
Volume	3519.7(2) $Å^3$
Z	2
Density (calculated)	1.123 Mg/m^3
Absorption coefficient	0.511 mm^{-1}
F(000)	1288
Crystal size	0.557 x 0.372 x 0.307 mm^3
Theta range for data collection	1.421 to 28.892°.
Index ranges	-15<=h<=15, -19<=k<=17, -29<=l<=29
Reflections collected	64193
Independent reflections	18283 [R(int) = 0.0294]
Completeness to theta = 25.242°	99.6 %
Absorption correction	Semi-empirical from equivalents
Max. and min. transmission	0.7458 and 0.7090
Refinement method	Full-matrix least-squares on F^2
Data / restraints / parameters	18283 / 244 / 1143
Goodness-of-fit on F^2	1.028
Final R indices [I>2sigma(I)]	R1 = 0.0385, wR2 = 0.0941
R indices (all data)	R1 = 0.0533, wR2 = 0.1015
Extinction coefficient	n/a
Largest diff. peak and hole	0.606 and -0.446 $e.Å^{-3}$

7.4.7. Crystal Data and Structure Refinement for Heavier Cyclopentenylidene Analogue 134

Identification code	sh3607
Empirical formula	C70 H110 Ge N2 Si2 x 1.25(C5 H12)
Formula weight	1188.47
Temperature	143(2) K
Wavelength	0.71073 Å
Crystal system	Monoclinic
Space group	$P2_1/n$
Unit cell dimensions	a = 12.6352(3) Å α= 90°.
	b = 23.8472(6) Å β= 101.5350(10)°.
	c = 25.5287(7) Å γ = 90°.
Volume	7536.8(3) $Å^3$
Z	4
Density (calculated)	1.047 Mg/m^3
Absorption coefficient	0.477 mm^{-1}
F(000)	2586
Crystal size	0.517 x 0.509 x 0.378 mm^3
Theta range for data collection	1.180 to 28.596°.
Index ranges	-17<=h<=16, -31<=k<=32, -34<=l<=31
Reflections collected	75564
Independent reflections	19229 [R(int) = 0.0316]
Completeness to theta = 25.242°	100.0 %
Absorption correction	Semi-empirical from equivalents
Max. and min. transmission	0.7457 and 0.6890
Refinement method	Full-matrix least-squares on F^2
Data / restraints / parameters	19229 / 42 / 763
Goodness-of-fit on F^2	1.107
Final R indices [I>2sigma(I)]	R1 = 0.0571, wR2 = 0.1648
R indices (all data)	R1 = 0.0789, wR2 = 0.1777
Extinction coefficient	n/a
Largest diff. peak and hole	1.135 and -0.460 e.$Å^{-3}$

7.4.8. Crystal Data and Structure Refinement for Cyclic Germylene 138

Identification code	sh3579
Empirical formula	C71H104 Ge N3 Si2 x 0.5 C7 H8
Formula weight	1173.39
Temperature	143(2) K
Wavelength	0.71073 Å
Crystal system	Monoclinic
Space group	$P2_1/n$
Unit cell dimensions	a = 12.7844(8) Å α= 90°.
	b = 22.7467(13) Å β= 94.490(3)°.
	c = 23.4180(11) Å γ = 90°.
Volume	6789.1(7) $Å^3$
Z	4
Density (calculated)	1.148 Mg/m^3
Absorption coefficient	0.529 mm^{-1}
F(000)	2540
Crystal size	0.927 x 0.066 x 0.038 mm^3
Theta range for data collection	1.250 to 26.431°.
Index ranges	-10<=h<=15, -28<=k<=28, -29<=l<=24
Reflections collected	50088
Independent reflections	13888 [R(int) = 0.0829]
Completeness to theta = 25.242°	100.0 %
Absorption correction	Semi-empirical from equivalents
Max. and min. transmission	0.7454 and 0.6187
Refinement method	Full-matrix least-squares on F^2
Data / restraints / parameters	13888 / 0 / 771
Goodness-of-fit on F^2	1.010
Final R indices [I>2sigma(I)]	R1 = 0.0523, wR2 = 0.0960
R indices (all data)	R1 = 0.1008, wR2 = 0.1096
Extinction coefficient	n/a
Largest diff. peak and hole	0.475 and -0.484 $e.Å^{-3}$

7.4.9. Crystal Data and Structure Refinement for Cyclic Germylene 143

Identification code	sh3675
Empirical formula	C71 H103 Ge N3 Si2 x 2(C5 H12)
Formula weight	1271.62
Temperature	152(2) K
Wavelength	0.71073 Å
Crystal system	Monoclinic
Space group	$P2_1/n$
Unit cell dimensions	a = 13.2550(5) Å α = 90°.
	b = 25.4218(8) Å β = 101.111(2)°.
	c = 23.7680(8) Å γ = 90°.
Volume	7858.9(5) $Å^3$
Z	4
Density (calculated)	1.075 Mg/m^3
Absorption coefficient	0.462 mm^{-1}
F(000)	2776
Crystal size	0.696 x 0.404 x 0.260 mm^3
Theta range for data collection	1.185 to 29.658°.
Index ranges	-18<=h<=18, -35<=k<=34, -29<=l<=33
Reflections collected	90578
Independent reflections	22144 [R(int) = 0.0325]
Completeness to theta = 25.242°	100.0 %
Absorption correction	Semi-empirical from equivalents
Max. and min. transmission	0.7459 and 0.7079
Refinement method	Full-matrix least-squares on F^2
Data / restraints / parameters	22144 / 305 / 887
Goodness-of-fit on F^2	1.042
Final R indices [I>2sigma(I)]	R1 = 0.0523, wR2 = 0.1323
R indices (all data)	R1 = 0.0723, wR2 = 0.1430
Extinction coefficient	n/a
Largest diff. peak and hole	0.867 and -0.593 $e.Å^{-3}$

7.4.10. Crystal Data and Structure Refinement for Phenylene-Bridged Bis-Germylene 146

Identification code	sh3470	
Empirical formula	C122 H182 Cl2 Ge2 N4 Si4	
Formula weight	2033.15	
Temperature	152(2) K	
Wavelength	0.71073 Å	
Crystal system	Triclinic	
Space group	P -1	
Unit cell dimensions	a = 13.0560(7) Å	α = 99.027(3)°.
	b = 13.1770(6) Å	β = 91.770(3)°.
	c = 21.8439(10) Å	γ = 92.430(3)°.
Volume	3705.4(3) $Å^3$	
Z	1	
Density (calculated)	0.911 Mg/m^3	
Absorption coefficient	0.511 mm^{-1}	
F(000)	1096	
Crystal size	0.259 x 0.178 x 0.038 mm^3	
Theta range for data collection	0.945 to 26.371°.	
Index ranges	-16<=h<=16, -15<=k<=16, -27<=l<=27	
Reflections collected	39440	
Independent reflections	13272 [R(int) = 0.0873]	
Completeness to theta = 25.242°	88.8 %	
Absorption correction	Semi-empirical from equivalents	
Refinement method	Full-matrix least-squares on F^2	
Data / restraints / parameters	13272 / 180 / 669	
Goodness-of-fit on F^2	1.440	
Final R indices [I>2sigma(I)]	R1 = 0.0894, wR2 = 0.2602	
R indices (all data)	R1 = 0.1747, wR2 = 0.2849	
Extinction coefficient	n/a	
Largest diff. peak and hole	1.128 and -0.504 $e.Å^{-3}$	

7.4.11. Crystal Data and Structure Refinement for Bis-Silyl Carbene 185

Identification code	sh3504	
Empirical formula	C41 H64 Cl4 N2 Si2	
Formula weight	782.92	
Temperature	133(2) K	
Wavelength	0.71073 Å	
Crystal system	Monoclinic	
Space group	P 21/n	
Unit cell dimensions	a = 9.6076(3) Å	α = 90°.
	b = 16.3497(5) Å	β = 95.7776(12)°.
	c = 27.6262(8) Å	γ = 90°.
Volume	4317.5(2) $Å^3$	
Z	4	
Density (calculated)	1.204 Mg/m^3	
Absorption coefficient	0.360 mm^{-1}	
F(000)	1680	
Crystal size	0.267 x 0.164 x 0.113 mm^3	
Theta range for data collection	1.449 to 27.151°.	
Index ranges	-12<=h<=11, -20<=k<=20, -35<=l<=32	
Reflections collected	36632	
Independent reflections	9534 [R(int) = 0.0547]	
Completeness to theta = 25.242°	100.0 %	
Absorption correction	Semi-empirical from equivalents	
Refinement method	Full-matrix least-squares on F^2	
Data / restraints / parameters	9534 / 0 / 698	
Goodness-of-fit on F^2	1.009	
Final R indices [I>2sigma(I)]	R1 = 0.0405, wR2 = 0.0811	
R indices (all data)	R1 = 0.0681, wR2 = 0.0910	
Extinction coefficient	n/a	
Largest diff. peak and hole	0.371 and -0.257 $e.Å^{-3}$	

7.4.12. Crystal Data and Structure Refinement for Disilyl Germylene 200

Identification code	sh3463a	
Empirical formula	C47 H66 Ge N2 Si2	
Formula weight	787.78	
Temperature	153(2) K	
Wavelength	0.71073 Å	
Crystal system	Monoclinic	
Space group	$P2_1/n$	
Unit cell dimensions	a = 14.2024(10) Å	α = 90°.
	b = 15.1956(12) Å	β = 93.956(2)°.
	c = 20.3915(15) Å	γ = 90°.
Volume	4390.3(6) $Å^3$	
Z	4	
Density (calculated)	1.192 Mg/m^3	
Absorption coefficient	0.785 mm^{-1}	
F(000)	1688	
Crystal size	0.532 x 0.203 x 0.092 mm^3	
Theta range for data collection	1.673 to 27.103°.	
Index ranges	-18<=h<=15, -19<=k<=19, -26<=l<=26	
Reflections collected	39764	
Independent reflections	9697 [R(int) = 0.0497]	
Completeness to theta = 25.242°	100.0 %	
Absorption correction	Milti-scan	
Refinement method	Full-matrix least-squares on F^2	
Data / restraints / parameters	9697 / 189 / 525	
Goodness-of-fit on F^2	1.014	
Final R indices [I>2sigma(I)]	R1 = 0.0443, wR2 = 0.0967	
R indices (all data)	R1 = 0.0775, wR2 = 0.1086	
Extinction coefficient	n/a	
Largest diff. peak and hole	0.411 and -0.312 $e.Å^{-3}$	

7.4.13. Crystal Data and Structure Refinement for Triaryl Germane 209

Identification code	sh3694	
Empirical formula	C45 H70 Ge	
Formula weight	683.60	
Temperature	222(2) K	
Wavelength	0.71073 Å	
Crystal system	Orthorhombic	
Space group	Pbcn	
Unit cell dimensions	a = 22.7691(9) Å	α = 90°.
	b = 20.9403(9) Å	β = 90°.
	c = 19.0560(8) Å	γ = 90°.
Volume	9085.7(7) $Å^3$	
Z	8	
Density (calculated)	0.999 Mg/m^3	
Absorption coefficient	0.699 mm^{-1}	
F(000)	2976	
Crystal size	0.593 x 0.472 x 0.420 mm^3	
Theta range for data collection	1.321 to 31.616°.	
Index ranges	-33<=h<=33, -30<=k<=30, -19<=l<=28	
Reflections collected	168472	
Independent reflections	15176 [R(int) = 0.0336]	
Completeness to theta = 25.242°	100.0 %	
Absorption correction	Semi-empirical from equivalents	
Max. and min. transmission	0.7462 and 0.6599	
Refinement method	Full-matrix least-squares on F^2	
Data / restraints / parameters	15176 / 5 / 449	
Goodness-of-fit on F^2	1.121	
Final R indices [I>2sigma(I)]	R1 = 0.0469, wR2 = 0.1428	
R indices (all data)	R1 = 0.0734, wR2 = 0.1657	
Extinction coefficient	n/a	
Largest diff. peak and hole	0.955 and -0.494 $e.Å^{-3}$	

7.4.14. Crystal Data and Structure Refinement for Digermenide 90

Identification code	sh3701	
Empirical formula	C53 H89 Ge2 Li O4	
Formula weight	942.36	
Temperature	122(2) K	
Wavelength	0.71073 Å	
Crystal system	Triclinic	
Space group	P-1	
Unit cell dimensions	a = 10.6247(7) Å	α = 77.769(4)°.
	b = 11.6930(8) Å	β = 86.480(4)°.
	c = 22.6251(17) Å	γ = 80.451(4)°.
Volume	2708.0(3) $Å^3$	
Z	2	
Density (calculated)	1.156 Mg/m^3	
Absorption coefficient	1.149 mm^{-1}	
F(000)	1012	
Crystal size	0.180 x 0.123 x 0.089 mm^3	
Theta range for data collection	0.921 to 26.632°.	
Index ranges	-13<=h<=13, -14<=k<=14, -28<=l<=28	
Reflections collected	42528	
Independent reflections	11149 [R(int) = 0.0787]	
Completeness to theta = 25.242°	99.9 %	
Absorption correction	Semi-empirical from equivalents	
Max. and min. transmission	0.7454 and 0.6973	
Refinement method	Full-matrix least-squares on F^2	
Data / restraints / parameters	11149 / 54 / 564	
Goodness-of-fit on F^2	1.014	
Final R indices [I>2sigma(I)]	R1 = 0.0528, wR2 = 0.1065	
R indices (all data)	R1 = 0.1080, wR2 = 0.1246	
Extinction coefficient	n/a	
Largest diff. peak and hole	0.881 and -0.449 $e.Å^{-3}$	

7.4.15. Crystal Data and Structure Refinement for Phenylene-Bridged Tetragermabutadiene 216

Identification code	sh3717	
Empirical formula	C96 H142 Ge4 x C5 H12	
Formula weight	1658.59	
Temperature	132(2) K	
Wavelength	0.71073 Å	
Crystal system	Monoclinic	
Space group	C2/c	
Unit cell dimensions	a = 33.389(3) Å	α = 90°.
	b = 16.0281(11) Å	β = 100.565(6)°.
	c = 18.0745(12) Å	γ = 90°.
Volume	9508.7(12) $Å^3$	
Z	4	
Density (calculated)	1.159 Mg/m^3	
Absorption coefficient	1.295 mm^{-1}	
F(000)	3552	
Crystal size	0.300 x 0.229 x 0.112 mm^3	
Theta range for data collection	1.241 to 27.926°.	
Index ranges	-43<=h<=43, -21<=k<=21, -23<=l<=23	
Reflections collected	69755	
Independent reflections	11331 [R(int) = 0.0405]	
Completeness to theta = 25.242°	99.8 %	
Absorption correction	Semi-empirical from equivalents	
Max. and min. transmission	0.7456 and 0.6886	
Refinement method	Full-matrix least-squares on F^2	
Data / restraints / parameters	11331 / 39 / 512	
Goodness-of-fit on F^2	1.050	
Final R indices [I>2sigma(I)]	R1 = 0.0391, wR2 = 0.0968	
R indices (all data)	R1 = 0.0568, wR2 = 0.1043	
Extinction coefficient	n/a	
Largest diff. peak and hole	0.747 and -0.514 $e.Å^{-3}$	

7.4.16. Crystal Data and Structure Refinement for Digermenyl Borate 219

Identification code	sh3730	
Empirical formula	C53 H89 B Ge2 Li O4 x C5 H12	
Formula weight	1025.31	
Temperature	293(2) K	
Wavelength	0.71073 Å	
Crystal system	Triclinic	
Space group	P-1	
Unit cell dimensions	a = 13.2371(8) Å	α = 74.390(2)°.
	b = 13.2748(8) Å	β = 85.281(3)°.
	c = 20.3077(13) Å	γ = 65.726(3)°.
Volume	3131.4(3) $Å^3$	
Z	2	
Density (calculated)	1.087 Mg/m^3	
Absorption coefficient	0.998 mm^{-1}	
F(000)	1106	
Crystal size	0.743 x 0.536 x 0.182 mm^3	
Theta range for data collection	1.042 to 31.626°.	
Index ranges	-19<=h<=19, -19<=k<=19, -28<=l<=29	
Reflections collected	75930	
Independent reflections	20713 [R(int) = 0.0329]	
Completeness to theta = 25.242°	99.5 %	
Absorption correction	Semi-empirical from equivalents	
Max. and min. transmission	0.7462 and 0.6310	
Refinement method	Full-matrix least-squares on F^2	
Data / restraints / parameters	20713 / 84 / 666	
Goodness-of-fit on F^2	1.032	
Final R indices [I>2sigma(I)]	R1 = 0.0424, wR2 = 0.1051	
R indices (all data)	R1 = 0.0701, wR2 = 0.1181	
Extinction coefficient	n/a	
Largest diff. peak and hole	1.210 and -0.553 e.$Å^{-3}$	

7.4.17. Crystal Data and Structure Refinement for Boryl Digermene 222 and Isomer 223

Identification code	sh3727	
Empirical formula	C57 H79 B Cl Ge2 N	
Formula weight	969.65	
Temperature	122(2) K	
Wavelength	0.71073 Å	
Crystal system	Monoclinic	
Space group	$P2_1/n$	
Unit cell dimensions	a = 14.9475(7) Å	α = 90°.
	b = 17.3173(8) Å	β = 90.032(3)°.
	c = 20.9587(10) Å	γ = 90°.
Volume	5425.2(4) $Å^3$	
Z	4	
Density (calculated)	1.187 Mg/m^3	
Absorption coefficient	1.192 mm^{-1}	
F(000)	2056	
Crystal size	0.548 x 0.278 x 0.212 mm^3	
Theta range for data collection	1.525 to 34.928°.	
Index ranges	-24<=h<=23, -27<=k<=24, -33<=l<=33	
Reflections collected	167845	
Independent reflections	23568 [R(int) = 0.0419]	
Completeness to theta = 25.242°	100.0 %	
Absorption correction	Semi-empirical from equivalents	
Max. and min. transmission	0.7468 and 0.6564	
Refinement method	Full-matrix least-squares on F^2	
Data / restraints / parameters	23568 / 0 / 587	
Goodness-of-fit on F^2	1.039	
Final R indices [I>2sigma(I)]	R1 = 0.0418, wR2 = 0.1021	
R indices (all data)	R1 = 0.0624, wR2 = 0.1100	
Extinction coefficient	n/a	
Largest diff. peak and hole	1.214 and -1.187 e.Å	